

IOWA STATE UNIVERSITY
Digital Repository

Graduate Theses and Dissertations

Iowa State University Capstones, Theses and
Dissertations

2020

**Combining synthesis, computation, and spectroscopy to
investigate dicyanomethyl radical dimerization**

Joshua Peterson
Iowa State University

Follow this and additional works at: <https://lib.dr.iastate.edu/etd>

Recommended Citation

Peterson, Joshua, "Combining synthesis, computation, and spectroscopy to investigate dicyanomethyl radical dimerization" (2020). *Graduate Theses and Dissertations*. 17857.
<https://lib.dr.iastate.edu/etd/17857>

This Thesis is brought to you for free and open access by the Iowa State University Capstones, Theses and Dissertations at Iowa State University Digital Repository. It has been accepted for inclusion in Graduate Theses and Dissertations by an authorized administrator of Iowa State University Digital Repository. For more information, please contact digirep@iastate.edu.



Combining synthesis, computation, and spectroscopy to investigate dicyanomethyl radical dimerization

by

Joshua Peterson

A dissertation submitted to the graduate faculty
in partial fulfillment of the requirements for the degree of
DOCTOR OF PHILOSOPHY

Major: Organic Chemistry

Program of Study Committee:
Arthur Winter, Major Professor
William Jenks
Levi Stanley
Brett Van Veller
Aaron Rossini

The student author, whose presentation of the scholarship herein was approved by the program of study committee, is solely responsible for the content of this dissertation. The Graduate College will ensure this dissertation is globally accessible and will not permit alterations after a degree is conferred.

Iowa State University

Ames, Iowa

2020

Copyright © Joshua Peterson, 2020. All rights reserved.

DEDICATION

I dedicate this dissertation to my late grandmother, Mabel Peterson. She is sorely missed, and I am forever in debt for the kindness, compassion, and guidance she gave me in my early childhood.

TABLE OF CONTENTS

	Page
LIST OF FIGURES	v
LIST OF TABLES.....	viii
ACKNOWLEDGMENTS	ix
ABSTRACT.....	xi
CHAPTER 1. INTRODUCTION	1
1.1 General Introduction	1
1.2 Thesis Organization.....	2
1.3 References	3
CHAPTER 2. EFFECT OF SUBSTITUENTS ON THE BOND STRENGTH OF AIR-STABLE DICYANOMETHYL RADICAL THERMOCHROMES	5
2.1 Abstract.....	5
2.2 Introduction	5
2.3 Results and Discussion	6
2.4 Conclusions	10
2.5 Experimental Section.....	10
2.6 References	15
CHAPTER 3. EFFECT OF STRUCTURE ON THE SPIN-SPIN INTERACTIONS OF TETHERED DICYANOMETHYL DIRADICALS	17
3.1 Abstract.....	17
3.2 Introduction	18
3.3 Results and Discussion	20
3.4 Materials and Methods	28
3.5 Conclusions	30
3.6 References	30
CHAPTER 4. SOLVENT EFFECTS ON THE STABILITY AND DELOCALIZATION OF ARYL DICYANOMETHYL RADICALS: THE CAPTODATIVE EFFECT REVISITED	33
4.1 Abstract.....	33
4.2 Introduction	34
4.3 Results and Discussion	36
4.4 Computational and Experimental Methods	45
4.5 Conclusions	46
4.6 References	47

CHAPTER 5. EFFECT OF STRUCTURE ON THE SPIN SWITCHING AND MAGNETIC BISTABILITY OF SOLID-STATE ARYL DICYANOMETHYL MONORADICALS AND DIRADICALS	50
5.1 Abstract.....	50
5.2 Introduction	51
5.3 Results and Discussion	52
5.4 Conclusions	57
5.5 Experimental Section.....	57
5.6 References	59
CHAPTER 6. SPIN DELOCALIZATION, POLARIZATION, AND LONDON DISPERSION FORCES GOVERN THE FORMATION OF DIRADICAL PIMERS	61
6.1 Abstract.....	61
6.2 Introduction	62
6.3 Results and Discussion	66
6.4 Computational and Experimental Methods	81
6.5 Conclusions	84
6.6 References	86
CHAPTER 7. GENERAL CONCLUSION	91
APPENDIX A. SUPPORTING INFORMATION FOR CHAPTER 2	94
APPENDIX B. SUPPORTING INFORMATION FOR CHAPTER 3	115
APPENDIX C. SUPPORTING INFORMATION FOR CHAPTER 4	242
APPENDIX D. SUPPORTING INFORMATION FOR CHAPTER 5	255
APPENDIX E. SUPPORTING INFORMATION FOR CHAPTER 6.....	266

LIST OF FIGURES

	Page
Figure 2-1. Structures of example dimer species (top row). Variable-temperature EPR study (second row). Variable-temperature UV-vis study (third row). Insets show the temperature cycling at 5 and 95 °C for 30 min each. Pictures demonstrating thermochromism open to air (bottom row). Pictures are shown to display full thermochromic behavior and may not represent all temperatures studied via EPR	7
Figure 2-2. Computed structure [B98D/6-31+G(d,p)] of dimer species 1 (A, side view; B, top view). Visualized by IboView. ^{14,15} Computed Mulliken atomic spin densities for compounds (C) 1, (D) 9, (E) 8, and (F) 6 and visualized total spin density.....	9
Figure 3-1. (Top) The 14 linked diradicals synthesized and studied in this paper. (Bottom) Generation and considered equilibria for diradicals.....	19
Figure 3-2. Electron paramagnetic resonance spectra of the diradical species of each compound with variable-temperature stimulation to study thermodynamic parameters.....	22
Figure 3-3. UV/vis spectroscopy showing the color change of compound 5O-JUL as it cools, signifying the formation of a pimer band by the peak growing in from 850 nm.....	23
Figure 3-4. (a) Crystal structures for 2,4,6-trimethoxy untethered diradical dimer and (b) 4O. (c) Computational screen of density functionals for accuracy in modeling p-fluorophenyl dicyanomethyl radical dimerization free energy. (d) Using the ωB97XD method to evaluate accuracy of dimerization thermodynamics over a small test set. (e) Suggested qualitative σ-dimer–pimer PES for varying substituents. (f) HOMO of julolidine pimer showing pi overlap.	26
Figure 3-5. (Top) Amino-substituted diradical photochemistry that transforms the diradical into a rhodamine dye derivative. (Bottom) UV-vis at different times of irradiation (Rayonet, 5×10^{-5} M in toluene).	27
Figure 4-1. (Top) MO model for the captodative effect, ^{3,4} showing the stabilization of a radical with an electron acceptor (a), an electron donor (c), and the combined effect (b). (Bottom) Resonance model depicting zwitterionic structures unique to captodative radicals.	34

Figure 4-2. (A) Radical/dimer equilibrium for dicyanomethyl systems; (B) example VT-EPR with van't Hoff plot insert for 1-NMe ₂ ; (C) binding data of representative compounds in a nonpolar (toluene) and polar (DMF) solvent.	37
Figure 4-3. Computed Mulliken spin densities (ω B97XD,6-31+G(d,p), SMD) on the benzylic carbon of differently substituted dicyanomethyl radicals in solvents of varying dielectric (left); spin density comparison of the benzylic carbon and para nitrogen in the NMe ₂ radical system as a function of solvent dielectric (center); spin density distributions across 1-DMA in a nonpolar and polar solvent (right). JUL = julolidine.....	39
Figure 4-4. Computed (left) EPR spectra using the computed A hyperfine coupling (h.f.c.) values from (B3LYP/EPR-III, SMD) compared to experimental EPR spectra (middle) and simulated values for the 1-NMe ₂ radical.	41
Figure 4-5. Plot of computed spin density on the benzylic carbon versus the experimentally derived binding constants on a log scale.	42
Figure 4-6. (Top) Select bond lengths (Å) for 1-DMA and 1-CN in toluene and DMF (ω B97XD/6-31+G(d,p), SMD). Dimethylaniline radical cation is shown as a reference. (Bottom) Grouped Mulliken atomic charges for 1-DMA and 1-CN in toluene and DMF (ω B97XD/ 6-31+G(d,p), SMD).	43
Figure 4-7. Plot of select computed Mulliken spin density (ω B97XD,6- 31+G(d,p), SMD) for the radicals showing no captodative solvent effect (top) in water and gas phase and modified structures with stronger donors and another acceptor, showing a larger solvent effect.....	44
Figure 5-1. Radical–dimer equilibria for all subsets of compounds (top left); crystal structure for thiomethyl, trimethoxy (reproduced from ref 7), and 4O dimers (top right) (reproduced from ref 7); and all VT-EPR data for the 16 solid-state samples in this work (bottom).	52
Figure 5-2. Spin counts at various temperatures for ortho tethers (A), para tethers (B), and monoradicals (C) with fold increases from 298 to 398 K to the right of each.	53
Figure 5-3. Single-crystal EPR data at 400 K for 2,4,6-trimethoxy- and p-thiomethyl-substituted dimers with amorphous powder EPR spectra for each compound below.	55
Figure 6-1. Examples of radicals that form sigma ^{13–17} and π-dimers. ^{16,18–21}	62
Figure 6-2. Known modes of dimerization for the dimethylamino ³¹ and julolidine ³² substituted dicyanomethyl radicals.....	63

Figure 6-3. Schematic of spin delocalization hypothesis for maximizing covalent bonding, polarization hypothesis for maximizing Coulombic interactions, and dispersion hypothesis for maximizing London dispersion forces.....	67
Figure 6-4. Radicals studied here with crystal structures of the radical dimers (crystal structures for 3 and 15 are reproduced from prior work, ^{31,32} while crystals of 4, 7, and 9 were crystallized from chloroform and their structures are new to this study). Radicals 1, 3, 6, and 15 were previously reported, ^{31,32} while the other 11 radicals are new to this study.....	68
Figure 6-5. UV-vis of 6 showing σ -dimerization (a). Low temperature UV-vis of 13 showing pimerization (b).....	71
Figure 6-6. Plot of the log of binding constant vs computed benzylic carbon spin density (top) and a plot of benzylic carbon spin density vs normalized dispersion stabilization energy (middle). In both graphs, red circles signify observed π -dimers and blue triangles represent observed σ -dimers. Versions of these plots with radical labels can be found in Appendix E.....	73
Figure 6-7. (A) Effect of radical polarization on pimer geometry. (B) Resonance model showing stabilization of polarizable captodative radicals by polar solvents (or the presence of another polarizable radical). (C) Mulliken charge distributions of the pimers of a weakly polarizable radical 2 and a highly polarizable radical 15. Insets show the computed Mulliken spin densities for the free radical as a function of solvent dielectric (SMD), with increasing contributions of zwitterionic resonance structures in polar solvents for highly polarizable radicals, which lead to diminished benzylic spin density.....	76
Figure 6-8. Dimerization of compounds 10 and 11 (a), UV-vis spectra of compounds 10 and 11 (b), and benzylic carbon spin density plot and visualized HOMO (IboView) ^{42,43} for compounds 10 and 11 (c).	78

LIST OF TABLES

	Page
Table 2-1. Thermodynamic Binding Parameters and a Plot of the Log of the Binding Constant versus the Hammett σ Parameter.....	6
Table 3-1. Thermodynamic Parameters for <i>o</i> -Linked (a), <i>p</i> -Linked (b), and Julolidine (c)	21
Table 6-1. Thermodynamic Data Obtained through VT-EPR, and Computed Mulliken Benzylid Spin Densities (ω B97XD/6-31+G (d,p)) and Estimates of the Relative Pimer Dispersion Energy (Defined As the Sigma Dimer– Pimer Energy Difference Computed at B98 vs B97D, Relative to Radical 2)	70

ACKNOWLEDGMENTS

I would like to thank my major professor, Dr. Arthur Winter. Upon acceptance into the graduate program at Iowa State I had no idea what type of chemistry I wanted to do, and Art was able to convince me that joining his group was the correct path. Art, you are a remarkable professor and over the years you have proven time and time again how deserving you are of the title Professor. Thank you for the years of mentoring and for teaching me that organic chemistry can have an exciting spin to it. I hope the research in your lab continues to grow and spread as it has during the years I have been a part of your group.

I would also like to extend thanks to current and former Winter group members. Having a positive work environment in graduate school may be the most important factor in keeping happy during the years. To Mark Juetten and Margarita Geraskina, I thank you both for introducing me to a graduate school level work environment and helping me out during my first year here. To Logan Fischer and Pradeep Shrestha, I wish the best of luck on all future work in the Winter Group and I hope the two of you are able to graduate soon and begin to share your knowledge of chemistry in bigger and better places. When all three of joined the group together in late 2015 I wasn't sure how doubling the size of the lab in one semester would go down, but I wouldn't have had it any other way. Thanks for being great co-workers over the years.

To the rest of my thesis committee, Dr. William Jenks, Dr. Levi Stanley, Dr. Brett Van Veller, and Dr. Aaron Rossini, I would like to mention how much I appreciate the diversity of your combined backgrounds. With my project, I was always able to come speak with one of you if I needed help with something outside of my normal niche. Thank you for serving on my committee and for all the support over the years.

I would also like to extend my thanks to the many friends I have made in Ames during my time here. Playing both intramural sports through the University or city-wide recreational leagues were some of the best times I've ever had. Mark, Dave, and Zak; thank you for the invitations to play poker and disc-golf (maybe not Zak for the disc-golf). I hope that many of the friendships I've made in Ames continue even after I've left.

It would not be a true acknowledgments section without the following: I would like to give my personal thanks to Dr. Sarah Cady of the Iowa State Chemical Instrumentation Facility. Sarah is fantastic at assisting with EPR studies and over the years she has taught me many important lessons about instrument maintenance, such as how to keep the EPR up and running, and happy. Not only that, but Sarah is a phenomenal friend and is always willing to talk or help in any way she can. Thank you very much for all you do Sarah, you are truly a great asset in not only the Chemistry Department, but to everyone who uses the department's facilities.

ABSTRACT

The work contained in this dissertation sheds a light on a previously under-investigated class of stable radicals; aryl dicyanomethyl radicals. Organic compounds with spin unpaired electrons, dubbed free radicals, are often reactive and tend to decompose quickly under normal atmospheric conditions. If organic radicals are stabilized, they are attractive candidates for stimuli responsive materials. If these stabilized radicals are to be useful in future materials applications, studies must be performed to learn as much as possible. This work will describe the journey from start to dissertation on the synthesis and analysis of new various dicyanomethyl radicals for their stimuli responsive properties.

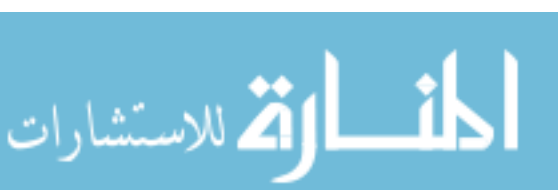
Aryl dicyanomethyl radicals exist in an equilibrium between a closed shell diamagnetic dimer and two open shell paramagnetic radicals. The equilibrium of each different dicyanomethylene radical is dependent upon both the substituents on the aryl ring as well as the solvent these radicals are studied in. Another factor that determines the equilibrium of these compounds is temperature. Thermal stimulation, in both solution and the solid-state, leads to homolysis of the radical-radical sigma bond into two identical radicals for intermolecular dimers. Each compound is investigated by variable temperature electron paramagnetic resonance spectroscopy (VT-EPR) in order to determine thermodynamic values. With thermodynamic data, binding constants for each compound can be calculated from a generated van't Hoff plot. In addition to VT-EPR analysis, some of these radicals have vibrant absorbances in the visible region, so variable temperature UV-Vis spectroscopy can also be performed on select radicals. Various other methods of dimerization other than normal “sigma-dimerization” have been studied as well. This class of organic radicals proves to be rich in potential for stimuli responsive materials.

CHAPTER 1. INTRODUCTION

1.1 General Introduction

In organic chemistry, free radicals can be classified based on reactivity. Unstable radicals are reactive intermediates that play important roles in various organic reactions and biological processes. However, radicals can be stabilized for applications relying on the unique properties of a spin unpaired electron. A few examples are organic spin-crossover materials,¹ turn on magnetic resonance contrast reagents,² stimuli-responsive soft materials,³ spintronics,⁴ and dynamic covalent assemblies derived from stable radical building blocks.⁵ The process of stabilizing a radical is not new to chemistry, Gomberg in 1900 on triphenylmethyl radicals stated, “The radical so formed is apparently stable, for it can be kept both in solution and in the dry crystalline state for weeks”.⁶ The addition of bulky substituents near the radical center and delocalizing spin density through a pi system are two ways in which reactive radicals can be stabilized.

To develop materials that exhibit stimuli responsive behavior, our strategy uses an air stable radical as a building block. A sub-set of radicals, dicyanomethyl radicals, exist in different forms dependent upon various stimuli in the environment. In 1966, Hartzler reported on the *para* functionalization of an aryl dicyanomethylene unit to stabilize the oxidized aryl dicyanomethyl radical.⁷ The addition of a nitro substituent in the *para* substituent inhibited a head-to-tail dead dimerization product. Studies of the homo-dimer of the *para*-nitro dicyanomethyl radical concluded that the dimer was heavily favored in an apparent equilibrium between radical and sigma dimer. Fifty years later, no other investigation into aryl dicyanomethyl radicals has occurred. In 2016, the Seki lab reopened the investigation of aryl dicyanomethyl radicals with a paper that highlighted a dynamic equilibrium between radical and dimer that could be altered with varying the temperature of the compound in solution.⁸ The compounds published in this work centered on



an electronically donating *para* substituent from the dicyanomethyl radical center. The work in this dissertation begins with the investigation into why Hartzler, in 1966, had such different results from Seki and coworkers in 2016 by functionalizing the radical differently.

1.2 Thesis Organization

The following dissertation is a summary of the re-opened investigation on dicyanomethyl radicals and their exciting ability to equilibrate between a closed shell diamagnetic dimer and an open shell paramagnetic radical. This project has evolved from an investigation of substituent effects to a project that questions the fundamental understanding of the behavior these radicals exhibit under varying environmental stimuli.

Chapter 2 contains the first published work of this dissertation, from the *Journal of Organic Chemistry*, and it focuses on altering substituents in the *para* position from the radical center in order to understand the effect on dimerization. After synthesizing 11 new *para*-substituted dicyanomethyl radicals, we find that electron donation into the aryl rings stabilizes the radical in the equilibrium by orders of magnitude more than withdrawing substituents.

Chapter 3 focuses on a publication, from the *Journal of the American Chemical Society*, highlighting the linking of two dicyanomethyl radicals together via an alkoxy alkyl alkoxy chain to form non-conjugated diradicals. Selected radicals bearing donating groups were tethered together with varying lengths of atoms in either the *para* or *ortho* position, relative to the dicyanomethyl radical center. Linker length, position, and donating ability all led to different results, and the first tethered π -dimer dicyanomethyl radical was synthesized and studied.

Chapter 4 focuses on a publication, from the *Journal of the American Chemical Society*, focusing on the captodative stabilization of radicals by altering dielectric constant of solvent. With experimental data from Chapters 2 and 3 and a computational investigation using the SMD solvent model, there is a captodative stabilization of strongly donating dicyanomethyl radicals in solvents

of high polarity. This work was applied to radicals other than dicyanomethyl radicals and helps provide an answer for questions from previously unsuccessful studies in the literature.

Chapter 5 contains a publication, in *ACS Omega*, highlighting the solid-state magnetic bistability of both tethered and non-tethered dicyanomethyl radicals. This work focused on a serendipitous discovery that dicyanomethyl radicals exhibit similar thermal homolysis of dimer to radical in the solid state as in solution. Both amorphous powders and crystalline samples were studied, and there were both similarities and differences with respect to previous works in solution.

Chapter 6 contains a publication, from the *Journal of the American Chemical Society*, in which modes of dimerization were investigated to determine structural characteristics necessary for the formation of π -dimers over σ -dimers, or vice versa. A new library of 15 differently substituted dicyanomethyl radicals, with moderate to strong electron donation, were analyzed experimentally and computationally. Computational results hint that spin delocalization, solvent dispersion, and polarizability of each radical contribute in some way to the preferred mode of dimerization. Experimentally, binding constant determination and low temperature UV-Vis studies helped validate computational data in the search for pimerization preferences.

1.3 References

- (1) Abe, M. *Chem. Rev.* 2013, 113, 7011–7088. Juetten, M. J.; Buck, A. T.; Winter, A. H. *Chem. Commun.* 2015, 51, 5516–5519. Buck, A. T.; Paletta, J. T.; Khindurangala, S. A.; Beck, C. L.; Winter, A. H. *J. Am. Chem. Soc.* 2013, 135, 10594–10597. Geraskina, M. R.; Buck, A. T.; Winter, A. H. *J. Org. Chem.* 2014, 79, 7723–7727.
- (2) Nguyen, H. V.-T.; Chen, Q.; Rajca, A.; Johnson, J. A. *ACS Cent. Sci.* 2017, 3, 800–811. Rajca, A.; Wang, Y.; Boska, M.; Paletta, J. T.; Olankitwanit, A.; Swanson, M. A.; Mitchell, D. G.; Eaton, S. S.; Eaton, G. R.; Rajca, S. *J. Am. Chem. Soc.* 2012, 134, 15724–15727. Sowers, M. A.; McCombs, J. R.; Wang, Y.; Paletta, J. T.; Morton, S. W.; Dreaden, E. C.; Boska, M. D.; Ottaviani, M. F.; Hammond, P. T.; Rajca, A.; Johnson, J. A. *Nat. Commun.* 2014, 5, 5460.

- (3) Nishida, S.; Morita, Y.; Fukui, K.; Sato, K.; Shiomi, D.; Takui, T.; Nakasuji, K. *Angew. Chem.* 2005, 117, 7443–7446. Wojtecki, R. J.; Meador, M. A.; Rowan, S. *J. Nat. Mater.* 2011, 10, 14–27.
- (4) Morita, Y.; Suzuki, S.; Sato, K.; Takui, T. *Nat. Chem.* 2011, 3, 197–204. Alcon, I.; Vin̄es, F.; Moreira, I.; Bromley, S. T. *Nat. Commun.* 2017, 8, 1957. Shishlov, N. M. *Russ. Chem. Rev.* 2006, 75, 863–884.
- (5) Rajca, A. *Chem. Rev.* 1994, 94, 871–893. Jin, Y.; Yu, C.; Denman, R. J.; Zhang, W. *Chem. Soc. Rev.* 2013, 42, 6634–6654. Rowan, S. J.; Cantrill, S. J.; Cousins, G. R. L.; Sanders, J. K. M.; Stoddart, J. F. *Angew. Chem., Int. Ed.* 2002, 41, 898–952.
- (6) Gomberg, M., *J. Am. Chem. Soc.*, 1900, 22 (11), 757-771.
- (7) Hartzler, H. D. *J. Org. Chem.*, 1966, 31 (8), 2654–2658.
- (8) Kobashi, T.; Sakamaki, D.; Seki, S. *Angew. Chem., Int. Ed.* 2016, 55, 8634.

CHAPTER 2. EFFECT OF SUBSTITUENTS ON THE BOND STRENGTH OF AIR-STABLE DICYANOMETHYL RADICAL THERMOCHROMES

Adapted with permission from: J. P. Peterson, M. R. Geraskina, R. Zhang, A. H. Winter. *J. Org. Chem.* **2017**, 82 (12), 6497–6501, Copyright (2020) American Chemical Society.

2.1 Abstract

A series of substituted aryl dicyanomethyl radicals were synthesized, and the bonding thermodynamic parameters for self-dimerization were determined from van't Hoff plots obtained from variable-temperature electron paramagnetic resonance and ultraviolet-visible spectroscopy. At low temperatures, the radicals dimerize, but the colored, air-stable free radicals return upon heating. Heating and cooling cycles (5–95 °C) can be repeated without radical degradation and with striking thermochromic behavior. We find a linear free energy relationship between the Hammett para substituent parameter and the dimerization equilibrium constant, with para electron-donating substituents leading to a weaker bond and electron-withdrawing substituents leading to stronger bonds, following a captodative effect. Density functional theory investigations [B98D/6-31+G(d,p)] reveal that the dimers prefer a slip-stacked geometry and feature elongated bonds.

2.2 Introduction

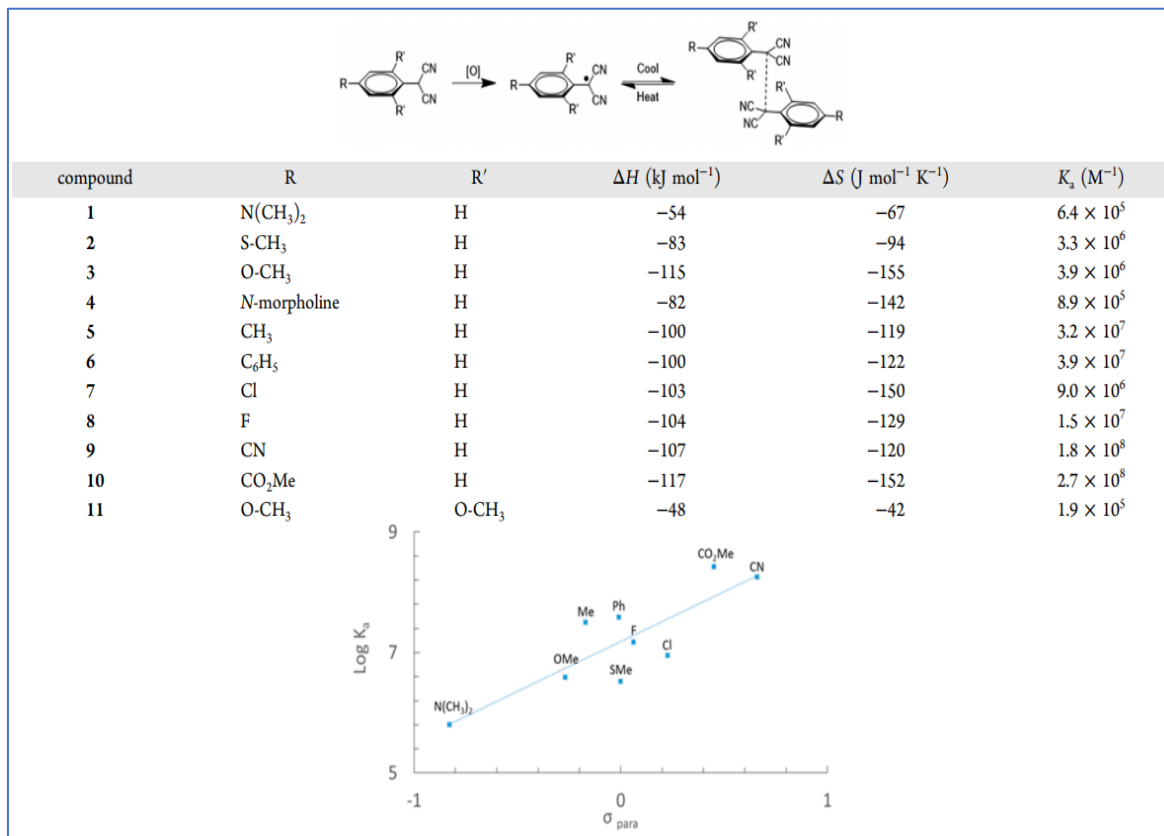
Dynamic materials that adapt their properties to environmental cues or external stimuli are increasingly being pursued. We have been interested in achieving such stimulus-responsive behavior by exploiting changes in spin state upon a stimulus because of the unique properties of radicals.^{1–3} However, this approach is made challenging because many radicals lack air and thermal stability.^{4–9} We were intrigued by reports of stable dicyanomethyl radicals and related radicals in the literature,^{4,6,7} as well as a recent report by Kobashi et al. describing stable

thermochromic triaryl amino-dicyanomethyl radicals.⁹ We thus set out to perform a systematic investigation of the effect of the structure of the dicyanomethyl radical on the strength of the radical bonding interaction, with an eye toward identifying potential new building blocks for stimulus-responsive materials.

2.3 Results and Discussion

A set of 11 aryl dicyanomethyl radicals were synthesized (Table 2.1), and the thermodynamic parameters were evaluated using van't Hoff plots generated from variable-temperature EPR and UV-vis spectroscopy experiments. The radicals were synthesized via palladium cross coupling reactions of varying aryl bromides with malononitrile, followed by oxidation to the radical using potassium ferricyanate. Remarkably, these radicals and/or radical

Table 2-1. Thermodynamic Binding Parameters and a Plot of the Log of the Binding Constant versus the Hammett σ Parameter



dimers can be purified by a low-temperature biphasic separation between acetonitrile and hexane under air.

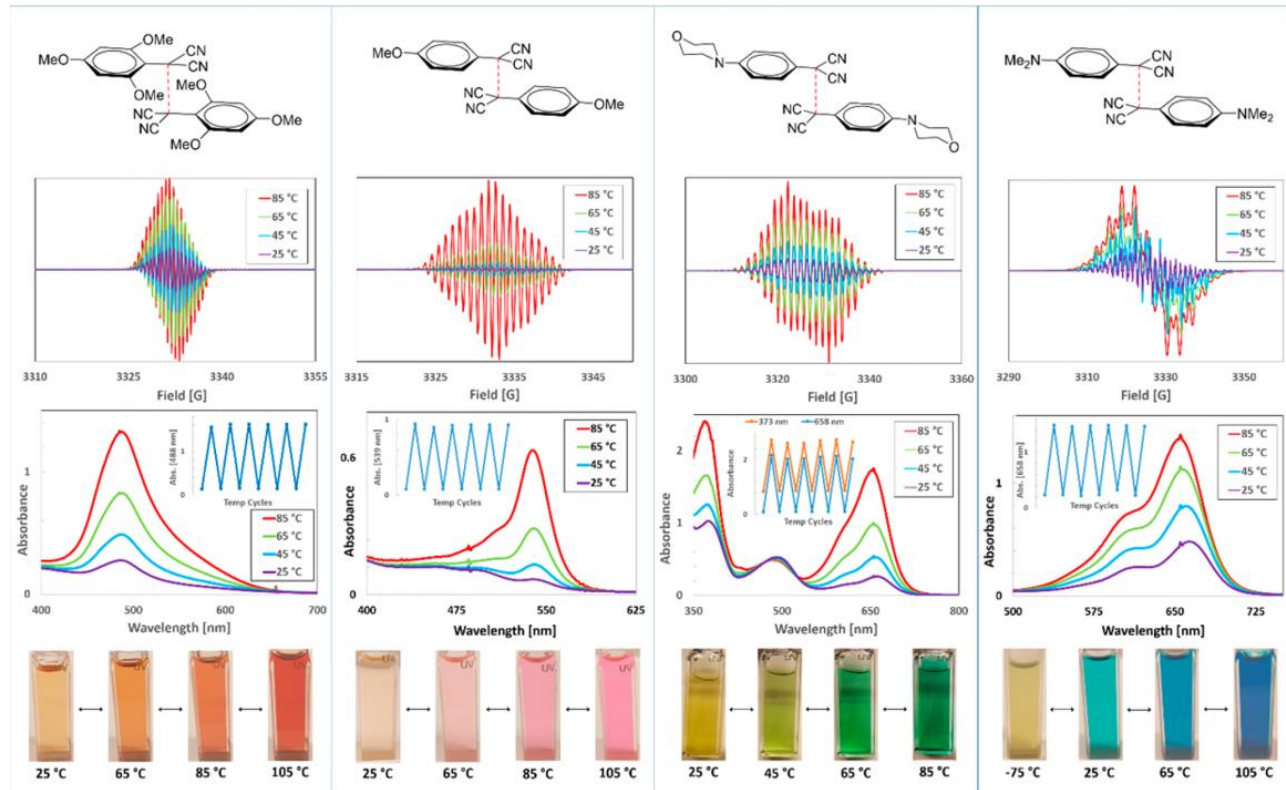


Figure 2-1. Structures of example dimer species (top row). Variable-temperature EPR study (second row). Variable-temperature UV-vis study (third row). Insets show the temperature cycling at 5 and 95 °C for 30 min each. Pictures demonstrating thermochromism open to air (bottom row). Pictures are shown to display full thermochromic behavior and may not represent all temperatures studied via EPR.

All the radicals exhibit qualitatively the same behavior. At low temperatures, the radical dimerizes, as evidenced by a lack of an EPR signal, yielding a yellow or colorless solution. As the temperature is increased, a signal corresponding to the radical grows in the EPR and UV-vis spectrum. The radicals have absorption bands in the visible region of the optical spectrum. Example variable-temperature EPR and UV-vis data are shown in Figure 2.1 for radicals 1, 3, 4, and 11 (all data, including a video demonstrating the thermochromic behavior, can be found in the Supporting Information). Each radical in Figure 2.1 has a different color, leading to striking

thermochromic behavior that is highly dependent on the radical structure. To test the durability of the radical species, temperature cycling studies in which a sample was monitored for 30 min at 5 °C followed by 30 min at 95 °C were performed. After six cycles, there was no decrease in absorbance at 95 °C, confirming that the radical was thermally stable (see UV-vis insets in Figure 2.1).

The thermodynamic bonding parameters for all the radicals were obtained from van't Hoff plots following the growth of the EPR signal as a function of temperature and are listed in Table 1. All thermodynamic data are the average of three separate runs and fits. Inspection of the binding constants shows that better electronic donors, such as compounds 1–4, have binding constants ($K_a = 10^5 - 10^6 \text{ M}^{-1}$) that are lower than those of radicals bearing either weaker donating substituents or withdrawing substituents, such as compounds 5–10 ($K_a > 10^7 \text{ M}^{-1}$).

To test if substituent effects were additive, we synthesized 11, a trimethoxy derivative. Indeed, this radical showed the weakest dimer bond of all molecules studied ($K_a = 1.9 \times 10^5 \text{ M}^{-1}$), suggesting that substituent effects are additive. The compounds with less electron donation exhibit stronger binding. Compounds 5–8 are interesting because the halogenated derivatives 7 and 8 bind less tightly than the alkyl-substituted derivatives 5 and 6. The ability of halogens to be both π -electron donors and σ -withdrawing groups may play a role in the weaker dimerization. Derivatives containing electron-withdrawing groups (e.g., CN and CO₂Me) were found to have the highest binding constants ($\sim 10^8 \text{ M}^{-1}$) and even have resolved NMR spectra at room temperature. The other dimers exhibit NMR signals only at low temperatures because of fast exchange.

A plot of the Hammett σ para parameter¹⁰ for each monomer unit against the log of the binding constant showed a positive, relatively linear trend (Table 2.1). The existence of the captodative effect has been debated,^{11,12} but this model predicts that radicals containing both

donating and withdrawing groups would be stabilized. Given that donating substituents lead to the weakest binding (and, presumably, the most stabilized radicals), our data are consistent with the captodative model.

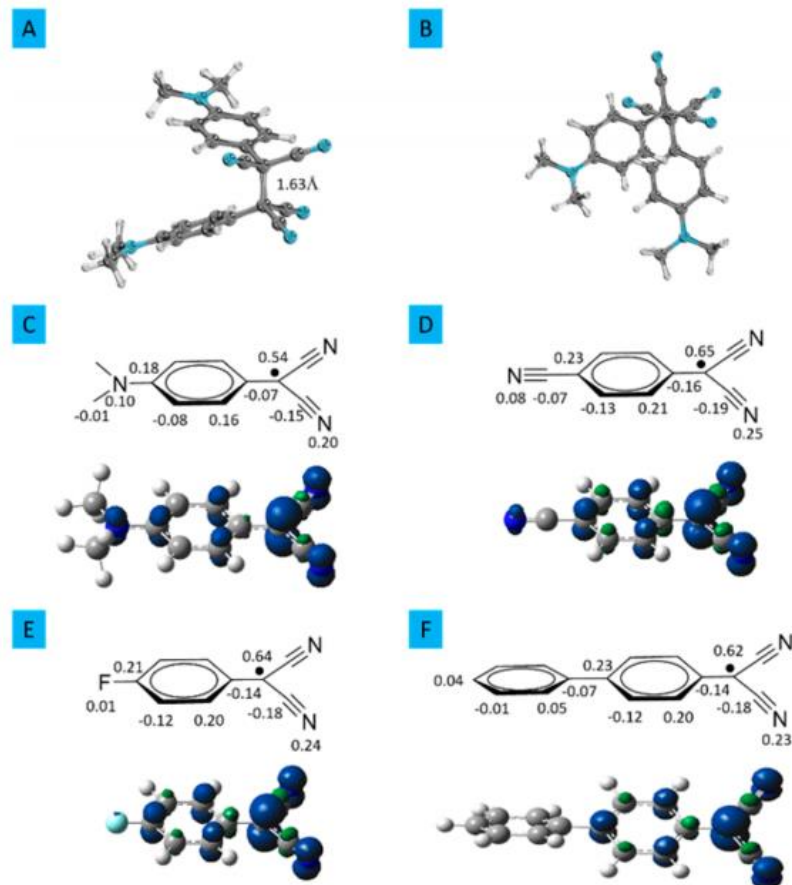


Figure 2-2. Computed structure [B98D/6-31+G(d,p)] of dimer species 1 (A, side view; B, top view). Visualized by IboView.^{14,15} Computed Mulliken atomic spin densities for compounds (C) 1, (D) 9, (E) 8, and (F) 6 and visualized total spin density.

Computational studies were performed on select dimer species to improve our understanding of the orientation of the two units with respect to the σ bond formed between two radicals (Figure 2.2).¹³ Surprisingly, the dihedral angle between the two molecules is only $\sim 60^\circ$. Only minor variance was observed between differently substituted compounds and the calculated dihedral angle. Figure 2.2 shows the computed structures, at two different viewpoints, for dimer

1, as well as the Mulliken spin densities for compounds 1, 9, 8, and 6. Each dimer features an exceptionally long computed σ bond of $\sim 1.63 \text{ \AA}$.

2.4 Conclusions

In conclusion, we have synthesized a set of stable aryl dicyanomethyl radicals that exhibit thermochromic properties and have a bond strength that is highly dependent on the substituents. The bond strengths can be tuned from 10^5 to 10^8 M^{-1} based on the nature of the para substituent. It is possible that these radicals could be incorporated into polymeric materials leading to bulk materials with temperature-responsive behavior or find use in dynamic covalent chemistries.

2.5 Experimental Section

General Methods. ^1H nuclear magnetic resonance (^1H NMR) and ^{13}C nuclear magnetic resonance (^{13}C NMR) spectra were recorded on a Bruker DRX-500 instrument. NMR spectra were recorded in CDCl_3 at room temperature except where noted. The NMR data were presented accordingly: chemical shifts in parts per million with deuterated chloroform (CDCl_3 , δ 7.26) for ^1H NMR and the chloroform residue (δ 77.0) for ^{13}C NMR as internal standards, multiplicity labels (s, singlet; d, doublet; t, triplet; m, multiplet), J splitting (hertz), and integration. EPR spectra were recorded on a Bruker FT-EPR instrument. UV-vis spectra were recorded on an Agilent 8453 spectrometer. Mass spectra were recorded on an Agilent QTOF 6540 instrument. Melting points were determined on a DigiMelt SRS apparatus. The crystal structure was obtained on a BRUKER APEX II diffractometer equipped with an APEX II CCD detector. All reactions were performed under an argon atmosphere in oven-dried glassware. Xylenes were dried under activated molecular sieves (0.4 nm). Flash column chromatography was performed with 40–63 μm silica gel (230–400 mesh) from SILICYCLE. All other chemical reagents were purchased from commercial sources and used without purification.

General Procedure for Coupling of Malononitrile to Aryl Bromide. To a 50 mL three-neck round-bottom flask with a magnetic stir bar was added NaOtBu (13 mmol) under an ambient atmosphere. The flask was sealed and placed under an argon atmosphere. To the flask was then added 20 mL of xylenes (dried by 0.4 nm activated molecular sieves), and the contents of the flask were stirred for 5 min to produce a uniform solution. To the flask was next added CH₂(CN)₂ (6.6 mmol) via syringe, and the resulting mixture was stirred for 60 min. To a separate 100 mL conical-bottom flask was added the aryl bromide of the reaction mixture (4.4 mmol) under an ambient atmosphere. The flask was pumped into a glovebox to add 0.2 g of [Pd(PPh₃)₂]Cl₂ catalyst (6.5 mol %). To the conical-bottom flask was then added 10–15 mL of dried xylenes, and the mixture was stirred for 5–10 min. The conical flask was cannulated into the round-bottom flask. The reaction mixture was stirred at 130 °C and the reaction monitored by TLC (CHCl₃ as eluent) until it reached completion. The resulting reaction was then quenched with a 10% HCl aqueous solution. The mixture was then filtered through Celite and extracted with ethyl acetate (3 × 50 mL). The organic layers were combined and dried with Na₂SO₄, and the solvent was removed by rotary evaporation. The crude product was then purified by flash chromatography (CHCl₃ as the eluent) to afford the product.

Procedure for Oxidation of 1-11. To a 50 mL Schlenk flask was added the aryl malononitrile (0.3 mmol) dissolved in 15 mL of CH₂Cl₂ along with a magnetic stir bar. The flask was flushed with argon and kept under an inert atmosphere. Separately in a 50 mL round-bottom flask was placed 15 mL of a 0.3 M KOH solution that was purged with argon. To the round-bottom flask was added K₃[Fe(CN)₆] (1.5 mmol) as the oxidant. The solution was allowed to mix for 5 min before the solution was cannulated into the Schlenk flask containing the aryl malononitrile. The solution was mixed while being vigorously stirred for 10 min. The mixture was then exposed

to air; the organic layer was separated and dried with Na_2SO_4 , and the solvent was removed by rotary evaporation. The crude product was then purified by cold extraction (-78°C) between hexanes and acetonitrile. The dimer product was kept in the solid acetonitrile, and impurities remained in the hexanes.

EPR Studies. All EPR studies were performed on samples purged with argon to view the hyperfine coupling of the radical species. Samples were allowed to equilibrate at each temperature for 5 min before data were acquired. The following EPR parameters were utilized for all samples unless otherwise noted: modulation frequency, 100 kHz; receiver gain, 50 dB; modulation amplitude, 0.5; time constant, 0.01 s; center field, 3300 G; sweep width, 200 G; microwave attenuation, 20 dB; microwave power, 2 mW; number of data points, 2048; average number of scans, 8. The sweep time and conversion time varied from sample to sample and are mentioned below for each compound.

UV-Vis Studies. To a 3 mL quartz cuvette was added a known concentration of dimer species dissolved in toluene for study. Identical results were obtained regardless of whether samples were purged with argon or under air. All samples were studied in the temperature range of 5–95 °C. A temperature-controlled water circulating bath was used to monitor the temperature, and at each data point, the sample was allowed to equilibrate to the current temperature for 5 min.

Compound Characterization. 1_{H} . The general procedure produced a green/yellow solid (0.383 g, 47% yield): mp 168–170 °C; ^1H NMR (500 MHz, CDCl_3) δ 7.98 (d, $J = 7.6$ Hz, 2H), 6.70 (d, $J = 7.6$ Hz, 2H), 3.16 (s, 1H); ^{13}C NMR (500 MHz, CDCl_3) δ 151.4, 128.2, 112.8, 112.6, 112.4, 40.3, 27.6. 1_{D} . Following the general oxidation procedure, a brilliant blue organic solution yielded a dark red solid. For EPR spectroscopy, a conversion time of 2.56 ms and a sweep time of 5.24 s were used.

2_H. The general procedure produced a pale yellow powder (0.151 g, 20% yield): ¹H NMR (500 MHz, CDCl₃) δ 7.37 (d, J = 8.35 Hz, 2H), 7.30 (d, J = 8.5 Hz, 2H), 5.04 (s, 1H), 2.50 (s, 3H); ¹³C NMR (500 MHz, CDCl₃) δ 142.4, 127.6, 127.0, 122.2, 111.9, 27.7, 15.2; HRMS (ESI-TOF) m/z calcd for C₁₀H₇N₂S 187.0335, found 187.0339 [M – H]. **2_D.** Following the general oxidation procedure, a green organic solution was isolated as a yellow powder. For EPR spectroscopy, a conversion time of 2.56 ms and a sweep time of 5.24 s were used.

3_H. The general procedure produced a pink solid (0.124 g, 15% yield): ¹H NMR (500 MHz, CDCl₃) δ 7.38 (d, J = 8.3 Hz, 2H), 6.97 (d, J = 7.6 Hz, 2H), 5.03 (s, 1H), 3.82 (s, 3H); ¹³C NMR (500 MHz, CDCl₃) δ 160.9, 128.6, 117.9, 115.3, 112.3, 55.5, 27.4. **3_D.** Following the general oxidation procedure, a pink organic solution yielded a pale yellow solid.

4_H. The general procedure produced a beige powder (0.120 g, 12% yield): mp 153–155 °C; ¹H NMR (500 MHz, CDCl₃) δ 7.34 (d, J = 7.3 Hz, 2H), 6.94 (d, J = 7.3 Hz, 2H), 5.00 (s, 1H), 3.84 (t, J = 4.0 Hz, 4H), 3.20 (t, J = 4.0 Hz, 4H); ¹³C NMR (500 MHz, CDCl₃) δ 152.5, 128.3, 116.1, 116.0, 112.3, 66.7, 48.4, 27.5; HRMS (ESI-TOF) m/z calcd for C₁₃H₁₄N₃O 228.1131, found 228.1136 [M + H]. **4_D.** Following the general oxidation procedure, a yellow/brown organic solution yielded a brown solid. For EPR spectroscopy, a conversion time of 2.56 ms and a sweep time of 5.24 s were used. This sample used a receiver gain of 40 dB and a modulation amplitude of 1.0.

5_H. The general procedure produced a pale yellow powder (0.570 g, 83% yield): mp 56–58 °C; ¹H NMR (500 MHz, CDCl₃) δ 7.38 (d, J = 8.0 Hz, 2H), 7.30 (d, J = 8.0 Hz, 2H), 5.02 (s, 1H), 2.40 (s, 3H); ¹³C NMR (500 MHz, CDCl₃) δ 140.7, 130.7, 127.1, 123.2, 111.9, 27.8, 21.2. **5_D.** Following the general oxidation procedure, a yellow organic solution yielded a pale yellow powder.

6_H. The general procedure produced a white crystalline solid (0.288 g, 30% yield): mp 105–108 °C; ¹H NMR (500 MHz, CDCl₃) δ 7.71 (d, J = 8.3 Hz, 2H) 7.58 (m, J = 8.3, 7.8 Hz, 4H), 7.49 (t, J = 7.8, 7.2 Hz, 2H), 7.43 (t, J = 7.2 Hz, 1H), 5.12 (s, 1H); ¹³C NMR (500 MHz, CDCl₃) δ 143.5, 139.4, 129.1, 128.7, 128.3, 127.7, 127.3, 125.0, 111.9, 27.9; HRMS (ESI-TOF) m/z calcd for C₁₅H₉N₂ 217.0771, found 217.0776 [M – H]. **6_D.** Following the general oxidation procedure, a clear organic solution yielded a white powder. For EPR spectroscopy, a modulation amplitude of 2.0, a conversion time of 2.56 ms, and a sweep time of 5.24 s were used.

7_H. The general procedure produced a pale orange solid (0.536 g, 69% yield): mp 72–75 °C; ¹H NMR (500 MHz, CDCl₃) δ 7.50 (d, J = 8.7 Hz, 2H), 7.46 (d, J = 8.7 Hz, 2H), 5.05 (s, 1H); ¹³C NMR (500 MHz, CDCl₃) δ 137.2, 130.7, 129.0, 125.0, 111.7, 28.0. **7_D.** Following the general oxidation procedure, a yellow organic solution yielded a pale yellow powder.

8_H. The general procedure produced a white crystalline solid (0.218 g, 31% yield): ¹H NMR (500 MHz, CDCl₃) δ 7.51 (dd, J = 7.0 Hz, 2H), 7.21 (t, J = 7.0 Hz, 2H), 5.06 (s, 1H); ¹³C NMR (500 MHz, CDCl₃) δ 163.8, 129.4, 122.2, 117.4, 111.7, 27.6; HRMS (ESI-TOF) m/z calcd for C₉H₄FN₂ 159.0359, found 159.0366 [M – H]. **8_D.** Following the general oxidation procedure, a yellow organic solution yielded a pale yellow powder. For EPR spectroscopy, a modulation amplitude of 2.0 was used.

9_H. The general procedure produced a slightly pink crystalline solid (0.331 g, 45% yield): mp 98–100 °C; ¹H NMR (500 MHz, CDCl₃) δ 7.83 (d, J = 10 Hz, 2H), 7.68 (d, J = 10 Hz, 2H), 5.21 (s, 1H); ¹³C NMR (500 MHz, CDCl₃) δ 133.8, 131.1, 128.3, 117.4, 114.9, 110.9, 28.2; HRMS (ESI-TOF) m/z calcd for C₁₀H₄N₃ 166.0411, found 166.0411 [M – H]. **9_D.** Following the general oxidation procedure, a clear organic solution yielded a white powder. For EPR spectroscopy, a modulation amplitude of 2.0 was used.

^{10H}. The general procedure produced a white crystalline solid (0.088 g, 10% yield): ¹H NMR (500 MHz, CDCl₃) δ 8.14 (d, J = 7.5 Hz, 2H), 7.59 (d, J = 7.5 Hz, 2H), 5.22 (s, 1H), 3.94 (s, 3H). ^{10D}. Following the general oxidation procedure, a clear organic solution yielded a white powder. For EPR spectroscopy, a modulation amplitude of 2.0 was used: ¹³C NMR (500 MHz, CDCl₃) δ 165.2, 134.4, 130.9, 128.7, 128.6, 109.9, 53.0, 52.6; HRMS (ESI-TOF) m/z calcd for C₁₁H₇N₂O₂ 199.0508, found 199.0511 [M/2].

^{11H}. The general procedure produced a white crystalline solid (0.092 g, 9% yield): mp 106–108 °C; ¹H NMR (500 MHz, CDCl₃) δ 6.15 (s, 2H), 5.52 (s, 1H), 3.90 (s, 6H), 3.82 (s, 3H); ¹³C NMR (500 MHz, CDCl₃) δ 163.4, 158.3, 112.5, 95.7, 91.0, 56.2, 55.6, 16.6; HRMS (ESI-TOF) m/z calcd for C₁₂H₁₃N₂O₃ 233.0921, found 233.0919 [M + H]. ^{11D}. Following the general oxidation procedure, a dark red organic solution yielded an orange powder.

2.6 References

- (1) Buck, A. T.; Paletta, J. T.; Khindurangala, S. A.; Beck, C. L.; Winter, A. H. J. Am. Chem. Soc. 2013, 135 (29), 10594–10597.
- (2) Geraskina, M. R.; Buck, A. T.; Winter, A. H. J. Org. Chem. 2014, 79 (16), 7723–7727.
- (3) Juettent, M. J.; Buck, A. T.; Winter, A. H. Chem. Commun. 2015, 51 (25), 5516–5519.
- (4) Hartzler, H. D. J. Org. Chem. 1966, 31 (8), 2654–2658.
- (5) Peterson, L. I. J. Am. Chem. Soc. 1967, 89 (11), 2677–2681.
- (6) de Jongh, H. A. P.; de Jonge, C. R. H. I.; Sinnige, H. J. M.; de Klein, W. J.; Huysmans, W. G. B.; Mijs, W. J.; van den Hoek, W. J.; Smidt, J. J. Org. Chem. 1972, 37 (12), 1960–1966.
- (7) Suzuki, H.; Koide, H.; Ogawa, T. Bull. Chem. Soc. Jpn. 1988, 61, 501–504.
- (8) de Jongh, H. A. P.; de Jonge, C. R. H. I.; Mijs, W. J. J. Org. Chem. 1971, 36 (21), 3160–3168.

- (9) Kobashi, T.; Sakamaki, D.; Seki, S. *Angew. Chem., Int. Ed.* 2016, 55, 8634.
- (10) McDaniel, D. H.; Brown, H. C. *J. Org. Chem.* 1958, 23, 420.
- (11) Leroy, G.; Dewispelaere, J. P.; Benkadour, H.; Riffi Temsamani, D.; Wilante, C. *Bull. Soc. Chim. Belg.* 1994, 103 (7–8), 367–378.
- (12) Tanaka, H. *Trends Polym. Sci.* 1993, 1 (11), 361–365.
- (13) Frisch, M. J.; Trucks, G. W.; Schlegel, H. B.; Scuseria, G. E.; Robb, M. A.; Cheeseman, J. R.; Scalmani, G.; Barone, V.; Mennucci, B.; Petersson, G. A.; Nakatsuji, H.; Caricato, M.; Li, X.; Hratchian, H. P.; Izmaylov, A. F.; Bloino, J.; Zheng, G.; Sonnenberg, J. L.; Hada, M.; Ehara, M.; Toyota, K.; Fukuda, R.; Hasegawa, J.; Ishida, M.; Nakajima, T.; Honda, Y.; Kitao, O.; Nakai, H.; Vreven, T.; Montgomery, J. A., Jr.; Peralta, J. E.; Ogliaro, F.; Bearpark, M.; Heyd, J. J.; Brothers, E.; Kudin, K. N.; Staroverov, V. N.; Kobayashi, R.; Normand, J.; Raghavachari, K.; Rendell, A. P.; Burant, J. C.; Iyengar, S. S.; Tomasi, J.; Cossi, M.; Rega, N.; Millam, N. J.; Klene, M.; Knox, J. E.; Cross, J. B.; Bakken, V.; Adamo, C.; Jaramillo, J.; Gomperts, R.; Stratmann, R. E.; Yazyev, O.; Austin, A. J.; Cammi, R.; Pomelli, C.; Ochterski, J. W.; Martin, R. L.; Morokuma, K.; Zakrzewski, V. G.; Voth, G. A.; Salvador, P.; Dannenberg, J. J.; Dapprich, S.; Daniels, A. D.; Farkas, Ö.; Foresman, J. B.; Ortiz, J. V.; Cioslowski, J.; Fox, D. J. Gaussian 09; Gaussian, Inc.: Wallingford, CT, 2009.
- (14) Knizia, G. *J. Chem. Theory Comput.* 2013, 9, 4834.
- (15) Knizia, G.; Klein, J. E. M. N. *Angew. Chem., Int. Ed.* 2015, 54, 5518–5522.

CHAPTER 3. EFFECT OF STRUCTURE ON THE SPIN-SPIN INTERACTIONS OF TETHERED DICYANOMETHYL DIRADICALS

Adapted with permission from: R. Zhang*, J. P. Peterson* L. J. Fischer, A. Ellern, A. H. Winter. *J.*

Am. Chem. Soc. **2018**, 140 (43), 14308-14313. Copyright (2020) American Chemical Society.

*Co-first author

3.1 Abstract

Stable organic radicals with switchable spin states have attracted attention for a variety of applications, but a fundamental understanding of how radical structure effects the weak bonding interactions between organic radicals is limited. To evaluate the effect of chemical structure on the strength and nature of such spin interactions, a series of 14 tethered aryl dicyanomethyl diradicals were synthesized, and the structure and thermodynamic properties of the diradicals were investigated. These studies indicate that the nature of the dimer and the equilibrium thermodynamic parameters of the diradical–dimer equilibria are highly sensitive to the attachment point of the linker, the length of the linker, and the substituents on the radical itself. Values of the intramolecular K_a vary from as small as 5 to as high as 10^5 depending on these variables. An X-ray crystal structure for a linked ortho-substituted diradical shows that the diradical forms an intramolecular sigma dimer in the crystalline state with an elongated C–C bond (1.637 Å). Subtle changes to the radical structure influences the nature of the spin interactions, as fixing the dimethylamino substituent on the radical into a ring to make a julolidine-derived diradical leads to the weakest bonding interaction observed ($\Delta G_{\text{bonding}} = 1 \text{ kcal mol}^{-1}$) and changes the spin-paired species from a sigma dimer to a diradical pimer. This work has implications for the design of

stimuli responsive materials that can reversibly switch between the dramatically different properties of closed-shell species and the unique properties of diradicals.

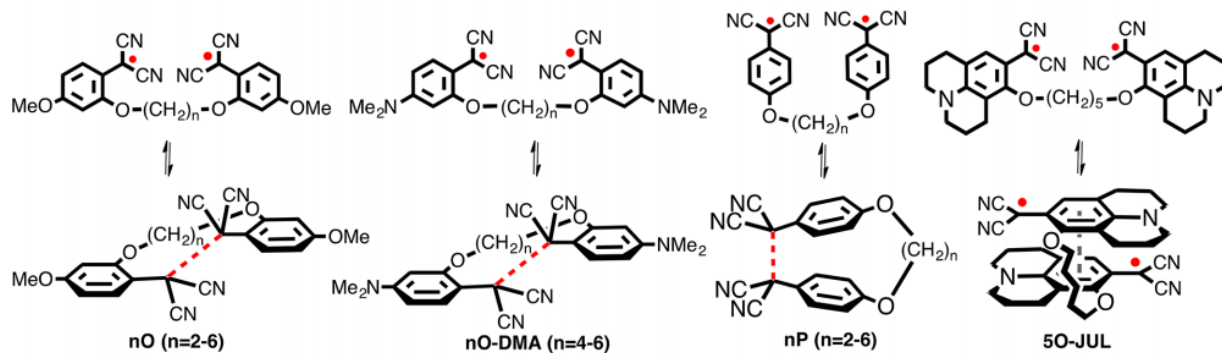
3.2 Introduction

The ability of open-shell species to form weak self-association complexes has made organic radicals attractive for a variety of applications including organic spin-crossover materials,¹ turn on magnetic resonance contrast reagents,² stimuli-responsive soft materials,³ spintronics,⁴ and dynamic covalent assemblies derived from stable radical building blocks.⁵ However, a fundamental understanding of how radical structure affects the weak bonding interactions between organic radicals is limited by the scarcity of radicals that engage in this behavior with sufficient stability for detailed study.

Aryl dicyanomethyl radicals make attractive candidates for such studies.⁶ These radicals, and related species, have been known for many years to persist long enough to collect electron paramagnetic resonance (EPR) spectra, but were long overlooked for applications because they undergo an irreversible “head-to-tail” dimerization⁶ that destroys the radical. However, in 2016 Seki and co-workers demonstrated that these radicals become indefinitely air and thermally stable species provided that para substituents are added to block this dead-end head-to-tail dimerization pathway.⁶ Normally, to achieve air stability, organic radicals must be substituted with sterically blocking groups near the radical center.⁷ That these aryl dicyanomethyl radicals do not require such sterically blocking groups for stability is unusual and permits these stable radicals to form weak-bonding spin–spin interactions in solution as diamagnetic dimers, straddling the knife-edge between normal closed-shell molecules and stable diradicals in both structure and properties. As a result, they are intriguing building blocks for stimuli-responsive materials that can switch between the dramatically different properties of closed-shell species and the unique properties of diradicals.

Following Seki's discovery, we performed structure–activity relationships on aryl dicyanomethyl monoradicals and found that electron-donating groups appended to the aryl ring shift the equilibrium toward the diradical,⁸ while withdrawing groups shift the equilibrium toward diamagnetic dimers. With para substituents, the bond strength is correlated with the Hammett σ_{para} substituent parameter. Thus, the radical–radical interaction can be tuned by substituents. However, whether these radicals can be used in larger structures featuring multiple radical centers remains unknown. A key problem in achieving this objective is understanding how the radicals interact when covalently linked.

■ **Linked diradicals studied and proposed equilibria**



■ **Generation and considered equilibria (50-DMA shown as example)**

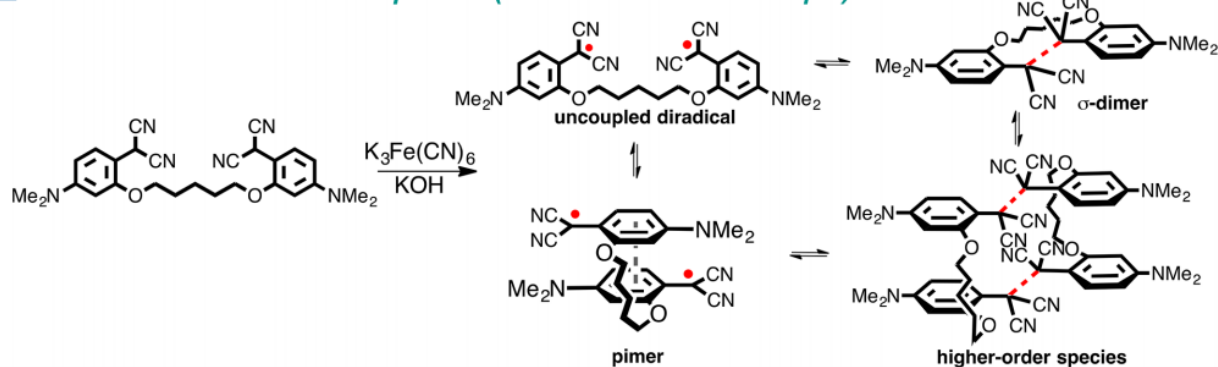


Figure 3-1. (Top) The 14 linked diradicals synthesized and studied in this paper. (Bottom) Generation and considered equilibria for diradicals.

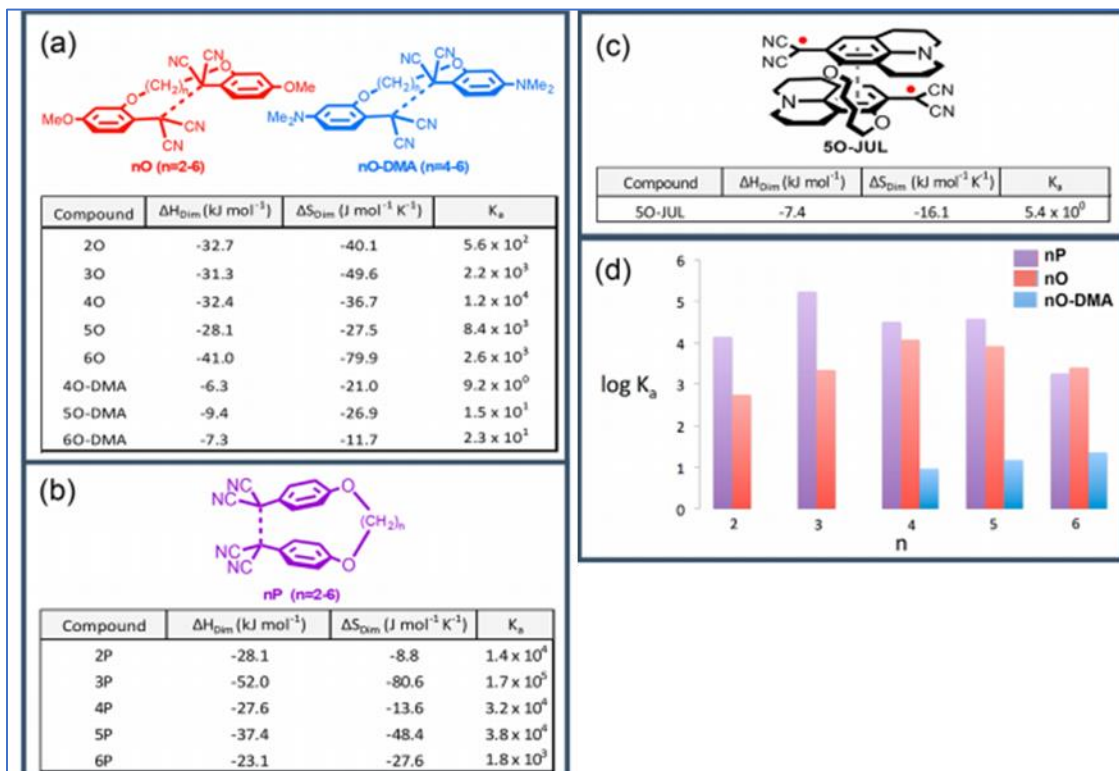
Here we report a detailed study of the effect of chemical structure on the strength and nature of the spin–spin interactions for linked aryl dicyanomethyl diradicals. A series of 14 tethered aryl dicyanomethyl diradicals were synthesized (Figure 3.1), and the thermodynamic bonding parameters were elucidated using variable-temperature EPR and UV–vis spectroscopy, X-ray crystallography, and computational analysis (Table 3.1). We find that the strength of the intramolecular spin–spin interaction is exquisitely sensitive to the structure of the radical, the substitution position of the linker, and the length of the linker, with the association constant varying over 5 orders of magnitude by changing these variables. Subtle changes to the radical structure are found to alter the nature of the spin–spin interaction, as a *p*-dimethylamino-substituted tethered diradical 5O-DMA forms a sigma dimer with an elongated bond, while a structurally related julolidine derivative 5O-JUL forms an exceedingly weakly bonded pimer ($\Delta G_{\text{bonding}} = 1 \text{ kcal/mol}$). Furthermore, a serendipitously discovered photochemical coupling reaction allows the radicals to be irreversibly locked upon irradiation via formation of a long-wavelength-absorbing rhodamine dye derivative ($\lambda_{\text{max}} \approx 725 \text{ nm}$) and formal loss of a dicyanomethyl group, providing a potentially useful tool for both irreversibly phototrapping metastable dynamic covalent assemblies and providing an optical readout. Overall, this work shows how structural changes can be used to control the strength and nature of intramolecular spin–spin interactions, which has implications for dynamic covalent assemblies and stimuli responsive polymers using this new class of stable diradicals as building blocks.

3.3 Results and Discussion

Determination of Equilibrium Species. The diradicals shown in Figure 3.1 were generated by quantitative oxidation of malononitrile-substituted arenes with potassium ferricyanide and the diradical purified from the inorganic byproducts by partitioning between water and dichloromethane. Prior to any quantitative measurements, we needed to identify the

species present in the equilibrium with the diradicals. Four different equilibrium species shown in Figure 3.1 were considered: the free diradical, a sigma dimer, a pi dimer (pimer), and higher-order aggregates. (See Figure 3.1, bottom.)

Table 3-1. Thermodynamic Parameters for *o*-Linked (a), *p*-Linked (b), and Julolidine (c)



To evaluate whether higher-order aggregates are formed, the spin concentration as a function of diradical concentration was plotted for representative radicals 5O, 5P, and 6O-DMA, at concentrations ranging from 50 μM to 10 mM. The spin concentrations were determined by double integration of the radical EPR signal. In all three cases, a linear plot was observed, indicating that the percent radical is independent of concentration, which is not consistent with the formation of higher-order diamagnetic species. Intermolecular dimerization would be concentration dependent and would be expected to lead to a curved binding isotherm similar to what we observed for the intermolecular dimerization of the monoradicals.⁸ Thus, while higher-

order species may be contributors to the equilibrium at higher concentrations than those studied, they are not expected to be relevant species to the equilibria at the concentrations used here.

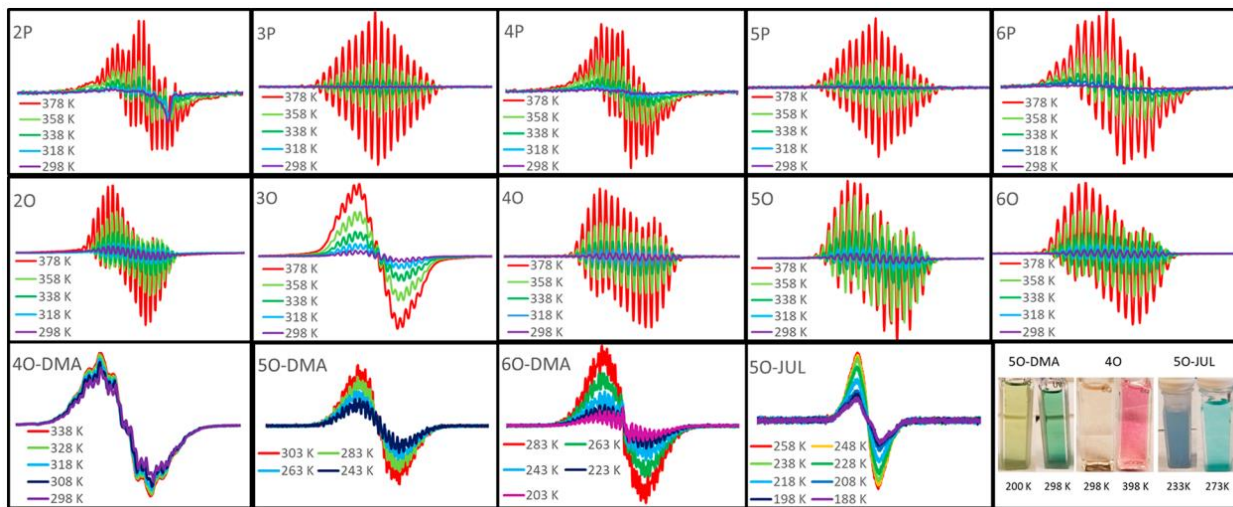


Figure 3-2. Electron paramagnetic resonance spectra of the diradical species of each compound with variable-temperature stimulation to study thermodynamic parameters.

Next, we considered whether the diradicals were forming sigma or pi dimers. Both are possible modes of dimerization for stabilized free radicals. While both sigma and pi dimers are diamagnetic and EPR silent, sigma dimers break the conjugation of the radical and are generally colorless (or slightly yellow), whereas pimers feature near-IR absorption bands and are often colored species. Diradicals 2-6O, 4-6ODMA, and 2-6P have qualitatively the same behavior. At low temperatures, the solutions are colorless or faintly colored, while upon heating the solutions turn brightly colored and are accompanied by the growth of an EPR signal (Figure 3.2 shows representative photos from each class of diradical) and a UV-vis band corresponding to the diradical. This heating/cooling can be reversibly switched. This temperature-responsive behavior

is consistent with an enthalpically favored sigma dimer in equilibrium with an entropically favored diradical.

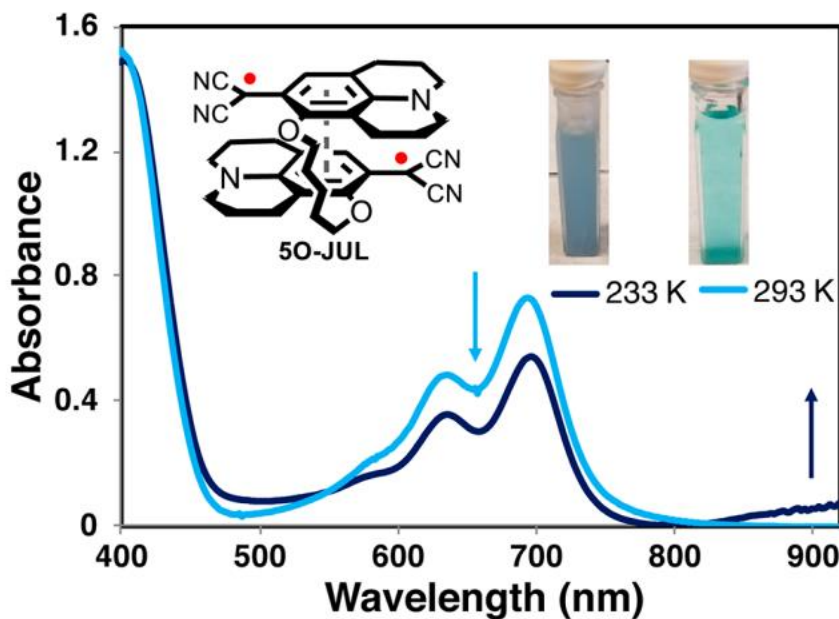


Figure 3-3. UV/vis spectroscopy showing the color change of compound 5O-JUL as it cools, signifying the formation of a pimer band by the peak growing in from 850 nm.

In contrast, 5O-JUL has qualitatively different behavior. At room temperature the solution is aqua-colored, which becomes darker blue upon cooling with a growth of a near-IR band >900 nm (Figure 3.3). As the temperature is decreased, the EPR signal also decreases and the UV-vis band associated with the diradical decreases. This behavior is consistent with an enthalpically favored diamagnetic diradical pimer existing in equilibrium with an entropically favored diradical and is also consistent with what Seki and co-workers observed for the monoradical.⁶ Computational modeling of the pimer is described below. Thermal population of a sigma dimer cannot be ruled out, as the sigma dimer is not visible by EPR or UV-vis spectroscopy. From a practical point of view, the thermodynamic parameters determined in Table 3.1 for this species can be viewed as the EPR-active diradical–EPR-inactive diamagnetic dimer equilibrium

thermodynamic parameters, with the diamagnetic dimer species possibly consisting of a Boltzmann population of at least the diamagnetic pimer and possibly the diamagnetic sigma dimer.

Effect of Linker Attachment Position and Length on the Spin–Spin Interaction

Thermodynamics and Equilibria. Having established the nature of the equilibrium species, we next evaluated the effect of changing the linker size for three different substituted radicals (with differing para substituents) and two different linker attachment positions, at the *ortho* (2-6O) and *para* position (2-6P) to the radical center. We determined the thermodynamic intramolecular dimerization parameters (ΔG° , ΔH° , ΔS° , K_a) for these diradicals from van 't Hoff plots measuring spin concentration determined by EPR spectroscopy (double integration) as a function of temperature. See Table 3.1.

Several conclusions can be made from the thermodynamic data. First, attachment position matters. In general, *ortho*-linked diradicals feature lower association constants for dimerization than the *para*-linked diradicals. For example, 3O has a weaker binding constant than 3P by nearly 2 orders of magnitude ($K_a = 2.2 \times 10^3$ vs 1.7×10^5 , respectively). This can be attributed to strains experienced by the *ortho*-linked species with an insufficiently long linker. Second, longer linkers generally favor the diradical, leading to lower association constants. The exception is that shorter linkers with two or three carbons for the *ortho*-linked (2-6O diradicals) and two carbons in the case of the *para*-linked (2-6P diradicals) have weaker binding constants. This can be attributable to the macrocyclic ring strains encountered with an insufficiently long linker. The four-carbon linker for the *ortho*-substituted diradical and the three-carbon linker for the *para*-substituted diradical feature the largest association constants, suggesting that these tethers represent the “ideal” linker size for a trade-off between added ring strain (in the case of a short linker) and entropic penalty of binding (in the case of a longer alkyl linker). Interestingly, there is an

alternating “even–odd” effect of linker size on the ΔH° in the 2-6O series, with all even numbers of carbons in the linker having more negative ΔH° values than odd linker numbers. This even–odd effect does not manifest itself in the K_a values, however, as a likely result of entropy–enthalpy compensation attenuation and other effects being larger. In the para series 2-6P, it is the odd number of carbons that always has a lower ΔH° . A similar even–odd effect has been seen in the case of linked viologen cation radicals.¹⁰ In the cases of the 4-6O-DMA series, featuring a stronger donating dimethylamino group in the para position, these diradicals all feature similarly extremely weak bonding interactions (e.g., ΔG° bonding < 2 kcal/mol), making trends difficult to discern. A striking result of this study is that changing the *para*-methoxy group to a *para*-dimethylamino group leads to a smaller K_a by 3–4 orders of magnitude.

Only one julolidine derivative (5O-JUL) was synthesized due to synthetic difficulties of making the diradical precursors. Briefly, the palladium-catalyzed cross-coupling of the diaryl dibromide is poisoned by the extremely electron-rich tethered diaryl substrate, leading to mostly reduction of Br to H rather than substitution with malononitrile. The julolidine is a more electron-donating substituent than dimethylamino because it locks the nitrogen into a planar conformation, forcing conjugation with the pi system of the arene. This julolidine-derived diradical features the weakest spin–spin interaction (ΔG° bonding = 1 kcal/mol) of the series, showing that more electron-donating substituents shift the equilibrium toward the diradical ($\text{OMe} \ll \text{NMe}_2 < \text{julolidine}$). As described above, the nature of the spin–spin bonding interaction also switches from an elongated sigma dimer to a pi dimer (pimer).

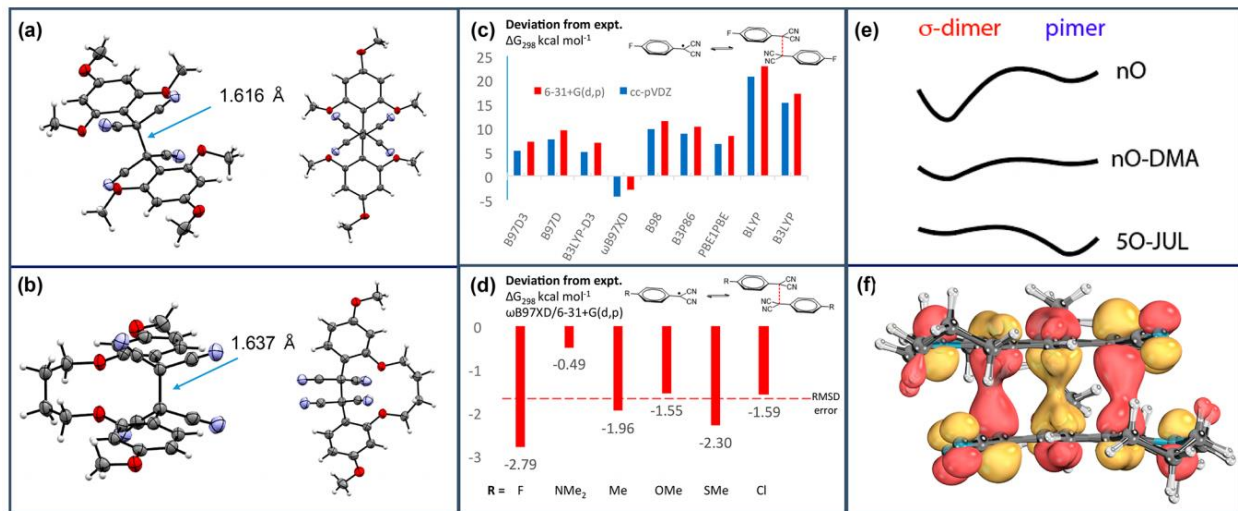


Figure 3-4. (a) Crystal structures for 2,4,6-trimethoxy untethered diradical dimer and (b) 4O. (c) Computational screen of density functionals for accuracy in modeling p-fluorophenyl dicyanomethyl radical dimerization free energy. (d) Using the ωB97XD method to evaluate accuracy of dimerization thermodynamics over a small test set. (e) Suggested qualitative σ-dimer–pimer PES for varying substituents. (f) HOMO of julolidine pimer showing pi overlap.

Computational Studies of the Nature of the Radical– Radical Interaction. To gain insight into the nature of the bonding interaction between the radicals, we turned to computational analysis. First, we sought to identify a computational method capable of handling such diradical interactions. To do this, we screened a variety of density functionals to see if any could reproduce our previously published⁸ intermolecular binding free energies of the fluoro substituted aryl dicyanomethyl monoradical (Figure 3.4C). Functionals lacking dispersion corrections give nonsensical predictions of the binding free energy, predicting it to be unfavorable and underestimating it by 5–25 kcal/mol. The Head-Gordon functional, ωB97XD/6-31+G(d,p), which includes a dispersion correction, was found to best reproduce the binding energy of this radical to within 3 kcal/mol. We then evaluated this level of theory against six different substituted monoradicals, for which we have previously determined experimental intermolecular binding free energies⁸ and span a range of binding enthalpies (24.6 kcal mol⁻¹ for Cl to 12.7 kcal mol⁻¹ for NMe₂). The RMSD error for the six radicals was less than 2 kcal mol⁻¹ with the fluoro being the

poorest predicted. The reasonable prediction of the binding free energies using this level of theory gives us confidence in using this method to evaluate new radicals, as yet unsynthesized. Regrettably, this method erroneously predicts the sigma dimer of 5O-JUL to be lower in energy than the pimer by 6.5 kcal/mol. In contrast, B97D/6-31+G(d,p), which gave good predictions of the pimerization of the viologen cation radical,⁹ predicts the pimer to be more stable than the sigma dimer by 4.5 kcal/mol. Thus, while ω B97XD appears to accurately describe the diradical–sigma dimer bonding thermodynamics, it fails for describing the sigma-dimer–pimer equilibrium. A computationally feasible method that can accurately handle the sigma dimer–pimer equilibrium is currently being investigated.

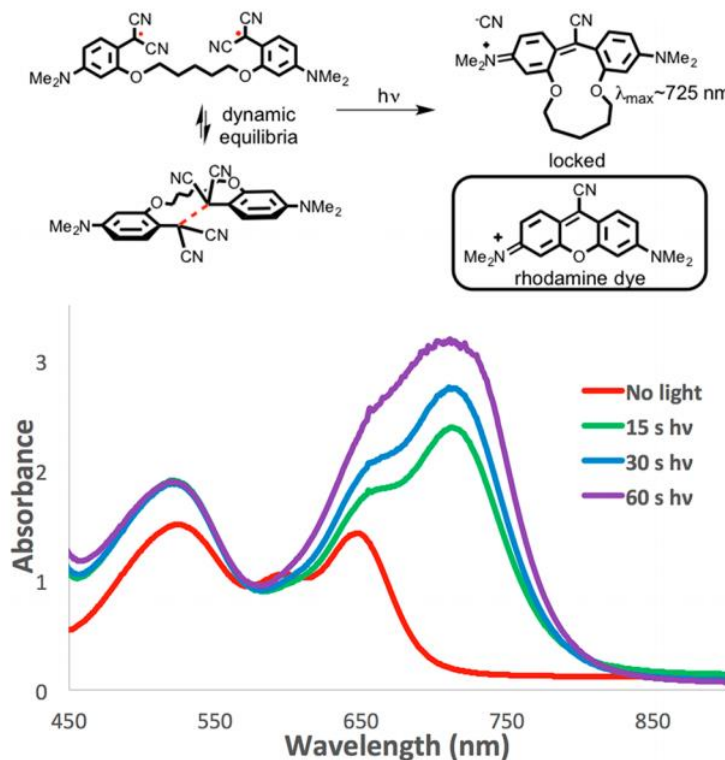


Figure 3-5. (Top) Amino-substituted diradical photochemistry that transforms the diradical into a rhodamine dye derivative. (Bottom) UV–vis at different times of irradiation (Rayonet, 5×10^{-5} M in toluene).

Radical Stability and Photochemical Reactivity. In general, the diradicals described in this study feature remarkable air and thermal stability. For example, solutions of 2-6O and 2-6P

were stable for at least 12 months. Heat/cool cycles can be performed multiple times without decomposition with two exceptions. Compounds 4-6O-DMA and 5O-JUL derivatives show some thermal instability at high temperature (above 60 and 40 °C, respectively). We serendipitously discovered a photoreaction of the amino-containing diradicals. Holding up tubes of the colored diradicals to bright sunshine led to a rapid color change and irreversible loss of all EPR signal. UV-vis experiments show the formation of a species with a λ max \approx 725 nm, a remarkably red-shifted absorption for a diamagnetic closed-shell species. Mass spectroscopy and NMR data are consistent with a xanthene dye-like structure corresponding to loss of a dicyanomethyl group, leading us to propose the structure shown in Figure 3.5, a derivative of the long-wavelength absorbing rhodamine dye. Growth of this absorption band occurs only for the amino derivatives. This photoreaction could prove to be useful for photochemically locking metastable dynamic covalent chemistry intermediates derived from these radicals in a way that can be monitored optically following the growth of the 725 nm absorption band.

3.4 Materials and Methods

Variable-Temperature EPR Experiments and van't Hoff Plots. Variable-temperature EPR studies were performed on all diradicals to elucidate the bonding thermodynamic parameters for each diradical/dimer equilibria. All diradicals were investigated in toluene solvent with concentrations ranging from 1 to 5 mM, with the exception of compounds 5-6O-DMA, requiring dichloromethane as solvent. During the EPR experiments, measurements were made using temperature increments of 10 K after allowing the sample to equilibrate for 5 min at each temperature from 298 to 378 K. A follow-up EPR scan was performed after increasing the temperature to ensure that no decomposition occurred. Diradicals 4-6O-DMA and 5O-JUL all showed signs of decomposition at elevated temperatures and in light. In the case of the more electron-donating compounds (4-6O-DMA and 5O-JUL), EPR experiments were performed by

lowering the temperature to as low as 188 K and then slowly raising the temperature up to 278 K to calculate thermodynamic parameters.

For each sample studied, toluene or dichloromethane was added to the solid sample to make a 1–5 mM solution of radical/dimer species. This solution was then purged and cannulated into a pre-purged quartz EPR tube. EPR studies were then performed at 10-degree increments (298–378 K for toluene and 208–298 K for dichloromethane) with an equilibration time of 5 min for each temperature increment. The following instrument parameters were generally followed for each sample: modulation frequency, 100 kHz; receiver gain, 50 dB; modulation amplitude, 0.5; time constant, 0.01 s; center field, 3330 G; sweep width, ~200 G; microwave attenuation, 20 dB; microwave power, 2 mW; number of data points, 2048; average number of scans, 15.

UV–Vis Spectrum for 50-JUL. A 50 μ M solution of 5O-JUL in toluene was carefully prepared to avoid any light, air, or other contamination to detect the presence of a pimer band growing in the near-IR region as the temperature was lowered to 233 K. Low temperature spectra were made possible by a liquid nitrogen cooler with a nitrogen blow off to avoid condensation on the quartz cell walls.

Computational Methods. All computations were carried out in Gaussian16.¹¹ Non-tethered dimers and radicals for the computational benchmark were optimized using multiple theoretical methods, BLYP,¹² B3LYP,¹³ PBE1PBE,¹⁴ B3P86,¹⁵ B98,¹⁶ ω B98XD,¹⁷ B3LYP-D3,¹⁸ B97D3,¹⁸ and B97D¹⁹ under both Pople's 6-31+G(d,p) basis set and Dunning's correlation-consistent cc-pVDZ basis set.²⁰

All optimized structures had zero imaginary frequencies. Computed free energies of dimerization were conducted by separately calculating the dimer and diradical and using a frequency calculation to convert the electronic energies to free energies. Intermolecular

dimerization free energies were corrected to the solution standard state of 1 M. Because implicit solvent models have difficulties with very low dielectric solvents such as toluene ($\epsilon = 2$), the solvent used for experimentally determining dimerization free energies, computations were carried out in the gas phase. Contributions to the free energy from higher-energy conformations were ignored.

3.5 Conclusions

In conclusion, we have investigated the intramolecular binding thermodynamics for a series of tethered dicyanomethyl diradicals and determined that these diradicals are promising building blocks for stimuli-responsive polymers and plastics, as well as dynamic covalent assemblies, possessing remarkable stability. Stronger para donating groups weaken the bonding interaction and lower the energy of the pimer relative to the sigma dimer. These diradical compounds have an advantage to the monoradical dimer species in that they exhibit orders of magnitude weaker binding, leading to an increase in the amount of radical at lower temperatures, in addition to having a spin–spin interaction that is concentration-independent. In all cases, temperature-responsive switching was observed, and the sensitivity can be tuned by both the attachment point and the length of the linker by changing the bonding thermodynamic parameters. Incorporation of these diradical building blocks into solid-state materials is currently being explored.

3.6 References

- (1) Abe, M. *Chem. Rev.* 2013, 113, 7011–7088. Juetten, M. J.; Buck, A. T.; Winter, A. H. *Chem. Commun.* 2015, 51, 5516–5519. Buck, A. T.; Paletta, J. T.; Khindurangala, S. A.; Beck, C. L.; Winter, A. H. *J. Am. Chem. Soc.* 2013, 135, 10594–10597. Geraskina, M. R.; Buck, A. T.; Winter, A. H. *J. Org. Chem.* 2014, 79, 7723–7727.

- (2) Nguyen, H. V.-T.; Chen, Q.; Rajca, A.; Johnson, J. A. ACS Cent. Sci. 2017, 3, 800–811. Rajca, A.; Wang, Y.; Boska, M.; Paletta, J. T.; Olankitwanit, A.; Swanson, M. A.; Mitchell, D. G.; Eaton, S. S.; Eaton, G. R.; Rajca, S. J. Am. Chem. Soc. 2012, 134, 15724–15727. Sowers, M. A.; McCombs, J. R.; Wang, Y.; Paletta, J. T.; Morton, S. W.; Dreaden, E. C.; Boska, M. D.; Ottaviani, M. F.; Hammond, P. T.; Rajca, A.; Johnson, J. A. Nat. Commun. 2014, 5, 5460.
- (3) Nishida, S.; Morita, Y.; Fukui, K.; Sato, K.; Shiomi, D.; Takui, T.; Nakasaji, K. Angew. Chem. 2005, 117, 7443–7446. Wojtecki, R. J.; Meador, M. A.; Rowan, S. J. Nat. Mater. 2011, 10, 14–27.
- (4) Morita, Y.; Suzuki, S.; Sato, K.; Takui, T. Nat. Chem. 2011, 3, 197–204. Alcon, I.; Vinces, F.; Moreira, I.; Bromley, S. T. Nat. Commun. 2017, 8, 1957. Shishlov, N. M. Russ. Chem. Rev. 2006, 75, 863–884.
- (5) Rajca, A. Chem. Rev. 1994, 94, 871–893. Jin, Y.; Yu, C.; Denman, R. J.; Zhang, W. Chem. Soc. Rev. 2013, 42, 6634–6654. Rowan, S. J.; Cantrill, S. J.; Cousins, G. R. L.; Sanders, J. K. M.; Stoddart, J. F. Angew. Chem., Int. Ed. 2002, 41, 898–952.
- (6) Okino, K.; Hira, S.; Inoue, Y.; Sakamaki, D.; Seki, S. Angew. Chem., Int. Ed. 2017, 56, 16597–16601. Kobashi, T.; Sakamaki, D.; Seki, S. Angew. Chem., Int. Ed. 2016, 55, 8634–8638. Yuan, L.; Han, Y.; Tao, T.; Phan, H.; Chi, C. Angew. Chem., Int. Ed. 2018, 57, 1–6. Li, H.; et al. Chem. - Eur. J. 2017, 23, 13776–13783.
- (7) Rajca, A.; Wongsriratanakul, J.; Rajca, S. Science 2001, 294, 1503–1505. Rajca, A.; Utamapanya, S.; Thayumanavan, S. J. Am. Chem. Soc. 1992, 114, 1884–1885. Rajca, A.; Janicki, S. J. Org. Chem. 1994, 59, 7099–7107. Rajca, A.; Utamapanya, S.; Xu, J. J. Am. Chem. Soc. 1991, 113, 9235–9241.
- (8) Peterson, J. P.; Geraskina, M. R.; Zhang, R.; Winter, A. H. J. Org. Chem. 2017, 82, 6497–6501.
- (9) Geraskina, M.; Dutton, A. S.; Juetten, M. J.; Wood, S. A.; Winter, A. H. Angew. Chem. 2017, 129 (32), 9563–9567.
- (10) Shimomura, M.; Utsugi, K.; Horikoshi, J.; Okuyama, K.; Hatozaki, O.; Oyama, N. Langmuir 1991, 7, 760–765.

- (11) Frisch, G. W. T. M. J.; Schlegel, H. B.; Scuseria, G. E.; Robb, J. R. C. M. A.; Scalmani, G.; Barone, V.; Mennucci, B.; Petersson, H. N. G. A.; Caricato, M.; Li, X.; Hratchian, H. P.; Izmaylov, J. B. A. F.; Zheng, G.; Sonnenberg, J. L.; Hada, M.; Ehara, K. T. M.; Fukuda, R.; Hasegawa, J.; Ishida, M.; Nakajima, T.; Honda, O. K. Y.; Nakai, H.; Vreven, T.; Montgomery, J. A., Jr.; Peralta, F. O. J. E.; Bearpark, M.; Heyd, J. J.; Brothers, E.; Kudin, V. N. S. K. N.; Keith, T.; Kobayashi, R.; Normand, J.; Raghavachari, A. R. K.; Burant, J. C.; Iyengar, S. S.; Tomasi, J.; Cossi, N. R. M.; Millam, J. M.; Klene, M.; Knox, J. E.; Cross, J. B.; Bakken, C. A. V.; Jaramillo, J.; Gomperts, R.; Stratmann, R. E.; Yazyev, A. J. A. O.; Cammi, R.; Pomelli, C.; Ochterski, J. W.; Martin, K. M. R. L.; Zakrzewski, V. G.; Voth, G. A.; Salvador, J. J. D. P.; Dapprich, S.; Daniels, A. D.; Farkas, J. B. F. O.; Ortiz, J. V.; Cioslowski, J.; A, D. J. Gaussian16; Gaussian, Inc.: Wallingford, CT, 2013.
- (12) (a) Becke, A. D. Phys. Rev. A: At., Mol., Opt. Phys. 1988, 38, 3098–3100. (b) Lee, C. T.; Yang, W. T.; Parr, R. G. Phys. Rev. B: Condens. Matter Mater. Phys. 1988, 37, 785–789.
- (13) Becke, A. D. J. Chem. Phys. 1993, 98, 98.
- (14) Perdew, J. P.; Burke, K.; Wang, Y. Phys. Rev. B: Condens. Matter Mater. Phys. 1996, 54, 16533–16539.
- (15) Perdew, J. P. Phys. Rev. B: Condens. Matter Mater. Phys. 1986, 33, 8822–8824.
- (16) Schmider, H. L.; Becke, A. D. J. Chem. Phys. 1998, 108, 9624– 9631.
- (17) Chai, J. D.; Head-Gordon, M. Phys. Chem. Chem. Phys. 2008, 10, 6615–6620.
- (18) Grimme, S.; Antony, J.; Ehrlich, S.; Krieg, H. J. Chem. Phys. 2010, 132, 132.
- (19) Grimme, S. J. Comput. Chem. 2006, 27, 1787–1799.
- (20) Dunning, T. H. J. Chem. Phys. 1989, 90, 1007–1023.

CHAPTER 4. SOLVENT EFFECTS ON THE STABILITY AND DELOCALIZATION OF ARYL DICYANOMETHYL RADICALS: THE CAPTODATIVE EFFECT REVISITED

Adapted with permission from: J. P. Peterson, A. H. Winter. *J. Am. Chem. Soc.* **2019**, 141, 32, 12901-12906. Copyright (2020) American Chemical Society.

4.1 Abstract

The captodative effect postulates that radicals substituted with both electron donating and accepting groups enjoy a special enhanced stabilization, a model given theoretical support by simple MO and resonance arguments. A key prediction from theory is that captodative stabilization of radicals is larger in polar solvents than in nonpolar solvents or the gas phase, which can be viewed in the resonance model as solvent stabilization of charge-separated resonance forms. Yet, several experimental studies have failed to observe a solvent effect on radical stability, casting doubt on key aspects of the captodative effect. Here, we examine in detail the effect of solvent on the stability of structurally related captodative aryl dicyanomethyl radicals. An attractive feature of these radicals is that they exist as stable steady state populations of radicals in equilibrium with their dimers, allowing us to directly characterize from experiment their thermodynamic stabilities and spin delocalization in solvents of varying polarity. In contrast to the prior studies, we find that captodative radicals are indeed stabilized by polar solvents, as measured by a shift in the radical–dimer association constants by up to 100-fold toward the radical upon going from nonpolar toluene to more polar DMF. Moreover, in polar solvents, the spin is shifted onto the donor substituent and away from the benzylic carbon. Within the resonance model, these results can be explained by the increased contributions of the zwitterionic resonance structures to the overall

hybrid. These results provide experimental support to a key prediction from theory that had previously been dismissed.

4.2 Introduction

Radicals substituted with both donor and acceptor groups have been postulated to be specially stabilized and are termed captodative radicals (or merostabilized or push–pull radicals). The effect was hinted at by Dewar in the early 1950s¹ and subsequently investigated in more detail by Viehe and others.² From simple MO models, interactions of radicals with either neighboring donor groups or acceptor groups are stabilizing, and the combination of both donors and acceptors is further stabilized³ (see Figure 4.1). Within the resonance model, radicals featuring both donors and acceptors have additional charge-separated resonance structures that radicals substituted either with multiple donors or multiple acceptors do not. These additional resonance structures hint at the possibility of cooperative stabilizing effects enjoyed by radicals featuring both donors and acceptors. Evidence both for^{4,5} and against^{6–8} the captodative effect has been presented, and while there is some agreement on the existence of the captodative effect

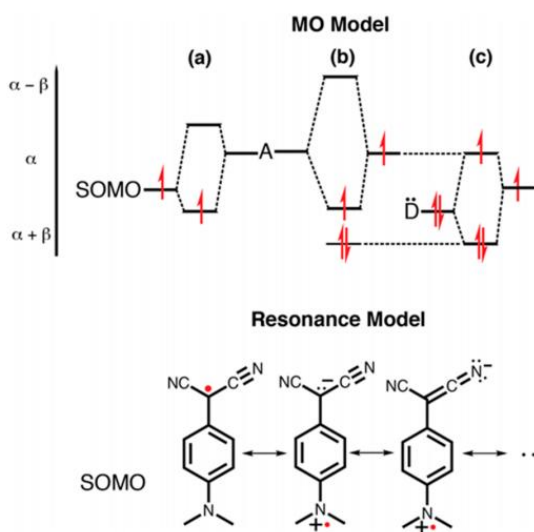


Figure 4-1. (Top) MO model for the captodative effect,^{3,4} showing the stabilization of a radical with an electron acceptor (a), an electron donor (c), and the combined effect (b). (Bottom) Resonance model depicting zwitterionic structures unique to captodative radicals.

in a general sense, like other conceptual models such as aromaticity, there is little agreement on the magnitude of the effect and its importance for specific radicals.

A particularly interesting prediction from early theoretical work by Katritzky and coworkers⁹ was that captodative stabilization should be large in high-dielectric solvents but minimal in low dielectric solvents, leading them to call the captodative phenomenon “mostly a solvent effect”.¹⁰ These predictions are easily understood from the resonance model by solvent screening of the unique charge-separated resonance structures that exist only for radicals bearing both donor and acceptor substituents. However, subsequent experimental work by Beckhaus and Rüchardt¹¹ showed no solvent dependence on the barriers for dissociation of alkoxy cyanomethyl radical homodimers into the free radicals, providing “unequivocal evidence in disfavor of the postulated increase in the “merostabilization” by polar solvents” for these radicals (emphasis added). A later study by Rhodes and Roduner¹² on cyclohexadienyl radicals containing both donor and acceptor groups also “argued against the prediction that a highly polar medium has a significant promoting influence on the captodative phenomenon”. A study by Viehe and coworkers¹³ on E/Z isomerization of cyclopropane derivatives proceeding through captodative diradicals found no solvent effect on the free energy barriers. These experiments have cast doubt on key aspects of the captodative effect. One can reasonably ask, if there is no solvent stabilization of the radicals, as would be expected from the charge-separated resonance structures and theory, is there a cooperative captodative effect at all? Here, we examine the effect of solvent on the stability of structurally related captodative aryl dicyanomethyl radicals. These radicals have seen recent interest upon Seki and coworkers’ discovery^{14–16} that a para substituent on the aryl group blocks an irreversible head-to-tail dimerization, leading to air and thermally stable steady state populations of radicals that can be directly detected by electron paramagnetic resonance (EPR)

spectroscopy. Because these radicals can be directly detected rather than existing as fleeting intermediates, we were able to evaluate the effect of solvent on their stability and radical delocalization using direct measurements. We measured the equilibrium constants of the radical with its dimer in solvents of varying polarity to probe relative radical stabilities as a function of solvent dielectric constant and as a function of the donating ability of the aryl ring. We also measured the change in the spin densities as a function of solvent by measuring EPR hyperfine coupling constants. We find that, in contrast to the work of Beckhaus and Rüchardt and Rhodes and Roduner, polar solvents do indeed stabilize these radicals, as shown by a change in the radical–dimer association constant by ~100-fold for radicals bearing a strong donating group upon changing from nonpolar to polar solvents, an effect whose magnitude is directly correlated to the strength of the donating aryl ring. Furthermore, we observe the increased delocalization of the radical in polar solvents by changes in the EPR hyperfine coupling as solvent polarity is increased, providing experimental evidence in favor of the theoretical prediction that polar solvents can stabilize captodative radicals, a claim that was thought to be discredited.

4.3 Results and Discussion

Solvent Effects on the Radical–Dimer Equilibrium Constants. Aryl dicyanomethyl radicals containing a very strong donating group (*para*-dimethylamino, 1-DMA), a less strong donating group (*para*-methoxy, 1-OMe), and a withdrawing group (*para*-cyano, 1-CN) were prepared by oxidation of the corresponding aryl malononitriles by known methods.^{17,18} These paramagnetic radicals exist in equilibrium with their diamagnetic EPR-silent dimers. To evaluate the effect of solvent on the stability of these radicals, we determined the association constant, K_a , for dimerization of each of these radicals in varying solvents as an indicator of relative radical stability.

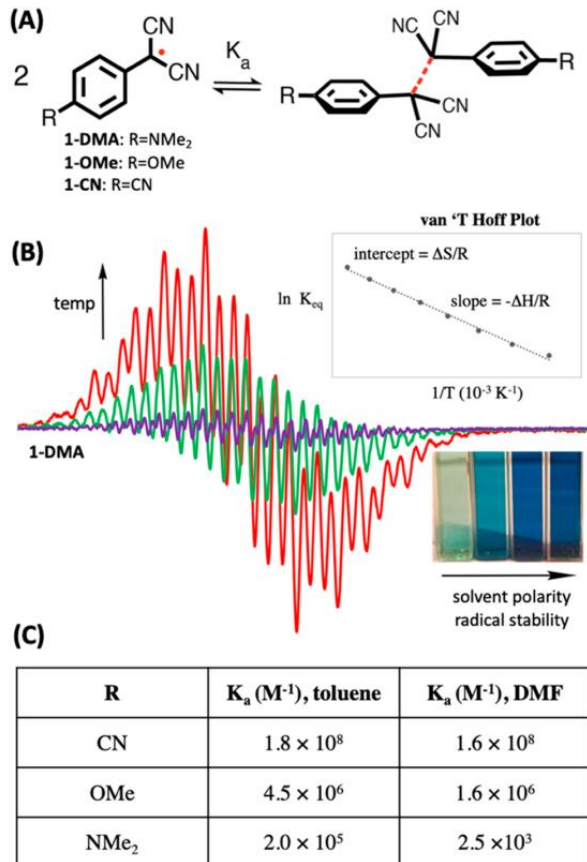


Figure 4-2. (A) Radical/dimer equilibrium for dicyanomethyl systems; (B) example VT-EPR with van't Hoff plot insert for 1-NMe₂; (C) binding data of representative compounds in a nonpolar (toluene) and polar (DMF) solvent.

Association constants for radical dimerization were determined by EPR spectroscopy using van't Hoff plots (example shown in Figure 4.2B; all others are included in the Supporting Information). Given that we are modifying the para position distant from the C–C bond, changing the substituents is anticipated to have a negligible steric effect on the dimer stability, so the radical–dimer equilibrium constant is a useful experimental probe of relative radical stability. In contrast to the prior work, we observe a significant solvent effect on radical stability with strong donors. The simple resonance model predicts that captodative radicals should be stabilized in polar solvents due to screening of the unique charge-separated resonance structures that exist only for captodative radicals. Indeed, that is what we observe experimentally. For the very strongly

donating p-dimethylamino-phenyl-substituted radical, 1-DMA, we observe a remarkable \sim 100-fold change in the association constant upon going from nonpolar toluene to more polar DMF (2.0×10^5 to $2.5 \times 10^3 \text{ M}^{-1}$) in favor of the radical (see Figure 4.2C). The shift in the equilibrium toward the radical is also readily apparent simply from visual inspection of solutions of these radicals in solvents of varying polarity, which are dark blue in polar solvents, indicating large amounts of the colored radical, and faintly blue in nonpolar solvents, indicating mostly uncolored dimer (inset in Figure 4.2B). With the less donating *p*-methoxyphenyl-substituted radical, 1-OMe, the association constant is an order of magnitude larger than that for 1-DMA in toluene, indicating less radical stability. Moreover, the solvent effect on the equilibrium is drastically diminished with a change in K_a of only \sim 3-fold (4.5×10^6 to $1.6 \times 10^6 \text{ M}^{-1}$ in toluene and DMF, respectively). Thus, 1-OMe and 1-DMA are an order of magnitude apart in equilibrium constant in toluene but three orders of magnitude in polar DMF, where 1-DMA radical is strongly stabilized by solvent, while 1-OMe is less stabilized. With the withdrawing *p*-cyanophenyl-substituted radical, 1-CN, which is no longer a captodative radical, the association constant is larger by two orders of magnitude than 1-OMe in toluene, indicating further diminished radical stability. For this radical, effectively no solvent effect on radical stability is observed (1.8×10^8 to $1.6 \times 10^8 \text{ M}^{-1}$ in toluene and DMF, respectively). These studies indicate that radicals substituted with very strong polarizable donors with strong acceptors have large solvent effects on radical stability. The solvent effect is drastically attenuated by substituting a very strong donor (e.g., NMe₂) with merely a strong donor (e.g., OMe) and is negligible with a withdrawing group.

Computational and Experimental Evaluation of Spin Delocalization as a Function of Solvent Dielectric. The simple resonance model suggests that, in polar solvents, radical stability increases due to solvent screening of zwitterionic resonance structures. If this is true, then the

rationalization for the enhanced stability of 1-DMA in polar solvents is radical delocalization. The prediction, then, is that spin density should shift from the benzylic carbon to the donating substituent in the para position in more polar solvents, as the zwitterionic resonance structures contribute more to the overall hybrid. All of the zwitterionic resonance structures feature spin sites that are delocalized off of the benzylic carbon (see Figure 4.2A).

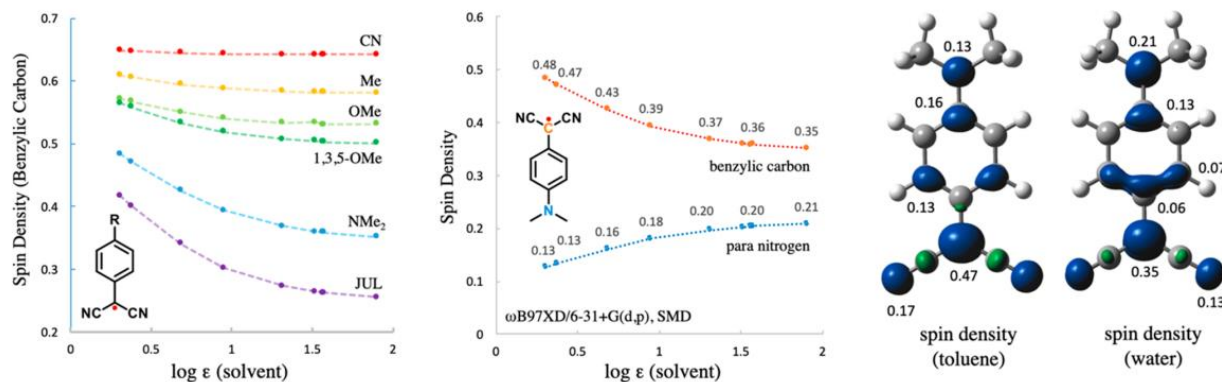


Figure 4-3. Computed Mulliken spin densities (ω B97XD,6-31+G(d,p), SMD) on the benzylic carbon of differently substituted dicyanomethyl radicals in solvents of varying dielectric (left); spin density comparison of the benzylic carbon and para nitrogen in the NMe₂ radical system as a function of solvent dielectric (center); spin density distributions across 1-DMA in a nonpolar and polar solvent (right). JUL = julolidine.

To test this prediction, we computationally evaluated the spin densities of a series of radicals bearing varying substituents using density functional theory (ω B97XD,6-31+G(d,p)) and in solvents of varying dielectric using the SMD solvation model (see Figure 4.3). From these computations, the spin density on the benzylic carbon decreases as the aryl substituent becomes more donating. Furthermore, the change in the spin density on the benzylic carbon as the solvent polarity is largest with strong donating groups, modest with less strong donors, and nonexistent with withdrawing groups. Figure 4.3 (middle) shows the spin density on the dimethylamino substituted radical, 1-DMA, as solvent polarity is increased. In toluene, the computed (Mulliken) spin density on the benzylic carbon is 0.47, while in water, the spin density decreases to 0.35. Concomitantly, the spin density on the dimethylamino nitrogen increases from 0.13 to 0.21 upon

changing solvent from toluene to water. This computational result supports the idea of increased contribution of zwitterionic resonance structures to the hybrid in polar solvents, which rationalizes the increased radical stability in polar solvents.

We also evaluated spin densities experimentally using the EPR hyperfine coupling constants for these radicals. Estimates of the spin densities for planar π radicals can be obtained from the McConnell equation,¹⁹ where the hyperfine coupling constant to spin-active nuclei is directly proportional to the spin density, following the equation $A = Q\rho$, where A is the hyperfine coupling constant, ρ is the pi spin density, and Q is the McConnell constant (~ 22 for planar carbon pi radicals²⁰). The EPR spectrum for the *p*-dimethylaminophenyl dicyanomethyl radical, 1-DMA, is shown in toluene, dichloromethane, and acetone in Figure 4.4. The hyperfine coupling varies as a function of solvent, indicating changes in spin density for this radical as a function of solvent. We found that the para-nitrogen Mulliken spin density from computation correlates strongly with spin densities estimated from computed A values and using the McConnell equation ($Q = 22$). The Mulliken spin densities for toluene, dichloromethane, and acetone were computed to be 0.14, 0.18, and 0.20, respectively. Using the McConnell equation with computed G values, the spin densities were calculated to be 0.14, 0.19, and 0.20 for toluene, dichloromethane, and acetone, respectively.

The EPR spectrum simulated directly from the A values predicted by computation (B3LYP/EPR-III, SMD) without modification is shown to the left of the experimentally obtained spectrum, which shows surprisingly reasonable agreement. A purely simulated spectrum to best match the experimental spectrum is shown to the right. In the case of toluene, the computed nitrogen A value is 3.2 G, while in acetone, it is 4.4 G, indicating an increase in spin density onto the substituent as the solvent polarity is increased.

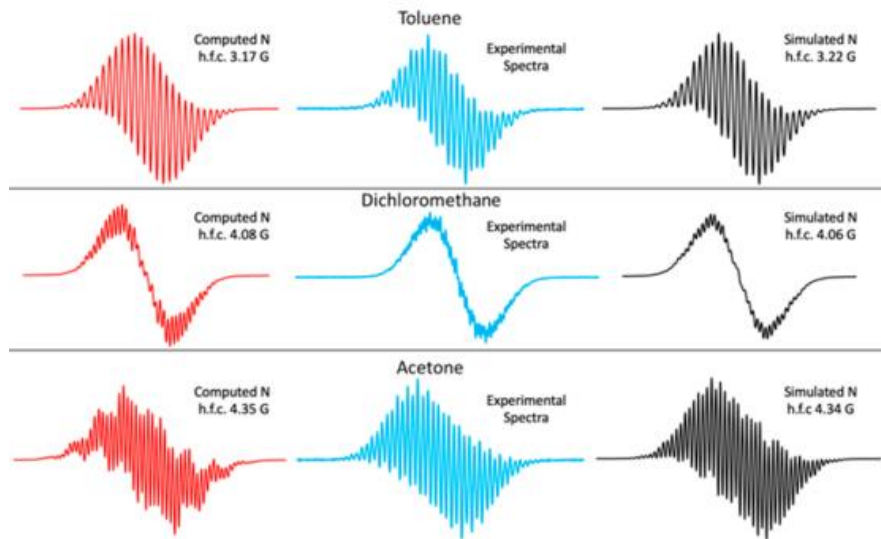


Figure 4-4. Computed (left) EPR spectra using the computed A hyperfine coupling (h.f.c.) values from (B3LYP/EPR-III, SMD) compared to experimental EPR spectra (middle) and simulated values for the 1-NMe₂ radical.

In contrast, the computed ¹³C hyperfine coupling constant for the benzylic carbon decreases from 11.6 gauss to 8.6 gauss, indicating delocalization off the benzylic carbon with increasing solvent polarity. We also simulated the EPR spectra by adjusting the A values to best match the experimental spectra. Only small variations in the computed A values led to good fits (see Figure 4.4). These results provide a rationalization for the dimerization equilibrium measurements above, which indicate that the captodative effect is largest with strong donating groups and polar solvents and requires highly polarizable radicals and polar solvents for maximal effect. In more polar solvents, the radical is stabilized by additional delocalization off of the benzylic carbon and onto the donating substituent.

Benzylic Carbon Spin Density as a Proxy for Radical Stability. Our results above suggest an inverse correlation between the amount of spin density on the benzylic carbon and radical stability. To evaluate the nature of this correlation, we plotted the experimentally determined association constants on a log scale vs the DFT-predicted spin density on the benzylic

carbon (ω B97XD,6-31+G(d,p), SMD). The results are shown in Figure 4.5. A striking correlation is observed, suggesting that radical delocalization may be useful as a direct proxy for radical stability. The trend shows that the less computed spin density on the benzylic carbon, the more radical is observed experimentally in the radical–dimer equilibrium.

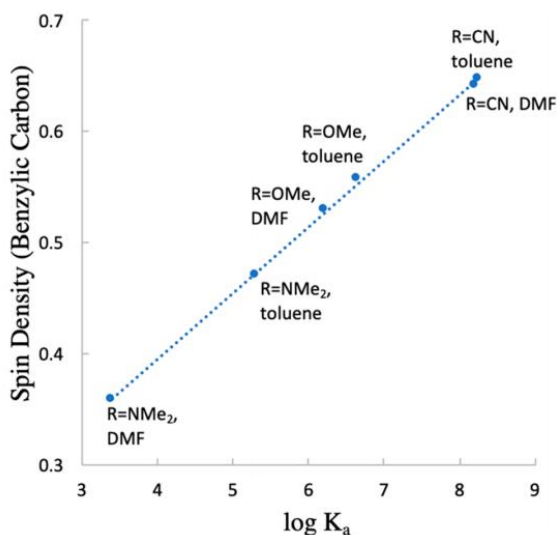


Figure 4-5. Plot of computed spin density on the benzylic carbon versus the experimentally derived binding constants on a log scale.

That is, radicals with more spin delocalization are more stable. Furthermore, this correlation may allow the estimation of radical dimerization binding constants simply by computing the spin density on the benzylic carbon of the free radical without computing the dimer, which may prove to be highly useful as the dimer is notoriously difficult to model accurately (having a C–C bond length $> 1.6 \text{ \AA}$), requiring expensive computational methods with high levels of correlation.

Effect of Solvent on Radical Geometries and Atomic Charges. In addition to changing spin densities of captodative radicals, we considered the possibility that the molecular geometries of the radicals might change in solvents of varying polarity due to the electronic reorganization of the radical as the solvent polarity is increased. In more polar solvents, as more zwitterionic

character is incorporated into the electronic hybrid, the molecular geometries would be expected to change. Thus, we evaluated the computed geometries for 1-DMA and 1-CN in toluene and DMF using the SMD solvation model. Select bond lengths are shown in Figure 4.6. Surprisingly, there are few geometric effects in the solvents of large difference in polarity. For 1-CN, the geometries are effectively identical, which is not surprising given that this is not a captodative radical, but with 1- DMA, there is only a tiny decrease in the length of the C–N bond (by ~0.01 Å). This is surprising because if greater zwitterionic character is mixing into the overall hybrid, the geometry would be expected to change more toward that of a zwitterion geometry. In the zwitterionic resonance form, the nitrogen takes on radical cation character, and the benzylic carbon takes on anion character. However, through examination of the geometry of the dimethylanilinium radical cation (Figure 4.6, right), it can be seen that the C–N bond and the adjacent C– C ring bonds are effectively the same as those for the radical in the gas phase. This result suggests that the lack of geometric change of the radical upon increasing the solvent polarity is due to the zwitterionic form having essentially the same preferred geometry as that of the neutral radical.

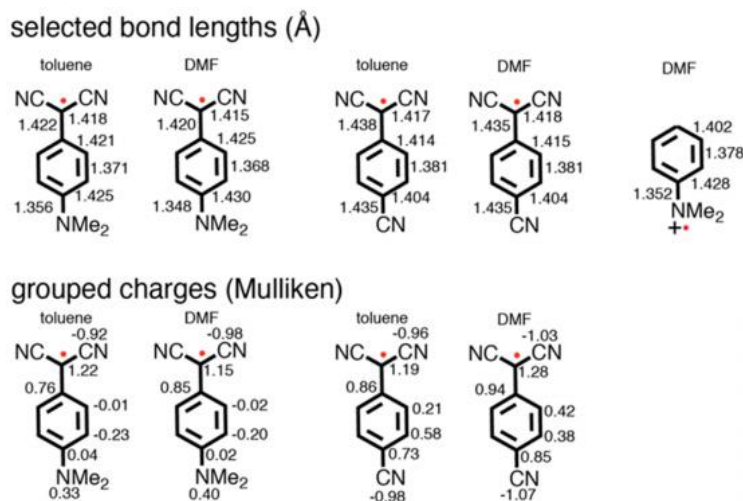


Figure 4-6. (Top) Select bond lengths (Å) for 1-DMA and 1-CN in toluene and DMF (ω B97XD/6-31+G(d,p), SMD). Dimethylaniline radical cation is shown as a reference. (Bottom) Grouped Mulliken atomic charges for 1-DMA and 1-CN in toluene and DMF (ω B97XD/ 6-31+G(d,p), SMD).

The computed Mulliken atomic charges provide more convincing evidence of the increased contribution of zwitterionic character into 1-DMA in polar solvents (Figure 4.6, bottom). Upon going from toluene to DMF, the dicyanomethyl group becomes more negative by 0.19 charge units. Concomitantly, the dimethylamino group becomes more positive by 0.07 charge units. This result is suggestive of increased contribution of charge separated resonance structures. In contrast, for 1-CN, which is not a captodative radical, the charges change slightly upon going from toluene to DMF, but in the other direction (e.g., the dicyanomethyl group becomes more positive).

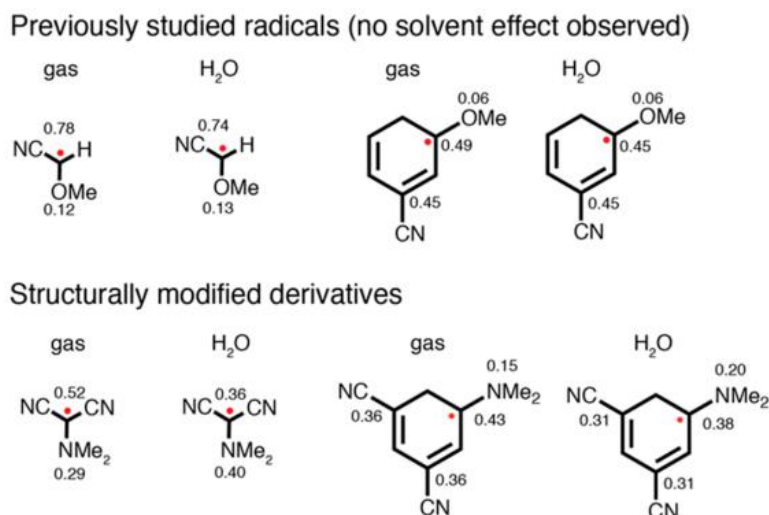


Figure 4-7. Plot of select computed Mulliken spin density ($\omega\text{B}97\text{XD},6-31+\text{G(d,p)}$, SMD) for the radicals showing no captodative solvent effect (top) in water and gas phase and modified structures with stronger donors and another acceptor, showing a larger solvent effect.

Investigating the Failure of Prior Studies to Identify a Solvent Effect on the Stability of Captodative Radicals.

The radicals featured in the two major studies^{11,12} failing to observe a solvent effect on the stability of captodative radicals are shown in Figure 4.7. We computationally evaluated the effect of solvent on the spin densities for these radicals and find that, in contrast to 1-DMA described here, these radicals show little change in spin density as a function of solvent dielectric constant, indicating that no solvent effect is expected. Given that these previously studied radicals featured donors not as strong as NMe₂ (e.g., OMe), and that we have shown here that very

strong donors are required to see a significant solvent effect, we evaluated computationally what would happen if very strong donor groups (e.g., NMe₂) would have been chosen along with an extra withdrawing nitrile group. The results are shown in Figure 4.7 (bottom). In these cases, a significant change in the spin density is predicted for these alternative radicals as a function of the solvent polarity, suggesting that the two prior studies unluckily chose insufficiently strong donors and acceptors to observe a solvent effect. A solvent effect would be expected for these proposed derivatives.

4.4 Computational and Experimental Methods

All compounds were initially optimized at the U_ωB97XD/6-31+G- (d,p) level of theory²¹ using Gaussian16²² using the SMD solvation model.²³ This functional and basis set were previously determined to be accurate and suitable for investigating dicyanomethyl radicals.^{17,18,24} The Mulliken spin density population scheme was used to determine how the spin density throughout the pi-system varies with solvent for different compounds (other population schemes are available, but we are interested mostly in changes in spin density, for which the Mulliken population scheme is suitable). For the computation of hyperfine coupling values for the NMe₂ radical across all solvents, we used the B3LYP/EPR-III level of theory.^{25,26}

To obtain the binding constants for the radical–dimer equilibria, the EPR spectrum of the dissolved radicals were recorded to determine the equilibrium constant between the radical and dimer at varying temperatures. To determine the equilibrium constants, the amount of radical at each temperature was quantified by double integration of the EPR signal (an example is shown in Figure 4.2B). From a van't Hoff plot ($\ln K_{eq}$ vs $1/T$, Figure 4.2B, inset), all of the equilibrium parameters (ΔH° and ΔS° , and subsequently ΔG° and K_a) were obtained. All van't Hoff plots in all solvents are shown in the Supporting Information. Radical/dimers were obtained by quantitative oxidation of aryl malononitrile C–H precursors as described previously.^{18,19}

Following the synthesis previously published in our group, a fresh sample of each radical precursor compound was synthesized by palladium-catalyzed cross coupling from the starting aryl bromide. After purification by column chromatography (80:20 hexanes:EtOAc), pure compounds were dissolved into the solvent of study, and a 10-fold excess of PbO₂ was added to the mixture. After 30 min of stirring, the samples were centrifuged multiple times until all of the lead oxidant was removed from the solution. The resulting radicals in solution were then purged with nitrogen gas and added to pre-purged quartz EPR tubes.

After the oxidation and preparation of radicals into EPR tubes, the following measurements were performed under the following settings. All samples were allowed to equilibrate for 5 min at each temperature before running a scan. A minimum of 8 scans were recorded at each temperature point; more scans were sometimes necessary for samples with low radical content. Solutions of toluene allowed the use of 3 mm quartz EPR tubes while all other solvents needed a specially designed 1 mm quartz EPR tube due to the higher dielectric constant of the solvent. The instrument parameters were set as follows: modulation frequency, 100 kHz; receiver gain, 50 dB; modulation amplitude, 0.5 G; time constant, 0.01 s; center field, 3335 G; sweep width, 150 G; microwave attenuation, 20 dB; microwave power, 2 mW; number of data points, 2048.

4.5 Conclusions

In summary, we demonstrated that for captodative radicals bearing very strong polarizable donors and acceptors, radical stability is solvent dependent. Within polar solvents, the radical is stabilized, which can be rationalized by increased contributions from zwitterionic canonical structures within the resonance model. This model is supported by increased spin delocalization in polar solvents, the change in the computed atomic charges in different solvents, and the correlation of the benzylic carbon radical spin density and the radical–dimer equilibrium constant. Although the theoretical predictions by Katritzky and coworkers^{10,12} appear to be wrong for

specific cases, and their claim that the captodative stabilization is “mostly a solvent effect” is highly suspect, the previous experimental studies that dismissed the importance of solvent stabilization on captodative radicals appear to have unluckily chosen example radicals substituted with insufficiently polarizable donors and acceptors. Had they studied slight structural variants, our computations (Figure 4.7) indicate that a solvent effect may have been observed. It is important to note that the concept of polarizability is fundamental to the captodative effect and has far-reaching consequences that extend to the reactivity of radicals and diradicals. On the basis of this work, we conclude that Katritzky and coworkers’ general prediction that polar solvents can stabilize captodative radicals was correct, vindicating a key prediction from theory.

4.6 References

- (1) Dewar, M. J. S. A Molecular Orbital Theory of Organic Chemistry. IV. Free Radicals. *J. Am. Chem. Soc.* 1952, 74, 3353.
- (2) Viehe, H. G.; Janousek, Z.; Merenyi, R.; Stella, L. The captodative effect. *Acc. Chem. Res.* 1985, 18 (5), 148–154.
- (3) Klessinger, M. Captodative Substituent Effects and the Chromophoric System of Indigo. *Angew. Chem., Int. Ed. Engl.* 1980, 19 (11), 908–909.
- (4) Crans, D.; Clark, T.; von Ragué Schleyer, P. A theoretical evaluation of the synergetic capto-dative stabilisation of free radicals. *Tetrahedron Lett.* 1980, 21 (38), 3681–3684.
- (5) Baldock, R. W.; Hudson, P.; Katritzky, A. R.; Soti, F. Stable free radicals. Part I. A new principle governing the stability of organic free radicals. *J. Chem. Soc., Perkin Trans. 1* 1974, No. 0, 1422–1427.
- (6) Leroy, G.; Peeters, D.; Sana, M.; Wilante, C. A Theoretical Approach to Substituent Effects in Radical Chemistry. In *Substituent Effects in Radical Chemistry*; Viehe, H. G., Janousek, Z., Merenyi, R., Eds.; Springer: Dordrecht, Netherlands, 1986; pp 1–48.
- (7) Pasto, D. J. Radical stabilization energies of disubstituted methyl radicals. A detailed theoretical analysis of the captodative effect. *J. Am. Chem. Soc.* 1988, 110 (24), 8164–8175.

- (8) Viehe, H. G.; Janousek, Z.; Merenyi, R. 'Substituent Effects in Radical Chemistry; Springer: Netherlands, 2012.
- (9) Korth, H.-G.; Sustmann, R.; Merenyi, R.; Viehe, H. G. Absolute' rates for dimerization of capto-dative substituted methyl radicals in solution: absence of kinetic stabilization. *J. Chem. Soc., Perkin Trans. 2* 1983, No. 1, 67–74.
- (10) Katritzky, A. R.; Zerner, M. C.; Karelson, M. M. A quantitative assessment of the merostabilization energy of carbon-centered radicals. *J. Am. Chem. Soc.* 1986, 108 (23), 7213–7214.
- (11) Karelson, M.; Tamm, T.; Katritzky, A. R.; Szafran, M.; Zerner, M. C. Reaction Field Effects on the Electronic Structure of Carbon Radical and Ionic Centers. *Int. J. Quantum Chem.* 1990, 37, 1–13.
- (12) Beckhaus, H.-D.; Rüchardt, C. The Effect of Solvent on the Stability of mero-Substituted Alkyl Radicals. *Angew. Chem., Int. Ed. Engl.* 1987, 26 (8), 770–771.
- (13) Rhodes, C. J.; Roduner, E. Muon Spin Rotation Studies of the Role of Solvent in Captodative Interactions of Cyclohexadienyl Radicals. *Hyperfine Interact.* 1991, 65, 975–978.
- (14) Merenyi, R.; Janousek, Z.; Viehe, H. G. Studies on the' Captodative Effect. Entropy/Enthalpy Compensation as Solvent Effect in Radical Forming Reactions. A Relative Radical Stabilisation Scale. In *Substituent Effects in Radical Chemistry*; Viehe, H. G.; Janousek, Z., Merenyi, R., Eds.; Springer: Dordrecht, Netherlands, 1986; pp 301 – 324.
- (15) Kobashi, T.; Sakamaki, D.; Seki, S. N-Substituted Dicyanomethylphenyl Radicals: Dynamic Covalent Properties and Formation of Stimuli-Responsive Cyclophanes by Self-Assembly. *Angew. Chem., Int. Ed.* 2016, 55 (30), 8634–8638.
- (16) Okino, K.; Hira, S.; Inoue, Y.; Sakamaki, D.; Seki, S. The Divergent Dimerization Behavior of N-Substituted Dicyanomethyl Radicals: Dynamically Stabilized versus Stable Radicals. *Angew. Chem.* 2017, 129 (52), 16824–16828.
- (17) Okino, K.; Sakamaki, D.; Seki, S. Dicyanomethyl Radical-Based Near-Infrared Thermochromic Dyes with High Transparency in the Visible Region. *ACS Mater. Lett.* 2019, 1, 25–29.
- (18) Peterson, J. P.; Geraskina, M. R.; Zhang, R.; Winter, A. H. Effect of Substituents on the Bond Strength of Air-Stable Dicyanomethyl Radical Thermochromes. *J. Org. Chem.* 2017, 82 (12), 6497–6501.

- (19) Zhang, R.; Peterson, J. P.; Fischer, L. J.; Ellern, A.; Winter, A. H. Effect of Structure on the Spin–Spin Interactions of Tethered Dicyanomethyl Diradicals. *J. Am. Chem. Soc.* 2018, 140 (43), 14308–14313.
- (20) McConnell, H. M. Molecular Orbital Approximation to Electron Coupled Interaction between Nuclear Spins. *J. Chem. Phys.* 1956, 24 (2), 460–467.
- (21) Xie, C.; Lahti, P. M.; George, C. Modulating Spin Delocalization in Phenoxy Radicals Conjugated with Heterocycles. *Org. Lett.* 2000, 2 (22), 3417–3420.
- (22) Chai, J.-D.; Head-Gordon, M. Long-range corrected hybrid density functionals with damped atom–atom dispersion corrections. *Phys. Chem. Chem. Phys.* 2008, 10 (44), 6615–6620.
- (23) Frisch, M. J.; Trucks, G. W.; Schlegel, H. B.; Scuseria, G. E.; Robb, M. A.; Cheeseman, J. R.; Scalmani, G.; Barone, V.; Petersson, G. A.; Nakatsuji, H.; Li, X.; Caricato, M.; Marenich, A. V.; Bloino, J.; Janesko, B. G.; Gomperts, R.; Mennucci, B.; Hratchian, H. P.; Ortiz, J. V.; Izmaylov, A. F.; Sonnenberg, J. L.; Williams; Ding, F.; Lipparini, F.; Egidi, F.; Goings, J.; Peng, B.; Petrone, A.; Henderson, T.; Ranasinghe, D.; Zakrzewski, V. G.; Gao, J.; Rega, N.; Zheng, G.; Liang, W.; Hada, M.; Ehara, M.; Toyota, K.; Fukuda, R.; Hasegawa, J.; Ishida, M.; Nakajima, T.; Honda, Y.; Kitao, O.; Nakai, H.; Vreven, T.; Throssell, K.; Montgomery, Jr., J. A.; Peralta, J. E.; Ogliaro, F.; Bearpark, M. J.; Heyd, J. J.; Brothers, E. N.; Kudin, K. N.; Staroverov, V. N.; Keith, T. A.; Kobayashi, R.; Normand, J.; Raghavachari, K.; Rendell, A. P.; Burant, J. C.; Iyengar, S. S.; Tomasi, J.; Cossi, M.; Millam, J. M.; Klene, M.; Adamo, C.; Cammi, R.; Ochterski, J. W.; Martin, R. L.; Morokuma, K.; Farkas, O.; Foresman, J. B.; Fox, D. J. Gaussian 16 Rev. B.01; Gaussian, Inc.: Wallingford, CT, 2016.
- (24) Marenich, A. V.; Cramer, C. J.; Truhlar, D. G. Universal Solvation Model Based on Solute Electron Density and on a Continuum Model of the Solvent Defined by the Bulk Dielectric Constant and Atomic Surface Tensions. *J. Phys. Chem. B* 2009, 113 (18), 6378–6396.
- (25) Geraskina, M. R.; Dutton, A. S.; Juetten, M. J.; Wood, S. A.; Winter, A. H. The Viologen Cation Radical Pimer: A Case of Dispersion-Driven Bonding. *Angew. Chem., Int. Ed.* 2017, 56 (32), 9435–9439.
- (26) Barone, V. Structure, Magnetic Properties and Reactivities of Open-Shell Species From Density Functional and Self-Consistent Hybrid Methods. In Recent Advances in Density Functional Methods; World Scientific Publishing Co. Pte. Ltd.: River Edge, NJ, 1995; pp 287–334.

CHAPTER 5. EFFECT OF STRUCTURE ON THE SPIN SWITCHING AND MAGNETIC BISTABILITY OF SOLID-STATE ARYL DICYANOMETHYL MONORADICALS AND DIRADICALS

Adapted with permission from: J. P. Peterson, R. Zhang, A. H. Winter. *ACS Omega*, **2019**, 4, 8, 13538-13542. Copyright (2020) American Chemical Society.

5.1 Abstract

Stable organic radicals with switchable spin states have applications in medicine, biology, and material science. An emerging class of such spin-switchable radicals is based on dicyanomethyl radicals, which are typically thermally and air-stable species that form weakly bonded (closed-shell singlet) dimers at a lower temperature that rupture into electron paramagnetic resonance-active diradicals at a higher temperature. However, thus far, the study of these dicyanomethyl radicals has focused on their solution-phase behavior. An understanding of how chemical structure affects the solid-state spin switching behavior for these radicals is unknown. Here, we examine the solid-state spin crossover behavior of 6 monoradicals and 10 tethered diradicals and demonstrate that these species also undergo spin switching in the solid state. We find that the susceptibility for solid-state spin switching for the intermolecular dimers is weakly correlated to the solution-phase Gibbs free energies of dimerization, but no apparent correlations are seen between the solution-state free energies for the intramolecular dimerization and the solid-state behavior. Furthermore, intramolecular diradical dimers have greatly enhanced temperature-responsive behavior compared to their intermolecular counterparts. Crystalline and amorphous powders of the same radicals feature similar spin switching behavior, but the crystalline materials have slower bond-rupture kinetics at higher temperatures, suggesting that solid-state packing

effects are an important kinetic consideration. An interesting feature of these systems is that, upon cooling down to room temperature after heating, some radicals remain trapped in the solids, indicating magnetic bistability, while others partially or fully return to the diamagnetic dimers. This work provides insights into how chemical structure affects spin crossover in the solid state for this new class of air-stable radicals, the knowledge of importance for the construction of dynamically responsive solid-state materials, and organic spin crossover polymers.

5.2 Introduction

Organic radicals with switchable spin states are emerging materials with applications in turn-on magnetic resonance contrast reagents, spintronics, dynamic covalent assemblies, and stimuli-responsive polymers and plastics.^{1–5} Such spin-switchable materials undergo a change in spin state in response to external stimuli or environmental cues. Switching between the standard properties of closed-shell molecules to spin-unpaired radicals leads to large changes in the optical, magnetic, and conductivity properties of these materials with relatively mild external stimuli, making this spin switching strategy an attractive one for the design of stimuli-responsive materials. A critical barrier toward the development of such spin crossover organic materials is the requirement for stable organic radicals that can switch between spin states. Regrettably, most stable organic radicals do not show such spin switching behavior. However, dicyanomethyl radicals have recently been demonstrated as promising building blocks for such spin-switchable materials because they are air- and thermally stable species and can switch between weakly bonded closed-shell forms and spin-unpaired forms.^{6–10} Furthermore, the strength of the spin–spin interaction can be tuned by substituents.⁶ The nature of the spin–spin interaction for these dicyanomethyl radicals is typically a very weak sigma dimer (with a C–C distance >1.6 Å) or an anti-ferromagnetically spin-coupled pi dimer. There are cases of organic radicals investigated in the solid state;^{11–16} however, detailed studies of dicyanomethyl organic radicals have been mostly

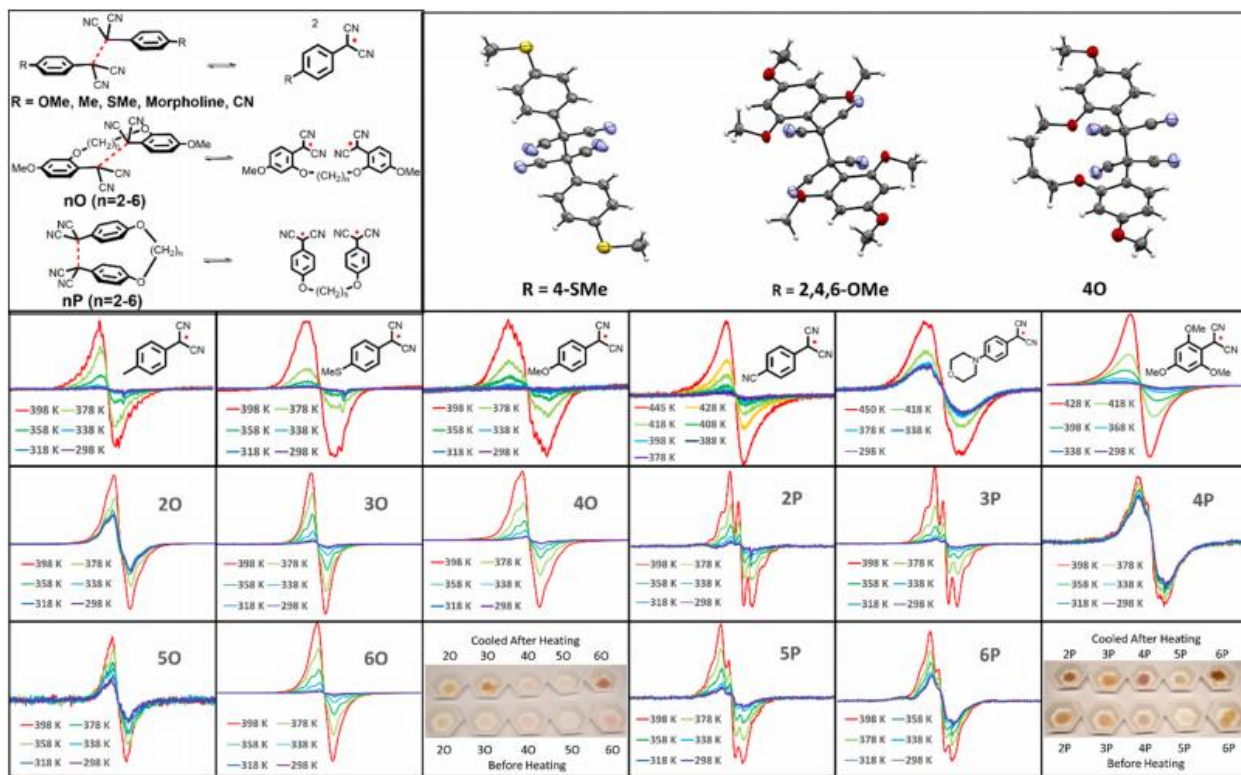


Figure 5-1. Radical–dimer equilibria for all subsets of compounds (top left); crystal structure for thiomethyl, trimethoxy (reproduced from ref 7), and 4O dimers (top right) (reproduced from ref 7); and all VT-EPR data for the 16 solid-state samples in this work (bottom).

limited to the solution phase. To understand how the structure affects spin crossover in the solid state, here, we report a study of a family of dicyanomethyl monoradicals and tethered diradicals using variable-temperature electron paramagnetic resonance (EPR), allowing the comparison of the solid-state behavior of 6 monoradicals and 10 tethered diradicals (Figure 5.1) to their previously reported solution-phase behavior.

5.3 Results and Discussion

All of the monoradicals and linked diradicals (shown in Figure 5.1) in this study exhibit qualitatively similar temperature responsive behavior in the solid state. At low temperatures, either no EPR signal or a very small one is observed. In all cases, an EPR signal grows in as the temperature is increased. This increase in the EPR signal is accompanied by a color change in the solid from typically a light powder to a darkly colored one. Except where noted, after a brief

temperature equilibration period, the EPR signal is stable. These features are consistent with rupturing of the colorless sigma dimers into their colored diradical forms as the temperature is increased, similar to their solution-phase behavior.

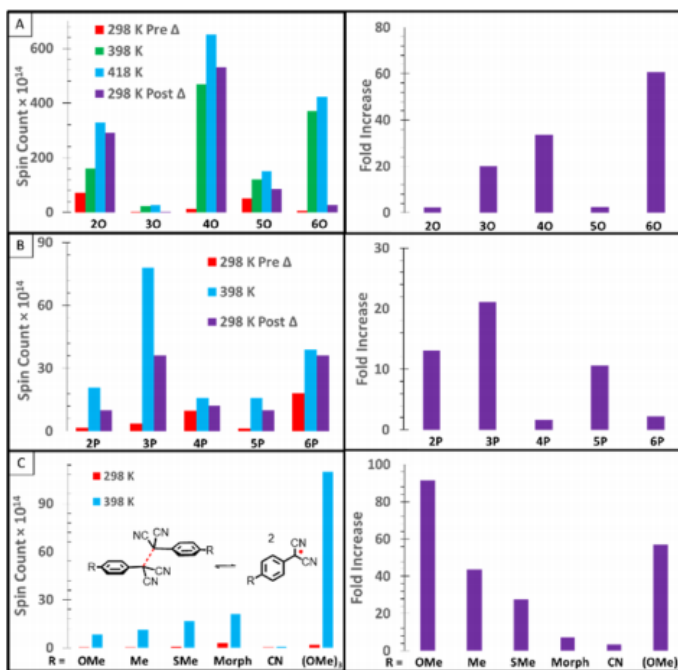


Figure 5-2. Spin counts at various temperatures for ortho tethers (A), para tethers (B), and monoradicals (C) with fold increases from 298 to 398 K to the right of each.

Correlation between Solution-Phase Radical Dimerization K_a and Solid-State Radical Behavior.

We were interested in whether there is a correlation between the solution-phase equilibrium constants for the radicals and the corresponding solid-state spin switching behavior. Intuitively, one expects radicals with weaker bonding interactions in the solution phase to have a higher susceptibility for solid-state spin crossover. To test this hypothesis, we evaluated six monoradicals with varying para substituents (OMe, Me, SMe, morpholine, CN, and 2,4,6-OMe) that have varying solution phase K_a values for dimerization. Radicals featuring donating substituents appended to the aryl ring have lower solution phase K_a values for dimerization, while those with withdrawing groups (e.g., CN) have a stronger interaction. A Hammett plot of the σ^+ of

the para substituent vs the K_a shows a positive correlation.⁶ Indeed, a comparison of the solution-state K_a values vs the sample spin count observed at 398 K shows a negative correlation. The 2,4,6-trimethoxy monoradical, which has the lowest binding constant ($1.9 \times 10^5 \text{ M}^{-1}$), has the highest percentage of spins, while the p-cyano derivative, which has the highest solution binding constant ($1.8 \times 10^8 \text{ M}^{-1}$), has the lowest percentage of spins. In general, however, the spin count observed for the solid monoradicals is orders of magnitude lower than the spin count observed in solution from 3 to 5 mM measured at the same temperature. For the intramolecular dimers, however, the spin count is about 2 orders of magnitude higher in the solid state than for the monoradicals, and in some cases, it is higher than that observed for the same diradicals in solution. For example (see Figure 5.2), 4O, 3P, and 4P show a greater spin count in the solid state than in solution at all temperatures studied. However, for these intramolecular diradical cases, there is no discernible correlation between the intramolecular K_a determined in solution and the solid-state spin switching behavior. Indeed, in the solid state, the temperature-responsive spin switching curves are all relatively similar, despite differences in the solution K_a between these linked diradicals. Given that the primary difference in these linked diradicals is the linker length, which leads to large changes in solution phase entropy, this is perhaps not so surprising because in solution, the diradical is free to sample conformational space, which is not the case in the confined solid-state environment. Thus, the differences are larger in the solution state for these tethered diradicals than in the solid state.

Reversibility of Spin Crossover. A major difference between solution-state and solid-state spin crossovers is the reversibility of spin crossover. In solution, rapid equilibration ensures a Boltzmann population of spin-paired and spin unpaired species. Upon lowering the temperature, radicals immediately return to the dimers. In contrast, we find that in the solid state, some of the

radicals show magnetic bistability (e.g., stay trapped in the paramagnetic state) despite lowering the temperature. After performing variable-temperature EPR on the *ortho* and *para* tethered diradicals, we evaluated the ability of the samples to return back to their diamagnetic dimers upon cooling. In solution, all compounds return completely to their starting equilibrium spin concentration upon cooling and can be reversibly cycled. This is not so in the solid state (see Figure 2). Some of the tethered diradicals tested here in the solid state show increases in radical concentration at elevated temperatures, but upon cooling, the radical concentrations remained elevated for over 12 months of extended sitting under air (evidenced by the after-heated pictures in Figure 1). Examples of this type include 2O, 4O, and 6P. Others (e.g., 2P, 3P, 5P, 5O) show a partial return. In still other cases (e.g., 3O, 6O), we observed a nearly complete return to the starting radical concentration upon cooling.

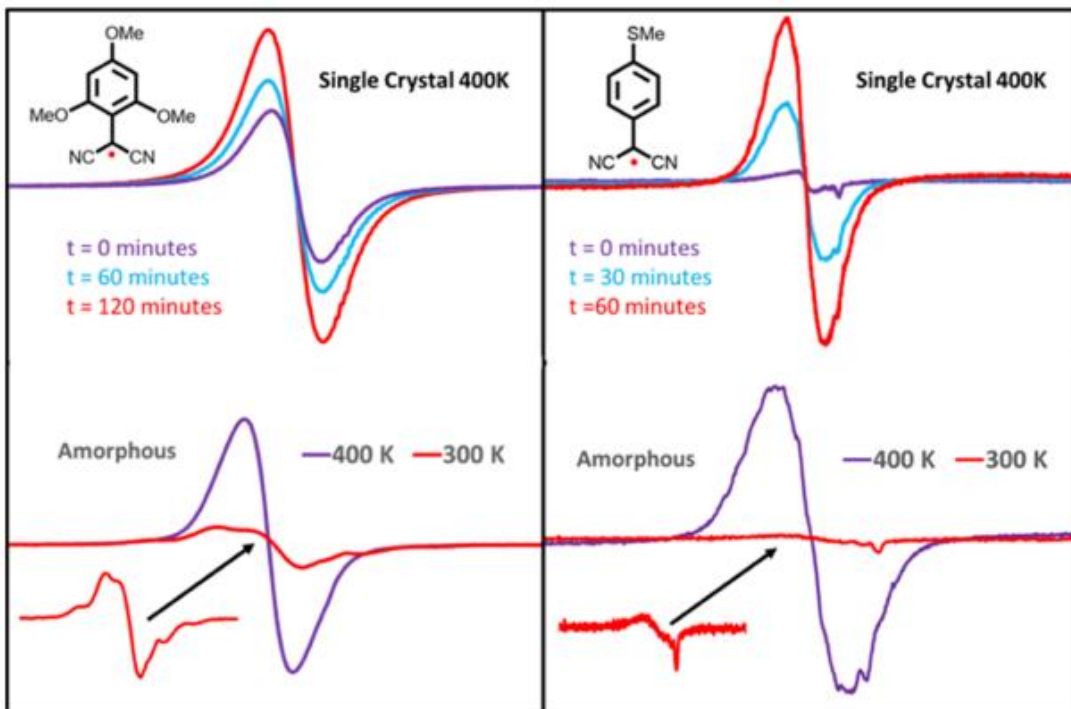


Figure 5-3. Single-crystal EPR data at 400 K for 2,4,6-trimethoxy- and p-thiomethyl-substituted dimers with amorphous powder EPR spectra for each compound below.

Difference between Crystalline and Amorphous Materials. The samples tested in Figure 5.1 are amorphous powders. We asked the question of whether there would be a difference in the spin switching behavior if the samples were crystalline solids. For two of the monoradicals, we obtained sufficient quantities of X-ray quality single crystals of the materials (see Figure 5.1) to perform solid-state VT-EPR measurements. In these two cases, we compared the temperature-responsive behavior of the amorphous powders compared to that of the single crystals (see Figure 5.3). The most striking difference is that, at higher temperatures, the crystalline compound shows further growth in the EPR signal over time after our short-temperature equilibration in the EPR cavity, while the amorphous samples do not show any further increase in their EPR signal. Essentially, the compound does not reach a quick equilibrium at elevated temperatures and the radical continues to form slowly over time. In the case of the thiomethyl monoradical, the further increase is substantial. Thus, the kinetics of bond rupture appear to be altered by solid-state morphology, and there appears to be a barrier for spin crossover in crystalline materials not present in the amorphous solids. By analyzing the combined data (i.e., spin counts at various temperatures) for all 16 compounds (Figure 5.2), some interesting trends were observed. Compounds 4O and 6O showed largest increases for those diradicals substituted at the ortho position, while 3P and 5P show the largest increase in the spin count for the para-substituted diradical series. Compound 2P is much less flexible than other compounds, and we hypothesize that it behaves differently because of this. An alternative possibility is that some of these diradicals form higher-order aggregates (dimer, trimer, oligomer, etc.) in the solid state. In the non-tethered series, the donating ability of each substituent correlated well with the fold increase in the amount from 398 to 298 K with the exception of the morpholine substitute compound. As noted in our previous work, the para-

nitrogen-containing dicyanomethyl radicals can suffer decomposition at elevated temperatures, and this also occurred in the solid state for this radical.

5.4 Conclusions

In conclusion, we have investigated the effect of structure on the spin crossover behavior of a family of dicyanomethyl monoradicals and linked diradicals. All radicals and diradicals show a 10- to 100-fold increase in spin counts upon being heated, with the linked diradicals being much more susceptible to spin crossover than the monoradicals. For the monoradicals, the solution-state K_a correlates weakly with the solid-state spin switching behavior, but there is no correlation for the linked dimers, which all show similar behavior due to a reduction of the importance of conformational entropy in the solid state. The kinetics of spin crossover differ between crystalline samples and amorphous powders, suggesting the importance of crystal packing and hinting at cooperative effects. The reversibility of spin crossover varies greatly among the radical structures, with some powders trapping the radicals generated upon heating and showing magnetic bistability, while others showing either partially or fully reversible behavior. These studies with discrete well-defined radicals lay the groundwork for using these radicals and diradicals as the building blocks for stimuli-responsive spin crossover polymers and bulk materials.

5.5 Experimental Section

General Procedure in the Preparation of Amorphous Powder Solid-State EPR Experiments. All of the compounds in this paper, the 6 intermolecular dimers and the 10 tethered intramolecular dimers, were all synthesized according to previous reports by our lab.^{6,7} At the time for each experiment, a fresh sample of each compound was oxidized from the precursor $-CH$ adduct to generate the radical/dimer species. Upon workup for these oxidations, during solvent removal of the purification step, freshly purified potassium chloride salt was added to the mixture to make an even dispersion in the sample tube. When all solvents were removed, the desired

compounds were then mixed with KCl salt and finely ground using a mortar and pestle. Compounds were added to EPR tubes and then sealed under normal atmospheric conditions. The ratio of KCl to compound in question was kept constant in all samples for consistency. A known weight of oxidized compound contained within the EPR window was calculated for spin count calculations. After EPR experiments, all samples were saved and placed into vials for future experiments because these compounds do not decompose over time, as evidenced by investigating samples many months after initial oxidation and EPR study. Compounds tested in the solid state can be dissolved and analyzed in solution to yield the exact same data from our previously published papers. This is also useful because it allows a “reset” to the dimer after spin switching to the diradical in the solid state, some of which is not reversible.

General Procedure in the Preparation of Single Crystal Solid-State EPR Experiments. For the 2,4,6-trimethoxy and thiomethyl-substituted compounds, sufficient amounts of single crystals were formed to allow for direct EPR characterization on the single crystals themselves. Crystals were grown by slow evaporation of compounds dissolved in toluene; this process occurred serendipitously over the course of a few months after initial solution EPR experiments. Single crystals were carefully added with a spatula to a 3 mm EPR tube, and the tube was sealed under atmospheric conditions. For the longer kinetic scans on the crystals, a built-in kinetics parameter on the instrument allowed for scanning the sample over a long period of time at various time increments while at the elevated temperature.

EPR Instrument Parameters. The following parameters were used on the EPR instrument for variable-temperature acquisitions: modulation frequency, 100 kHz; receiver gain, 50 dB; modulation amplitude, 0.5–1 G; time constant, 0.1 s; center field, 3330 G; sweep width, 300 G; microwave attenuation, 20 dB; microwave power, 2 mW; number of data points, 2048. For

the determination of spin count, a calibration curve was generated using a sample of TEMPO at various concentrations.

Variable-Temperature EPR Experiments. Variable-temperature EPR studies were performed on all compounds, radicals and diradicals, to elucidate the effect of temperature on the homolytic bond cleavage to generate each, in the solid state. All compounds were investigated in the solid state, with a portion of each sample, ranging from 5 to 10 mg, in a sealed quartz EPR tube. During experiments on the EPR spectrometer, a spectrum was recorded at 10 K intervals after allowing 5 min for the sample to reach an equilibrated temperature. The temperature range for each sample was from 298 to 418 K at minimum; some samples were investigated at even higher temperatures up to 450 K. Follow-up EPR scans were performed after the samples were cooled back to room temperature to gauge the reversibility for each sample to return to starting temperature radical concentrations.

5.6 References

- (1) Grossel, M. C.; Weston, S. C. Synthesis of materials for molecular electronic applications. *Contemp. Org. Synth.* 1994, 1, 367 – 386.
- (2) Hughes, B. K.; Braunecker, W. A.; Bobela, D. C.; Nanayakkara, S. U.; Reid, O. G.; Johnson, J. C. Covalently Bound Nitroxyl Radicals in an Organic Framework. *J. Phys. Chem. Lett.* 2016, 7, 3660 –3665.
- (3) Li, L. H.; Feng, X. L.; Cui, X. H.; Ma, Y. X.; Ding, S. Y.; Wang, W. Salen-Based Covalent Organic Framework. *J. Am. Chem. Soc.* 2017, 139, 6042 –6045.
- (4) Ma, Y. X.; Li, Z. J.; Wei, L.; Ding, S. Y.; Zhang, Y. B.; Wang, W. A Dynamic Three-Dimensional Covalent Organic Framework. *J. Am. Chem. Soc.* 2017, 139, 4995 –4998.
- (5) Montoro, C.; Rodríguez-San-Miguel, D.; Polo, E.; Escudero-Cid, R.; Ruiz-Gonzalez, M. L.; Navarro, J. A. R.; Oco'n, P.; Zamora, F. Ionic Conductivity and Potential Application for Fuel Cell of a Modified Imine-Based Covalent Organic Framework. *J. Am. Chem. Soc.* 2017, 139, 10079 –10086.

- (6) Peterson, J. P.; Geraskina, M. R.; Zhang, R.; Winter, A. H. Effect of Substituents on the Bond Strength of Air-Stable Dicyanomethyl Radical Thermochromes. *J. Org. Chem.* 2017, 82, 6497 –6501.
- (7) Zhang, R.; Peterson, J. P.; Fischer, L. J.; Ellern, A.; Winter, A. H. Effect of Structure on the Spin –Spin Interactions of Tethered Dicyanomethyl Diradicals. *J. Am. Chem. Soc.* 2018, 140, 14308 – 14313.
- (8) Kobashi, T.; Sakamaki, D.; Seki, S. N-Substituted Dicyanomethylphenyl Radicals: Dynamic Covalent Properties and Formation of Stimuli-Responsive Cyclophanes by Self-Assembly. *Angew. Chem., Int. Ed.* 2016, 55, 8634 –8638.
- (9) Okino, K.; Hira, S.; Inoue, Y.; Sakamaki, D.; Seki, S. The Divergent Dimerization Behavior of N-Substituted Dicyanomethyl Radicals: Dynamically Stabilized versus Stable Radicals. *Angew. Chem., Int. Ed.* 2017, 129, 16824 –16828.
- (10) Hartzler, H. D. Polycyano Radicals. *J. Org. Chem.* 1966, 31, 2654 –2658.
- (11) Hicks, R. G. A new spin on bistability. *Nat. Chem.* 2011, 3, 189.
- (12) Bag, P.; Pal, S. K.; Itkis, M. E.; Sarkar, A.; Tham, F. S.; Donnadieu, B.; Haddon, R. C. Synthesis of Tetrachalcogenide Substituted Phenalenyl Derivatives: Preparation and Solid-State Characterization of Bis(3,4,6,7-tetrathioalkyl-phenalenyl)boron Radicals. *J. Am. Chem. Soc.* 2013, 135, 12936–12939.
- (13) Leitch, A. A.; Lekin, K.; Winter, S. M.; Downie, L. E.; Tsuruda, H.; Tse, J. S.; Mito, M.; Desgreniers, S.; Dube, P. A.; Zhang, S.; Liu, Q.; Jin, C.; Ohishi, Y.; Oakley, R. T. From Magnets to Metals: The Response of Tetragonal Bisdiselenazolyl Radicals to Pressure. *J. Am. Chem. Soc.* 2011, 133, 6051 –6060.
- (14) Morita, Y.; Suzuki, S.; Fukui, K.; Nakazawa, S.; Kitagawa, H.; Kishida, H.; Okamoto, H.; Naito, A.; Sekine, A.; Ohashi, Y.; Shiro, M.; Sasaki, K.; Shiomi, D.; Sato, K.; Takui, T.; Nakasaji, K. Thermochromism in an organic crystal based on the coexistence of σ - and π -dimers. *Nat. Mater.* 2008, 7, 48.
- (15) Sarkar, A.; Pal, S. K.; Itkis, M. E.; Tham, F. S.; Haddon, R. C. Sulfur and selenium substituted spiro-biphenalenyl-boron neutral radicals. *J. Mater. Chem.* 2012, 22, 8245 –8256.
- (16) Fourmigue, M.; Lieffrig, J. Organizing radical species in the solid state with halogen bonding. *Top. Curr. Chem.* 2015, 359, 91 – 113.

CHAPTER 6. SPIN DELOCALIZATION, POLARIZATION, AND LONDON DISPERSION FORCES GOVERN THE FORMATION OF DIRADICAL PIMERS

Adapted with permission from: J. P. Peterson, A. Ellern, A. H. Winter. *J. Am. Chem. Soc.*

2020, 142, 11, 5304-5313. Copyright (2020) American Chemical Society.

6.1 Abstract

Some free radicals are stable enough to be isolated, but most are either unstable transient species or exist as metastable species in equilibrium with a dimeric form, usually a spin-paired sigma dimer or a pi dimer (pimer). To gain insight into the different modes of dimerization, we synthesized and evaluated a library of 15 aryl dicyanomethyl radicals in order to probe what structural and molecular parameters lead to sigma versus pi dimerization. We evaluated the divergent dimerization behavior by measuring the strength of each radical association by variable-temperature EPR spectroscopy, determining the mode of dimerization (sigma or pi dimer) by UV-Vis spectroscopy and X-ray crystallography, and performing computational analysis. We evaluated three different hypotheses to explain the difference in the dimerization behavior: (1) that the dimerization behavior is dictated by radical spin densities; (2) that it is dictated by radical polarizability; (3) that it is dictated by London dispersion stabilization of the pimer. However, no single parameter model in itself was predictive. Two-parameter models incorporating either the computed degree of spin delocalization or the radical polarizability as well as computed estimates for the attractive London dispersion forces in the pi dimers lead to improved forecasts of sigma vs. pi dimerization mode, and suggests that a balance of spin delocalization of the isolated radical, as well as attractive forces between the stacked radicals, govern the formation of diradical pimers.

6.2 Introduction

Free radicals pervade all aspects of chemistry, from synthetic mechanisms to materials science to biological chemistry. Some free radicals can be stabilized sufficiently to make them isolable. Just below this point of indefinite persistence are metastable radicals that exist in a dynamic equilibrium with dimers. An example of such a meta-stable radical is the trityl radical, the first detected free radical, which famously exists in a solution-phase equilibrium with a head-to-tail sigma dimer.¹ This radical dimerization can be an annoyance when attempting to make ferromagnetic plastics, but is an attractive feature when using these radicals as building blocks for stimuli responsive materials, dynamic covalent assemblies, chemical sensors with optical or magnetic resonance contrast, or organic spin-crossover materials.²⁻¹⁰

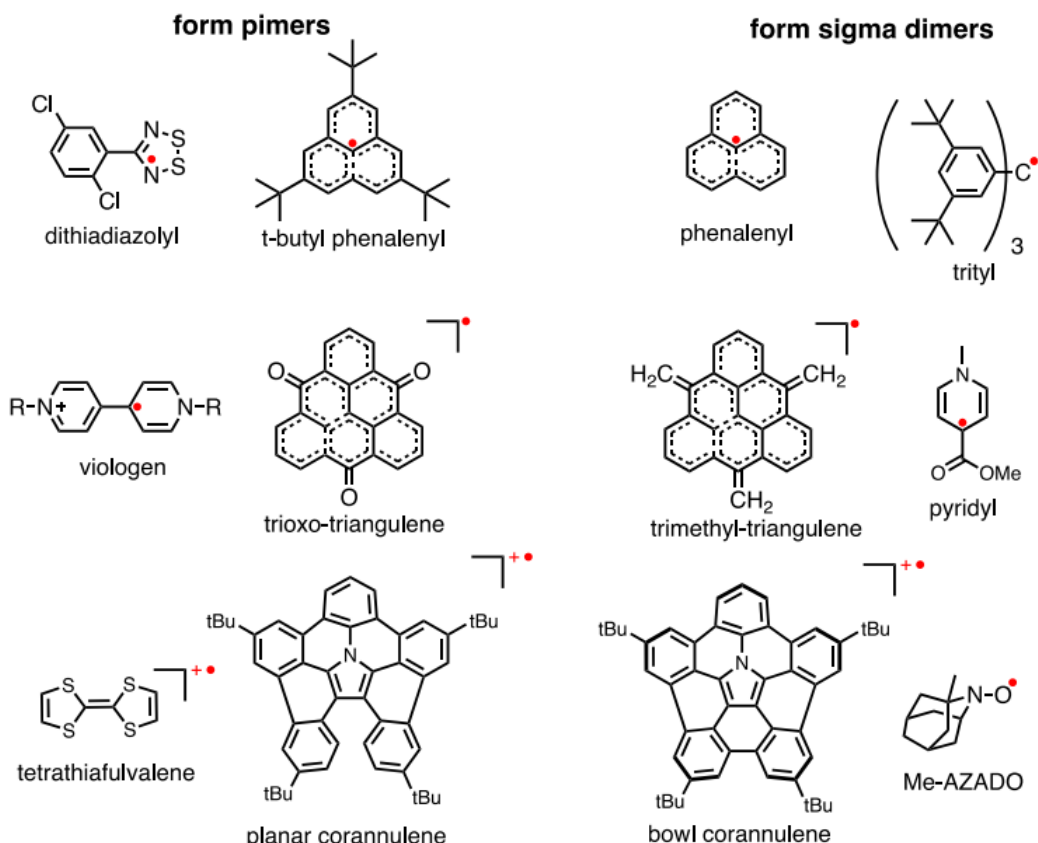


Figure 6-1. Examples of radicals that form sigma¹³⁻¹⁷ and π-dimers.^{16,18-21}

A wealth of literature on such meta-stable radical species shows that they form either weak sigma dimers or multi-centered pi dimers (pimers).^{11, 12} The radical—radical bond found in these pimers is fascinating for its unusual multicenter covalent bonding pattern that brings the atoms closer than the van der Waals radii but much longer than a conventional two-atom bond (>2.8 Å), while straddling the knife edge between van der Waals interactions and conventional chemical bonds in strength and properties. Unfortunately, models to understand why some meta-stable radicals form sigma dimers while others form pimers are lacking.

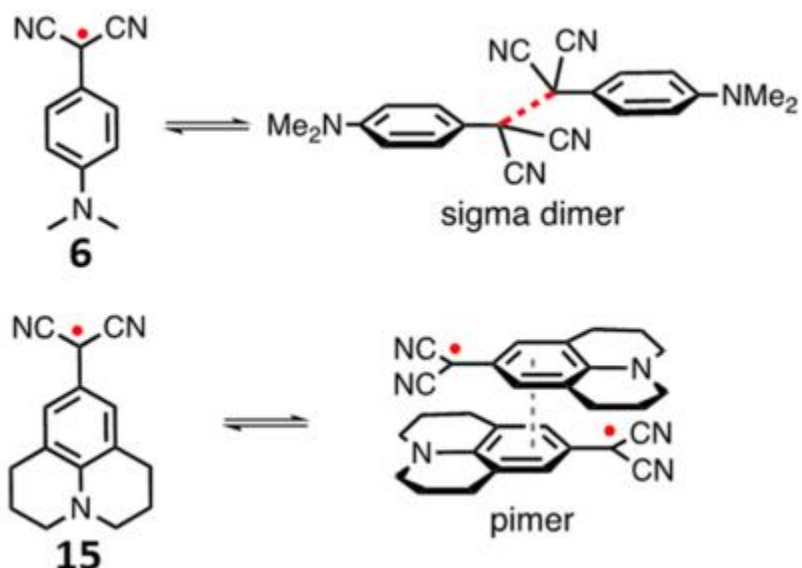


Figure 6-2. Known modes of dimerization for the dimethylamino³¹ and julolidine³² substituted dicyanomethyl radicals.

Understanding this divergent dimerization behavior would aid in the application of these radicals into useful materials, because the properties of the two types of radical dimers show remarkable differences. For example, sigma dimers usually absorb mostly in the UV region of the optical spectrum and have properties that are more consistent with “normal” closed-shell organic molecules. In contrast, diradical pimers are typically colored species that absorb visible to near-

infrared light and feature unusual conductive and magnetic properties.^{18, 22, 23} Such radical pimers, or ‘pancake dimers’,²¹ are distinct from normal pi-stacked dimers between closed-shell aromatics because they often prefer face-to-face sandwich geometries rather than slip stacked geometries. Moreover, unlike normal pi stacked dimers, they can have strong orientational geometric preferences, are stabilized by p orbital interactions (rather than being repulsive), have fluxional geometries, and often show large intramolecular and layer-to-layer charge transporting properties with broader energy bands than typical organic semiconductors.

Select examples of meta-stable radicals are shown in Figure 6.1, along with their preferred mode of dimerization. For example, phenalenyl radicals and triangulene radicals can form either sigma or pi dimers depending on the substitution.^{20, 24-26} Examples of radicals that form sigma dimers include trityl radicals,^{13, 14} pyridyl radicals,²⁷ and aza-adamantyl nitroxyl radicals.¹⁷ Radicals that form pimers include halo-phenyl dithiazolyl radicals,¹⁹ planar corranulene-derived cation radicals¹⁶ viologen cation radicals,¹⁸ pi radical anions such as tetracyanoquinodimethane (TCNQ)¹¹ and naphthalene diimide radical anions,¹² although many others are known.²⁸⁻³⁰

To understand what structural and molecular parameters dictate whether a sigma or pi dimer is formed for that radical, a library of aryl dicyanomethyl radicals was synthesized and evaluated. As shown by Seki and coworkers,³²⁻³⁴ and subsequently by us,^{31, 35-37} this class of radicals are indefinitely stable provided a para substituent is added to block an irreversible head-to-tail dimerization reaction. They exist as stable steady state populations of radical in equilibrium with dimers. These radicals are attractive for such a study because they are known to dimerize to form either a sigma dimer or a pimer depending on the attached substituents. For example, a p

dimethylamino derivative forms a sigma dimer, while a structurally-related julolidine derivative forms a pimer, with no obvious explanation for the difference. (See Figure 6.2).

To elucidate the structural and molecular parameters that direct the formation of sigma and pi dimerization, a library of radicals was investigated using variable temperature EPR spectroscopy, VT-UV-Vis spectroscopy, X-ray crystallography, and computational analysis. The synthesized library is shown in Figure 6.4 and explores the structural region around these two known radicals (6, 15) featuring different dimerization modes. We evaluated three competing hypotheses—one based on spin delocalization, one based on radical polarizability, and one based on London dispersion forces—to explain the divergent modes of dimerization, with the hopes of developing a predictive model that could be used to both explain the modes of dimerization for known radicals, and ideally allow forecasts of the dimerization mode for novel radicals (Figure 6.3) and provide fundamental insight into the important properties driving the formation of the two different types of dimers.

This investigation reveals that radical spin delocalization is a key parameter for predicting sigma or pi dimerization. For example, all radicals in this work with highly localized spin densities form sigma dimers. However, with delocalized spin densities, either pi dimers or sigma dimers can form. Within this regime, spin delocalization is an insufficiently predictive parameter in isolation. A two-parameter model incorporating either the computed spin density or the radical polarizability, and a computational estimate of the dispersion forces in the stacked pimers, leads to improved two-parameter models for predicting the mode of dimerization, and suggests that both

spin delocalization and attractive forces between the stacked radicals are critical to understanding the dimerization mode of meta-stable radicals.

6.3 Results and Discussion

Structural Effects on the Radical-Dimer Equilibrium Constants. A library of aryl dicyanomethyl radicals with para substituted electron donating groups were prepared by oxidation of the precursor aryl malononitriles by previously reported experimental methods^{31,32} (Figure 6.4). The library was made to span the structural space between radicals 6 and 15 (Figure 6.2). All synthetic procedures are provided in the Supporting Information.

In order to decouple steric effects of the substituents, with the exception of 3, substituents were appended to the meta and para positions relative to the radical center. Consequently, these substituents are anticipated to have little steric effect on the stability of the sigma dimer (See Figure 6.4 for crystal structures of some of the dimers). Eleven of the fifteen radicals in Figure 4 are new structures, while four of them have been previously reported either by us (1, 3, 6)³¹ or Seki and coworkers (15)³². Radical association constants for dimerization were determined from van'T Hoff plots obtained by determining the radical/dimer equilibrium constants at varying temperatures using variable-temperature EPR spectroscopy (Table 6.1 shows an example van'T Hoff plot; all van'T Hoff plots are shown in the Supporting Information).

As can be seen in Table 1, the electronic donating ability of the para substituent is inversely correlated with the dimerization association constant. Thus, radicals with strong donating groups are stabilized and feature lower K_a values for dimerization than radicals substituted with less strong donors. With less strongly electron donating substituents, such as oxo-substitution in the para position, K_a values between 10^5 and 10^6 M^{-1} were obtained irrespective of whether the substituent was freely rotating (radicals 1-3) or locked in a fused ring (radicals 4 and 5). These radicals form sigma dimers as shown by variable temperature UV-Vis experiments described later and by crystal

structures determined for 3 and 4 (see Figure 4). For all radicals that form sigma dimers, at low temperature the solution is clear or yellow and becomes brightly colored upon heating as the colored radical is liberated.

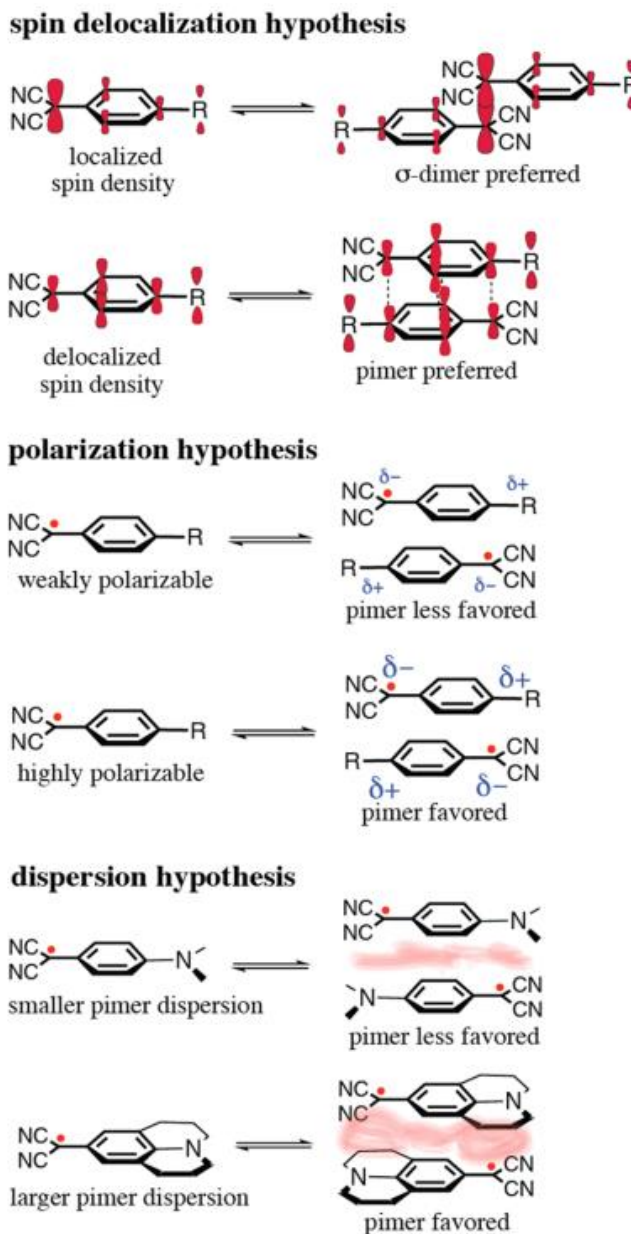


Figure 6-3. Schematic of spin delocalization hypothesis for maximizing covalent bonding, polarization hypothesis for maximizing Coulombic interactions, and dispersion hypothesis for maximizing London dispersion forces.

In contrast, para amino substituents stabilize the radical by orders of magnitude compared to oxo-substituents.^{31, 36} Radicals 6-14 are examples of radicals that feature a para amino substituent, with 6-8 having free substituent rotation while 9-14 are constrained by a ring that both hinders free rotation and nitrogen pyramidalization. Hindering pyramidalization of the amino substituent certainly favors more delocalization into the aromatic ring by maximizing p character without the usual energetic penalty for rehybridization at nitrogen.^{38,39} For radicals 6-8 and 11-14, association constants for these radicals range from $10^2 - 10^4 \text{ M}^{-1}$. Thus, in contrast to radicals with oxo substituents, at room temperature a large fraction of the sample exists as the free radical rather than the dimer and the solutions are highly colored even at room temperature (at millimolar or lower concentrations). Radicals 9 and 10, indole derivatives, are exceptional cases, and feature larger association constants, more similar to the oxo-substituted dicyanomethyl radical ($K_a \sim 10^6 \text{ M}^{-1}$), than typical amino substituents. In these cases, the para nitrogen in the indole ring is no longer as strong a donor as a typical amino substituent due to lost electron donation into the aromatic indole ring. These radicals are discussed in more detail below.

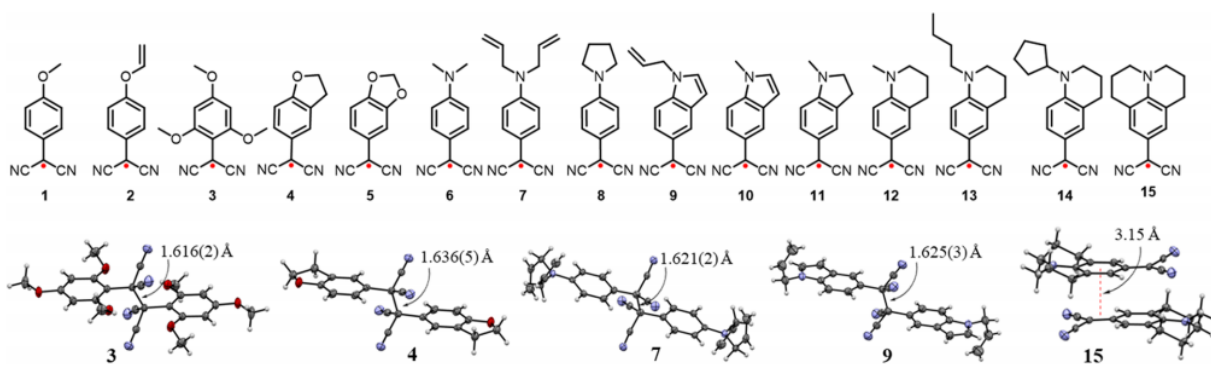


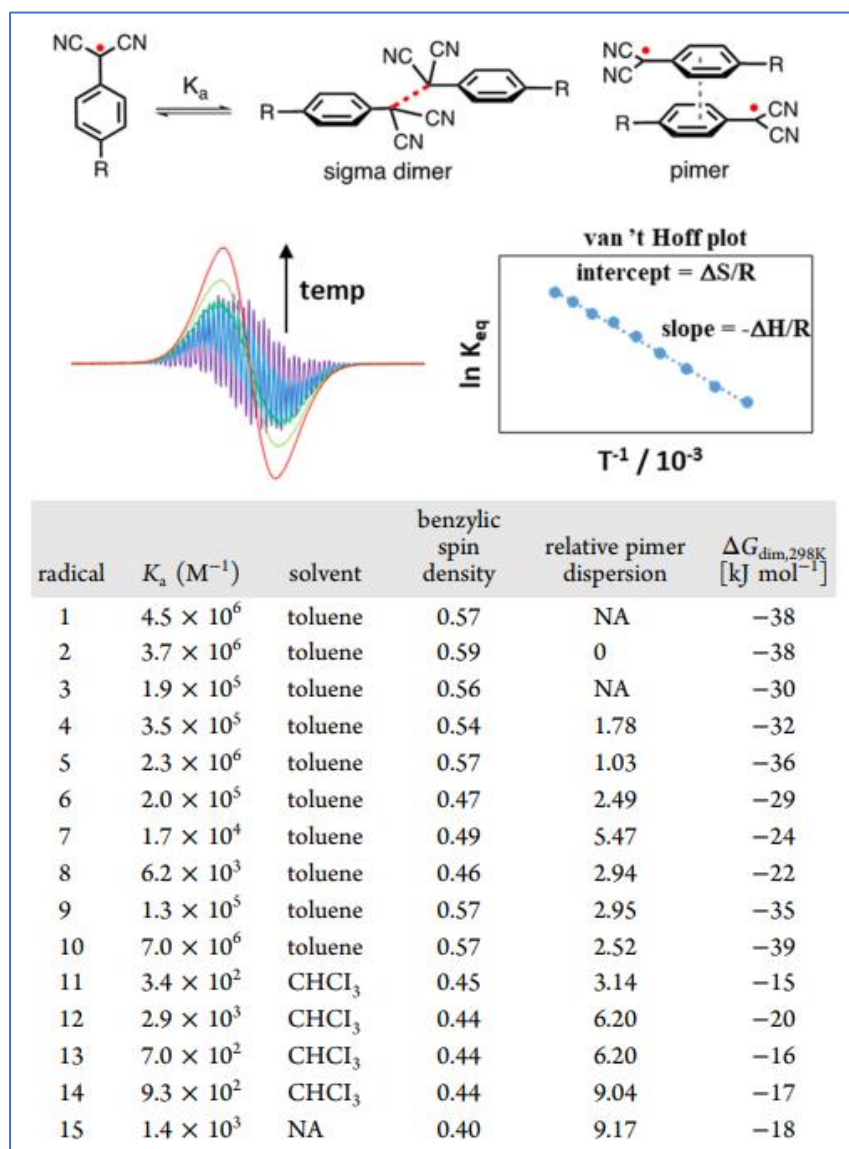
Figure 6-4. Radicals studied here with crystal structures of the radical dimers (crystal structures for 3 and 15 are reproduced from prior work,^{31,32} while crystals of 4, 7, and 9 were crystallized from chloroform and their structures are new to this study). Radicals 1, 3, 6, and 15 were previously reported,^{31,32} while the other 11 radicals are new to this study.

Predictive Power and Failures of the Spin Delocalization Hypothesis. A parameter potentially important for directing the mode of radical dimerization is radical spin delocalization. The hypothesis is that radicals with highly localized spins on the benzylic carbon have a greater likelihood for making a sigma dimer because orbital overlap would be maximized in making the two-atom bond (Figure 6.3, top). However, as the radical becomes more delocalized, the sigma bond should get weaker due to diminished overlap. Eventually, in radicals where the spin density becomes highly delocalized, there may come a tipping point where forming a multi-centered pimer becomes energetically preferred, where the sum of many weaker p-p stacked SOMO orbital interactions (plus other attractive non-covalent forces and entropic effects) exceeds that of forming one more strongly-overlapping two-atom s-dimer. This hypothesis is related to one suggested by Passmore, White, and coworkers⁴⁰ who suggested that there is an energetic penalty for making sigma dimers with highly delocalized radicals, which they used to explain the pimerization of sulfur-containing radicals⁴⁰. Consistent with this notion, the recently prepared more localized phosphorous analogs form sigma dimers.⁴¹

To test this hypothesis, we computed the Mulliken spin densities for each of the radicals in Figure 6.4, and determined whether the radical forms a sigma dimer or a pimer in solution. Fortunately, it is simple to determine whether the radical makes a sigma dimer or a pimer, because cooling solutions of the colored radical leads to the dimerized form, as shown by a loss of the EPR signal for the radical upon cooling. If the radical forms a sigma dimer, the solution turns clear or yellow upon cooling because the sigma dimer disrupts the π conjugation. The sigma dimer has absorptions mostly in the UV region of the optical spectrum. In contrast, if the radical forms a pimer, the solution becomes more darkly colored than the free radical, as the pimers typically have slightly increased absorptions in the visible region of the optical spectrum. Additionally, the pimers

show growth of a new band in the near-IR region of the optical spectrum ~850-900 nm. An example of the difference between a radical forming a sigma dimer and a radical forming a pimer is shown in Figure 6.5. TD-DFT computations of the UV-Vis spectra of the pimers match well with the experimentally determined spectra (see Appendix E).

Table 6-1. Thermodynamic Data Obtained through VT-EPR, and Computed Mulliken Benzyllic Spin Densities (ω B97XD/6-31+G (d,p)) and Estimates of the Relative Pimer Dispersion Energy (Defined As the Sigma Dimer–Pimer Energy Difference Computed at B98 vs B97D, Relative to Radical 2)



In all cases, the mode of dimerization in solution matches the mode of dimerization observed in the crystal structure. Radicals 3, 4, 7, and 9 form sigma dimers in the crystal, and these radicals were found to also form sigma dimers in solution. The most noteworthy features of the solid state structures is that the sigma dimers feature elongated C-C single bonds ($>1.6 \text{ \AA}$) and adopt an anti conformation. In the case where a crystal structure of a pimer was obtained by Seki and coworkers (15),³² this radical also forms a pimer in solution.

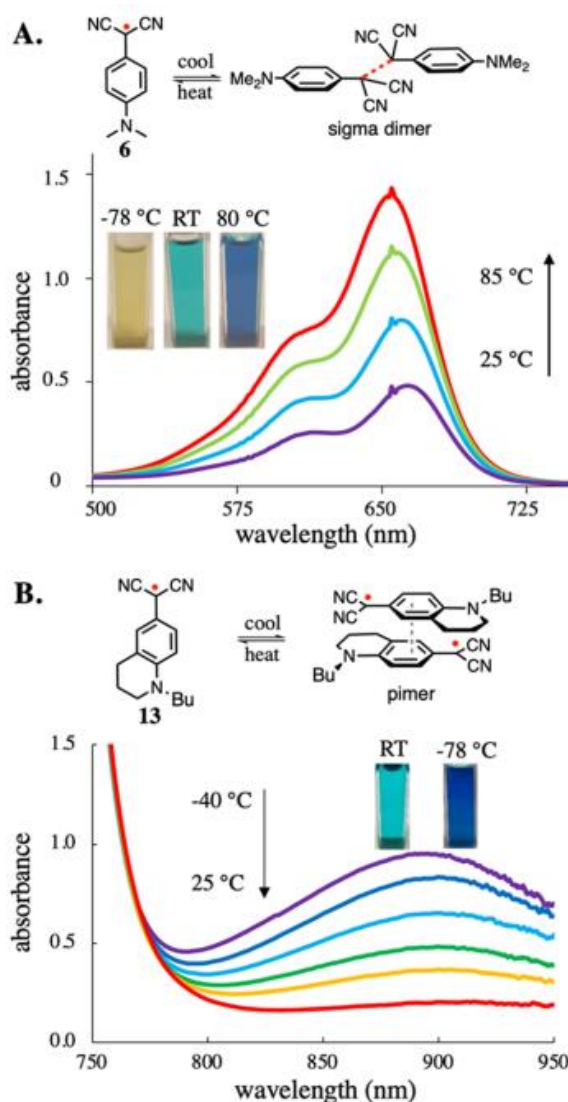


Figure 6-5. UV-vis of 6 showing σ -dimerization (a). Low temperature UV-vis of 13 showing pimerization (b).

To evaluate whether there is a correlation between the spin density and the radical dimerization mode, we plotted the computed benzylic spin density for each of the radicals versus the experimentally determined association constants for radical dimerization (Figure 6.6, top). Radicals that were observed to form sigma dimers when the solutions were cooled are depicted as blue triangles while those that were observed to form pimers are depicted with red circles.

As can be seen from Figure 6.6, there is a strong direct correlation between the K_a and the computed spin density on the benzylic carbon. Thus, radicals with large spin densities on the benzylic carbon form stronger bonds. Furthermore, all the aryl dicyanomethyl radicals in this work with a high spin density on the benzylic carbon (>45%) formed sigma dimers, in line with the spin delocalization hypothesis. Also consistent with the hypothesis, all radicals that formed pimers had <45% computed spin density on the benzylic carbon.

However, a number of radicals with <45% spin density also formed sigma dimers. Thus, while the spin delocalization hypothesis shown in Figure 6.5 explains many of our observations, it cannot, on its own, explain all of the observed radical behavior. Within the regime of radicals having highly delocalized spin densities, it fails to be predictive.

Effect of Pimer Dispersion Stabilization Energy: Incorporation into 2-Parameter Predictive Models. As noted above, the spin delocalization hypothesis fails to be predictive for radicals that feature highly delocalized spins. Thus, we considered that other effects other than spin delocalization may be playing a role in directing the relative energetics of the sigma dimer and pimer. It is known that a variety of pimers such as TCNQ and TCNE radical anions as well as viologen cation radical pimers are stabilized by dispersion forces,^{11,12,18} so we considered that perhaps some radicals stack better in the pimers than others, leading to larger stabilizing dispersion

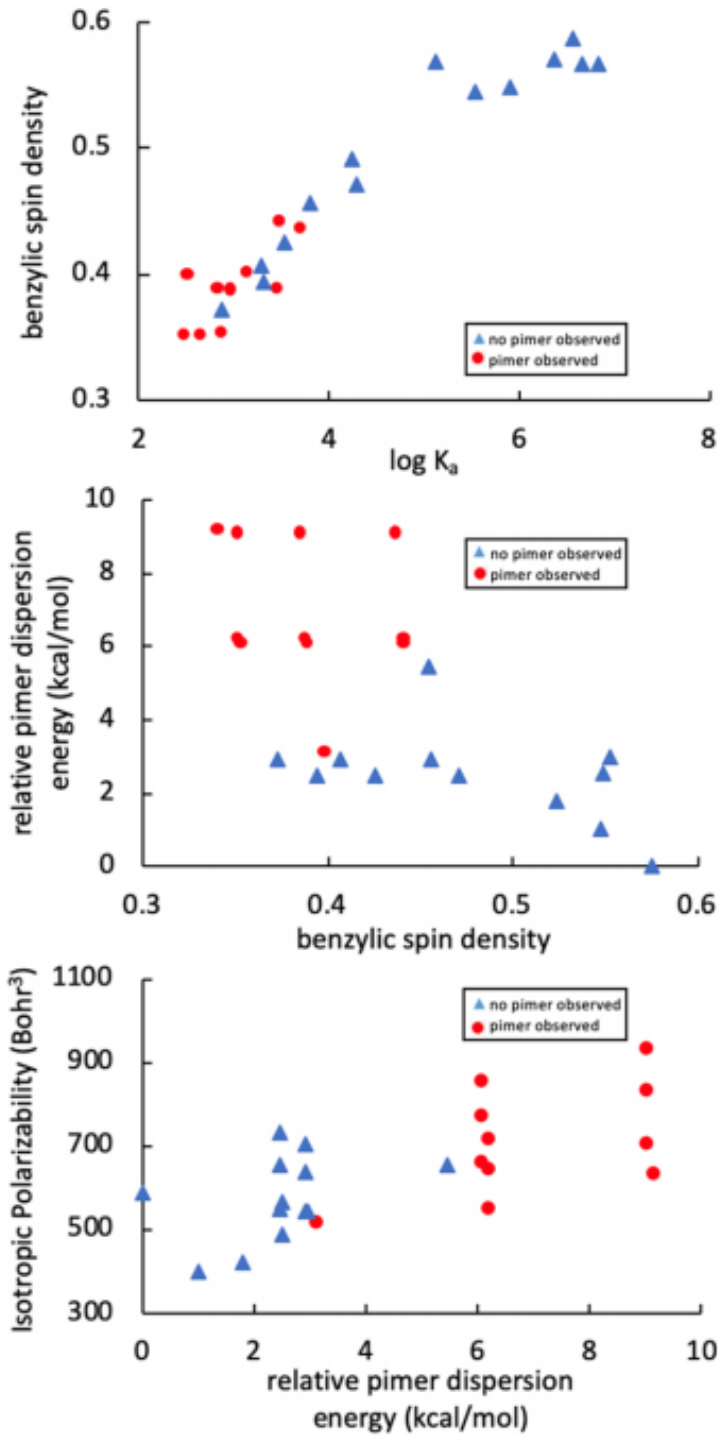


Figure 6-6. Plot of the log of binding constant vs computed benzylic carbon spin density (top) and a plot of benzylic carbon spin density vs normalized dispersion stabilization energy (middle). In both graphs, red circles signify observed π -dimers and blue triangles represent observed σ -dimers. Versions of these plots with radical labels can be found in Appendix E.

energies. We hypothesized that differences in these dispersion forces could explain the differing mode of dimerization for radicals that have similar spin delocalization.

To computationally estimate the dispersion stabilization, we computed the relative energy of the π -dimer and σ -dimer for each radical with two different density functionals, one including a dispersion correction (B97D), and the other without a dispersion correction (B98). The difference in energies gives a “dispersion energy” parameter of the pimer relative to the sigma dimer. These absolute dispersion energies were converted to relative dispersion energies by subtracting the dispersion energy for radical 2, which had the lowest computed pimer dispersion energy value. Thus, radical 2 has a “relative pimer dispersion” of zero.

A single-parameter model using just the relative pimer dispersion energies (shown in Appendix E) to predict the mode of radical dimerization is imperfect because, while in general radicals that form pimers have large computed pimer dispersion energies, it is not always true. For example, radical 11 has a small computed pimer dispersion, but forms a pimer in solution. However, when these relative pimer dispersion energies were plotted against the computed spin density to give the two-parameter model shown in Figure 6.6 (middle), this new two-parameter model is significantly improved compared to the model containing just the spin delocalization parameter (Figure 6.6, top) or just the pimer dispersion energy (Appendix E). All radicals with experimentally observed π -dimers were all computed to have a relative dispersion stabilization energy greater than 6 kcal/mol, with radical 11 being an exception. Radical 11 has a low pimer dispersion energy but compensates by having sufficient spin delocalization to make the pimer preferred. Intuitively, this result makes sense because radical 11 has a smaller substituent and so would not be expected to have as large a pimer dispersion energy. Yet, having the nitrogen locked

into a small ring should make the substituent a very strong donor and lead to larger spin delocalization, favoring the pimer.

Despite some regions of ambiguity at the interface, in general radicals featuring low benzylic spin density and large dispersion energies form pimers, while radicals with high benzylic spin density and low pimer dispersion energies form sigma dimers. This two-parameter model, while imperfect, is clearly an improvement over the model including just the spin density (Figure 6.6, top), which is non-predictive in the regime of radicals having low computed benzylic spin density.

Importance of Radical Polarizability: Effect on Pimer Geometries and Energies. We also considered that the polarizability of the radical could play a role in stabilizing the pimer (hypothesis 2 in Figure 6.3). If the radical is highly polarizable, it should be able to delocalize its electron density in response to a neighboring electric field, such as a polar solvent or another radical, and potentially allow for attractive electrostatic interactions in the pi dimer. Additionally, donor-substituted radical pimers may also be stabilized by $3e^-$ radical stabilization (lone pair with radical³⁹).

To test this hypothesis, we computed the isotropic radical polarizability for each radical, and also examined the computed charge populations of the free radical relative to the pimer. For weakly polarizable radicals, such as 2 shown in Figure 4, relatively small changes in the charge distribution are observed between the free radical and the pimer. With highly polarizable radicals, such as julolidine-derivative 15, large changes in the computed Mulliken atomic charges are observed between the free radical and the pimer. For example, the nitrogen and the two adjacent carbons become more positive by 0.78 charge units, while the dicyanomethyl group becomes more negative by 0.30 charge units upon going from the free radical to the pimer.

Two parameter models including the computed radical isotropic polarizability versus the relative pimer dispersion energy is shown in Figure 6.6 (bottom). This two-parameter model is better than the model containing just the spin delocalization parameter, but radical 11 is a major outlier. As noted above, this radical has a low computed pimer dispersion energy, but is observed to form a pimer. For this radical, the two-parameter model fails.

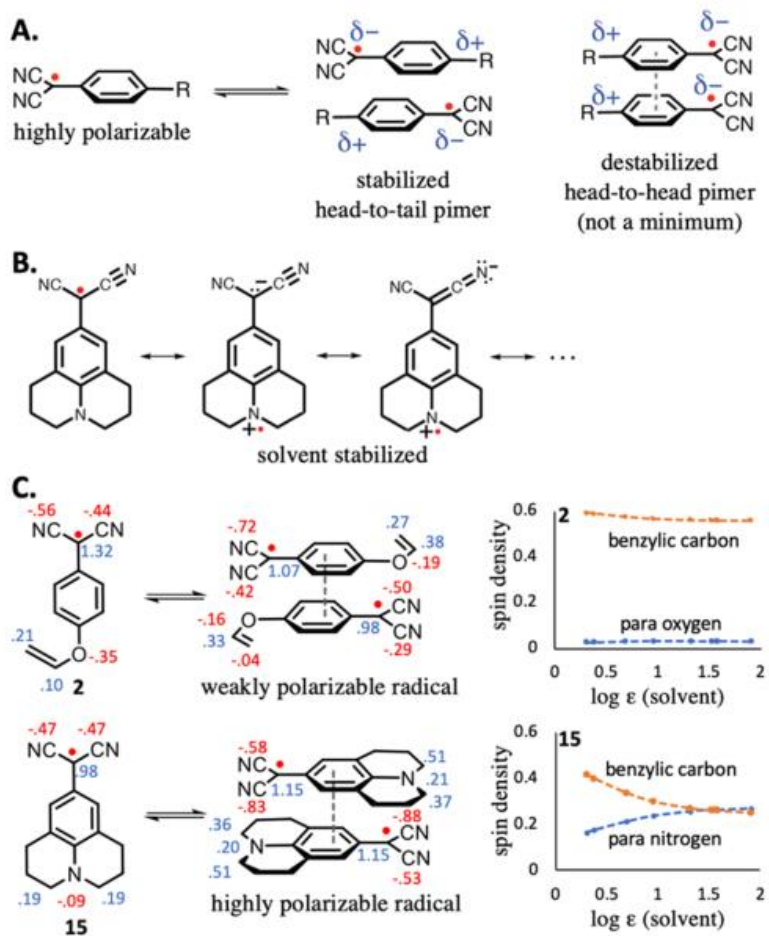


Figure 6-7. (A) Effect of radical polarization on pimer geometry. (B) Resonance model showing stabilization of polarizable captodative radicals by polar solvents (or the presence of another polarizable radical). (C) Mulliken charge distributions of the pimers of a weakly polarizable radical 2 and a highly polarizable radical 15. Insets show the computed Mulliken spin densities for the free radical as a function of solvent dielectric (SMD), with increasing contributions of zwitterionic resonance structures in polar solvents for highly polarizable radicals, which lead to diminished benzylic spin density

While this two-parameter radical polarizability/pimer dispersion model is insufficient in some cases, this polarization effect explains the observed head-to-tail geometry seen in the crystal structure of pimer 15. Our attempts to optimize the geometry of head-to-head pimers failed, as these geometries optimized to the gauche sigma dimer minimum, suggesting that the head-to head pimer may not be even a minimum on the potential energy surface. Intuitively, this result makes sense when considering that a perfect sandwich-stacked pimer would feature repulsive electrostatic interactions, which become favorable in the head to-tail pimer (See Figure 6.7A).

It should be noted that the radical spin delocalization, polarizability, and pimer dispersion energies are not decoupled parameters. Radicals that are highly delocalized off of the benzylic carbon are also highly polarizable. This interconnectedness of these parameters can be clearly observed from a plot of the benzylic spin density versus the computed radical polarizability (See Appendix E) and by the solvent-dependence of the computed spin densities of the radicals. For highly polarizable radicals, the spins become more delocalized off of the benzylic carbon and onto the donating para substituent as the solvent dielectric increases (See Figure 6.7 for an example of the spin density plotted against the solvent dielectric with a highly polarizable and less polarizable radical). With weakly polarizable radicals, the spin densities are more localized and do not change significantly as a function of solvent dielectric. This polarizability can be explained by solvent screening of the charge-separated resonance structures that are unique to captodative radicals (Figure 6.7B). Thus, the spin delocalization parameter “encodes” within it information about the radical polarizability. This feature explains why the two-parameter model containing just the delocalization and dispersion parameters can be successful even though it ignores the effect of radical polarizability, because the polarizability is partially integrated into the spin delocalization parameter.

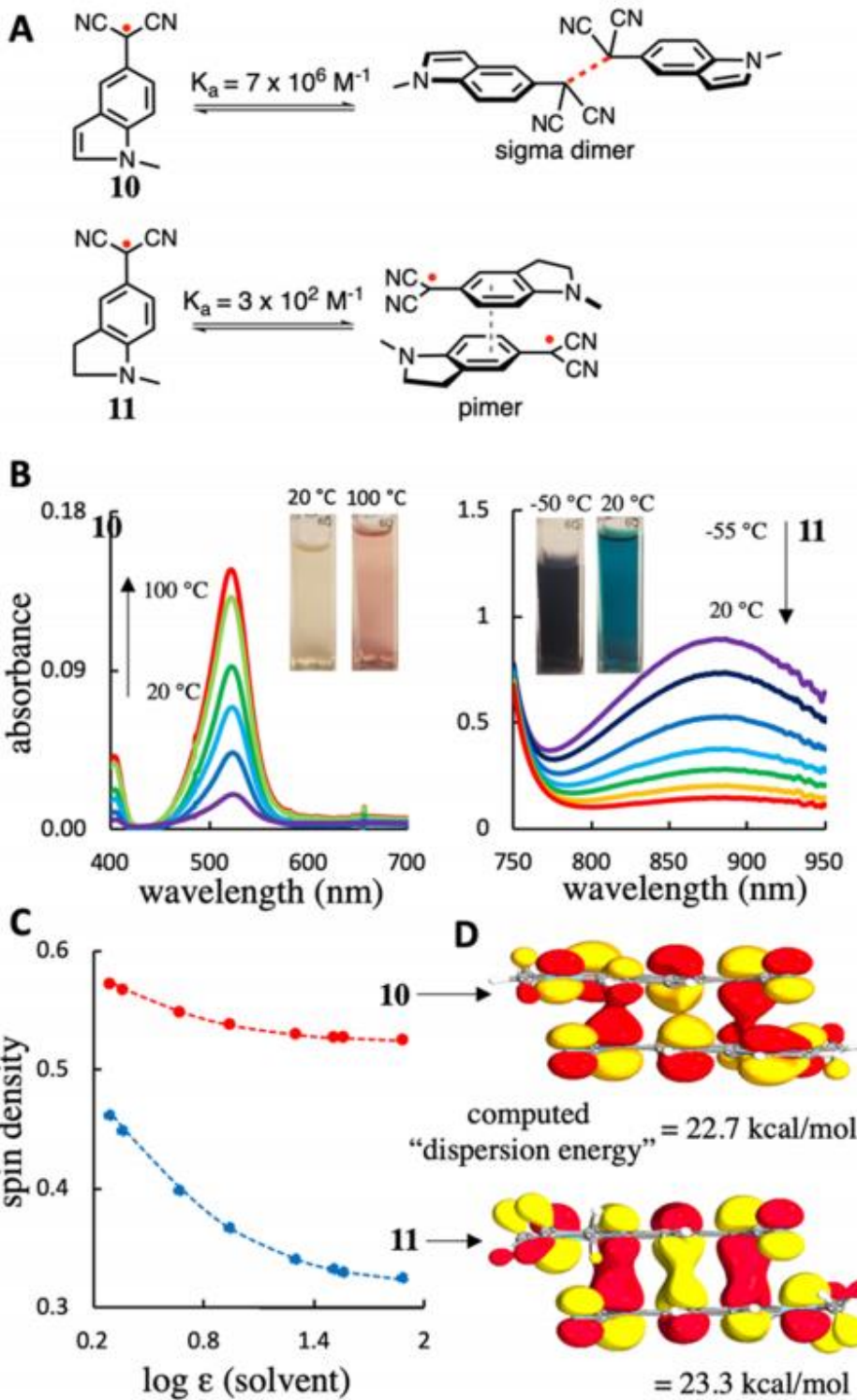


Figure 6-8. Dimerization of compounds 10 and 11 (a), UV-vis spectra of compounds 10 and 11 (b), and benzylic carbon spin density plot and visualized HOMO (IboView)^{42,43} for compounds 10 and 11 (c).

The other parameter, the pimer dispersion energy, should also be dependent on both the geometry of the pimer and the polarizability of the two interacting species, with more highly polarizable species leading to higher dispersion energies. Yet, in a practical sense the computed dispersion energy does not really account for the polarizability of the radical itself. This is because the dispersion corrections included in this B97D functional are akin to a patched-on summation of all the attractive pairwise $1/r^6$ terms in a Lennard-Jones potential added to the DFT energy, with an atom-dependent parameterized coefficient and a damping function to prevent singularities at small r values.⁴⁶ This coefficient includes the static dipolar polarizability of the atom, but it is ignorant of the electronic polarizability of the atom in the radical itself. The coefficient will be poorly chosen if the polarizability of the atom in the molecular environment is much different than for the isolated atom, from which the coefficients were obtained. It would not be surprising if atoms in molecular free radicals had different polarizabilities than those for the isolated atoms, as free radicals are expected to be more polarizable than closed-shell species as a general rule. Thus, the dispersion estimates obtained from our DFT model are in reality more decoupled from the polarizability for the predictive model than they would be if more accurate dispersion energies were available.

However, none of our models are successful without including this term, which is the only parameter that has a dependence on the geometry of the pimer. The polarizability and spin delocalization terms are obtained from computations of the isolated free radicals. Thus, as improvements are made to DFT dispersion corrections to take into account the specifics of the molecular electronic environment, which could be as simple as adjusting the atom-dependent parameterized coefficients, it may be the case that models incorporating the computed dispersion energy will also improve.

Spin Delocalization Effects: What a Difference a Double Bond Makes! From the 2-parameter models shown in Figure 6.6, the pimer dispersion energy appears to be an important parameter in dictating the preferred mode of radical dimerization. We asked the question of whether spin delocalization or dispersion effects were more important in determining the preferred dimerization mode. To answer this question, radicals 10 and 11 were evaluated (Figure 6.8). These radicals are identical except 10 has an extra double bond. Not surprisingly, then, the computed dispersion energies for the pimers are essentially identical (within 0.6 kcal/mol). Yet, because the indole radical 10 has its lone pair tied into an aromatic ring, it is a much weaker donor than 11. For example, the computed benzylic carbon spin densities (see Figure 6.8C) for 10 range from 57-52 % (indicating it is weakly polarizable) while 11 spans the range of 46-32 % (indicating it is highly polarizable), depending on the solvent polarity. We anticipated that if dispersion forces directed pimer formation, then both 10 and 11 might form pimers. If spin delocalization was a more important parameter, than 11 might form a pimer, while 10 would not.

The latter outcome proves to be the case. We observe that 10 forms a sigma dimer while 11 forms a pimer (See Figure 6.8). Indeed, 10 has the largest association constant of all the radicals we tested ($\sim 7 \times 10^6 \text{ M}^{-1}$) while 11 has the smallest value ($3 \times 10^2 \text{ M}^{-1}$) of all radicals tested—a factor of greater than four orders of magnitude difference in radical stability! UV-Vis spectroscopy (Figure 6.8B) shows that 10 exists mostly as σ -dimer at room temperature and upon heating liberates the free radical with a $\lambda_{\text{max}} = 525 \text{ nm}$ ($K_d \sim 1 \times 10^{-7} \text{ M}$). Conversely, 11 exists as a significant portion of radical at room temperature evidenced by large radical band between 600-700 nm ($K_d \sim 3 \times 10^{-3} \text{ M}$). When cooled, radical 11 shows a pimer band grow in $\sim 880 \text{ nm}$ (Figure 8B) and shows no decrease in the visible region absorption. Visually, the two radicals have ‘radically’ different behavior, with 10 appearing slightly yellow at room temperature (mostly

sigma dimer) and becoming pink as the free radical is liberated at high temperature. In contrast, 11 is blue at room temperature as a result of a large thermal population of free radical and becomes a darker blue upon cooling as the pimer forms. Given that the pimer dispersion energy is computed to be essentially identical for these radicals, but these radicals have drastically different spin delocalization/polarization, we conclude that dispersion effects in the pimer cannot be exclusively the driving force for pimerization, and are perhaps subordinate to the electronic substituent effects that lead to spin delocalization/polarization.

6.4 Computational and Experimental Methods

Computational Methods. To compute spin density and polarizabilities for each radical, geometries were optimized at the ω B97XD44/6-31+G(d,p) level of theory using Gaussian16⁴⁵ using the SMD solvation model. Previous work had determined this functional and basis set accurate for obtaining the free radical/s dimer equilibrium thermodynamic values for dicyanomethyl radicals.³⁷ Mulliken spin densities were used to determine how the spin density varied with solvent for different radicals. For the computation of the π -dimer dispersion stabilization energy, all radicals were optimized at both their σ -dimer and π -dimer geometries at the ω B97XD/6-31+G(d,p) level of theory and then a single-point energy computation was conducted using both B97D⁴⁶/6-31+G(d,p) and B98⁴⁷/6-31+G(d,p) for the π -dimer and σ -dimer. The difference in the s-dimer/pimer equilibrium DE values between the two functionals were given relative to radical 2 to give the “relative pimer dispersion energy” parameter. Radical 2 had the lowest computed pimer dispersion energy so it was defined as zero. It should be noted that the pimers are unstable with respect to an RHF-UHF perturbation. Thus, we also optimized the pimers using a broken-symmetry unrestricted singlet approach to allow for singlet diradical character and calculated the “dispersion energies” at those new geometries. An alternative plot for Figure 6.6 (pimer dispersion energy vs. spin density) is shown in Appendix E with the dispersion energies

calculated at these new geometries. Although some differences are observed, they are qualitatively similar.

Oxidation to Generate Radicals. The C-H aryl malononitrile precursors were oxidized to form the radical/dimers using previously reported methods.^{31, 33} For radicals 1-5 and 9-10, a biphasic oxidation between basic aqueous potassium ferricyanate and dichloromethane was used. For all other radicals, 6-8 and 11-14, the aryl malononitrile was dissolved in the solvent of study, then lead(IV) oxide was added in excess and the resulting mixture was mixed for 5-10 minutes. After removal of all excess solids by centrifugation, quantitative oxidation to radicals was indicated by absence of starting material peaks in the ¹H NMR spectrum.

Association constants and van't Hoff Plots. The dimerization thermodynamic parameters for each of the radicals was determined by variable temperature EPR. From the double integration of each EPR spectra, equilibrium constants were obtained. Intermolecular binding constants were calculated from a van't Hoff plot. An example is shown in Table 1 and all plots are included in the Supporting Information. The EPR instrument was calibrated with a TEMPO standard. A van't Hoff plot ($\ln K_{eq}$ vs $1/T$) provides the equilibrium parameters (ΔH° and ΔS° , which lead to ΔG° and K_a values) for each system. It is important to note that EPR spectroscopy is blind to the nature of spin-paired species (sigma dimer or pimer) so the K_a value is really measuring the equilibrium between EPR-inactive diamagnetic dimers and spin-unpaired free radicals (or possibly thermally populated triplet excited states of the pimers, at high temperatures).

Determining Mode of Radical Dimerization and Low Temperature UV-Vis Measurements. In general, the mode of dimerization for each radical was determined by change in color of the solutions. For sigma dimers, the solution turns clear or yellow upon cooling in a dry ice/acetone bath, while for pimers the solutions turn darker blue. These results were also

observable using a UV-Vis spectrometer with low-temperature capability. All UV-Vis experiments started with a known concentration of radical prepared by oxidation of the malononitrile derivative. A UV-Vis spectrometer with liquid nitrogen cooling capabilities was used under inert atmosphere to avoid water vapor condensation. A temperature curve calibration was used to determine accurate temperature measurements at various data points. Sampling intervals were performed at 0.2 nm increments and equilibration of temperature was allowed for 5 minutes prior to each spectrum being acquired. Because both the sigma dimer and pimer are in equilibrium, observation of a pimer does not rule out the possibility of a low-energy or near degenerate sigma dimer that may also be present in the equilibrium at higher temperatures. In some cases, pimers were observed at higher concentrations but not low concentrations, suggesting in these cases that, while the sigma dimer is likely the lower energy form, the pimer is close enough in energy to be thermally populated, which can be observed at higher concentrations, and suggesting these dimeric forms are nearly degenerate. We listed these in the graphs as “pimer observed”, although the near-degeneracy of the two dimers is likely, and the sigma dimer form may even be the lower energy form.

EPR Measurements and Parameters. After oxidation of each radical precursor to generate the radical, solutions of each radical were purged and placed under an inert atmosphere to remove oxygen. Solutions of toluene allowed the use of a 3 mm quartz EPR tube. When performing variable temperature EPR analysis, solutions were allowed to equilibrate at each temperature for 5 minutes before each scan. Every data point is an average of a minimum of 8 scans, with more scans used in cases where small radical signals were observed. The following instrument parameters were utilized for all compounds at all temperatures: modulation frequency, 100 kHz; receiver gain, 50 dB; modulation amplitude, 0.5 G; time constant, 0.01 s; center field,

3335 G; sweep width, 150 G; microwave attenuation, 20 dB; microwave power, 2 mW; number of data points, 2048.

6.5 Conclusions

In conclusion, we have demonstrated that the mode of dimerization of dicyanomethyl radicals can be reasonably predicted by two parameter models using computational predictions of spin density delocalization or the radical polarizability and computational estimates of the π -dimer dispersion stabilization energy. The importance of polarization can be seen by the change in the charge densities upon pimerization, and the preferred geometry of the pimer as a head-to-tail dimer, while the head-to-head pimer is not even a minimum on the potential energy surface. Care was taken to isolate electronic effects by choosing neutral radicals that are planar and not sterically hindered at the radical center. This can be viewed as both a strength and a weakness of this study. The strength is that electronic effects can be more clearly elucidated. A weakness of this study, then, is that steric effects or charge repulsion effects that could be important for radicals that are not planar, have bulky groups attached, or are charged, are not considered here. For example, a radical that forms a sigma dimer might prefer to form a pimer if bulky substituents are attached adjacent to the radical center (see Figure 1 for an example of this with the phenalenyl radical). We find that for radicals with greater than 45% spin density on the benzylic dicyanomethyl carbon, only σ -dimerization is observed. Such highly localized spins correlates to radical/dimer binding constants of 10^5 M^{-1} or greater. In contrast, with more delocalized radicals (<45 % spin density on the benzylic carbon), either sigma dimerization or pimerization can occur, with radicals with strong pimer dispersion energies forming pimers while those with weak dispersion interactions forming sigma dimers. While we have yet to identify a computational method that can accurately predict the radical—sigma dimer— pimer thermodynamics for these radicals, simple models that can explain and predict the interactions of such radicals, such as the ones developed in this paper, may

prove to be useful for explaining and predicting the properties of new radicals. Importantly, this work suggests that both radical delocalization, polarization, and dispersion forces are important in dictating the mode of dimerization for meta-stable radicals, and provides a theoretical framework for explaining the behavior of known radicals and predicting the behavior of novel radicals.

At present, some humility in our ability to conceptually understand the features that lead to small changes in relative energy is needed. For a few of the radicals in our library, at low concentrations of the radical we observe visually the sigma dimer at low temperature, as indicated by the colored solutions of radical turning clear or yellow as the temperature is lowered. Yet, at much higher concentrations, the solutions turn darker blue upon cooling, the hallmark indicator for formation of the pimer. This observation suggests that, for these radicals, the sigma dimer and pimer forms are nearly degenerate. Most likely, at low temperatures there is still a thermal population of the higher-energy pimer form that can only be observed visually at high concentrations. In this regime, where the two radical dimeric forms may be separated by less than 1 kcal/mol in free energy, the subtle features that lead to a small change in the relative stability of the sigma dimer/pimer may not be perfectly captured by relatively crude indices such as “polarizability,” “spin delocalization,” and “dispersion,” that relate mostly to enthalpy and ignore entropy.

Furthermore, models can be useful and predictive without being built on any bedrock truth. Therefore, the imperfect but somewhat surprising success of the two-parameter models described here does not necessarily mean that the parameters themselves are important directing features. They may be merely indicators. Nevertheless, it is tempting to interpret the clear correlation and predictive power of the computed spin density on the benzylic carbon with the experimentally-determined K_a values (Figure 6.6, top) as demonstrating the importance of spin (de)localization on

the stability of the free radical relative to either dimeric form. Less clear are the importance of polarizability and dispersion forces, although none of our models are successful without including pimer dispersion estimates, and the polarizability hypothesis explains nicely why the pimer adopts the head-to-tail structure, and why the head to-head pimer does not appear to be a local minimum. Subject to the usual caveats about models and reality, it is reasonable to suggest that (at least) these three effects are important in governing the formation of diradical pimers.

6.6 References

- (1) Gomberg, M., An Instance of Trivalent Carbon: Triphenylmethyl. *J. Am. Chem. Soc.* 1900, 22 (11), 757-771.
- (2) Grossel, M. C.; Weston, S. C., Synthesis of materials for molecular electronic applications. *Contemp. Org. Synth.* 1994, 1 (5), 367-386.
- (3) Hughes, B. K.; Braunecker, W. A.; Bobela, D. C.; Nanayakkara, S. U.; Reid, O. G.; Johnson, J. C., Covalently Bound Nitroxyl Radicals in an Organic Framework. *J. Phys. Chem. Lett.* 2016, 7 (18), 3660-5.
- (4) Li, L. H.; Feng, X. L.; Cui, X. H.; Ma, Y. X.; Ding, S. Y.; Wang, W., Salen-Based Covalent Organic Framework. *J. Am. Chem. Soc.* 2017, 139 (17), 6042-6045.
- (5) Juetten, M. J.; Buck, A. T.; Winter, A. H., A radical spin on viologen polymers: organic spin crossover materials in water. *Chem Commun. (Camb)* 2015, 51 (25), 5516-9.
- (6) Rajca, A., Organic Diradicals and Polyradicals: From Spin Coupling to Magnetism? *Chem. Rev.* 1994, 94 (4), 871-893.
- (7) Rowan, S. J.; Cantrill, S. J.; Cousins, G. R. L.; Sanders, J. K. M.; Stoddart, J. F., Dynamic Covalent Chemistry. *Angew. Chem., Int. Ed.* 2002, 41 (6), 898-952.
- (8) Jin, Y.; Yu, C.; Denman, R. J.; Zhang, W., Recent advances in dynamic covalent chemistry. *Chem. Soc. Rev.* 2013, 42 (16), 6634-6654.
- (9) Morita, Y.; Suzuki, S.; Sato, K.; Takui, T., Synthetic organic spin chemistry for structurally well defined open-shell graphene fragments. *Nat. Chem.* 2011, 3 (3), 197-204.

- (10) Rajca, A.; Wang, Y.; Boska, M.; Paletta, J. T.; Olankitwanit, A.; Swanson, M. A.; Mitchell, D. G.; Eaton, S. S.; Eaton, G. R.; Rajca, S., Organic Radical Contrast Agents for Magnetic Resonance Imaging. *J. Am. Chem. Soc.* 2012, 134 (38), 15724-15727.
- (11) Kobayashi, H.; Danno, T.; Saito, Y., The Crystal structure of bis(trimethylammonium) tris(7,7,8,8- tetracyanoquinodimethanide), (TMA⁺)₂ (TCNQ)₃ 2-. *Acta Crystallogr. Sect. B: Struct. Crystallogr. Cryst. Chem.* 1973, 29 (12), 2693-2699.
- (12) Penneau, J. F.; Stallman, B. J.; Kasai, P. H.; Miller, L. L., An imide anion radical that dimerizes and assembles into .pi.-stacks in solution. *Chem. Mater.* 1991, 3 (5), 791-796.
- (13) Rösel, S.; Becker, J.; Allen, W. D.; Schreiner, P. R., Probing the Delicate Balance between Pauli Repulsion and London Dispersion with Triphenylmethyl Derivatives. *J. Am. Chem. Soc.* 2018, 140 (43), 14421-14432.
- (14) Rösel, S.; Balestrieri, C.; Schreiner, P. R., Sizing the role of London dispersion in the dissociation of allmeta tert-butyl hexaphenylethane. *Chemical Science* 2017, 8 (1), 405-410.
- (15) Lekin, K.; Phan, H.; Winter, S. M.; Wong, J. W. L.; Leitch, A. A.; Laniel, D.; Yong, W.; Secco, R. A.; Tse, J. S.; Desgreniers, S.; Dube, P. A.; Shatruk, M.; Oakley, R. T., Heat, Pressure and Light-Induced Interconversion of Bisdithiazolyl Radicals and Dimers. *J. Am. Chem. Soc.* 2014, 136 (22), 8050-8062.
- (16) Yokoi, H.; Hiroto, S.; Shinokubo, H., Reversible σ-Bond Formation in Bowl-Shaped π-Radical Cations: The Effects of Curved and Planar Structures. *J. Am. Chem. Soc.* 2018, 140 (13), 4649-4655.
- (17) Dragulescu-Andrasi, A.; Filatov, A. S.; Oakley, R. T.; Li, X.; Lekin, K.; Huq, A.; Pak, C.; Greer, S. M.; McKay, J.; Jo, M.; Lengyel, J.; Hung, I.; Maradzike, E.; DePrince, A. E.; Stoian, S. A.; Hill, S.; Hu, Y.-Y.; Shatruk, M., Radical Dimerization in a Plastic Organic Crystal Leads to Structural and Magnetic Bistability with Wide Thermal Hysteresis. *J. Am. Chem. Soc.* 2019.
- (18) Geraskina, M. R.; Dutton, A. S.; Juetten, M. J.; Wood, S. A.; Winter, A. H., The Viologen Cation Radical Pimer: A Case of Dispersion-Driven Bonding. *Angew. Chem., Int. Ed.* 2017, 56 (32), 9435-9439.
- (19) Constantinides, C. P.; Carter, E.; Eisler, D.; Beldjoudi, Y.; Murphy, D. M.; Rawson, J. M., Effects of Halo-Substitution on 2'-Chloro-5'-halo-phenyl-1,2,3,5-dithiadiazolyl Radicals: A Crystallographic, Magnetic, and Electron Paramagnetic Resonance Case Study. *Cryst. Growth Des.* 2017, 17 (6), 3017-3029.

- (20) Mou, Z.; Kertesz, M., Sigma- versus Pi Dimerization Modes of Triangulene. *Chem – Eur. J.* 2018, 24 (23), 6140-6147.
- (21) Kertesz, M., Pancake Bonding: An Unusual PiStacking Interaction. *Chem –Eur. J.* 2019, 25 (2), 400-416.
- (22) Pal, S. K.; Itkis, M. E.; Tham, F. S.; Reed, R. W.; Oakley, R. T.; Haddon, R. C., Resonating Valence-Bond Ground State in a Phenalenyl-Based Neutral Radical Conductor. *Science* 2005, 309 (5732), 281.
- (23) Fujita, W.; Awaga, a. K., Room-Temperature Magnetic Bistability in Organic Radical Crystals. *Science* 1999, 286 (5438), 261.
- (24) Mou, Z.; Kubo, T.; Kertesz, M., Hetero- π -Dimers of Phenalenyls. *Chem. - Eur. J.* 2015, 21 (50), 18230- 18236.
- (25) Mou, Z.; Uchida, K.; Kubo, T.; Kertesz, M., Evidence of σ - and π -Dimerization in a Series of Phenalenyls. *J. Am. Chem. Soc.* 2014, 136 (52), 18009-18022.
- (26) Uchida, K.; Mou, Z.; Kertesz, M.; Kubo, T., Fluxional σ -Bonds of the 2,5,8-Trimethylphenalenyl Dimer: Direct Observation of the Sixfold σ -Bond Shift via a π -Dimer. *J. Am. Chem. Soc.* 2016, 138 (13), 4665-4672.
- (27) Kosower, E. M.; Poziomek, E. J., Stable Free Radicals. I. Isolation and Distillation of 1-Ethyl-4- carbomethoxypyridinyl. *J. Am. Chem. Soc.* 1964, 86 (24), 5515-5523.
- (28) Itkis, M. E.; Chi, X.; Cordes, A. W.; Haddon, R. C., Magneto-Opto-Electronic Bistability in a PhenalenylBased Neutral Radical. *Science* 2002, 296 (5572), 1443.
- (29) Koivisto, B. D.; Ichimura, A. S.; McDonald, R.; Lemaire, M. T.; Thompson, L. K.; Hicks, R. G., Intramolecular π -Dimerization in a 1,1'- Bis(verdazyl)ferrocene Diradical. *J. Am. Chem. Soc.* 2006, 128 (3), 690-691.
- (30) Melen, R. L.; Less, R. J.; Pask, C. M.; Rawson, J. M., Structural Studies of Perfluoroaryldiselenadiazolyl Radicals: Insights into Dithiadiazolyl Chemistry. *Inorg. Chem.* 2016, 55 (22), 11747-11759.
- (31) Peterson, J. P.; Geraskina, M. R.; Zhang, R.; Winter, A. H., Effect of Substituents on the Bond Strength of Air-Stable Dicyanomethyl Radical Thermochromes. *J. Org. Chem.* 2017, 82 (12), 6497-6501.
- (32) Okino, K.; Hira, S.; Inoue, Y.; Sakamaki, D.; Seki, S., The Divergent Dimerization Behavior of N-Substituted Dicyanomethyl Radicals: Dynamically Stabilized versus Stable Radicals. *Angew. Chem.* 2017, 129 (52), 16824-16828.

- (33) Kobashi, T.; Sakamaki, D.; Seki, S., N-Substituted Dicyanomethylphenyl Radicals: Dynamic Covalent Properties and Formation of Stimuli-Responsive Cyclophanes by Self-Assembly. *Angew. Chem. Int. Ed.* 2016, 55 (30), 8634-8638.
- (34) Okino, K.; Sakamaki, D.; Seki, S., Dicyanomethyl Radical-Based Near-Infrared Thermochromic Dyes with High Transparency in the Visible Region. *ACS Materials Letters* 2019, 25-29.
- (35) Peterson, J. P.; Zhang, R.; Winter, A. H., Effect of Structure on the Spin Switching and Magnetic Bistability of Solid-State Aryl Dicyanomethyl Monoradicals and Diradicals. *ACS Omega* 2019.
- (36) Peterson, J. P.; Winter, A. H., Solvent Effects on the Stability and Delocalization of Aryl Dicyanomethyl Radicals: The Captodative Effect Revisited. *J. Am. Chem. Soc.* 2019.
- (37) Zhang, R.; Peterson, J. P.; Fischer, L. J.; Ellern, A.; Winter, A. H., Effect of Structure on the Spin-Spin Interactions of Tethered Dicyanomethyl Diradicals. *J. Am. Chem. Soc.* 2018.
- (38) Alabugin, I. V., *Stereoelectronic Effects: A Bridge Between Structure and Reactivity*. Wiley: 2016.
- (39) Syroeshkin, M. A.; Kuriakose, F.; Saverina, E. A.; Timofeeva, V. A.; Egorov, M. P.; Alabugin, I. V., Upconversion of Reductants. *Angew. Chem., Int. Ed.* 2019, 58 (17), 5532-5550.
- (40) Awere, E. G.; Burford, N.; Haddon, R. C.; Parsons, S.; Passmore, J.; Waszczak, J. V.; White, P. S., Xray crystal structures of the 1,3,2-benzodithiazolyl dimer and 1,3,2-benzodithiazolium chloride sulfur dioxide solvate: comparison of the molecular and electronic structures of the 10-.pi.-electron C₆H₄S₂N⁺ cation and the C₆H₄S₂N.bul. radical and dimer and a study of the variable -temperature magnetic behavior of the radical. *Inorg. Chem.* 1990, 29 (23), 4821 -4830.
- (41) Ould, D. M. C.; Tran, T. T. P.; Rawson, J. M.; Melen, R. L., Structure –property - reactivity studies on dithiaphospholes. *Dalton Transactions* 2019, 48 (45), 16922 - 16935.
- (42) Knizia, G., Intrinsic Atomic Orbitals: An Unbiased Bridge between Quantum Theory and Chemical Concepts. *J. Chem. Theory Comput.* 2013, 9 (11), 4834 - 4843.

- (43) Knizia, G.; Klein, J. E. M. N., Electron Flow in Reaction Mechanisms — Revealed from First Principles. *Angew. Chem., Int. Ed.* 2015, 54 (18), 5518 - 5522.
- (44) Chai, J. -D.; Head -Gordon, M., Long -range corrected hybrid density functionals with damped atom– atom dispersion corrections. *Phys. Chem. Chem. Phys.* 2008, 10 (44), 6615 -6620.
- (45) Frisch, M. J.; Trucks, G. W.; Schlegel, H. B.; Scuseria, G. E.; Robb, M. A.; Cheeseman, J. R.; Scalmani, G.; Barone, V.; Petersson, G. A.; Nakatsuji, H.; Li, X.; Caricato, M.; Marenich, A. V.; Bloino, J.; Janesko, B. G.; Gomperts, R.; Mennucci, B.; Hratchian, H. P.; Ortiz, J. V.; Izmaylov, A. F.; Sonnenberg, J. L.; Williams; Ding, F.; Lipparini, F.; Egidi, F.; Goings, J.; Peng, B.; Petrone, A.; Henderson, T.; Ranasinghe, D.; Zakrzewski, V. G.; Gao, J.; Rega, N.; Zheng, G.; Liang, W.; Hada, M.; Ehara, M.; Toyota, K.; Fukuda, R.; Hasegawa, J.; Ishida, M.; Nakajima, T.; Honda, Y.; Kitao, O.; Nakai, H.; Vreven, T.; Throssell, K.; Montgomery Jr, J. A.; Peralta, J. E.; Ogliaro, F.; Bearpark, M. J.; Heyd, J. J.; Brothers, E. N.; Kudin, K. N.; Staroverov, V. N.; Keith, T. A.; Kobayashi, R.; Normand, J.; Raghavachari, K.; Rendell, A. P.; Burant, J. C.; Iyengar, S. S.; Tomasi, J.; Cossi, M.; Millam, J. M.; Klene, M.; Adamo, C.; Cammi, R.; Ochterski, J. W.; Martin, R. L.; Morokuma, K.; Farkas, O.; Foresman, J. B.; Fox, D. J. *Gaussian 16 Rev. C.01*, Wallingford, CT % ! *Gaussian 16*, 2016.
- (46) Grimme, S., Semiempirical GGA -type density functional constructed with a long -range dispersion correction. *J. Comput. Chem.* 2006, 27 (15), 1787 -1799.
- (47) Schmider, H. L.; Becke, A. D., Optimized density functionals from the extended G2 test set. *J. Chem. Phys.* 1998, 108 (23), 9624 -9631.

CHAPTER 7. GENERAL CONCLUSION

The work in this dissertation focuses on the synthetic, spectroscopic, and computational investigation into the stimuli responsive behavior of aryl dicyanomethyl radicals. Dicyanomethyl radicals are a bridge for applying the stimuli responsiveness of spin-unpaired electrons to the stability of a spin-paired dimeric form. The project began with a substituent effect study in the *para* position of an aryl dicyanomethylene unit. Electronic donating substituents resulted in a weaker association of the dimer and withdrawing substituents led to a tighter binding and larger association constant. By plotting the Hammett parameter to experimentally derived association constants, we were able to show stabilization of dicyanomethyl radicals with electronic donating substituents in the *para* position.

After concluding that good electron donation into the aryl ring lowered the binding constant, a set of tethered diradicals were synthesized with either methoxy or dimethylamino substitution in the *para* position to probe the intramolecular dimerization tendencies of diradicals. By altering the length of an alkyl linker between the aryl radical units, an even/odd effect was found that switched when the radicals were tethered in the *para* or *ortho* position. *Ortho* tethered diradicals consistently favored the radical more than the *para* tethered counterpart, likely attributable to a steric effect. Dimethylamino tethered diradicals had the weakest associations of all compounds investigated and a julolidine tethered diradical was found to form a pimer conformation at lower temperatures.

A computational investigation into the effect of solvent on dicyanomethyl radicals was performed. By plotting the computed benzylic spin density of dicyanomethyl radicals against the dielectric constants of solvents, a trend was observed for strong electronically donating radicals. As the solvent polarity increases for strong donating radicals, the spin density of the system

switches from being primarily localized on the benzylic carbon to delocalization of spin density into the aryl ring. With this information, coupled with experimental data, it is now possible to predict an association constant for a novel dicyanomethyl radical prior to synthesis and experimental testing. Also, by implementing the computational methods of this work, other radical systems show a solvent effect when a captodative model is considered, contrary to previous failed methods.

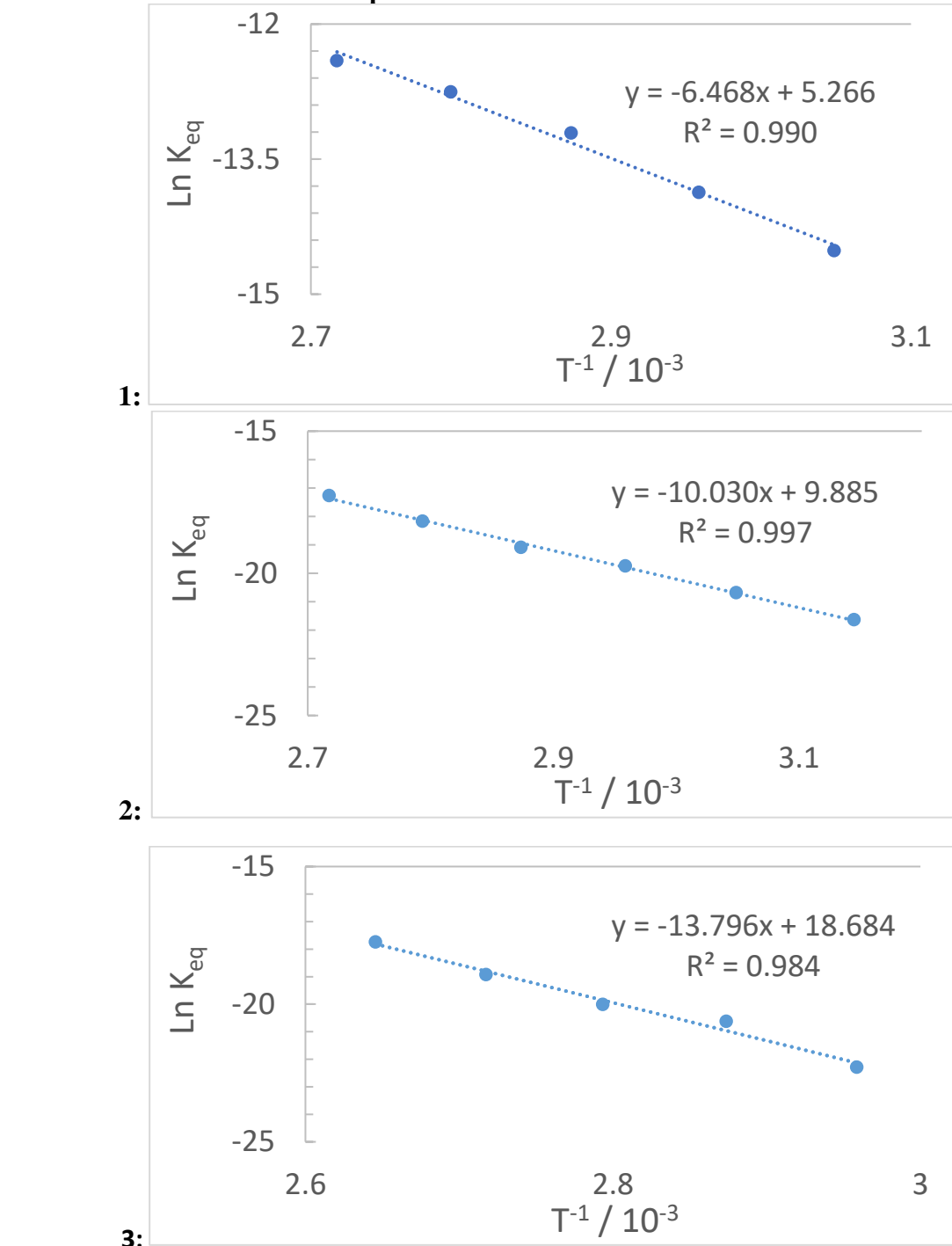
Dicyanomethyl radicals and diradicals also show thermal stimuli responsive character in the solid state. Upon heating of a crystalline or amorphous sample, thermal homolysis of the radical-radical sigma bonds occurs and color changes can be observed. When comparing crystalline and amorphous samples, amorphous powders show a regular homolysis and recombination when heated. Crystalline samples; however, show a kinetic effect. Crystalline samples of dicyanomethyl radicals show a slow increase in radical concentration when heated and the radical concentration slowly continues to increase over extended times at elevated temperatures. Magnetic bistability was observed for some of the tethered diradicals when investigated. These compounds showed elevated radical concentrations after thermal experiments that remained stable for long periods of time after experiment.

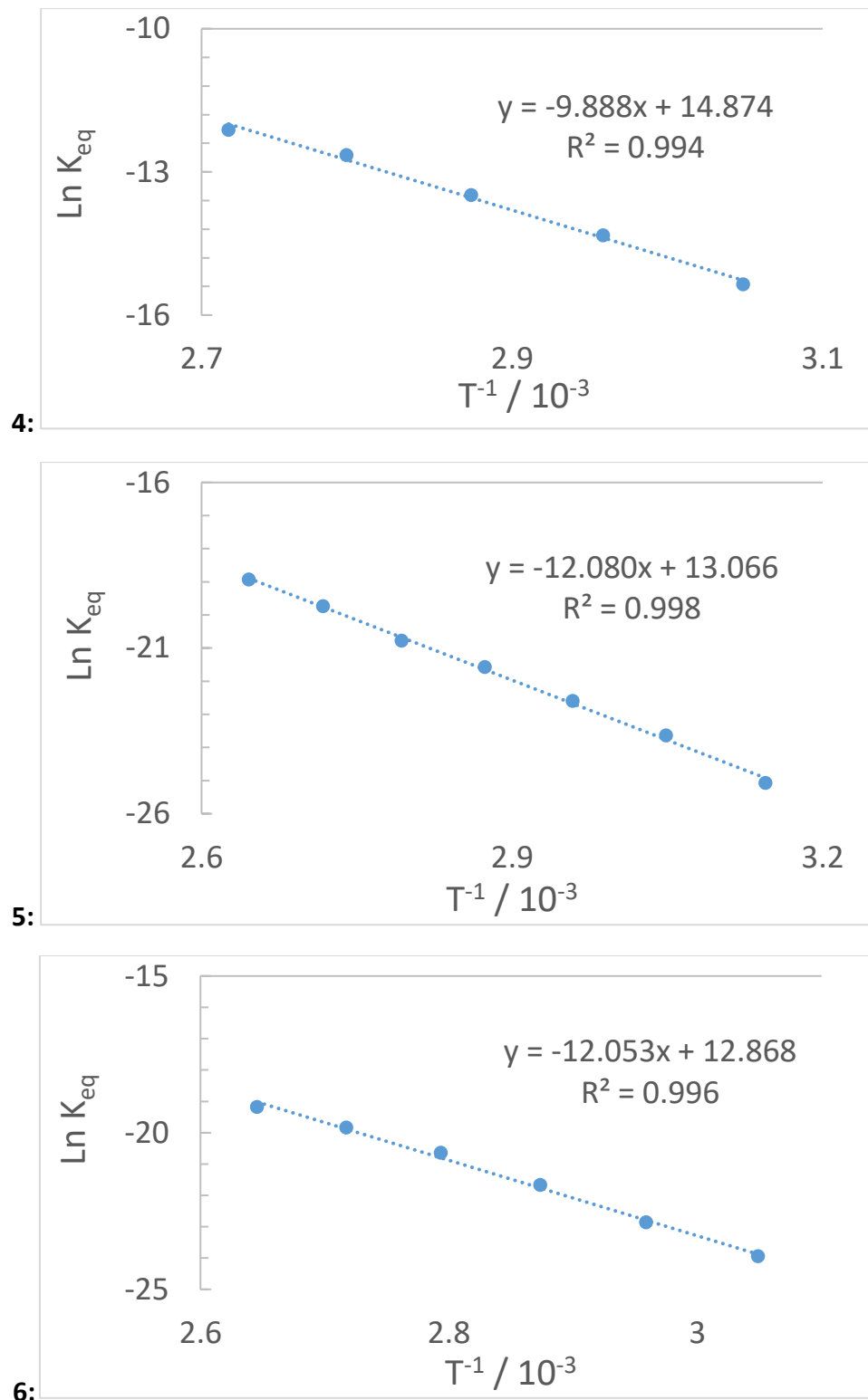
Finally, the formation of pimers versus sigma dimers was investigated both experimentally and computationally. A library of 15 dicyanomethyl radicals was synthesized with a substituent emphasis on strong electron donation. There are many potential factors in stabilizing a pimer over a sigma dimer. Benzylic spin density, London dispersion forces, and polarizability all influence the mode of dimerization. Low spin densities on the benzylic carbon, high dispersion stabilization, and a large polarizability all contribute some degree of stabilization towards a pimer species. Structurally, a *para* nitrogen unit fixed in a cycloalkyl ring is mandatory for forming a pimer as

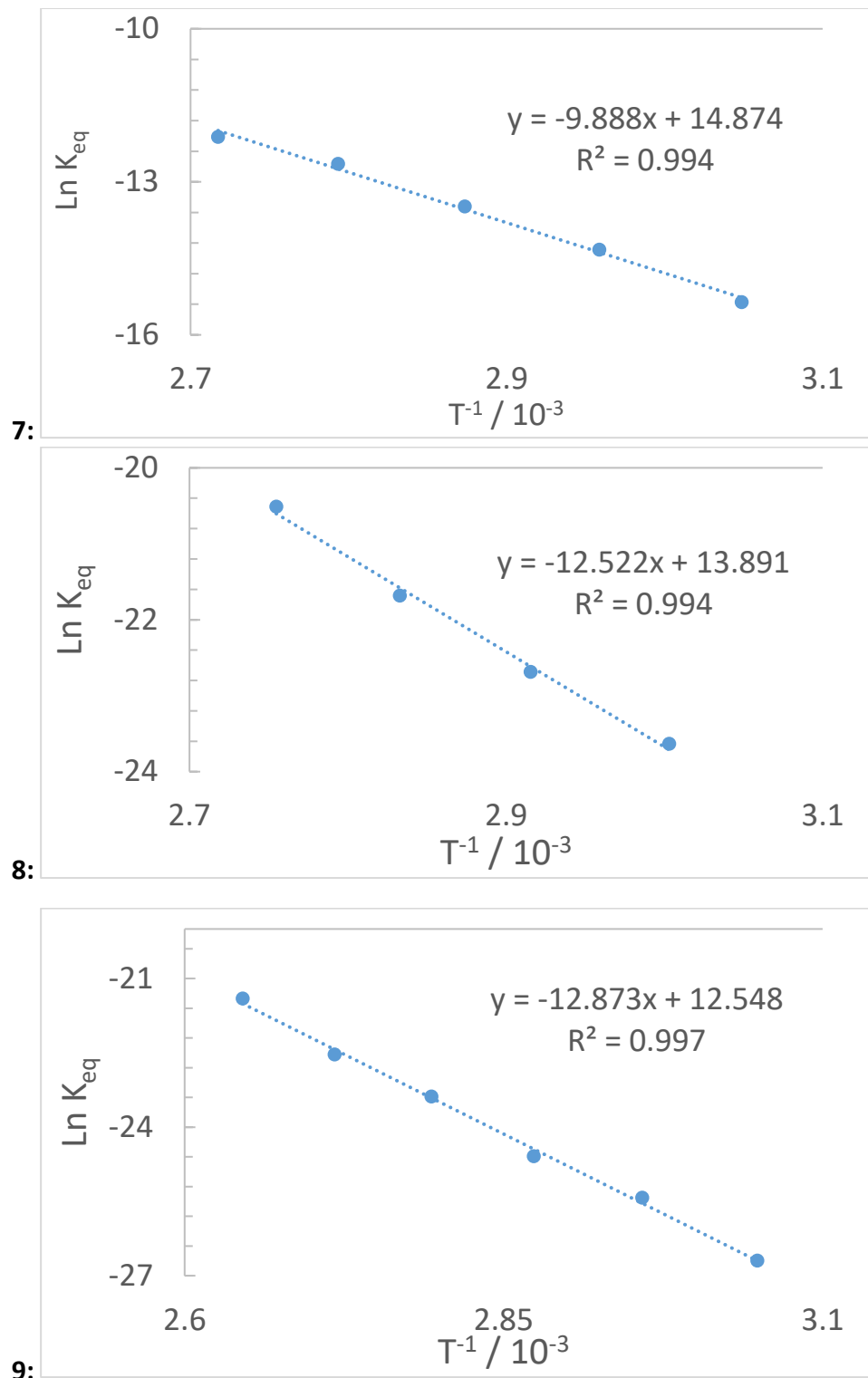
opposed to sigma dimer. Aryl dicyanomethyl radicals can be readily synthesized and investigated both experimentally and computationally. This work has shown that these radicals, existing in equilibrium with a closed shell dimer, are attractive candidates for use in a variety of stimuli responsive applications.

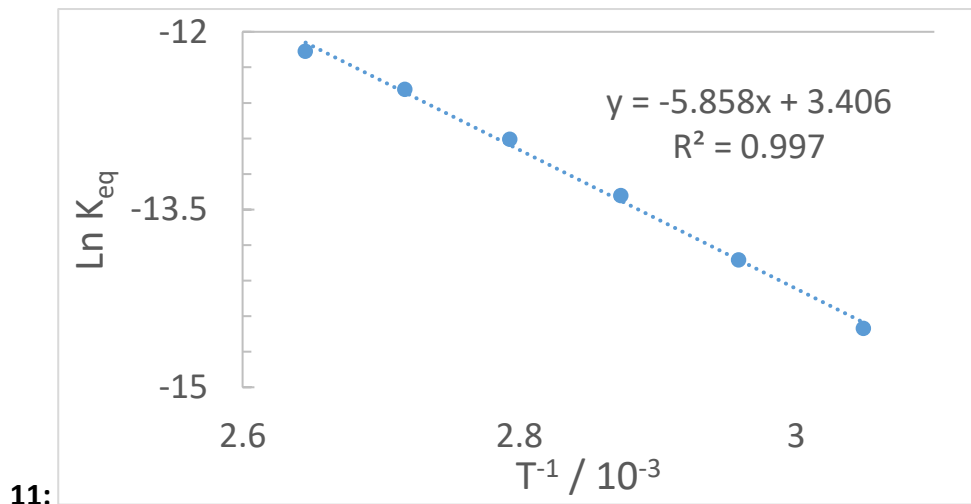
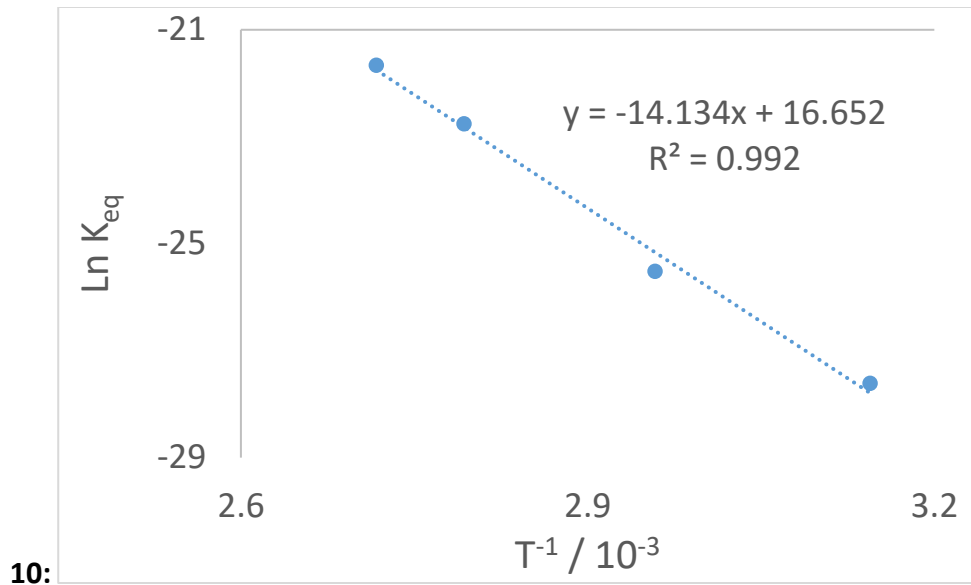
APPENDIX A. SUPPORTING INFORMATION FOR CHAPTER 2

Van 't Hoff Plots for Each Compound:

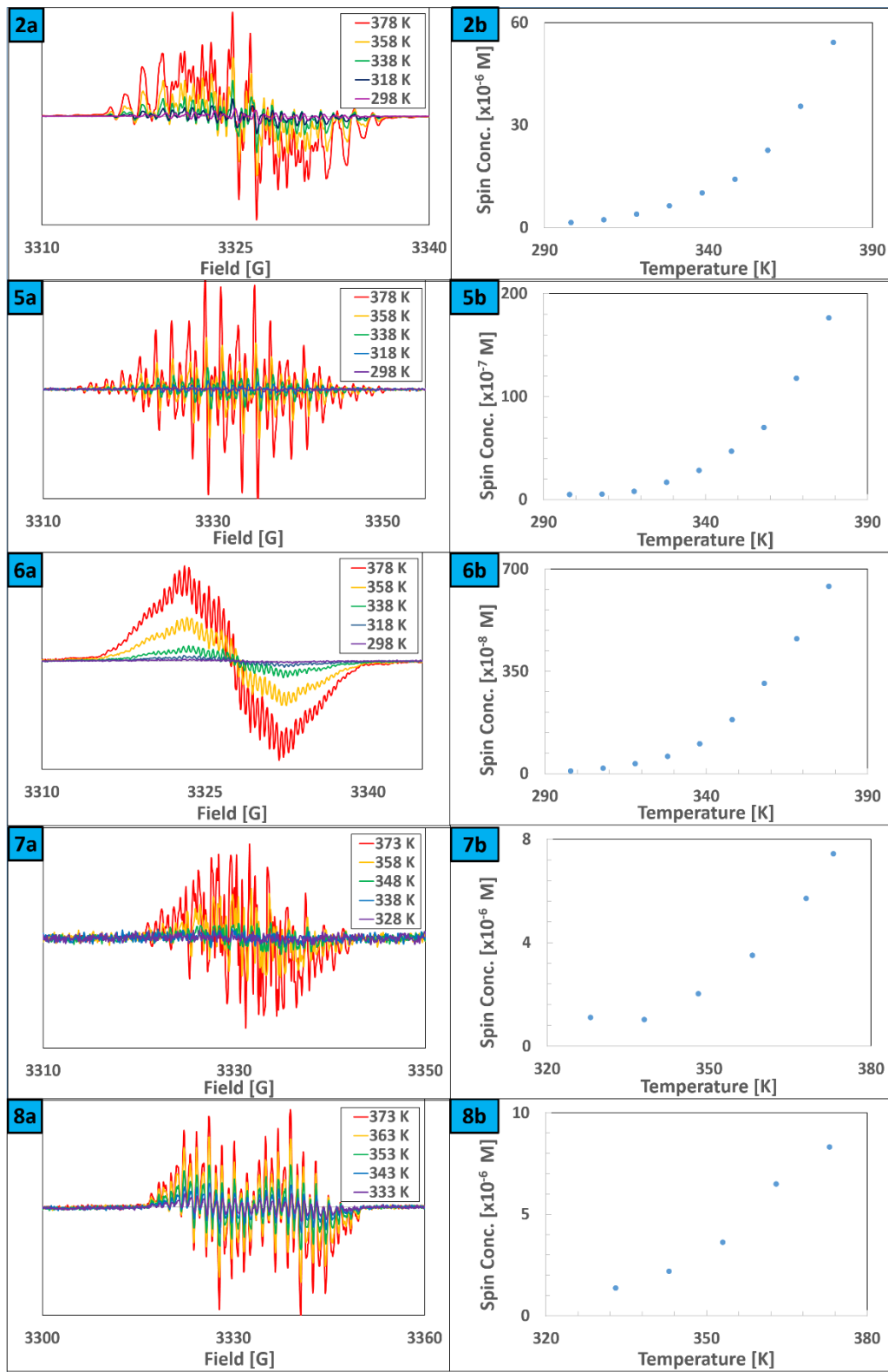


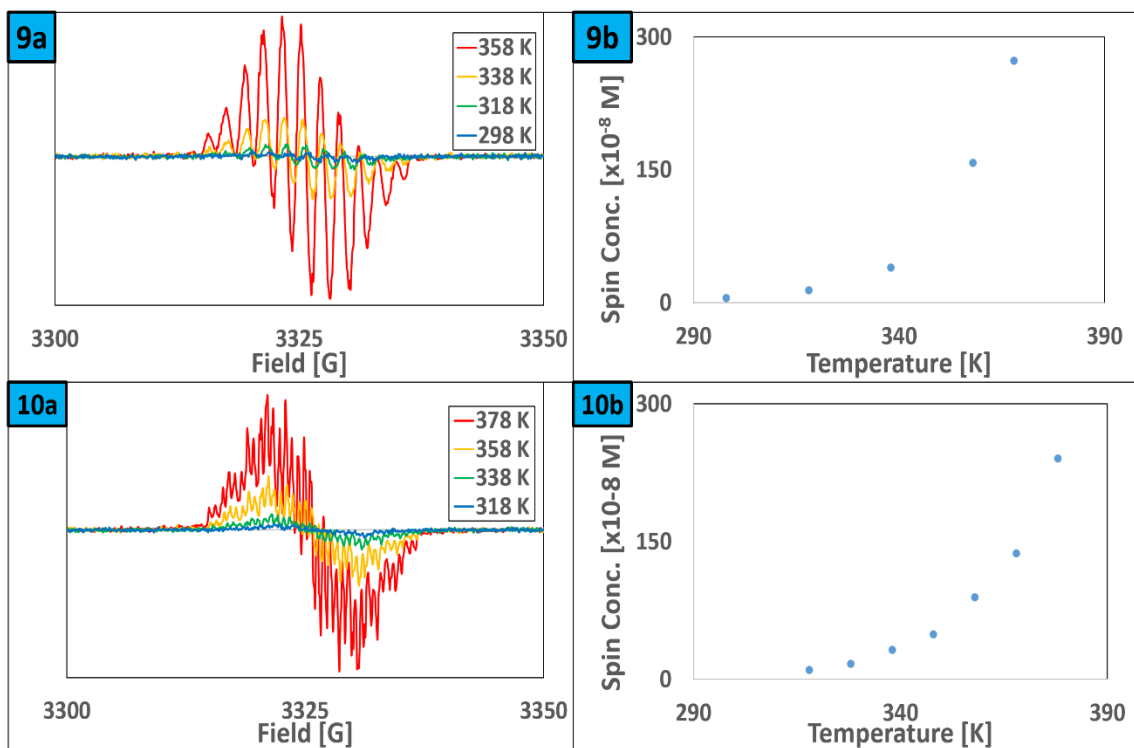




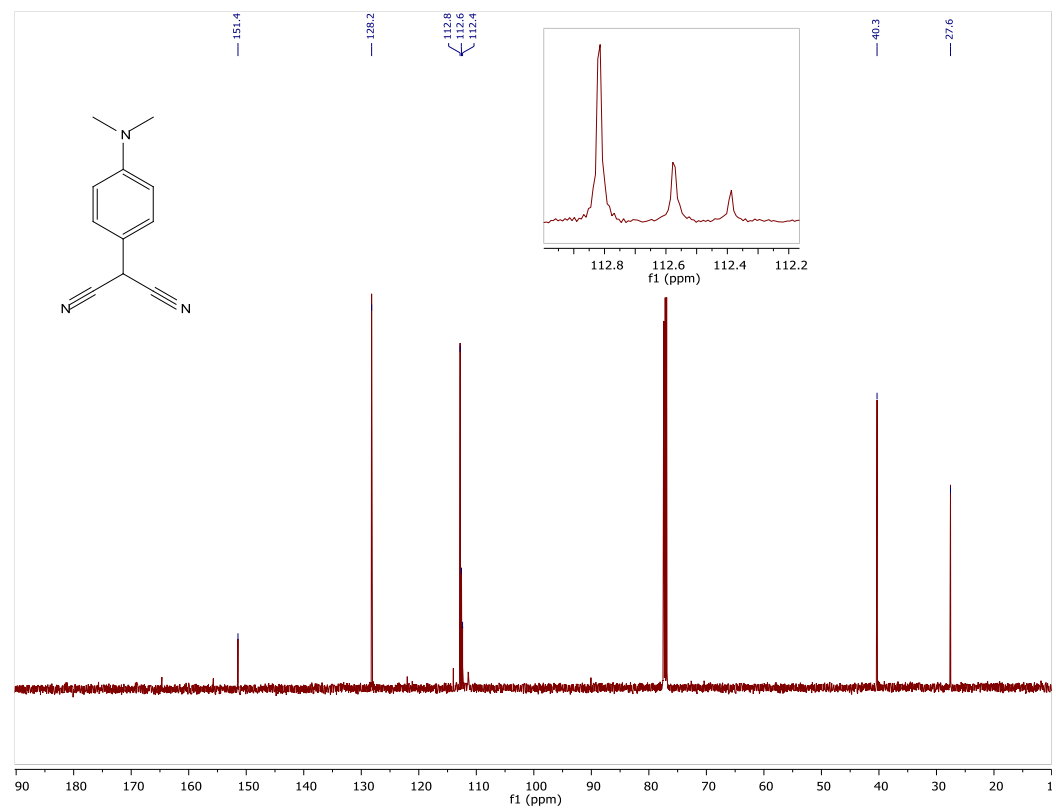
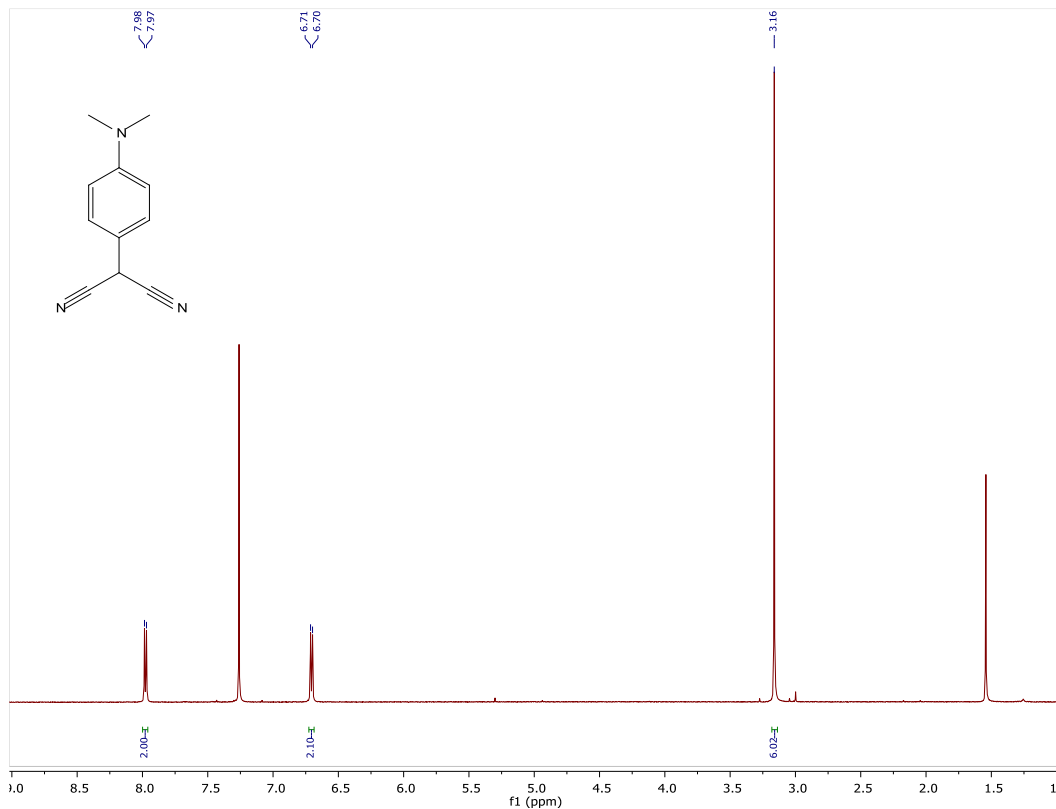


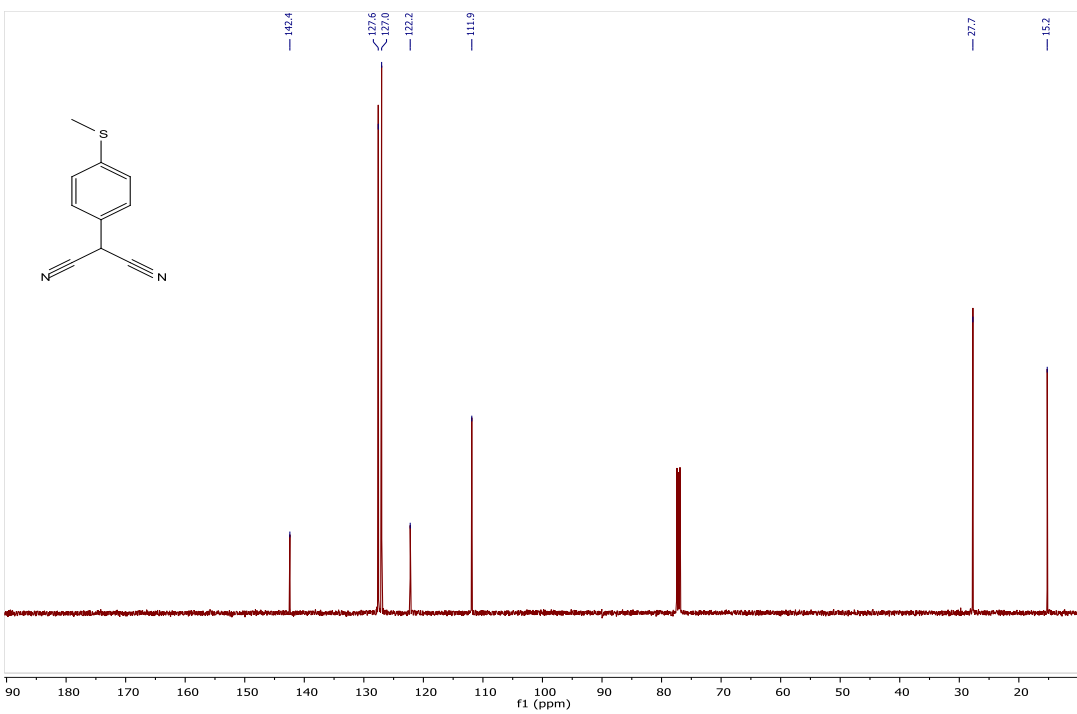
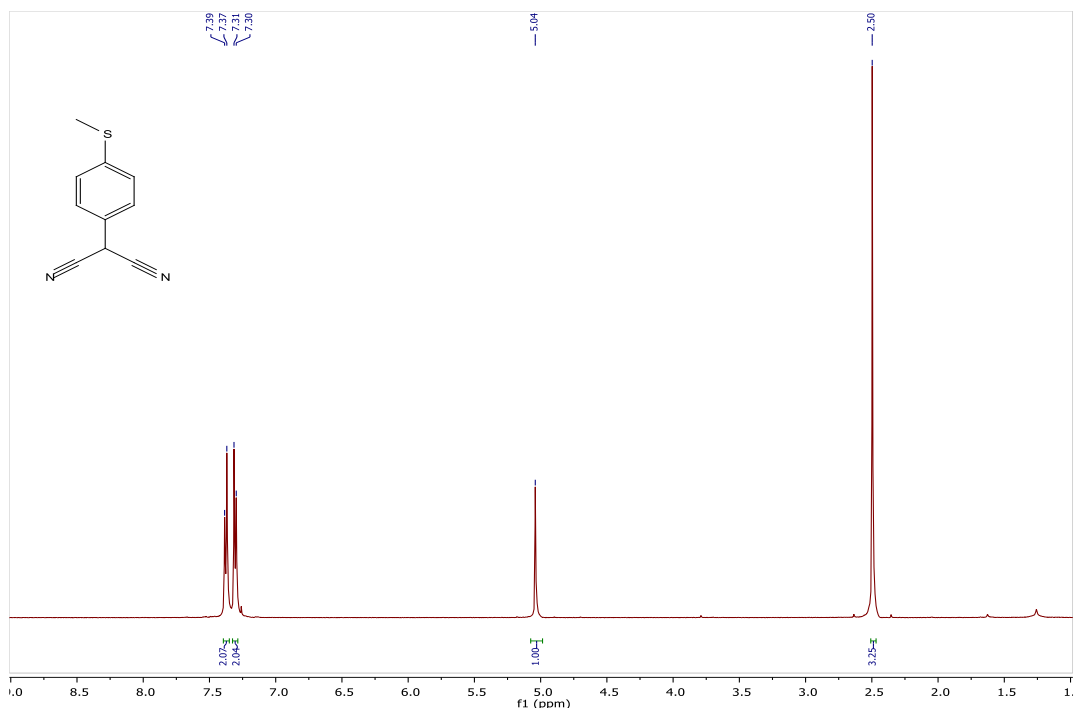
EPR Data:

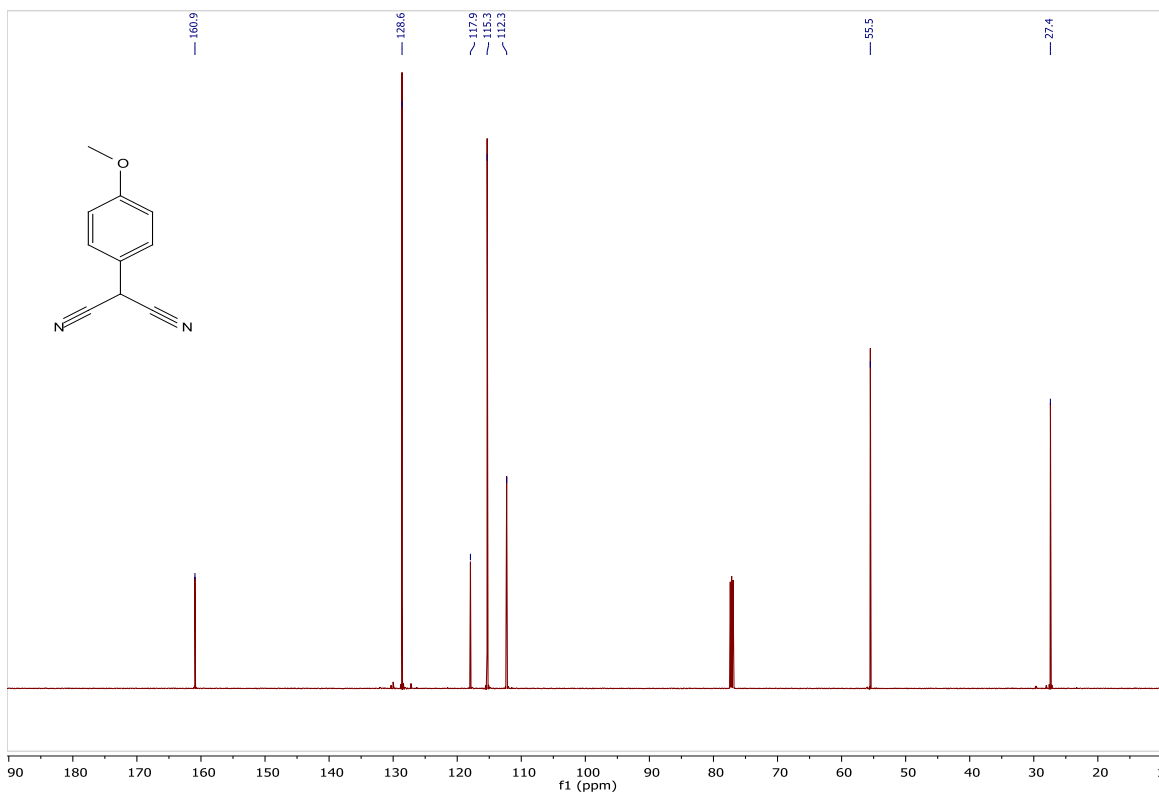
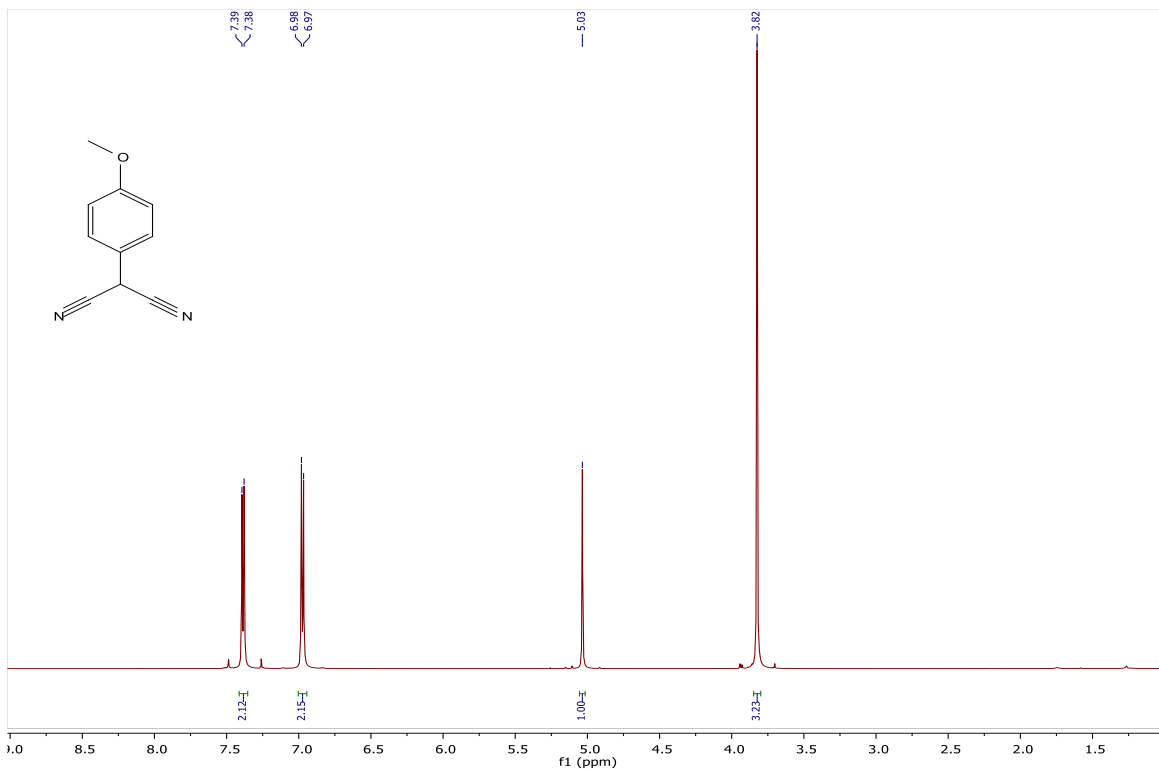


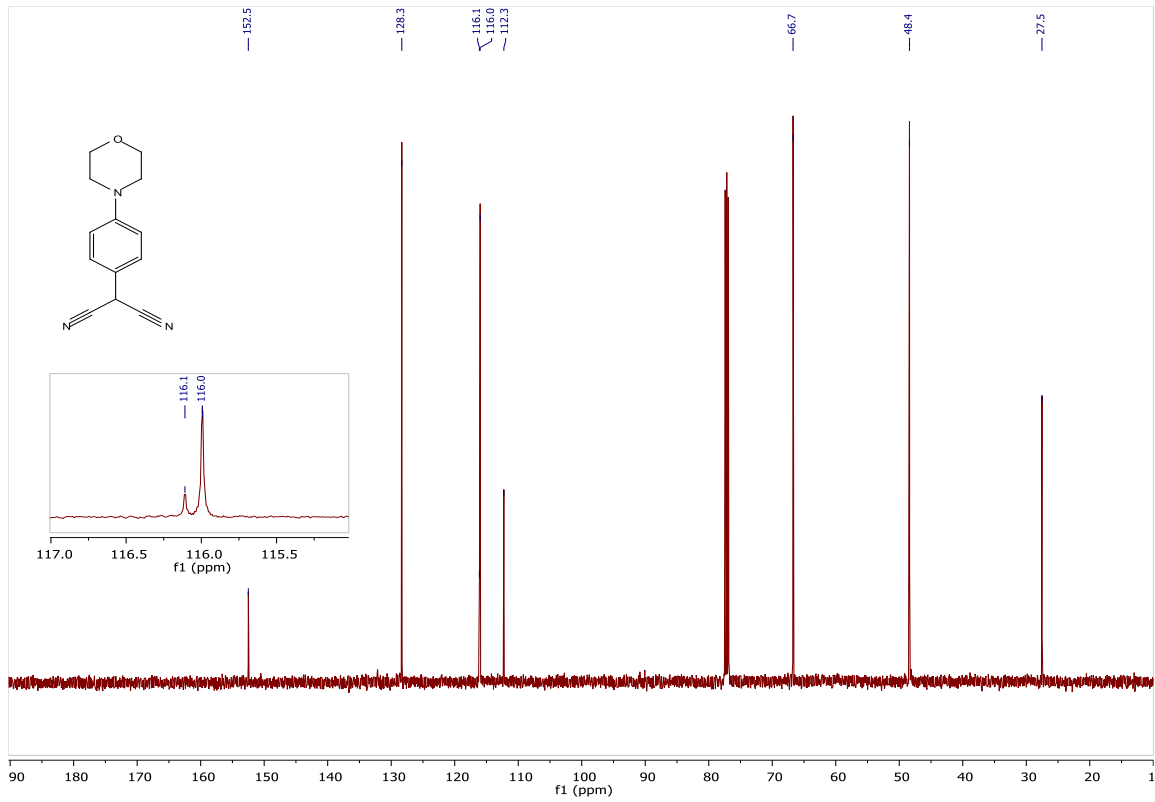
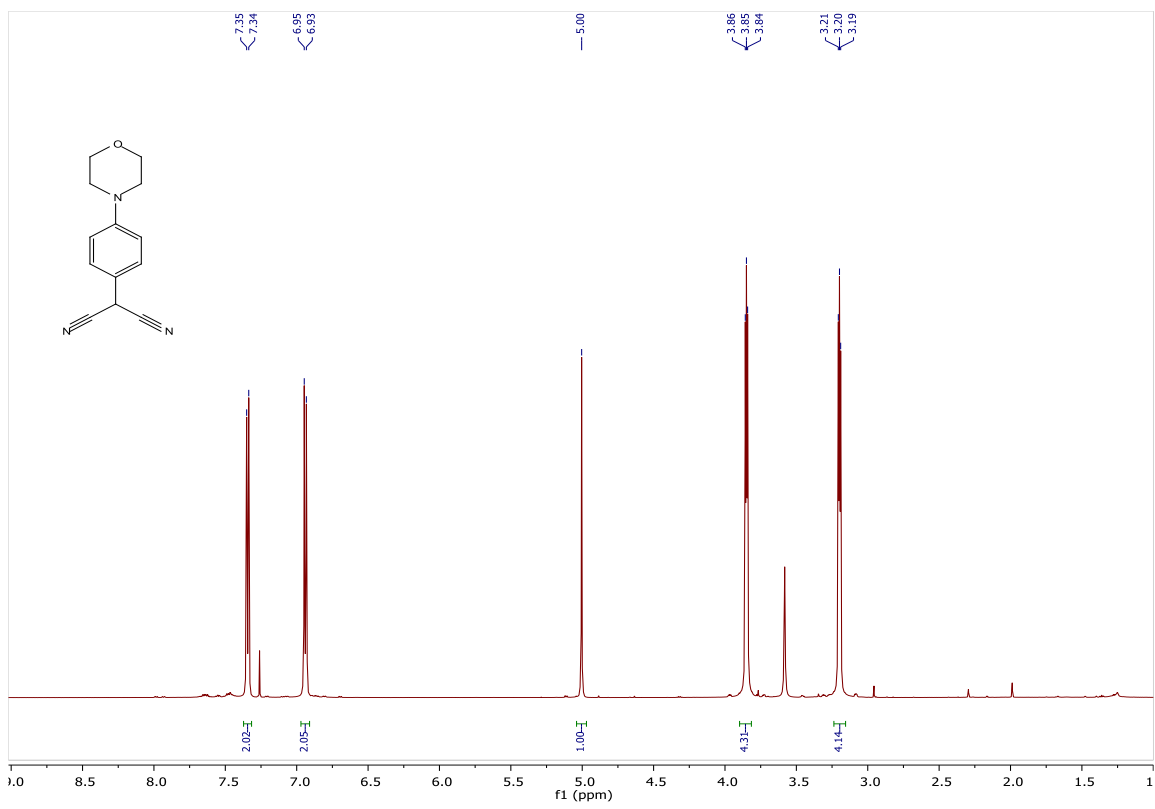


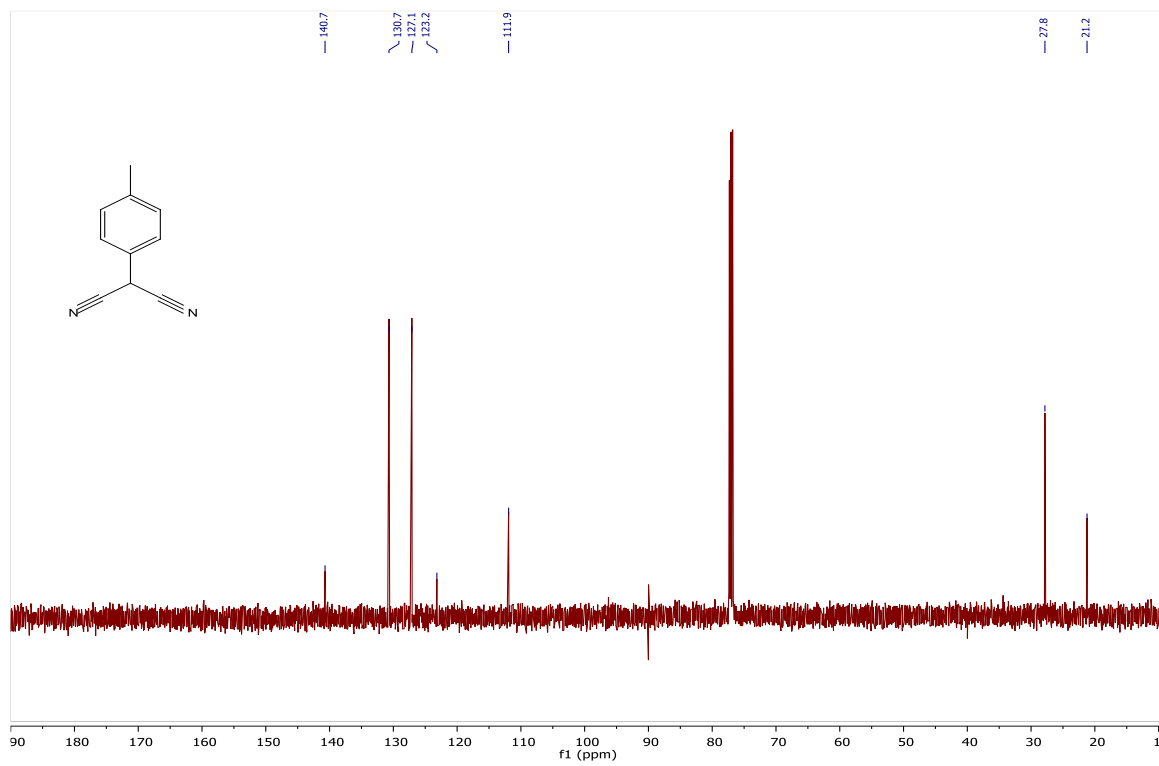
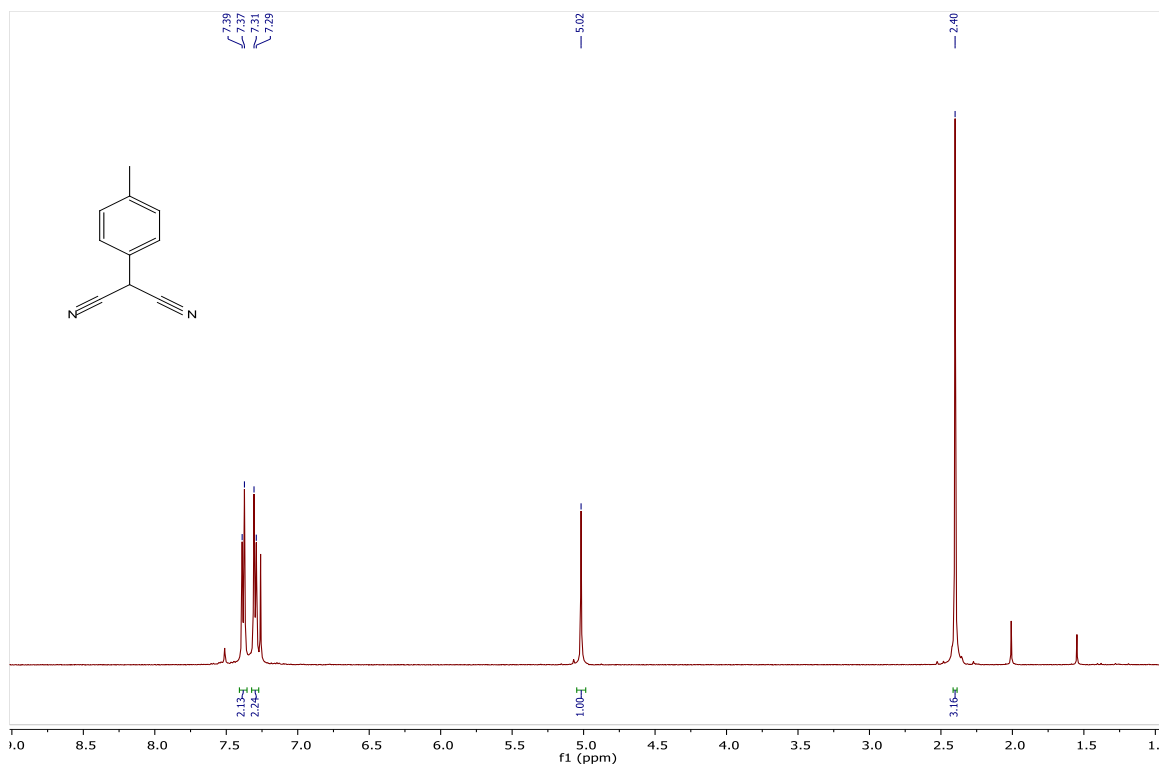
¹H and ¹³C Spectra:

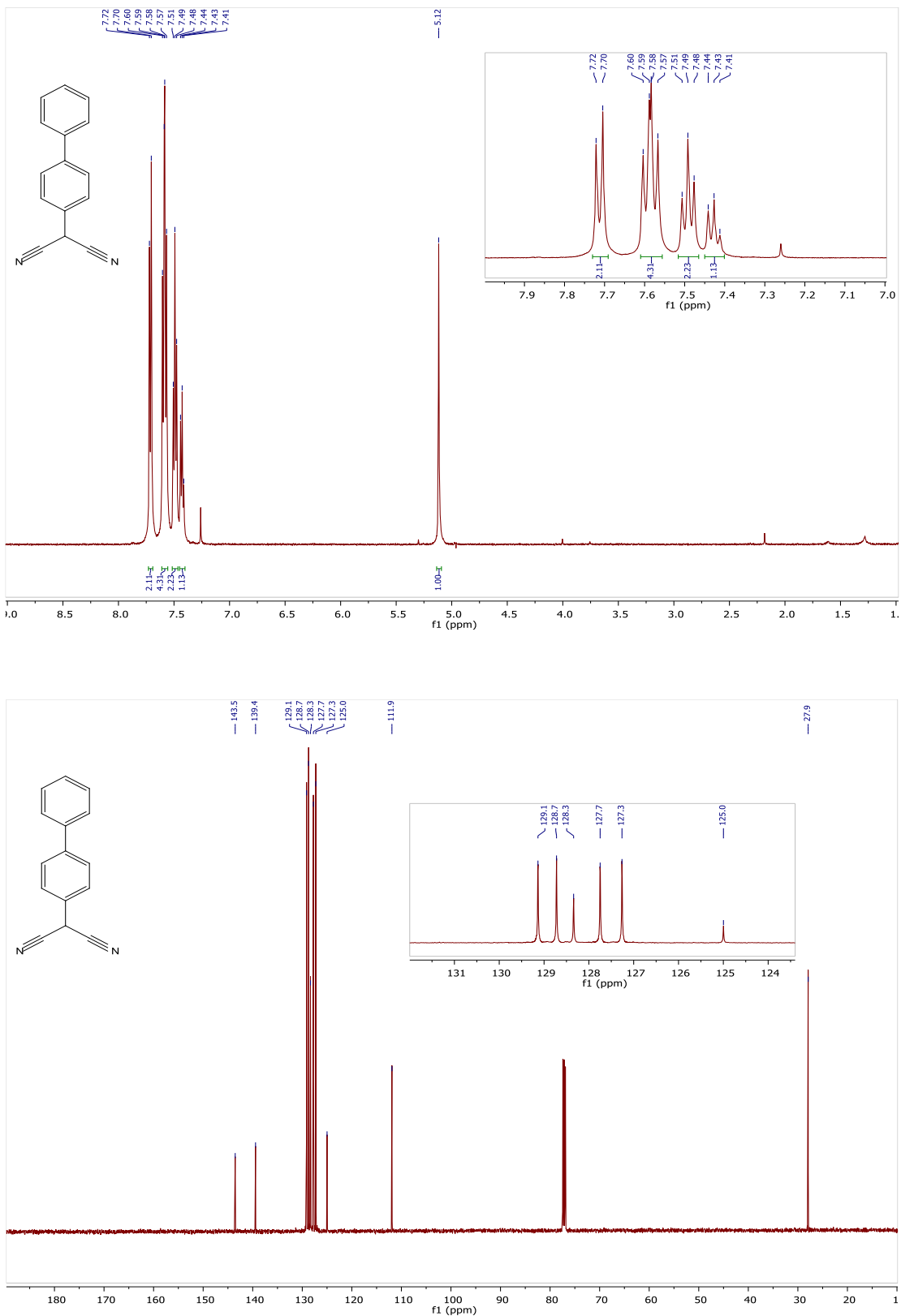


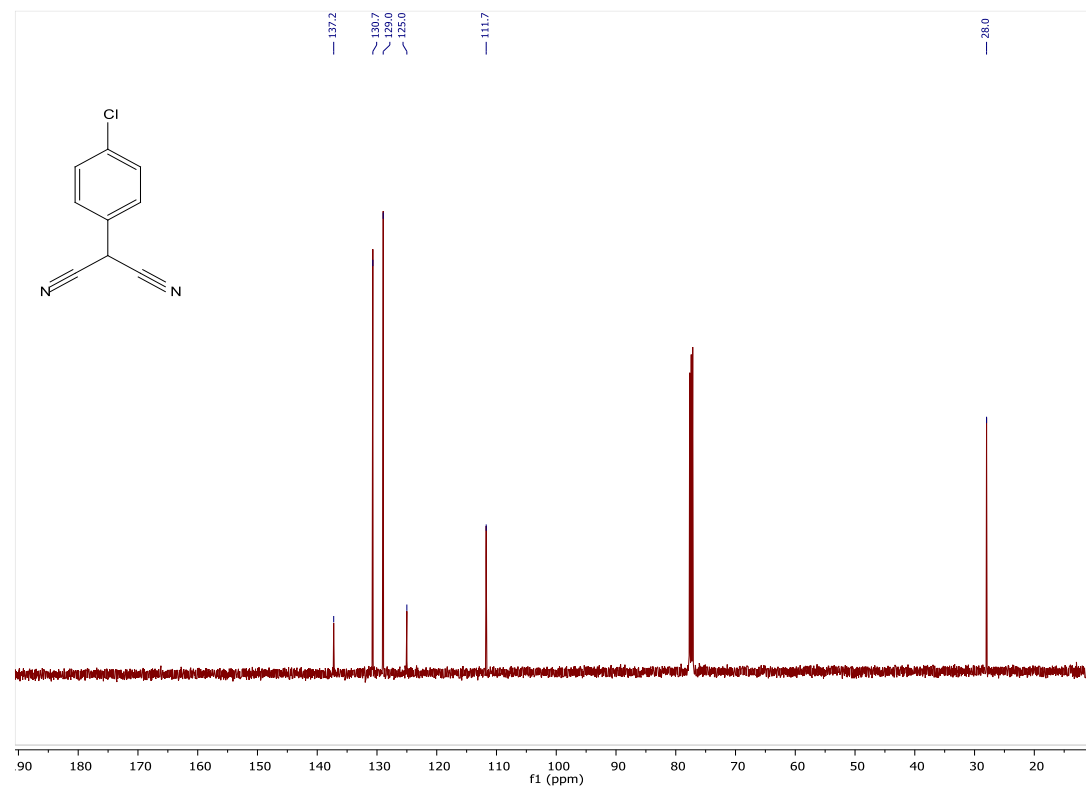
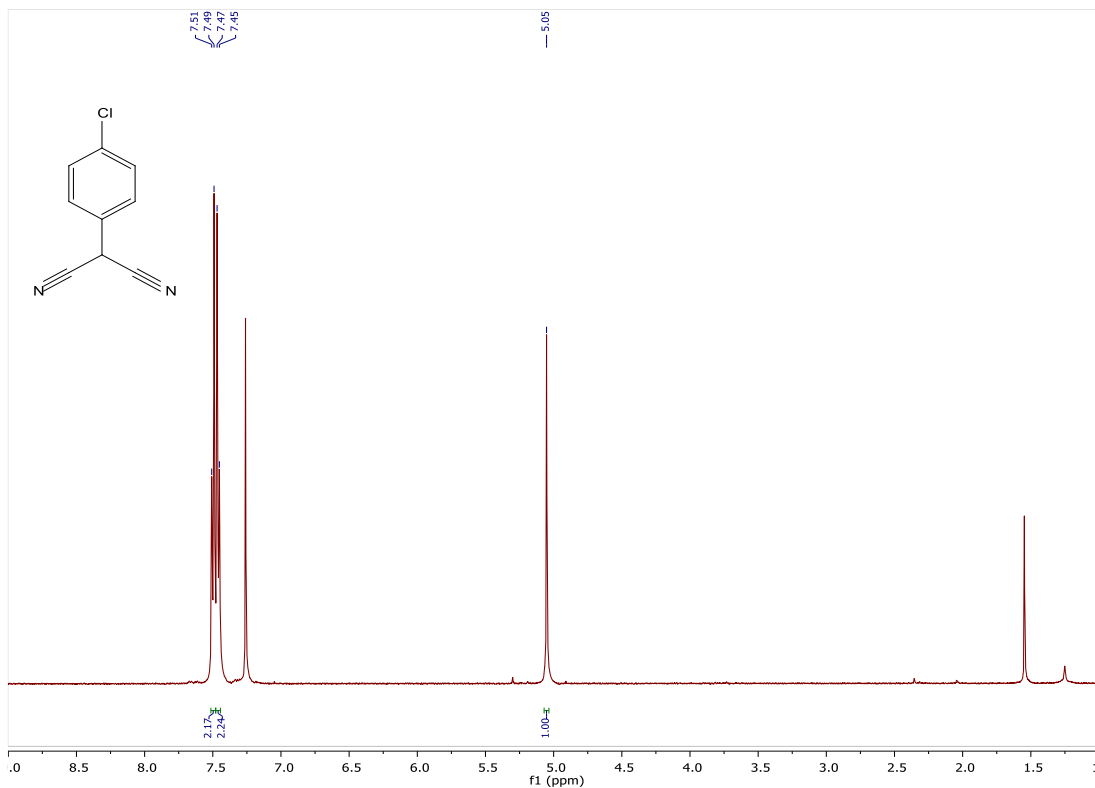


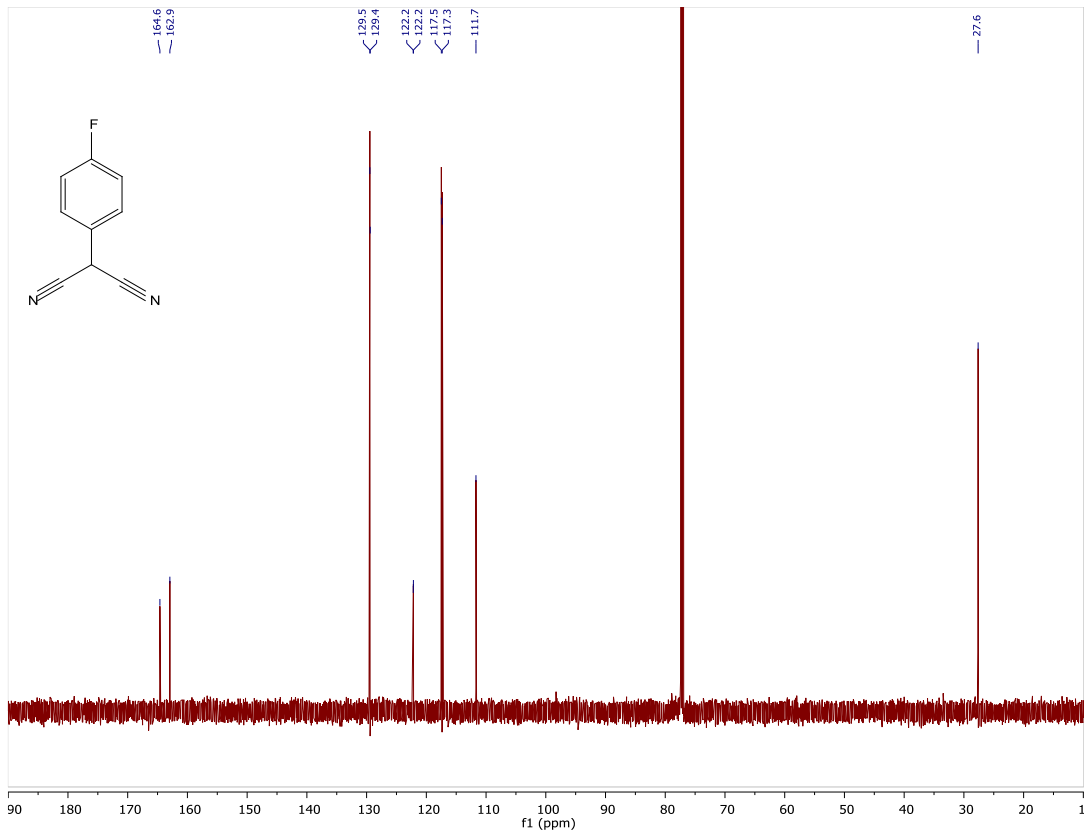
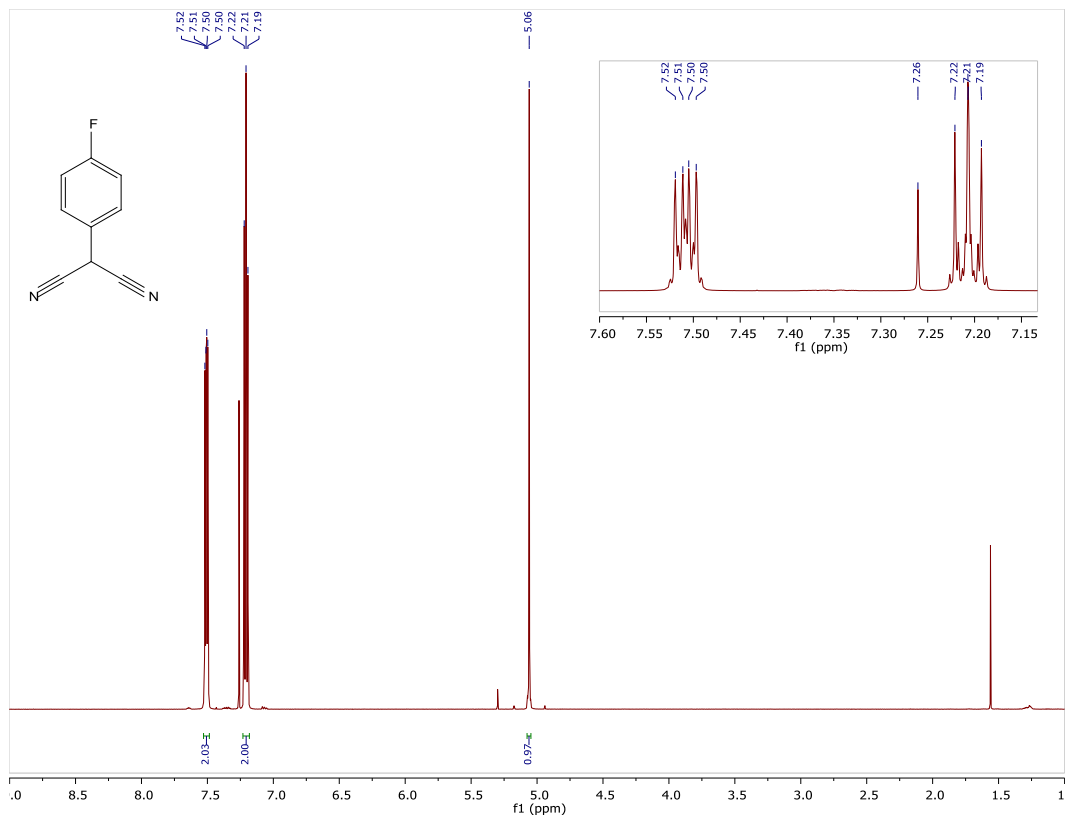


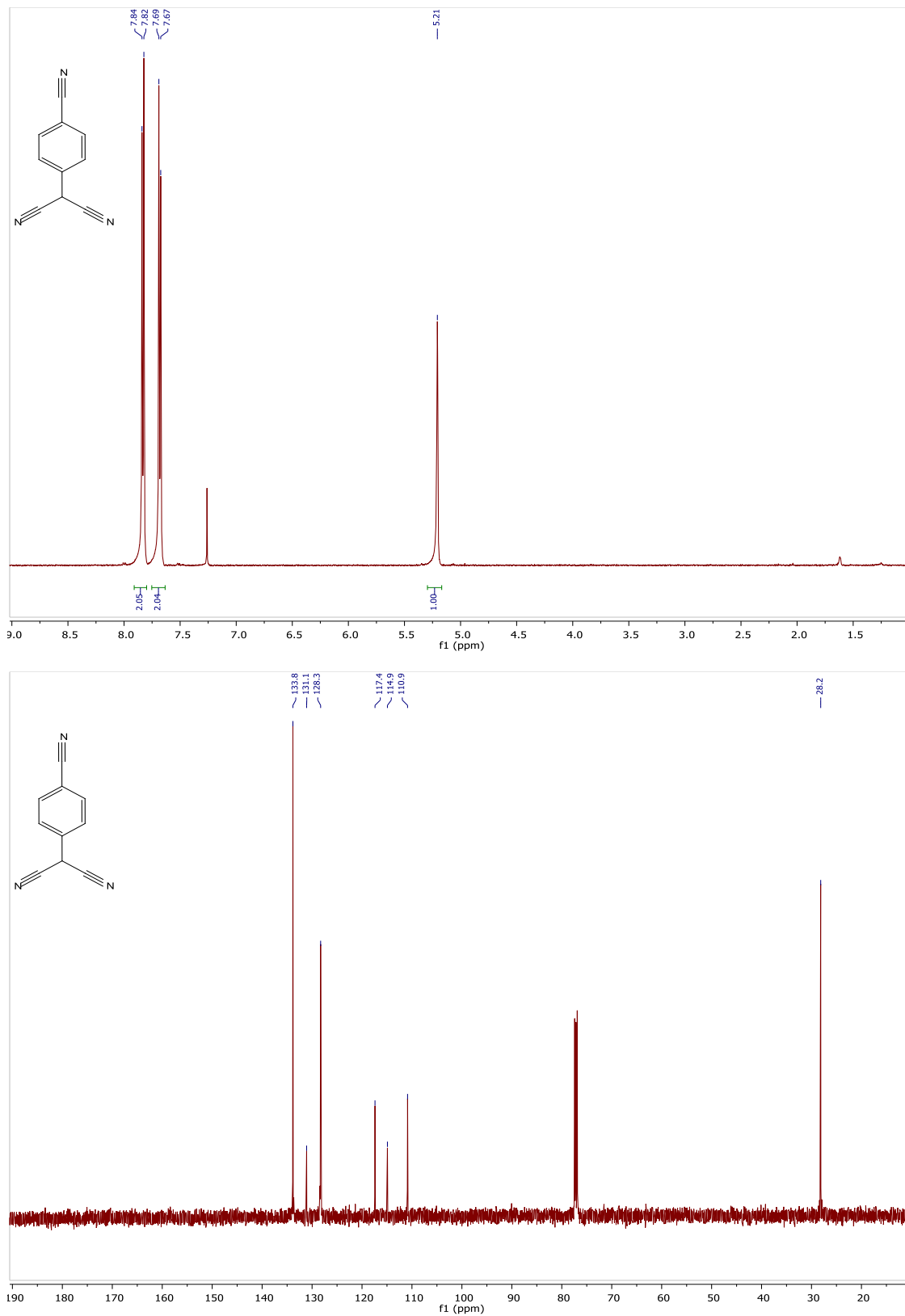


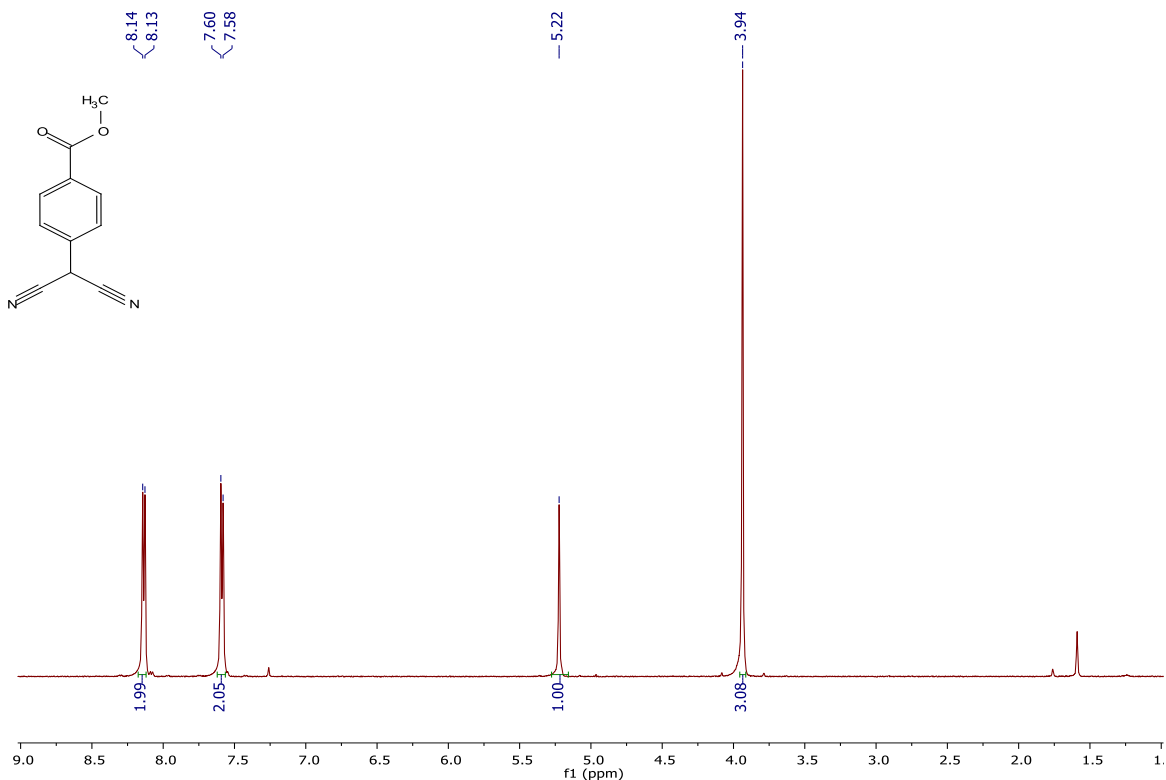


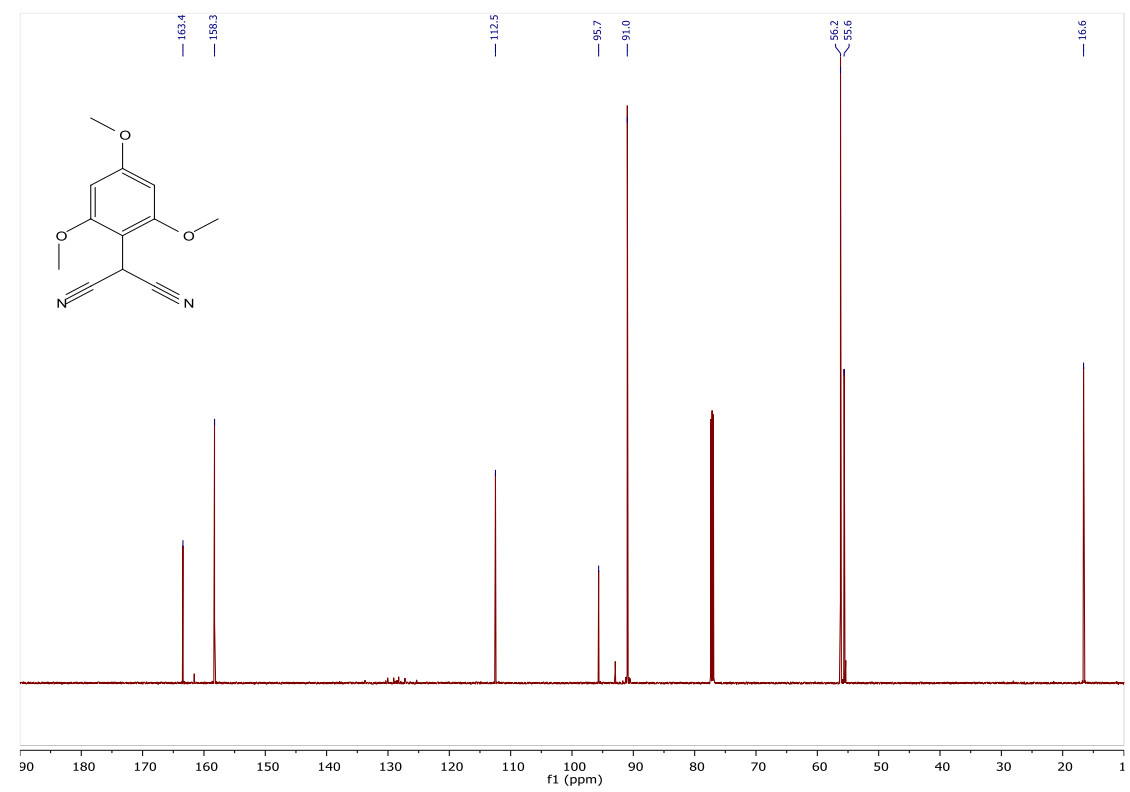
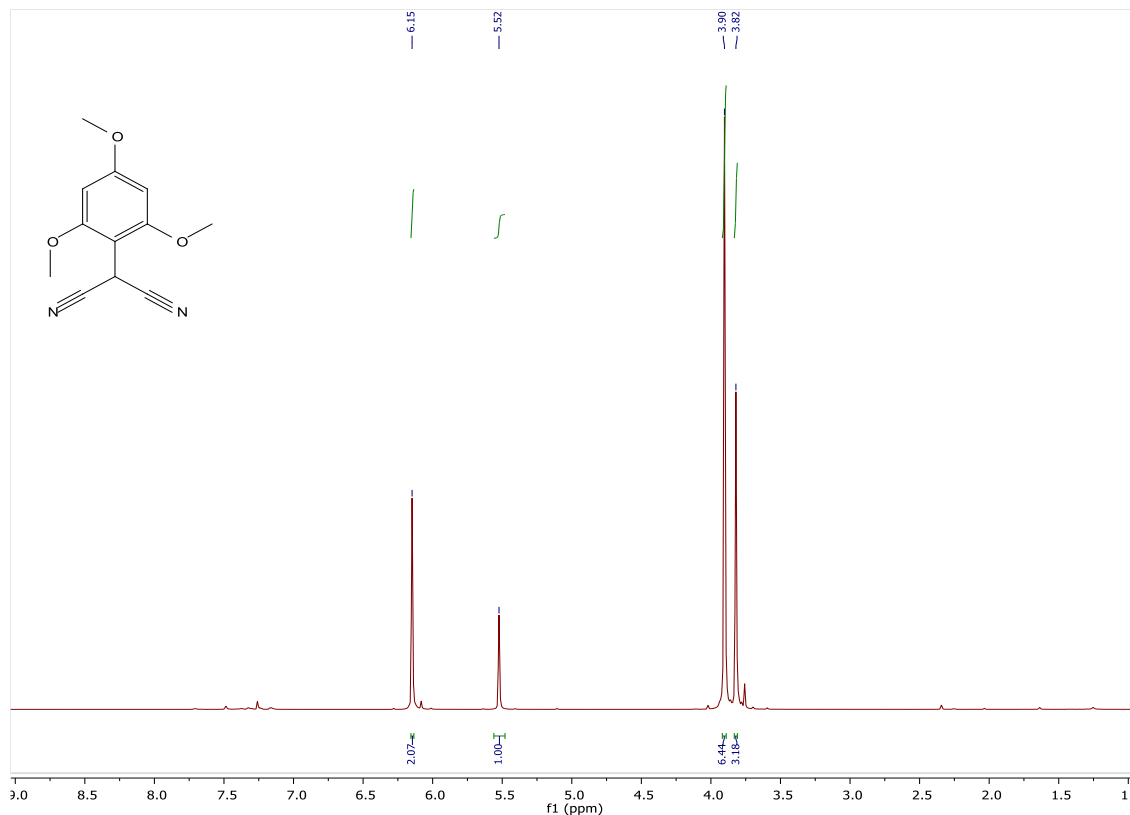




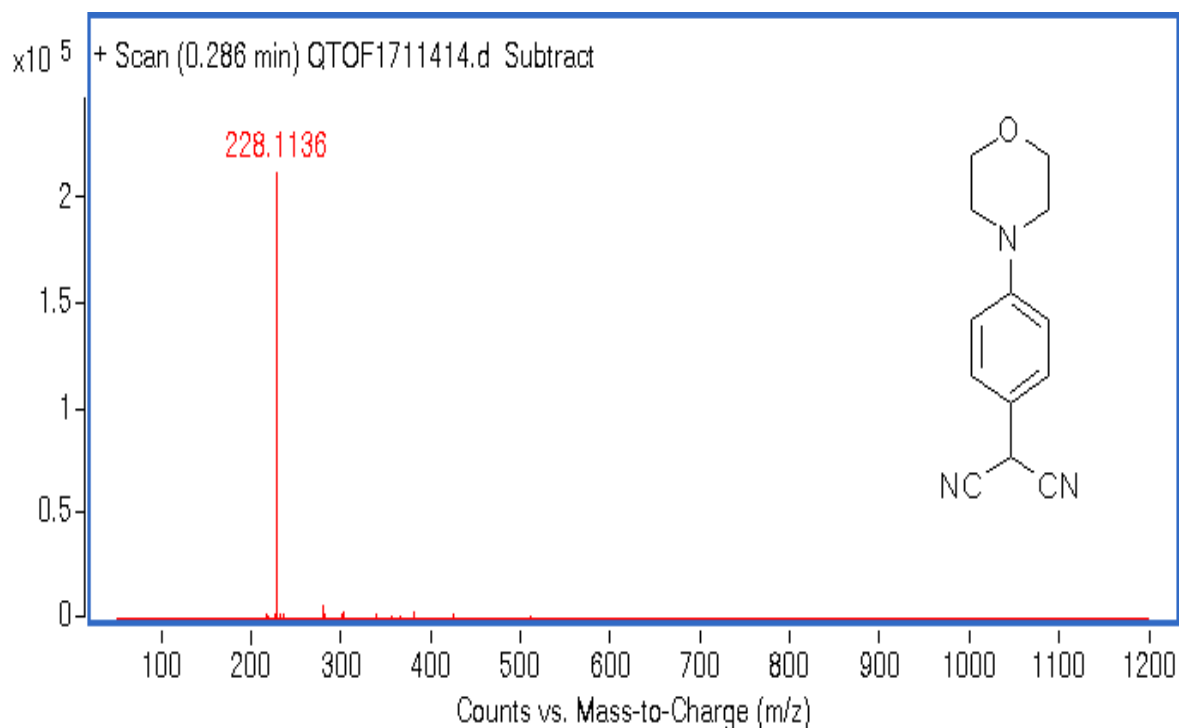
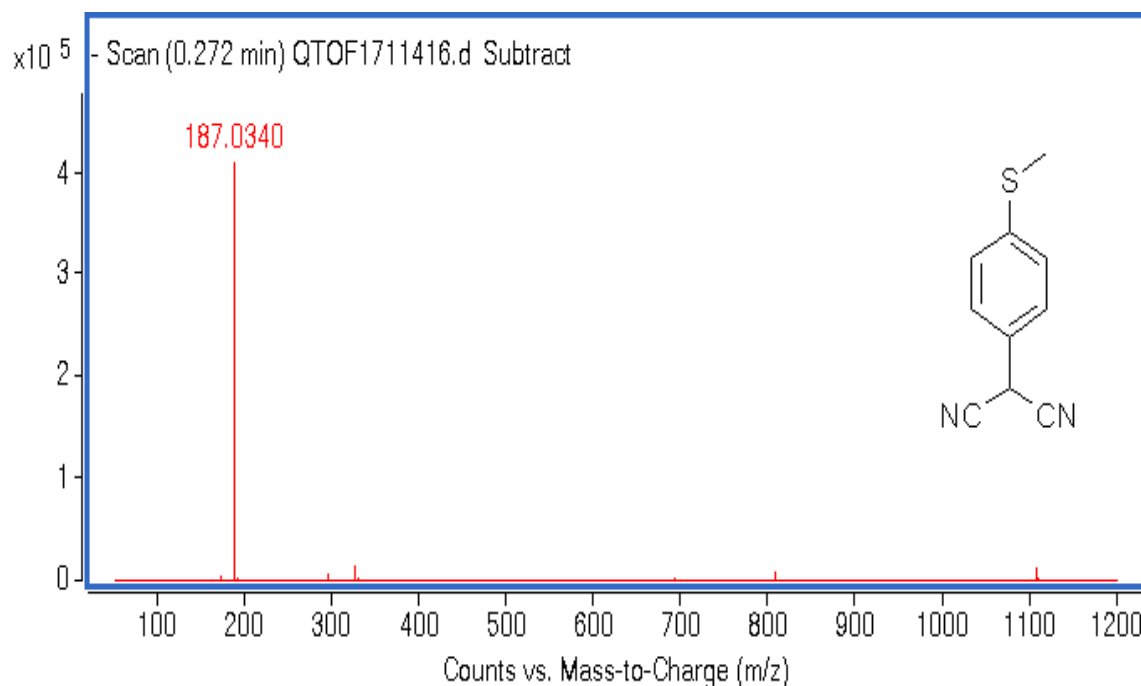


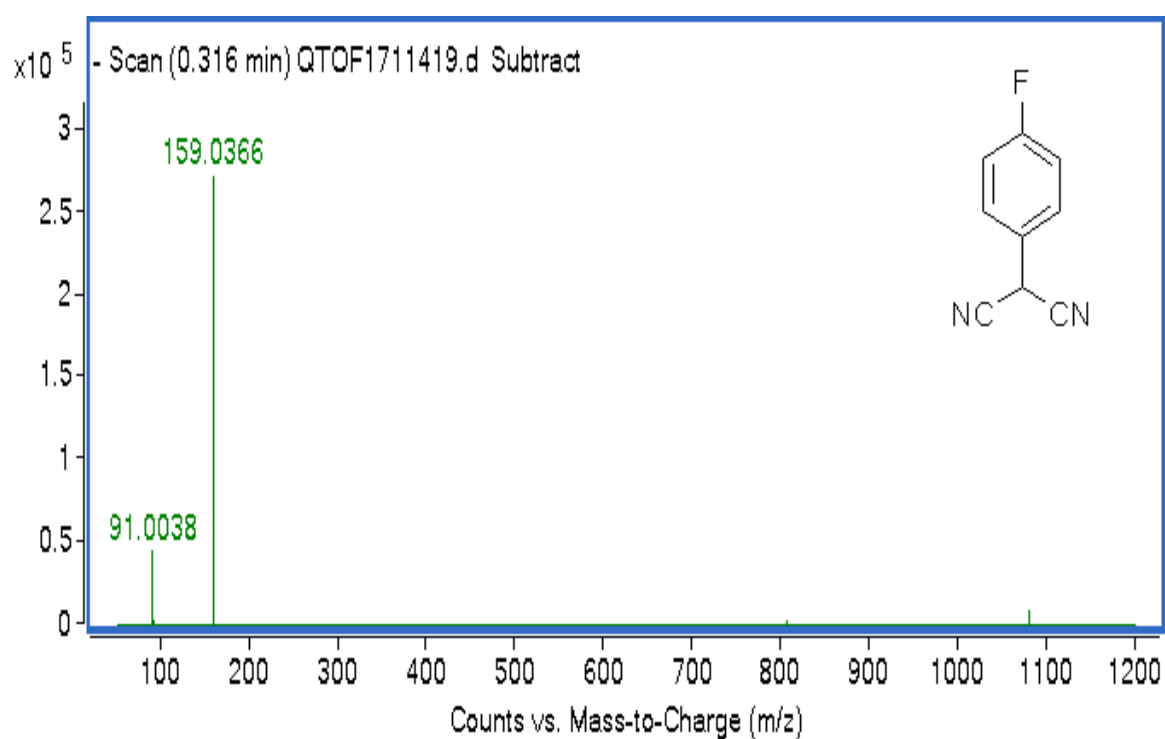
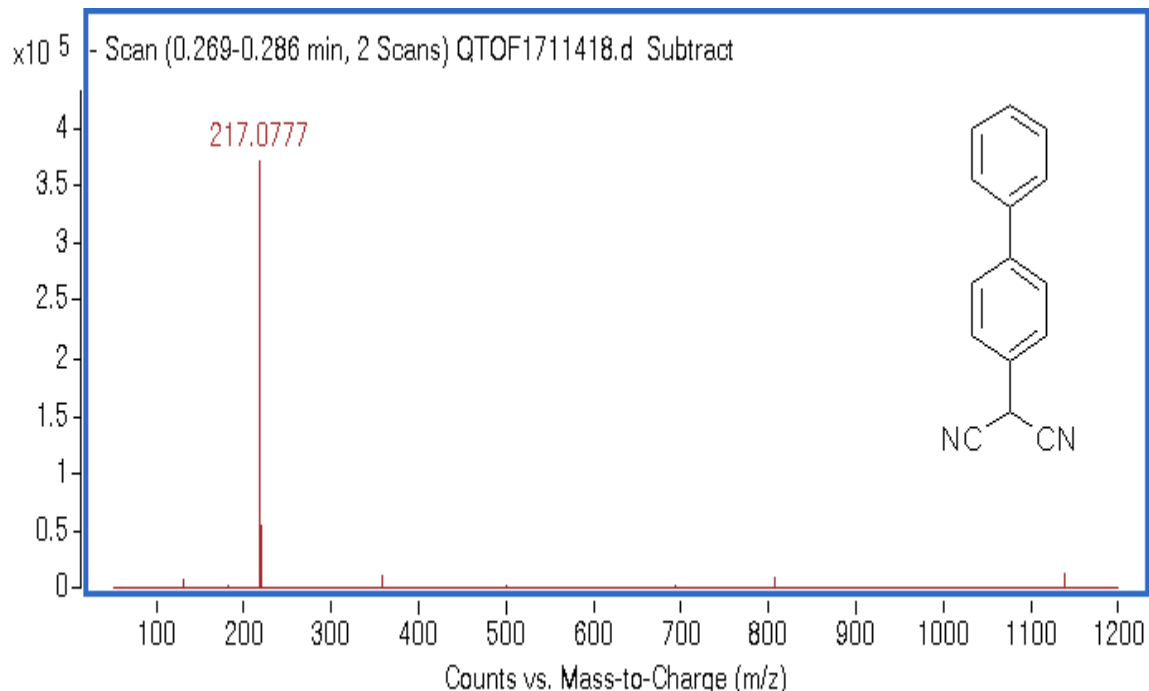


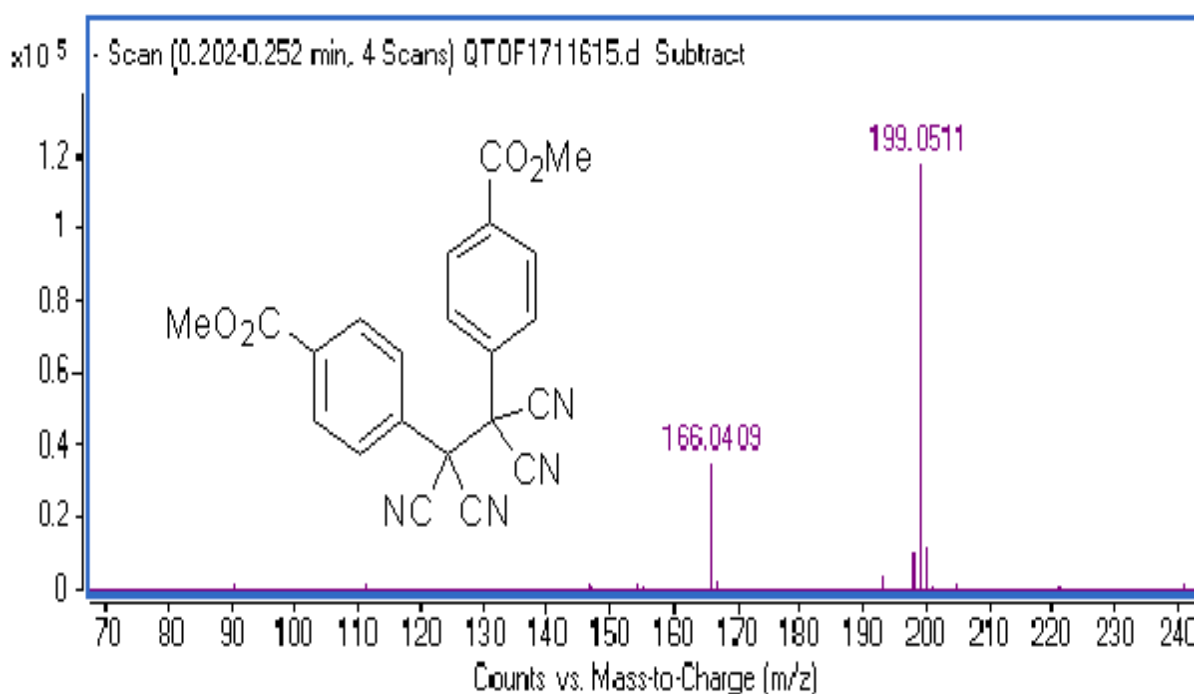
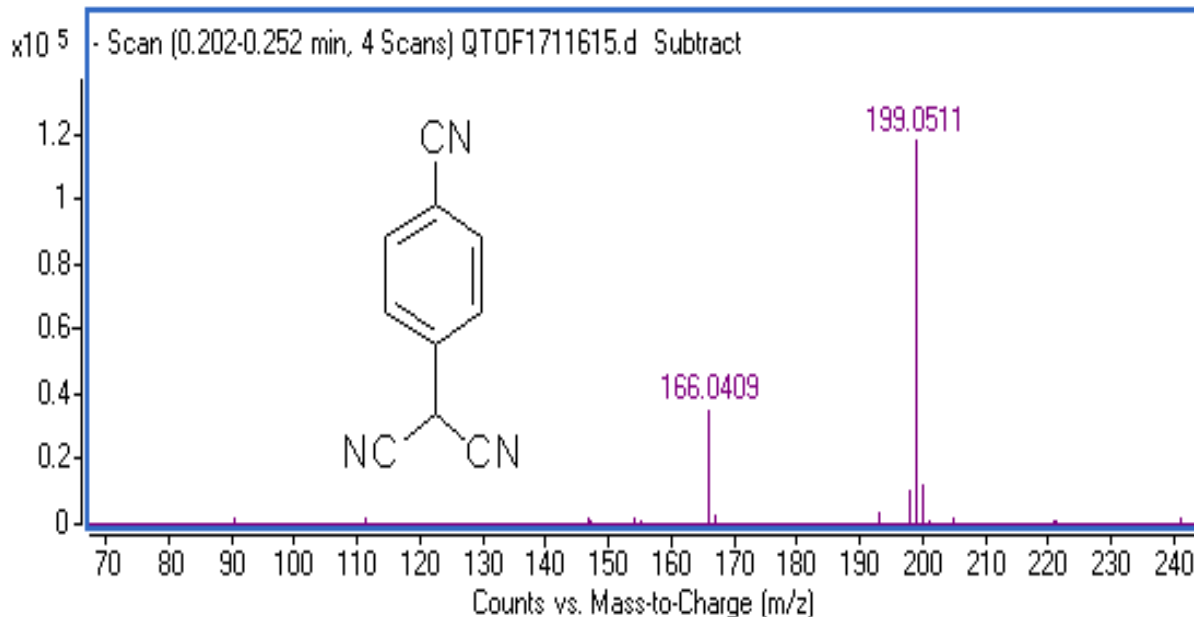


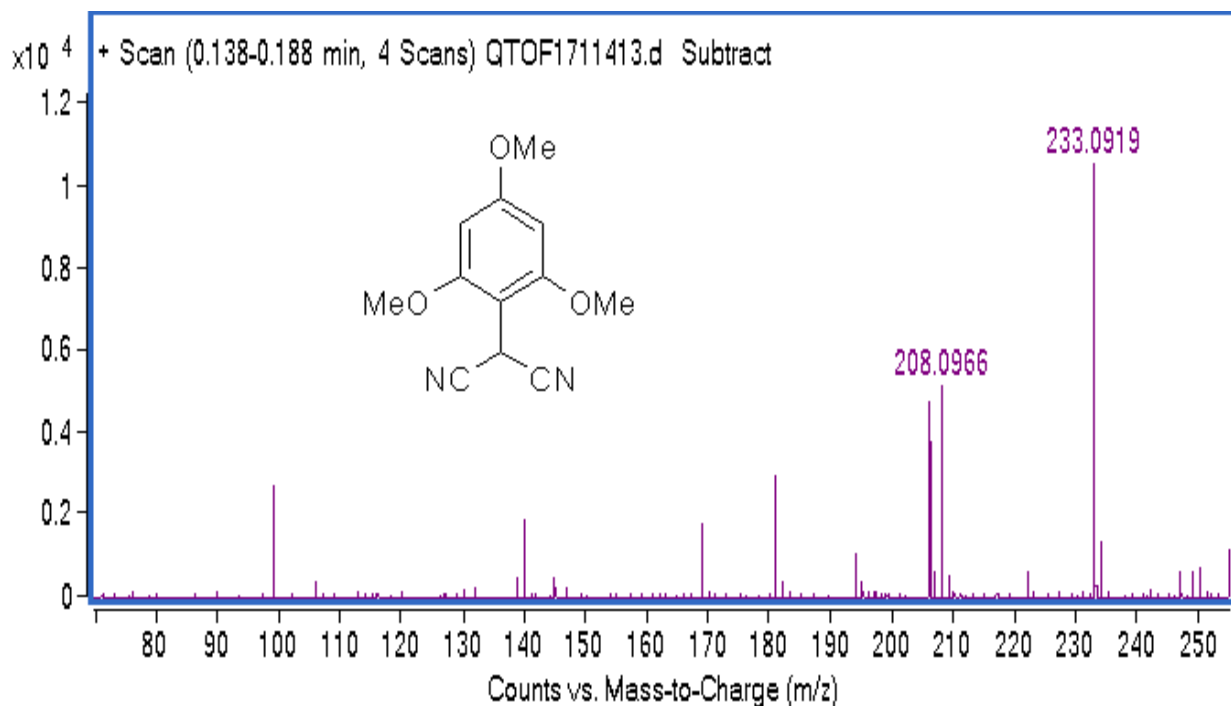


High Resolution Mass Spectra:

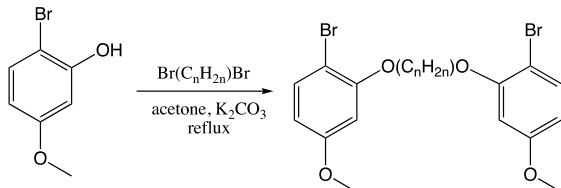








APPENDIX B. SUPPORTING INFORMATION FOR CHAPTER 3

General Procedure for linking bromophenol:

To a 50 mL round-bottom flask, equipped with a stir bar, was added 2-bromo-5-methoxyphenol (1.005 g, 5 mmol), dried acetone (15 mL), 1,6-dibromohexane (0.605 g, 2.5mmol), and K_2CO_3 (2.070 g, 15 mmol). The reaction mixture was refluxed for 24 h. The mixture was filtered and washed with acetone. The solvent was removed by rotary evaporation. The crude product was purified by recrystallization to afford white solid (0.820g, 67%)

6O-Br: The general procedure produced a white solid. ^1H NMR (500 MHz, Chloroform-*d*) δ (ppm) 7.43 (d, J = 8.4 Hz, 2H), 6.51 (d, J = 2.9 Hz, 2H), 6.47 – 6.35 (m, 2H), 4.04 (t, J = 6.4 Hz, 4H), 3.82 (s, 6H), 1.91 (m, 4H), 1.64 (m, 4H). ^{13}C NMR (151 MHz, CDCl_3) δ (ppm) 160.1, 156.1, 133.1, 106.0, 103.1, 100.9, 68.9, 55.6, 28.9, 25.7. HRMS(ESI). Calcd. for $[\text{C}_{20}\text{H}_{24}\text{Br}_2\text{O}_4 + \text{H}]^+$: 487.0114. Found: 487.0113. m.p. 90 – 93°C.

5O-Br: The general procedure produced a white solid (0.902 g, 76%). ^1H NMR (600 MHz, Chloroform-*d*) δ (ppm) 7.43 (d, J = 8.6 Hz, 2H), 6.51 (d, J = 2.7 Hz, 2H), 6.42 (dd, J = 8.6, 2.7 Hz, 2H), 4.06 (t, J = 6.4 Hz, 4H), 3.81 (s, 6H), 2.01 – 1.92 (m, 4H), 1.85 – 1.72 (m, 2H). ^{13}C NMR (151 MHz, CDCl_3) δ (ppm) 160.1, 156.1, 133.1, 106.0, 103.1, 100.9, 68.9, 55.6, 28.7, 22.7. HRMS(ESI). Calcd. for $[\text{C}_{19}\text{H}_{22}\text{Br}_2\text{O}_4 + \text{H}]^+$: 472.9958. Found: 472.9961. m.p. 113 – 116 °C.

4O-Br: The general procedure produced a white solid (0.930 g, 81%). ^1H NMR (600 MHz, Chloroform-*d*) δ (ppm) 7.42 (d, J = 8.7 Hz, 2H), 6.52 (d, J = 2.7 Hz, 2H), 6.42 (dd, J = 8.7, 2.8 Hz, 2H), 4.44 – 4.02 (m, 4H), 3.81 (s, 6H), 2.33 – 1.99 (m, 4H). ^{13}C NMR (151 MHz, CDCl_3) δ (ppm) 160.1, 156.0, 133.1, 106.2, 103.0, 100.9, 68.7, 55.6, 25.9. HRMS(ESI). Calcd. for $[\text{C}_{18}\text{H}_{20}\text{Br}_2\text{O}_4 + \text{H}]^+$: 458.9801. Found: 458.9800. m.p. 116 – 122 °C.

3O-Br: The general procedure produced a white solid (0.880 g, 79%). ^1H NMR (600 MHz, Chloroform-*d*) δ (ppm) 7.42 (dd, J = 8.8, 0.7 Hz, 2H), 6.56 (d, J = 2.8 Hz, 2H), 6.43 (ddd, J = 8.7, 2.8, 0.6 Hz, 2H), 4.28 (t, J = 6.0 Hz, 4H), 3.81 (s, 6H), 2.61 – 2.21 (m, 2H). ^{13}C NMR (151 MHz, CDCl_3) δ (ppm) 160.2, 155.8, 133.1, 106.5, 103.0, 101.0, 65.4, 55.6, 29.1. HRMS(ESI). Calcd. for $[\text{C}_{17}\text{H}_{18}\text{Br}_2\text{O}_4 + \text{H}]^+$: 444.9645. Found: 444.9646. m.p. 111 – 115 °C.

2O-Br: The general procedure produced a white solid (0.862 g, 80%). ^1H NMR (600 MHz, Chloroform-*d*) δ (ppm) 7.44 (d, J = 8.7 Hz, 2H), 6.65 (d, J = 2.8 Hz, 2H), 6.47 (dd, J = 8.7, 2.7 Hz, 2H), 4.44 (s, 4H), 3.82 (s, 6H). ^{13}C NMR (151 MHz, CDCl_3) δ (ppm) 160.2, 155.8, 133.3, 107.2, 103.4, 102.0, 67.9, 55.7. HRMS(ESI). Calcd. for $[\text{C}_{16}\text{H}_{16}\text{Br}_2\text{O}_4 + \text{H}]^+$: 430.9488. Found: 430.9488. m.p. 108 – 114 °C.

6P-Br: The general procedure produced a white solid (0.548 g, 64%). ^1H NMR (500 MHz, Chloroform-*d*) δ (ppm) 7.40 (d, J = 8.9 Hz, 4H), 6.80 (d, J = 9.0 Hz, 4H), 3.97 (t, J = 6.4 Hz, 4H), 1.83 (d, J = 7.3 Hz, 4H), 1.68 – 1.43 (m, 4H). ^{13}C NMR (126 MHz, CDCl₃) δ (ppm) 158.2, 132.3, 116.3, 112.7, 68.1, 29.1, 25.8. Elem. Anal. Calcd. for C₁₈H₂₀Br₂O₂: C 50.49, H 4.71. Found: C 50.47, H 4.62. m.p. 98 – 102 °C.

5P-Br: The general procedure produced a white solid (0.596 g, 72%). ^1H NMR (500 MHz, Chloroform-*d*) δ 7.40 (d, J = 9.1 Hz, 4H), 6.81 (d, J = 9.0 Hz, 4H), 3.98 (t, J = 6.4 Hz, 4H), 1.88 (p, J = 6.7 Hz, 4H), 1.64–1.70 (m, 2H). ^{13}C NMR (126 MHz, CDCl₃) δ (ppm) 158.2, 132.3, 116.3, 112.7, 68.0, 29.0, 22.7. HRMS(ESI). Calcd. for [C₁₇H₁₈Br₂O₄ - H]⁺: 410.9601. Found: 410.9591. m.p. 56 – 58 °C.

4P-Br: The general procedure produced a white solid (0.456 g, 57%). ^1H NMR (500 MHz, Chloroform-*d*) δ (ppm) 7.43 (d, J = 8.8 Hz, 4H), 6.87 (d, J = 8.8 Hz, 4H), 4.31 (s, 5H). ^{13}C NMR (126 MHz, CDCl₃) δ (ppm) 158.1, 132.3, 116.3, 112.8, 67.7, 25.9. Elem. Anal. Calcd. for C₁₆H₁₆Br₂O₂: C 48.03, H 4.03. Found: C 47.93, H 4.15. m.p. 119 – 120 °C.

3P-Br: The general procedure produced a white solid (0.409 g, 53%). ^1H NMR (500 MHz, Chloroform-*d*) δ (ppm) 7.40 (d, J = 8.9 Hz, 4H), 6.82 (d, J = 8.9 Hz, 4H), 4.15 (t, J = 6.0 Hz, 4H), 2.47 – 2.04 (m, 2H). ^{13}C NMR (126 MHz, CDCl₃) δ (ppm) 157.9, 132.3, 116.3, 113.0, 64.6, 29.2. Elem. Anal. Calcd. for C₁₅H₁₄Br₂O₂: C 46.66, H 3.16. Found: C 46.42, H 3.11. m.p. 139 – 143 °C.

2P-Br: The general procedure produced a white solid (0.357 g, 48%). ^1H NMR (500 MHz, Chloroform-*d*) δ (ppm) 7.57 – 7.38 (m, 4H), 6.87 (d, J = 8.8 Hz, 4H), 4.31 (s, 4H). ^{13}C NMR (126 MHz, CDCl₃) δ 157.7, 132.4, 116.5, 113.5, 66.7. Elem. Anal. Calcd. for C₁₄H₁₂Br₂O₂: C 45.20, H 3.25. Found: C 45.49, H 3.06. m.p. 120 – 125 °C.

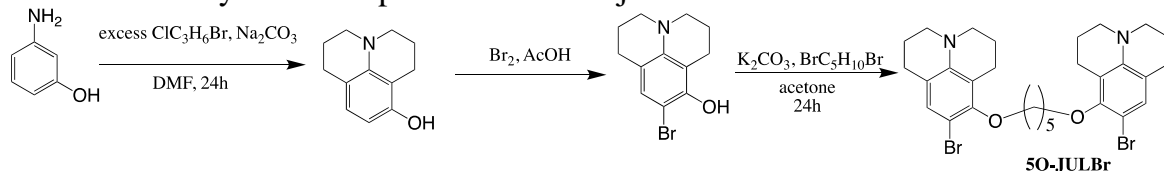
6O-DMA-Br: The general procedure produced red solid (0.668 g, 65%). ^1H NMR (500 MHz, Chloroform-*d*) δ (ppm) 7.34 (d, J = 8.8 Hz, 2H), 6.29 (d, J = 2.8 Hz, 2H), 6.24 (dd, J = 8.8, 2.8 Hz, 2H), 4.07 (t, J = 6.4 Hz, 4H), 2.97 (s, 12H), 2.00 – 1.89 (m, 4H), 1.77 – 1.56 (m, 4H); ^{13}C NMR (126 MHz, CDCl₃) δ (ppm) 155.9, 151.2, 132.9, 106.3, 98.8, 98.7, 68.9, 40.7, 29.1, 25.7. HRMS(ESI). Calcd. for [C₂₂H₃₀Br₂N₂O₂ + H]⁺: 513.0747. Found: 513.0743. m.p. 110 – 113 °C.

5O-DMA-Br: The general procedure produced purple solid (0.590 g, 59%). ^1H NMR (600 MHz, Chloroform-*d*) δ (ppm) 7.34 (d, J = 8.8 Hz, 2H), 6.29 (d, J = 2.8 Hz, 2H), 6.24 (dd, J = 8.8, 2.8 Hz, 2H), 4.09 (t, J = 6.4 Hz, 4H), 2.97 (s, 12H), 1.97 (dq, J = 8.2, 6.6 Hz, 4H), 1.89 – 1.73 (m, 2H). ^{13}C NMR (151 MHz, CDCl₃) δ (ppm) 155.9, 151.2, 132.9, 106.3, 98.8, 98.7, 68.9, 40.7, 28.9, 22.7. HRMS(ESI). Calcd. for [C₂₁H₂₈Br₂N₂O₂ + H]⁺: 499.0590. Found: 499.0590. m.p. 78 – 84 °C.

4O-DMA-Br: The general procedure produced purple solid (0.622 g, 64%). ^1H NMR (600 MHz, Chloroform-*d*) δ (ppm) 7.33 (d, J = 8.8 Hz, 2H), 6.30 (d, J = 2.8 Hz, 2H), 6.24 (dd, J = 8.8, 2.8 Hz, 2H), 4.17 (s, 4H), 2.96 (s, 12H), 2.13 (s, 4H); ^{13}C NMR (151 MHz, CDCl₃) δ (ppm) 155.8,

151.2, 132.9, 106.3, 98.6, 98.6, 68.6, 40.7, 26.1. HRMS(ESI). Calcd. for $[C_{20}H_{26}Br_2N_2O_2 + H]^+$: 485.0434. Found: 485.0433. m.p. 155 – 158 °C.

5O-JUL-Br: The synthesis of pentane-tethered julolidine

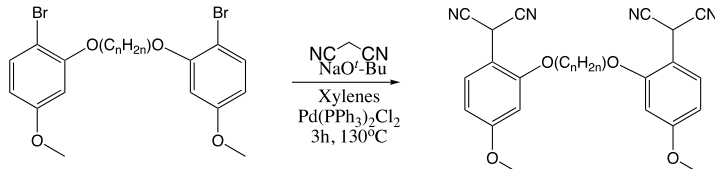


3-aminophenol (2.18 g, 20 mmol), 1-bromo-3-chloropropane (9.42 g, 60 mmol), sodium carbonate (7.42 g, 70 mmol), and 20 mL DMF were added to a round bottom flask and refluxed for 24 h. The reaction mixture was cooled to room temperature, filtered and extracted with DCM (250 mL). The organic phase was washed with brine (5×150 mL) and dried with Na_2SO_4 . Flash chromatography purification after evaporation gave the product as white solid (2.46 g, 65%). 1H NMR (500 MHz, Chloroform-*d*) δ (ppm) 6.70 (d, *J* = 8.0 Hz, 1H), 6.10 (d, *J* = 8.0 Hz, 1H), 4.56(s, 1H), 3.15-3.13 (m, 4H), 2.75-2.69 (m, 4H), 2.05-1.99 (m, 4H); ^{13}C NMR (126 MHz, $CDCl_3$) δ (ppm) 151.78, 144.00, 126.79, 114.39, 107.89, 102.99, 50.27, 49.60, 27.25, 22.42, 21.65, 21.01.

8-hydroxyljulolidine (1.89g, 10mmol) was dissolved in 20 mL acetic acid, and bromine (0.51 mL, 10 mmol) mixed with 10 mL acetic acid was added dropwise at 0°C. The mixture was warmed to room temperature for 1h. Acetic acid was removed by evaporation. The pH was changed to 8 with saturated sodium carbonate solution. The mixture was extracted with DCM (3×100 mL). The organic phase was dried with Na_2SO_4 . Flash chromatography purification after evaporation gave the product as yellow solid (1.66 g, 62%). 1H NMR (500 MHz, Chloroform-*d*) δ (ppm) 6.93 (s, 1H), 3.87 (t, *J* = 6.6 Hz, 2H), 3.10 (q, *J* = 5.5 Hz, 5H), 2.77 (t, *J* = 6.5 Hz, 2H), 2.68 (t, *J* = 6.6 Hz, 2H), 2.16 – 1.81 (m, 8H).

9-bromo-8-hydroxyljulolidine (1.34 g, 5mmol) 1,5-dibromopentane (0.58 g, 2.5mmol), potassium carbonate (1.38 g, 10 mmol), and acetone (10 mL) were added into a round bottom flask. The mixture was refluxed for 24 h. After filtration and evaporation, flash chromatography purification after evaporation gave the product as white solid (1.24 g, 52%). 1H NMR (500 MHz, Chloroform-*d*) δ (ppm) 6.93 (s, 2H), 3.87 (t, *J* = 6.6 Hz, 4H), 3.10 (q, *J* = 5.5 Hz, 8H), 2.77 (t, *J* = 6.5 Hz, 4H), 2.68 (t, *J* = 6.6 Hz, 4H), 2.16 – 1.81 (m, 12H); ^{13}C NMR (126 MHz, $CDCl_3$) δ (ppm) 151.92, 143.15, 129.99, 119.03, 116.68, 102.12, 72.42, 49.83, 49.52, 30.05, 27.24, 22.68, 22.33, 21.95, 21.56.

General procedure for Coupling of Malononitrile to Aryl Bromide:



To a dried 50 mL three-neck round bottom flask, which was equipped with a magnetic stirring bar, was added malononitrile (0.21 mL, 3.8 mmol), $\text{NaO}'\text{Bu}$ (0.644 g, 6.7 mmol) and xylenes (10 mL) and stirred under a nitrogen atmosphere for 0.5 h at room temperature. 1,6-bis(2-bromo-5-methoxyphenoxy)hexane (0.486 g, 1mmol) and $\text{Pd}(\text{PPh}_3)_2\text{Cl}_2$ (0.100 g) were added and the reaction was stirred at 130 °C for 3 h. The reaction mixture was cooled down to room temperature and quenched by 10% HCl aqueous solution. The resulting mixture was filtered through celite and extracted with CH_2Cl_2 (3×50 mL). The organic layers were combined and dried with Na_2SO_4 , and the solvent was removed by rotary evaporation. The crude product was purified by chromatography on silica gel (hexane: CH_2Cl_2 = 1:1 as eluent) to afford **6CS** (0.124 g, 27%).

6O: ^1H NMR (600 MHz, CDCl_3) δ (ppm) 7.40 (d, J = 8.5 Hz, 2H), 6.57 (dd, J = 8.5, 2.4 Hz, 2H), 6.53 (d, J = 2.4 Hz, 2H), 5.18 (s, 2H), 4.10 (t, J = 6.2 Hz, 4H), 3.86 (s, 6H), 1.94 (t, J = 6.4 Hz, 4H), 1.66 – 1.62 (m, 4H); ^{13}C NMR (151 MHz, CDCl_3) δ (ppm) 162.8, 156.7, 129.3, 112.2, 106.9, 105.3, 99.7, 68.5, 55.7, 28.9, 25.7, 23.2. HRMS(ESI). Calcd. for $[\text{C}_{26}\text{H}_{26}\text{N}_4\text{O}_4 - \text{H}]^-$: 457.1881. Found: 457.1886. m.p. 67 – 72°C.

5O: The general procedure produced a white solid (0.098 g, 22%). ^1H NMR (600MHz, CDCl_3) δ (ppm) 7.38 – 7.41 (m, 2H), 6.55 – 6.58 (m, 2H), 6.53 – 6.54 (m, 2H), 5.20 – 5.21 (m, 2H), 4.12 (td, J = 6.0, 1.7 Hz, 4H), 3.85 – 3.87 (m, 6H), 1.96 – 2.00 (m, 4H), 1.81 – 1.85 (m, 2H); ^{13}C NMR (151 MHz, CDCl_3) δ 162.3, 156.7, 129.4, 112.4, 106.7, 105.1, 99.6, 68.5, 55.7, 28.8, 23.4, 23.1. HRMS(ESI). Calcd. for $[\text{C}_{25}\text{H}_{24}\text{N}_4\text{O}_4 - \text{H}]^-$: 443.1725. Found: 443.1729. m.p. 84 – 92°C.

4O: The general procedure produced a white solid (0.104 g, 24%). ^1H NMR (600 MHz, CD_3CN) δ (ppm) 7.39 (d, J = 8.5 Hz, 2H), 6.70 (d, J = 2.4 Hz, 2H), 6.64 (dd, J = 8.5, 2.4 Hz, 2H), 5.47 (s, 2H), 4.24 – 4.26 (m, 4H), 3.85 (s, 6H), 2.13 – 2.15 (m, 4H); ^{13}C NMR (151 MHz, CD_3CN) δ (ppm) 162.7, 157.1, 129.9, 113.1, 107.3, 105.5, 99.6, 68.3, 55.4, 25.5, 23.5. HRMS(ESI). Calcd. for $[\text{C}_{24}\text{H}_{22}\text{N}_4\text{O}_4 - \text{H}]^-$: 429.1568. Found: 429.1570. m.p. 158 – 163°C.

3O: The general procedure produced a pink solid (0.087 g, 21%). ^1H NMR (600 MHz, CDCl_3) δ (ppm) 7.36 (d, J = 8.5 Hz, 2H), 6.63 (d, J = 2.4 Hz, 2H), 6.58 (dd, J = 8.5, 2.4 Hz, 2H), 5.10 (s, 2H), 4.40 (t, J = 6 Hz, 4H), 3.84 (s, 6H), 2.49 (p, J = 6 Hz, 2H); ^{13}C NMR (151MHz, CD_3CN) δ (ppm) 162.8, 156.9, 129.8, 113.1, 107.4, 105.9, 99.6, 65.4, 55.4, 28.6, 23.5. HRMS(ESI). Calcd. For $[\text{C}_{23}\text{H}_{20}\text{N}_4\text{O}_4 - \text{H}]^-$: 415.1412. Found: 415.1417. m.p. 147 – 153°C.

2O: The general procedure produced a red solid (0.062 g, 15%). ^1H NMR (600MHz, CDCl_3) δ (ppm) 7.45 (d, $J = 8.6$ Hz, 2H), 6.64 (dd, $J = 8.6, 2.4$ Hz, 2H), 6.60 (d, $J = 2.4$ Hz, 2H), 5.26 (s, 2H), 4.52 (s, 4H), 3.89 (s, 6H); ^{13}C NMR (151MHz, CDCl_3) δ (ppm) 162.8, 156.1, 129.6, 112.1, 107.2, 105.7, 99.9, 66.6, 55.7, 23.4. HRMS(ESI). Calcd. for $[\text{C}_{22}\text{H}_{18}\text{N}_4\text{O}_4 - \text{H}]^-$: 401.1255. Found: 401.1257. m.p. 145 – 149°C.

6P: The general procedure produced a pale pink solid (0.069 g, 17%). ^1H NMR (600 MHz, CDCl_3) δ (ppm) 7.42 (dd, $J = 6.5, 2.2$ Hz, 4H), 7.00 (dd, $J = 6.5, 2.2$ Hz, 4H), 5.04 (s, 2H), 4.03 (t, $J = 6.4$ Hz, 4H), 1.86 – 1.89 (m, 4H), 1.58 – 1.60 (m, 4H); ^{13}C NMR (151MHz, CDCl_3) δ (ppm) 160.5, 128.6, 117.7, 115.9, 112.1, 68.1, 29.0, 27.5, 25.8. HRMS(ESI). Calcd. for $[\text{C}_{24}\text{H}_{22}\text{N}_4\text{O}_2 - \text{H}]^-$: 397.1670. Found: 397.1675. m.p. 92 – 96 °C.

5P: The general procedure produced a red solid (0.104 g, 28%). ^1H NMR (600MHz, CDCl_3) δ (ppm) 7.42 (dd, $J = 6.5, 2.2$ Hz, 4H), 7.00 (dd, $J = 6.5, 2.2$ Hz, 4H), 5.04 (s, 2H), 4.05 (t, $J = 6.3$ Hz, 4H), 1.90 – 1.94 (m, 4H), 1.68 – 1.73 (m, 2H); ^{13}C NMR (151 MHz, CDCl_3) δ 160.5, 128.6, 117.8, 115.9, 112.1, 68.0, 28.8, 27.5, 22.7. HRMS(ESI). Calcd. for $[\text{C}_{23}\text{H}_{20}\text{N}_4\text{O}_2 - \text{H}]^-$: 385.1513. Found: 385.1520. m.p. 60 – 63°C.

4P: The general procedure produced a red solid (0.067 g, 18%). ^1H NMR (600 MHz, CDCl_3) δ (ppm) 7.43 (dd, $J = 6.5, 2.2$ Hz, 4H), 7.00 (dd, $J = 6.5, 2.2$ Hz, 4H), 5.03 (s, 2H), 4.10 – 4.12 (m, 4H), 2.04 – 2.05 (m, 4H); ^{13}C NMR (151 MHz, CDCl_3) δ (ppm) 160.4, 128.6, 117.9, 115.9, 112.0, 67.7, 27.5, 25.8. HRMS(ESI). Calcd. for $[\text{C}_{22}\text{H}_{18}\text{N}_4\text{O}_2 - \text{H}]^-$: 369.1357. Found: 369.1359. m.p. 166 – 169 °C.

3P: The general procedure produced a red solid (0.043 g, 12%). ^1H NMR (600 MHz, CDCl_3) δ (ppm) 7.43 (d, $J = 8.7$ Hz, 4H), 7.03 (d, $J = 8.7$ Hz, 4H), 5.03 (s, 2H), 4.23 (t, $J = 6$ Hz, 4H), 2.34 (p, $J = 6$ Hz, 2H); ^{13}C NMR (151MHz, CDCl_3) δ (ppm) 160.2, 128.7, 118.1, 115.9, 112.0, 64.5, 29.0, 27.5. HRMS(ESI). Calcd. for $[\text{C}_{21}\text{H}_{16}\text{N}_4\text{O}_2 - \text{H}]^-$: 355.1200. Found: 355.1205. m.p. 98 – 112 °C.

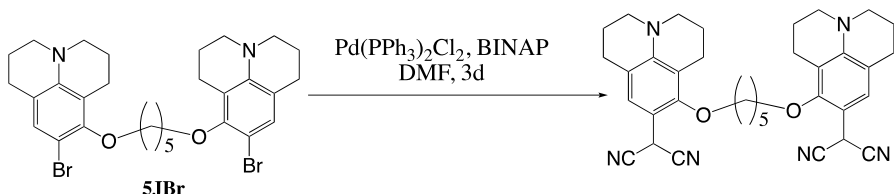
2P: Added PCy₃ (0.157 g, 56%) as ligand. The reaction mixture was refluxed for 48 h. After purification, the product was obtained as a red solid (0.055 g, 16%). ^1H NMR (600 MHz, CDCl_3) δ (ppm) 7.47 (d, $J = 8.8$ Hz, 4H), 7.08 (d, $J = 8.8$ Hz, 4H), 5.05 (s, 2H), 4.41 (s, 4H); ^{13}C NMR (151 MHz, CDCl_3) δ (ppm) 159.9, 128.7, 118.6, 116.1, 112.0, 66.6, 27.5. HRMS(ESI). Calcd. for $[\text{C}_{20}\text{H}_{14}\text{N}_4\text{O}_2 - \text{H}]^-$: 341.1044. Found: 341.1045. m.p. 140 – 143°C.

6O-DMA: The general procedure produced a blue solid (0.058 g, 12%). ^1H NMR (500 MHz, Chloroform-*d*) δ (ppm) 7.28 (d, $J = 8.7$ Hz, 2H), 6.33 (dd, $J = 8.7, 2.5$ Hz, 2H), 6.23 (d, $J = 2.4$ Hz, 2H), 5.15 (s, 2H), 4.12 (t, $J = 6.3$ Hz, 4H), 3.03 (s, 12H), 1.95 (s, 4H), 1.67 (s, 4H); ^{13}C NMR (126 MHz, CDCl_3) δ 156.7, 153.3, 128.9, 112.7, 104.5, 101.4, 95.8, 68.0, 40.4, 29.1, 25.7, 23.1. HRMS(ESI). Calcd. for $[\text{C}_{28}\text{H}_{32}\text{N}_6\text{O}_2 - \text{H}]^-$: 483.2514. Found: 483.2519. m.p. 148 – 150 °C.

5O-DMA: The general procedure produced a purple solid (0.099 g, 21%). ^1H NMR (500 MHz, Chloroform-*d*) δ (ppm) 7.27 (d, $J = 8.7$ Hz, 2H), 6.34 (d, $J = 2.4$ Hz, 2H), 6.24(s, 2H), 5.16 (s, 2H), 4.16 (t, $J = 6.1$ Hz, 5H), 3.03 (s, 12H), 2.00 (t, $J = 7.5$ Hz, 4H), 1.84 (p, $J = 8.0$ Hz, 2H); ^{13}C

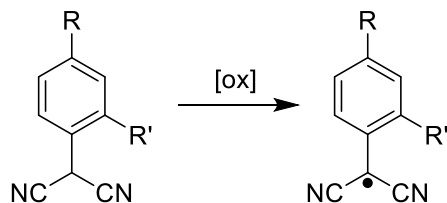
NMR (126 MHz, CDCl₃) δ (ppm) 156.7, 153.3, 129.0, 112.8, 104.5, 101.4, 95.8, 68.1, 40.4, 28.9, 23.3, 22.9. HRMS(ESI). Calcd. for [C₂₇H₃₀N₆O₂ + H]⁺: 471.2503. Found: 471.2507. m.p. 95 – 102 °C.

4O-DMA: The general procedure produced a purple solid (0.068 g, 15%). ¹H NMR (500 MHz, Chloroform-*d*) δ (ppm) 7.27 (d, *J* = 8.3 Hz, 2H), 6.34 (dd, *J* = 8.5, 2.2 Hz, 2H), 6.25 (d, *J* = 2.5 Hz, 2H), 5.12 (s, 2H), 4.22 (s, 4H), 3.04 (d, *J* = 1.8 Hz, 12H), 2.19 (s, 4H); ¹³C NMR (126 MHz, CDCl₃) δ (ppm) 156.6, 153.3, 129.1, 112.6, 104.6, 95.8, 67.6, 40.4, 25.9, 23.3. HRMS(ESI). Calcd. for [C₂₆H₂₈N₆O₂ + H]⁺: 457.2347. Found: 457.2337. m.p. 205 – 209 °C.



5O-JUL: To a dried 50 mL three-neck round bottom flask, which was equipped with a magnetic stirring bar, was added malononitrile (0.21 mL, 3.8 mmol), NaO'Bu (0.644 g, 6.7 mmol) and DMF (10 mL) and stirred under a nitrogen atmosphere for 0.5 h at room temperature. 5O-JULBr (0.546 g, 1 mmol) Pd(PPh₃)₂Cl₂ (0.14g, 20%) and BINAP (0.124 g, 20%) were added and the reaction was refluxed for 3d. The reaction mixture was cooled down to room temperature and quenched by 10% HCl aqueous solution. The resulting mixture was filtered through celite and extracted with CH₂Cl₂ (3×50 mL). After extracted with DCM and evaporation, flash chromatography purification after evaporation gave the product as blue solid (0.024g, 5%).

5O-JUL: ¹H NMR (500 MHz, Chloroform-*d*) δ (ppm) 7.02 (s, 2H), 5.27 (s, 2H), 3.95 (t, *J* = 6.3 Hz, 4H), 3.27 (s, 8H), 2.81 (m, 2H), 2.07 (p, *J* = 6.2 Hz, 4H), 1.96 (p, *J* = 6.7 Hz, 2H), 1.89 – 1.63 (m, 2H). ¹³C NMR (126 MHz, CDCl₃) δ (ppm) 152.70, 141.86, 126.66, 122.06, 119.13, 112.69, 110.85, 73.37, 50.99, 50.62, 31.61, 29.93, 26.76, 22.92, 22.68, 22.51, 21.79, 20.69, 20.20, 14.16.



General Oxidation Procedure:

Quantities of each substrate for each oxidation often varied greatly but this general procedure scales without any detrimental effects. To a 50 mL round bottom flask was added 0.3 mmol of tethered substrate dissolved in 10 mL of dichloromethane. The flask was then sealed and purged on a Schlenk line to introduce nitrogen as an inert atmosphere. In a separate 25 mL round bottom flask was added 3 mmol of K₃[Fe(CN)₆]. The flask was then purged and 10 mL of 0.3 M KOH_(aq) was added. This mixture was allowed to mix for 5 minutes before transferal to the 50 mL round bottom. After mixing the oxidant with the substrate the reaction was allowed to proceed for 10-15 minutes. The mixture was exposed to air, extracted with dichloromethane (3 X 20 mL), dried with Na₂SO₄, and the solvent removed by rotary evaporation.

General Procedure for EPR Studies:

Variable temperature EPR studies were performed for each compound in order to understand the binding characteristics and thermodynamic properties for each system. For each sample studied, toluene or dichloromethane was added to the solid sample to make a 1-5 mM solution of radical/dimer species. This solution was then purged and cannulated into a pre-purged quartz EPR tube. EPR studies were then performed at 10 degrees increments (298-378 K for toluene and 208-298 K for dichloromethane) with an equilibration time of 5 minutes for each temperature increment. The following instrument parameters were generally followed for each sample; modulation frequency, 100 kHz; receiver gain, 50 dB; modulation amplitude, 0.5; time constant, 0.01 s; center field, 3330 G; sweep width, ~200 G; microwave attenuation, 20 dB; microwave power, 2 mW; number of data points, 2048; average number of scans, 15. Other parameters such as sweep time and conversion time varied from sample to sample depending on the signal received from each compound.

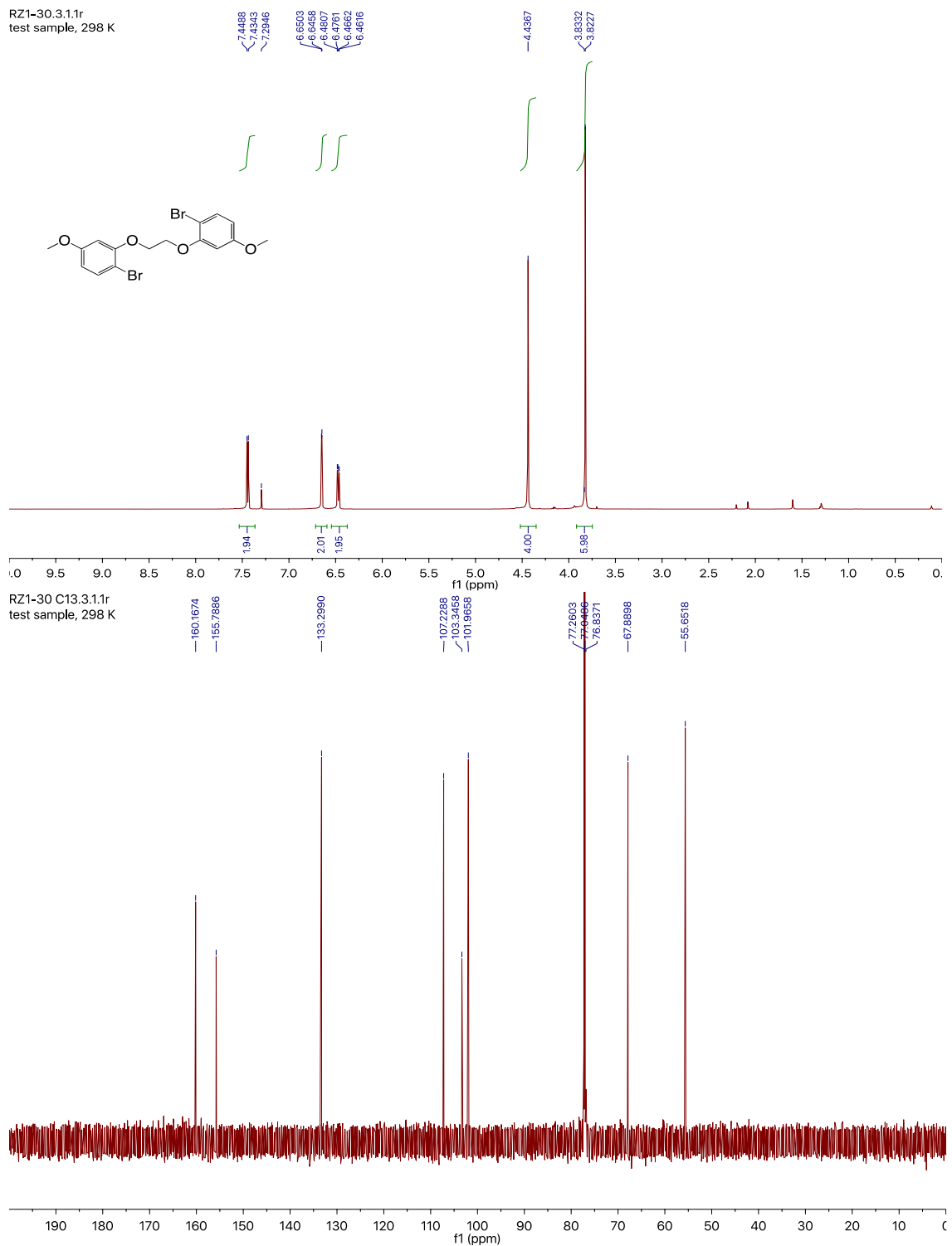
General Procedure for UV/Vis Studies:

Variable temperature UV/Vis studies were performed by dissolving each compound into a suitable solvent (mostly toluene), and using a circulating water bath as the medium for heating each sample. A representative sample for each different type of compound was investigated from 25-85° C.

NMR Spectra:

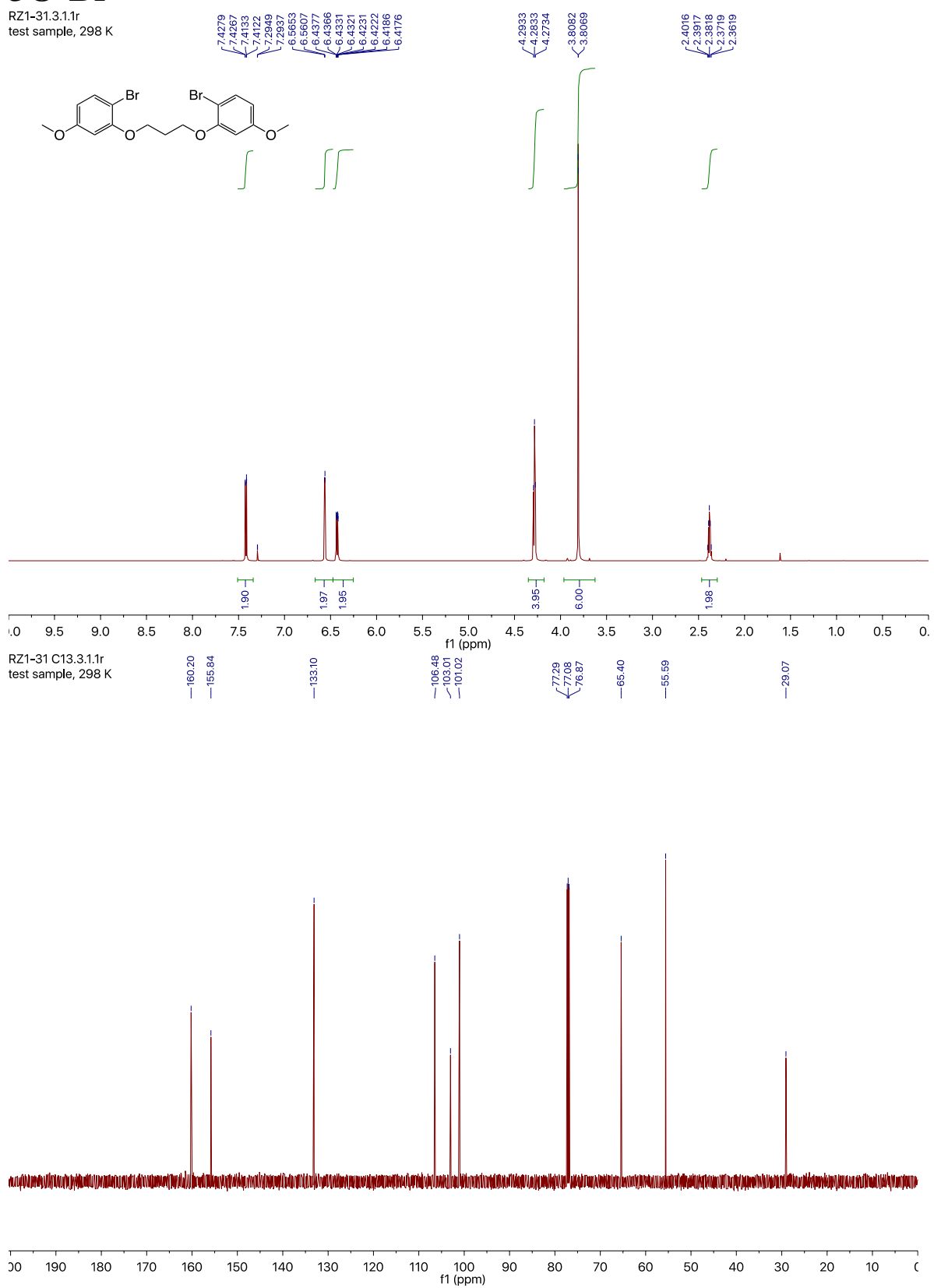
2O-Br

RZ1-30.3.1.1r
test sample, 298 K



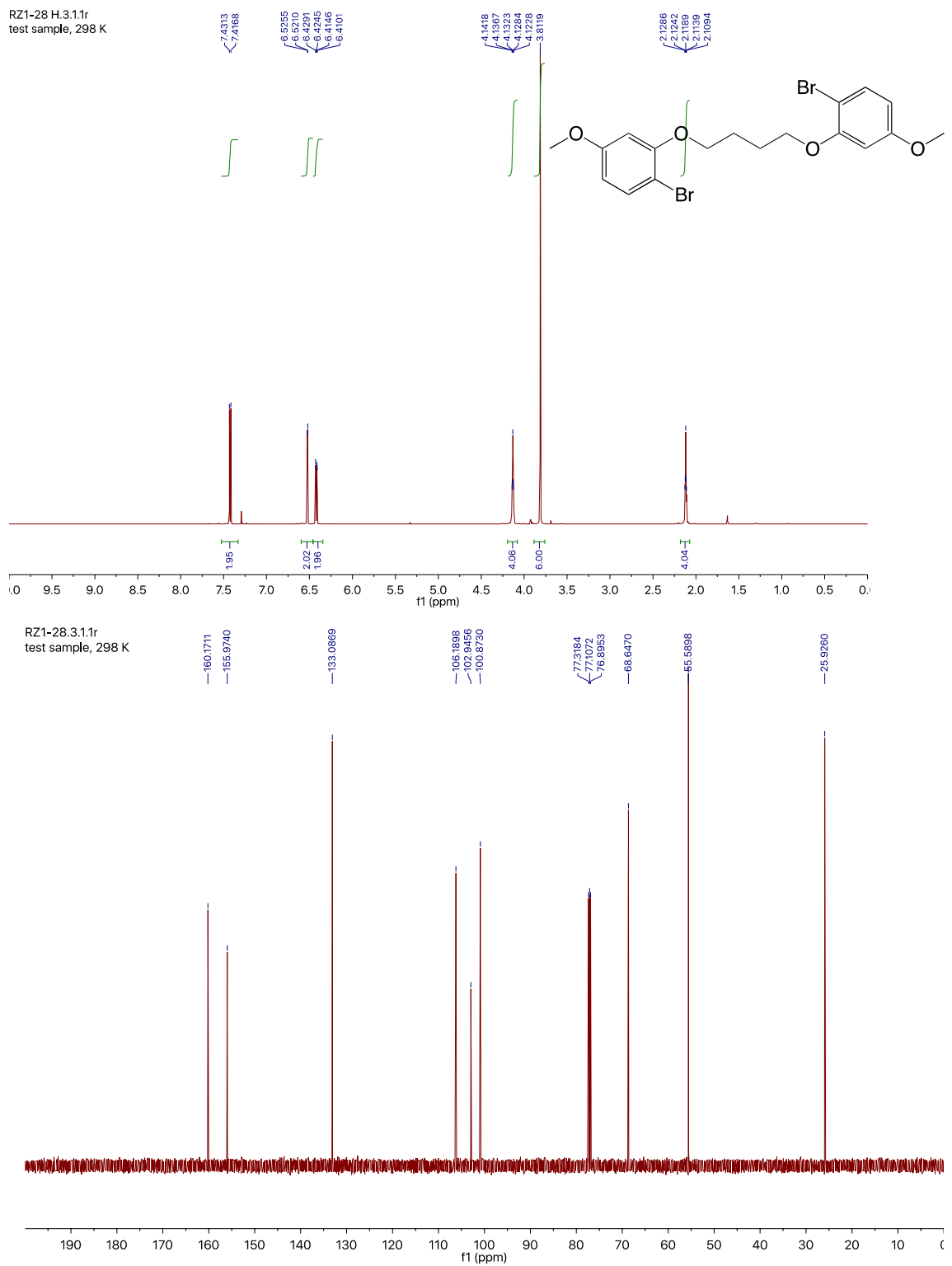
3O-Br

RZ1-31.3.1r
test sample, 298 K



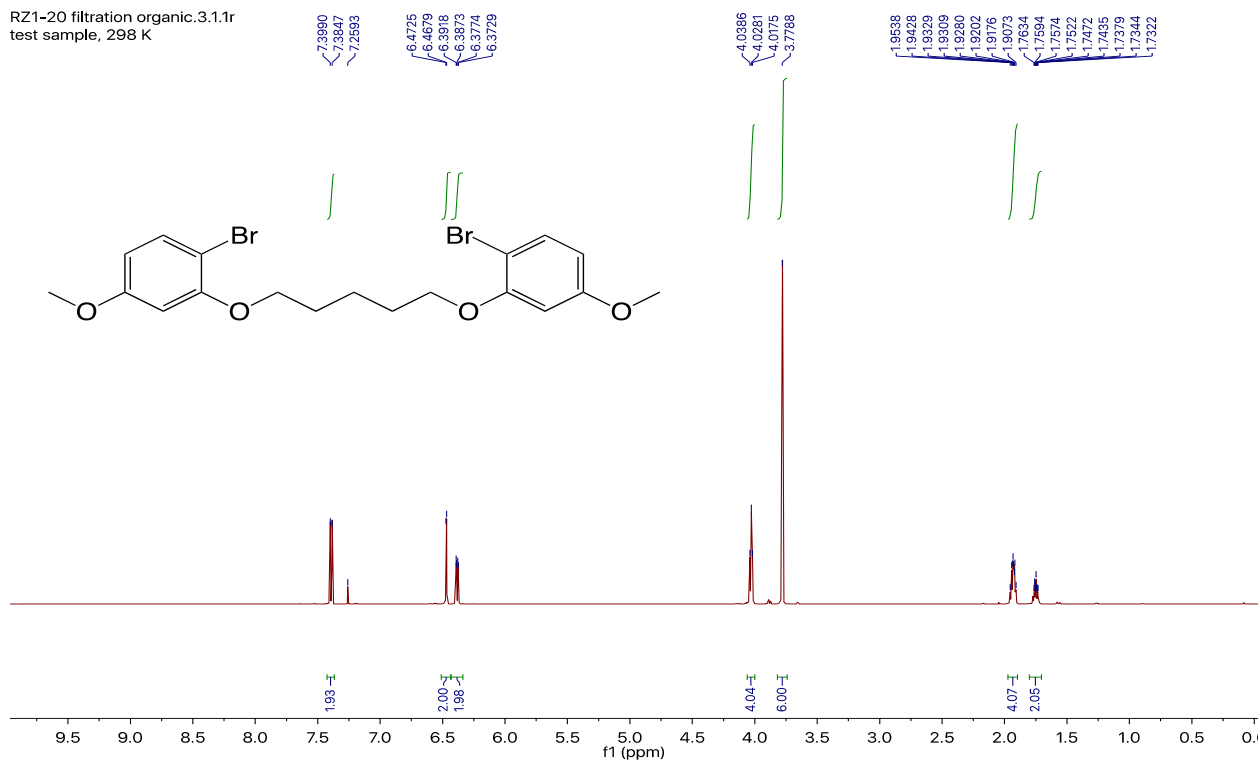
4O-Br

RZ1-28 H.3.1.1r
test sample, 298 K

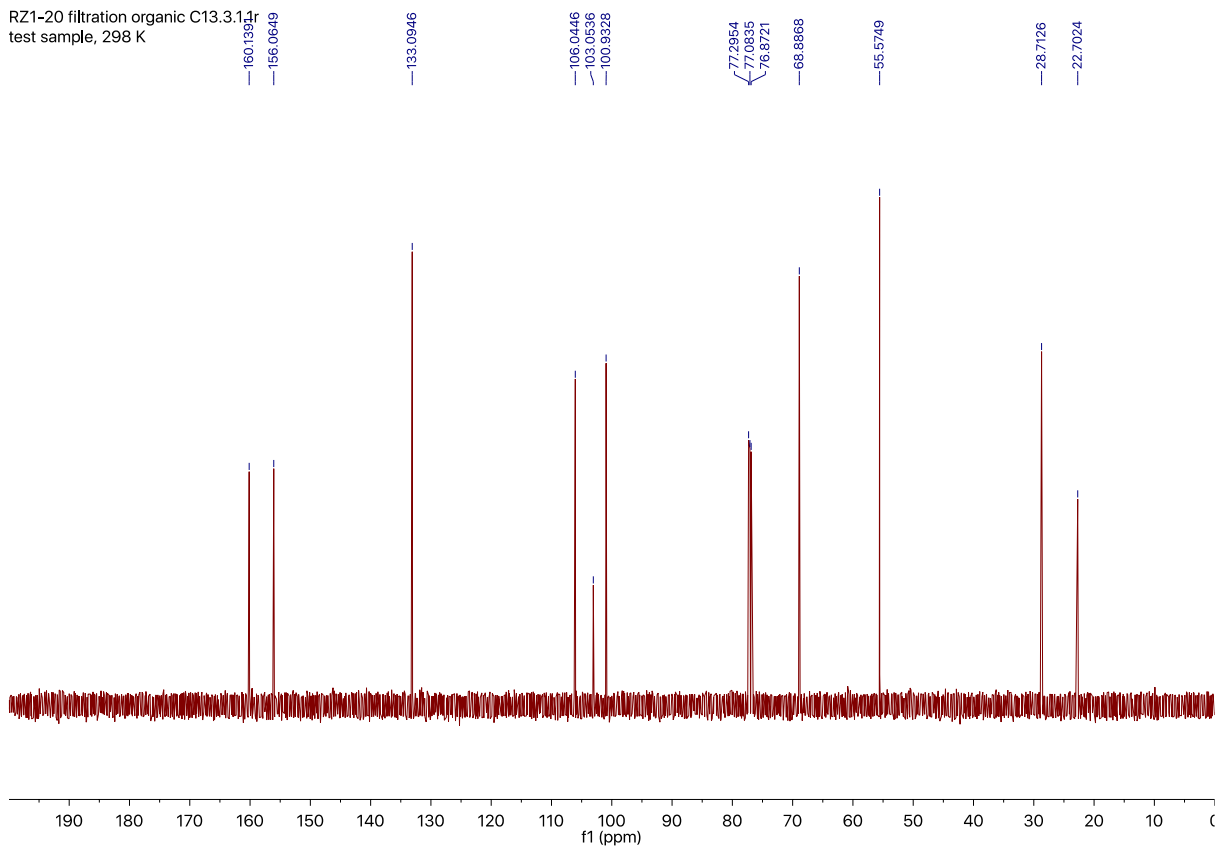


5O-Br

RZ1-20 filtration organic.3.1.1r
test sample, 298 K

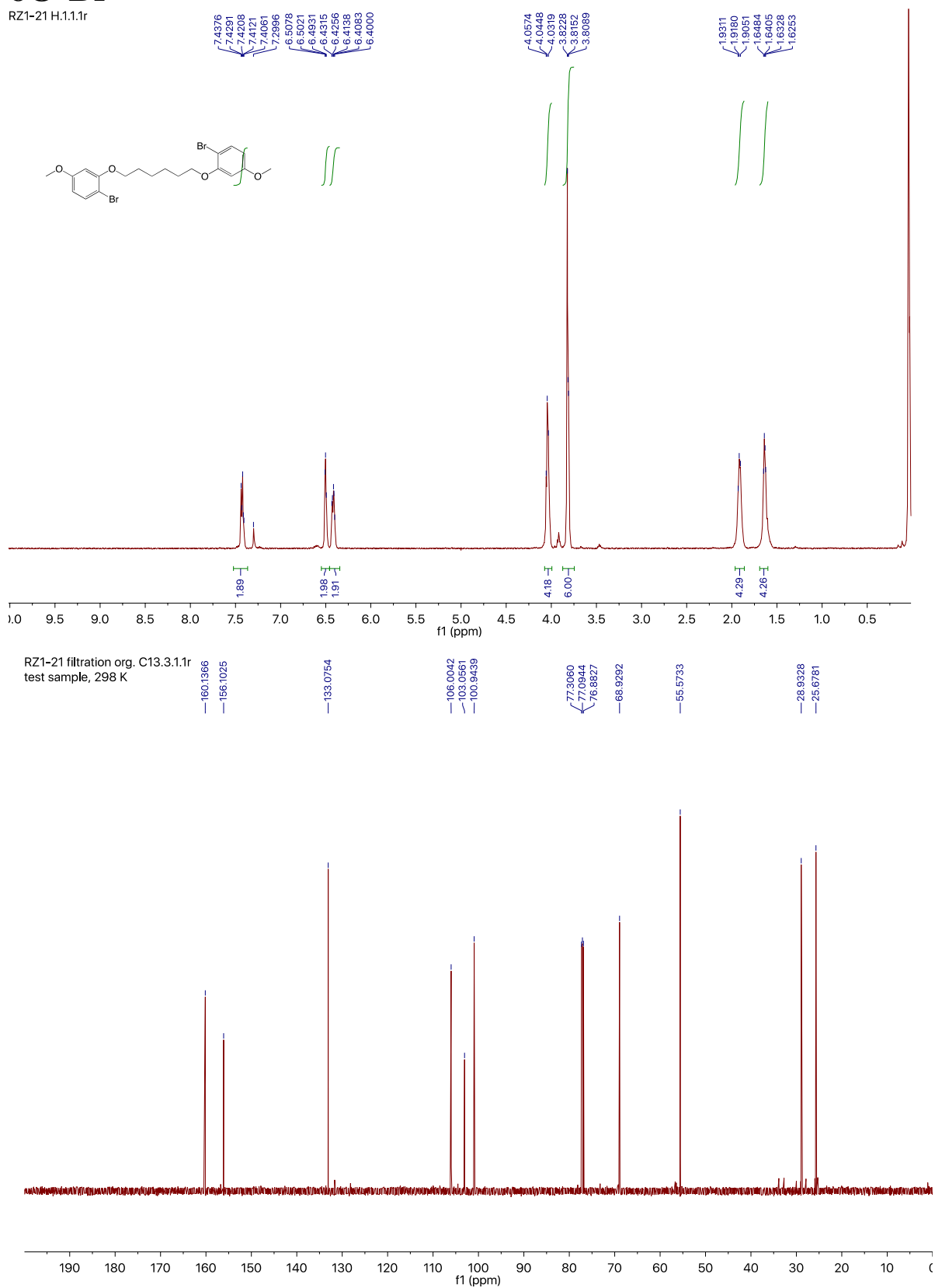


RZ1-20 filtration organic C13.3.1.1r
test sample, 298 K



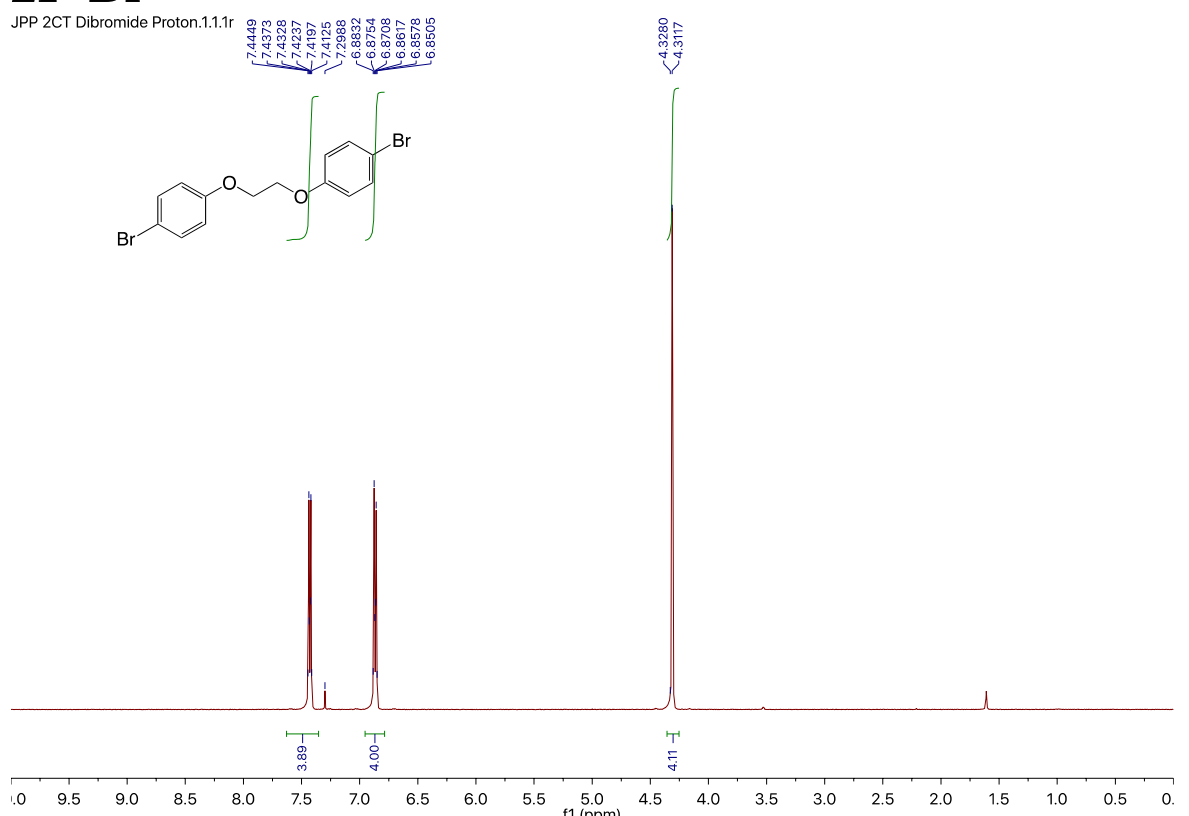
6O-Br

RZ1-21 H.1.1.1r

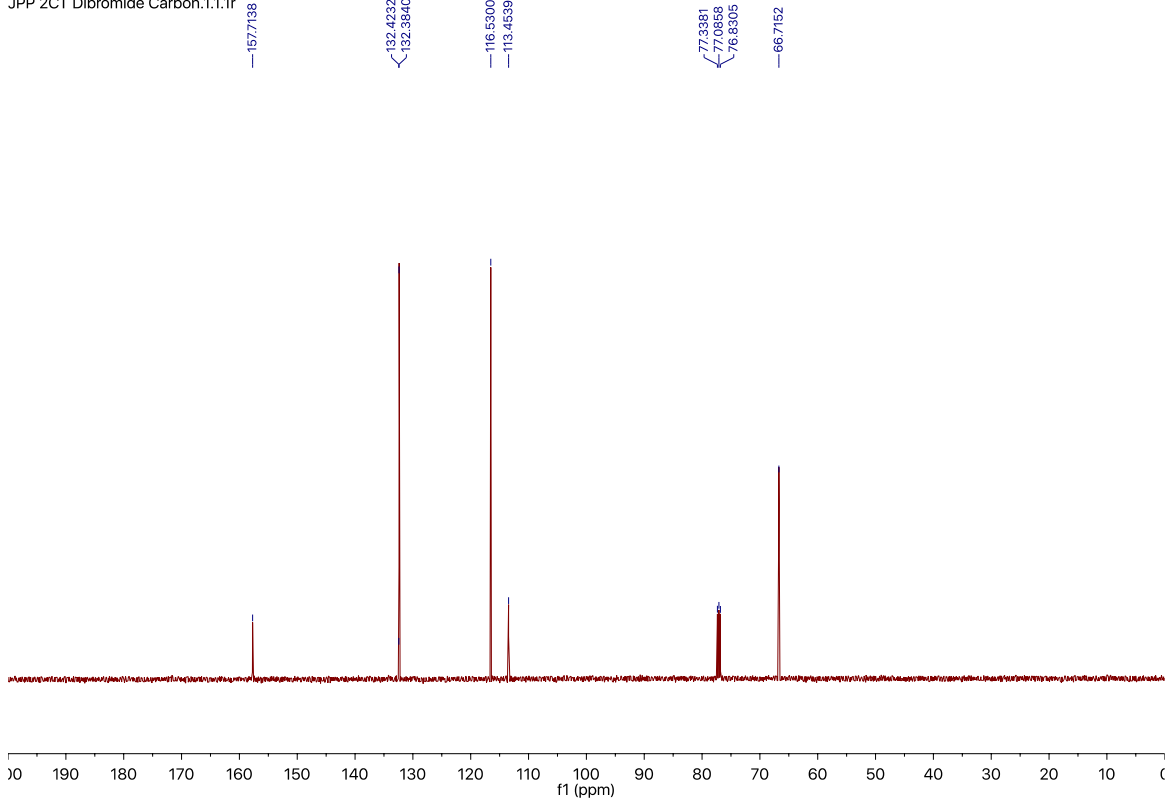


2P-Br

JPP 2CT Dibromide Proton.1.1.1r

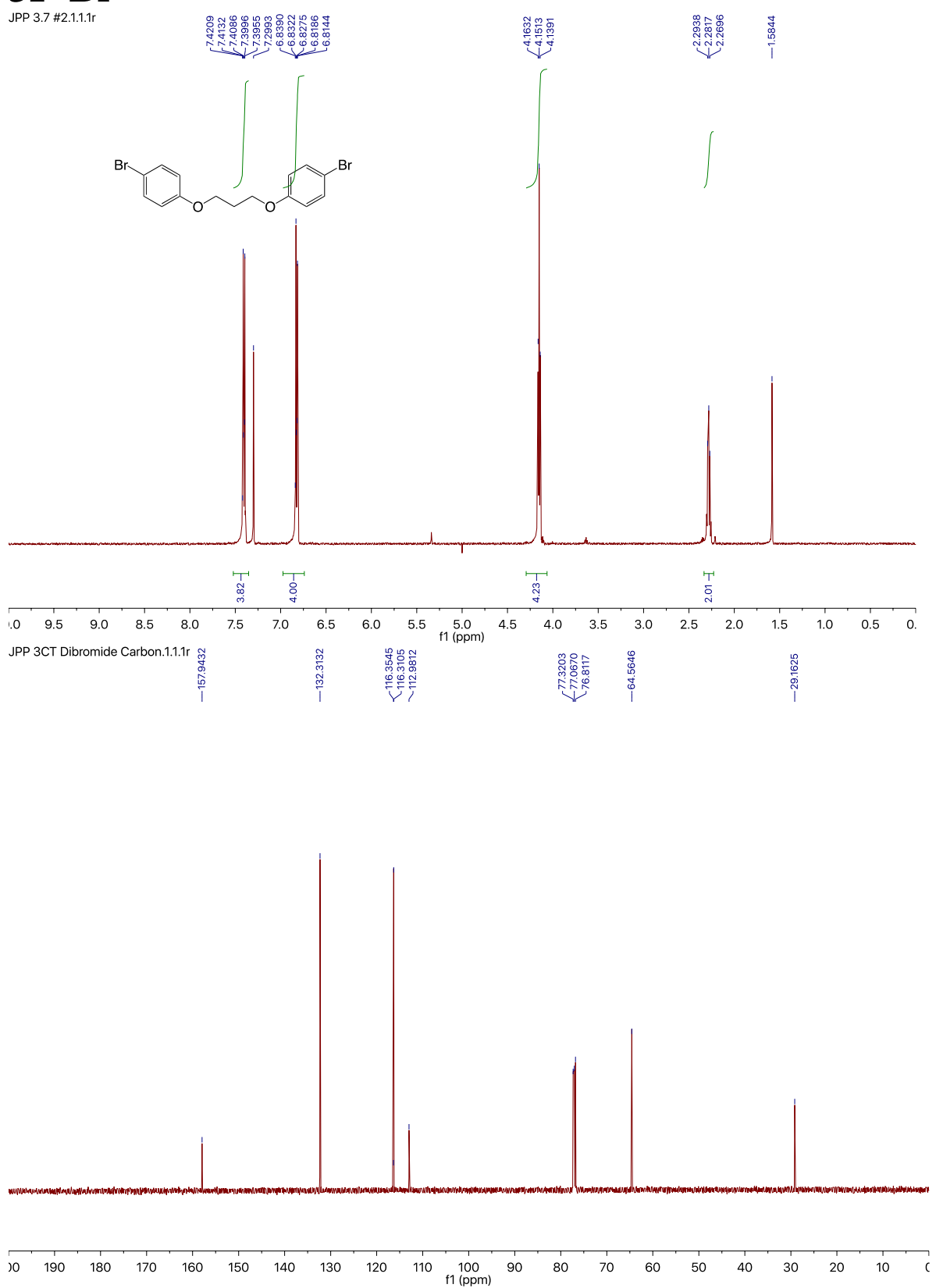


JPP 2CT Dibromide Carbon.1.1.1r



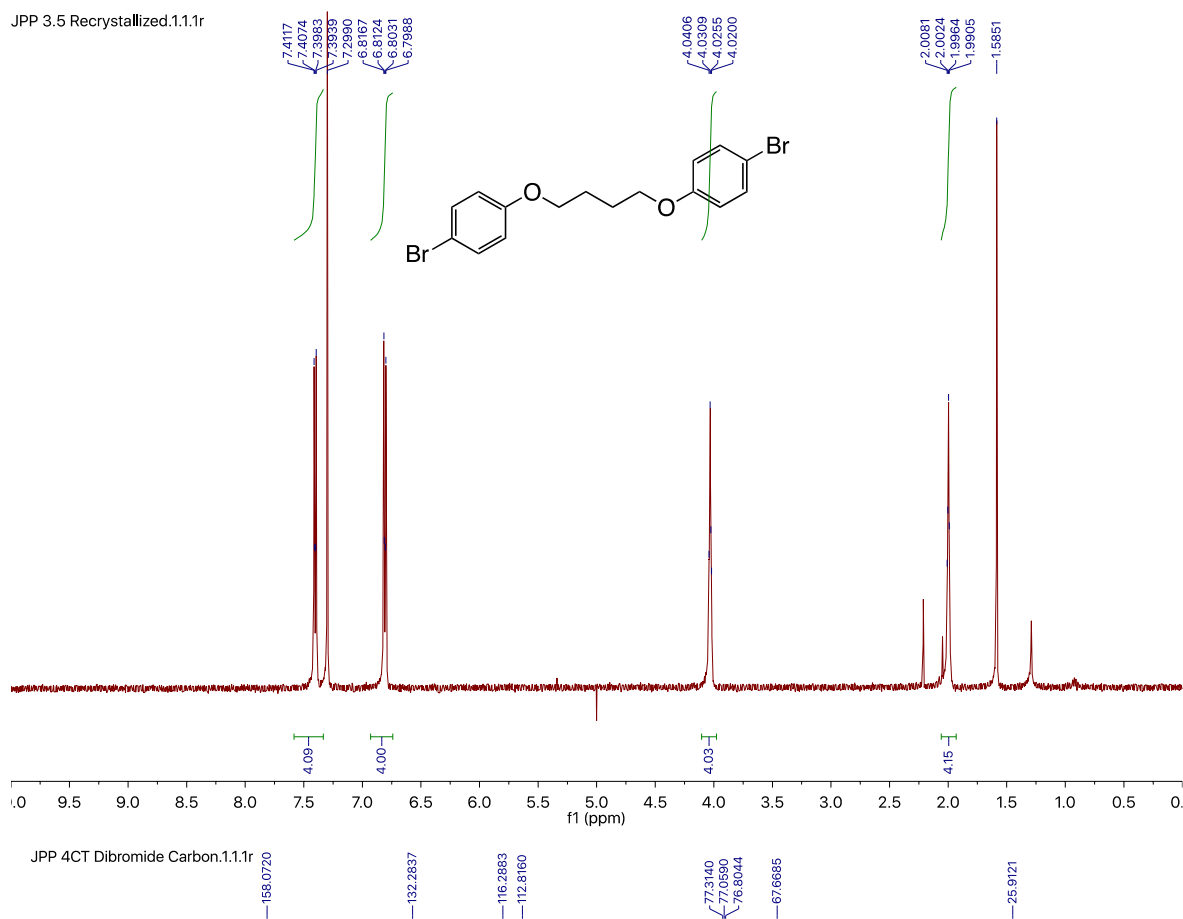
3P-Br

JPP 3.7 #2.1.1r

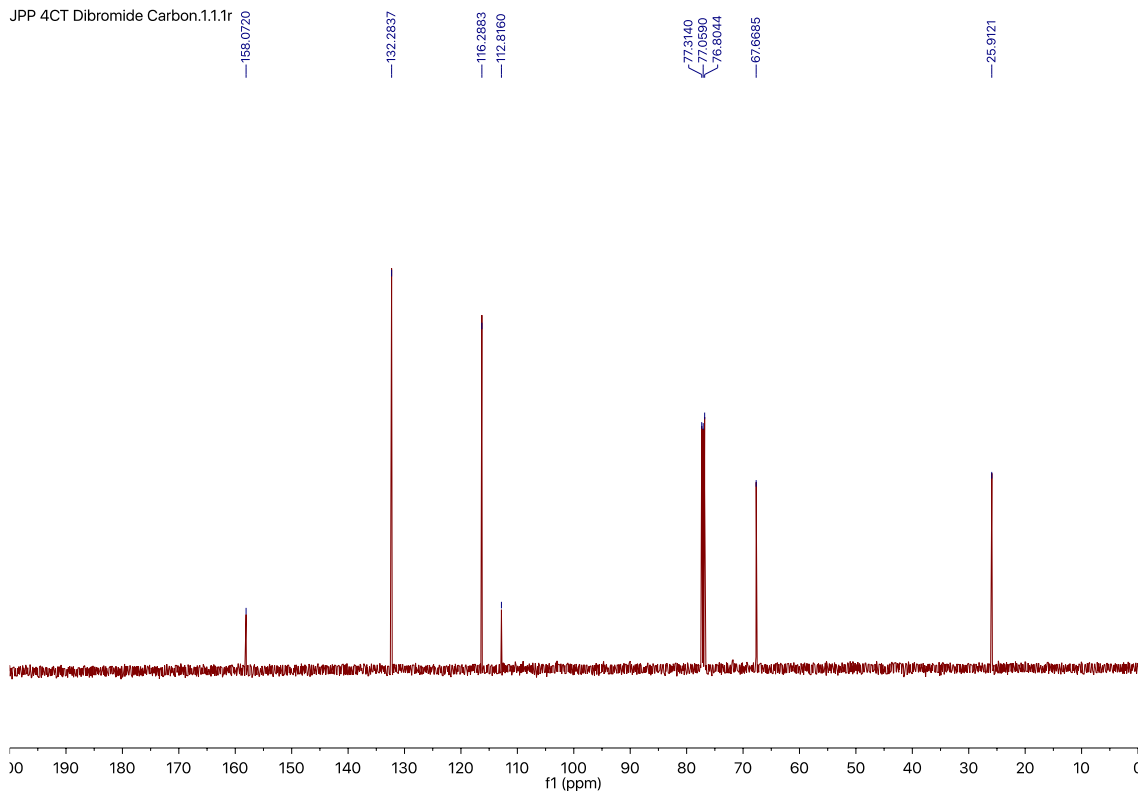


4P-Br

JPP 3.5 Recrystallized.1.1.1r

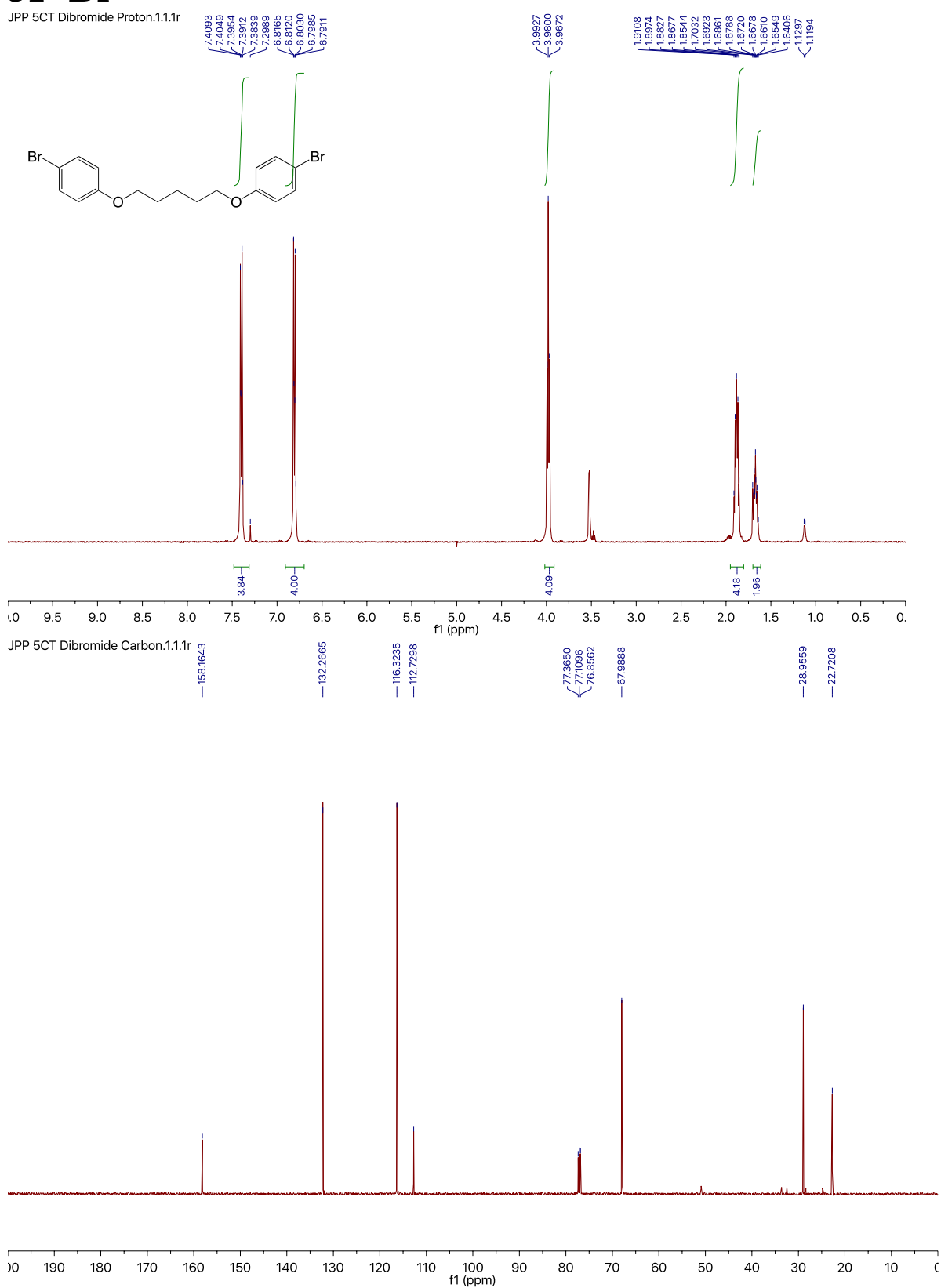


JPP 4CT Dibromide Carbon.1.1.1r



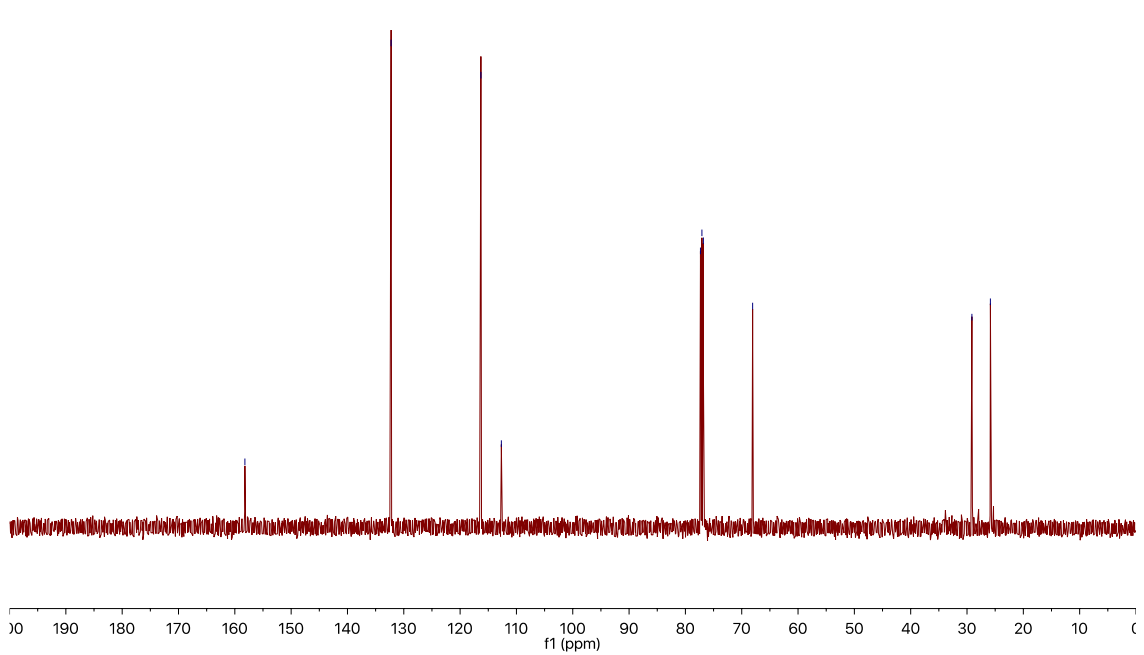
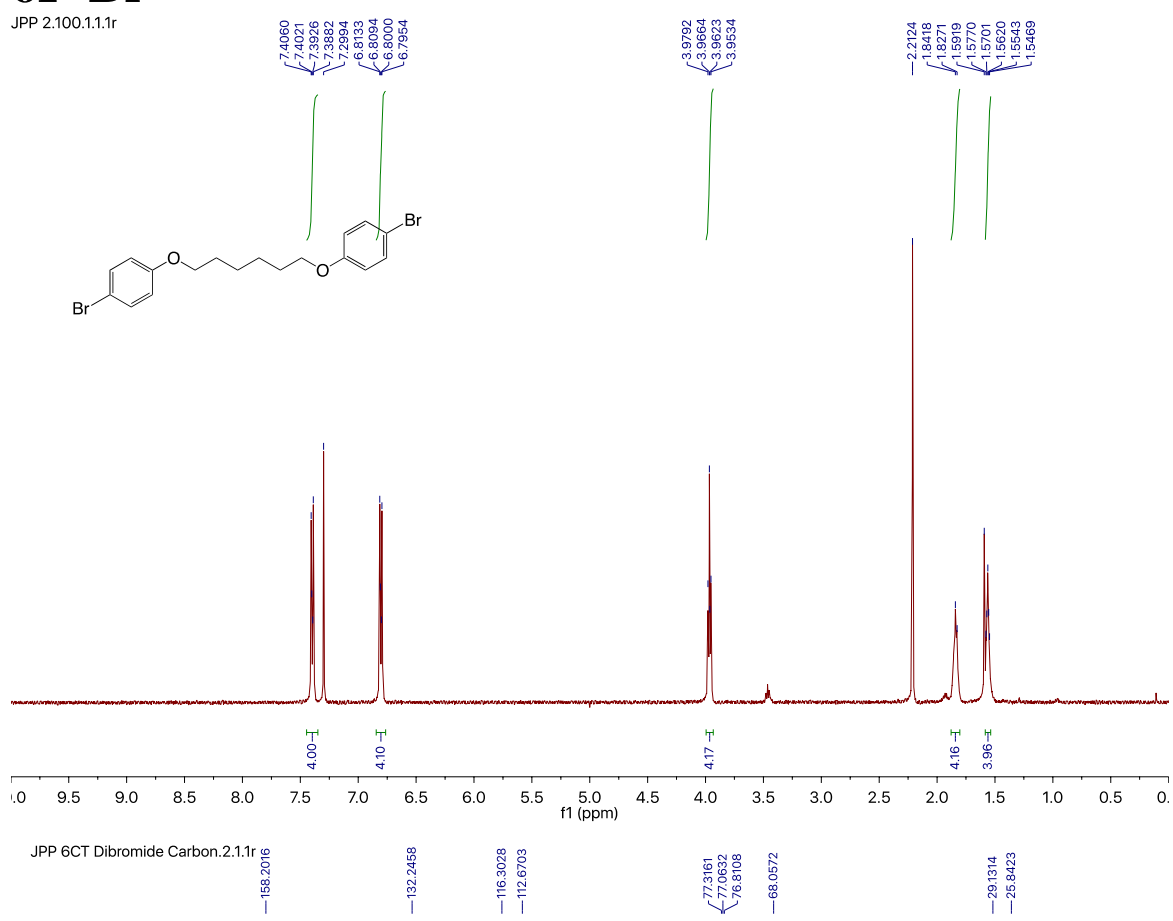
5P-Br

JPP 5CT Dibromide Proton.1.1.1r



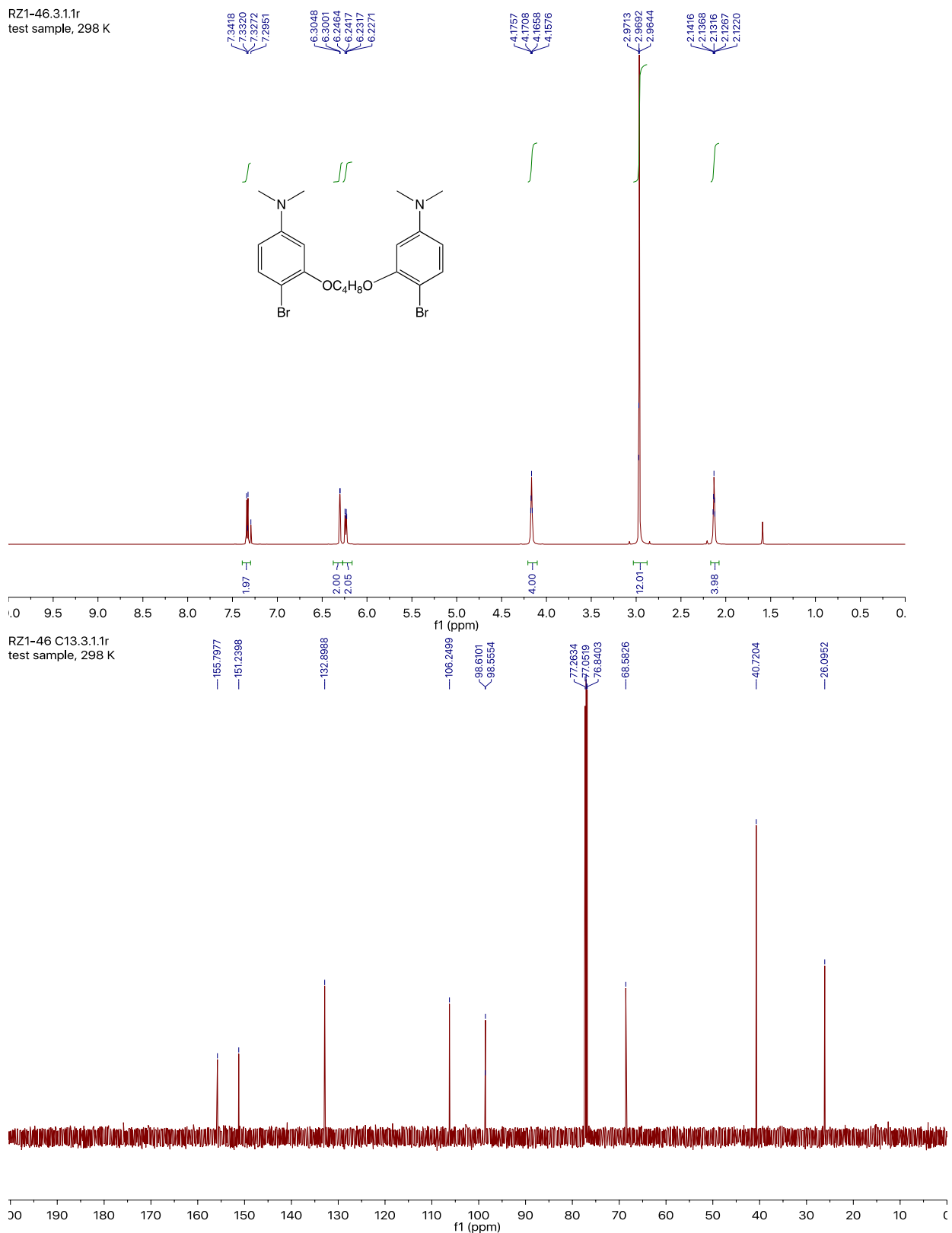
6P-Br

JPP 2.100.1.1.1r



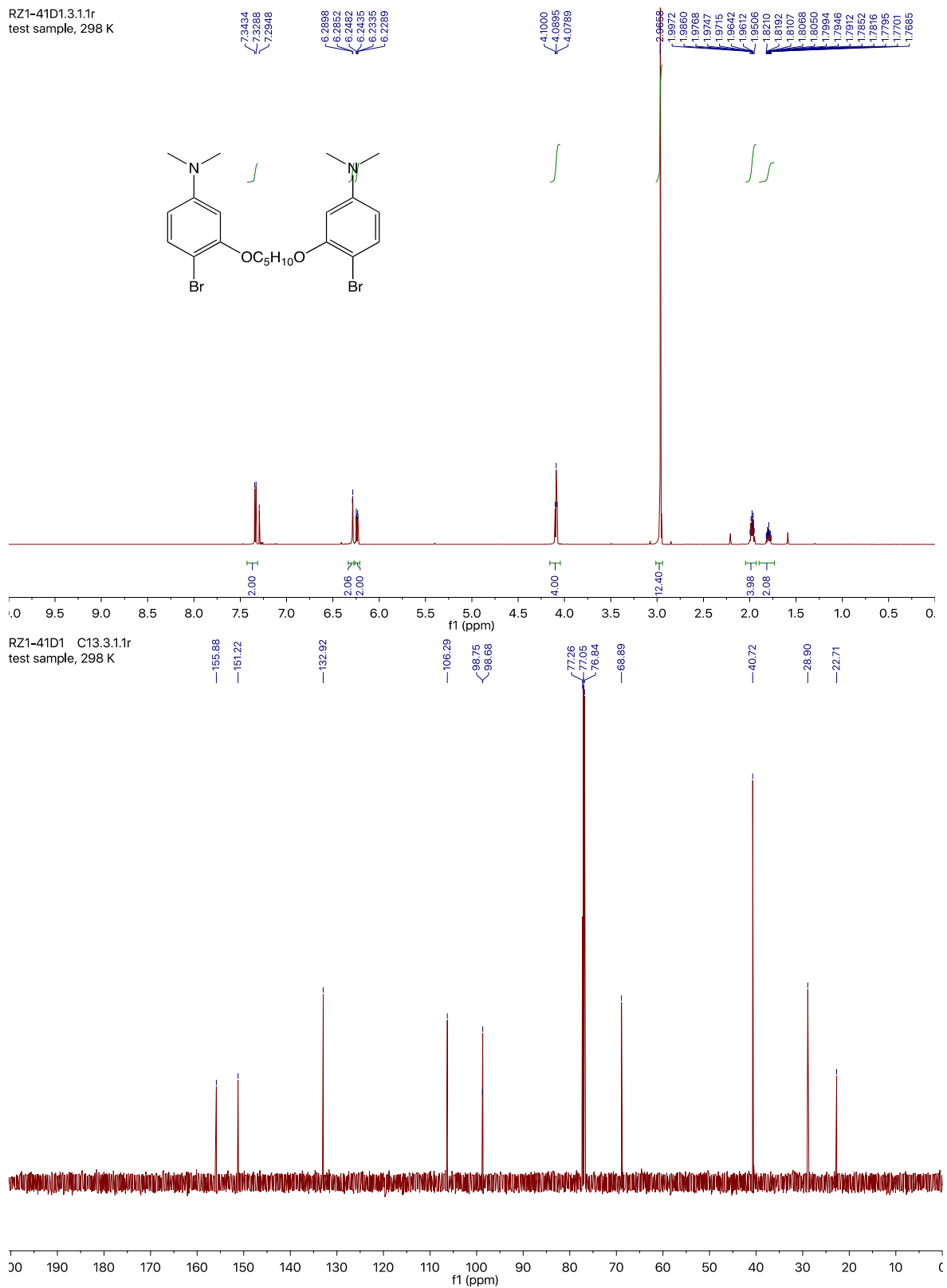
4O-DMA-Br

RZ1-46.3.1.1r
test sample, 298 K



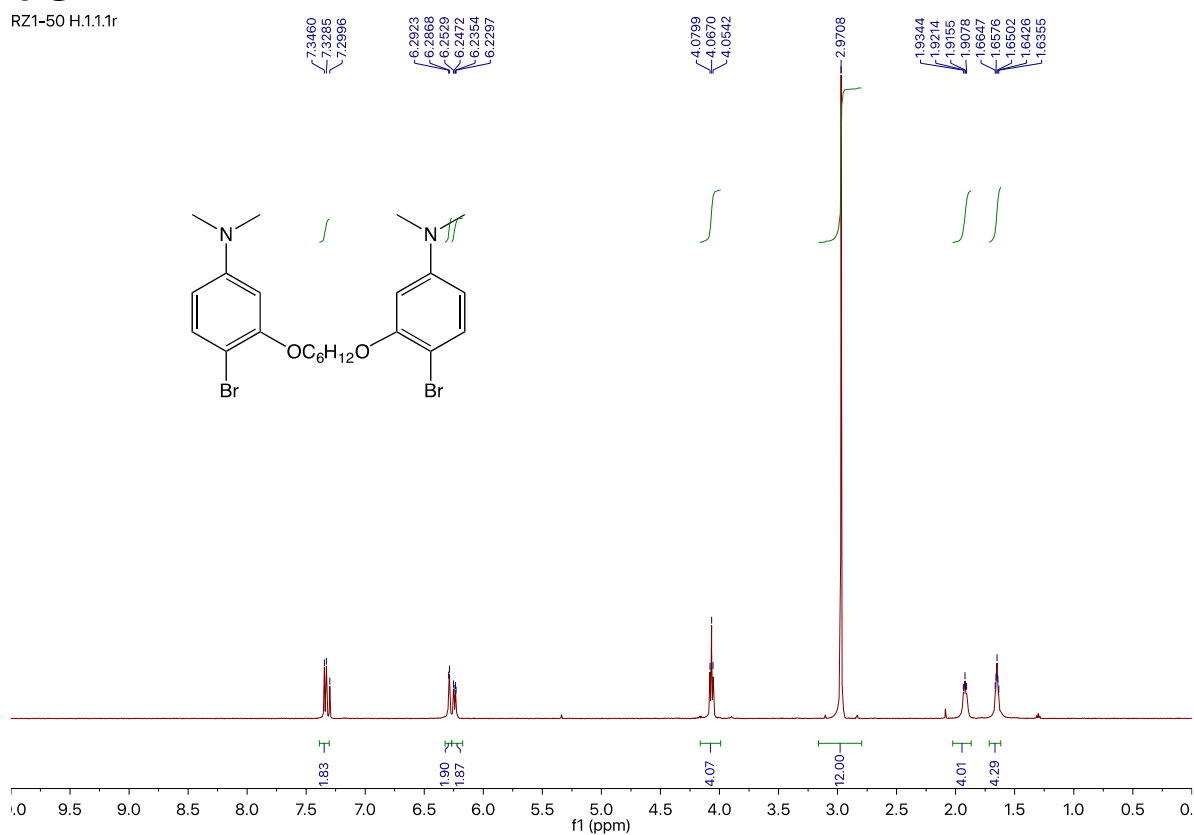
5O-DMA-Br

RZ1-41D1.3.1.1r
test sample, 298 K

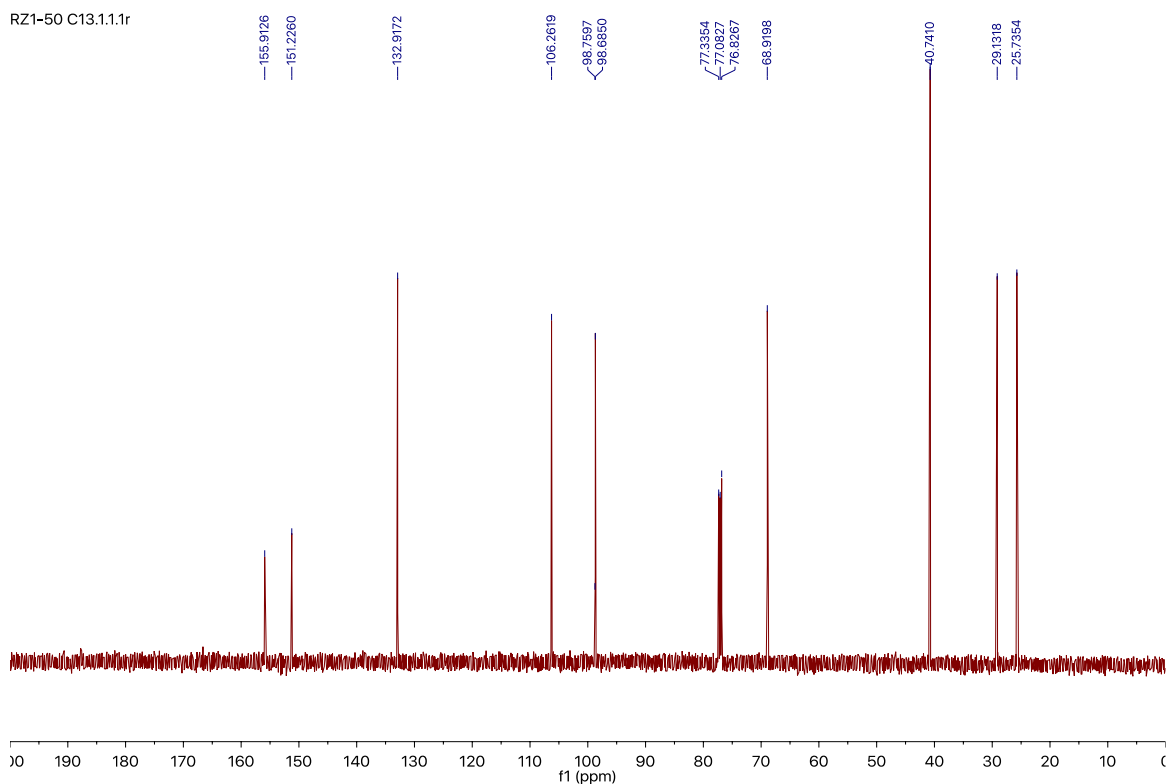


6O-DMA-Br

RZ1-50 H.1.1.1r

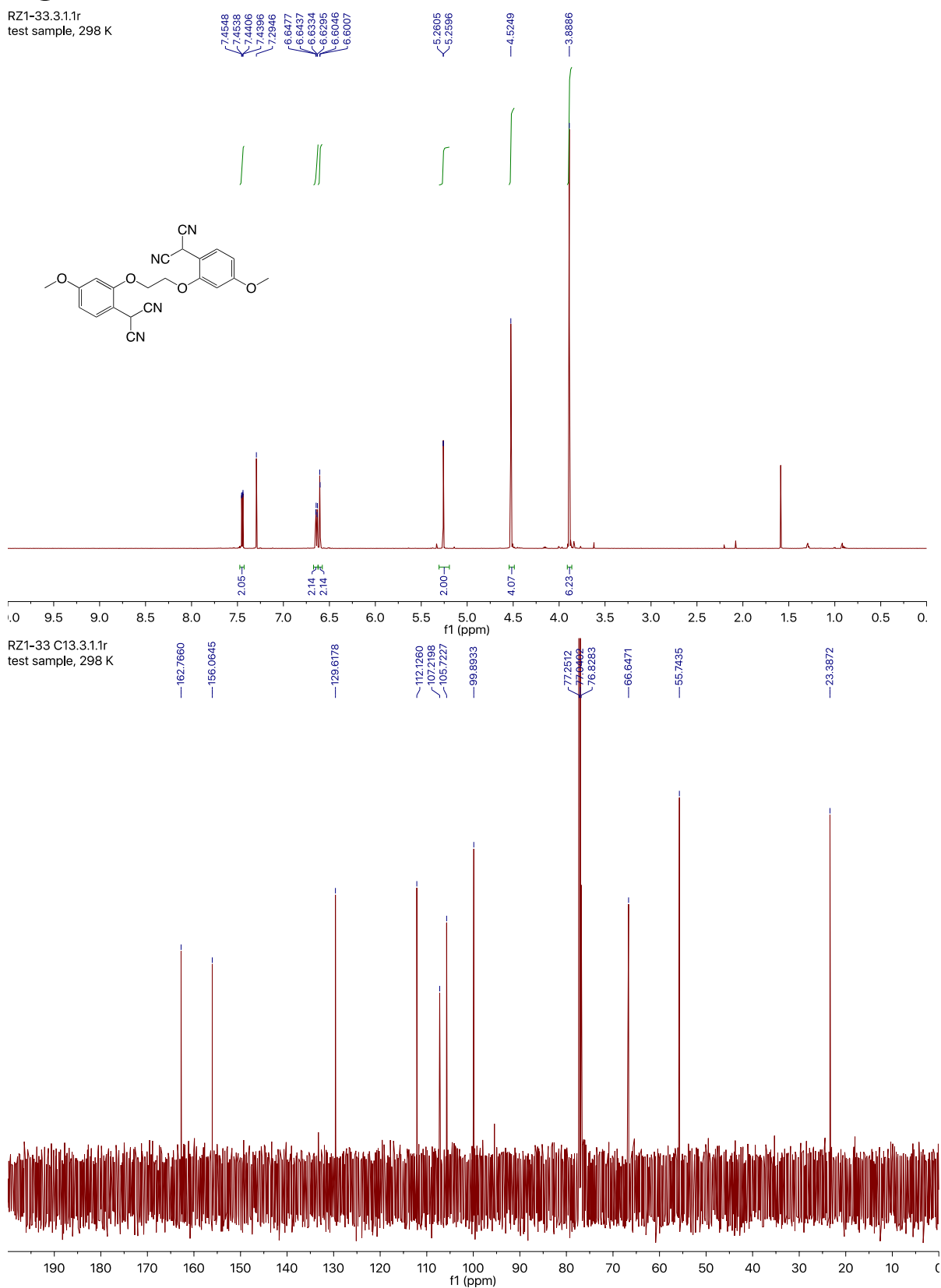


RZ1-50 C13.1.1.1r



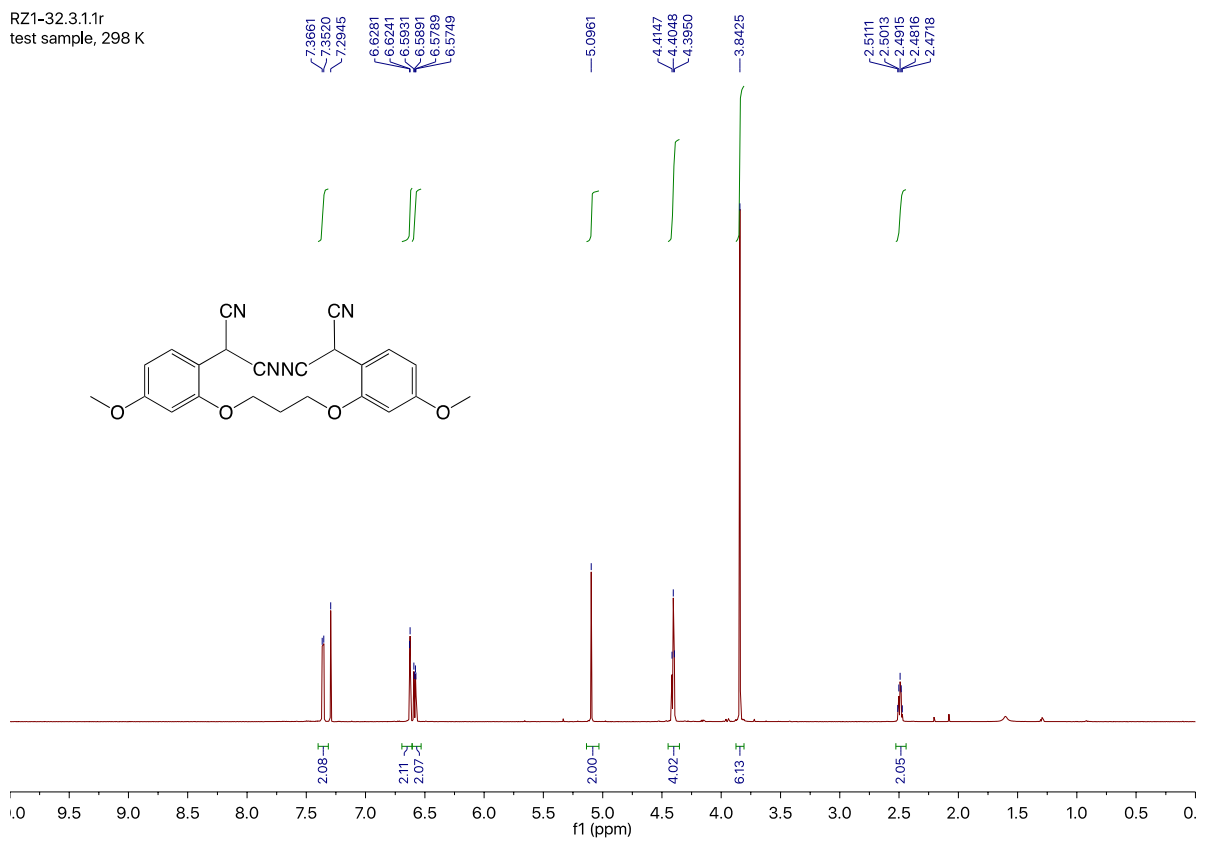
20

RZ1-33.3.1r
test sample, 298 K

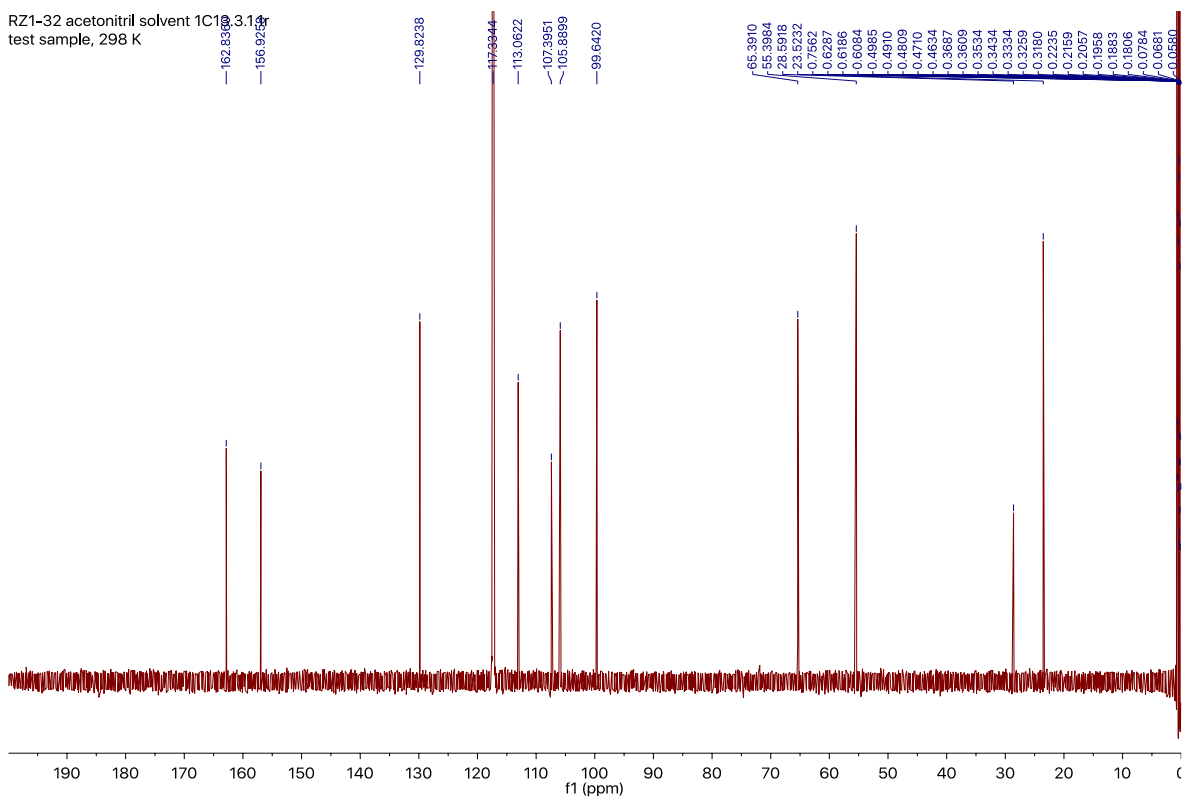


30

RZ1-32.3.1.1r
test sample, 298 K

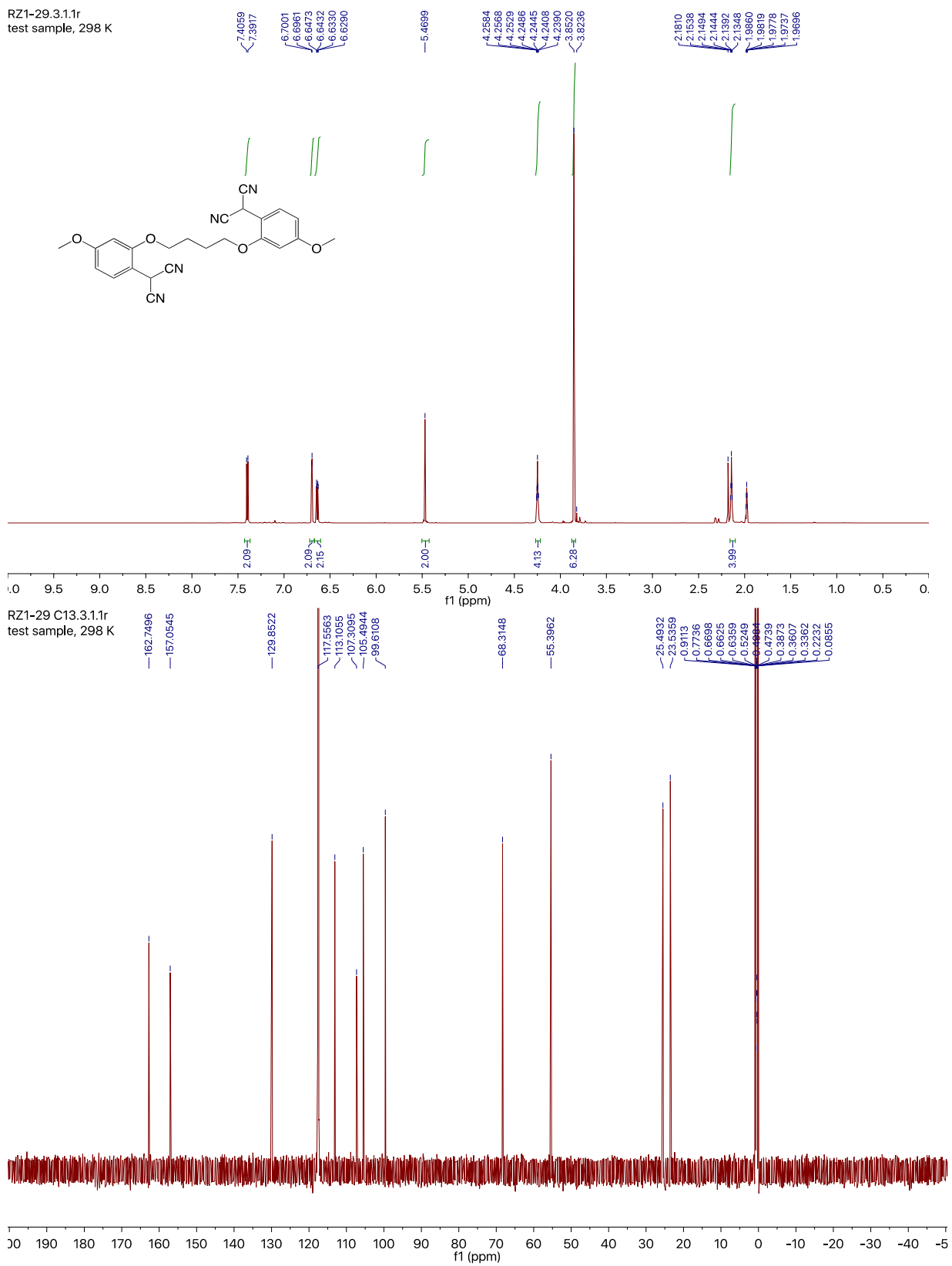


RZ1-32 acetonitril solvent 1C18.3.14r
test sample, 298 K



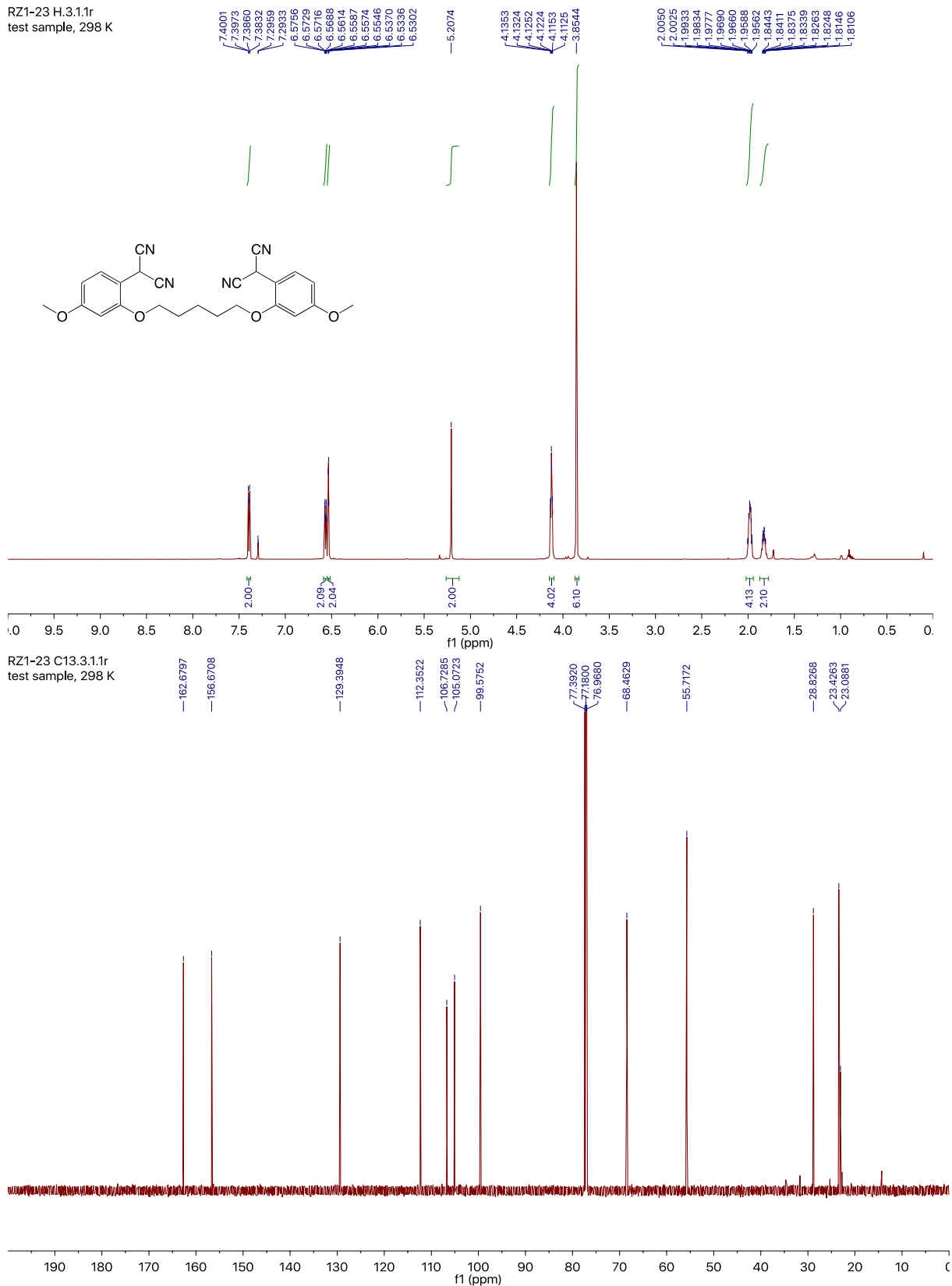
40

RZ1-29.3.1r
test sample, 298 K



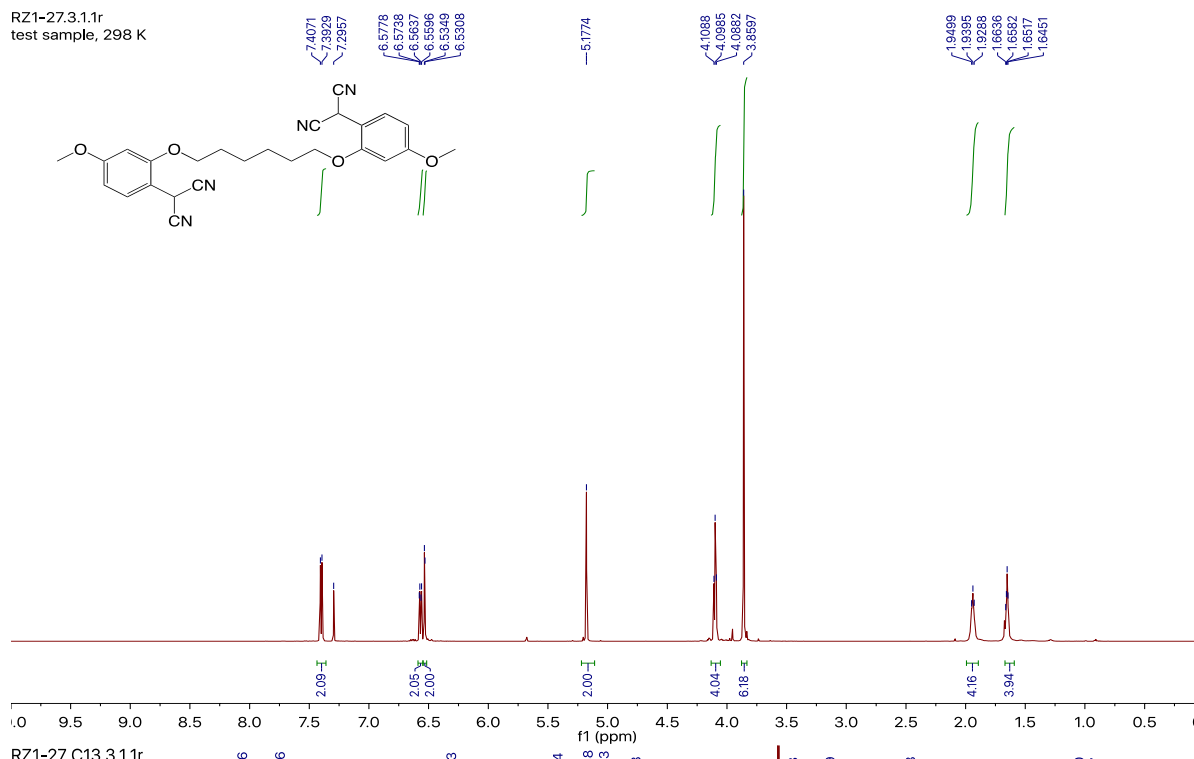
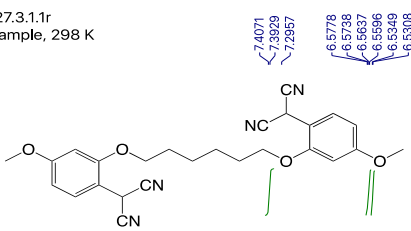
50

RZ1-23 H.3.1.1r
test sample, 298 K

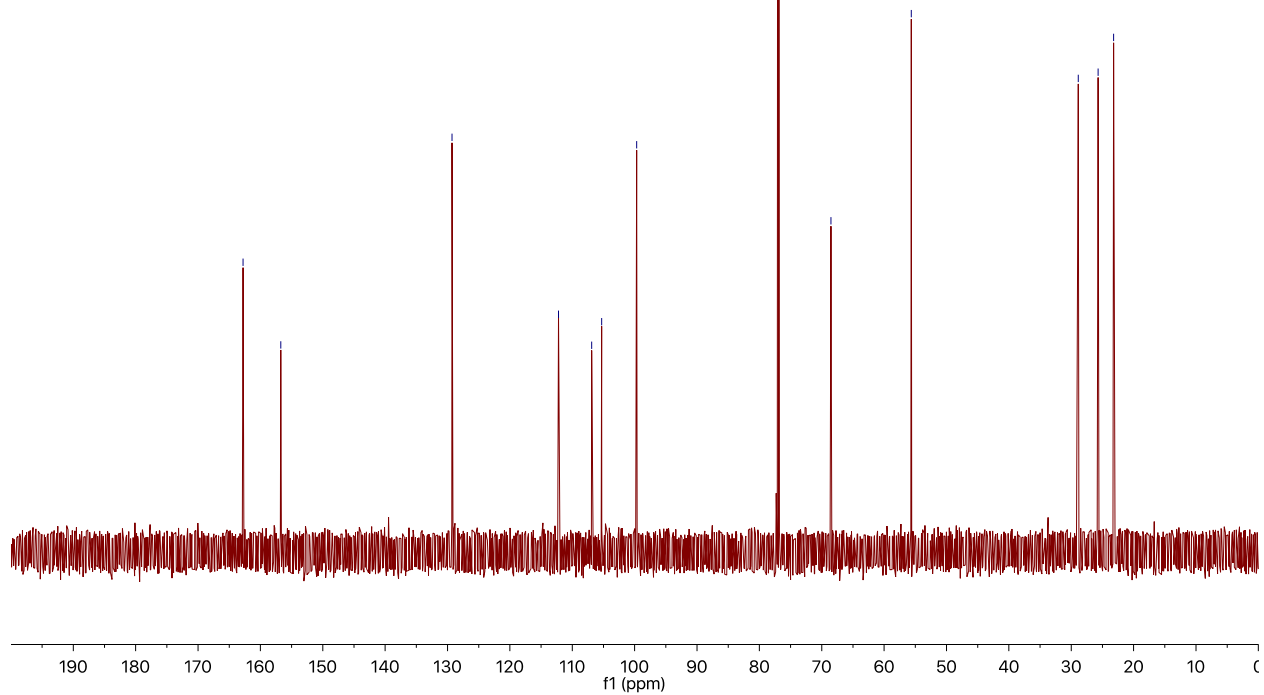


60

RZ1-27.3.1.1r
test sample, 298 K

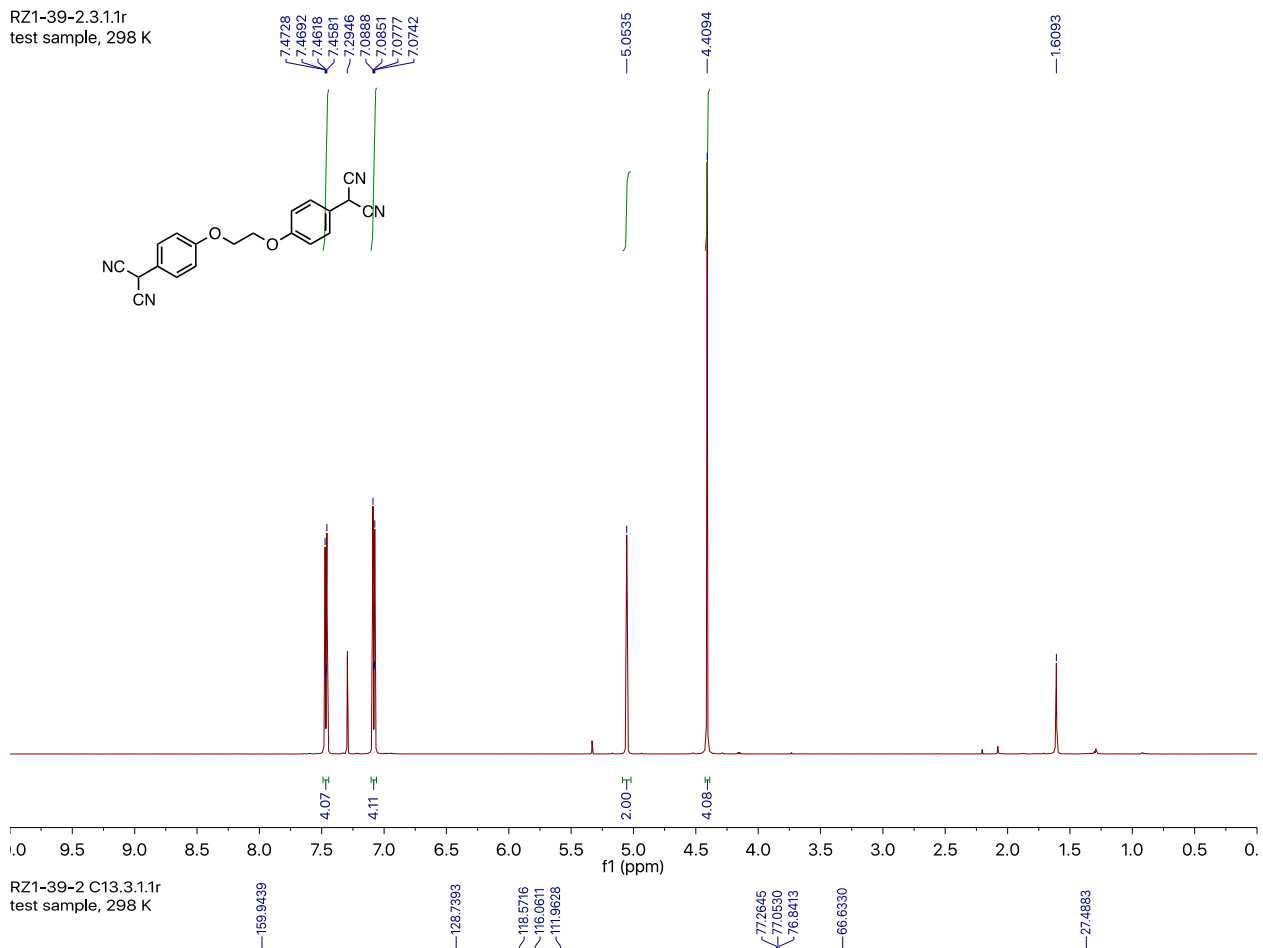


RZ1-27 C13.3.1.1r
test sample, 298 K

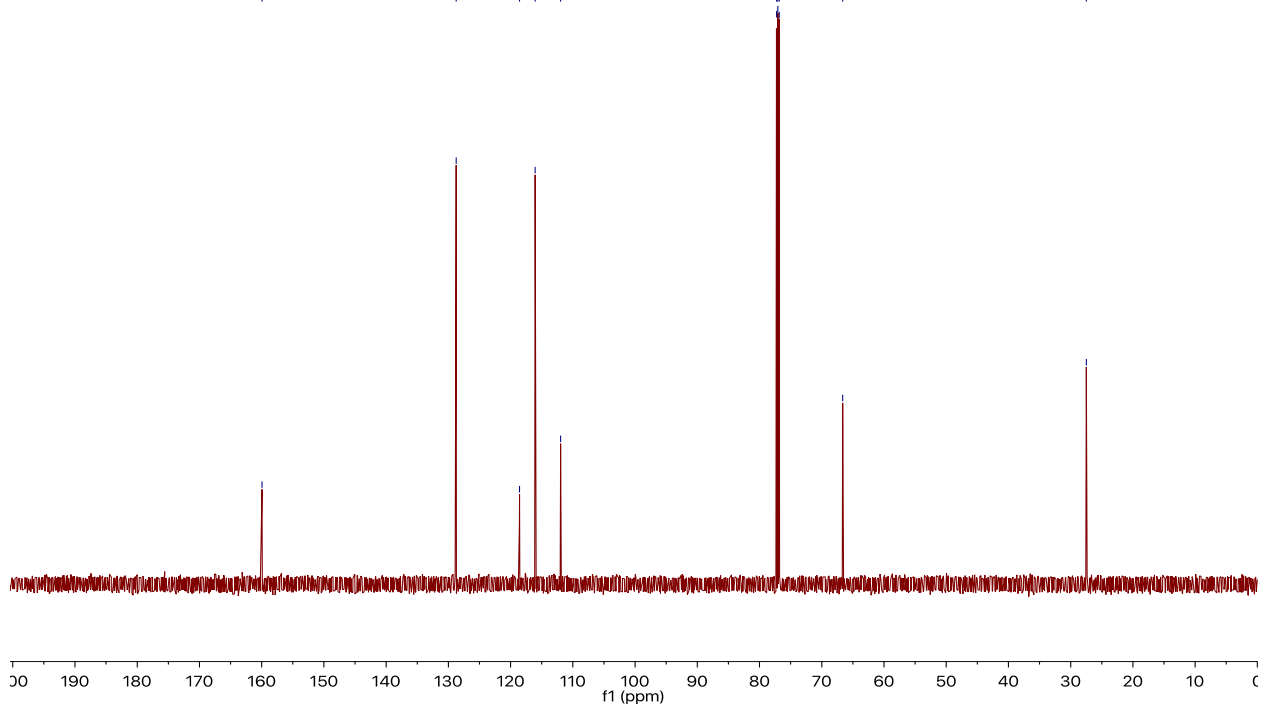


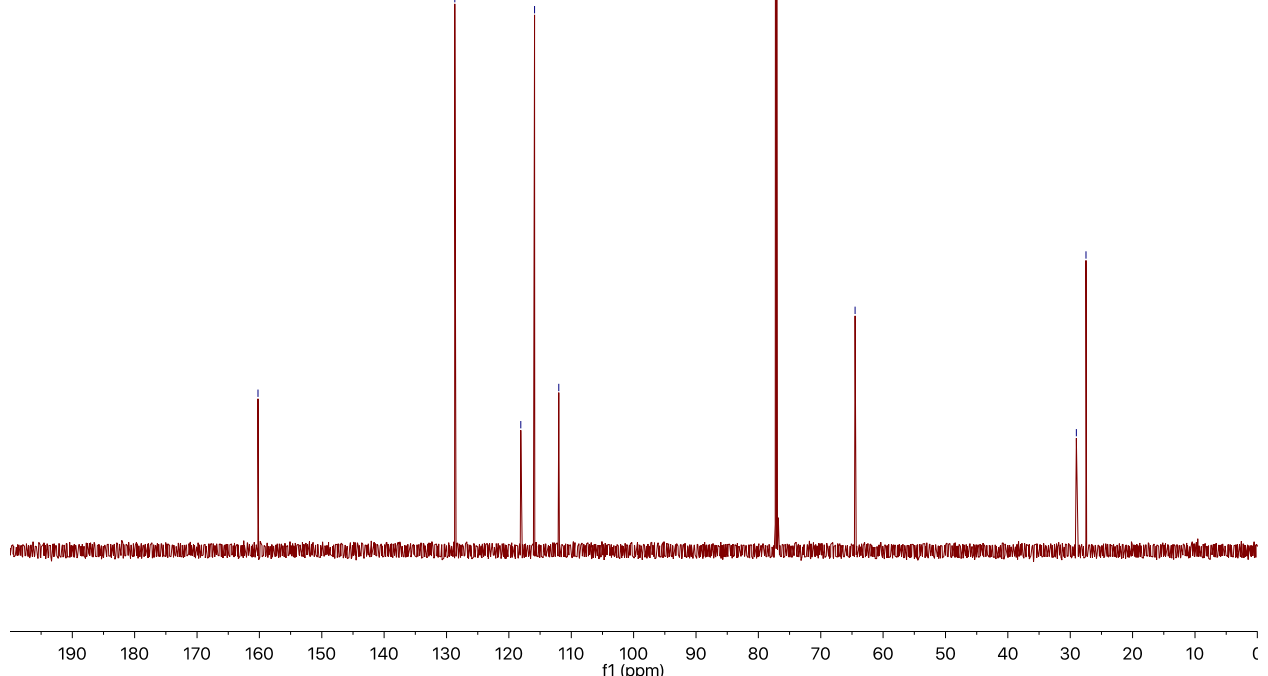
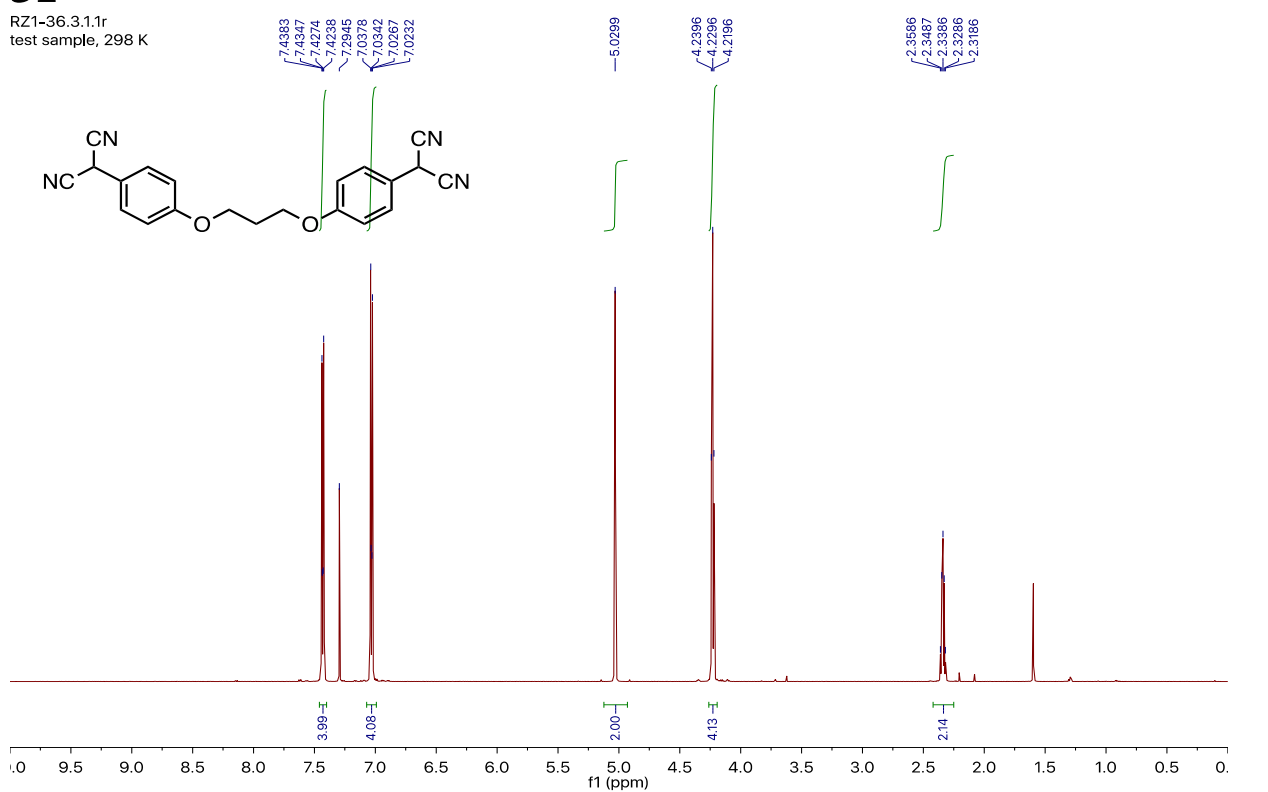
2P

RZ1-39-2,3.1.1r
test sample, 298 K



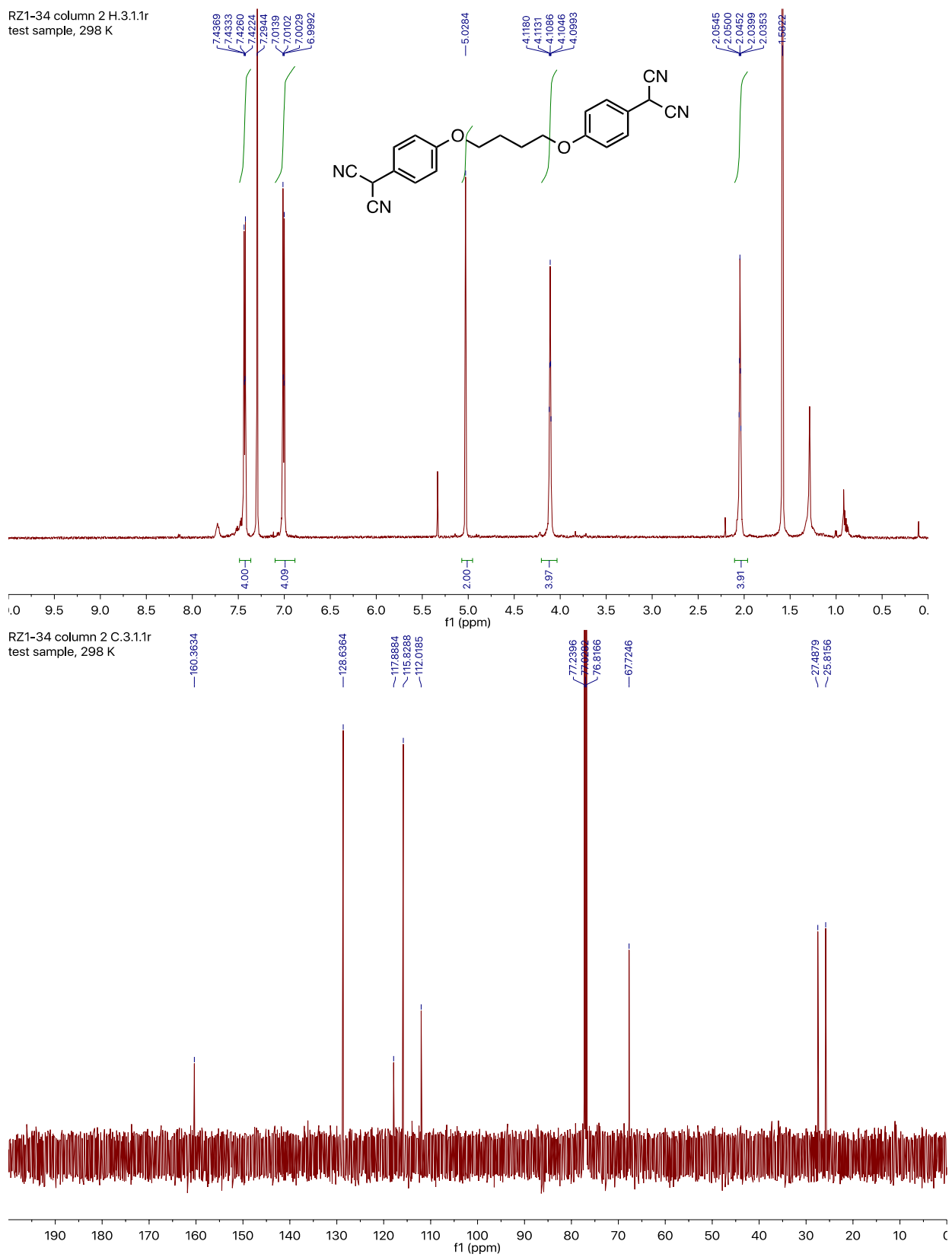
RZ1-39-2 C13.3.1.1r
test sample, 298 K

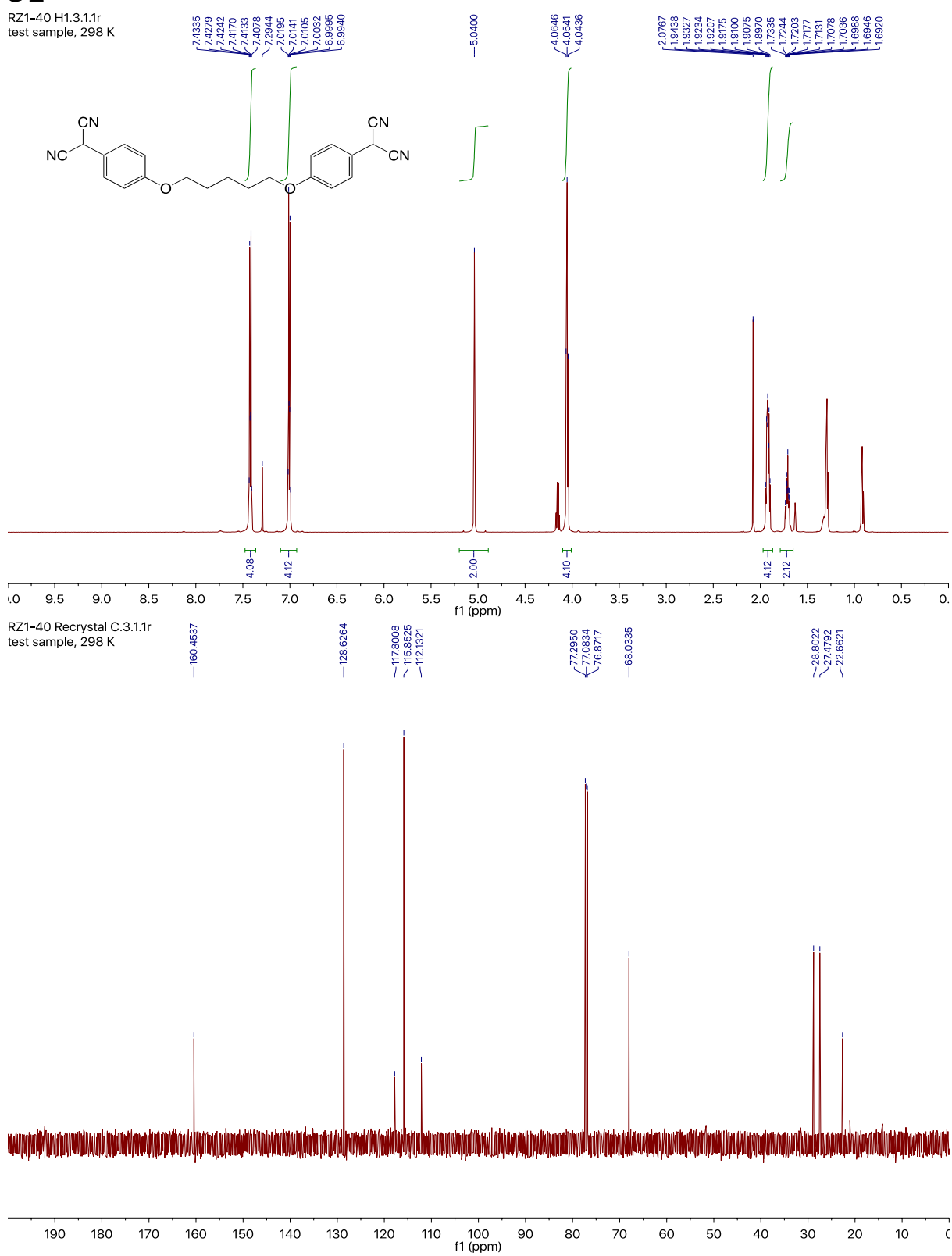


3PRZ1-36.3.1r
test sample, 298 K

4P

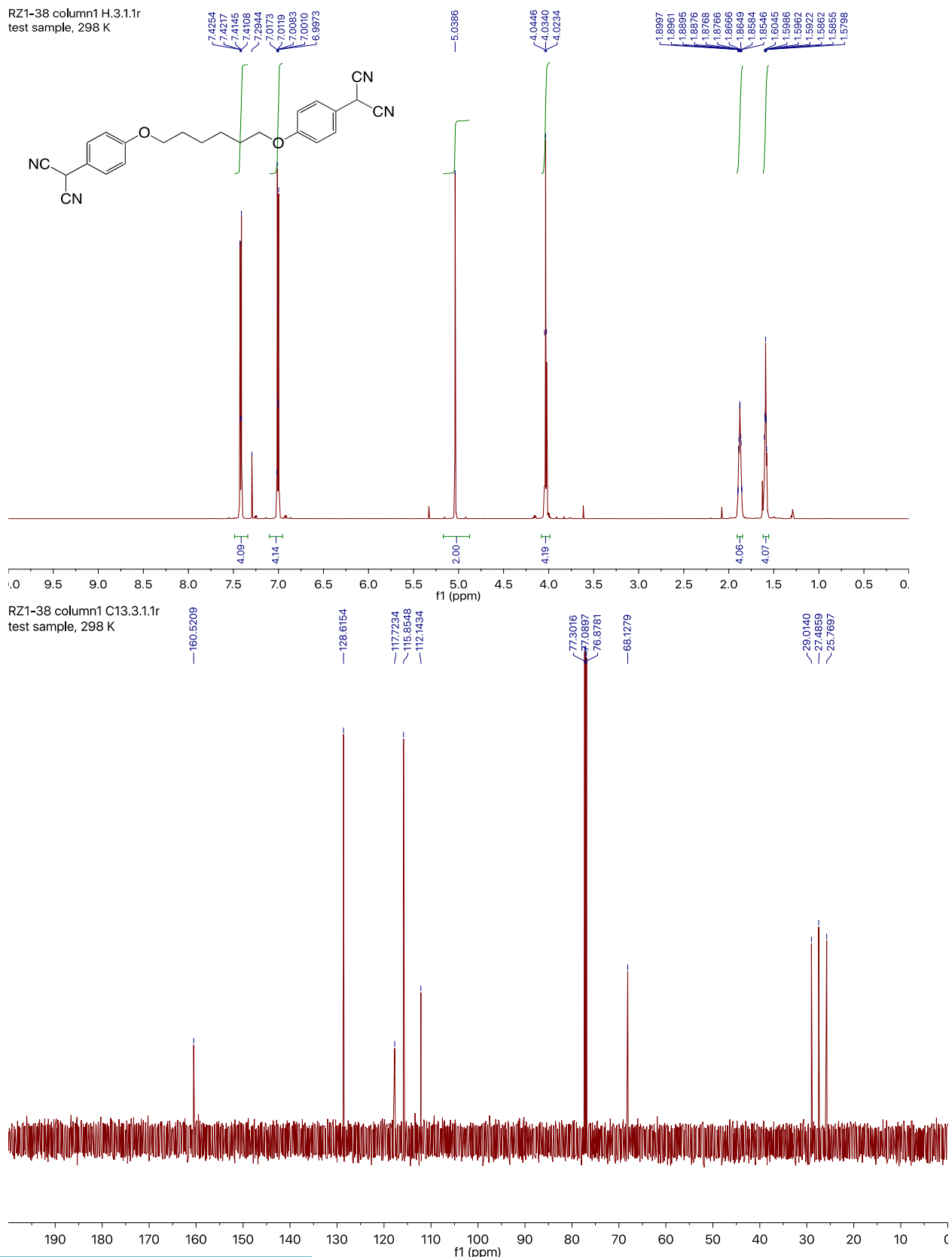
RZ1-34 column 2 H.3.1.1r
test sample, 298 K



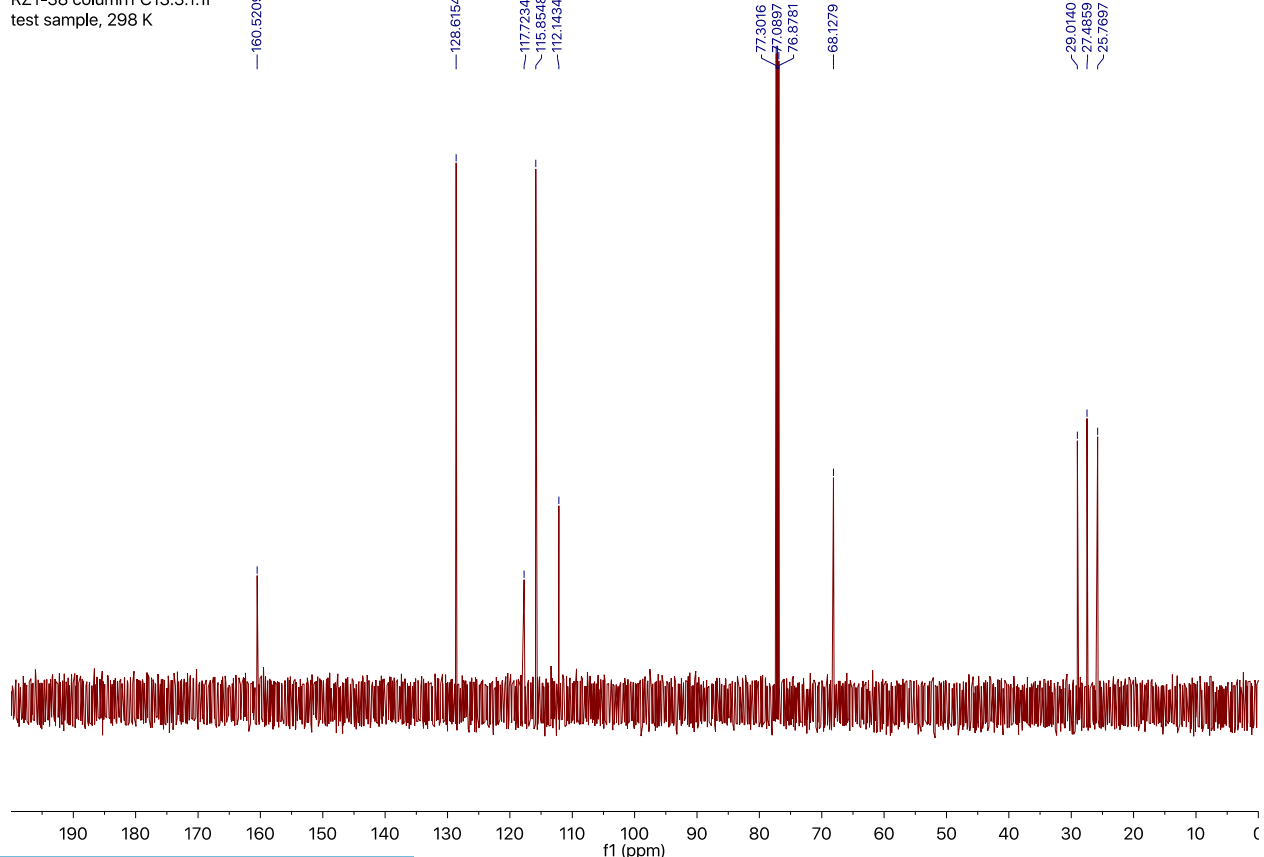
5PRZ1-40 H1.3.1.1r
test sample, 298 K

6P

RZ1-38 column1 H.3.1.1r
test sample, 298 K

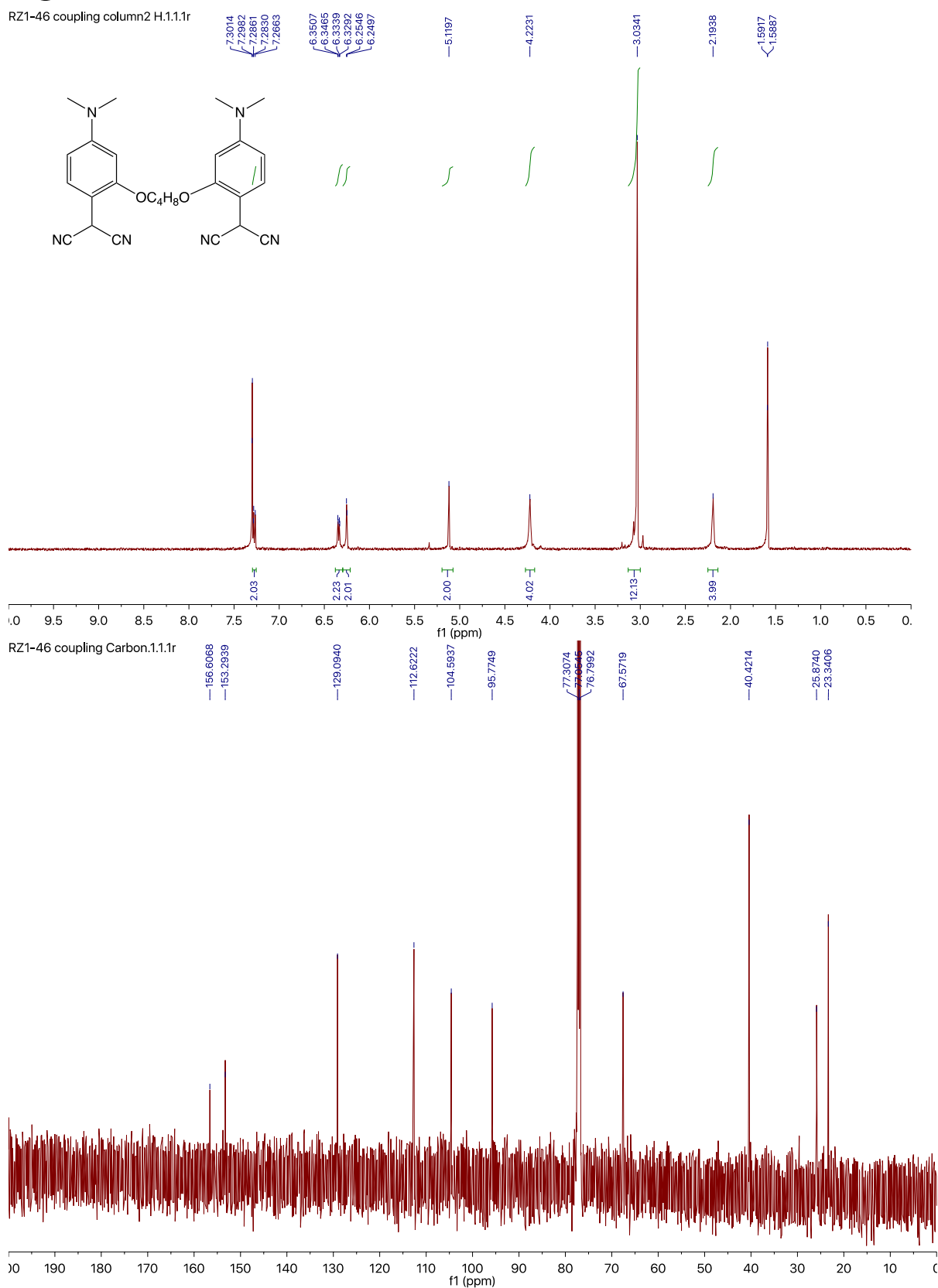


RZ1-38 column1 C13.3.1.1r
test sample, 298 K



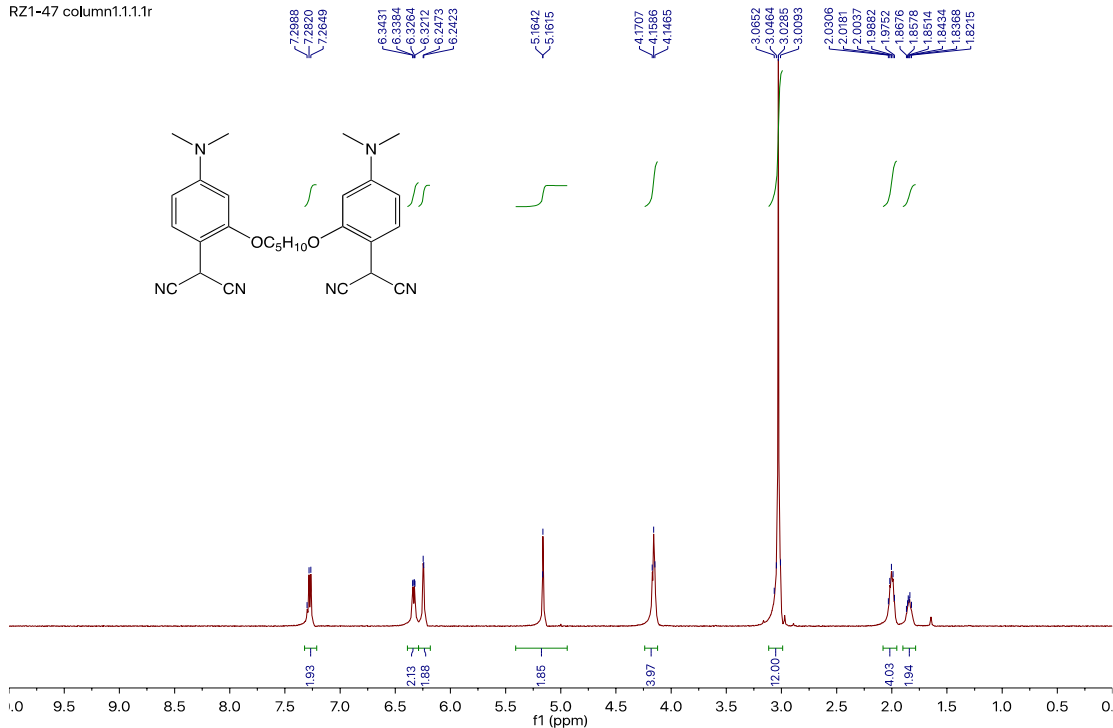
4O-DMA

RZ1-46 coupling column2 H.1.1.1r

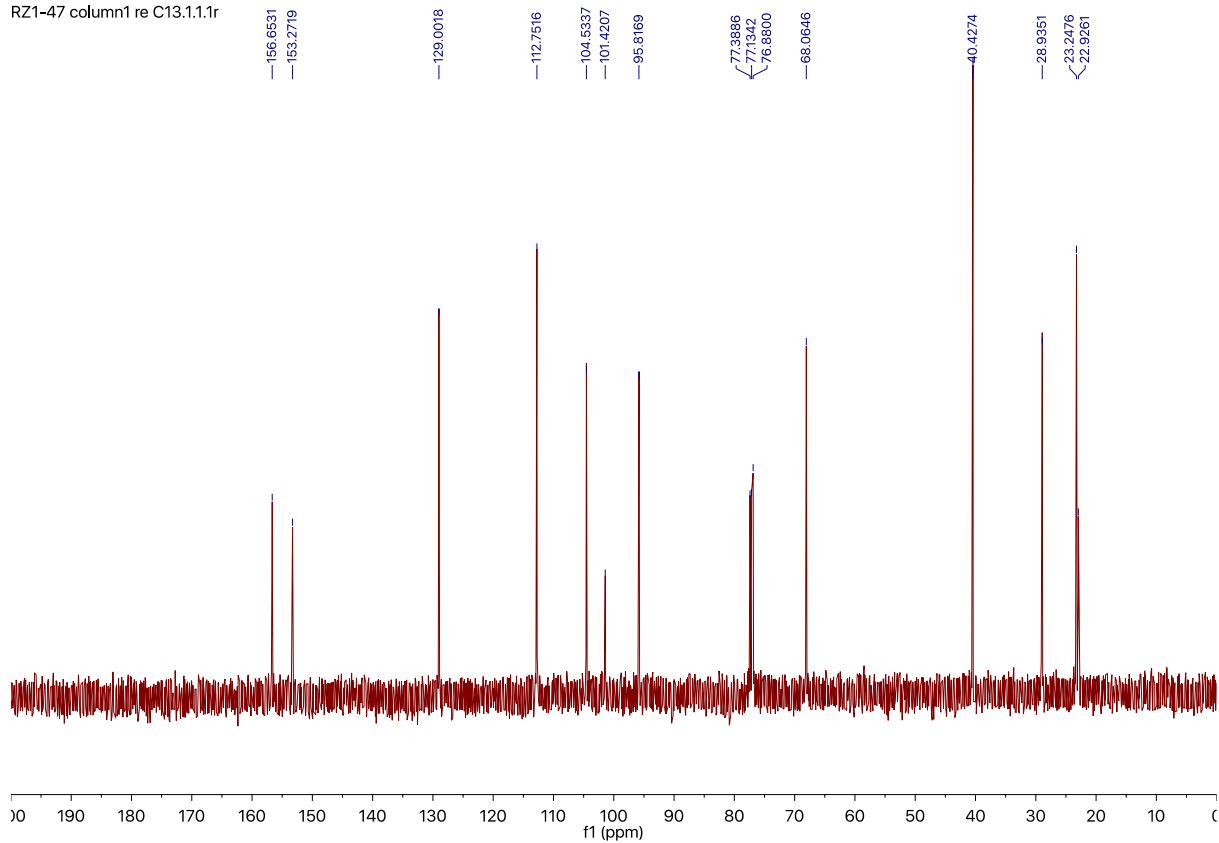


5O-DMA

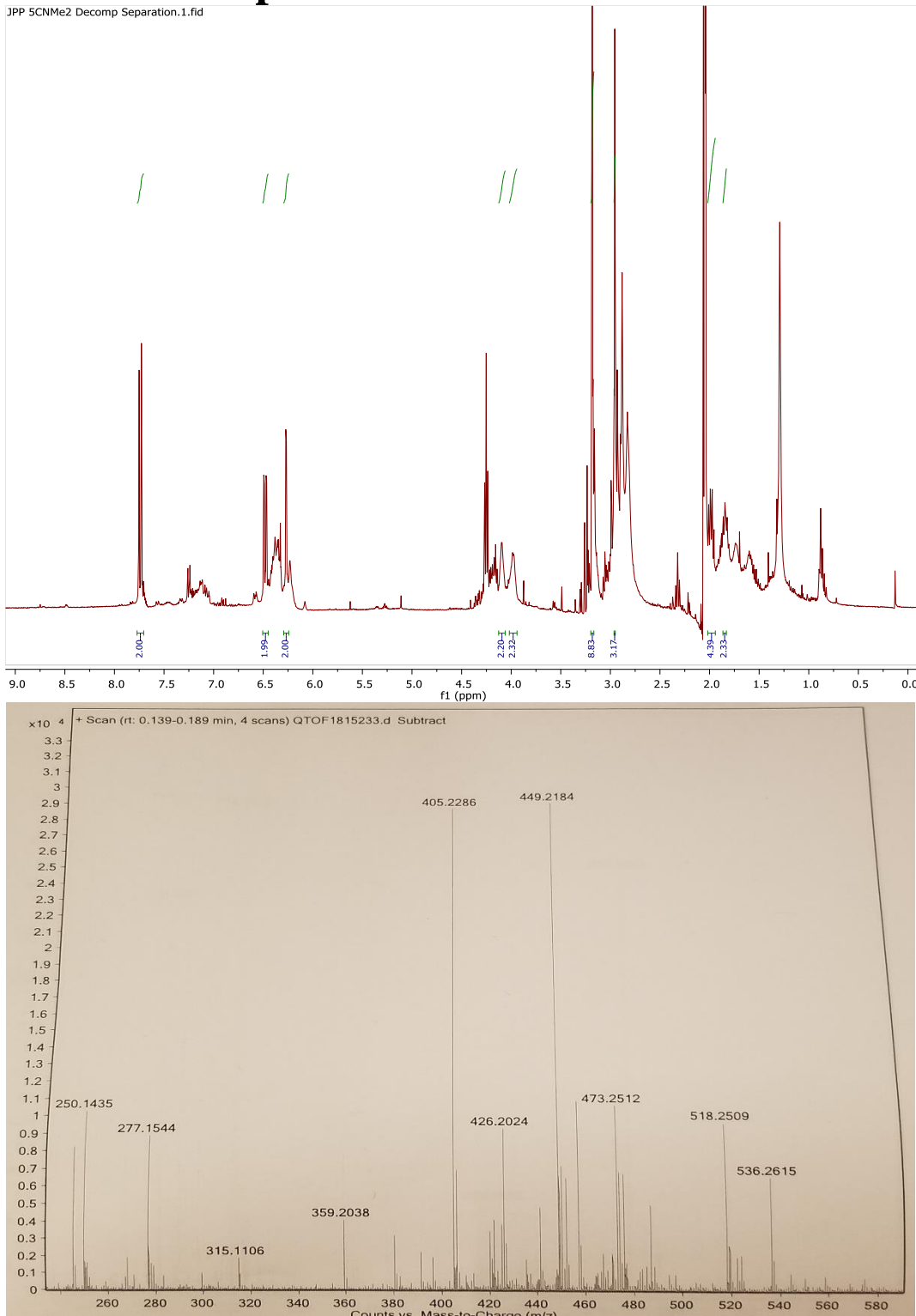
RZ1-47 column1.1.1r



RZ1-47 column1 re C13.1.1.1r

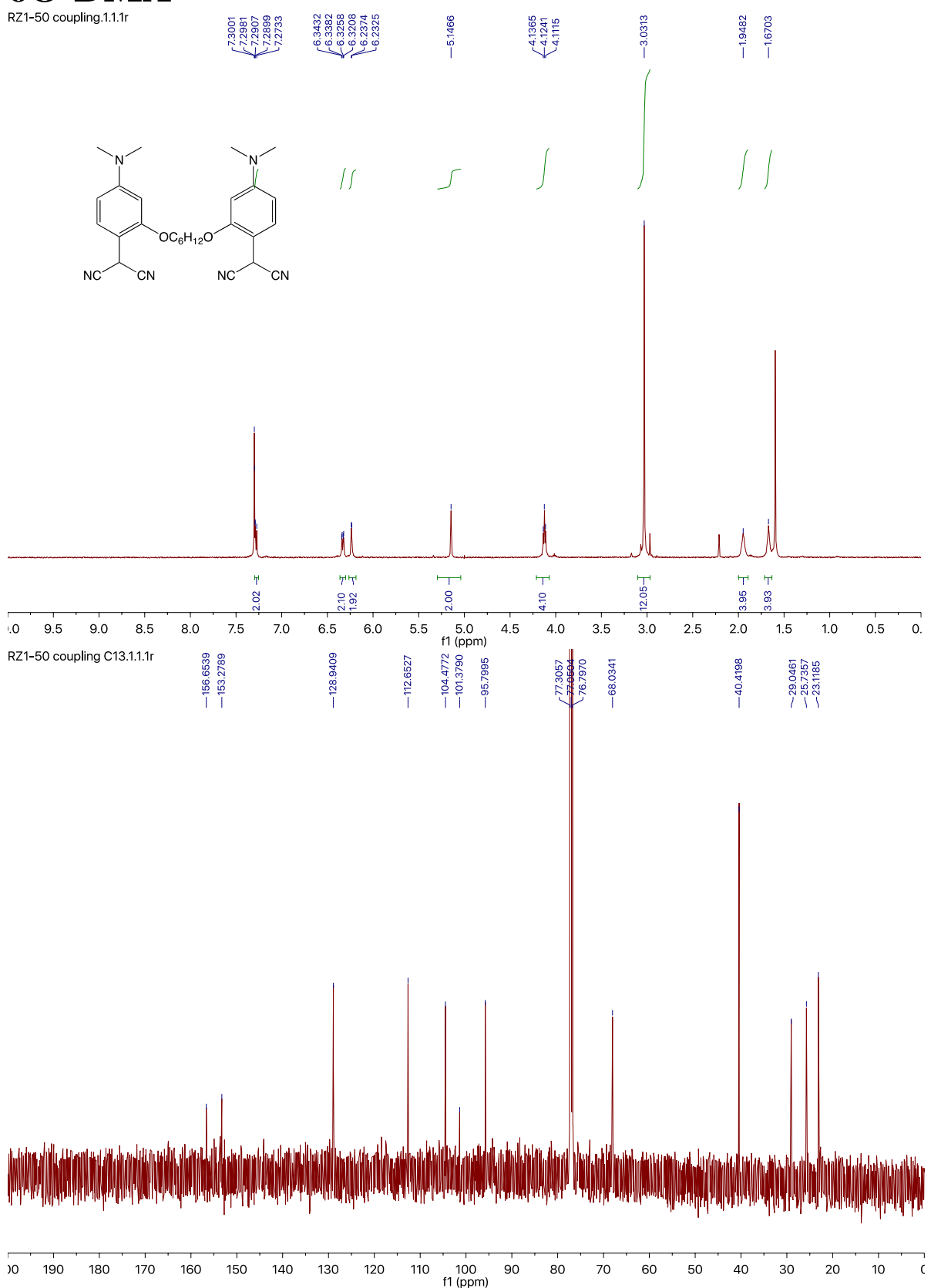


50-DMA Decomposition



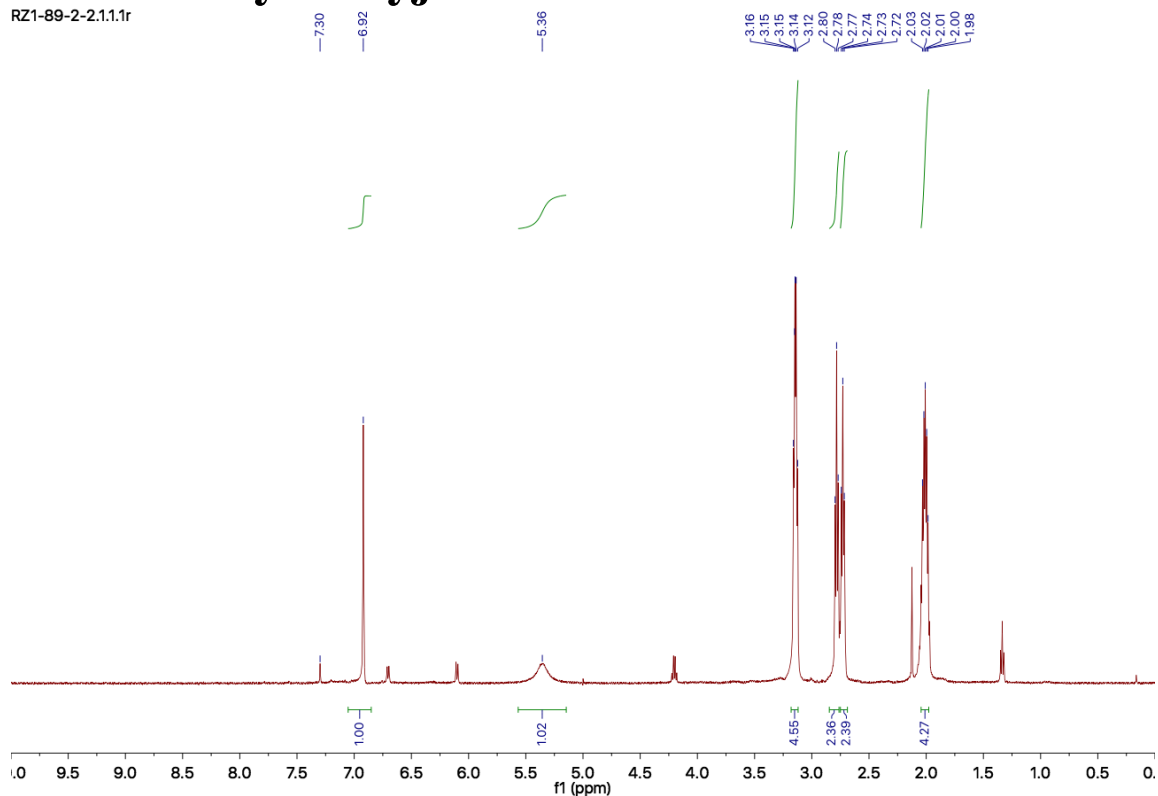
6O-DMA

RZ1-50 coupling.1.1.1r



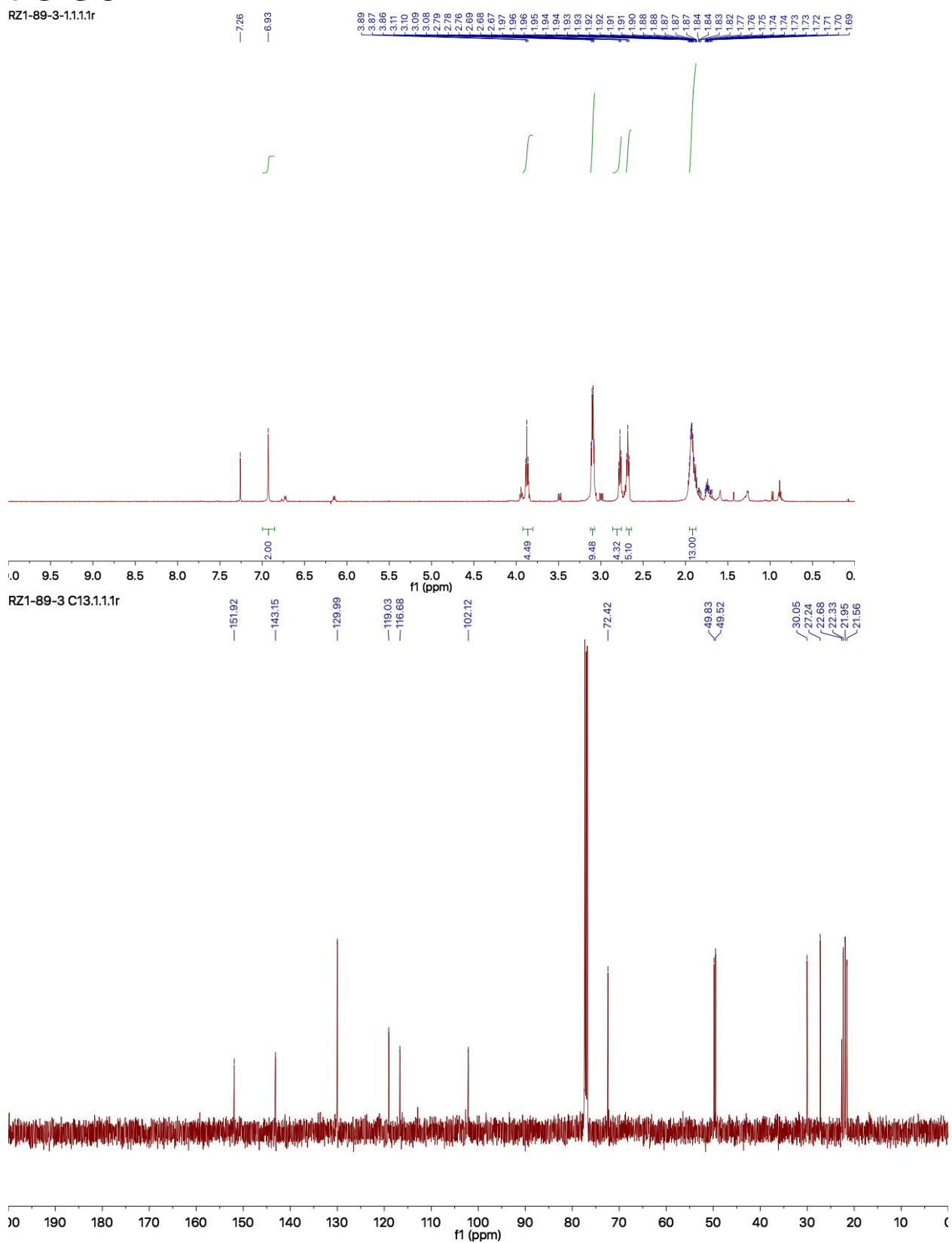
8-bromo-hydroxyjulolidine

RZ1-89-2-2.1.1.1r



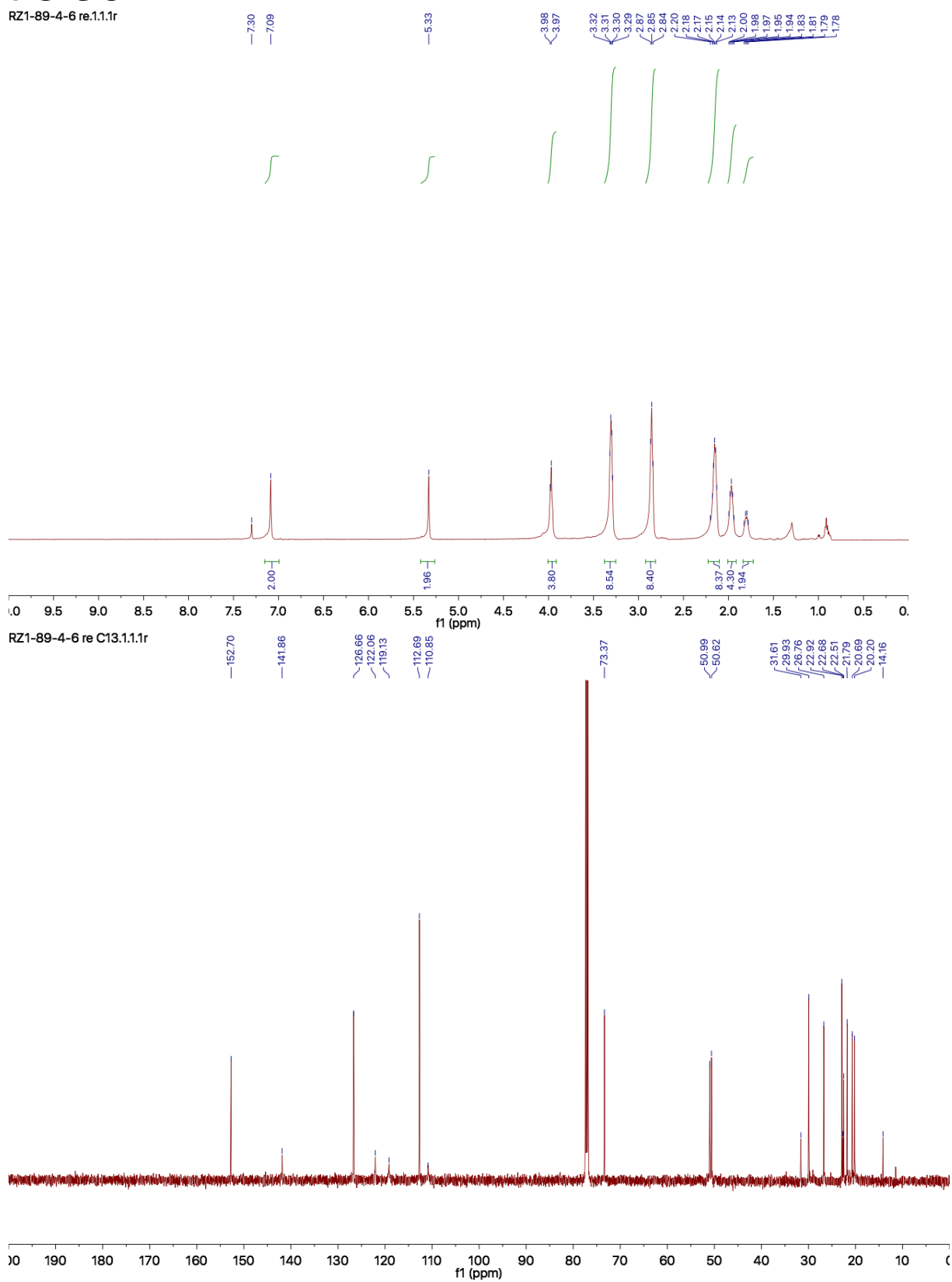
50-JUL-Br

RZ1-89-3-1.1.1r

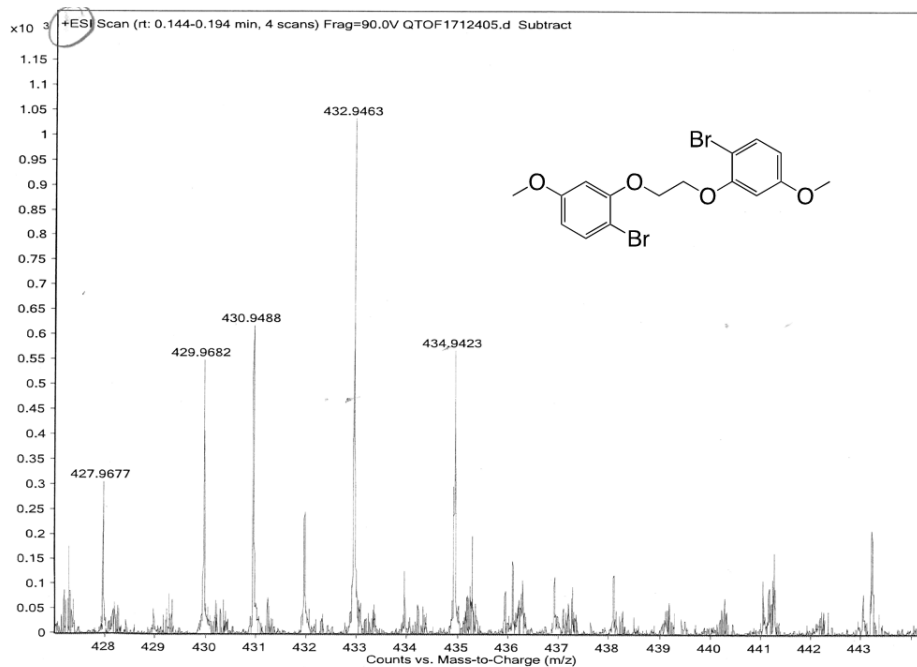


50-JUL

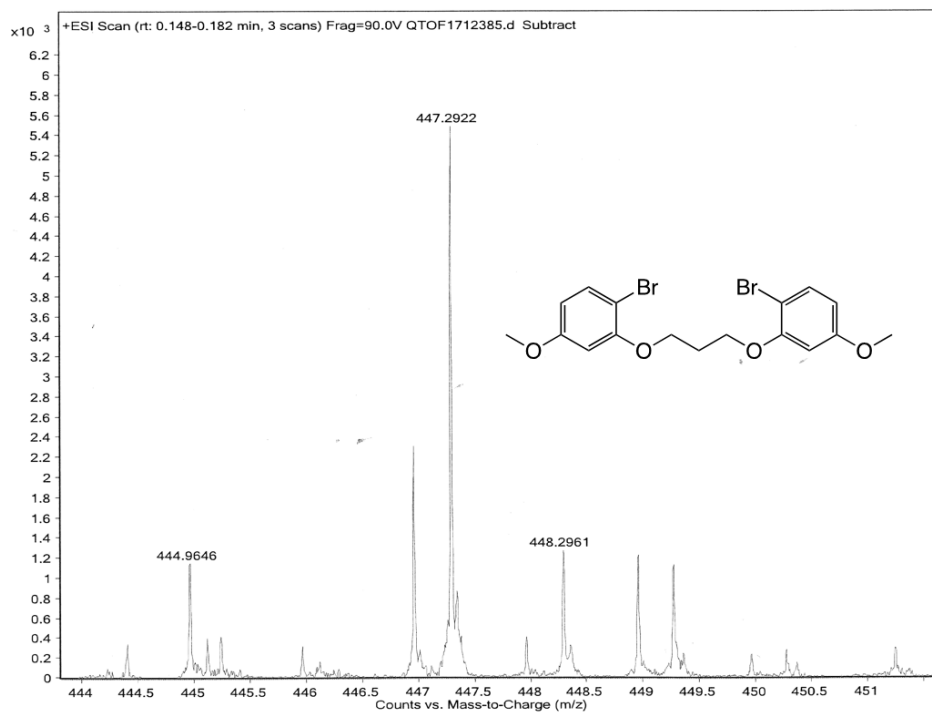
RZ1-89-4-6 re.1.1.1r

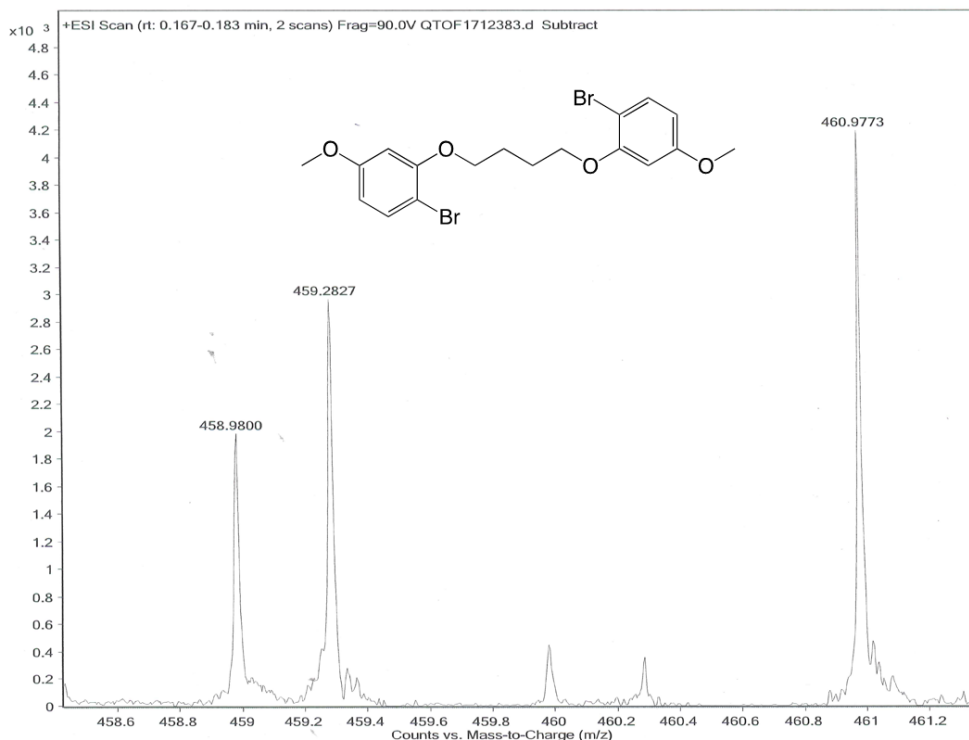
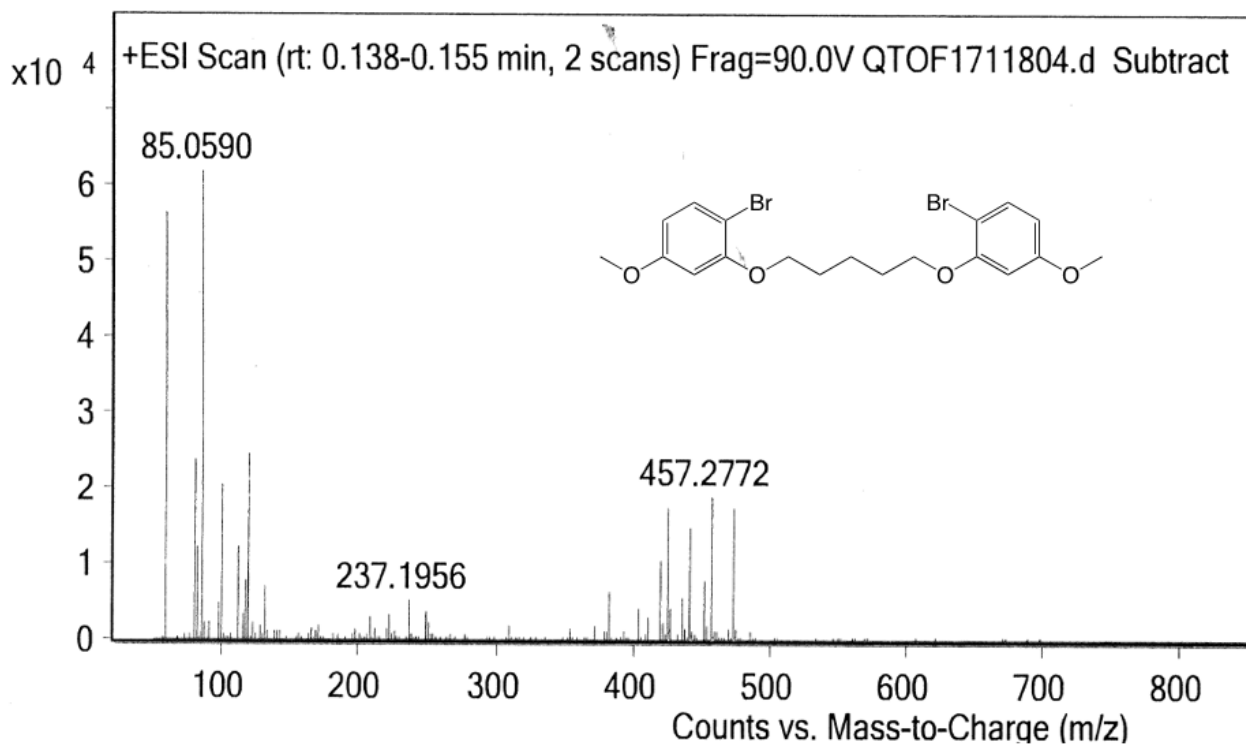


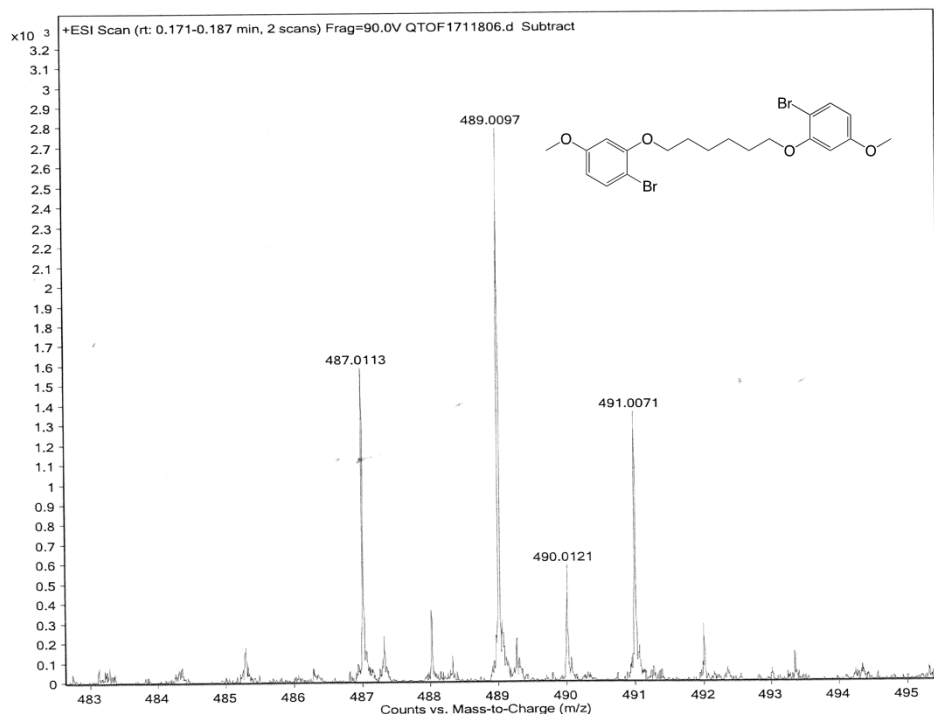
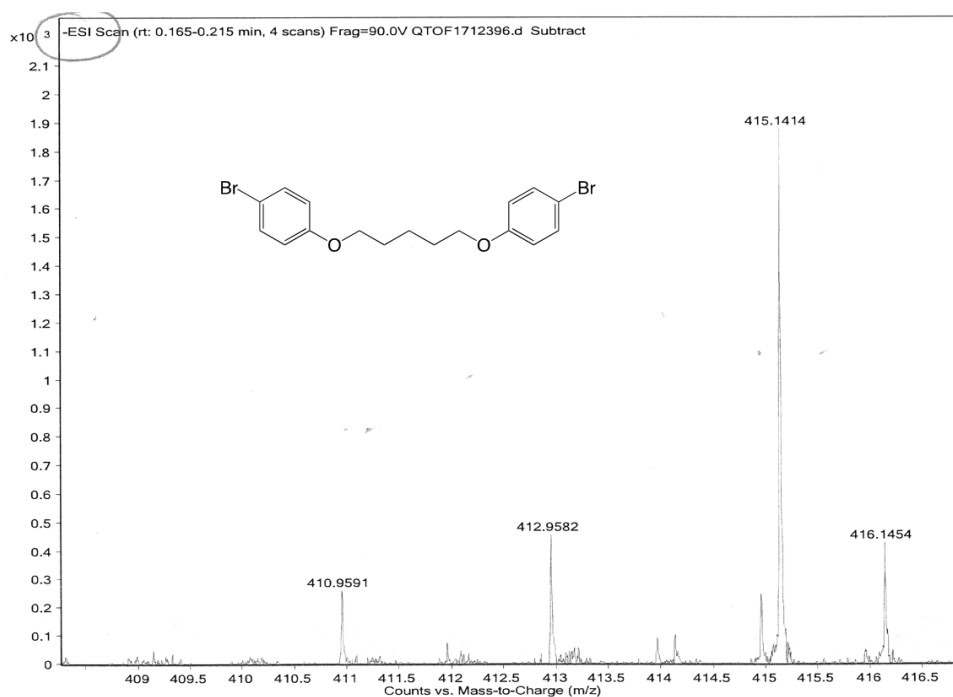
Mass Spectra: 2O-Br



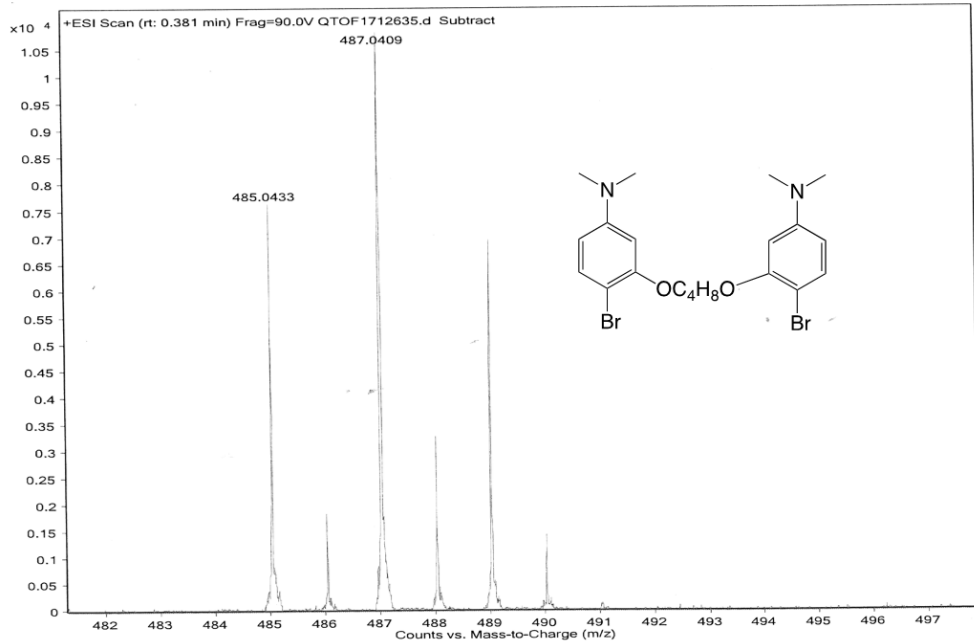
3O-Br



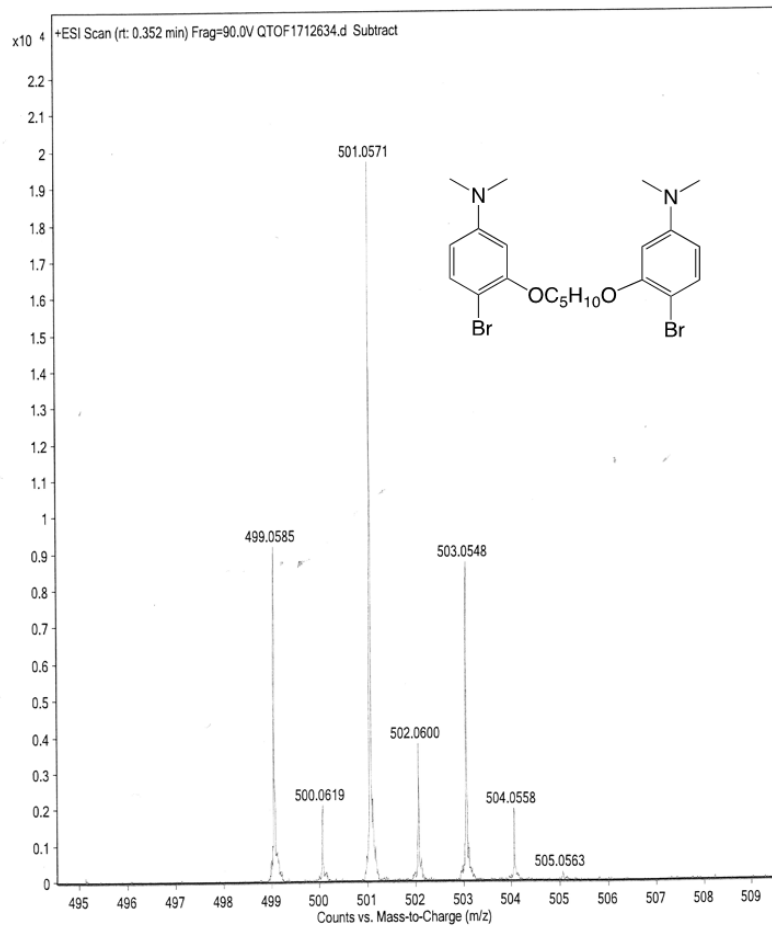
4O-Br**5O-Br**

6O-Br**5P-Br**

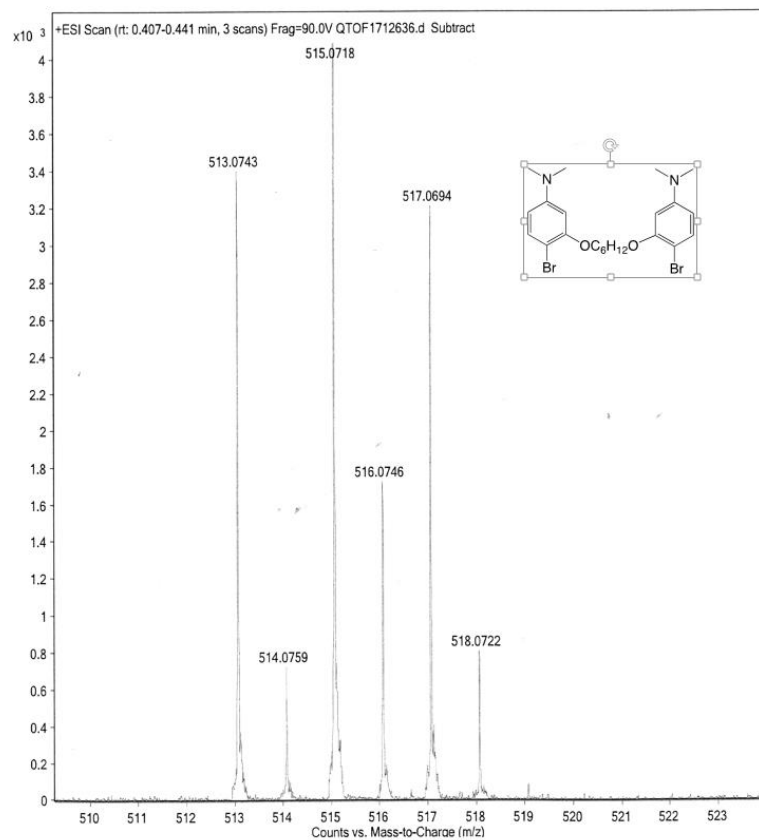
4O-DMA-Br



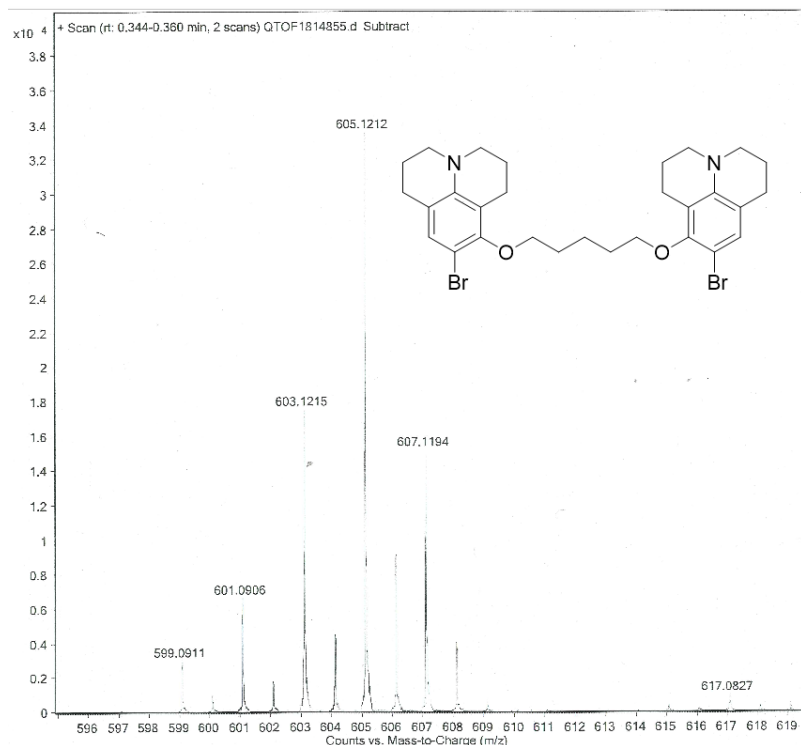
5O-DMA-Br

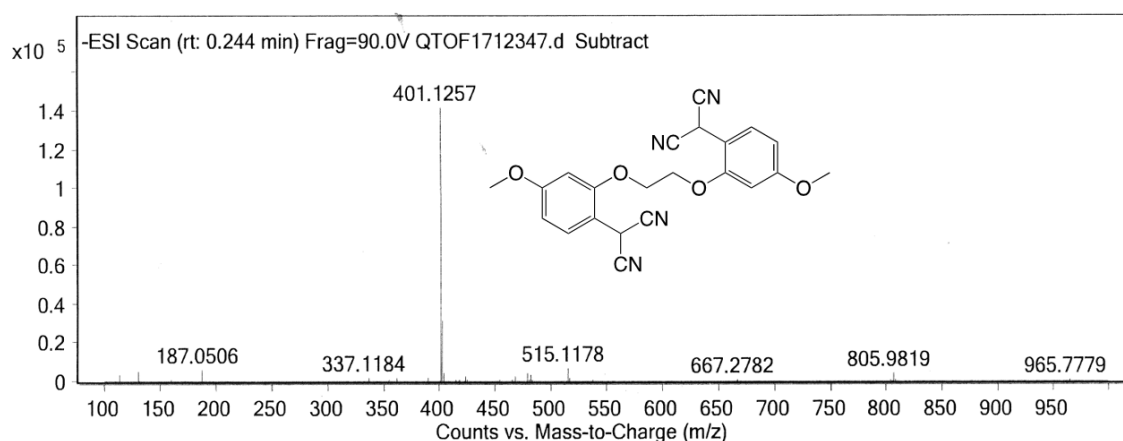
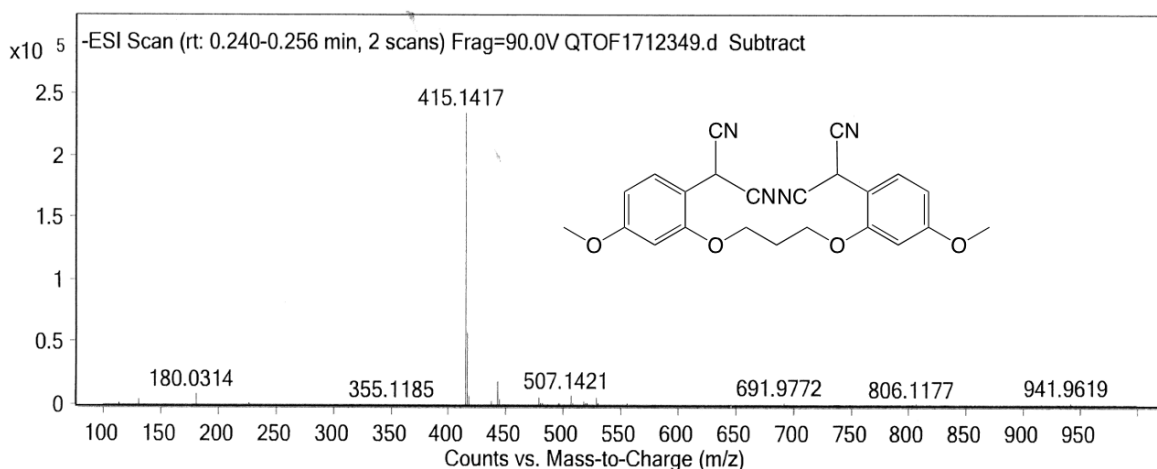
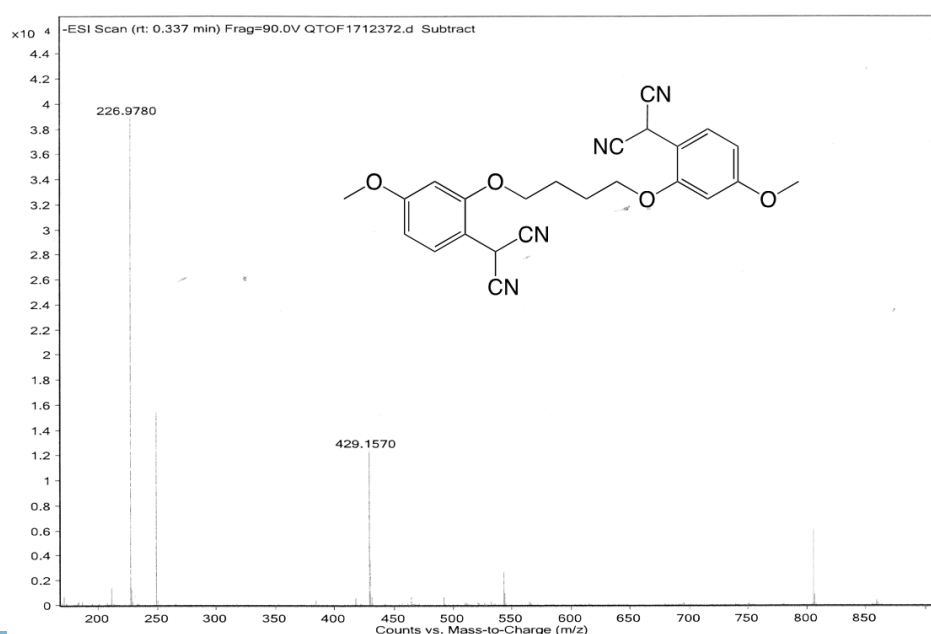


6O-DMA-Br

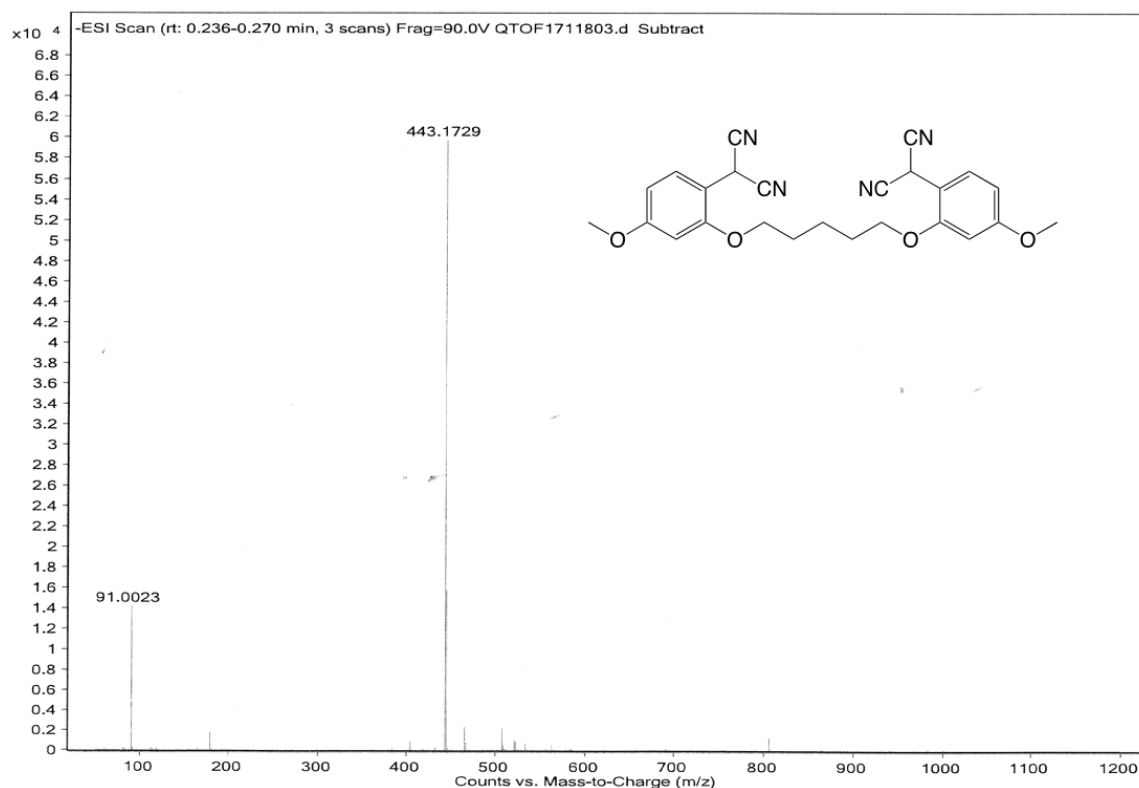


5O-JUL-Br

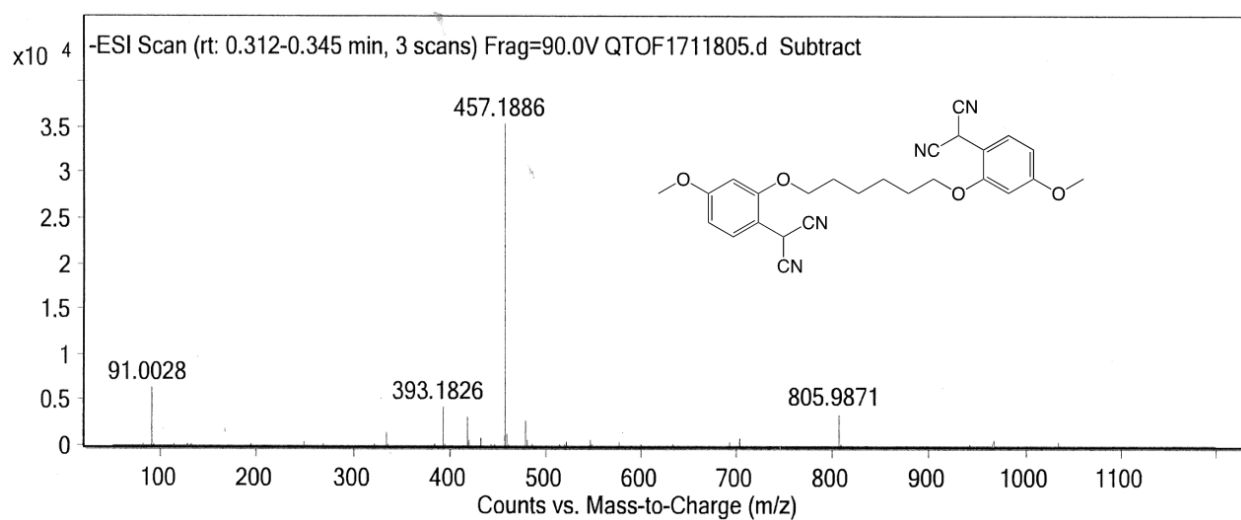


20**30****40**

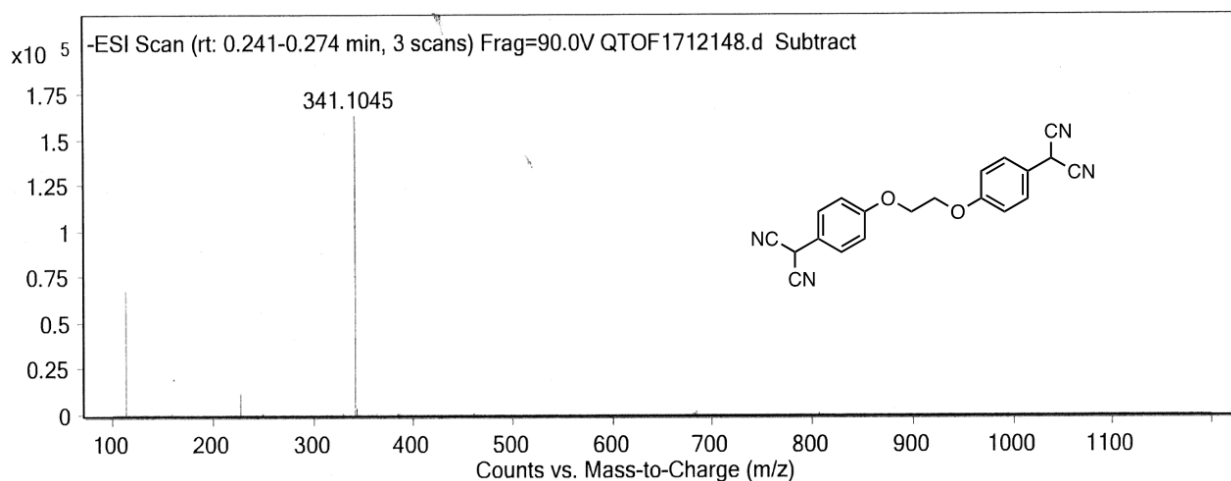
50



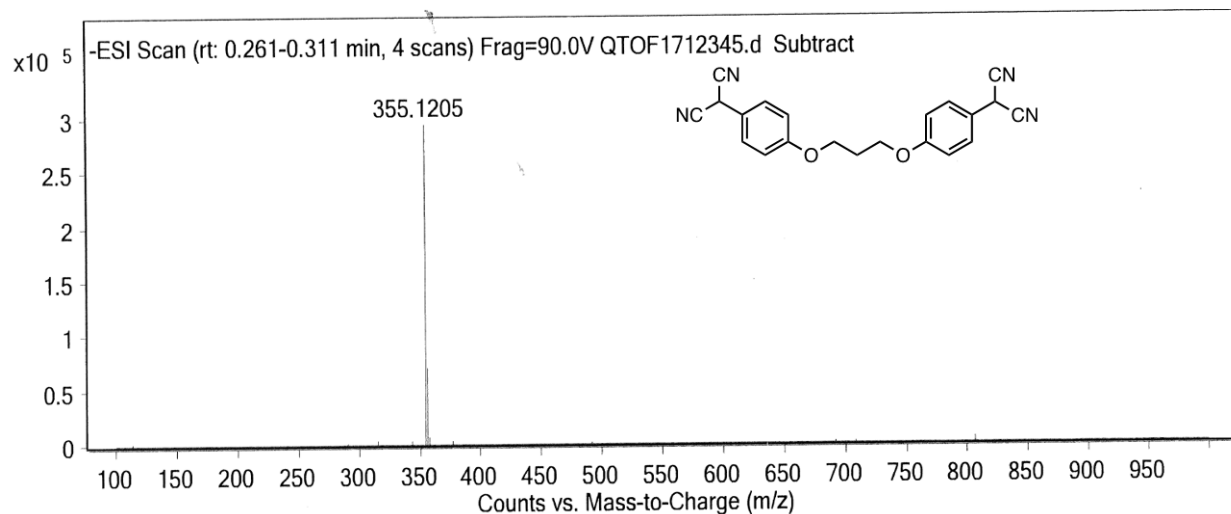
60



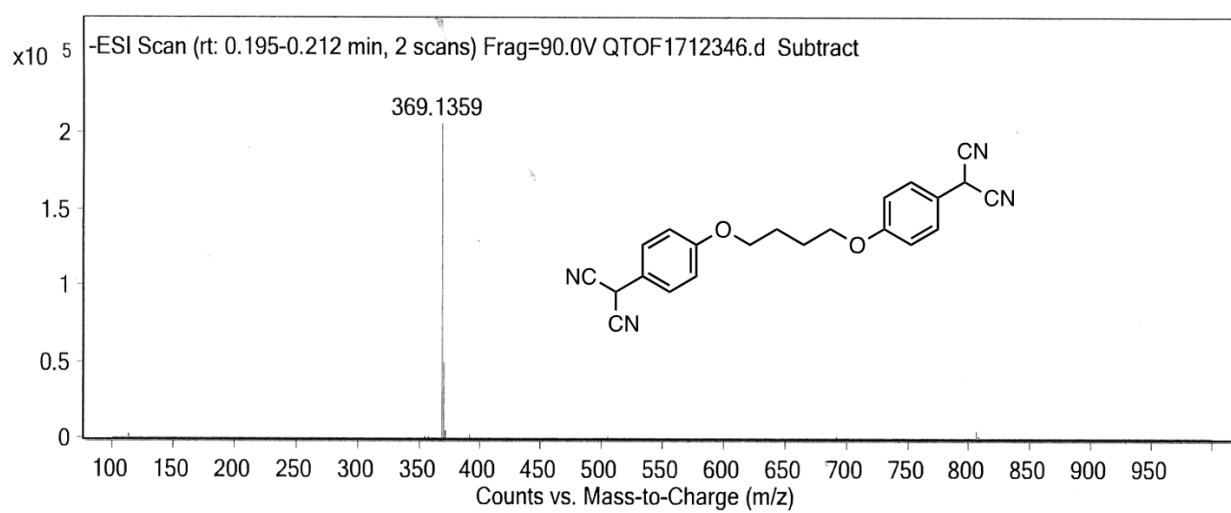
2P

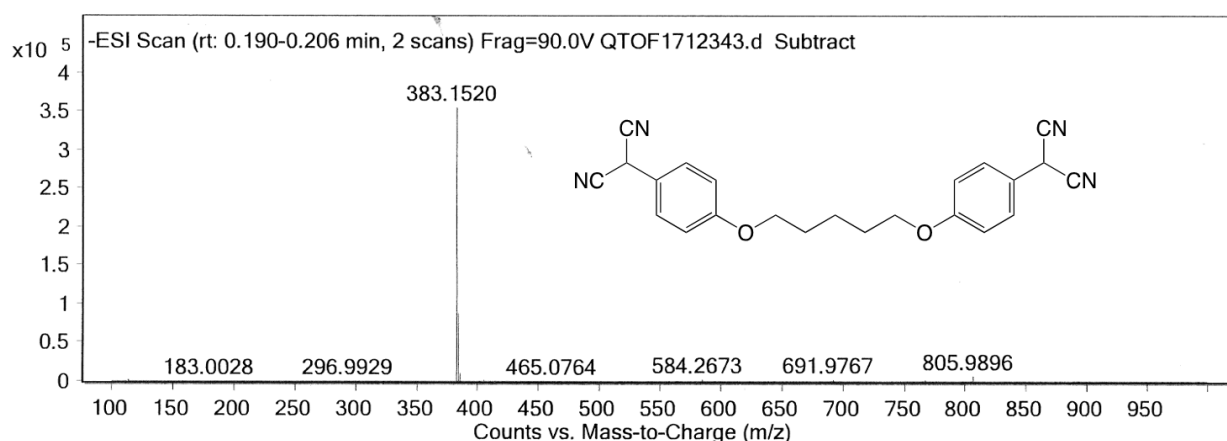
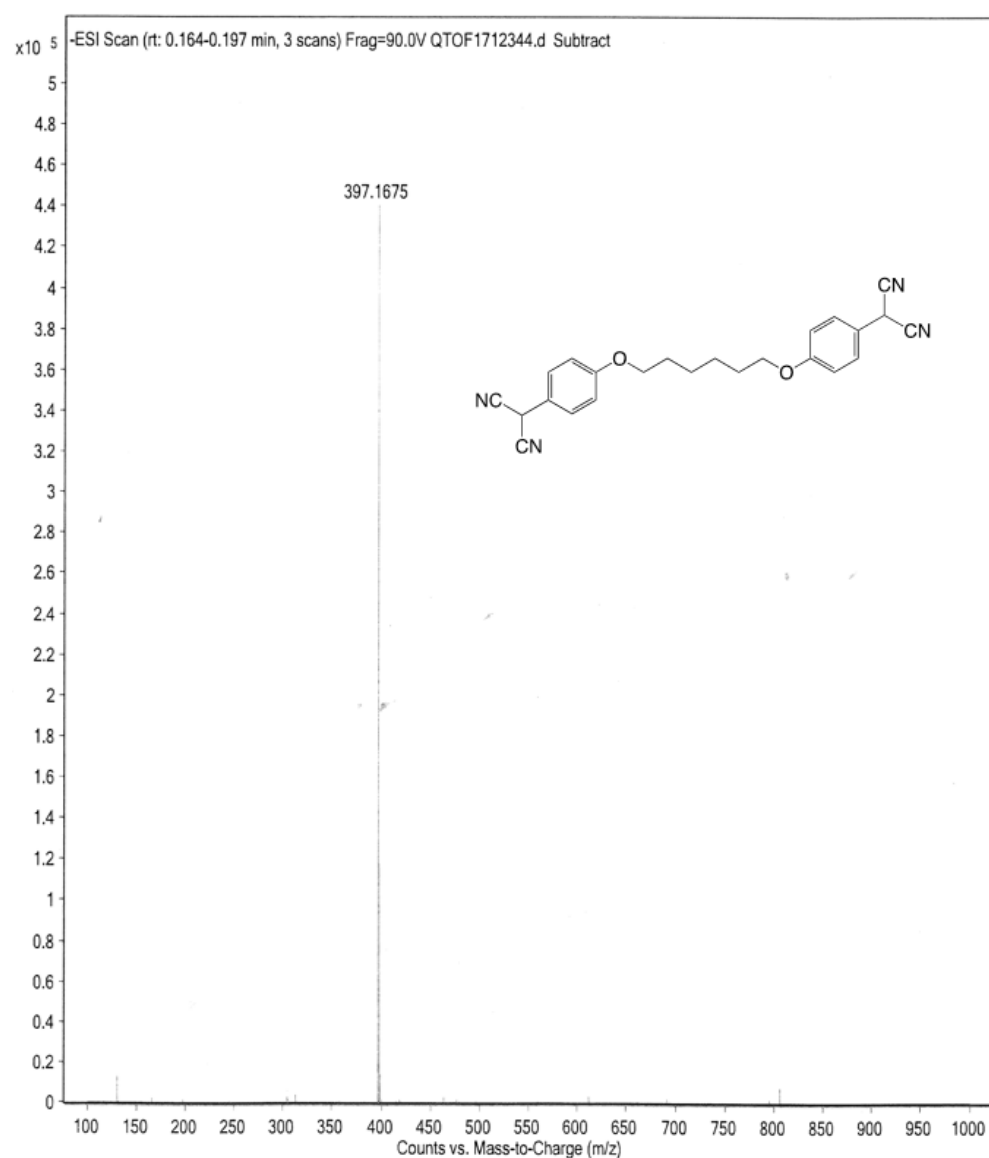


3P

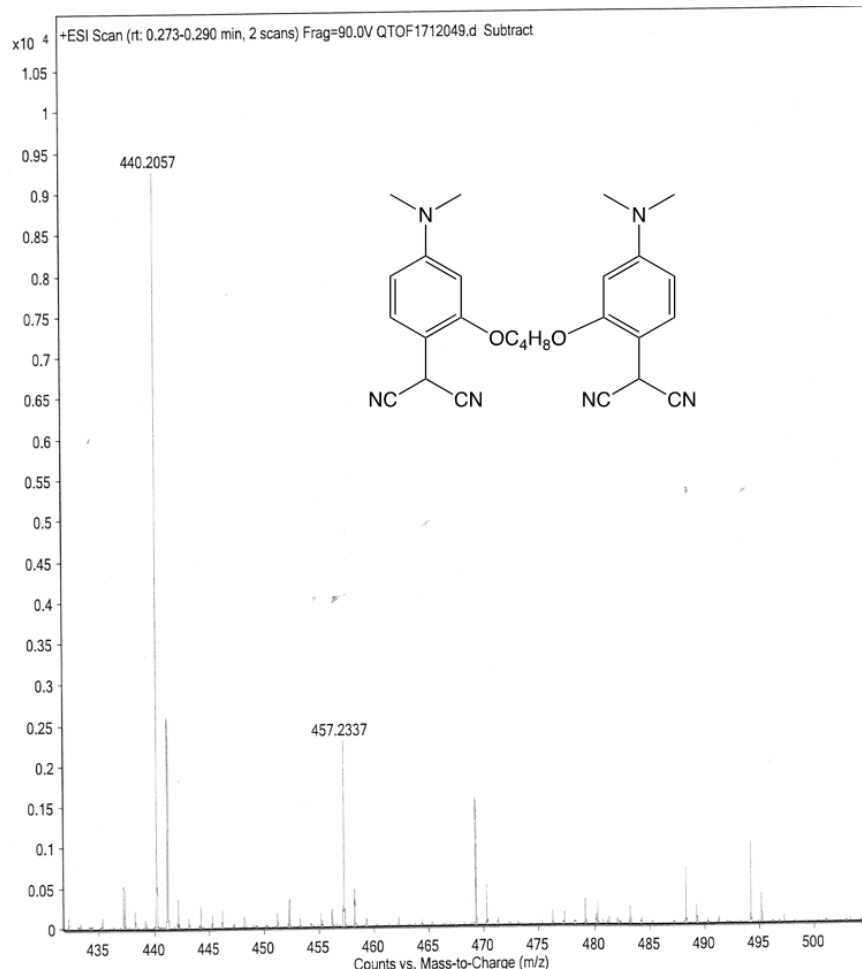


4P

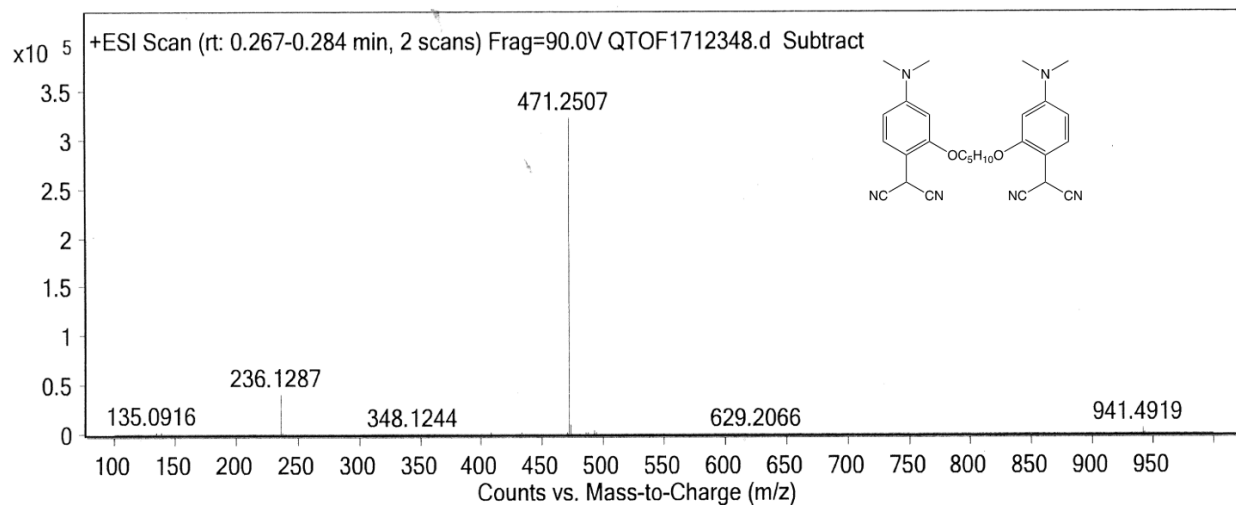


5P**6P**

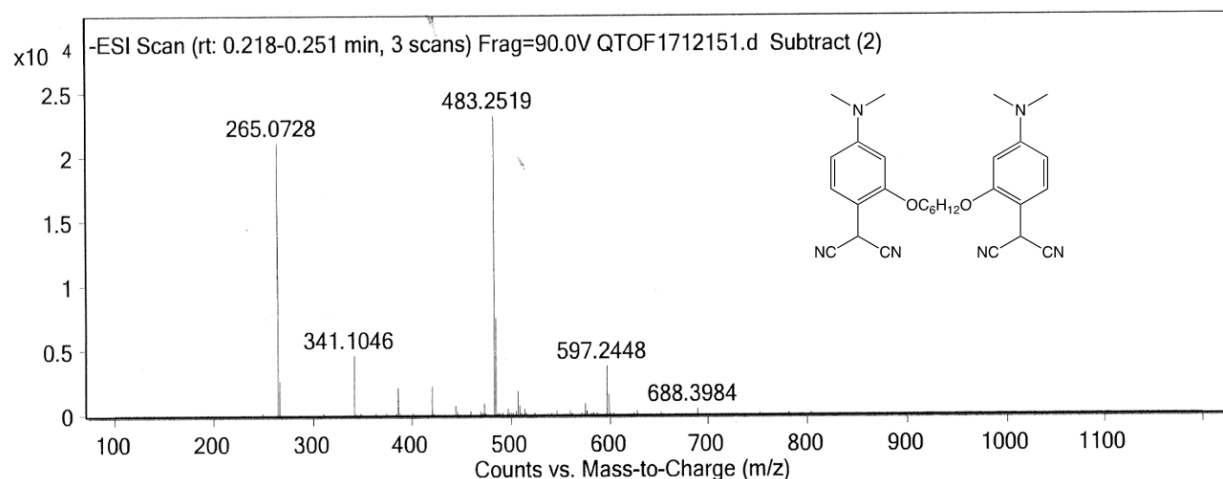
4O-DMA



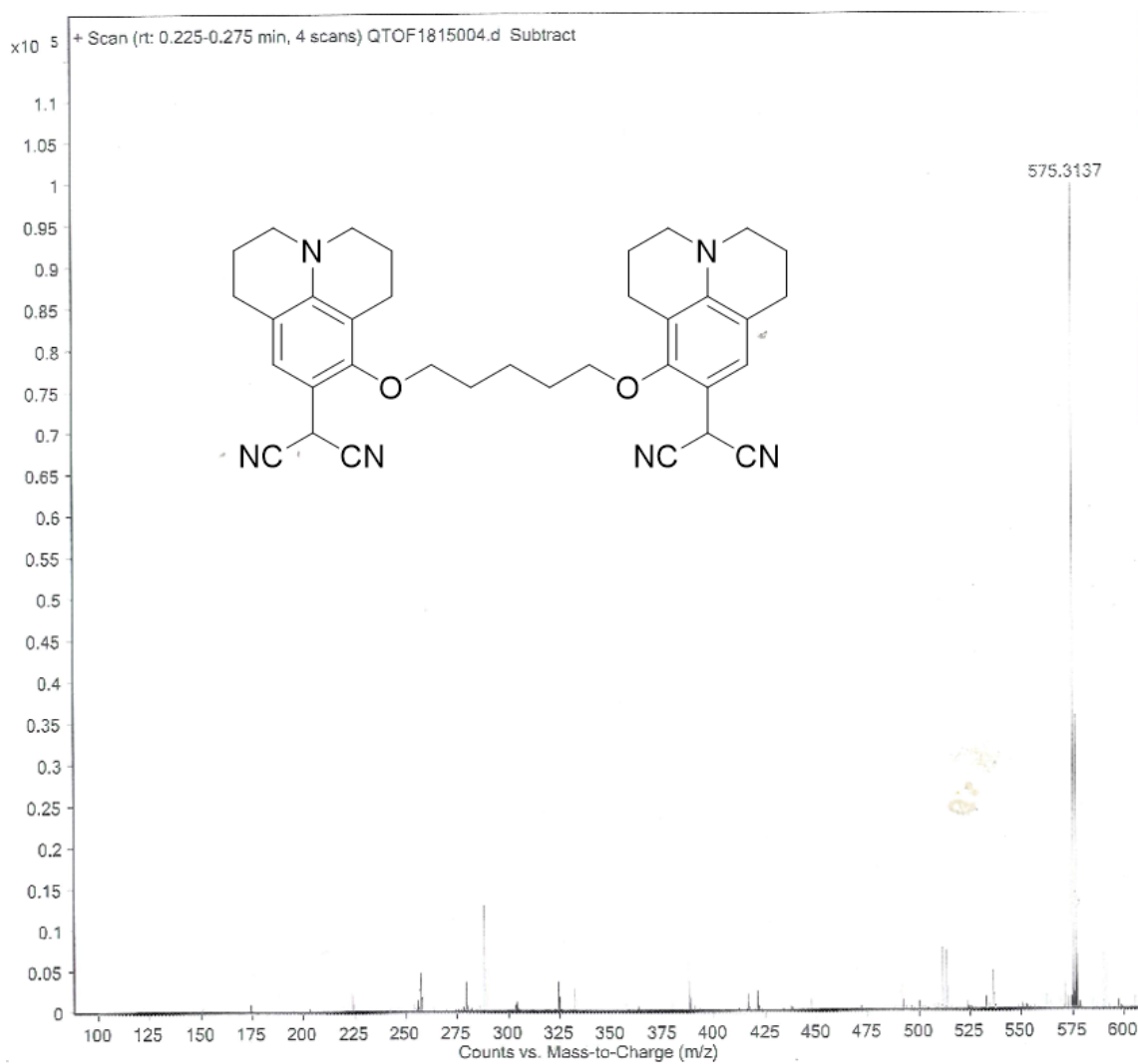
5O-DMA



6O-DMA

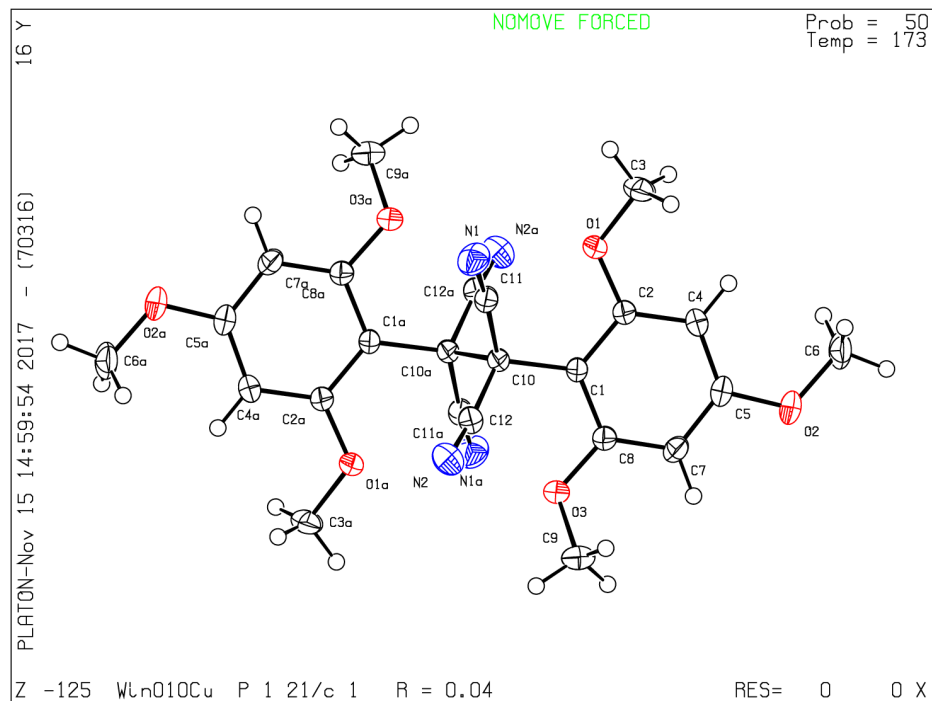


5O-JUL

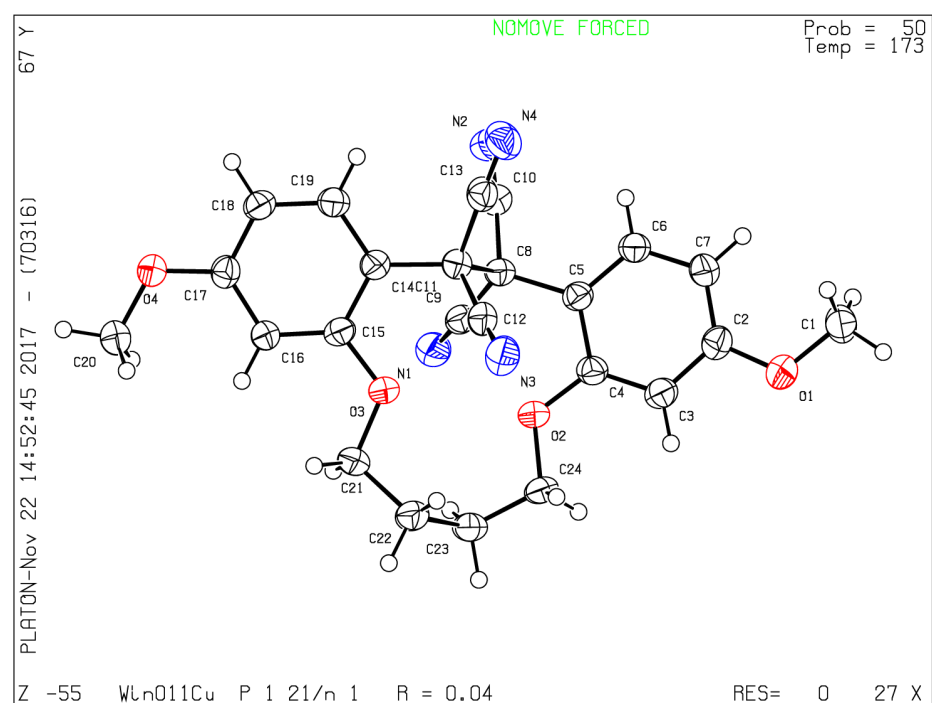


Crystallographic Plots

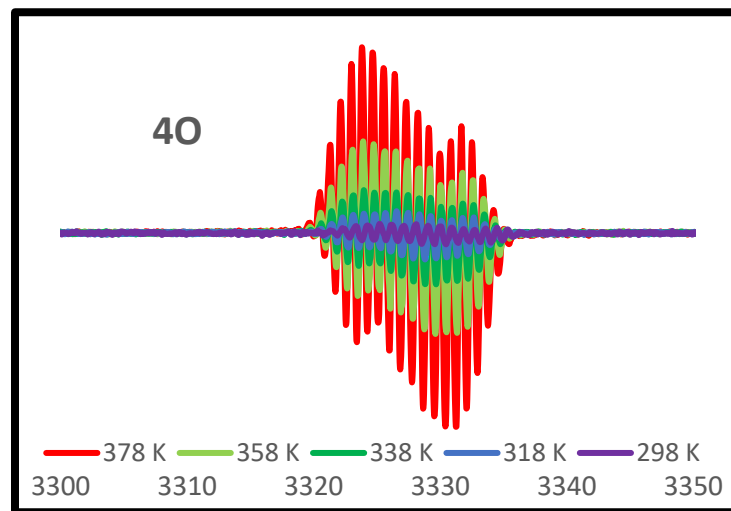
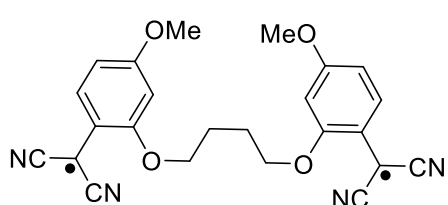
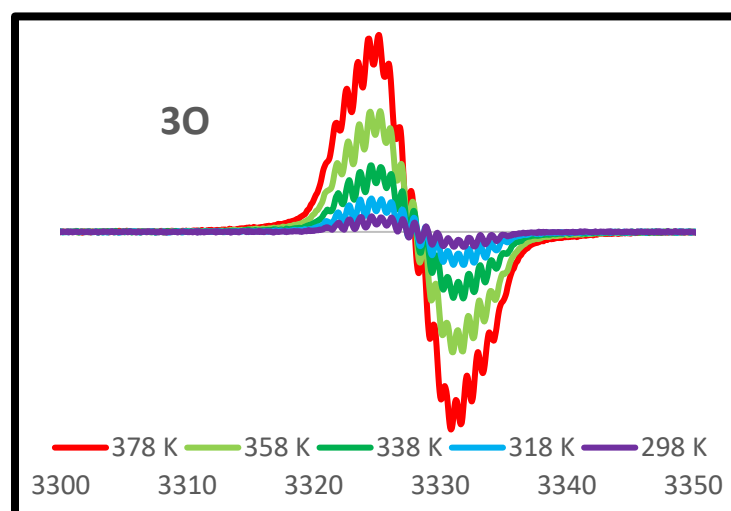
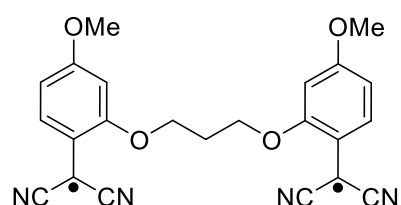
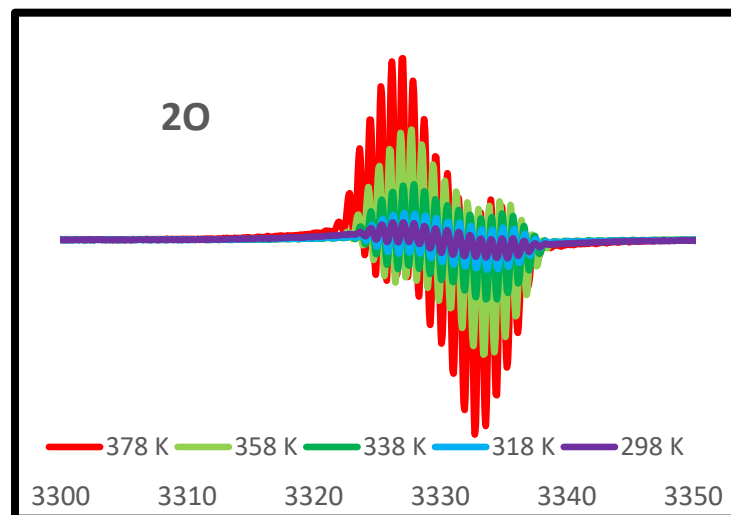
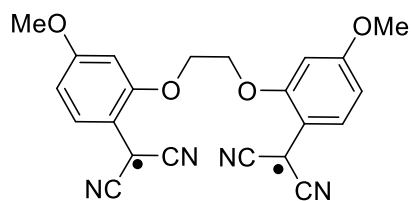
Trimethoxy

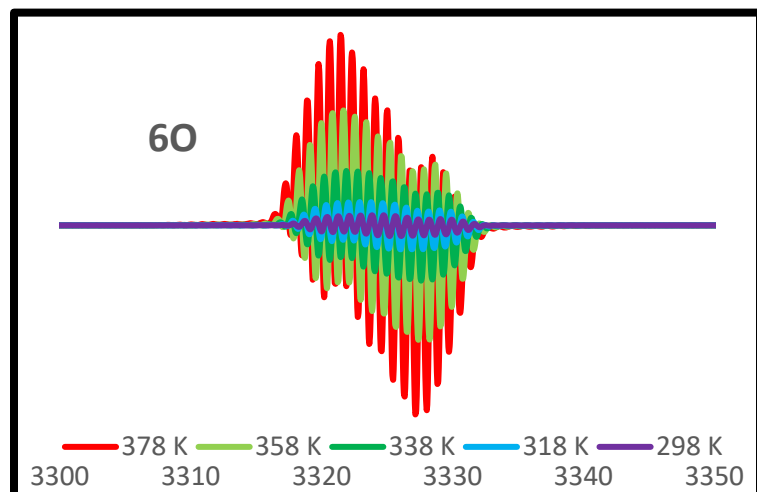
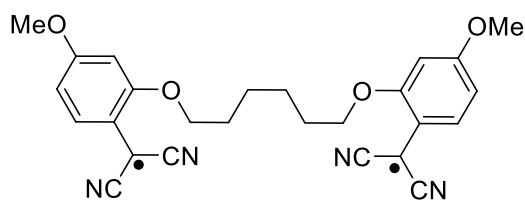
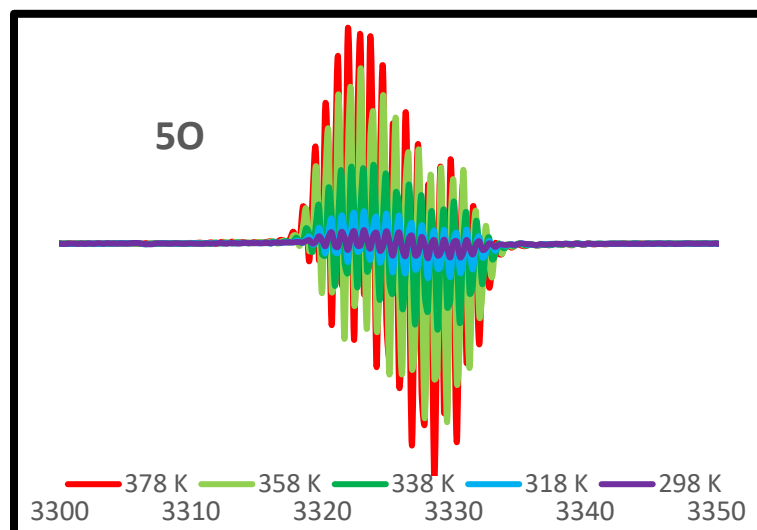
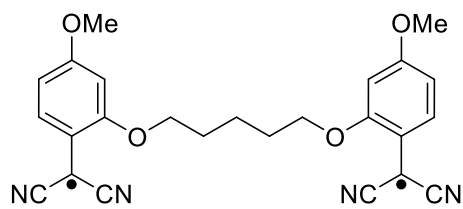


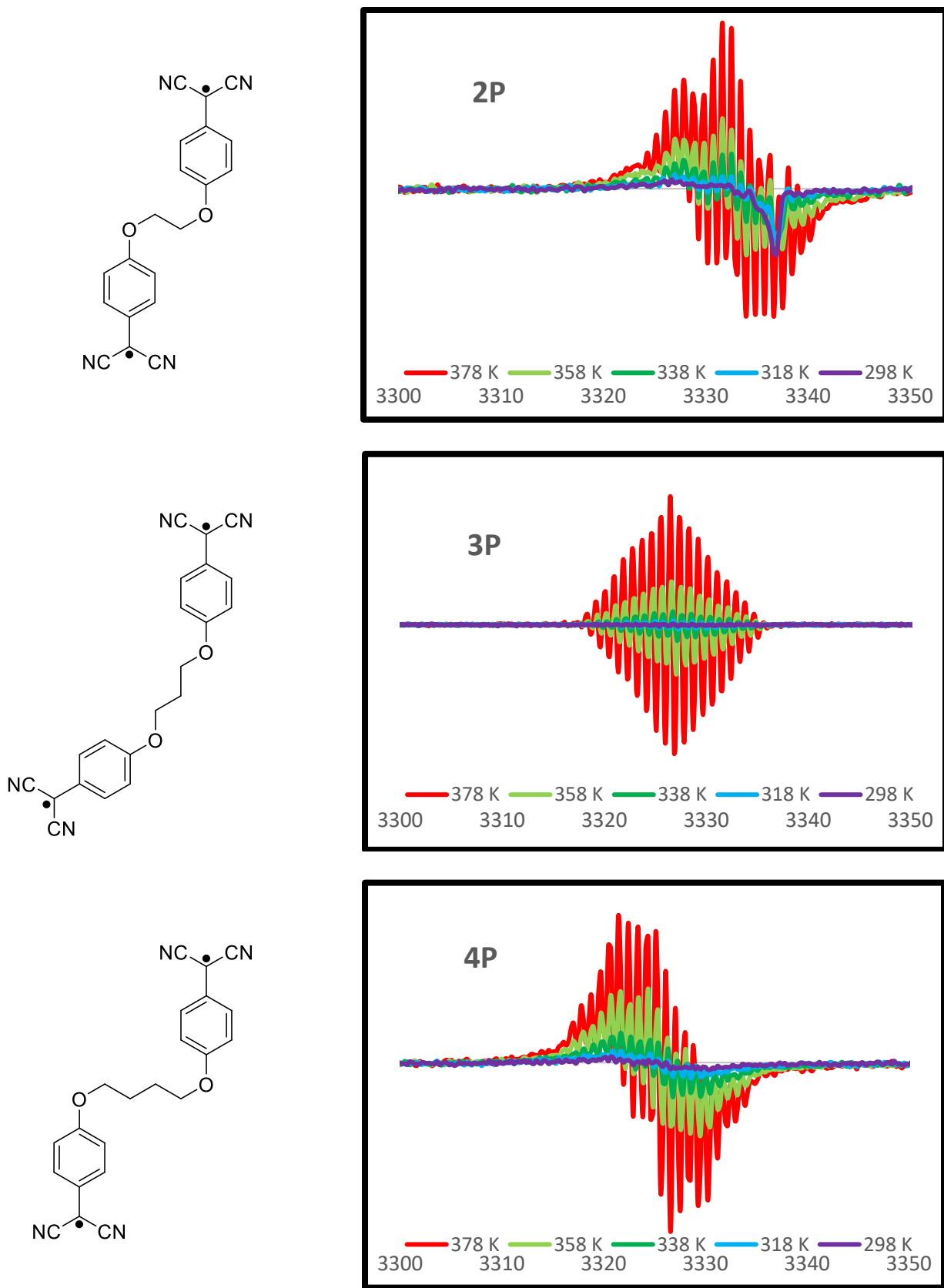
40

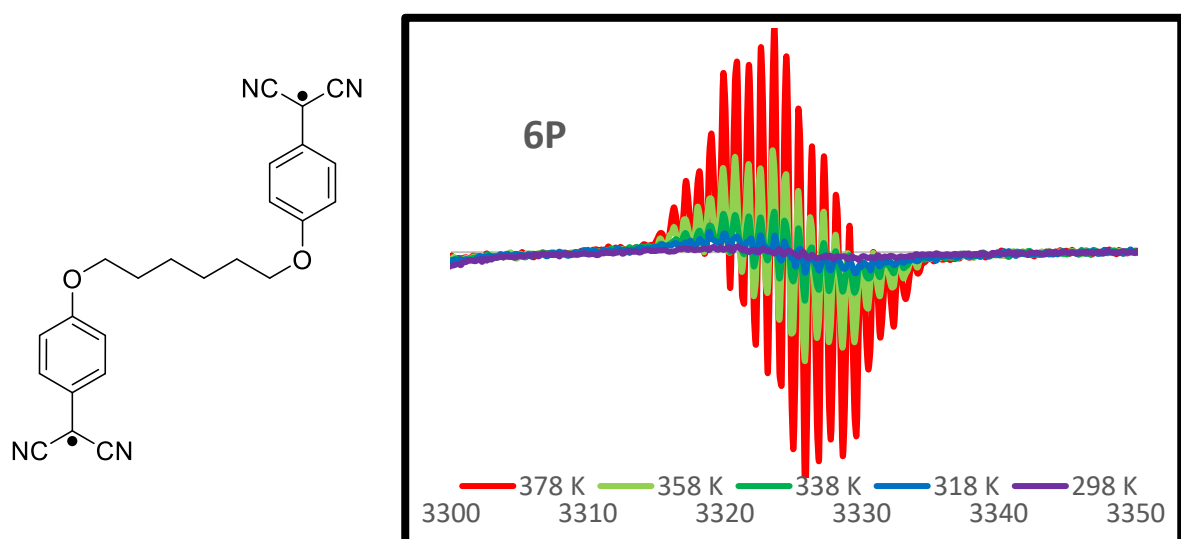
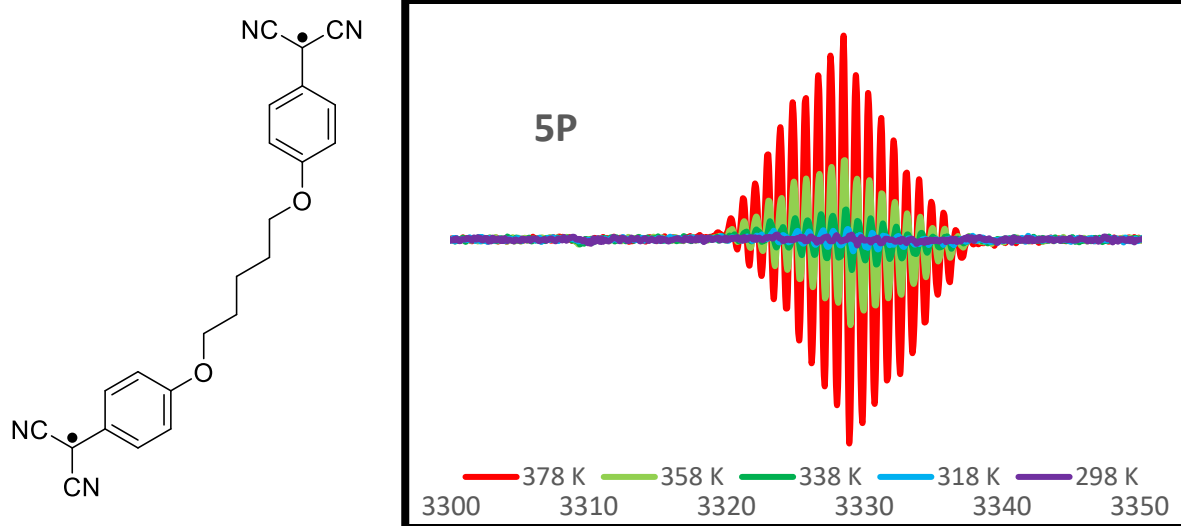


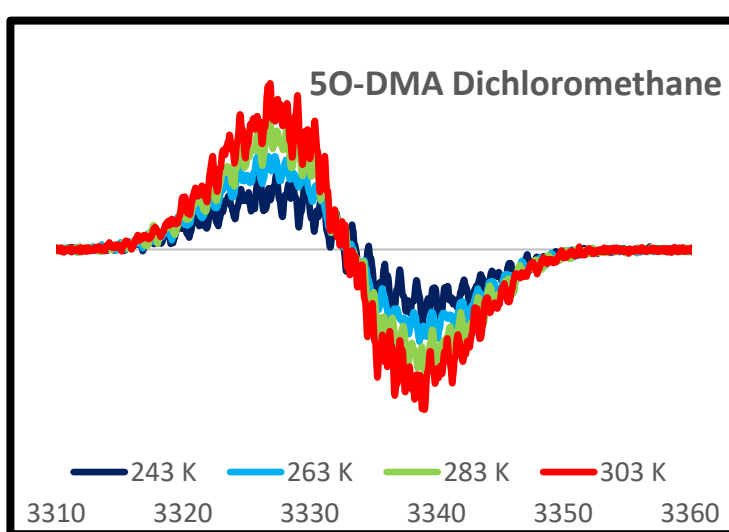
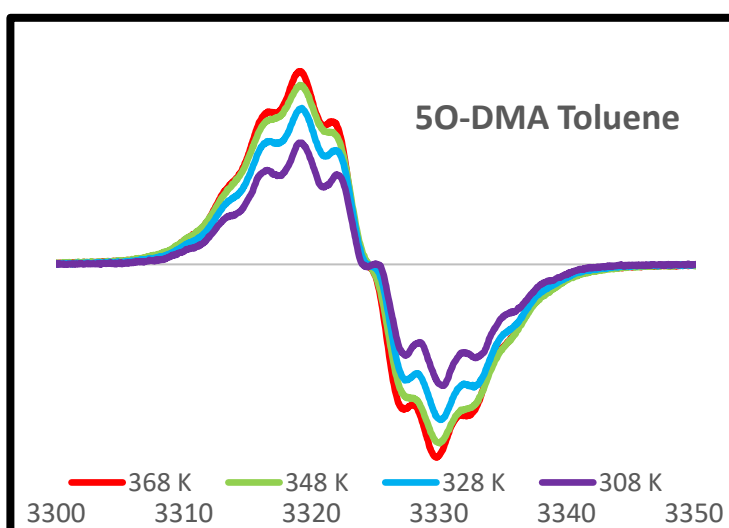
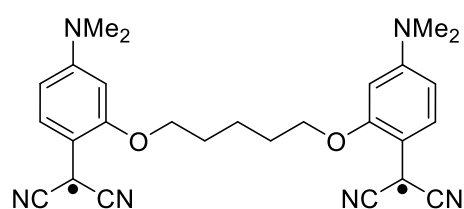
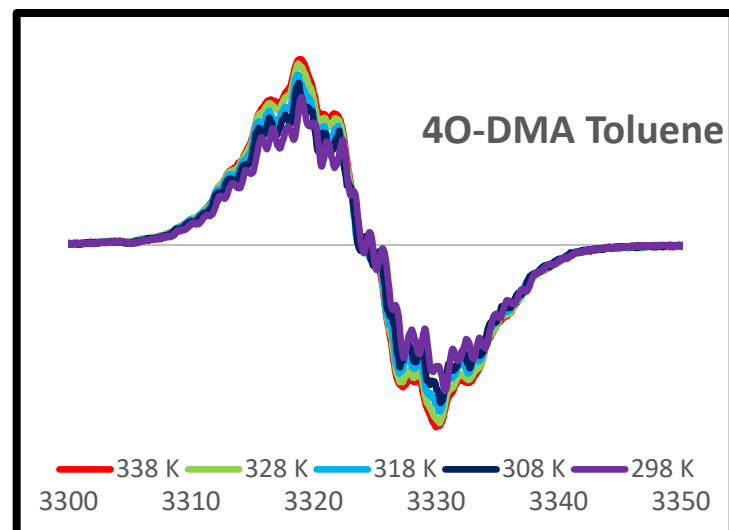
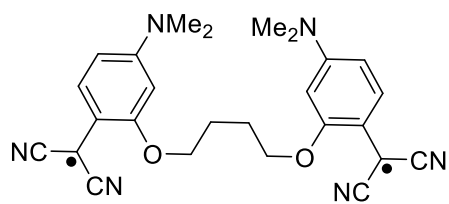
EPR Spectra:

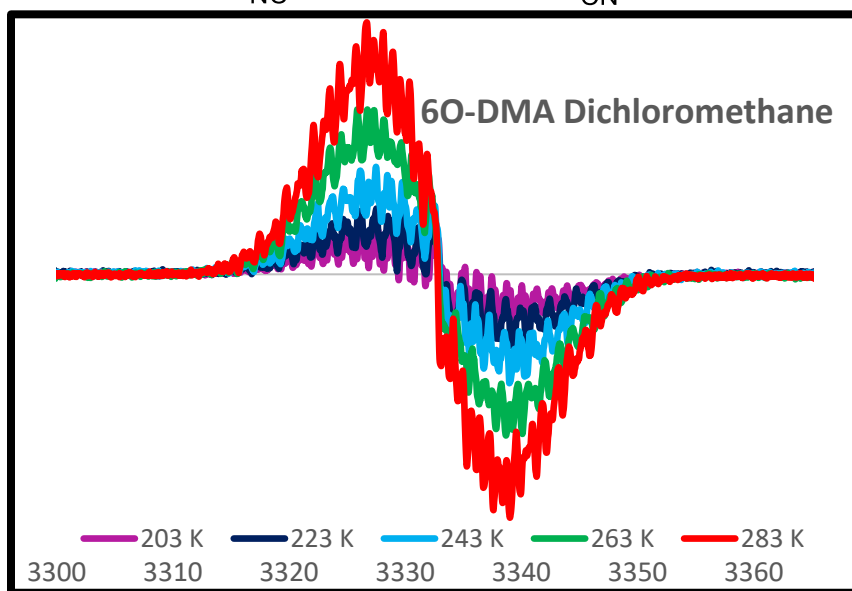
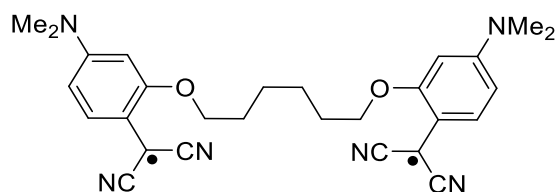
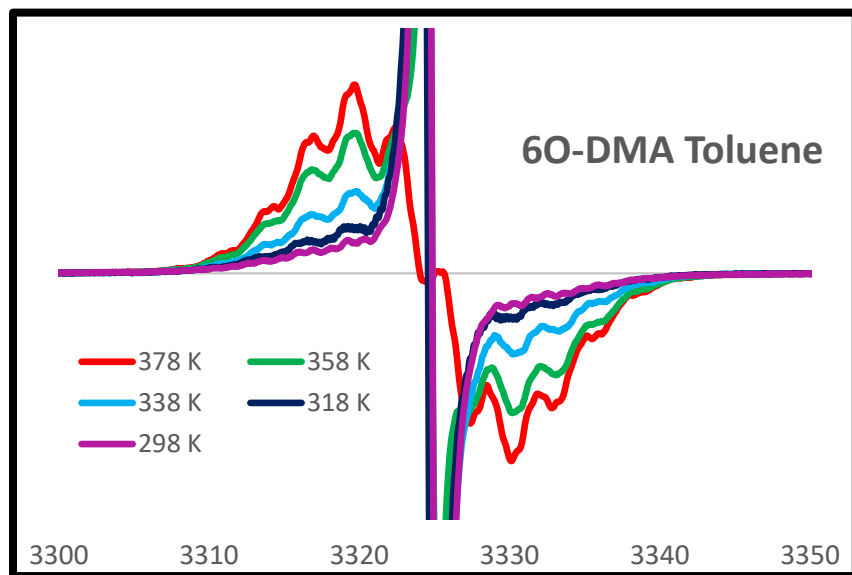


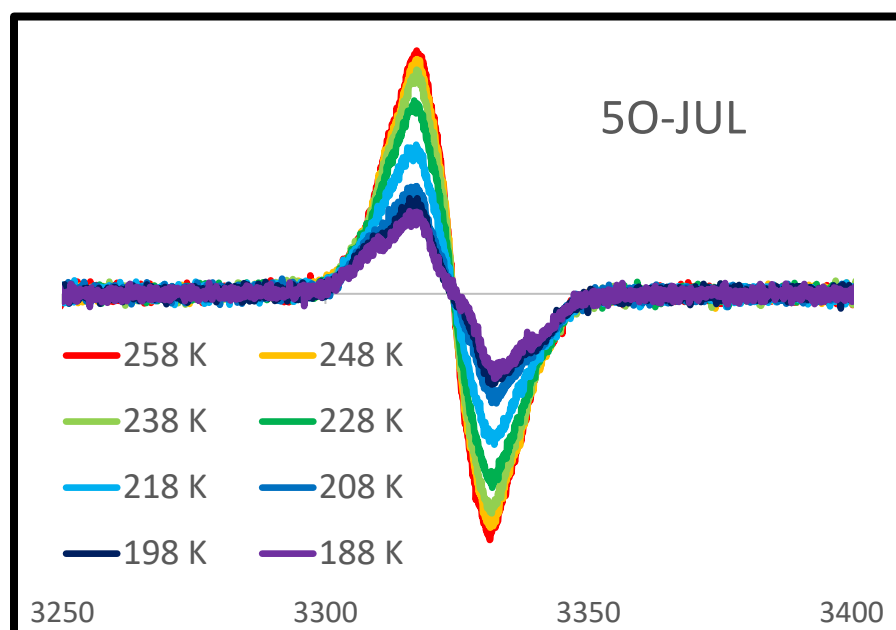
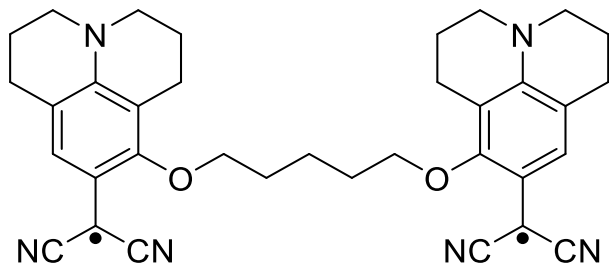






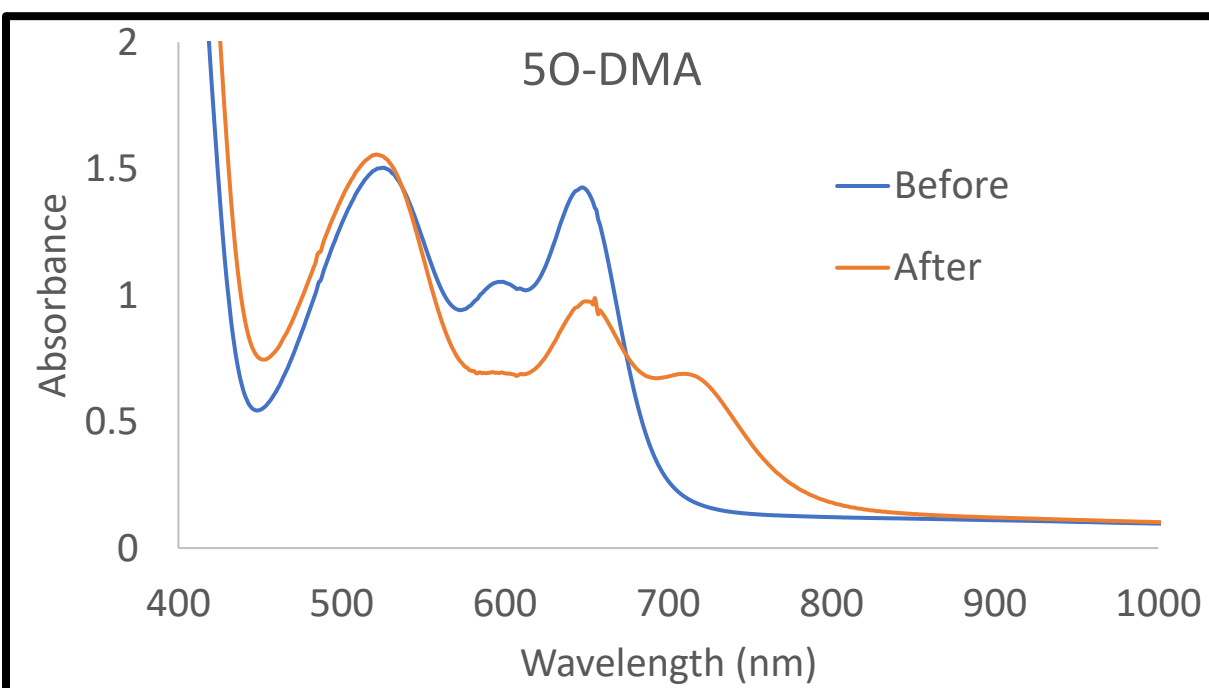
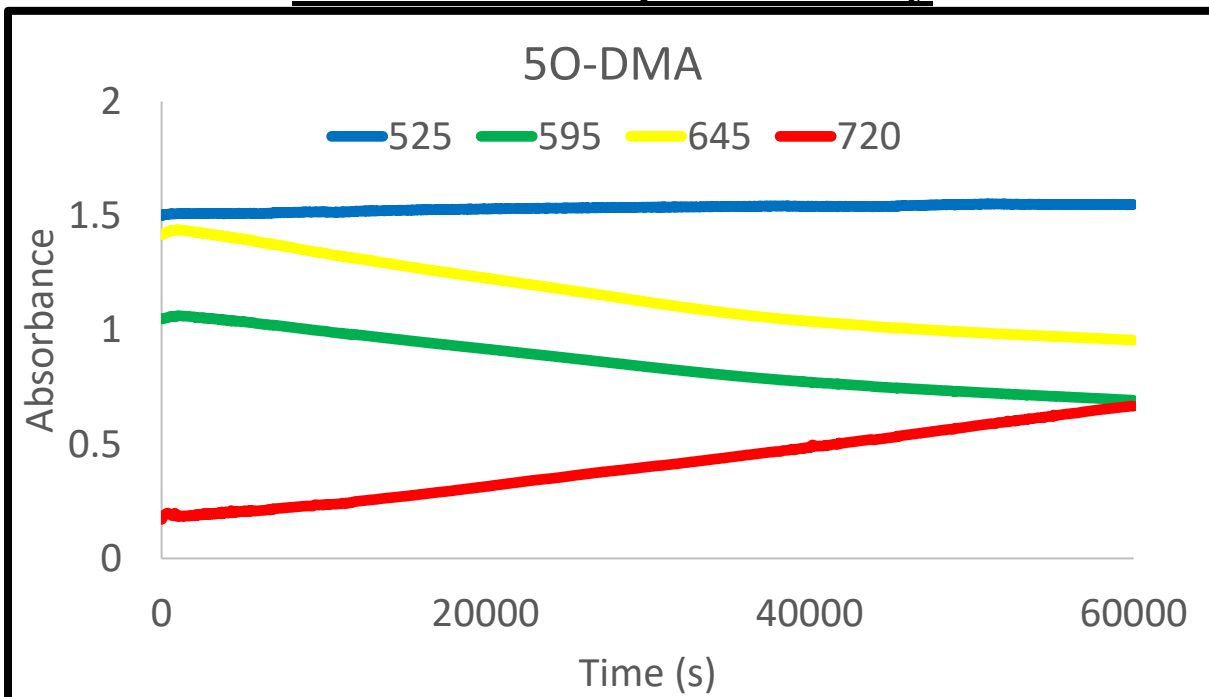


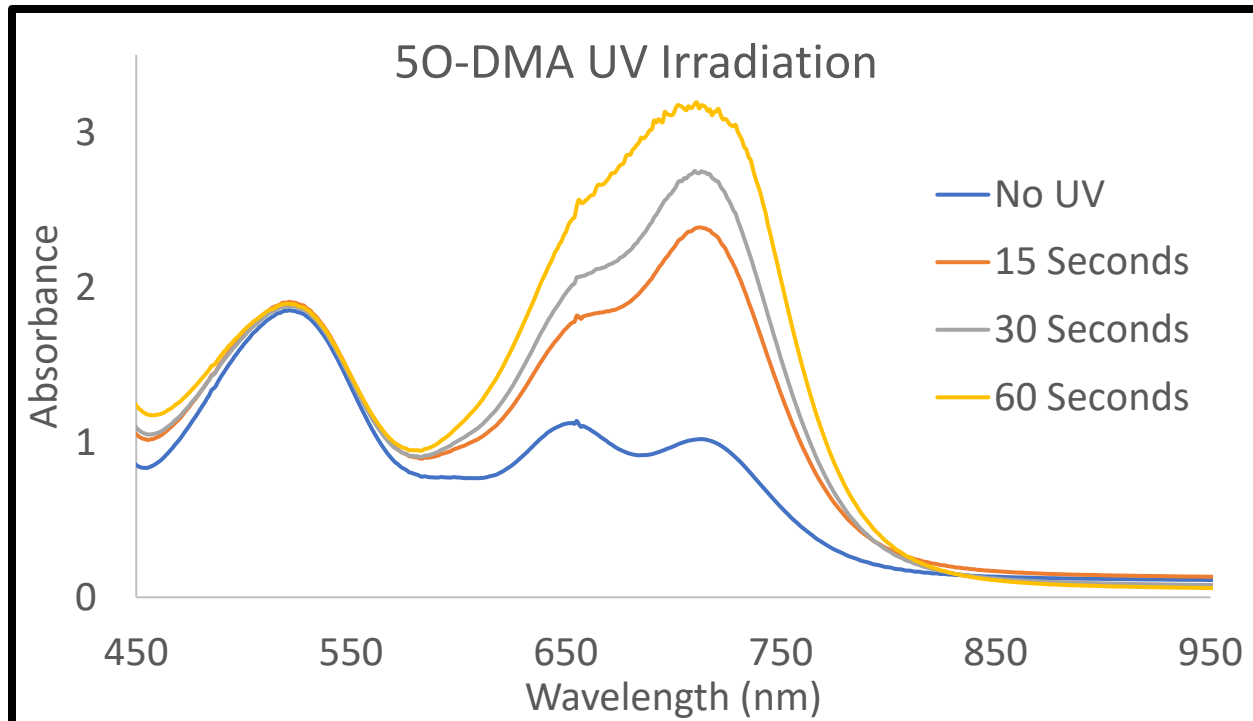




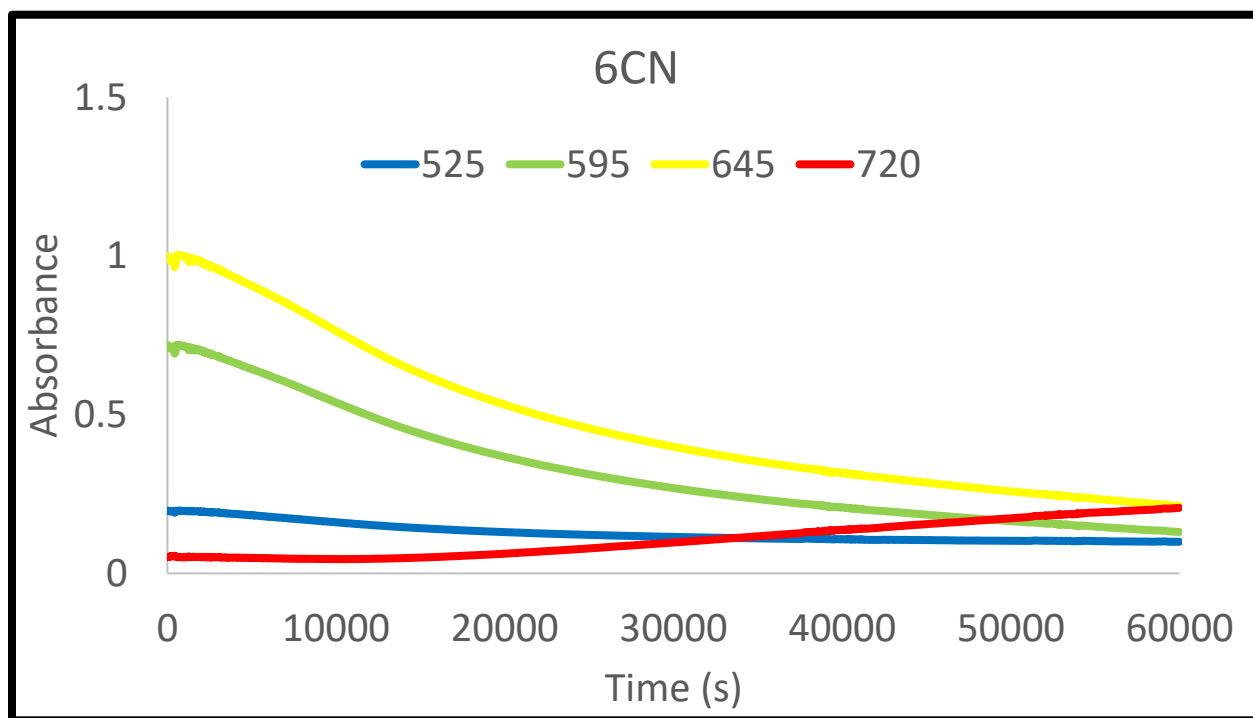
UV/Vis Spectra:

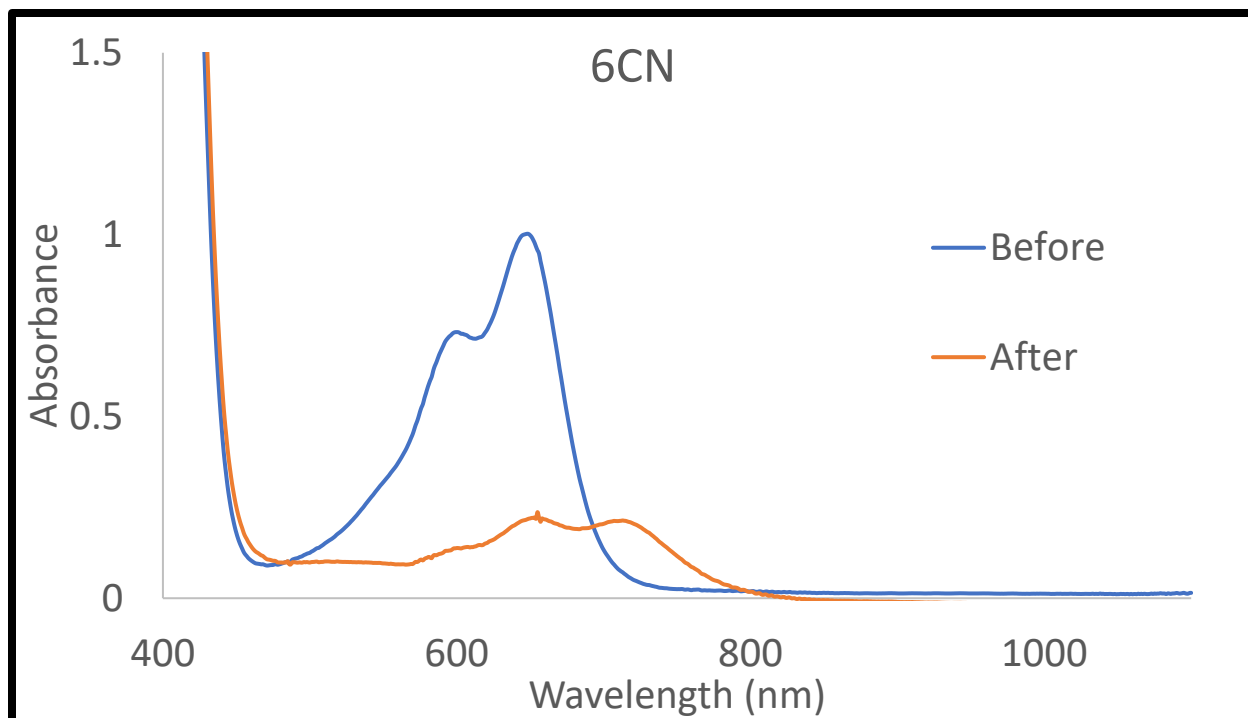
5O-DMA Decomposition Study





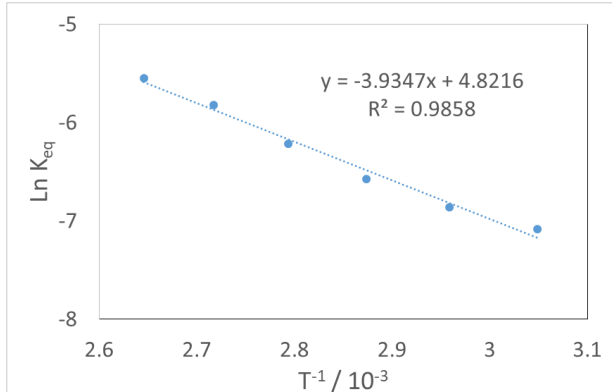
60-DMA Decomposition Study



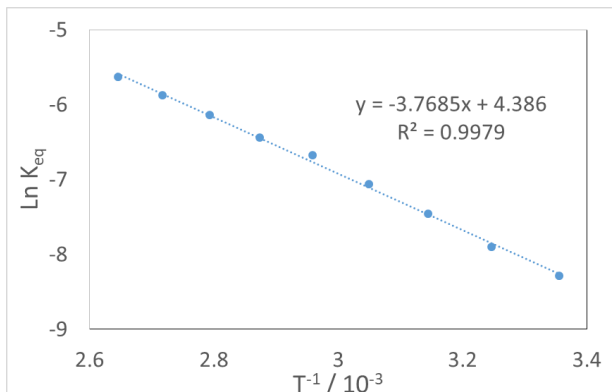


Van 't Hoff Plots

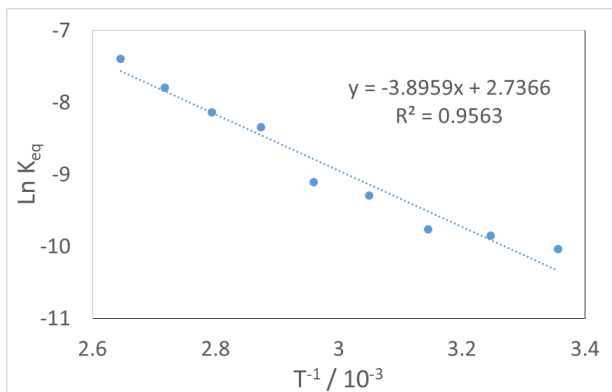
20:



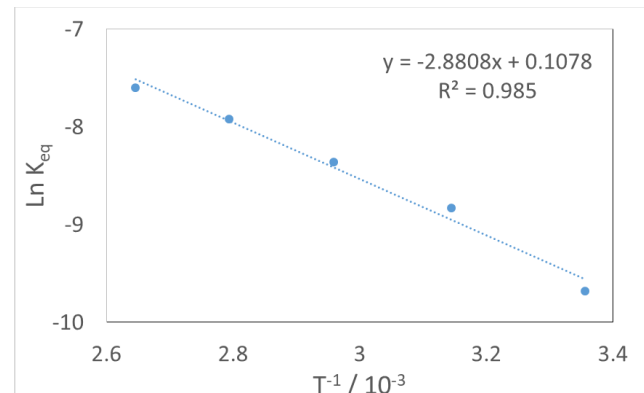
30:



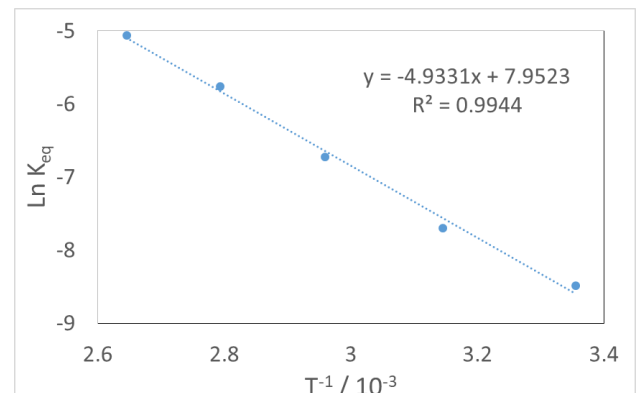
40:

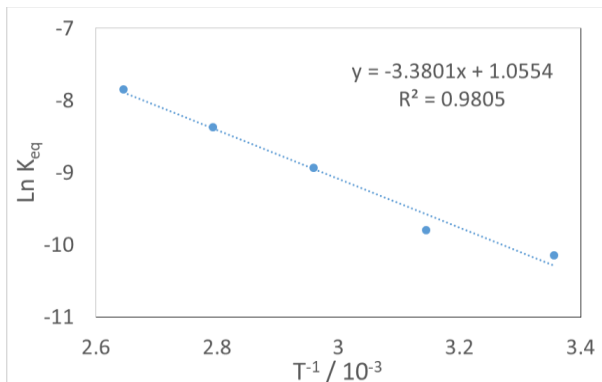
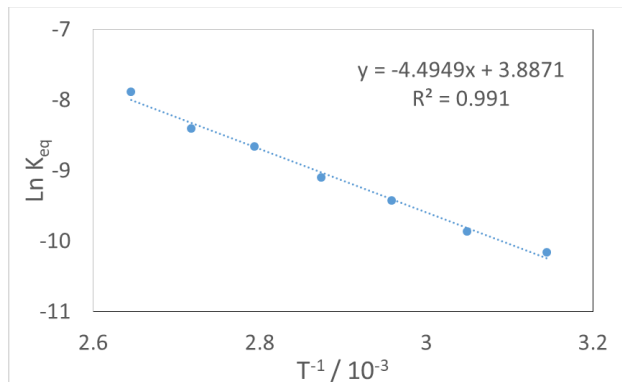
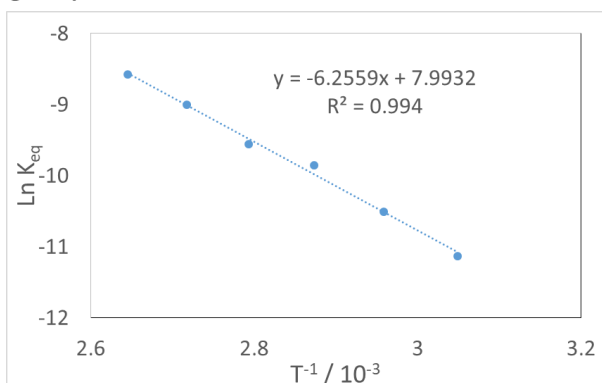
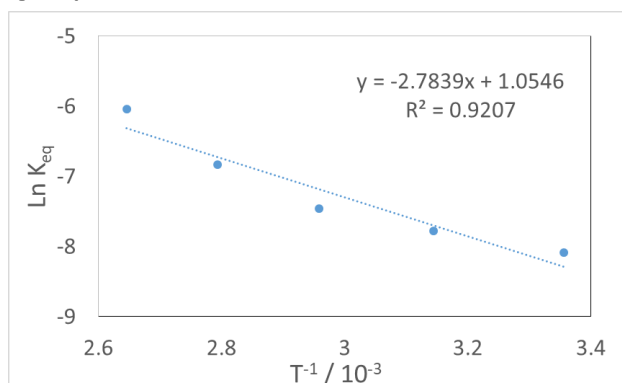
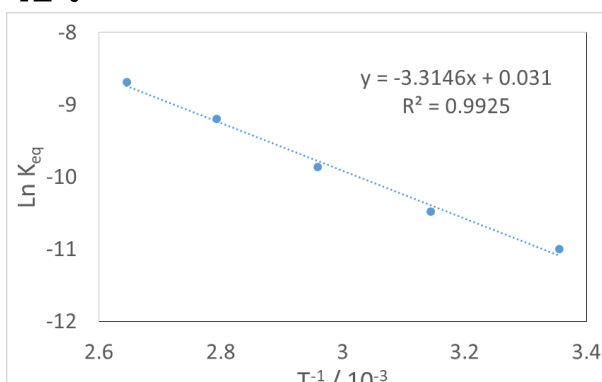


50:



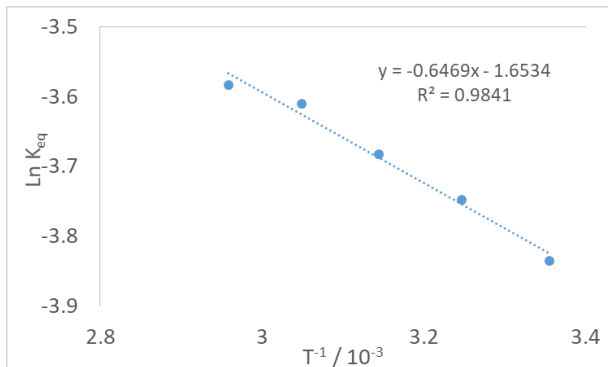
60:



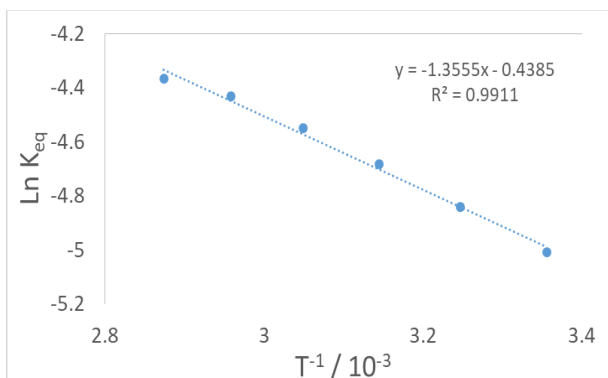
2P:**5P:****3P:****6P:****4P:**

*** - Dichloromethane
solvent**

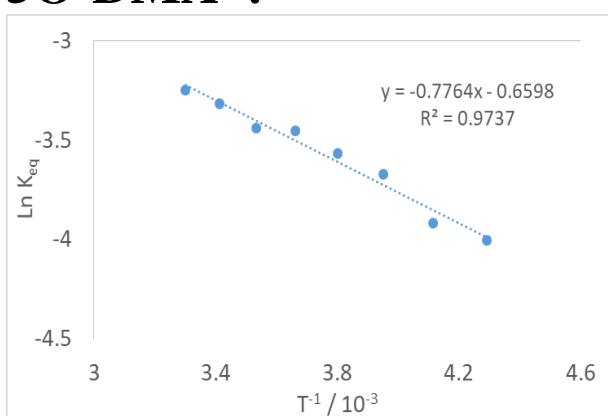
4O-DMA:



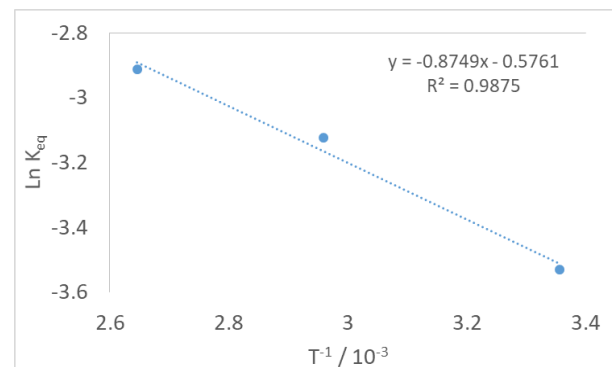
5O-DMA:



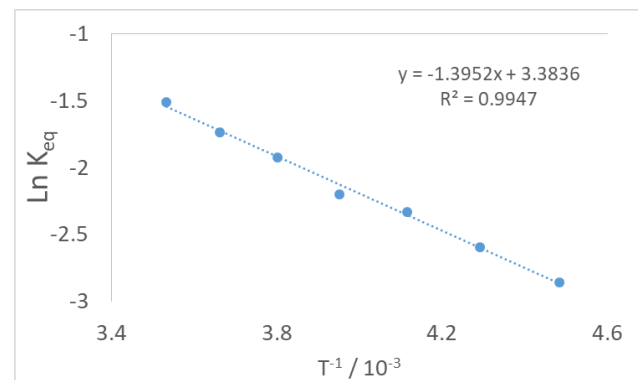
5O-DMA*:



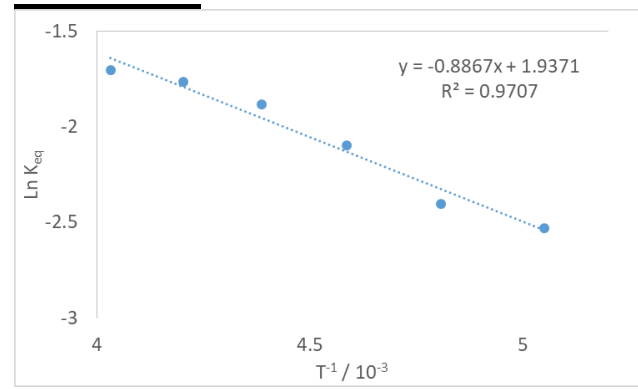
6O-DMA:

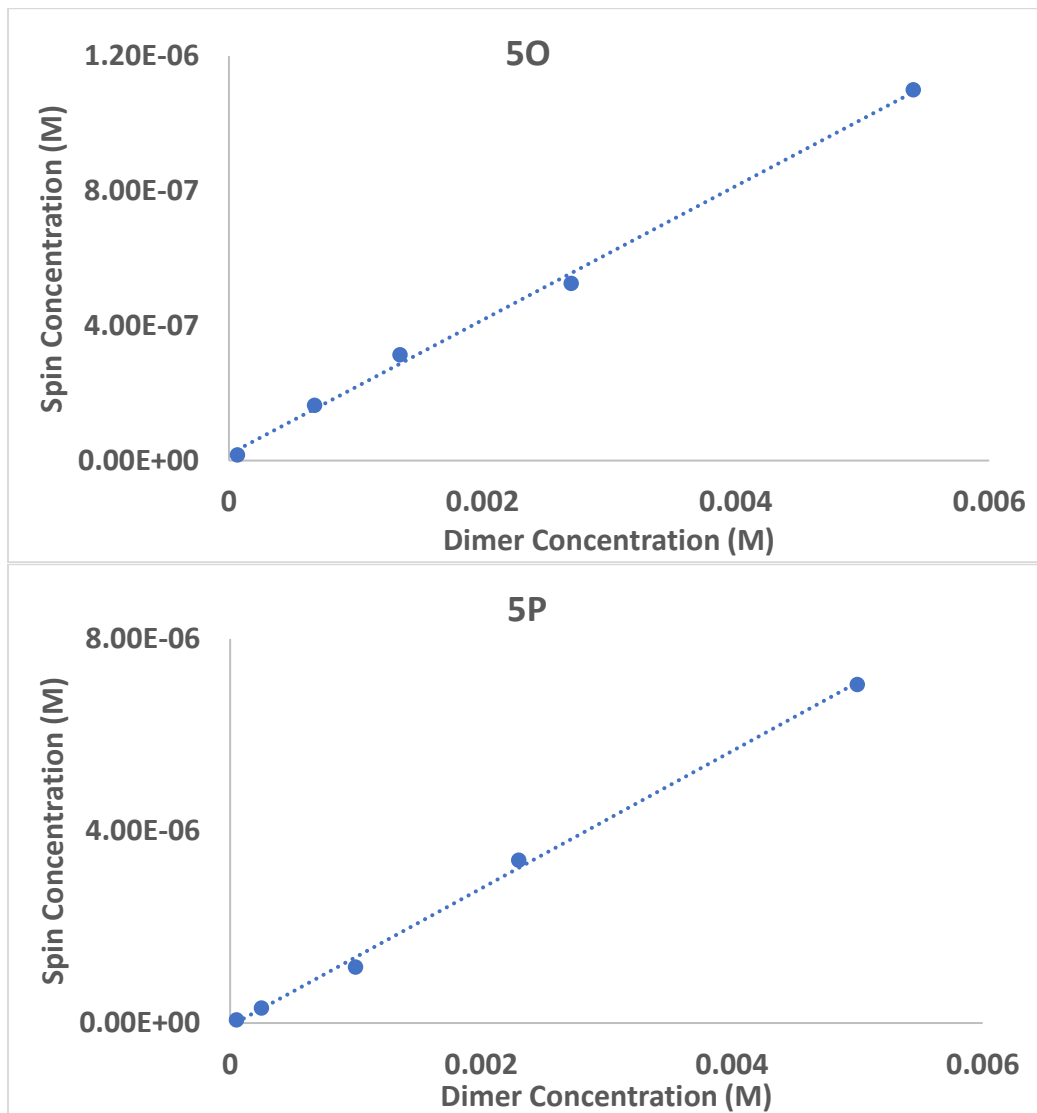


6O-DMA*:



5O-JUL





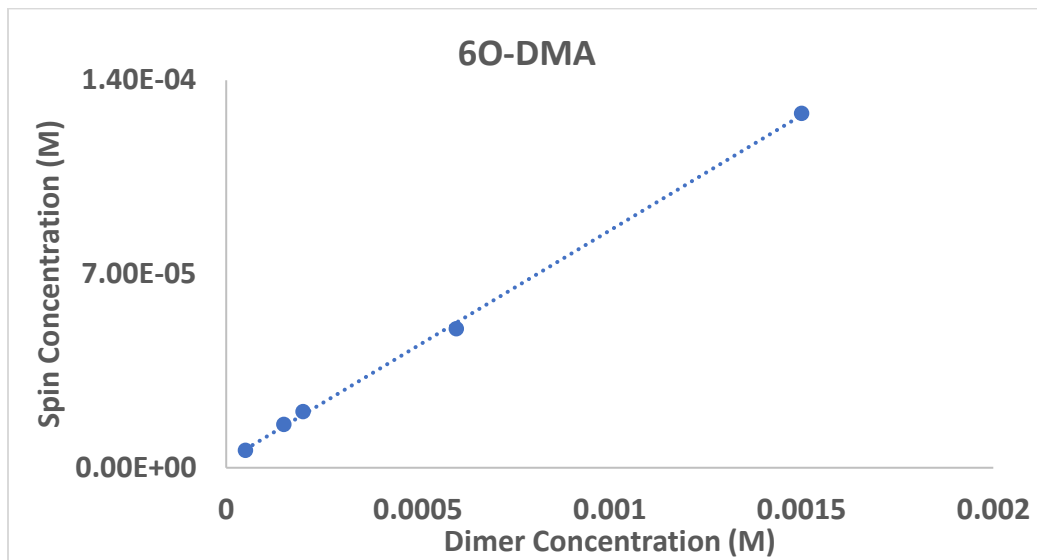
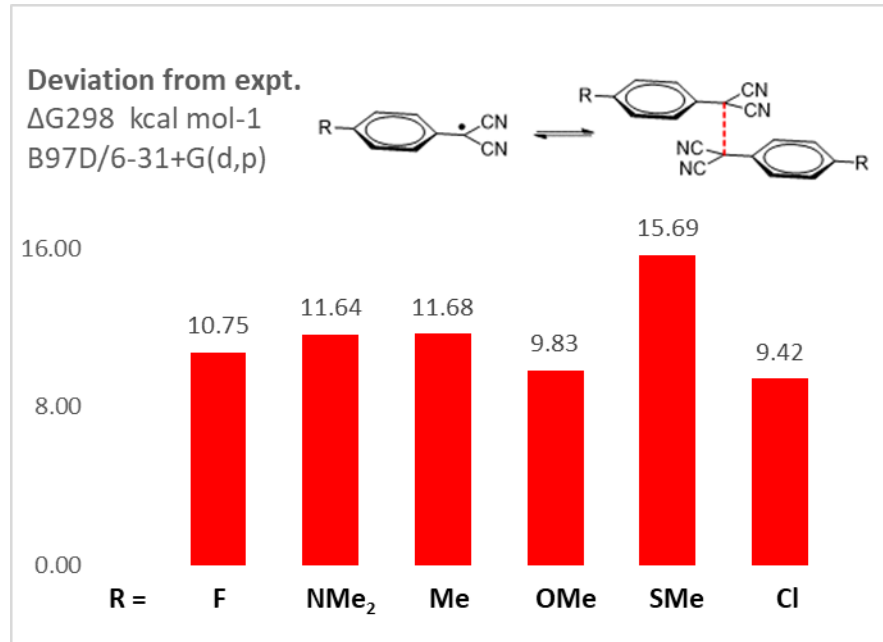


Table of Absolute Energies for Computed Radicals and Dimers

Fluorine Dimer		
Functional	6-31+G(d,p)	cc-pVDZ
B3LYP	-1109.192149	-1109.207056
BLYP	-1108.892874	-1108.895063
PBE1PBE	-1107.944329	-1107.977360
B3P86	-1112.058042	-1112.090692
B98	-1108.752373	-1108.785060
ω B97XD	-1108.821366	-1108.851594
B3LYP-D3	-1109.231774	-1109.246705
B97D	-1108.441235	-1108.480890
B97D3	-1108.511615	-1108.551219
Fluorine Radical		
Functional	6-31+G(d,p)	cc-pVDZ
uB3LYP	-554.603146	-554.609099
uBLYP	-554.458043	-554.457467
uPBE1PBE	-553.972199	-553.987424
uB3P86	-556.030696	-556.045786
uB98	-554.378835	-554.393838
uwB97XD	-554.401935	-554.415814
uB3LYP-D3	-554.614809	-554.620753
uB97D	-554.221599	-554.239903
uB97D3	-554.255006	-554.273259
Functional Group Test - ω B97XD/6-31+G(d,p)		
R	Dimer	Radical
NMe ₂	-1178.126616	-589.057888
OMe	-1139.309126	-569.647126
SMe	-1785.279410	-892.632271
Me	-988.947889	-494.465709
Cl	-1829.555060	-914.768947



Optimized Geometry Coordinates

F-Dimer B3LYP/6-31+G(d,p)

```

C      0.429295 -0.000133 -0.707888
C      1.952622 -0.000072 -0.470979
C      0.018587 -1.191372 -1.477449
C      0.018558  1.190823 -1.477870
C      2.647062 -1.212008 -0.346383
C      2.646989  1.211923 -0.346520
N     -0.288225 -2.139584 -2.070567
N     -0.288278  2.138813 -2.071331
C      4.016728 -1.217811 -0.087920
H      2.130318 -2.159249 -0.453902
C      4.016653  1.217837 -0.088057
H      2.130186  2.159121 -0.454142
C      4.673985  0.000039  0.038126
H      4.567956 -2.146036  0.010515
H      4.567828  2.146104  0.010277
F      6.003975  0.000096  0.283670
C     -0.429295  0.000101  0.707898
C     -1.952622  0.000066  0.470984

```

C -0.018574 1.191324 1.477476
C -0.018577 -1.190873 1.477864
C -2.647045 1.212018 0.346431
C -2.647002 -1.211912 0.346469
N 0.288249 2.139522 2.070611
N 0.288238 -2.138874 2.071316
C -4.016707 1.217848 0.087960
H -2.130289 2.159248 0.453992
C -4.016667 -1.217800 0.087998
H -2.130212 -2.159122 0.454052
C -4.673981 0.000010 -0.038138
H -4.567926 2.146082 -0.010443
H -4.567850 -2.146058 -0.010376
F -6.003969 -0.000014 -0.283691

F-Dimer 6-31+G(d,p)/B3LYP-D3

C 0.41488500 0.00043800 -0.71451200
C 1.93701800 0.00024600 -0.49482000
C -0.01283900 -1.19032700 -1.47209200
C -0.01275900 1.19212700 -1.47068500
C 2.62760100 -1.21271000 -0.36496600
C 2.62785900 1.21302300 -0.36464100
N -0.33865000 -2.14695100 -2.04004200
N -0.33848200 2.14946000 -2.03748800
C 3.99586800 -1.21856500 -0.10044700
H 2.10710100 -2.15839800 -0.46721100
C 3.99612500 1.21851200 -0.10012500
H 2.10756200 2.15884800 -0.46664500
C 4.65218400 -0.00011400 0.02792600
H 4.54826600 -2.14520800 0.00374500
H 4.54872400 2.14500700 0.00431300
F 5.98098500 -0.00028500 0.28057900
C -0.41488500 -0.00035600 0.71452000
C -1.93701700 -0.00022600 0.49482200

C	0.01280600	1.19044900	1.47205600
C	0.01278700	-1.19200700	1.47073800
C	-2.62765000	1.21269300	0.36487900
C	-2.62780500	-1.21303900	0.36472500
N	0.33856700	2.14710400	2.03997900
N	0.33854700	-2.14930900	2.03757300
C	-3.99591400	1.21846900	0.10035700
H	-2.10718700	2.15841000	0.46705200
C	-3.99607200	-1.21860900	0.10020100
H	-2.10747000	-2.15883600	0.46680400
C	-4.65218000	-0.00002000	-0.02793500
H	-4.54835500	2.14507800	-0.00390800
H	-4.54862800	-2.14513700	-0.00416900
F	-5.98098000	0.00008400	-0.28059400

F-Dimer 6-31+G(d,p)/B3P86

C	0.41864000	0.00023700	-0.70303600
C	1.93343400	0.00008700	-0.47501500
C	0.00425600	-1.18791300	-1.46392800
C	0.00440800	1.18874900	-1.46344200
C	2.62328700	-1.20955800	-0.35095500
C	2.62345900	1.20958700	-0.35045700
N	-0.30529000	-2.13974000	-2.04859700
N	-0.30502600	2.14086100	-2.04770700
C	3.98892700	-1.21541900	-0.09247400
H	2.10299100	-2.15542800	-0.46002300
C	3.98909700	1.21514500	-0.09197700
H	2.10329800	2.15557500	-0.45913500
C	4.64516100	-0.00021100	0.03421300
H	4.54059400	-2.14306400	0.00597400
H	4.54090000	2.14266800	0.00685800
F	5.96632400	-0.00035100	0.27894000
C	-0.41863900	0.00001700	0.70304200
C	-1.93343300	-0.00004200	0.47501800

C -0.00439700 1.18828100 1.46383100
C -0.00427000 -1.18838200 1.46355300
C -2.62340000 1.20949700 0.35052800
C -2.62334200 -1.20964900 0.35088200
N 0.30504100 2.14020000 2.04840700
N 0.30525700 -2.14040600 2.04791300
C -3.98903800 1.21513400 0.09204300
H -2.10319300 2.15545400 0.45925700
C -3.98898100 -1.21543000 0.09239700
H -2.10309100 -2.15554900 0.45990000
C -4.64515800 -0.00018300 -0.03422000
H -4.54079600 2.14268900 -0.00674200
H -4.54069100 -2.14304300 -0.00610600
F -5.96632000 -0.00024800 -0.27895300

F-Dimer 6-31+G(d,p)/B97D

C 0.41193800 -0.00015300 -0.73714800
C 1.93695100 -0.00000400 -0.52465500
C -0.03864900 -1.19429400 -1.48215900
C -0.03890400 1.19393100 -1.48210400
C 2.62932300 -1.21969900 -0.38638900
C 2.62912700 1.21983400 -0.38676500
N -0.38188700 -2.16073700 -2.04385500
N -0.38236500 2.16032200 -2.04375300
C 4.00247300 -1.22587000 -0.11162200
H 2.10468300 -2.16808700 -0.49053900
C 4.00228100 1.22631100 -0.11200300
H 2.10432400 2.16810100 -0.49120300
C 4.66156200 0.00029600 0.02136600
H 4.55410400 -2.15775000 -0.00226900
H 4.55376400 2.15831400 -0.00295100
F 5.99508100 0.00044100 0.28461700
C -0.41193700 -0.00024900 0.73713200
C -1.93695100 -0.00006200 0.52464800

C	0.03891700	1.19372900	1.48224900
C	0.03864700	-1.19449300	1.48198000
C	-2.62910500	1.21979300	0.38679300
C	-2.62934900	-1.21974000	0.38636800
N	0.38237600	2.16004500	2.04402700
N	0.38189700	-2.16102000	2.04352400
C	-4.00226100	1.22630300	0.11204400
H	-2.10428200	2.16804800	0.49124400
C	-4.00250200	-1.22587800	0.11161400
H	-2.10472800	-2.16814000	0.49050000
C	-4.66156800	0.00030400	-0.02134400
H	-4.55372700	2.15832000	0.00301600
H	-4.55415400	-2.15774500	0.00225100
F	-5.99508900	0.00048100	-0.28458000

F-Dimer 6-31+G(d,p)/B97-D3

C	0.40884500	-0.00012000	-0.72799100
C	1.92896700	0.00001200	-0.51468600
C	-0.03423500	-1.19464900	-1.46906100
C	-0.03445700	1.19439900	-1.46894600
C	2.62009100	-1.21752600	-0.38266200
C	2.61989700	1.21768000	-0.38287800
N	-0.37245000	-2.16274600	-2.02988500
N	-0.37285800	2.16248800	-2.02967200
C	3.99159900	-1.22374100	-0.11020600
H	2.09625100	-2.16469500	-0.49017600
C	3.99140600	1.22416400	-0.11042200
H	2.09590400	2.16474400	-0.49056700
C	4.65012000	0.00027700	0.02303400
H	4.54226800	-2.15542400	-0.00419200
H	4.54192600	2.15595500	-0.00458500
F	5.98365000	0.00040500	0.28446400
C	-0.40884600	-0.00026000	0.72798500
C	-1.92896800	-0.00007400	0.51468500

C 0.03446400 1.19411200 1.46917300
C 0.03423100 -1.19493400 1.46882100
C -2.61986200 1.21761800 0.38291000
C -2.62013200 -1.21758700 0.38263500
N 0.37286400 2.16208900 2.03009200
N 0.37246500 -2.16314500 2.02943700
C -3.99137100 1.22415200 0.11045900
H -2.09583700 2.16466300 0.49061700
C -3.99164100 -1.22375300 0.11018300
H -2.09632300 -2.16477500 0.49012900
C -4.65012400 0.00028900 -0.02302500
H -4.54186200 2.15596300 0.00464600
H -4.54233900 -2.15541600 0.00415100
F -5.98365500 0.00046500 -0.28445000

F-Dimer 6-31+G(d,p)/B98

C 0.42729400 -0.00032200 -0.70882800
C 1.95275600 -0.00007900 -0.47551900
C 0.01206500 -1.19465400 -1.47712100
C 0.01175000 1.19360900 -1.47756400
C 2.64705000 -1.21449300 -0.35047900
C 2.64662100 1.21454500 -0.35009500
N -0.29810500 -2.14630400 -2.06466200
N -0.29871800 2.14494000 -2.06546300
C 4.01854000 -1.21970900 -0.09038000
H 2.12907500 -2.16260900 -0.45866300
C 4.01810500 1.22015600 -0.08999500
H 2.12830500 2.16251100 -0.45795400
C 4.67768100 0.00031800 0.03705800
H 4.57011500 -2.14869300 0.00846200
H 4.56935500 2.14929900 0.00916100
F 6.00110300 0.00051800 0.28303700
C -0.42729100 -0.00011500 0.70873000
C -1.95276300 0.00004100 0.47546900

C -0.01173300 1.19404800 1.47709600
 C -0.01202600 -1.19420400 1.47737800
 C -2.64669200 1.21462800 0.35003400
 C -2.64701800 -1.21441000 0.35056800
 N 0.29877200 2.14557400 2.06466200
 N 0.29822600 -2.14568000 2.06515900
 C -4.01819200 1.22016400 0.09001400
 H -2.12841700 2.16262300 0.45783000
 C -4.01852300 -1.21970000 0.09055000
 H -2.12899900 -2.16249600 0.45879500
 C -4.67772200 0.00029000 -0.03693200
 H -4.56948900 2.14927800 -0.00915500
 H -4.57006500 -2.14871400 -0.00819400
 F -6.00116100 0.00041800 -0.28282100

F-Dimer 6-31+G(d,p)/BLYP

C 0.44327700 0.00006500 -0.72850900
 C 1.97369800 -0.00003800 -0.48215300
 C 0.02355200 -1.19742700 -1.49462800
 C 0.02371800 1.19752200 -1.49477600
 C 2.67381900 -1.22144300 -0.35441200
 C 2.67402400 1.22126800 -0.35464600
 N -0.29316700 -2.15558000 -2.09238200
 N -0.29284300 2.15565600 -2.09264200
 C 4.05254100 -1.22770500 -0.08928900
 H 2.15420700 -2.17433600 -0.46500600
 C 4.05275100 1.22735200 -0.08952900
 H 2.15456500 2.17422500 -0.46541100
 C 4.71318100 -0.00021800 0.03986200
 H 4.60609100 -2.16232600 0.01138500
 H 4.60645800 2.16190200 0.01095600
 F 6.06056000 -0.00031000 0.29321900
 C -0.44327700 0.00023300 0.72842300
 C -1.97370900 0.00006200 0.48211100

C -0.02370300 1.19787000 1.49439900
 C -0.02351800 -1.19707000 1.49481700
 C -2.67408700 1.22133700 0.35459400
 C -2.67380000 -1.22137400 0.35449200
 N 0.29292600 2.15615300 2.09199000
 N 0.29327700 -2.15507700 2.09276300
 C -4.05282800 1.22736000 0.08954600
 H -2.15466000 2.17431700 0.46530100
 C -4.05253600 -1.22769700 0.08943800
 H -2.15415600 -2.17424300 0.46512300
 C -4.71322200 -0.00023900 -0.03975200
 H -4.60657300 2.16188600 -0.01095200
 H -4.60606200 -2.16234200 -0.01115000
 F -6.06061600 -0.00038900 -0.29302900

F-Dimer 6-31+G(d,p)/PBE1PBE

C 0.41627800 -0.00041900 -0.70102400
 C 1.93129300 -0.00019300 -0.47544400
 C 0.00139300 -1.18915500 -1.46167400
 C 0.00121700 1.18755100 -1.46277200
 C 2.62128400 -1.20939900 -0.35094000
 C 2.62098700 1.20922800 -0.35138600
 N -0.30886800 -2.14105100 -2.04379800
 N -0.30919100 2.13885000 -2.04579100
 C 3.98671100 -1.21472000 -0.09284100
 H 2.10120500 -2.15623300 -0.45887700
 C 3.98641200 1.21497900 -0.09328500
 H 2.10067200 2.15589400 -0.45966100
 C 4.64317100 0.00023300 0.03333700
 H 4.53895500 -2.14269100 0.00599500
 H 4.53843000 2.14312000 0.00521300
 F 5.96162800 0.00044100 0.27740600
 C -0.41627800 0.00015600 0.70102300
 C -1.93129300 0.00014700 0.47544400

C	-0.00124800	1.18877900	1.46177000
C	-0.00136200	-1.18792700	1.46267400
C	-2.62113800	1.20946500	0.35120500
C	-2.62113600	-1.20916100	0.35112200
N	0.30913900	2.14058800	2.04397000
N	0.30892800	-2.13931200	2.04561700
C	-3.98656300	1.21500900	0.09310600
H	-2.10094300	2.15621200	0.45935400
C	-3.98656300	-1.21469100	0.09302200
H	-2.10093600	-2.15591500	0.45918400
C	-4.64317200	0.00016200	-0.03333600
H	-4.53869600	2.14306700	-0.00552500
H	-4.53869100	-2.14274400	-0.00568100
F	-5.96163000	0.00017200	-0.27740400

F-Dimer 6-31+G(d,p)/ωB97XD

C	0.40742300	-0.00022200	-0.70331600
C	1.92715100	-0.00005200	-0.48779400
C	-0.01512500	-1.19158100	-1.46360800
C	-0.01534100	1.19094500	-1.46379100
C	2.61548000	-1.20875600	-0.36063500
C	2.61526800	1.20883400	-0.36122200
N	-0.33397000	-2.14488000	-2.03435100
N	-0.33433400	2.14410100	-2.03468900
C	3.97981900	-1.21460000	-0.09946300
H	2.09606200	-2.15557300	-0.46444700
C	3.97960500	1.21504600	-0.10005200
H	2.09568100	2.15550700	-0.46550600
C	4.63504500	0.00031100	0.02766300
H	4.52993400	-2.14225800	0.00261600
H	4.52955800	2.14284900	0.00157100
F	5.95437600	0.00048900	0.27668200
C	-0.40742400	-0.00019700	0.70331100
C	-1.92715300	-0.00003800	0.48779200

C 0.01534000 1.19099900 1.46374100
C 0.01512900 -1.19152700 1.46364600
C -2.61527700 1.20884300 0.36121600
C -2.61547600 -1.20874600 0.36064700
N 0.33433500 2.14417700 2.03460000
N 0.33399100 -2.14480300 2.03441600
C -3.97961500 1.21504600 0.10004900
H -2.09569600 2.15552100 0.46549200
C -3.97981600 -1.21460000 0.09947900
H -2.09605300 -2.15556000 0.46446500
C -4.63504900 0.00030700 -0.02765600
H -4.52957400 2.14284600 -0.00157800
H -4.52992600 -2.14226200 -0.00259100
F -5.95438100 0.00047600 -0.27667000

F-Radical 6-31+G(d,p)/uB3LYP

C -1.68797500 0.00000000 -0.00002800
C -0.24530700 0.00000000 -0.00001800
C -2.42809800 -1.20711100 0.00003000
C -2.42809800 1.20711100 -0.00002900
C 0.47806500 -1.22113900 0.00002400
C 0.47806500 1.22113900 -0.00004600
N -3.02033800 -2.21429300 0.00007200
N -3.02033800 2.21429300 -0.00003300
C 1.86467800 -1.22366100 0.00003500
H -0.05954600 -2.16361300 0.00004700
C 1.86467800 1.22366100 -0.00003600
H -0.05954600 2.16361300 -0.00007700
C 2.53487600 0.00000000 0.00000400
H 2.43077600 -2.14842100 0.00006600
H 2.43077600 2.14842100 -0.00005800
F 3.88410700 0.00000000 0.00001500

F-Radical 6-31+G(d,p)/uB3LYP-D3

C -1.68943300 0.00000000 -0.00003800
 C -0.24728600 0.00000000 -0.00002500
 C -2.42867100 -1.20707900 0.00003300
 C -2.42867100 1.20707900 -0.00002700
 C 0.47580500 -1.22173800 0.00001900
 C 0.47580500 1.22173800 -0.00005100
 N -3.01161200 -2.21943300 0.00007800
 N -3.01161300 2.21943300 -0.00002700
 C 1.86241800 -1.22391900 0.00003400
 H -0.06124800 -2.16458700 0.00004100
 C 1.86241800 1.22391900 -0.00003600
 H -0.06124800 2.16458700 -0.00008300
 C 2.53242100 0.00000000 0.00000600
 H 2.43054700 -2.14724500 0.00006700
 H 2.43054700 2.14724500 -0.00005700
 F 3.88168200 0.00000000 0.00002000

F-Radical 6-31+G(d,p)/uB3P86

C -1.68241900 0.00000000 -0.00001500
 C -0.24500500 0.00000000 -0.00000900
 C -2.41781600 -1.20489300 0.00002700
 C -2.41781600 1.20489300 -0.00002800
 C 0.47407800 -1.21823100 0.00003000
 C 0.47407800 1.21823100 -0.00004200
 N -3.00464600 -2.21415700 0.00006000
 N -3.00464600 2.21415700 -0.00003900
 C 1.85699200 -1.22096900 0.00003600
 H -0.06651500 -2.15946400 0.00005500
 C 1.85699200 1.22096900 -0.00003600
 H -0.06651500 2.15946400 -0.00007100
 C 2.52609000 0.00000000 0.00000200
 H 2.42338500 -2.14522400 0.00006600
 H 2.42338500 2.14522400 -0.00006100
 F 3.86669400 0.00000000 0.00000800

F-Radical 6-31+G(d,p)/uB97D

```

C      -1.69714100  0.00000000  0.00002100
C      -0.24793000  0.00000000  0.00001400
C      -2.44023100 -1.20904100  0.00003100
C      -2.44023100  1.20904100 -0.00003100
C      0.47928400 -1.22833200  0.00004300
C      0.47928400  1.22833200 -0.00002500
N      -3.03077400 -2.22898700  0.00004100
N      -3.03077400  2.22898700 -0.00007500
C      1.87267600 -1.23150700  0.00003500
H      -0.06191100 -2.17417300  0.00007200
C      1.87267600  1.23150700 -0.00003300
H      -0.06191100  2.17417300 -0.00004800
C      2.54674800  0.00000000 -0.00000300
H      2.44075300 -2.16021200  0.00005800
H      2.44075300  2.16021200 -0.00006200
F      3.90248300  0.00000000 -0.00001000

```

F-Radical 6-31+G(d,p)/uB97-D3

```

C      -1.69493300  0.00000000 -0.00002200
C      -0.24898800  0.00000000 -0.00001400
C      -2.43218600 -1.20924600  0.00003000
C      -2.43218600  1.20924600 -0.00002700
C      0.47503800 -1.22609900  0.00002700
C      0.47503800  1.22609900 -0.00004400
N      -3.01918500 -2.23084000  0.00006500
N      -3.01918600  2.23083900 -0.00003700
C      1.86615200 -1.22927300  0.00003500
H      -0.06711700 -2.17006500  0.00005100
C      1.86615200  1.22927300 -0.00003600
H      -0.06711700  2.17006500 -0.00007500
C      2.53980100  0.00000000  0.00000300
H      2.43281500 -2.15769700  0.00006600

```

H 2.43281500 2.15769700 -0.00006000
 F 3.89487500 0.00000000 0.00001100

F-Radical 6-31+G(d,p)/uB98

C -1.68982300 0.00000000 -0.00002200
 C -0.24485800 0.00000000 -0.00001400
 C -2.43098300 -1.20957600 0.00002600
 C -2.43098300 1.20957600 -0.00002500
 C 0.47864700 -1.22347200 0.00002800
 C 0.47864700 1.22347200 -0.00004600
 N -3.02164000 -2.21839900 0.00006000
 N -3.02164100 2.21839900 -0.00003100
 C 1.86739300 -1.22577500 0.00003700
 H -0.05988100 -2.16690800 0.00005400
 C 1.86739300 1.22577500 -0.00003800
 H -0.05988100 2.16690800 -0.00007700
 C 2.53972000 0.00000000 0.00000300
 H 2.43368900 -2.15149200 0.00006900
 H 2.43368900 2.15149200 -0.00006300
 F 3.88271500 0.00000000 0.00001100

F-Radical 6-31+G(d,p)/uBLYP

C -1.70116300 0.00000000 0.00002700
 C -0.24759900 0.00000000 0.00001700
 C -2.44562900 -1.21133200 0.00003300
 C -2.44562900 1.21133200 -0.00003200
 C 0.48230500 -1.23032700 0.00004500
 C 0.48230500 1.23032700 -0.00002200
 N -3.04792800 -2.22845200 0.00003900
 N -3.04792800 2.22845200 -0.00008100
 C 1.87877500 -1.23345000 0.00003500
 H -0.05876700 -2.17858600 0.00007400
 C 1.87877500 1.23345000 -0.00003200
 H -0.05876700 2.17858600 -0.00004500

C	2.55290500	0.00000000	-0.00000300
H	2.44783900	-2.16444300	0.00005600
H	2.44783800	2.16444300	-0.00006200
F	3.92028600	0.00000000	-0.00001300

F-Radical 6-31+G(d,p)/uPBE1PBE

C	-1.68214200	0.00000000	-0.00001400
C	-0.24449000	0.00000000	-0.00000900
C	-2.41813200	-1.20546500	0.00002700
C	-2.41813200	1.20546500	-0.00002800
C	0.47424900	-1.21790000	0.00003000
C	0.47424900	1.21790000	-0.00004100
N	-3.00416500	-2.21390200	0.00006000
N	-3.00416500	2.21390200	-0.00004100
C	1.85717900	-1.22049100	0.00003500
H	-0.06606100	-2.15993200	0.00005600
C	1.85717900	1.22049100	-0.00003600
H	-0.06606100	2.15993200	-0.00007000
C	2.52665900	0.00000000	0.00000200
H	2.42391600	-2.14521400	0.00006500
H	2.42391600	2.14521400	-0.00006100
F	3.86476500	0.00000000	0.00000700

F-Radical 6-31+G(d,p)/uω97XD

C	-1.68334900	0.00000000	-0.00001000
C	-0.24497000	0.00000000	-0.00000700
C	-2.42101400	-1.20903000	0.00000700
C	-2.42101500	1.20902900	0.00000700
C	0.47354300	-1.21759100	0.00004500
C	0.47354300	1.21759100	-0.00005400
N	-2.99930800	-2.21882600	-0.00000300
N	-2.99931000	2.21882500	0.00000600
C	1.85660400	-1.22016900	0.00005100
H	-0.06360200	-2.16059600	0.00008400

C	1.85660400	1.22017000	-0.00005100
H	-0.06360200	2.16059600	-0.00009400
C	2.52497600	0.00000000	0.00000200
H	2.42170800	-2.14470100	0.00009400
H	2.42170800	2.14470200	-0.00009000
F	3.86495400	0.00000000	0.00000500

F-Dimer cc-pVDZ/B3LYP

C	0.42805500	0.00019800	-0.70550400
C	1.95011600	0.00009200	-0.46654500
C	0.01805000	-1.19228900	-1.47487400
C	0.01813100	1.19305400	-1.47434200
C	2.64577000	-1.21224000	-0.34206900
C	2.64589500	1.21233000	-0.34181600
N	-0.29162600	-2.14273900	-2.06440500
N	-0.29147600	2.14379500	-2.06344200
C	4.01654700	-1.21645700	-0.08763900
H	2.12389100	-2.16362200	-0.44765900
C	4.01666900	1.21635000	-0.08738600
H	2.12411600	2.16378700	-0.44721500
C	4.68171800	-0.00010200	0.03752000
H	4.57200100	-2.14962100	0.01008400
H	4.57222300	2.14943500	0.01053200
F	6.00411300	-0.00019100	0.27741300
C	-0.42805600	-0.00008800	0.70554000
C	-1.95011200	-0.00007600	0.46656200
C	-0.01812700	1.19244500	1.47487600
C	-0.01807500	-1.19290100	1.47441800
C	-2.64581500	1.21221300	0.34191100
C	-2.64583400	-1.21235600	0.34196200
N	0.29146800	2.14292900	2.06439600
N	0.29156300	-2.14360300	2.06356300
C	-4.01658300	1.21633700	0.08745100
H	-2.12397700	2.16363100	0.44738500

C -4.01660500 -1.21647000 0.08750400
 H -2.12401400 -2.16377800 0.44748500
 C -4.68170300 -0.00006500 -0.03756500
 H -4.57207800 2.14946300 -0.01040800
 H -4.57211200 -2.14959400 -0.01030900
 F -6.00409100 -0.00005600 -0.27749200

F-Dimer cc-pVDZ/B3LYP-D3

C 0.41390100 -0.00051500 -0.71218400
 C 1.93479000 -0.00028600 -0.49004000
 C -0.01292400 -1.19394600 -1.46741200
 C -0.01302900 1.19183500 -1.46905500
 C 2.62703800 -1.21338600 -0.35997500
 C 2.62670400 1.21301900 -0.36010200
 N -0.34182300 -2.15366900 -2.02987600
 N -0.34206200 2.15072700 -2.03285600
 C 3.99643900 -1.21710400 -0.09958200
 H 2.10170100 -2.16340200 -0.45990100
 C 3.99610300 1.21714000 -0.09970700
 H 2.10109800 2.16287900 -0.46010300
 C 4.66027500 0.00011600 0.02740000
 H 4.55339100 -2.14850500 0.00414100
 H 4.55280100 2.14870300 0.00392700
 F 5.98153800 0.00031300 0.27421700
 C -0.41390100 0.00042900 0.71218500
 C -1.93479000 0.00027700 0.49004100
 C 0.01297700 1.19382800 1.46743300
 C 0.01297500 -1.19195200 1.46903600
 C -2.62695700 1.21341200 0.35984500
 C -2.62678700 -1.21299300 0.36023200
 N 0.34196300 2.15351800 2.02990300
 N 0.34192600 -2.15087300 2.03283600
 C -3.99635500 1.21719400 0.09945000
 H -2.10155300 2.16340200 0.45966900

C -3.99618800 -1.21705000 0.09983600
 H -2.10124800 -2.16287900 0.46033500
 C -4.66027600 0.00000500 -0.02740300
 H -4.55324600 2.14862000 -0.00437400
 H -4.55294500 -2.14858800 -0.00370000
 F -5.98153700 -0.00012400 -0.27422200

F-Dimer cc-pVDZ/B3P86

C 0.41836700 0.00025900 -0.70052200
 C 1.93202200 0.00011500 -0.46996900
 C 0.00571700 -1.18881000 -1.46213100
 C 0.00583400 1.18979200 -1.46146800
 C 2.62349000 -1.20972100 -0.34625900
 C 2.62364200 1.20981700 -0.34575000
 N -0.30548900 -2.14157700 -2.04627700
 N -0.30528500 2.14292200 -2.04506700
 C 3.99028900 -1.21397600 -0.09154900
 H 2.09907200 -2.15984600 -0.45400400
 C 3.99043900 1.21379000 -0.09104000
 H 2.09934500 2.16005300 -0.45310000
 C 4.65352900 -0.00016200 0.03422200
 H 4.54566300 -2.14651100 0.00603700
 H 4.54593400 2.14621200 0.00693900
 F 5.96887000 -0.00029100 0.27393200
 C -0.41836700 -0.00007900 0.70052900
 C -1.93202100 -0.00008500 0.46997300
 C -0.00582000 1.18907300 1.46206100
 C -0.00573400 -1.18953000 1.46155000
 C -2.62355300 1.20967700 0.34585400
 C -2.62357700 -1.20986100 0.34615400
 N 0.30530800 2.14190500 2.04614200
 N 0.30545400 -2.14259700 2.04521700
 C -3.99034900 1.21377200 0.09113800
 H -2.09918400 2.15986500 0.45327700

C -3.99037500 -1.21399300 0.09144100
 H -2.09923000 -2.16003300 0.45382700
 C -4.65352700 -0.00012000 -0.03422900
 H -4.54577500 2.14624300 -0.00676800
 H -4.54581700 -2.14647900 -0.00622500
 F -5.96886600 -0.00013400 -0.27394500

F-Dimer cc-pVDZ/B97D

C 0.41075700 -0.00000800 -0.73373700
 C 1.93491400 0.00004000 -0.51893900
 C -0.03826800 -1.19523800 -1.47934100
 C -0.03837700 1.19530800 -1.47914300
 C 2.62859100 -1.21979700 -0.38135500
 C 2.62849100 1.21991500 -0.38122200
 N -0.38440900 -2.16328700 -2.03881300
 N -0.38462000 2.16341600 -2.03845100
 C 4.00278600 -1.22443300 -0.11098200
 H 2.09919700 -2.17213400 -0.48377100
 C 4.00268900 1.22463600 -0.11084700
 H 2.09901700 2.17221800 -0.48353500
 C 4.66957100 0.00012300 0.02094500
 H 4.55867600 -2.16093800 -0.00261800
 H 4.55850100 2.16117600 -0.00238700
 F 5.99550900 0.00016100 0.27795900
 C -0.41075700 -0.00016100 0.73374500
 C -1.93491200 -0.00004900 0.51894300
 C 0.03838800 1.19498800 1.47941300
 C 0.03824900 -1.19556000 1.47909000
 C -2.62844900 1.21985300 0.38126100
 C -2.62862600 -1.21986000 0.38131300
 N 0.38462900 2.16297200 2.03893600
 N 0.38437900 -2.16373900 2.03834400
 C -4.00264600 1.22462700 0.11088100
 H -2.09894500 2.17213700 0.48360400

C -4.00282100 -1.22444300 0.11093500
 H -2.09926300 -2.17221600 0.48370300
 C -4.66956700 0.00013900 -0.02095400
 H -4.55842800 2.16118800 0.00244900
 H -4.55874000 -2.16092700 0.00253800
 F -5.99550400 0.00022700 -0.27797400

F-Dimer cc-pVDZ/B97-D3

C 0.40801900 0.00003800 -0.72499700
 C 1.92706500 -0.00001700 -0.50902400
 C -0.03383200 -1.19569200 -1.46614200
 C -0.03373300 1.19573000 -1.46626200
 C 2.61943500 -1.21771000 -0.37755500
 C 2.61952900 1.21762000 -0.37754600
 N -0.37521300 -2.16553700 -2.02433000
 N -0.37502600 2.16554600 -2.02455400
 C 3.99192000 -1.22248400 -0.10946000
 H 2.09085500 -2.16874300 -0.48354000
 C 3.99201500 1.22228700 -0.10945000
 H 2.09102200 2.16869500 -0.48351900
 C 4.65819000 -0.00012400 0.02264500
 H 4.54671500 -2.15878700 -0.00440100
 H 4.54688100 2.15854700 -0.00438400
 F 5.98414500 -0.00017800 0.27796000
 C -0.40801900 0.00014000 0.72504600
 C -1.92705800 0.00004500 0.50904400
 C 0.03371200 1.19594300 1.46614500
 C 0.03382100 -1.19548400 1.46636800
 C -2.61954300 1.21766500 0.37751400
 C -2.61939300 -1.21766600 0.37756600
 N 0.37497000 2.16584200 2.02431300
 N 0.37516000 -2.16524700 2.02472400
 C -3.99202200 1.22229500 0.10938200
 H -2.09106000 2.16875300 0.48348000

C -3.99187100 -1.22247600 0.10943400
 H -2.09079100 -2.16868500 0.48357100
 C -4.65816700 -0.00013400 -0.02270600
 H -4.54690600 2.15854100 0.00428100
 H -4.54664000 -2.15879400 0.00437100
 F -5.98411300 -0.00022300 -0.27806300

F-Dimer cc-pVDZ/B98

C 0.42657800 0.00026300 -0.70599500
 C 1.95065900 0.00008400 -0.47033600
 C 0.01244300 -1.19473800 -1.47470000
 C 0.01263600 1.19563300 -1.47422900
 C 2.64607200 -1.21487300 -0.34550000
 C 2.64628100 1.21486900 -0.34495400
 N -0.30005900 -2.14799900 -2.05989200
 N -0.29971900 2.14918400 -2.05902600
 C 4.01868000 -1.21885600 -0.08959700
 H 2.12314200 -2.16701200 -0.45164200
 C 4.01888700 1.21850100 -0.08905100
 H 2.12351200 2.16714500 -0.45066300
 C 4.68501800 -0.00026400 0.03661700
 H 4.57404300 -2.15285100 0.00847400
 H 4.57441400 2.15235400 0.00944200
 F 6.00256700 -0.00042700 0.27688500
 C -0.42657900 0.00006500 0.70603500
 C -1.95065500 -0.00003100 0.47035600
 C -0.01263600 1.19521100 1.47461800
 C -0.01246700 -1.19516500 1.47439900
 C -2.64622100 1.21479000 0.34501500
 C -2.64611400 -1.21495200 0.34542700
 N 0.29970700 2.14858400 2.05971100
 N 0.29999300 -2.14860000 2.05932900
 C -4.01882100 1.21849300 0.08908000
 H -2.12341300 2.16703800 0.45077500

C -4.01871500 -1.21886500 0.08949300
 H -2.12322400 -2.16711900 0.45152600
 C -4.68500100 -0.00023700 -0.03666700
 H -4.57430700 2.15237500 -0.00938200
 H -4.57411500 -2.15283100 -0.00864500
 F -6.00254300 -0.00033300 -0.27697200

F-Dimer cc-pVDZ/BLYP

C 0.44044300 -0.00003400 -0.72463100
 C 1.96971300 -0.00003700 -0.47678100
 C 0.02170900 -1.19929600 -1.49043800
 C 0.02173300 1.19913600 -1.49060100
 C 2.67093600 -1.22155200 -0.34904200
 C 2.67096600 1.22147200 -0.34920200
 N -0.29782900 -2.16026100 -2.08332800
 N -0.29778000 2.16003300 -2.08361400
 C 4.05066300 -1.22578800 -0.08899800
 H 2.14571200 -2.17843100 -0.45678500
 C 4.05069600 1.22571200 -0.08915900
 H 2.14576000 2.17834900 -0.45706500
 C 4.72051200 -0.00003600 0.03872900
 H 4.60893700 -2.16513500 0.01101800
 H 4.60899100 2.16506000 0.01072500
 F 6.05767200 -0.00003900 0.28506200
 C -0.44044200 0.00008600 0.72456300
 C -1.96972000 0.00003400 0.47674700
 C -0.02172000 1.19938300 1.49032400
 C -0.02168300 -1.19904100 1.49056700
 C -2.67101200 1.22152100 0.34916700
 C -2.67092300 -1.22150300 0.34909700
 N 0.29783600 2.16038400 2.08314600
 N 0.29791200 -2.15990200 2.08359400
 C -4.05075200 1.22571700 0.08917900
 H -2.14582900 2.17841400 0.45699100

C -4.05065900 -1.22578300 0.08910600
 H -2.14567400 -2.17836600 0.45686400
 C -4.72054200 -0.00005200 -0.03864500
 H -4.60907600 2.16504800 -0.01070900
 H -4.60891600 -2.16514600 -0.01084700
 F -6.05771400 -0.00009600 -0.28491300

F-Dimer cc-pVDZ/PBE1PBE

C 0.41621300 -0.00027700 -0.69843500
 C 1.92991800 -0.00016600 -0.47026400
 C 0.00320000 -1.18964800 -1.45952600
 C 0.00317400 1.18845700 -1.46050700
 C 2.62140500 -1.20939800 -0.34625500
 C 2.62125300 1.20916100 -0.34634400
 N -0.30863100 -2.14308900 -2.04024600
 N -0.30869200 2.14140500 -2.04201600
 C 3.98766500 -1.21322300 -0.09187000
 H 2.09707700 -2.16009600 -0.45294900
 C 3.98751300 1.21317600 -0.09195700
 H 2.09680100 2.15978400 -0.45309000
 C 4.65081200 0.00002300 0.03345300
 H 4.54360500 -2.14572700 0.00604400
 H 4.54333800 2.14575600 0.00589400
 F 5.96357100 0.00011500 0.27255800
 C -0.41621600 0.00029000 0.69843300
 C -1.92992200 0.00017100 0.47026400
 C -0.00320100 1.18966500 1.45951800
 C -0.00317400 -1.18843900 1.46050900
 C -2.62140600 1.20939600 0.34617800
 C -2.62125900 -1.20916300 0.34642400
 N 0.30866500 2.14311100 2.04021200
 N 0.30868900 -2.14137500 2.04203900
 C -3.98766600 1.21320700 0.09179400
 H -2.09707500 2.16010000 0.45280800

C -3.98751900 -1.21319200 0.09203900
 H -2.09681000 -2.15978100 0.45323200
 C -4.65081600 -0.00004600 -0.03345100
 H -4.54360700 2.14570500 -0.00618000
 H -4.54334400 -2.14577800 -0.00575300
 F -5.96357500 -0.00014800 -0.27255300

F-Dimer cc-pVDZ/ωB97XD

C 0.40725300 -0.00008200 -0.70075400
 C 1.92592300 -0.00000800 -0.48317600
 C -0.01344300 -1.19229600 -1.46210000
 C -0.01355300 1.19209000 -1.46210600
 C 2.61583000 -1.20919100 -0.35634400
 C 2.61573900 1.20925400 -0.35659900
 N -0.33332000 -2.14628300 -2.03323300
 N -0.33351600 2.14604900 -2.03323700
 C 3.98151100 -1.21358700 -0.09852800
 H 2.09190300 -2.16016900 -0.45933900
 C 3.98142000 1.21380700 -0.09878500
 H 2.09174100 2.16017000 -0.45980600
 C 4.64355100 0.00014900 0.02801000
 H 4.53526200 -2.14634500 0.00246800
 H 4.53510400 2.14662800 0.00200700
 F 5.95722100 0.00022500 0.27224200
 C -0.40725400 -0.00011900 0.70071900
 C -1.92593000 -0.00003100 0.48316200
 C 0.01356500 1.19201000 1.46213000
 C 0.01345400 -1.19237200 1.46199600
 C -2.61574000 1.20923700 0.35661500
 C -2.61585100 -1.20920700 0.35634400
 N 0.33355500 2.14593800 2.03329800
 N 0.33337100 -2.14639000 2.03305500
 C -3.98142600 1.21380300 0.09882800
 H -2.09173300 2.16014800 0.45982100

C -3.98153800 -1.21359000 0.09855600
 H -2.09193200 -2.16019100 0.45932800
 C -4.64357000 0.00015100 -0.02796400
 H -4.53510500 2.14662900 -0.00194400
 H -4.53529900 -2.14634300 -0.00243200
 F -5.95724500 0.00024000 -0.27216300

F-Radical cc-pVDZ/uB3LYP

C -1.69081800 0.00000000 -0.00001900
 C -0.24730900 0.00000000 -0.00001200
 C -2.42930300 -1.20995400 0.00002700
 C -2.42930300 1.20995400 -0.00002600
 C 0.47741400 -1.22095000 0.00002900
 C 0.47741400 1.22095000 -0.00004400
 N -3.01860900 -2.21954900 0.00006100
 N -3.01861000 2.21954900 -0.00003500
 C 1.86447100 -1.22217500 0.00003600
 H -0.06438800 -2.16805900 0.00005400
 C 1.86447100 1.22217500 -0.00003700
 H -0.06438800 2.16805900 -0.00007500
 C 2.54174800 0.00000000 0.00000300
 H 2.43461700 -2.15183900 0.00006700
 H 2.43461700 2.15183900 -0.00006200
 F 3.88304000 0.00000000 0.00001000

F-Radical cc-pVDZ/u3LYP-D3

C -1.69195800 0.00000000 0.00001400
 C -0.24906300 0.00000000 0.00001000
 C -2.42971700 -1.20992700 0.00001100
 C -2.42971700 1.20992700 -0.00002100
 C 0.47519400 -1.22159300 0.00004700
 C 0.47519400 1.22159300 -0.00003500
 N -3.01071500 -2.22411600 0.00002200
 N -3.01071500 2.22411600 -0.00003700

C 1.86242600 -1.22252100 0.00004200
H -0.06584900 -2.16931100 0.00008200
C 1.86242600 1.22252100 -0.00004100
H -0.06584900 2.16931100 -0.00006600
C 2.53934300 0.00000000 -0.00000200
H 2.43417000 -2.15106800 0.00007300
H 2.43417000 2.15106800 -0.00007600
F 3.88095500 0.00000000 -0.00000700

F-Radical cc-pVDZ/uB3P86

C -1.68502700 0.00000000 -0.00001900
C -0.24689600 0.00000000 -0.00001200
C -2.41876700 -1.20729900 0.00003300
C -2.41876700 1.20729900 -0.00003100
C 0.47365900 -1.21802200 0.00002600
C 0.47365900 1.21802200 -0.00004100
N -3.00432000 -2.21843900 0.00007100
N -3.00432000 2.21843900 -0.00004600
C 1.85702800 -1.21953700 0.00003300
H -0.07077500 -2.16375300 0.00004900
C 1.85702800 1.21953700 -0.00003400
H -0.07077500 2.16375300 -0.00006900
C 2.53261800 0.00000000 0.00000300
H 2.42709700 -2.14860600 0.00006100
H 2.42709700 2.14860600 -0.00005600
F 3.86673600 0.00000000 0.00001000

F-Radical cc-pVDZ/uB97D

C -1.69975100 0.00000000 -0.00001400
C -0.25007500 0.00000000 -0.00000900
C -2.44125100 -1.21146700 0.00002500
C -2.44125100 1.21146800 -0.00002200
C 0.47857800 -1.22787600 0.00003300
C 0.47857800 1.22787600 -0.00004400

N -3.02851300 -2.23447300 0.00005000
 N -3.02851300 2.23447300 -0.00003300
 C 1.87221800 -1.22982100 0.00003800
 H -0.06623600 -2.17832600 0.00006100
 C 1.87221800 1.22982100 -0.00003900
 H -0.06623600 2.17832600 -0.00007500
 C 2.55331800 0.00000000 0.00000200
 H 2.44409600 -2.16327300 0.00007000
 H 2.44409600 2.16327300 -0.00006600
 F 3.90088700 0.00000000 0.00000700

F-Radical cc-pVDZ/uB97-D3

C -1.69689000 0.00000000 0.00000800
 C -0.25093200 0.00000000 0.00000600
 C -2.43313500 -1.21159300 0.00001000
 C -2.43313500 1.21159300 -0.00001700
 C 0.47431800 -1.22576700 0.00004600
 C 0.47431800 1.22576700 -0.00003900
 N -3.01740900 -2.23574700 0.00002100
 N -3.01740900 2.23574700 -0.00002900
 C 1.86578100 -1.22777300 0.00004400
 H -0.07137600 -2.17445700 0.00008100
 C 1.86578100 1.22777300 -0.00004200
 H -0.07137600 2.17445700 -0.00007100
 C 2.54617900 0.00000000 -0.00000100
 H 2.43600600 -2.16110400 0.00007700
 H 2.43600500 2.16110500 -0.00007800
 F 3.89341700 0.00000000 -0.00000400

F-Radical cc-pVDZ/uB98

C -1.69233000 0.00000000 -0.00002000
 C -0.24675900 0.00000000 -0.00001300
 C -2.43197800 -1.21192500 0.00002900
 C -2.43197800 1.21192500 -0.00002600

C 0.47796100 -1.22327800 0.00002800
C 0.47796100 1.22327800 -0.00004400
N -3.02020700 -2.22299500 0.00006300
N -3.02020800 2.22299500 -0.00003700
C 1.86712500 -1.22442200 0.00003600
H -0.06452300 -2.17120100 0.00005300
C 1.86712500 1.22442200 -0.00003600
H -0.06452300 2.17120100 -0.00007400
C 2.54566200 0.00000000 0.00000300
H 2.43729600 -2.15487200 0.00006600
H 2.43729600 2.15487200 -0.00006100
F 3.88229200 0.00000000 0.00001000

F-Radical cc-pVDZ/uBLYP

C -1.70375100 0.00000000 -0.00001300
C -0.24980200 0.00000000 -0.00000900
C -2.44623500 -1.21458500 0.00002600
C -2.44623500 1.21458500 -0.00002400
C 0.48157800 -1.22992600 0.00003200
C 0.48157800 1.22992600 -0.00004300
N -3.04549400 -2.23395700 0.00005300
N -3.04549400 2.23395600 -0.00003700
C 1.87807000 -1.23152200 0.00003800
H -0.06377300 -2.18277900 0.00005900
C 1.87807000 1.23152200 -0.00003800
H -0.06377300 2.18277900 -0.00007400
C 2.56102400 0.00000000 0.00000200
H 2.45125500 -2.16750100 0.00006900
H 2.45125500 2.16750200 -0.00006500
F 3.91735300 0.00000000 0.00000700

F-Radical cc-pVDZ/uPBE1PBE

C -1.68463500 0.00000000 0.00001500
C -0.24656200 0.00000000 0.00001000

C -2.41877700 -1.20753600 0.00003200
 C -2.41877700 1.20753600 -0.00003200
 C 0.47344700 -1.21741500 0.00003900
 C 0.47344700 1.21741500 -0.00002700
 N -3.00207200 -2.21863300 0.00004600
 N -3.00207200 2.21863300 -0.00007100
 C 1.85656900 -1.21881800 0.00003400
 H -0.07065400 -2.16362000 0.00006700
 C 1.85656900 1.21881800 -0.00003300
 H -0.07065400 2.16362000 -0.00005000
 C 2.53221800 0.00000000 -0.00000200
 H 2.42693700 -2.14798400 0.00005700
 H 2.42693700 2.14798400 -0.00006000
 F 3.86393600 0.00000000 -0.00000700

F-Radical cc-pVDZ/uωB97XD

C -1.68600100 0.00000000 -0.00003600
 C -0.24659200 0.00000000 -0.00002400
 C -2.42232700 -1.21143700 0.00003900
 C -2.42232700 1.21143700 -0.00002600
 C 0.47338800 -1.21769800 0.00001800
 C 0.47338800 1.21769800 -0.00004800
 N -2.99991900 -2.22278700 0.00007900
 N -2.99992000 2.22278600 -0.00003600
 C 1.85712800 -1.21907100 0.00003300
 H -0.06774100 -2.16524300 0.00003900
 C 1.85712800 1.21907100 -0.00003400
 H -0.06774100 2.16524400 -0.00007900
 C 2.53181700 0.00000000 0.00000600
 H 2.42592900 -2.14852000 0.00006400
 H 2.42592900 2.14852000 -0.00005400
 F 3.86543100 0.00000000 0.00001900

JUL – σ-Dimer 6-31+G(d,p)/B97D

C 0.39757200 0.00020700 -0.77125000
C -0.09676400 -1.19320100 -1.48396400
C -0.09696800 1.19398200 -1.48324600
C 1.91430200 0.00022900 -0.62026700
C 2.62055900 -1.21000800 -0.48991000
C 3.99275600 -1.23076200 -0.23347300
C 4.70802800 0.00005600 -0.10859600
C 3.99313800 1.23095900 -0.23478300
C 2.62092200 1.21037700 -0.49119100
H 2.09808400 2.16294400 -0.58070900
C 6.75968400 -1.24076800 0.48445000
H 6.62974500 -1.42477100 1.57130900
N -0.47197000 -2.16219000 -2.02166200
N -0.47236600 2.16321300 -2.02036600
H 7.83587200 -1.10891400 0.29582900
C 6.76018200 1.24085600 0.48285800
H 6.63051000 1.42619200 1.56952400
H 7.83629300 1.10840900 0.29420200
N 6.08853400 -0.00007400 0.08776700
C 4.70416200 2.56422400 -0.06393900
H 4.53984400 2.93188000 0.96420900
H 4.25987700 3.31103700 -0.73928500
C 6.21461100 2.43115000 -0.31573100
H 6.40622700 2.25791700 -1.38628200
H 6.74252700 3.34866500 -0.01696000
C 4.70330600 -2.56408900 -0.06118600
H 4.53865400 -2.93066600 0.96729100
H 4.25888100 -3.31141400 -0.73587400
C 6.21385100 -2.43181500 -0.31284200
H 6.74139000 -3.34916000 -0.01288800
H 6.40574900 -2.25990500 -1.38355700
H 2.09742200 -2.16250000 -0.57846300
C -0.39762700 -0.00022800 0.77145400
C 0.09695500 1.19311800 1.48410800
C 0.09669700 -1.19406200 1.48352100

C -1.91434200 -0.00015500 0.62047200
 N 0.47241800 2.16205400 2.02171700
 N 0.47187000 -2.16333700 2.02072200
 C -2.62073600 -1.21029300 0.49004600
 C -2.62081600 1.21009200 0.49140800
 C -3.99293200 -1.23086800 0.23354000
 H -2.09771500 -2.16285300 0.57856500
 C -3.99301000 1.23085200 0.23492700
 H -2.09786800 2.16258800 0.58102700
 C -4.70803200 0.00003400 0.10862600
 C -4.70360400 -2.56413300 0.06120600
 C -4.70384500 2.56422000 0.06409100
 N -6.08853800 0.00007900 -0.08786200
 H -4.53866900 -2.93086500 -0.96716900
 H -4.25947200 -3.31142000 0.73613200
 C -6.21421300 -2.43168000 0.31239800
 H -4.53923500 2.93197400 -0.96397300
 H -4.25961500 3.31089700 0.73962400
 C -6.21436900 2.43132300 0.31552800
 C -6.75964700 -1.24050400 -0.48497500
 C -6.75989500 1.24109800 -0.48319200
 H -6.74176500 -3.34894600 0.01222600
 H -6.40642600 -2.25980800 1.38306200
 H -6.40626600 2.25810600 1.38603100
 H -6.74210000 3.34890600 0.01663900
 H -6.62927800 -1.42438300 -1.57180600
 H -7.83589600 -1.10857800 -0.29676900
 H -6.62987700 1.42638200 -1.56982600
 H -7.83607700 1.10880600 -0.29483800

Sum of electronic and thermal Free Energies= -1487.057904

NMe₂ – σ-Dimer 6-31+G(d,p)/ωB97XD

C 2.60896300 1.19939600 -0.48198400
 C 3.97837900 1.20613300 -0.27864300

C 4.70511300 0.00003800 -0.17063400
C 3.97841100 -1.20610500 -0.27854600
C 2.60900900 -1.19945800 -0.48188700
H 2.09242000 2.15104700 -0.55913700
H 4.47910500 2.16264000 -0.20359400
H 4.47919800 -2.16257400 -0.20341500
H 2.09251300 -2.15113900 -0.55896100
C 6.76169500 1.25224400 0.23795500
H 7.82369700 1.05149100 0.37826100
H 6.66168600 1.91740700 -0.62793800
H 6.39393400 1.78268700 1.12716900
C 6.76171400 -1.25211000 0.23810200
H 6.39392600 -1.78247000 1.12735100
H 6.66176000 -1.91735600 -0.62773400
H 7.82370300 -1.05131300 0.37844000
N 6.06461700 0.00005100 0.02384500
C 1.90168300 -0.00004300 -0.58212200
C 0.37885500 -0.00004500 -0.72067400
C -0.08112800 1.19055800 -1.46167500
C -0.08109400 -1.19067800 -1.46166600
N -0.42118100 2.14358100 -2.02094700
N -0.42111900 -2.14371500 -2.02093200
C -0.37885100 -0.00003000 0.72080000
C -1.90166500 -0.00003200 0.58218100
C 0.08109300 1.19059300 1.46179500
C 0.08106000 -1.19065300 1.46183400
C -2.60893800 1.19940500 0.48198400
C -2.60897700 -1.19945000 0.48189400
N 0.42101600 2.14365100 2.02108500
N 0.42095500 -2.14370400 2.02115400
C -3.97834400 1.20613800 0.27857700
H -2.09239700 2.15105800 0.55915400
C -3.97836900 -1.20610200 0.27848700
H -2.09247800 -2.15112900 0.55899000
C -4.70507000 0.00004000 0.17053800

H	-4.47907000	2.16264300	0.20350100
H	-4.47915100	-2.16257200	0.20333400
N	-6.06456100	0.00004800	-0.02401700
C	-6.76164400	1.25224200	-0.23811300
C	-6.76165600	-1.25211700	-0.23825200
H	-7.82363400	1.05148100	-0.37849300
H	-6.66169400	1.91737200	0.62781400
H	-6.39383600	1.78272500	-1.12728200
H	-6.39381600	-1.78252200	-1.12745400
H	-6.66175900	-1.91732400	0.62762100
H	-7.82363400	-1.05131900	-0.37866800

NMe₂ – σ-Dimer 6-31+G(d,p)/B97D

C	2.63360100	1.21070900	-0.47176100
C	4.00731900	1.21719000	-0.23302000
C	4.73687100	-0.00006400	-0.09286000
C	4.00747400	-1.21731700	-0.23378600
C	2.63375000	-1.21086700	-0.47251800
H	2.11417800	2.16378600	-0.56458400
H	4.51071300	2.17729800	-0.15433600
H	4.51099000	-2.17740800	-0.15565900
H	2.11445500	-2.16395800	-0.56590600
C	6.83375900	1.26040200	0.16191900
H	7.88227500	1.06329300	0.41259700
H	6.79177200	1.75661800	-0.82559800
H	6.42591500	1.95443800	0.91432500
C	6.83392300	-1.26045000	0.16079300
H	6.42644500	-1.95507200	0.91286400
H	6.79162300	-1.75597400	-0.82705400
H	7.88250900	-1.06337700	0.41119900
N	6.09340800	-0.00007300	0.16918100
C	1.92253400	-0.00008900	-0.59358600
C	0.40315200	-0.00005000	-0.75811100
C	-0.07712000	1.19388600	-1.48223100

C -0.07728600 -1.19410800 -1.48192400
 N -0.43781800 2.16339800 -2.02841200
 N -0.43817900 -2.16369100 -2.02784800
 C -4.73689300 -0.00005100 0.09288000
 C -4.00739000 1.21723600 0.23297300
 C -4.00743200 -1.21726600 0.23385700
 N -6.09344800 -0.00012100 -0.16910800
 C -2.63366000 1.21083200 0.47166900
 H -4.51082500 2.17732100 0.15427400
 C -2.63370300 -1.21074100 0.47254100
 H -4.51090300 -2.17738700 0.15582100
 C -6.83385800 1.26031700 -0.16174200
 C -6.83396000 -1.26049700 -0.16051000
 H -2.11428400 2.16394000 0.56442900
 C -1.92253300 0.00007800 0.59351300
 H -2.11436300 -2.16380000 0.56598200
 H -7.88238000 1.06315100 -0.41235800
 H -6.79183200 1.75650500 0.82578800
 H -6.42610500 1.95439200 -0.91415900
 H -6.42651700 -1.95521600 -0.91250500
 H -6.79163700 -1.75588800 0.82740500
 H -7.88255000 -1.06344300 -0.41091700
 C -0.40314100 0.00014400 0.75799500
 C 0.07714400 1.19426700 1.48180400
 C 0.07731800 -1.19372500 1.48209700
 N 0.43790800 2.16389200 2.02774000
 N 0.43831900 -2.16315300 2.02822400

Sum of electronic and thermal Free Energies= -1177.690921

NMe₂ – π-Dimer 6-31+G(d,p)/B97D

C 0.58202300 -1.40690000 -1.22669900
 C 1.94293100 -1.17517300 -1.22049900
 C 2.67445200 -1.05265700 0.00978700
 C 1.92775400 -1.18536200 1.22997400

C 0.56692200 -1.41563800 1.21719700
H 0.06150000 -1.49569700 -2.17951200
H 2.45584800 -1.06819600 -2.17182900
H 2.42874000 -1.08428500 2.18834300
H 0.03401900 -1.51027700 2.16260100
C 4.78495300 -0.83697500 -1.24071200
H 5.82659100 -0.58061700 -1.02170700
H 4.75672200 -1.82231200 -1.73826500
H 4.37845700 -0.07436800 -1.91651200
C 4.76907800 -0.87404500 1.29113300
H 4.37412200 -0.11027500 1.97270900
H 4.70778100 -1.86528400 1.77333700
H 5.82003200 -0.64373700 1.08877200
N 4.02702700 -0.86097700 0.02032600
C -0.16397900 -1.54714300 -0.00999100
C -1.56924600 -1.79502800 -0.01919900
C -2.29357400 -1.96292000 -1.23246700
C -2.31021300 -1.96860600 1.18307300
N -2.88693500 -2.09502500 -2.24179000
N -2.91892800 -2.10570800 2.18251500
C -2.67430400 1.05218900 0.01343700
C -1.94288700 1.17952000 -1.21641800
C -1.92751600 1.18057500 1.23403500
N -4.02683900 0.85996400 0.02324500
C -0.58200000 1.41127700 -1.22187800
H -2.45585600 1.07614900 -2.16811700
C -0.56667300 1.41094800 1.22200800
H -2.42840200 1.07626100 2.19210500
C -4.78503900 0.84246600 -1.23774300
C -4.76897500 0.86832000 1.29403000
H -0.06160200 1.50368000 -2.17441500
C 0.16414000 1.54694000 -0.00472900
H -0.03373600 1.50230900 2.16771500
H -5.82654100 0.58461600 -1.01982800
H -4.75724700 1.83047700 -1.73001900

H -4.37859400 0.08357200 -1.91775000
H -4.37235900 0.10374900 1.97368500
H -4.71003800 1.85851400 1.77872300
H -5.81936600 0.63594100 1.09106300
C 1.56940000 1.79497000 -0.01334000
C 2.29300400 1.96821600 -1.22630200
C 2.31067700 1.96417700 1.18935200
N 2.88527300 2.10488500 -2.23566800
N 2.91959800 2.09755500 2.18917300

Sum of electronic and thermal Free Energies= -1177.715603

NMe₂ – Radical 6-31+G(d,p)/uωB97XD

C -0.33350100 1.21013200 -0.00035900
C 1.04093900 1.21382600 -0.00048200
C 1.77896100 0.00000400 -0.00041900
C 1.04094200 -1.21381900 -0.00001100
C -0.33349800 -1.21012800 0.00012300
H -0.86429600 2.15725900 -0.00047200
H 1.55332100 2.16738300 -0.00072100
H 1.55332600 -2.16737400 0.00038200
H -0.86429000 -2.15725600 0.00048700
C 3.87490500 1.25449700 0.00121200
H 4.94381500 1.04522000 0.00172300
H 3.64775200 1.85297900 -0.88900200
H 3.64649000 1.85101000 0.89243800
C 3.87489200 -1.25450300 -0.00044000
H 3.64865500 -1.85108400 0.89132300
H 3.64554600 -1.85291200 -0.89011500
H 4.94380300 -1.04524200 -0.00269800
N 3.14338500 0.00000100 -0.00073100
C -1.07117100 0.00000100 -0.00008700
C -2.49687900 -0.00000100 0.00003800
C -3.23395500 1.21129000 -0.00005200
C -3.23395200 -1.21129200 0.00030300

N -3.80742500 2.22398600 -0.00013200
 N -3.80742000 -2.22399000 0.00053600

NMe₂ – Radical 6-31+G(d,p)/uB97D

C 0.33425500 -1.21929400 -0.00024700
 C -1.05188700 -1.22339500 -0.00033300
 C -1.79533000 -0.00000300 -0.00032000
 C -1.05188900 1.22338900 -0.00004400
 C 0.33425300 1.21929000 0.00005100
 H 0.86882700 -2.16932100 -0.00031200
 H -1.56858800 -2.18013700 -0.00047800
 H -1.56859300 2.18013000 0.00022600
 H 0.86882300 2.16931900 0.00030100
 C -3.90821600 -1.26562700 0.00099900
 H -4.98323500 -1.05741200 0.00117800
 H -3.66541700 -1.86404900 -0.89282400
 H -3.66472300 -1.86228800 0.89582300
 C -3.90820600 1.26563200 -0.00029800
 H -3.66644000 1.86233900 0.89498900
 H -3.66367100 1.86400400 -0.89365600
 H -4.98322600 1.05742800 -0.00225900
 N -3.17087300 -0.00000100 -0.00058600
 C 1.07757600 -0.00000100 -0.00008000
 C 2.51958700 0.00000000 0.00001000
 C 3.25983800 -1.21134900 -0.00005300
 C 3.25983600 1.21135100 0.00020000
 N 3.84310600 -2.23596000 -0.00010600
 N 3.84310200 2.23596400 0.00036400

Sum of electronic and thermal Free Energies= -588.852682

OMe – σ-Dimer 6-31+G(d,p)/ωB97XD

C -2.61354100 1.31863500 0.42250100
 C -3.97693400 1.31765400 0.19511800
 C -4.67214300 0.10732800 0.08019500

C -3.98220100 -1.10098600 0.20311900
 C -2.60964500 -1.08981300 0.43269000
 C -1.91376700 0.11114700 0.53891400
 H -2.09517800 2.26806800 0.50914500
 H -4.52668500 2.24724700 0.10319700
 H -4.49119200 -2.05331200 0.12487100
 H -2.09088700 -2.03843100 0.52664700
 O -5.99986700 0.21072400 -0.14184400
 C -6.75861000 -0.97704600 -0.27606800
 H -6.71990400 -1.57808300 0.63990600
 H -7.78396300 -0.65568500 -0.45435800
 H -6.41143700 -1.57521500 -1.12648800
 C -0.39136000 0.11204900 0.71285200
 C 0.05029700 1.30229500 1.46464300
 C 0.05272600 -1.07943300 1.46156600
 N 0.37924300 2.25424000 2.03206400
 N 0.38464800 -2.03305800 2.02449400
 C 0.39138200 0.11255000 -0.71286700
 C 1.91378600 0.11147600 -0.53893300
 C -0.05025100 1.30335000 -1.46379800
 C -0.05274300 -1.07836900 -1.46245300
 C 2.61366400 1.31888600 -0.42234000
 C 2.60956500 -1.08956000 -0.43290100
 N -0.37920600 2.25572500 -2.03049200
 N -0.38469000 -2.03156500 -2.02609300
 C 3.97705500 1.31775500 -0.19495300
 H 2.09538400 2.26837700 -0.50886100
 C 3.98212000 -1.10088400 -0.20332700
 H 2.09072500 -2.03811900 -0.52699300
 C 4.67216100 0.10735200 -0.08020600
 H 4.52688500 2.24728800 -0.10289500
 H 4.49103400 -2.05326500 -0.12524100
 O 5.99989400 0.21060200 0.14184500
 C 6.75848100 -0.97725300 0.27621000
 H 6.71993000 -1.57825700 -0.63979300

H 7.78382500 -0.65600500 0.45475400
H 6.41104200 -1.57541200 1.12652700

OMe – σ-Dimer 6-31+G(d,p)/B97D

C -2.54191400 -1.41072800 0.37641400
C -3.91169300 -1.48657000 0.13092700
C -4.68947600 -0.30867100 0.07456800
C -4.07440800 0.94522900 0.27343600
C -2.69660000 1.01094000 0.52061400
C -1.91851300 -0.15864000 0.57344900
H -1.95710100 -2.32878100 0.41241000
H -4.39868500 -2.44870700 -0.02163300
H -4.64905400 1.86773600 0.23805100
H -2.23546000 1.98648200 0.66876100
O -6.01890800 -0.48974100 -0.17176800
C -6.85471400 0.67623400 -0.25131700
H -6.52239800 1.34037500 -1.06615500
H -7.86248300 0.30071200 -0.46012200
H -6.84775300 1.22840300 0.70305500
C -0.39580100 -0.06897700 0.74753900
C 1.91851300 0.15864100 -0.57344900
C 2.54191400 1.41072700 -0.37641200
C 2.69660000 -1.01094100 -0.52061500
C 3.91169300 1.48657000 -0.13092500
H 1.95710200 2.32878200 -0.41240800
C 4.07440700 -0.94522900 -0.27343800
H 2.23546000 -1.98648100 -0.66876300
C 4.68947600 0.30867000 -0.07456700
H 4.39868500 2.44870700 0.02163500
H 4.64905400 -1.86773700 -0.23805500
O 6.01890800 0.48974000 0.17176800
C 6.85471300 -0.67623700 0.25131500
H 6.84775300 -1.22840300 -0.70305800
H 7.86248300 -0.30071400 0.46012000

H 6.52239800 -1.34037700 1.06615300
 C 0.39580000 0.06897800 -0.74753800
 C -0.15501800 1.26944800 -1.41016800
 C 0.00206500 -1.10895700 -1.54817400
 N -0.57658800 2.24056600 -1.90707900
 N -0.28835800 -2.06373100 -2.15792100
 C -0.00206500 1.10895900 1.54817400
 C 0.15501700 -1.26944600 1.41016900
 N 0.28835700 2.06373300 2.15792100
 N 0.57658900 -2.24056400 1.90708000

Sum of electronic and thermal Free Energies= -1138.903398

OMe – π-Dimer 6-31+G(d,p)/B97D

C -0.25390500 1.17984500 1.52308200
 C -1.62566100 1.06392600 1.63074800
 C -2.45272300 1.23939300 0.48580300
 C -1.86179000 1.54543100 -0.77140100
 C -0.48442200 1.66224400 -0.87534300
 C 0.36797600 1.50026300 0.26693700
 H 0.37031500 1.04761500 2.40573700
 H -2.10019100 0.82081400 2.57975700
 H -2.47994000 1.66629900 -1.65749900
 H -0.03737100 1.89908000 -1.83993300
 O -3.77889800 1.16015400 0.71189800
 C -4.69556700 1.38179400 -0.38938400
 H -4.53065500 0.64144100 -1.18269300
 H -5.69244000 1.25870900 0.04572500
 H -4.57362400 2.40432200 -0.77959700
 C 1.78451400 1.63337800 0.15513100
 C -0.36794000 -1.50081900 -0.26644300
 C 0.25289900 -1.18046500 -1.52314400
 C 0.48535300 -1.66251200 0.87517500
 C 1.62454700 -1.06434300 -1.63193400
 H -0.37206900 -1.04845900 -2.40530500

C 1.86262100 -1.54536100 0.77013400
 H 0.03915400 -1.89929300 1.84017000
 C 2.45250300 -1.23945400 -0.48760700
 H 2.09829700 -0.82124200 -2.58133800
 H 2.48147100 -1.66582400 1.65579600
 O 3.77848000 -1.15997600 -0.71479600
 C 4.69594300 -1.37930200 0.38630500
 H 4.57511900 -2.40135600 0.77805900
 H 5.69247900 -1.25593300 -0.04948100
 H 4.53058500 -0.63796800 1.17858800
 C -1.78437600 -1.63402300 -0.15357500
 C -2.63257200 -1.52702300 -1.29281600
 C -2.40863700 -1.98756600 1.07604900
 N -3.31533300 -1.42591900 -2.24682300
 N -2.90268200 -2.28007300 2.10385300
 C 2.40977800 1.98722000 -1.07387600
 C 2.63166200 1.52635100 1.29518200
 N 2.90478800 2.28005000 -2.10113000
 N 3.31336900 1.42544000 2.24996500

Sum of electronic and thermal Free Energies= -1138.913622

OMe – Radical 6-31+G(d,p)/uωB97XD

C -0.08363900 -1.32571500 0.00005900
 C 1.28541500 -1.44535900 0.00011300
 C 2.09945400 -0.29670300 0.00010100
 C 1.50992100 0.97619100 0.00002900
 C 0.13080400 1.09288300 -0.00002400
 C -0.70054100 -0.04818600 -0.00000600
 H -0.70011000 -2.21909300 0.00007500
 H 1.76374200 -2.41822500 0.00017000
 H 2.11451500 1.87453100 0.00000800
 H -0.31697200 2.08177300 -0.00008000
 O 3.42433300 -0.52264100 0.00014200
 C 4.31068700 0.58486300 0.00030900

H	4.17393800	1.19862500	0.89742400
H	5.31327900	0.16008300	0.00046600
H	4.17424200	1.19866600	-0.89682600
C	-2.12719400	0.08104700	-0.00006100
C	-2.97175900	-1.05688200	-0.00012900
C	-2.75271000	1.35286400	-0.00019400
N	-3.63954400	-2.00989100	-0.00019700
N	-3.23473100	2.41199700	-0.00031100

OMe – Radical 6-31+G(d,p)/uB97D

C	-0.08285800	-1.33658000	0.00006000
C	1.29756800	-1.45912000	0.00013300
C	2.11815900	-0.30088000	0.00014400
C	1.52272700	0.98448100	0.00007600
C	0.13437000	1.10234400	0.00000200
C	-0.70593000	-0.04905400	-0.00000500
H	-0.70409900	-2.23209500	0.00005400
H	1.77525000	-2.43811600	0.00018600
H	2.13401900	1.88419100	0.00008000
H	-0.31716500	2.09443400	-0.00005000
O	3.45646200	-0.53233200	0.00021700
C	4.34876500	0.59813700	0.00027600
H	4.19538600	1.21234000	0.90194400
H	5.35770000	0.17243400	0.00037300
H	4.19554600	1.21230800	-0.90144100
C	-2.14541400	0.08150200	-0.00008300
C	-2.99453000	-1.05593300	-0.00016900
C	-2.77539200	1.35376400	-0.00022400
N	-3.67432900	-2.01893200	-0.00024600
N	-3.26754500	2.42481900	-0.00034700

Sum of electronic and thermal Free Energies= -569.454644

SMe – Dimer 6-31+G(d,p)/ωB97XD

C	0.19445300	1.13202900	1.15194200
---	------------	------------	------------

C	1.38292800	1.82876400	0.96570800
C	1.45826600	2.85595700	0.02132600
C	0.31271200	3.17718600	-0.72109500
C	-0.87229300	2.48482300	-0.52928500
H	0.16682100	0.32842300	1.88114300
H	2.24184700	1.55257900	1.56499700
H	0.34634700	3.98008600	-1.45081000
H	-1.74466800	2.75933600	-1.11370800
C	4.11132700	3.15977200	0.87623300
H	3.77596600	3.31412400	1.90425200
H	4.33202300	2.10420500	0.70191800
H	5.02292400	3.73798400	0.71545800
C	-0.93803100	1.44887100	0.40608400
C	-2.21058300	0.60966000	0.54051900
C	-2.31012100	0.01671300	1.88736100
C	-3.41647400	1.43269000	0.32449700
N	-2.36523400	-0.46164100	2.93824800
N	-4.35222600	2.08115600	0.12363200
S	2.91317700	3.80043800	-0.31598800
C	-2.21058300	-0.60956000	-0.54049500
C	-0.93806700	-1.44882500	-0.40604900
C	-2.31012200	-0.01662400	-1.88734200
C	-3.41649500	-1.43257700	-0.32447600
C	0.19450400	-1.13191100	-1.15181500
C	-0.87242300	-2.48491400	0.52912000
N	-2.36529000	0.46175400	-2.93821600
N	-4.35225100	-2.08104300	-0.12362500
C	1.38291500	-1.82868400	-0.96559800
H	0.16691000	-0.32820600	-1.88090700
C	0.31257800	-3.17735400	0.72091700
H	-1.74481600	-2.75952200	1.11347300
C	1.45818600	-2.85601300	-0.02132000
H	2.24190600	-1.55249800	-1.56479200
H	0.34605900	-3.98039700	1.45048100
S	2.91303900	-3.80057600	0.31594300

C 4.11123800 -3.15983900 -0.87618100
 H 3.77593600 -3.31406300 -1.90423100
 H 4.33201600 -2.10430600 -0.70175500
 H 5.02279200 -3.73811800 -0.71537800

SMe – Dimer 6-31+G(d,p)/B97D

C -0.18922900 -1.08103700 1.17818300
 C -1.39711100 -1.76053700 0.98047600
 C -1.47951000 -2.80980300 0.03994300
 C -0.31716600 -3.16794400 -0.68620000
 C 0.88692800 -2.49234600 -0.47953400
 H -0.15593500 -0.26209200 1.89571300
 H -2.26580600 -1.45714400 1.56060300
 H -0.35317900 -3.98071400 -1.41250600
 H 1.76726700 -2.78602200 -1.04961600
 C -4.17739700 -3.01297100 0.86022700
 H -3.85581000 -3.15113200 1.90183500
 H -4.34893200 -1.94706500 0.65397700
 H -5.10929800 -3.56814300 0.69226200
 C 0.96176900 -1.43863600 0.45460700
 C 2.24839600 -0.61752800 0.58717100
 C 2.34853200 0.04156000 1.90459300
 C 3.45823500 -1.44472500 0.39833100
 N 2.39725900 0.57991500 2.94158700
 N 4.40615600 -2.10442500 0.21190200
 S -2.96010500 -3.72881300 -0.30552500
 C 2.24838900 0.61755700 -0.58717800
 C 0.96175300 1.43865100 -0.45460600
 C 2.34852600 -0.04152300 -1.90460300
 C 3.45821900 1.44476700 -0.39834100
 C -0.18922900 1.08106500 -1.17821300
 C 0.88688500 2.49232600 0.47957500
 N 2.39725300 -0.57986700 -2.94160400
 N 4.40614300 2.10446000 -0.21190100

C -1.39712100 1.76054700 -0.98050300
 H -0.15591400 0.26214600 -1.89577100
 C -0.31721900 3.16790400 0.68624400
 H 1.76721000 2.78598900 1.04968400
 C -1.47954700 2.80977900 -0.03993400
 H -2.26580200 1.45716800 -1.56065700
 H -0.35325300 3.98064700 1.41257900
 S -2.96015700 3.72876200 0.30554200
 C -4.17742300 3.01294800 -0.86025400
 H -3.85582300 3.15115300 -1.90185300
 H -4.34894500 1.94703100 -0.65404700
 H -5.10933400 3.56810000 -0.69228100

Sum of electronic and thermal Free Energies= -1784.943656

SMe – Radical 6-31+G(d,p)/uωB97XD

C 2.49802400 0.09268400 0.00011300
 C 1.07313400 -0.04042500 0.00015800
 C 3.34595300 -1.04323000 -0.00001800
 C 3.11991900 1.36662900 -0.00001300
 C 0.46014300 -1.31814900 0.00015300
 C 0.23730200 1.09907300 -0.00001100
 N 4.01724600 -1.99358900 -0.00012400
 N 3.60054500 2.42625200 -0.00008800
 C -0.91047200 -1.43999200 0.00007300
 H 1.07797600 -2.21059900 0.00016400
 C -1.13901200 0.97260000 -0.00003500
 H 0.68093700 2.08985300 0.00005200
 C -1.73788300 -0.29754800 -0.00008100
 H -1.35935900 -2.42844700 0.00006200
 H -1.74262700 1.87206200 0.00007600
 S -3.46958500 -0.58507000 -0.00010800
 C -4.18078100 1.07702900 0.00008500
 H -3.90209000 1.63253100 0.89802700
 H -3.90158200 1.63286900 -0.89744500

H -5.26239600 0.93219300 -0.00026100

SMe – Radical 6-31+G(d,p)/uB97D

C 2.51825300 0.09451200 0.00006000
 C 1.08133500 -0.04211600 0.00004100
 C 3.37182500 -1.03989500 -0.00000600
 C 3.14171000 1.37017800 -0.00000400
 C 0.46263700 -1.33068900 0.00002500
 C 0.23389100 1.10540100 0.00002900
 N 4.05450200 -2.00076000 -0.00007000
 N 3.62800000 2.44384900 -0.00006600
 C -0.91822700 -1.45856500 0.00000400
 H 1.08602700 -2.22476000 0.00003000
 C -1.15153100 0.97701200 0.00000900
 H 0.67931300 2.10037200 0.00003600
 C -1.75496100 -0.30668800 -0.00000200
 H -1.36383000 -2.45422400 -0.00000600
 H -1.76177600 1.87770700 -0.00000300
 S -3.49566700 -0.58998100 -0.00002500
 C -4.21093600 1.09553800 0.00003600
 H -3.91577000 1.64829900 0.90230900
 H -3.91554800 1.64845900 -0.90206800
 H -5.29923500 0.95409400 -0.00010800

Sum of electronic and thermal Free Energies= -892.475494

Me – Dimer 6-31+G(d,p)/ωB97XD

C 1.09390500 0.94342000 -1.18261700
 C 1.83120400 2.11036900 -1.02467300
 C 2.92531200 2.16316900 -0.15734500
 C 3.26293000 1.00508300 0.54831300
 C 2.53695600 -0.17013600 0.39441700
 H 0.24113000 0.93680800 -1.85416700
 H 1.54588600 2.99546900 -1.58576700
 H 4.11011500 1.01655600 1.22778400

H 2.82833700 -1.05405600 0.95276000
 C 1.44285000 -0.20387900 -0.47042200
 C 0.57997300 -1.46610200 -0.57028500
 C -0.08124800 -1.54958700 -1.88629800
 C 1.40034800 -2.68251100 -0.40713200
 N -0.61067600 -1.59560800 -2.91283200
 N 2.04760200 -3.62727500 -0.24927700
 C -0.58009300 -1.46604700 0.57026300
 C -1.44288000 -0.20376100 0.47040900
 C 0.08118900 -1.54953000 1.88624300
 C -1.40056100 -2.68240300 0.40718100
 C -1.09368300 0.94359800 1.18239000
 C -2.53716900 -0.17003000 -0.39419400
 N 0.61070000 -1.59552800 2.91273500
 N -2.04786000 -3.62714900 0.24939400
 C -1.83090000 2.11059400 1.02444500
 H -0.24076700 0.93699000 1.85376100
 C -3.26306400 1.00524200 -0.54809500
 H -2.82877000 -1.05399800 -0.95234400
 C -2.92518600 2.16338700 0.15733400
 H -1.54538300 2.99574100 1.58536400
 H -4.11039500 1.01669900 -1.22738400
 C -3.74175300 3.42090000 0.01269900
 H -4.13242200 3.52603300 -1.00287800
 H -4.59769200 3.40210800 0.69597400
 H -3.15006700 4.30952500 0.24687700
 C 3.74198500 3.42061000 -0.01267800
 H 4.59850800 3.40129900 -0.69520500
 H 3.15066500 4.30922300 -0.24782200
 H 4.13180700 3.52619900 1.00317900

Me – Dimer 6-31+G(d,p)/B97D

C 2.62774400 1.21648700 -0.41246700
 C 4.00331400 1.20857000 -0.14999700

C 4.71355100 -0.00031400 -0.00959000
 C 4.00300100 -1.20905200 -0.14965900
 C 2.62742800 -1.21668600 -0.41212900
 H 2.10453600 2.16620700 -0.51552500
 H 4.53230700 2.15814600 -0.05522900
 H 4.53174700 -2.15873900 -0.05462500
 H 2.10397500 -2.16630000 -0.51492300
 C 1.93122700 -0.00002900 -0.54280900
 C 0.40350800 0.00013900 -0.74039600
 C -0.05304700 1.19350200 -1.48369900
 C -0.05332700 -1.19322300 -1.48353100
 N -0.39623800 2.15686200 -2.05073100
 N -0.39677700 -2.15658700 -2.05039800
 C -0.40350900 0.00030600 0.74042400
 C -1.93122500 0.00007700 0.54282200
 C 0.05302200 1.19385200 1.48345200
 C 0.05333300 -1.19287700 1.48384300
 C -2.62777200 1.21656400 0.41240800
 C -2.62739000 -1.21660900 0.41218100
 N 0.39620100 2.15734800 2.05025900
 N 0.39676800 -2.15610100 2.05095700
 C -4.00333900 1.20859500 0.14991400
 H -2.10459200 2.16630400 0.51542900
 C -4.00295600 -1.20902700 0.14968800
 H -2.10390900 -2.16620400 0.51501600
 C -4.71354000 -0.00031300 0.00955300
 H -4.53235800 2.15815100 0.05508900
 H -4.53167200 -2.15873400 0.05468500
 C -6.19394700 -0.00053500 -0.30613600
 H -6.35509600 -0.00115100 -1.39710000
 H -6.68820700 -0.89364100 0.10273000
 H -6.68827600 0.89297200 0.10175800
 C 6.19396400 -0.00045800 0.30607400
 H 6.68812400 -0.89392400 -0.10212000
 H 6.68837900 0.89268900 -0.10250800

H 6.35513100 -0.00024300 1.39703600
 Sum of electronic and thermal Free Energies= -988.578755

Me – Radical 6-31+G(d,p)/uωB97XD

C 0.43432600 1.21440200 -0.00610000
 C 1.81688200 1.20420500 -0.01121200
 C 2.53688300 -0.00000300 -0.01128700
 C 1.81688100 -1.20421000 -0.01084900
 C 0.43432600 -1.21440500 -0.00572900
 H -0.10058800 2.15905700 -0.00751400
 H 2.35486600 2.14766800 -0.01666600
 H 2.35486500 -2.14767500 -0.01602100
 H -0.10059000 -2.15906000 -0.00685900
 C -0.28834400 -0.00000100 -0.00259900
 C -1.72470200 0.00000100 0.00085400
 C -2.46391300 1.20881000 0.00347500
 C -2.46391500 -1.20880700 0.00324400
 N -3.04568900 2.21656900 0.00560200
 N -3.04569400 -2.21656600 0.00518600
 C 4.04039200 0.00000200 0.01791300
 H 4.40090800 0.00019100 1.05291500
 H 4.44866100 -0.88667100 -0.47365800
 H 4.44866000 0.88649900 -0.47397900

Me – Radical 6-31+G(d,p)/uB97D

C -0.44072300 -1.22522000 -0.00659800
 C -1.83348000 -1.21478100 -0.01213200
 C -2.56060000 0.00000200 -0.01182100
 C -1.83347900 1.21478500 -0.01190100
 C -0.44072300 1.22522200 -0.00636800
 H 0.09817700 -2.17294200 -0.00870600
 H -2.37583700 -2.16171500 -0.01892300
 H -2.37583700 2.16171900 -0.01850400
 H 0.09817800 2.17294500 -0.00829600

C 0.29027600 0.00000100 -0.00252600
 C 1.73764400 0.00000000 0.00131000
 C 2.48203900 -1.20914500 0.00399900
 C 2.48204100 1.20914400 0.00406300
 N 3.07662100 -2.22661500 0.00614800
 N 3.07662300 2.22661300 0.00626800
 C -4.07036400 -0.00000200 0.01792700
 H -4.43414300 -0.00013400 1.05995600
 H -4.47951700 0.89437600 -0.47397100
 H -4.47951600 -0.89425600 -0.47419600

Sum of electronic and thermal Free Energies= -494.290540

Cl – Dimer 6-31+G(d,p)/ωB97XD

C -2.60599200 -1.20724500 -0.41862600
 C -3.97585800 -1.21087000 -0.18737800
 C -4.65080300 0.00002500 -0.07170400
 C -3.97582300 1.21088700 -0.18750300
 C -2.60595600 1.20719900 -0.41874700
 H -2.08639800 -2.15521800 -0.51090600
 H -4.51328500 -2.14767700 -0.09987400
 H -4.51322700 2.14771700 -0.10010100
 H -2.08632400 2.15514400 -0.51111800
 C -1.91476900 -0.00003600 -0.53020000
 C -0.39024900 -0.00006300 -0.71299700
 C 0.04827000 -1.19170100 -1.46349000
 C 0.04826600 1.19152700 -1.46356900
 N 0.37890300 -2.14501400 -2.02740200
 N 0.37888400 2.14481400 -2.02753300
 C 0.39024300 -0.00000900 0.71260100
 C 1.91480000 0.00000300 0.52999000
 C -0.04835900 -1.19159800 1.46312300
 C -0.04840200 1.19160600 1.46304800
 C 2.60604300 -1.20721100 0.41862100
 C 2.60602800 1.20723300 0.41871600

N	-0.37920900	-2.14487200	2.02697300
N	-0.37928000	2.14490300	2.02684200
C	3.97594900	-1.21084800	0.18762100
H	2.08642900	-2.15517500	0.51086900
C	3.97593900	1.21090800	0.18772600
H	2.08640900	2.15518800	0.51103800
C	4.65092200	0.00004000	0.07204000
H	4.51339600	-2.14765600	0.10025000
H	4.51336800	2.14773400	0.10043800
Cl	6.36773000	0.00005200	-0.21430700
Cl	-6.36755100	0.00006700	0.21499000

Cl – Dimer 6-31+G(d,p)/B97D

C	-2.61969700	1.21771800	0.44670100
C	-3.99857600	1.22219800	0.20291300
C	-4.67877300	-0.00022300	0.08119800
C	-3.99826900	-1.22251100	0.20254600
C	-2.61939200	-1.21775800	0.44633700
H	-2.09539900	2.16763800	0.53915300
H	-4.53664700	2.16374700	0.10894300
H	-4.53610400	-2.16416600	0.10829100
H	-2.09485600	-2.16757600	0.53850100
C	-1.92324500	0.00004900	0.56868100
C	-0.39347000	0.00022200	0.74709900
C	0.07320300	1.19481500	1.48103500
C	0.07347200	-1.19421800	1.48111400
N	0.42815600	2.16139700	2.03507800
N	0.42867900	-2.16068800	2.03519000
C	0.39347300	0.00023200	-0.74719000
C	1.92324100	0.00005700	-0.56872900
C	-0.07317600	1.19483600	-1.48112500
C	-0.07344200	-1.19420600	-1.48122600
C	2.61968700	1.21772500	-0.44670500
C	2.61937700	-1.21775200	-0.44634400

N -0.42810000 2.16142100 -2.03518300
 N -0.42858900 -2.16067800 -2.03533800
 C 3.99855500 1.22220200 -0.20285800
 H 2.09539200 2.16764600 -0.53916800
 C 3.99824500 -1.22250700 -0.20249500
 H 2.09484100 -2.16756800 -0.53851900
 C 4.67874700 -0.00022100 -0.08112100
 H 4.53662300 2.16375000 -0.10885800
 H 4.53607300 -2.16416300 -0.10821300
 Cl 6.40616300 -0.00039500 0.22137900
 Cl -6.40620400 -0.00039500 -0.22122300

Sum of electronic and thermal Free Energies= -1829.273073

Cl – Radical 6-31+G(d,p)/uωB97XD

C -0.00035700 0.04646000 -1.21597500
 C -0.00035700 1.42924100 -1.21640300
 C -0.00027500 2.11592700 0.00000000
 C -0.00035700 1.42924100 1.21640300
 C -0.00035700 0.04646000 1.21597500
 H -0.00018700 -0.48850500 -2.16030300
 H -0.00043700 1.97922800 -2.15026200
 H -0.00043700 1.97922800 2.15026200
 H -0.00018700 -0.48850500 2.16030300
 C -0.00041300 -0.67301300 0.00000000
 C 0.00015000 -2.11072200 0.00000000
 C 0.00049300 -2.84858100 -1.20900400
 C 0.00049300 -2.84858100 1.20900400
 N 0.00112200 -3.42764500 -2.21829000
 N 0.00112200 -3.42764500 2.21829000
 Cl -0.00050500 3.85217700 0.00000000

Cl – Radical 6-31+G(d,p)/uB97D

C -0.00012100 -0.04940600 1.22616800
 C -0.00012100 -1.44210800 1.22785800

C -0.00011100 -2.13708600 0.00000000
 C -0.00012100 -1.44210800 -1.22785800
 C -0.00012100 -0.04940600 -1.22616800
 H -0.00013200 0.48853900 2.17410200
 H -0.00013100 -1.99282700 2.16720600
 H -0.00013100 -1.99282700 -2.16720600
 H -0.00013200 0.48853900 -2.17410200
 C -0.00011600 0.67971800 0.00000000
 C -0.00010400 2.12722600 0.00000000
 C 0.00010200 2.87002800 1.20972900
 C 0.00010200 2.87002800 -1.20972900
 N 0.00042400 3.46160900 2.22884500
 N 0.00042400 3.46160900 -2.22884500
 Cl -0.00010300 -3.88325100 0.00000000

Sum of electronic and thermal Free Energies= -914.637782

5O-JUL σ-Dimer 6-31+G(d,p)/ωB97XD

C -6.83121900 -1.72012700 0.45744700
 H -7.06558300 -2.23445700 -0.49139100
 H -7.78414800 -1.45819200 0.92828700
 C -4.74671400 -0.53406100 -0.04923900
 C -4.06786900 0.59956500 -0.54758700
 C -2.69025900 0.54701000 -0.76847700
 C -1.95497800 -0.62243800 -0.52213600
 C -2.65563800 -1.73500200 -0.05039400
 H -2.12829800 -2.66916800 0.11976600
 C -4.01506000 -1.71822300 0.19854000
 C -0.44662200 -0.77218200 -0.74032000
 C 0.16328100 0.23896400 -1.62688500
 C -0.19769900 -2.04872100 -1.45100800
 C 0.42302900 -0.82129600 0.66433700
 C -0.17665700 0.10648200 1.64721600
 C 0.19380100 -2.15045500 1.27900100
 C 1.92757200 -0.64435800 0.44131500

C 2.62635500 0.55472700 0.65457400
C 4.01283200 0.62122800 0.47472700
C 4.71726400 -0.51085100 0.00362500
C 4.00664500 -1.70061300 -0.27871400
C 2.65032000 -1.74565200 -0.02271000
H 2.13924600 -2.68854300 -0.19481200
C 6.81859600 0.76462700 0.02351600
H 6.80056100 1.35294500 -0.91046000
C 1.80205500 2.78609100 0.28257900
H 1.42461400 2.44719900 -0.68392000
H 2.77279400 3.25868200 0.10759400
C 0.84238600 3.75876100 0.96517700
C -0.84905300 3.70330700 -1.00315100
C -1.51129100 2.52805700 -0.31553300
H -0.77216100 1.95838500 0.24755300
H -2.27313000 2.85223500 0.40889100
N 0.73833700 0.92896400 -2.35464600
N -0.01321100 -3.04471400 -2.00921200
N -0.72407200 0.71039000 2.46750300
N 0.02193900 -3.18520800 1.76609300
O -2.09869700 1.66772100 -1.29353800
O 1.94804500 1.64045300 1.13972800
H 7.86508700 0.52101300 0.23317800
C -6.89495400 0.60066700 -0.34843500
H -7.11080800 0.42046400 -1.41645200
H -7.85451100 0.62256500 0.17775100
C 6.76555900 -1.53136000 -0.88022000
H 6.67503200 -1.35732500 -1.96623400
H 7.83066300 -1.48716000 -0.63268000
N 6.09618400 -0.48354200 -0.12917600
N -6.10880300 -0.48354800 0.21160900
C 4.70542000 -2.92043500 -0.83531200
H 4.56232100 -2.95007600 -1.92345300
H 4.24046700 -3.82702200 -0.43605600
C 6.19725800 -2.89724500 -0.52374300

H 6.36511800 -3.08395800 0.54281300
 H 6.72219900 -3.67516600 -1.08602000
 C 4.76335300 1.88045700 0.84823700
 H 4.73086300 2.60033800 0.02028600
 H 4.27143400 2.35491700 1.70278700
 C 6.22390300 1.57898100 1.16060700
 H 6.78665800 2.50849100 1.28726600
 H 6.30558400 1.00787100 2.09198400
 C -4.81865900 1.86816900 -0.88817700
 H -4.22212200 2.74623100 -0.63176700
 H -4.96442500 1.91410700 -1.97512300
 C -6.16785700 1.92459200 -0.18104300
 H -6.02566600 2.11598600 0.88848300
 H -6.77804600 2.73721900 -0.58649600
 C -4.69820600 -2.97180100 0.69772600
 H -4.87097300 -3.65237800 -0.14636200
 H -4.03749700 -3.49788200 1.39368700
 C -6.03008500 -2.64362700 1.36234600
 H -6.60080700 -3.55623000 1.55771100
 H -5.86108300 -2.14300400 2.32214500
 C -0.03387700 4.55885600 -0.01520400
 H -0.20834400 3.31142000 -1.79919900
 H -1.60700800 4.32440800 -1.49229200
 H -0.71439000 5.17941900 0.57978900
 H 0.58656400 5.25511100 -0.59175900
 H 1.40401700 4.45529600 1.59621300
 H 0.21079200 3.18191100 1.64750600

Sum of electronic and thermal Free Energies= -1833.205393

5O-JUL π-Dimer 6-31+G(d,p)/ωB97XD

C 0.14228000 -0.47723400 -1.54098500
 C 0.89081000 0.68717600 -1.21232000
 C 2.20578400 0.63662400 -0.78130400
 C 2.85582700 -0.63229500 -0.66813900

C 2.13378400 -1.81873200 -1.01815000
 C 0.83421900 -1.71743900 -1.42879100
 C 2.93479200 1.90084900 -0.38731800
 N 4.15533800 -0.71802100 -0.27188100
 H 2.58871700 2.21403000 0.60347200
 H 2.68860300 2.71658900 -1.06718700
 C 4.79830700 0.42243300 0.36696400
 H 4.49261000 0.48042400 1.42099700
 H 5.87753000 0.24975500 0.34453300
 C -1.21262500 -0.45900800 -1.97432400
 C -2.02319500 0.69805500 -2.10240400
 N -2.75213700 1.59750800 -2.24194400
 C -1.81077500 -1.64922500 -2.46200700
 N -2.28268100 -2.64085000 -2.85404600
 C 4.44673500 1.70767000 -0.36122600
 H 4.92389300 2.55436200 0.13972700
 H 4.84297200 1.65622200 -1.38223200
 C 2.79753300 -3.16298100 -0.88355700
 H 2.62371500 -3.55035900 0.12933700
 H 2.35005100 -3.86923000 -1.58885700
 C 4.29923900 -3.03498400 -1.10867600
 H 4.80368800 -3.98860300 -0.93051200
 H 4.50213100 -2.73823800 -2.14441400
 C 4.86055000 -1.99362500 -0.15551700
 H 4.80208000 -2.35502300 0.87903200
 H 5.91383100 -1.80093200 -0.38552300
 C 0.41660700 2.77336900 -2.32724100
 H -0.13612300 2.40144300 -3.19777200
 H 1.47908700 2.81383200 -2.59426300
 C -0.04110800 -0.50247600 1.54677100
 C -0.92607600 0.64011000 1.40282300
 C -2.26489400 0.46886800 1.08461200
 C -2.73369400 -0.85611700 0.74004400
 C -1.84500900 -1.98629200 0.81422100
 C -0.56367000 -1.78418300 1.22292100

C	-3.27474900	1.59796800	1.05125700
N	-4.02931000	-1.07036100	0.40783700
H	-3.26189500	2.07162200	0.06378700
H	-3.03431400	2.35799700	1.78886600
C	-5.00060200	0.01409100	0.29661300
H	-4.99016200	0.41977900	-0.72358700
H	-5.98999800	-0.41363900	0.47859100
C	1.26548700	-0.39844700	2.05775100
C	1.87397500	0.77809500	2.58368500
N	2.45876200	1.67202600	3.04590500
C	2.03988100	-1.57450700	2.27485900
N	2.67056400	-2.53478600	2.46247500
C	-4.68725700	1.09606000	1.30506800
H	-5.40043100	1.91755600	1.19537500
H	-4.78753500	0.69566700	2.32077700
C	-2.31119000	-3.37765000	0.47415500
H	-2.07263500	-3.59138700	-0.57586300
H	-1.76650300	-4.10161300	1.08710500
C	-3.81323000	-3.51391500	0.66840300
H	-4.17177000	-4.46698900	0.27062000
H	-4.07122500	-3.47462300	1.73324800
C	-4.50096200	-2.37654300	-0.06372700
H	-4.33121700	-2.45844800	-1.14394400
H	-5.57926000	-2.40825300	0.10991700
C	-0.68432400	3.13014600	1.76156000
H	-1.48292200	3.18701000	2.50495700
H	0.19385000	3.61284000	2.20079900
H	0.30049200	-2.62904600	-1.68303300
H	0.09030000	-2.64377000	1.32972600
O	0.23615400	1.88124600	-1.22783400
O	-0.24852300	1.77357400	1.63692600
C	-0.09648000	4.14933200	-1.88969500
H	-1.15842400	4.23959700	-2.14282200
H	0.43292700	4.90825800	-2.47583500
C	0.08380400	4.40182800	-0.38163000

H 1.03853900 3.98421100 -0.04837700
H 0.13761600 5.48068800 -0.20086800
C -1.07241000 3.79727600 0.44181500
H -1.80717100 4.57935000 0.67024100
H -1.59004300 3.06595800 -0.17623600

Sum of electronic and thermal Free Energies= -1833.194981

5O-JUL σ-Dimer 6-31+G(d,p)/B97D

C -6.84143000 -1.65682200 0.55372300
H -7.28490500 -2.12464100 -0.34826900
H -7.66980500 -1.33632000 1.20295100
C -4.77171900 -0.53786300 -0.23728500
C -4.08860500 0.62138100 -0.73265100
C -2.73935500 0.53112400 -1.08309800
C -2.01783800 -0.70602800 -0.99818700
C -2.73728200 -1.84119800 -0.52374100
H -2.21354600 -2.79234500 -0.43088200
C -4.06589200 -1.78370900 -0.14156500
C -0.62843400 -0.85222600 -1.34708100
C 0.23961200 0.16384300 -1.82142200
C -0.02801000 -2.13769900 -1.46373700
C 0.63636200 -0.78004900 1.43716100
C -0.19495400 0.24008100 1.97484900
C 0.02550700 -2.05915400 1.58121500
C 2.00196100 -0.64551600 1.00847400
C 2.72026300 0.60006600 0.98335400
C 4.05194900 0.66532500 0.55330500
C 4.69990200 -0.51649200 0.06700900
C 3.98048800 -1.75966600 0.04136500
C 2.68988900 -1.80090400 0.53172900
H 2.16248500 -2.75407800 0.51454900
C 6.75694400 0.78778500 -0.40666500
H 6.57840900 1.27518200 -1.38582900
C 1.76977000 2.76591000 0.48369000

H 1.41864500 2.27032800 -0.42853900
 H 2.68087700 3.33144200 0.23549900
 C 0.70472900 3.68904100 1.07706700
 C -0.72717000 3.61749400 -1.10928000
 C -1.46428400 2.43133600 -0.50284900
 H -0.76790900 1.77173000 0.02356700
 H -2.22495400 2.75276800 0.23002500
 N 1.07236600 0.90427200 -2.20813800
 N 0.50597400 -3.18122900 -1.58293200
 N -1.00142000 0.96614800 2.43567900
 N -0.52048600 -3.09381500 1.72083800
 O -2.10855600 1.66329900 -1.56165800
 O 2.08171400 1.72096400 1.46147200
 H 7.83014500 0.55479000 -0.34085800
 C -6.88676400 0.74985200 -0.09376600
 H -7.31596200 0.70025300 -1.11476100
 H -7.72461200 0.75829300 0.61900700
 C 6.62861900 -1.62262900 -1.03434700
 H 6.38208200 -1.57550600 -2.11345700
 H 7.72002200 -1.52795500 -0.93664600
 N 6.02444600 -0.48071700 -0.33455300
 N -6.09116000 -0.45272500 0.17421900
 C 4.61228200 -3.01294200 -0.53522300
 H 4.31382600 -3.10906600 -1.59385700
 H 4.21828100 -3.89865900 -0.01677000
 C 6.14394700 -2.95275300 -0.44647800
 H 6.46749400 -3.01918900 0.60434500
 H 6.60402000 -3.78396700 -1.00042000
 C 4.81869800 1.97324400 0.62929100
 H 4.62201700 2.57782700 -0.27286500
 H 4.45720200 2.55484400 1.48921000
 C 6.32982300 1.72225300 0.72818900
 H 6.88643400 2.66770700 0.65400400
 H 6.57586200 1.25276400 1.69344900
 C -4.83130200 1.93612000 -0.89749100

H -4.15283800 2.78144300 -0.73378600
 H -5.18278300 2.02263700 -1.94090700
 C -6.03377600 2.01339700 0.05395400
 H -5.68484400 2.08973500 1.09563200
 H -6.64996500 2.89705800 -0.16749800
 C -4.76237100 -3.03330100 0.36644900
 H -5.13844300 -3.62175100 -0.48951100
 H -4.03529900 -3.66542400 0.89637200
 C -5.94335400 -2.66629600 1.27703900
 H -6.53380200 -3.55691200 1.53679700
 H -5.57330800 -2.21462500 2.21051900
 C -0.05362200 4.48795000 -0.01403900
 H 0.02170600 3.23194300 -1.81505700
 H -1.43207000 4.23610400 -1.68689100
 H -0.82283200 5.09227300 0.49410500
 H 0.62914400 5.19924500 -0.50790800
 H 1.16645400 4.38926300 1.79053900
 H -0.00803500 3.07942500 1.64607100

Sum of electronic and thermal Free Energies= -1832.512827

5O-JUL π-Dimer 6-31+G(d,p)/B97D

C 0.12190200 -0.52537000 -1.56584100
 C 0.86531700 0.65504200 -1.23767100
 C 2.19396500 0.61189000 -0.80431600
 C 2.85226000 -0.66464200 -0.68993900
 C 2.12707800 -1.86575700 -1.02369800
 C 0.81651100 -1.77087300 -1.43859900
 C 2.92537500 1.88242500 -0.40729000
 N 4.16363800 -0.74633700 -0.29558600
 H 2.59612800 2.18126500 0.59758200
 H 2.66235200 2.71005400 -1.07327300
 C 4.81902100 0.40975600 0.33383700
 H 4.51325500 0.47282900 1.39177500
 H 5.90341500 0.23496000 0.29961200

C -1.24499300 -0.50833900 -2.00503000
 C -2.04510100 0.65352300 -2.17298100
 N -2.77618200 1.55856300 -2.37103800
 C -1.87088700 -1.70658500 -2.44295200
 N -2.37213500 -2.71079300 -2.80730000
 C 4.45022200 1.69801400 -0.40443200
 H 4.93160600 2.55306300 0.09089000
 H 4.83171100 1.63872900 -1.43648000
 C 2.79241600 -3.21382200 -0.86470100
 H 2.63746500 -3.57146400 0.16753800
 H 2.32896300 -3.94074800 -1.54767100
 C 4.30378100 -3.09359900 -1.11375700
 H 4.81235300 -4.04919500 -0.92213400
 H 4.49371600 -2.80695800 -2.16055000
 C 4.87990200 -2.03152000 -0.17424300
 H 4.82571000 -2.37769400 0.87017300
 H 5.93486300 -1.83176000 -0.41870800
 C 0.40233400 2.76977400 -2.35147600
 H -0.21028400 2.44431200 -3.20700000
 H 1.46111800 2.74021200 -2.65360500
 C -0.04112600 -0.48693000 1.58198900
 C -0.91252400 0.66606200 1.41106500
 C -2.26606700 0.50607500 1.07151200
 C -2.75730400 -0.82916100 0.77462800
 C -1.87504900 -1.96836000 0.86348800
 C -0.57597100 -1.76891500 1.27058800
 C -3.25826800 1.65440300 0.95981500
 N -4.07776700 -1.04399900 0.46235700
 H -3.23983300 2.05171500 -0.06650400
 H -3.00864900 2.47012400 1.63732100
 C -5.03954100 0.05755300 0.30237800
 H -5.02942600 0.41015700 -0.74344800
 H -6.03976200 -0.34503100 0.51872900
 C 1.29459100 -0.38794800 2.09039100
 C 1.91313500 0.78721700 2.60200200

N 2.51601800 1.69342600 3.05724300
 C 2.08078100 -1.55941900 2.28353500
 N 2.73208000 -2.52692900 2.45618400
 C -4.69242900 1.19767400 1.25055500
 H -5.39094600 2.03168200 1.09218900
 H -4.79133500 0.85519900 2.29312300
 C -2.35142000 -3.36985300 0.54684000
 H -2.13202800 -3.59929900 -0.50911500
 H -1.79653000 -4.09132700 1.16478100
 C -3.86353800 -3.50138700 0.76182700
 H -4.23121900 -4.46480800 0.38096400
 H -4.10986100 -3.43546100 1.83376000
 C -4.55985500 -2.36673800 0.00900000
 H -4.38638800 -2.46627200 -1.07423700
 H -5.64359300 -2.39274200 0.18927400
 C -0.64956200 3.17692800 1.78703100
 H -1.46732800 3.20799400 2.52061100
 H 0.23090000 3.64049600 2.25583000
 H 0.28317300 -2.69174600 -1.67594400
 H 0.06873200 -2.63993500 1.38201400
 O 0.19366000 1.85238300 -1.25075500
 O -0.21047600 1.81101600 1.60930300
 C -0.00798000 4.18274800 -1.87945800
 H -1.06729300 4.35393900 -2.12473100
 H 0.57759800 4.91033100 -2.46359400
 C 0.19795600 4.41418200 -0.35840800
 H 1.11982300 3.91682100 -0.02904600
 H 0.33211700 5.49127800 -0.17408800
 C -1.00816600 3.89142800 0.47311300
 H -1.67409400 4.73306000 0.72815000
 H -1.59208200 3.20866300 -0.14840600

Sum of electronic and thermal Free Energies= -1832.519928

Computational References:

- [1] Gaussian 16, Revision A.03, M. J. Frisch, G. W. Trucks, H. B. Schlegel, G. E. Scuseria, M. A. Robb, J. R. Cheeseman, G. Scalmani, V. Barone, G. A. Petersson, H. Nakatsuji, X. Li, M. Caricato, A. V. Marenich, J. Bloino, B. G. Janesko, R. Gomperts, B. Mennucci, H. P. Hratchian, J. V. Ortiz, A. F. Izmaylov, J. L. Sonnenberg, D. Williams-Young, F. Ding, F. Lipparini, F. Egidi, J. Goings, B. Peng, A. Petrone, T. Henderson, D. Ranasinghe, V. G. Zakrzewski, J. Gao, N. Rega, G. Zheng, W. Liang, M. Hada, M. Ehara, K. Toyota, R. Fukuda, J. Hasegawa, M. Ishida, T. Nakajima, Y. Honda, O. Kitao, H. Nakai, T. Vreven, K. Throssell, J. A. Montgomery, Jr., J. E. Peralta, F. Ogliaro, M. J. Bearpark, J. J. Heyd, E. N. Brothers, K. N. Kudin, V. N. Staroverov, T. A. Keith, R. Kobayashi, J. Normand, K. Raghavachari, A. P. Rendell, J. C. Burant, S. S. Iyengar, J. Tomasi, M. Cossi, J. M. Millam, M. Klene, C. Adamo, R. Cammi, J. W. Ochterski, R. L. Martin, K. Morokuma, O. Farkas, J. B. Foresman, and D. J. Fox, Gaussian, Inc., Wallingford CT, 2016.
- [2] a)A. D. Becke, Physical Review A 1988, 38, 3098-3100; b) C. T. Lee, W. T. Yang, R. G. Parr, Physical Review B 1988, 37, 785-789.
- [3] A. D. Becke, Journal of Chemical Physics 1993, 98.
- [4] J. P. Perdew, K. Burke, Y. Wang, Physical Review B 1996, 54, 16533-16539.
- [5] J. P. Perdew, Physical Review B 1986, 33, 8822-8824.
- [6] H. L. Schmider, A. D. Becke, Journal of Chemical Physics 1998, 108, 9624-9631.
- [7] J. D. Chai, M. Head-Gordon, Physical Chemistry Chemical Physics 2008, 10, 6615-6620.
- [8] S. Grimme, J. Antony, S. Ehrlich, H. Krieg, Journal of Chemical Physics 2010, 132.
- [9] S. Grimme, Journal of Computational Chemistry 2006, 27, 1787-1799.
- [10] T. H. Dunning, Journal of Chemical Physics 1989, 90, 1007-1023

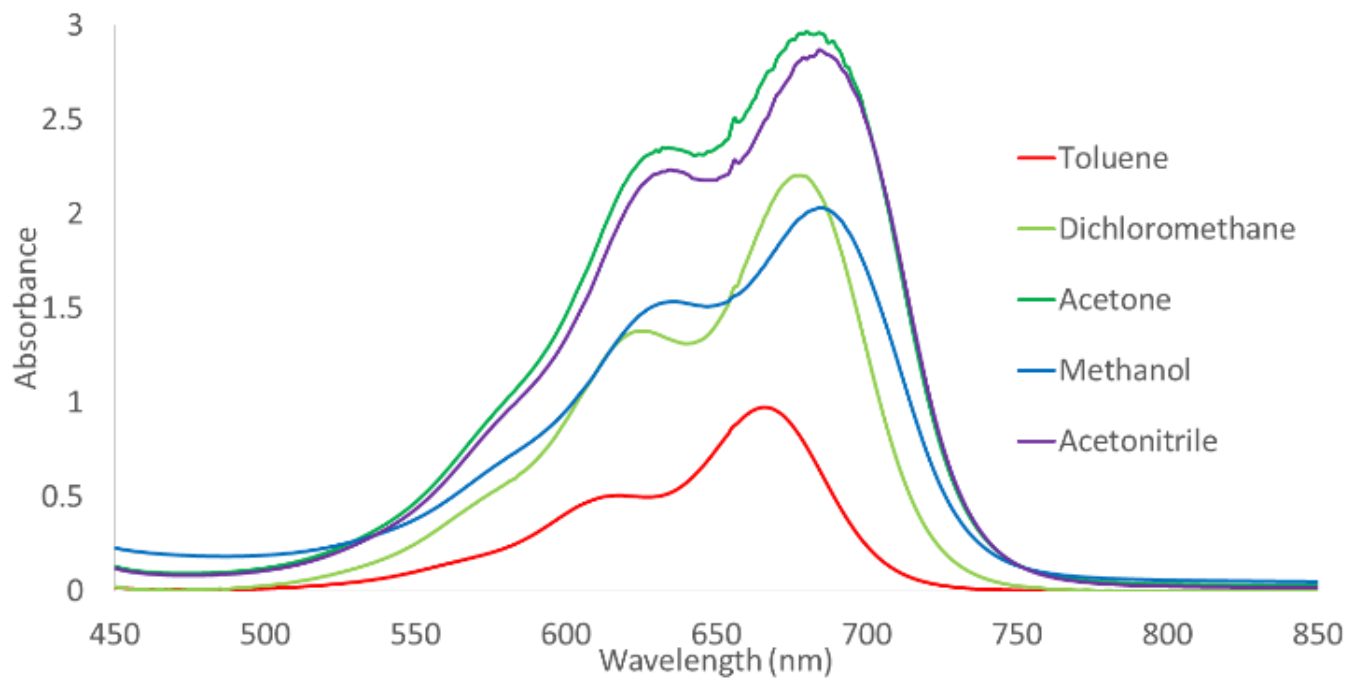
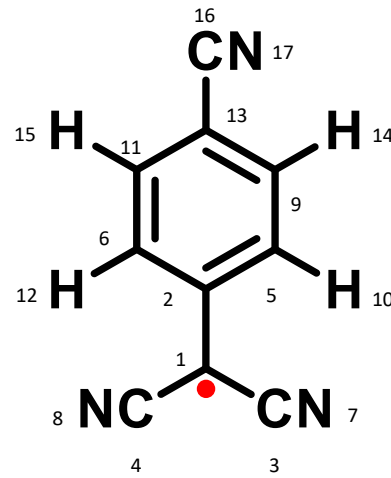
APPENDIX C. SUPPORTING INFORMATION FOR CHAPTER 4

Figure S1: Room temperature UV/Vis spectra of N,N-dimethylamino dicyanomethyl radical in different solvents ($\sim 75 \mu\text{M}$)

Optimized Geometry:

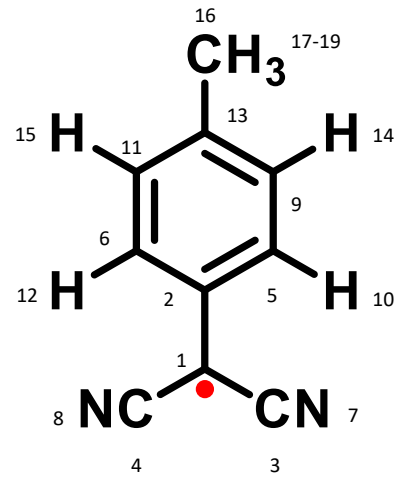
Atomic #	Atom	Coordinates (Angstroms)		
		X	Y	Z
6	1	-1.979944	-0.000000	0.000060
6	2	-0.540337	-0.000000	0.000046
6	3	-2.717340	-1.209151	-0.000148
6	4	-2.717340	1.209151	0.000127
6	5	0.175228	-1.218275	0.000252
6	6	0.175228	1.218275	-0.000179
7	7	-3.297728	-2.217497	-0.000294
7	8	-3.297728	2.217498	0.000191
6	9	1.556896	-1.217321	0.000228
1	10	-0.361608	-2.161261	0.000424
6	11	1.556896	1.217321	-0.000199
1	12	-0.361608	2.161260	-0.000336
6	13	2.255269	0.000000	0.000001
1	14	2.104333	-2.152954	0.000381
1	15	2.104333	2.152954	-0.000372
6	16	3.690720	0.000000	-0.000026
7	17	4.850154	0.000000	-0.000049



Mulliken Spin Density Cyano Radical									
	Acetone	CH ₃ CN	CHCl ₃	C ₆ H ₁₂	CH ₂ Cl ₂	DMF	CH ₃ OH	Toluene	H ₂ O
C 1	0.642473	0.642121	0.644940	0.648110	0.643489	0.642102	0.642166	0.647393	0.641858
C 2	-0.140614	-0.140074	-0.144500	-0.149893	-0.142192	-0.140043	-0.140143	-0.148617	-0.139670
C 3	-0.178494	-0.178092	-0.181235	-0.184668	-0.179638	-0.178069	-0.178144	-0.183891	-0.177788
C 4	-0.178495	-0.178093	-0.181236	-0.184669	-0.179638	-0.178070	-0.178144	-0.183892	-0.177789
C 5	0.213208	0.213310	0.212433	0.211274	0.212902	0.213316	0.213297	0.211555	0.213385
C 6	0.213208	0.213310	0.212433	0.211274	0.212902	0.213316	0.213297	0.211555	0.213385
N 7	0.230987	0.230381	0.235198	0.240730	0.232726	0.230347	0.230459	0.239447	0.229924
N 8	0.230988	0.230382	0.235199	0.240731	0.232727	0.230348	0.230460	0.239448	0.229925
C 9	-0.136214	-0.136277	-0.135680	-0.134790	-0.136012	-0.136281	-0.136269	-0.135012	-0.136322
H 10	-0.008374	-0.008375	-0.008367	-0.008353	-0.008372	-0.008375	-0.008374	-0.008356	-0.008375
C 11	-0.136214	-0.136277	-0.135680	-0.134790	-0.136012	-0.136281	-0.136269	-0.135012	-0.136322
H 12	-0.008374	-0.008375	-0.008367	-0.008353	-0.008372	-0.008375	-0.008374	-0.008356	-0.008375
C 13	0.237452	0.237598	0.236320	0.234595	0.237009	0.237606	0.237579	0.235015	0.237704
H 14	0.004581	0.004580	0.004587	0.004596	0.004583	0.004580	0.004580	0.004594	0.004580
H 15	0.004581	0.004580	0.004587	0.004596	0.004583	0.004580	0.004580	0.004594	0.004580
C 16	-0.066730	-0.066639	-0.067284	-0.067842	-0.066975	-0.066634	-0.066651	-0.067727	-0.066568
N 17	0.076031	0.075939	0.076651	0.077450	0.076291	0.075934	0.075951	0.077263	0.075869

Optimized Geometry:

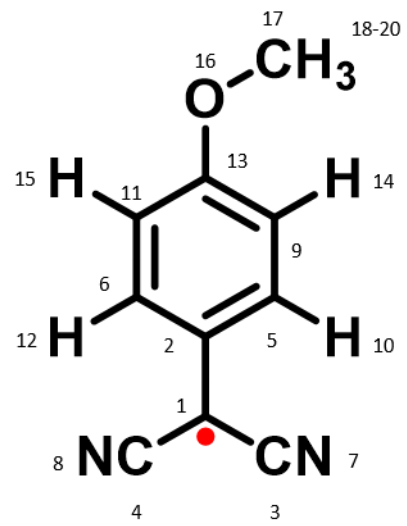
Atomic #	Atom	Coordinates (Angstroms)		
		X	Y	Z
6	1	-2.076541	-0.213017	-0.337516
6	2	-0.663693	0.046792	-0.339099
6	3	-3.022515	0.841934	-0.322416
6	4	-2.585556	-1.535361	-0.350985
6	5	-0.172393	1.370548	-0.325548
6	6	0.267493	-1.017799	-0.354269
7	7	-3.777822	1.727010	-0.309871
7	8	-2.976927	-2.631159	-0.362245
6	9	1.190829	1.610942	-0.327191
1	10	-0.868090	2.203822	-0.313781
6	11	1.623831	-0.757673	-0.355664
1	12	-0.087324	-2.043695	-0.364854
6	13	2.115278	0.558226	-0.342203
1	14	1.547996	2.636368	-0.316617
1	15	2.323973	-1.588202	-0.367413
6	16	3.597010	0.815365	-0.344038
1	17	4.071359	0.359870	0.531251
1	18	4.065661	0.380115	-1.232597
1	19	3.819905	1.884510	-0.332486



Mulliken Spin Density Methyl Radical									
	Acetone	CH ₃ CN	CHCl ₃	C ₆ H ₁₂	CH ₂ Cl ₂	DMF	CH ₃ OH	Toluene	H ₂ O
C 1	0.583346	0.581757	0.594512	0.609215	0.587936	0.581668	0.581961	0.605824	0.580565
C 2	-0.083134	-0.081662	-0.093513	-0.107424	-0.087390	-0.081579	-0.081851	-0.104179	-0.080557
C 3	-0.158598	-0.157851	-0.163834	-0.170740	-0.160753	-0.157809	-0.157947	-0.169142	-0.157290
C 4	-0.158526	-0.157786	-0.163717	-0.170566	-0.160662	-0.157744	-0.157881	-0.168981	-0.157230
C 5	0.205459	0.205189	0.207228	0.209259	0.206212	0.205174	0.205224	0.208819	0.204983
C 6	0.192973	0.192662	0.195011	0.197341	0.193840	0.192644	0.192702	0.196838	0.192425
N 7	0.210103	0.209238	0.216244	0.224614	0.212612	0.209189	0.209349	0.222644	0.208590
N 8	0.210965	0.210100	0.217107	0.225478	0.213474	0.210052	0.210211	0.223508	0.209452
C 9	-0.125633	-0.125483	-0.126563	-0.127477	-0.126041	-0.125474	-0.125502	-0.127298	-0.125367
H 10	-0.008445	-0.008436	-0.008502	-0.008563	-0.008470	-0.008436	-0.008437	-0.008550	-0.008429
C 11	-0.116407	-0.116185	-0.117849	-0.119443	-0.117025	-0.116172	-0.116214	-0.119106	-0.116015
H 12	-0.007806	-0.007795	-0.007876	-0.007953	-0.007836	-0.007794	-0.007796	-0.007936	-0.007786
C 13	0.247222	0.247716	0.243647	0.238656	0.245774	0.247744	0.247653	0.239839	0.248085
H 14	0.003904	0.003892	0.003987	0.004090	0.003938	0.003891	0.003893	0.004067	0.003883
H 15	0.003886	0.003874	0.003974	0.004084	0.003923	0.003873	0.003875	0.004059	0.003864
C 16	-0.020891	-0.020896	-0.020847	-0.020763	-0.020875	-0.020896	-0.020895	-0.020785	-0.020899
H 17	0.010637	0.010679	0.010336	0.009927	0.010514	0.010681	0.010674	0.010023	0.010711
H 18	0.010638	0.010680	0.010337	0.009929	0.010515	0.010683	0.010675	0.010024	0.010712
H 19	0.000308	0.000306	0.000320	0.000336	0.000313	0.000306	0.000306	0.000332	0.000305

Optimized Geometry:

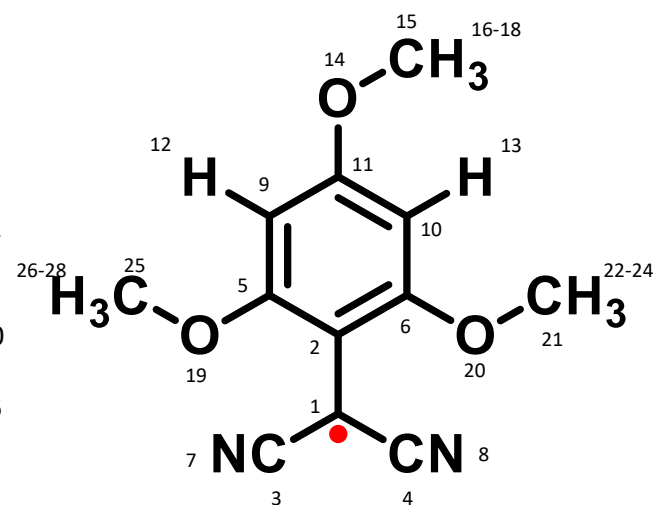
Atomic #	Atom	Coordinates (Angstroms)		
		X	Y	Z
6	1	-2.073638	-0.196723	-0.362989
6	2	-0.659765	0.033209	-0.347158
6	3	-2.995937	0.877355	-0.428229
6	4	-2.608239	-1.508471	-0.314028
6	5	-0.133453	1.349735	-0.397162
6	6	0.248888	-1.045659	-0.281395
7	7	-3.729077	1.779404	-0.482250
7	8	-3.014759	-2.598007	-0.272696
6	9	1.223710	1.565475	-0.381962
1	10	-0.810286	2.196930	-0.448054
6	11	1.616174	-0.832091	-0.265860
1	12	-0.129693	-2.062241	-0.242153
6	13	2.115524	0.477869	-0.316212
1	14	1.633324	2.568438	-0.419966
1	15	2.281800	-1.684844	-0.214865
8	16	3.421140	0.796816	-0.306719
6	17	4.383670	-0.243278	-0.241786
1	18	4.307070	-0.905096	-1.111329
1	19	5.352814	0.252997	-0.247010
1	20	4.274831	-0.823030	0.681279



Mulliken Spin Density Methoxy Radical									
	Acetone	CH ₃ CN	CHCl ₃	C ₆ H ₁₂	CH ₂ Cl ₂	DMF	CH ₃ OH	Toluene	H ₂ O
C	0.532912	0.530245	0.550517	0.572393	0.540183	0.530418	0.533944	0.567426	0.531872
C	-0.048451	-0.046185	-0.063589	-0.082898	-0.054677	-0.046304	-0.049013	-0.078458	-0.047227
C	-0.144659	-0.143606	-0.151670	-0.160548	-0.147550	-0.143655	-0.144724	-0.158518	-0.143879
C	-0.142370	-0.141310	-0.149504	-0.158633	-0.145304	-0.141350	-0.142505	-0.156535	-0.141657
C	0.156052	0.155518	0.160010	0.164770	0.157701	0.155437	0.157601	0.163661	0.157241
C	0.191302	0.190361	0.196862	0.203270	0.193605	0.190622	0.191866	0.201875	0.191182
N	0.194512	0.193342	0.202455	0.212896	0.197760	0.193389	0.194534	0.210466	0.193592
N	0.192374	0.191239	0.200121	0.210318	0.195543	0.191272	0.192468	0.207941	0.191556
C	-0.087392	-0.086745	-0.091710	-0.096626	-0.089200	-0.086776	-0.088721	-0.095516	-0.088268
H	-0.006470	-0.006453	-0.006605	-0.006768	-0.006527	-0.006449	-0.006530	-0.006729	-0.006518
C	-0.100030	-0.099576	-0.102991	-0.106360	-0.101254	-0.099650	-0.101321	-0.105597	-0.101037
H	-0.008120	-0.008088	-0.008312	-0.008528	-0.008200	-0.008096	-0.008136	-0.008481	-0.008111
C	0.209875	0.210390	0.207487	0.203587	0.208963	0.210123	0.212470	0.204393	0.212915
H	0.002665	0.002633	0.002877	0.003133	0.002753	0.002636	0.002709	0.003075	0.002686
H	0.002699	0.002675	0.002863	0.003065	0.002766	0.002676	0.002748	0.003018	0.002731
O	0.050899	0.051324	0.047195	0.043154	0.049323	0.051476	0.048484	0.044157	0.048776
C	-0.003391	-0.003410	-0.003198	-0.002985	-0.003308	-0.003424	-0.003248	-0.003040	-0.003262
H	0.003825	0.003850	0.003626	0.003411	0.003740	0.003855	0.003716	0.003462	0.003734
H	-0.000056	-0.000056	-0.000060	-0.000065	-0.000058	-0.000056	-0.000061	-0.000064	-0.000061
H	0.003826	0.003852	0.003627	0.003412	0.003742	0.003856	0.003718	0.003463	0.003736

Optimized Geometry:

Atomic #	Atom	Coordinates (Angstroms)		
		X	Y	Z
6	1	2.013038	0.063354	0.000413
6	2	0.585278	-0.061542	0.000295
6	3	2.920273	-1.033506	0.000634
6	4	2.715947	1.301009	0.000313
6	5	-0.064111	-1.338836	-0.000310
6	6	-0.273356	1.077122	0.000776
7	7	3.756063	-1.843799	0.000885
7	8	3.395093	2.246563	0.000173
6	9	-1.442200	-1.459063	-0.000408
6	10	-1.661940	0.963448	0.000662
6	11	-2.237570	-0.308288	0.000072
1	12	-1.935322	-2.421561	-0.000886
1	13	-2.276024	1.851524	0.001047
8	14	-3.566383	-0.529360	-0.000080
6	15	-4.448027	0.579302	0.000308
1	16	-4.311425	1.193848	-0.896716
1	17	-5.452624	0.158683	0.000031
1	18	-4.311598	1.193078	0.897886
8	19	0.760277	-2.392376	-0.000822
8	20	0.351708	2.260436	0.001387
6	21	-0.383988	3.468375	0.001909
1	22	-1.005978	3.550367	-0.896564
1	23	-1.006132	3.549498	0.900354
1	24	0.364489	4.259532	0.002351
6	25	0.238527	-3.708137	-0.001375
1	26	-0.361925	-3.891803	0.896354
1	27	-0.361909	-3.891054	-0.899269
1	28	1.109795	-4.361371	-0.001639

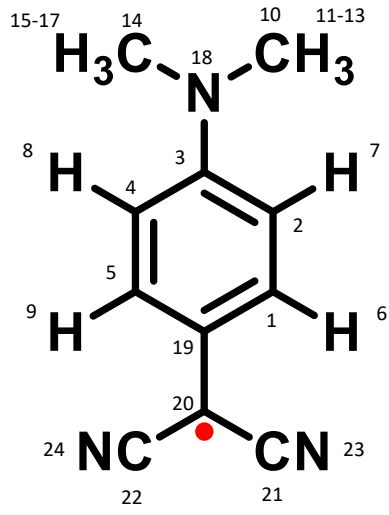


Mulliken Spin Density 1,3,5-Trimethoxy Radical									
	Acetone	CH ₃ CN	CHCl ₃	C ₆ H ₁₂	CH ₂ Cl ₂	DMF	CH ₃ OH	Toluene	H ₂ O
C 1	0.507144	0.502640	0.533629	0.564569	0.518497	0.503109	0.504503	0.558216	0.500822
C 2	0.050036	0.054649	0.022071	-0.012423	0.038185	0.054262	0.051664	-0.005099	0.055379
C 3	-0.155681	-0.154110	-0.164786	-0.175713	-0.159557	-0.154308	-0.154385	-0.173473	-0.153108
C 4	-0.157516	-0.155959	-0.166536	-0.177358	-0.161349	-0.156175	-0.156225	-0.175142	-0.154957
C 5	0.112049	0.111043	0.118840	0.126218	0.115036	0.110875	0.113431	0.124612	0.112635
C 6	0.141479	0.140253	0.149258	0.157922	0.144885	0.140184	0.142379	0.156094	0.141373
N 7	0.197126	0.195464	0.207096	0.219894	0.201310	0.195657	0.195812	0.217158	0.194468
N 8	0.198082	0.196437	0.207963	0.220602	0.202221	0.196646	0.196768	0.217906	0.195431
C 9	-0.072553	-0.071735	-0.077845	-0.083440	-0.074887	-0.071633	-0.073357	-0.082248	-0.072682
C 10	-0.080882	-0.080278	-0.085129	-0.089628	-0.082783	-0.080151	-0.081950	-0.088639	-0.081440
C 11	0.159641	0.159878	0.159300	0.158810	0.159497	0.159617	0.162419	0.158778	0.162676
H 12	0.002024	0.001987	0.002269	0.002540	0.002131	0.001983	0.002048	0.002482	0.002017

H 13	0.002155	0.002129	0.002337	0.002541	0.002235	0.002124	0.002191	0.002495	0.002169
O 14	0.036113	0.036520	0.032869	0.029737	0.034649	0.036706	0.034824	0.030454	0.035177
C 15	-0.002616	-0.002633	-0.002462	-0.002311	-0.002547	-0.002644	-0.002540	-0.002347	-0.002555
H 16	0.002839	0.002861	0.002684	0.002547	0.002768	0.002867	0.002788	0.002576	0.002807
H 17	-0.000056	-0.000056	-0.000062	-0.000068	-0.000059	-0.000055	-0.000060	-0.000066	-0.000059
H 18	0.002839	0.002861	0.002684	0.002547	0.002768	0.002867	0.002788	0.002576	0.002807
O 19	0.024085	0.024166	0.023448	0.022412	0.023841	0.024166	0.023711	0.022659	0.023746
O 20	0.031063	0.031223	0.029862	0.028216	0.030576	0.031258	0.030520	0.028605	0.030605
C 21	-0.003158	-0.003165	-0.003090	-0.002975	-0.003132	-0.003167	-0.003125	-0.003005	-0.003128
H 22	0.002293	0.002306	0.002215	0.002115	0.002261	0.002304	0.002287	0.002136	0.002295
H 23	0.002294	0.002307	0.002216	0.002116	0.002262	0.002305	0.002288	0.002137	0.002296
H 24	-0.000057	-0.000057	-0.000060	-0.000065	-0.000059	-0.000057	-0.000059	-0.000064	-0.000059
C 25	-0.002244	-0.002252	-0.002180	-0.002074	-0.002220	-0.002252	-0.002228	-0.002100	-0.002234
H 26	0.001773	0.001781	0.001728	0.001658	0.001756	0.001778	0.001776	0.001673	0.001781
H 27	0.001774	0.001782	0.001729	0.001659	0.001757	0.001779	0.001777	0.001673	0.001782
H 28	-0.000044	-0.000044	-0.000046	-0.000049	-0.000045	-0.000044	-0.000046	-0.000048	-0.000046

Optimized Geometry:

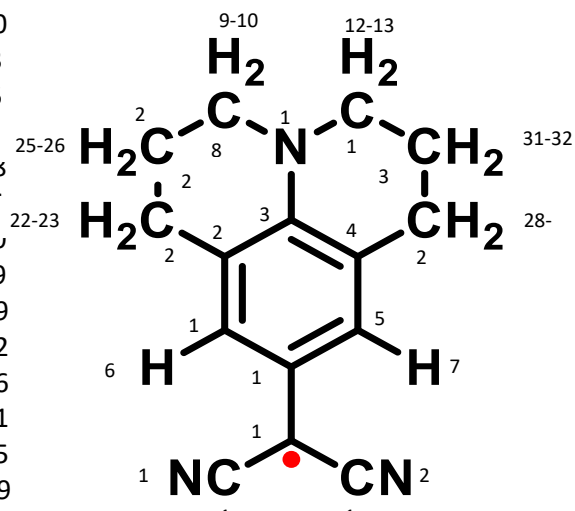
Atomic #	Atom	Coordinates (Angstroms)		
		X	Y	Z
6	1	-0.333127	1.210062	-0.000310
6	2	1.041317	1.213736	-0.000448
6	3	1.779491	-0.000004	-0.000364
6	4	1.041315	-1.213744	0.000123
6	5	-0.333130	-1.210067	0.000235
1	6	-0.863082	2.157589	-0.000459
1	7	1.553815	2.167238	-0.000750
1	8	1.553809	-2.167247	0.000584
1	9	-0.863087	-2.157593	0.000632
6	10	3.875285	1.254549	0.001237
1	11	4.944434	1.046200	0.001795
1	12	3.647726	1.852647	-0.889192
1	13	3.646422	1.850614	0.892711
6	14	3.875302	-1.254541	-0.000507
1	15	3.648849	-1.850600	0.891610
1	16	3.645353	-1.852650	-0.890291
1	17	4.944445	-1.046180	-0.003078
7	18	3.143928	0.000000	-0.000763
6	19	-1.071147	-0.000002	-0.000028
6	20	-2.497096	0.000000	0.000042
6	21	-3.234425	1.211198	-0.000066
6	22	-3.234429	-1.211195	0.000196
7	23	-3.808734	2.223390	-0.000146
7	24	-3.808740	-2.223386	0.000307



Mulliken Spin Density Dimethylamino Radical									
	Acetone	CH ₃ CN	CHCl ₃	C ₆ H ₁₂	CH ₂ Cl ₂	DMF	CH ₃ OH	Toluene	H ₂ O
C 1	0.075830	0.070892	0.104476	0.131831	0.088751	0.070606	0.071542	0.126235	0.067006
C 2	-0.003335	0.001439	-0.030694	-0.056265	-0.015746	0.001716	0.000810	-0.051081	0.005207
C 3	0.135477	0.132294	0.152660	0.167106	0.143494	0.132108	0.132716	0.164303	0.129742
C 4	-0.003333	0.001441	-0.030693	-0.056264	-0.015744	0.001717	0.000812	-0.051080	0.005209
C 5	0.075830	0.070892	0.104476	0.131831	0.088751	0.070606	0.071542	0.126235	0.067006
H 6	-0.003972	-0.003794	-0.004998	-0.005966	-0.004436	-0.003783	-0.003817	-0.005769	-0.003653
H 7	-0.000868	-0.001054	0.000216	0.001268	-0.000380	-0.001065	-0.001030	0.001051	-0.001201
H 8	-0.000868	-0.001054	0.000216	0.001268	-0.000380	-0.001065	-0.001030	0.001051	-0.001201
H 9	-0.003972	-0.003794	-0.004998	-0.005966	-0.004436	-0.003783	-0.003817	-0.005769	-0.003653
C 10	-0.014278	-0.014641	-0.012128	-0.009996	-0.013317	-0.014662	-0.014594	-0.010440	-0.014926
H 11	0.000476	0.000489	0.000400	0.000322	0.000442	0.000490	0.000487	0.000338	0.000499
H 12	0.012168	0.012490	0.010337	0.008644	0.011334	0.012508	0.012447	0.008986	0.012745
H 13	0.012174	0.012496	0.010344	0.008651	0.011341	0.012515	0.012454	0.008994	0.012751
C 14	-0.014278	-0.014641	-0.012128	-0.009996	-0.013317	-0.014662	-0.014594	-0.010440	-0.014926
H 15	0.012206	0.012529	0.010369	0.008670	0.011370	0.012548	0.012486	0.009014	0.012785
H 16	0.012136	0.012457	0.010313	0.008625	0.011306	0.012476	0.012415	0.008966	0.012711
H 17	0.000476	0.000489	0.000400	0.000322	0.000442	0.000490	0.000487	0.000338	0.000499
N 18	0.197127	0.203436	0.160911	0.126682	0.180720	0.203802	0.202605	0.133677	0.208418
C 19	0.052798	0.059370	0.012274	-0.031010	0.035052	0.059747	0.058512	-0.021727	0.064463
C 20	0.368335	0.358905	0.425261	0.483537	0.393527	0.358363	0.360140	0.471282	0.351560
C 21	-0.093239	-0.090390	-0.111034	-0.130481	-0.100981	-0.090227	-0.090762	-0.126275	-0.088190
C 22	-0.093239	-0.090390	-0.111034	-0.130481	-0.100981	-0.090227	-0.090762	-0.126276	-0.088190
N 23	0.138173	0.135069	0.157527	0.178833	0.146596	0.134892	0.135474	0.174192	0.132669
N 24	0.138174	0.135070	0.157527	0.178833	0.146597	0.134892	0.135475	0.174193	0.132669

Optimized Geometry:

Atomic #	Atom	Coordinates (Angstroms)		
		X	Y	Z
6	1	0.133944	1.567060	-0.791765
6	2	1.410300	1.170335	-0.474403
6	3	1.623324	-0.095799	0.146084
6	4	0.498562	-0.921571	0.440058
6	5	-0.766952	-0.482038	0.135804
1	6	-0.010482	2.529696	-1.274980
1	7	-1.614423	-1.118254	0.376740
6	8	4.080693	0.223015	0.048983
1	9	4.476816	0.777203	0.913415
1	10	4.841326	-0.512548	-0.23821
6	11	3.153639	-1.727857	1.215238
1	12	3.482597	-2.521229	0.526981
1	13	3.991529	-1.519741	1.891010
7	14	2.888143	-0.511872	0.455059
6	15	-0.998245	0.766705	-0.494819
6	16	-2.313998	1.199440	-0.816782
6	17	-2.544288	2.447973	-1.449306
6	18	-3.446161	0.398910	-0.517941
7	19	-2.695215	3.478556	-1.968635
7	20	-4.351538	-0.284450	-0.257399
6	21	2.600562	2.044766	-0.775284
1	22	2.830738	2.671259	0.097059
1	23	2.366231	2.722737	-1.600519
6	24	3.808878	1.173986	-1.105598
1	25	4.698983	1.783416	-1.284081
1	26	3.612044	0.599153	-2.017581
6	27	0.727471	-2.262845	1.088639
1	28	0.901534	-3.023808	0.315931
1	29	-0.166323	-2.568042	1.639607
6	30	1.941978	-2.189530	2.008946
1	31	1.745780	-1.484554	2.824683
1	32	2.157910	-3.163056	2.457476



Mulliken Spin Density Julolidine Radical

	Acetone	CH ₃ CN	CHCl ₃	C ₆ H ₁₂	CH ₂ Cl ₂	DMF	CH ₃ OH	Toluene	H ₂ O
C 1	0.042560	0.036699	0.079138	0.116519	0.058570	0.036364	0.037461	0.108792	0.032194
C 2	0.019717	0.025600	-0.015854	-0.049931	0.003901	0.025937	0.024832	-0.043100	0.030154
C 3	0.131821	0.127153	0.157422	0.177471	0.143762	0.126882	0.127770	0.173842	0.123455
C 4	0.019740	0.025625	-0.015840	-0.049925	0.003920	0.025962	0.024857	-0.043093	0.030181
C 5	0.042552	0.036689	0.079142	0.116535	0.058566	0.036354	0.037452	0.108806	0.032183
H 6	-0.002479	-0.002260	-0.003840	-0.005206	-0.003077	-0.002247	-0.002288	-0.004926	-0.002090
H 7	-0.002481	-0.002261	-0.003842	-0.005208	-0.003079	-0.002249	-0.002290	-0.004928	-0.002092
C 8	-0.017300	-0.017712	-0.014715	-0.012023	-0.016172	-0.017735	-0.017658	-0.012586	-0.018028

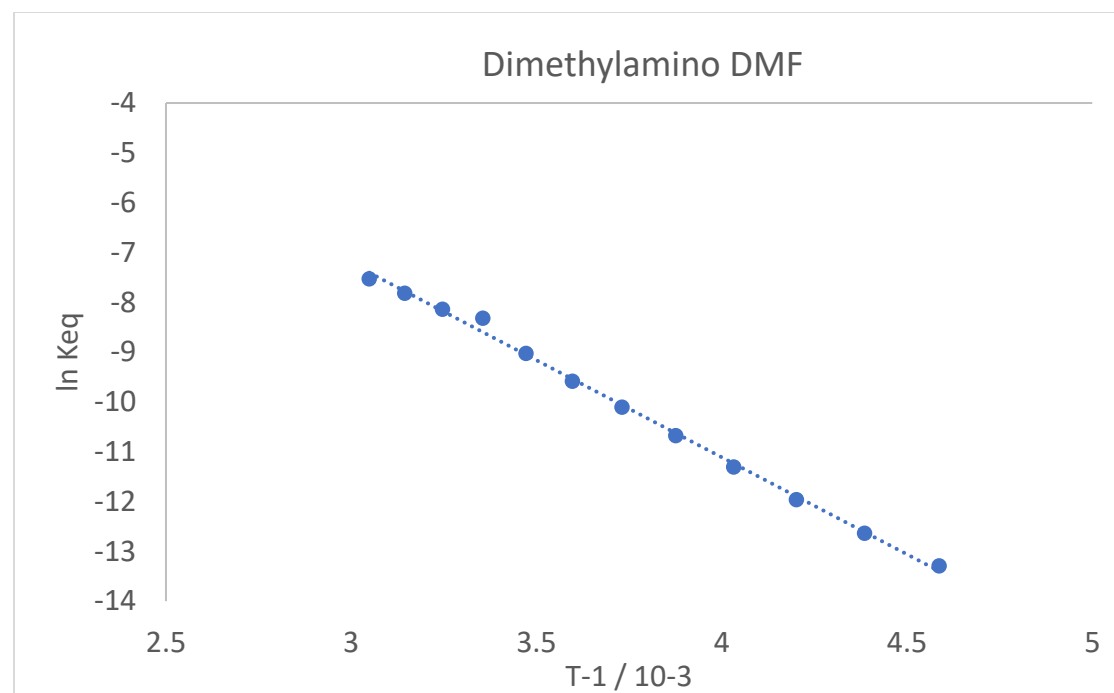
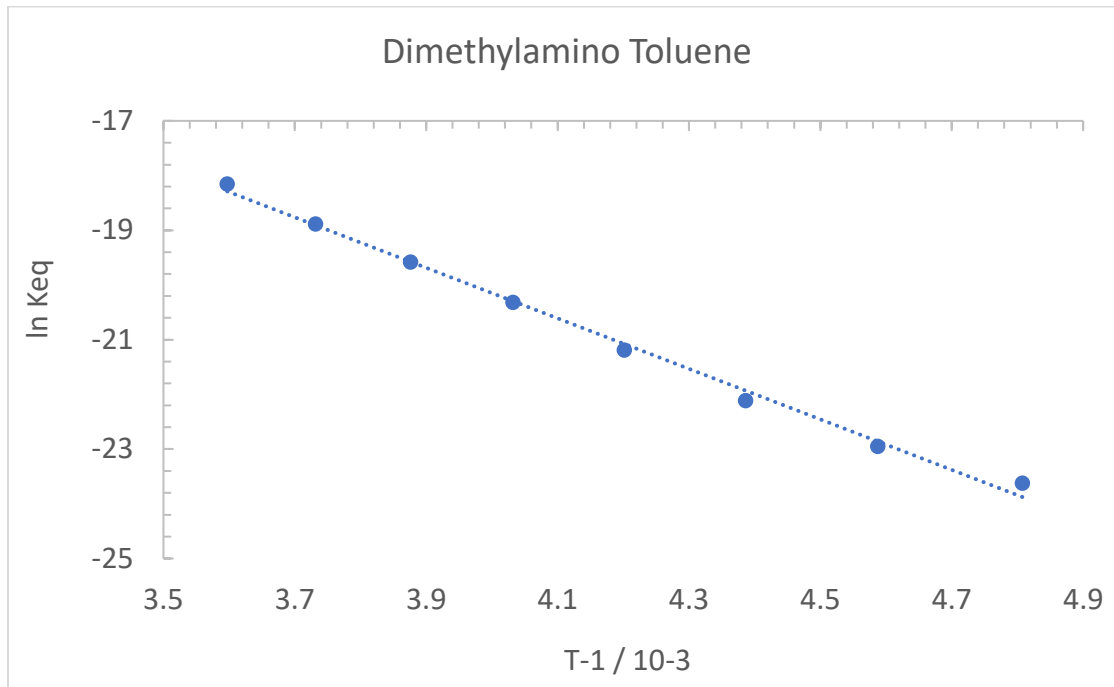
H 9	0.016211	0.016671	0.013460	0.010822	0.014983	0.016697	0.016610	0.011355	0.017028
H 10	0.008430	0.008664	0.007018	0.005641	0.007802	0.008678	0.008634	0.005922	0.008846
C 11	-0.017318	-0.017732	-0.014724	-0.012024	-0.016186	-0.017756	-0.017678	-0.012589	-0.018050
H 12	0.016239	0.016699	0.013486	0.010845	0.015010	0.016726	0.016639	0.011379	0.017057
H 13	0.008387	0.008621	0.006981	0.005610	0.007762	0.008634	0.008590	0.005889	0.008801
N 14	0.258925	0.266455	0.213005	0.167474	0.238617	0.266887	0.265473	0.176804	0.272280
C 15	0.131767	0.138844	0.083785	0.026860	0.111602	0.139243	0.137932	0.039387	0.144174
C 16	0.273281	0.262939	0.341152	0.417063	0.302263	0.262353	0.264276	0.400775	0.255088
C 17	-0.067564	-0.064632	-0.087392	-0.110916	-0.075903	-0.064466	-0.065010	-0.105736	-0.062421
C 18	-0.067561	-0.064629	-0.087391	-0.110918	-0.075902	-0.064464	-0.065007	-0.105738	-0.062418
N 19	0.108376	0.105141	0.130085	0.155702	0.117537	0.104959	0.105559	0.150055	0.102697
N 20	0.108376	0.105141	0.130085	0.155701	0.117536	0.104958	0.105558	0.150053	0.102696
C 21	-0.013285	-0.013702	-0.010556	-0.007522	-0.012118	-0.013725	-0.013648	-0.008172	-0.014019
H 22	0.001527	0.001753	0.000146	-0.001210	0.000917	0.001766	0.001723	-0.000935	0.001927
H 23	0.000620	0.000676	0.000275	-0.000068	0.000468	0.000680	0.000669	0.000002	0.000720
C 24	0.005985	0.006117	0.005147	0.004254	0.005621	0.006125	0.006100	0.004443	0.006219
H 25	-0.000580	-0.000591	-0.000516	-0.000454	-0.000552	-0.000591	-0.000589	-0.000466	-0.000599
H 26	-0.000111	-0.000116	-0.000078	-0.000047	-0.000096	-0.000116	-0.000115	-0.000053	-0.000120
C 27	-0.013294	-0.013712	-0.010562	-0.007523	-0.012125	-0.013735	-0.013658	-0.008175	-0.014029
H 28	0.001536	0.001761	0.000153	-0.001206	0.000925	0.001774	0.001732	-0.000930	0.001935
H 29	0.000626	0.000683	0.000279	-0.000066	0.000473	0.000686	0.000675	0.000004	0.000726
C 30	0.005991	0.006125	0.005148	0.004251	0.005625	0.006132	0.006107	0.004441	0.006227
H 31	-0.000112	-0.000117	-0.000078	-0.000047	-0.000097	-0.000117	-0.000116	-0.000053	-0.000121
H 32	-0.000582	-0.000593	-0.000517	-0.000455	-0.000553	-0.000594	-0.000592	-0.000467	-0.000601

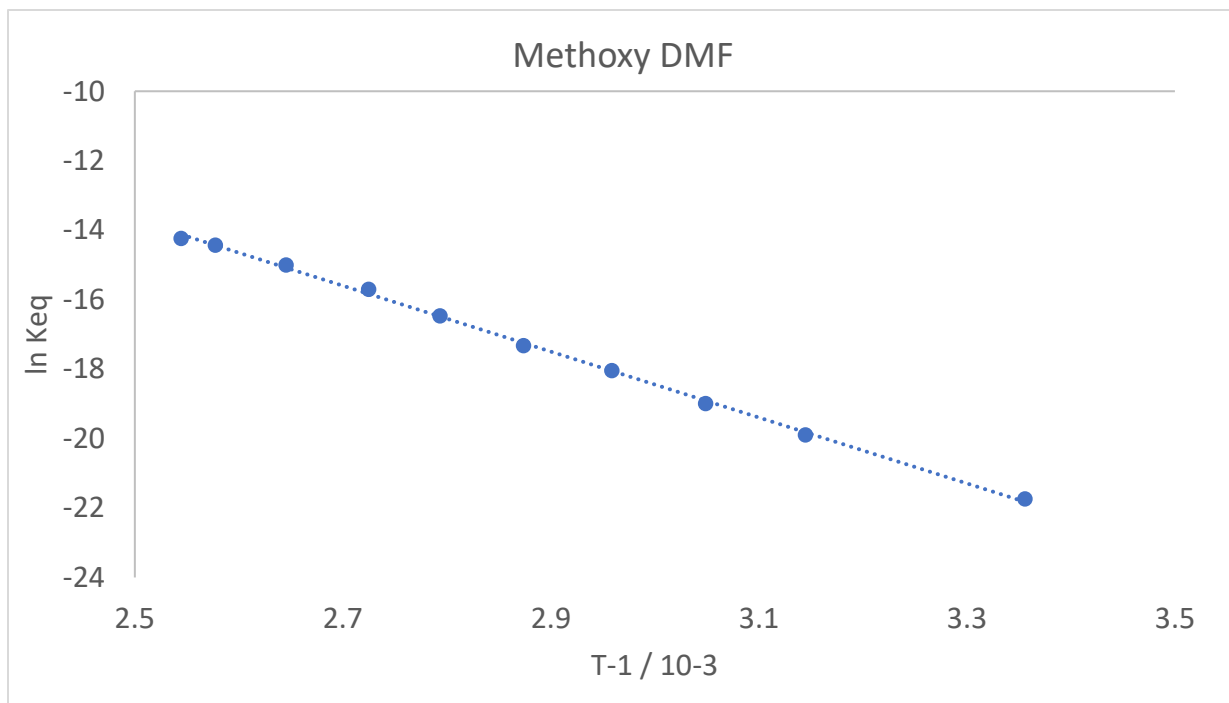
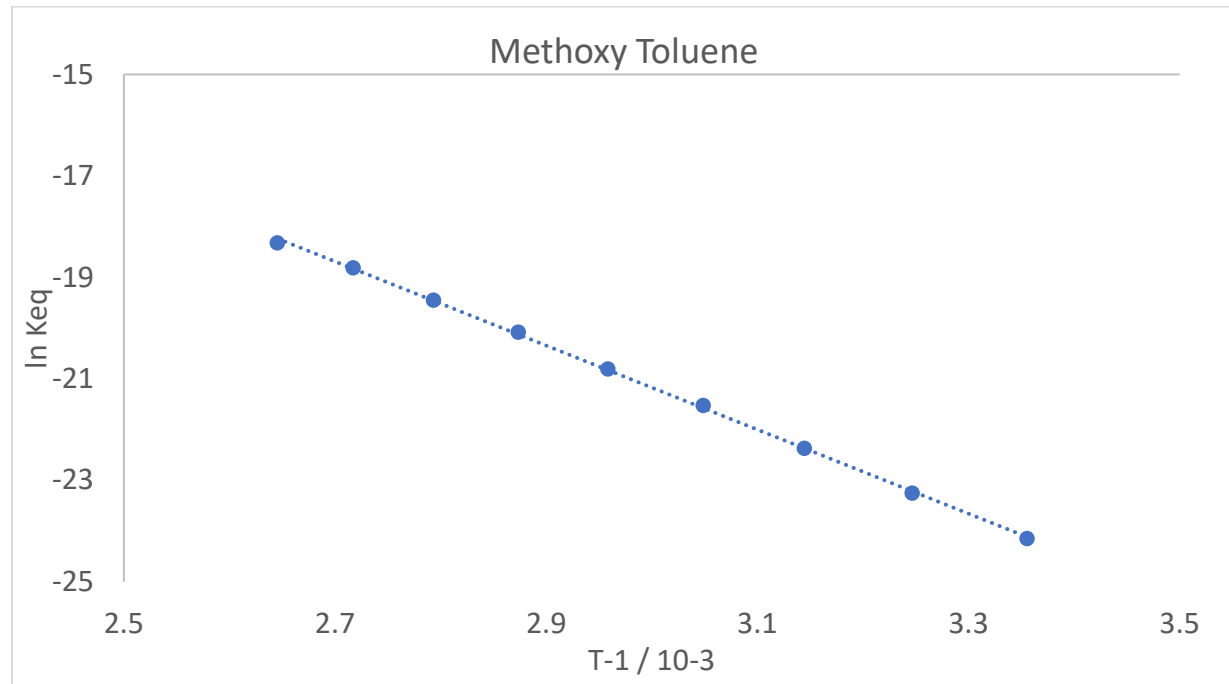
Computationally derived hyperfine coupling values for the NMe₂ radical in different solvents

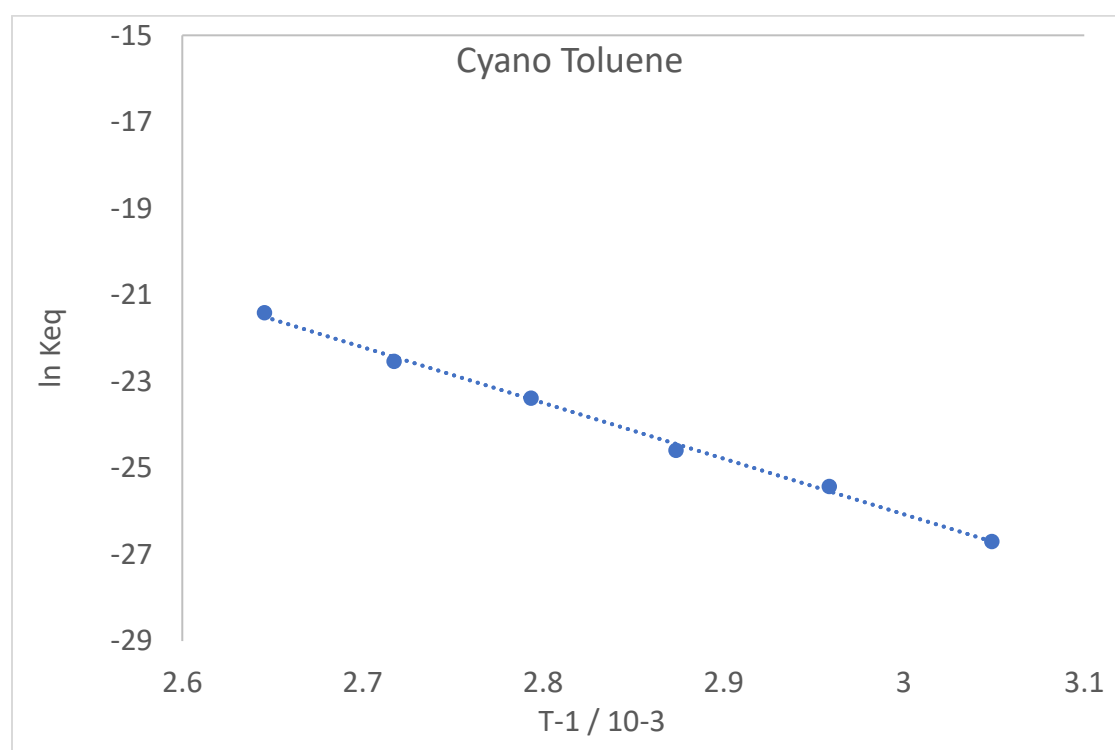
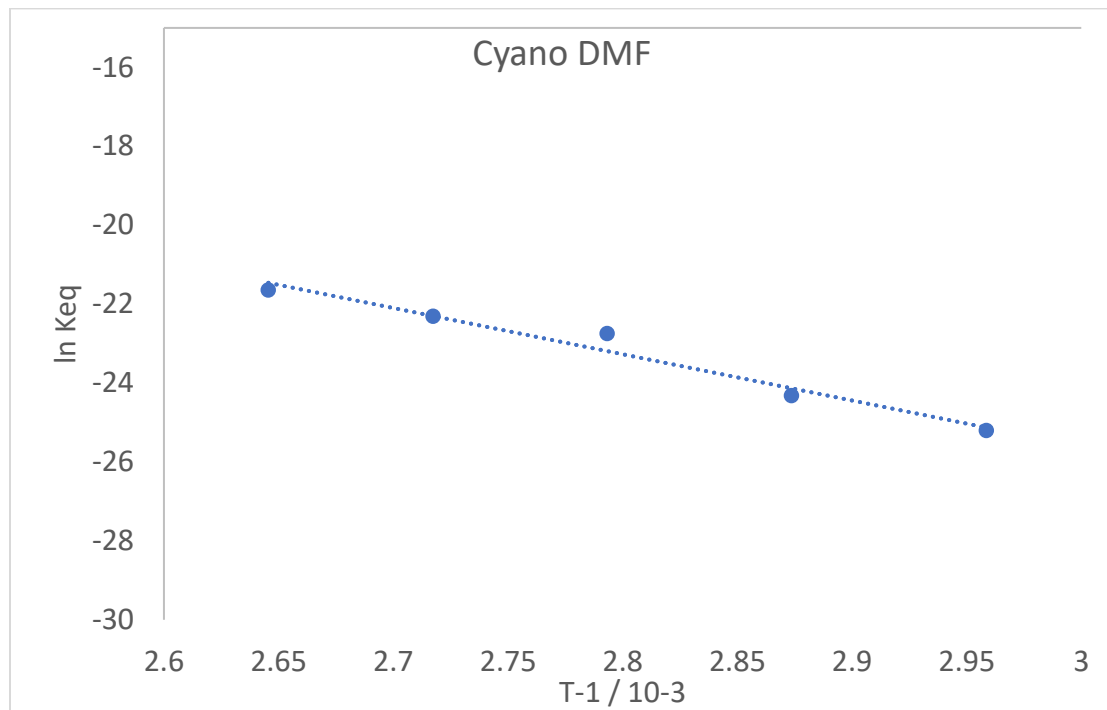
		Toluene	DCM	Acetone
Atom	# Equiv	A value (comp)		
H-1	2	-2.60	-2.04	-1.11
H-1	2	-0.29	-0.92	-1.87
N-14	2	1.41	1.22	1.16
N-14	1	3.17	4.08	4.35
H-1	6	4.40	4.50	4.75
C-13	2	-2.00	-1.02	-0.72
C-13	2	2.06	0.94	0.61
C-13	2	-10.23	-8.65	-8.19
C-13	1	0.84	-0.60	-1.05
C-13	1	-5.04	-3.00	-2.42
C-13	1	11.58	9.23	8.56

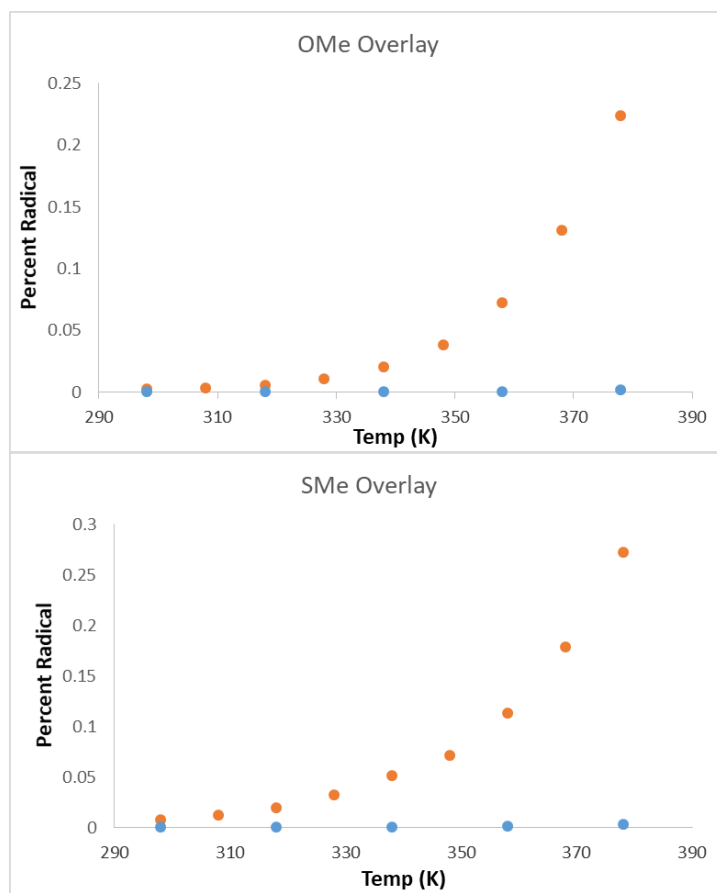
Simulated hyperfine coupling values for the NMe₂ radical in different solvents

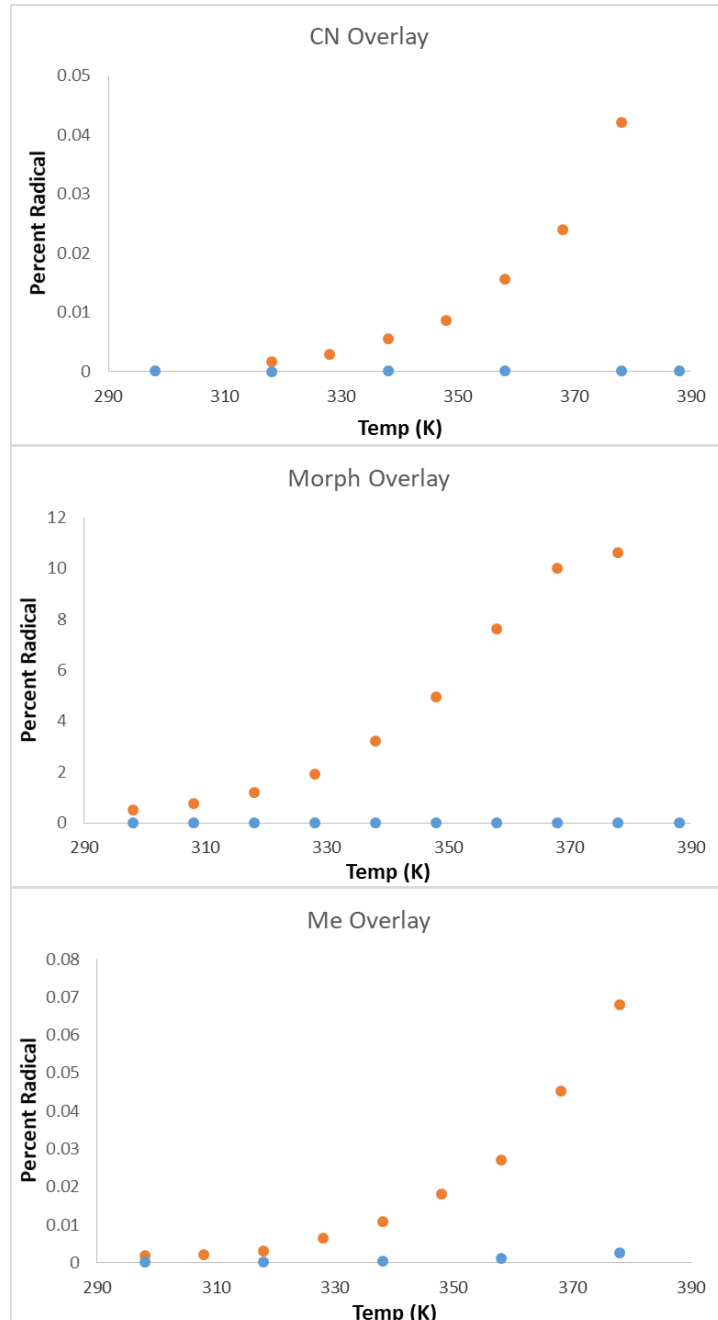
		Toluene	DCM	Acetone
Atom	# Equiv	A value (comp)		
H-1	2	-2.603	-2.050	-1.053
H-1	2	-0.350	-0.942	-1.895
N-14	2	1.401	1.222	1.190
N-14	1	3.222	4.055	4.355
H-1	6	4.422	4.440	5.140
C-13	2	-2.000	-1.020	-0.720
C-13	2	2.060	0.940	0.610
C-13	2	-10.23	-8.650	-8.190
C-13	1	0.840	-0.600	-1.050
C-13	1	-5.040	-3.000	-2.420
C-13	1	11.580	9.230	8.560





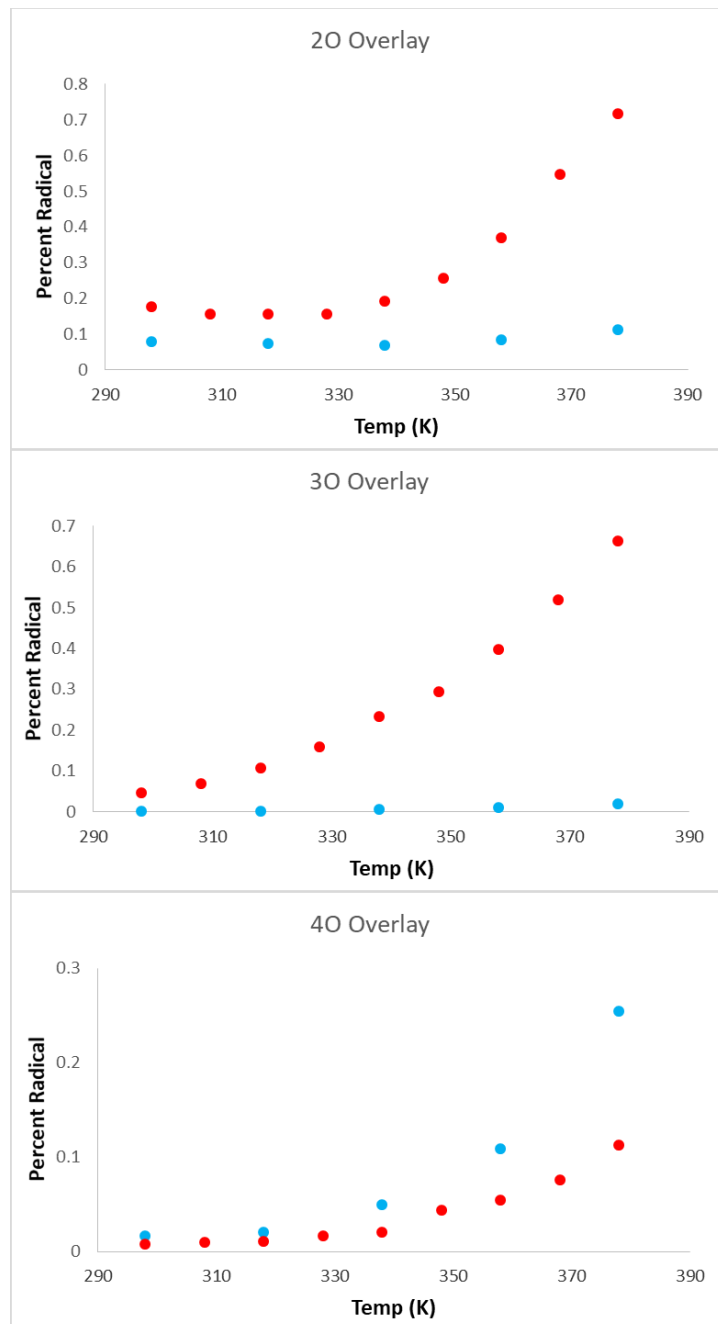


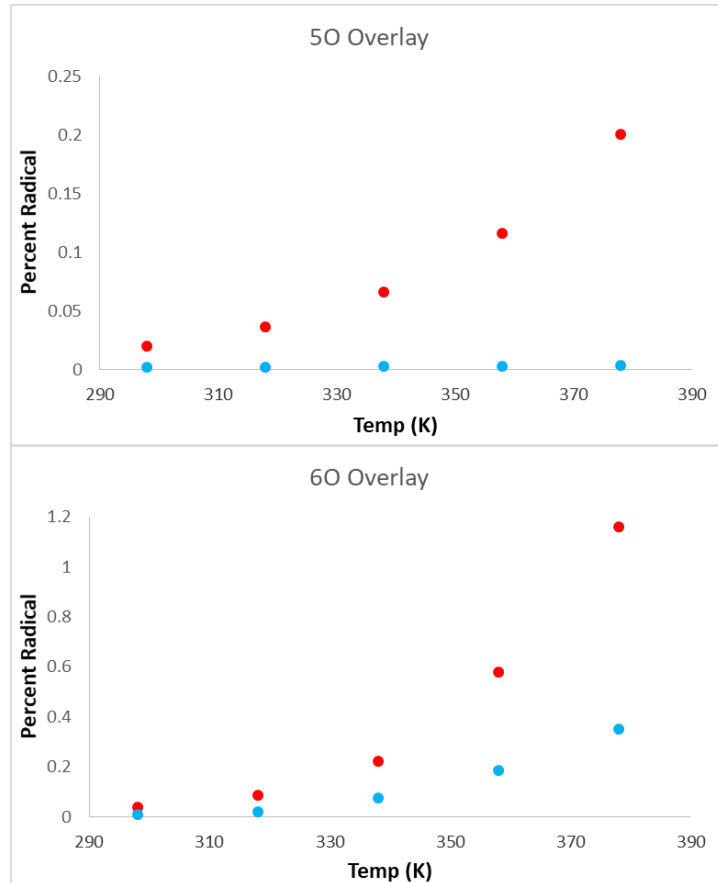
APPENDIX D. SUPPORTING INFORMATION FOR CHAPTER 5**Figure S1: Non-Tethered Dimer Variable Temperature Plots of Solution and Solid-State Samples**



Blue = Solid State
Orange = Solution State

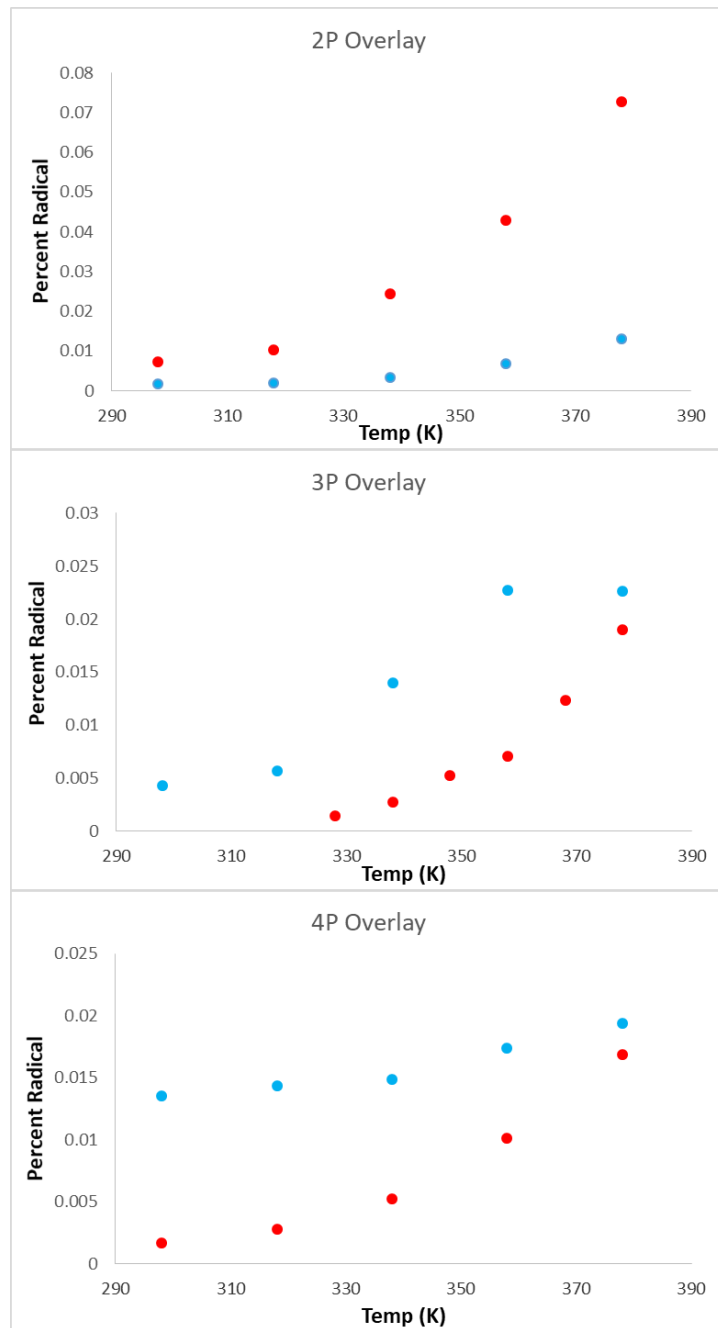
Figure S2: *Ortho* Tethered Dimer Variable Temperature Plots of Solution and Solid-State Samples

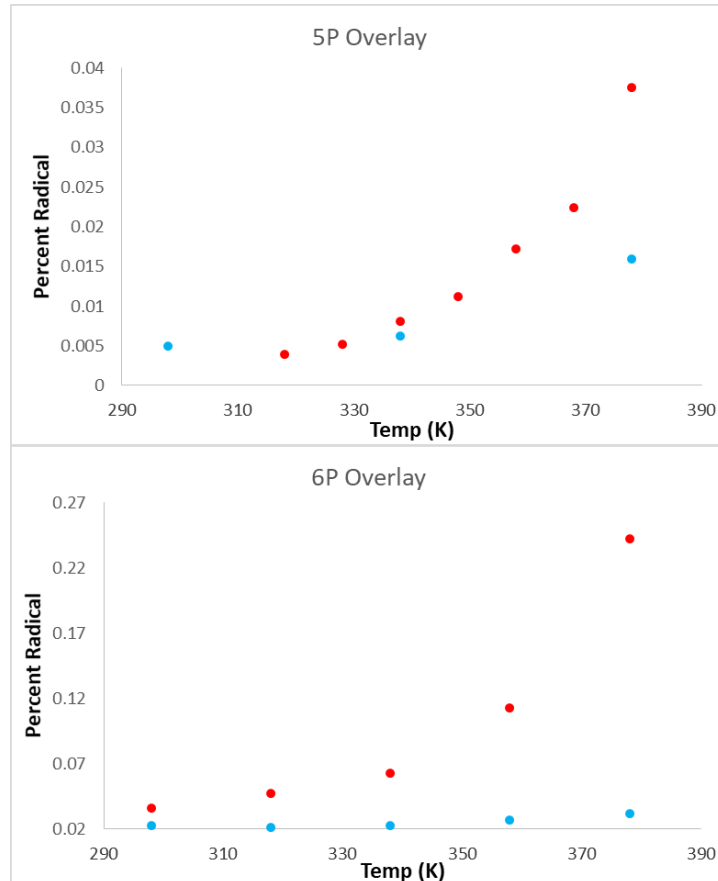




**Blue = Solid State
Red = Solution State**

Figure S3: Para Tethered Dimer Variable Temperature Plots of Solution and Solid-State Samples





Blue = Solid State
Red = Solution State

Figure S4: Plot of Radical Percentage at 398 K for Solid Samples versus the Binding Constant in Solution

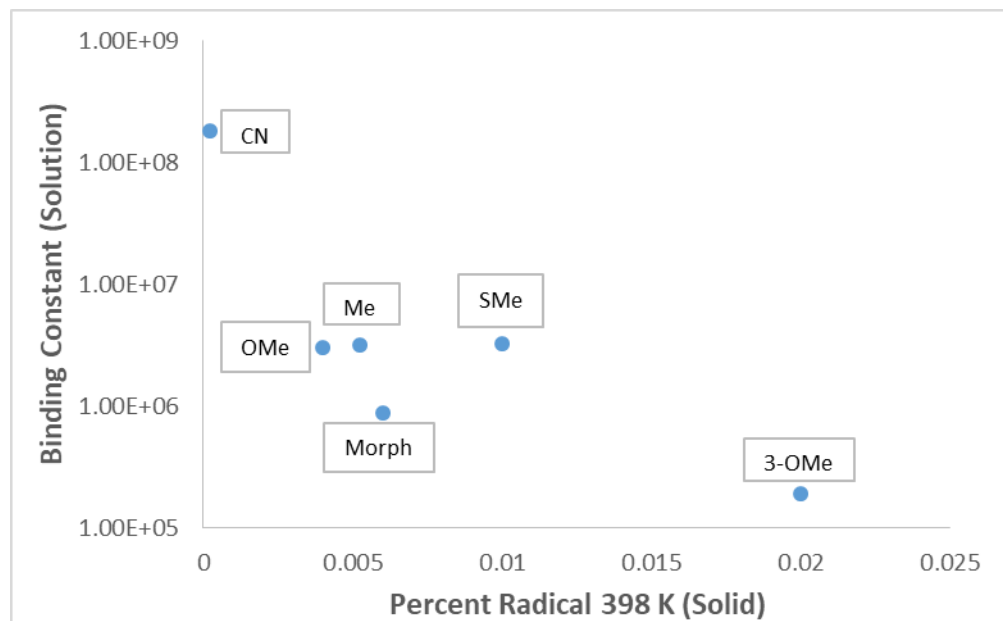
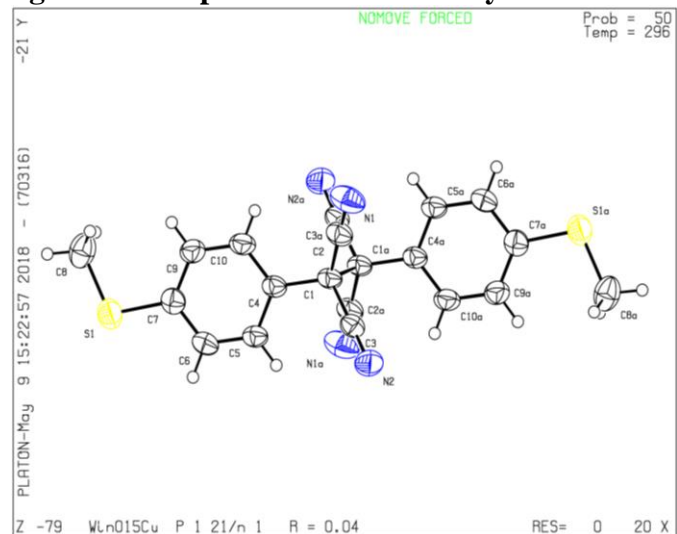


Figure S5: Ellipsoid Plot of SMe Crystal Structure

Crystal Preparation: A 5 mM solution of the compound in toluene solvent was tightly sealed and left to sit in the back of a fume hood for 60 days. Upon checking the sample, enough crystals were formed to both determine the crystal structure and to also perform a single crystal EPR experiment with.

Table 1. Sample and crystal data for Win015_233.

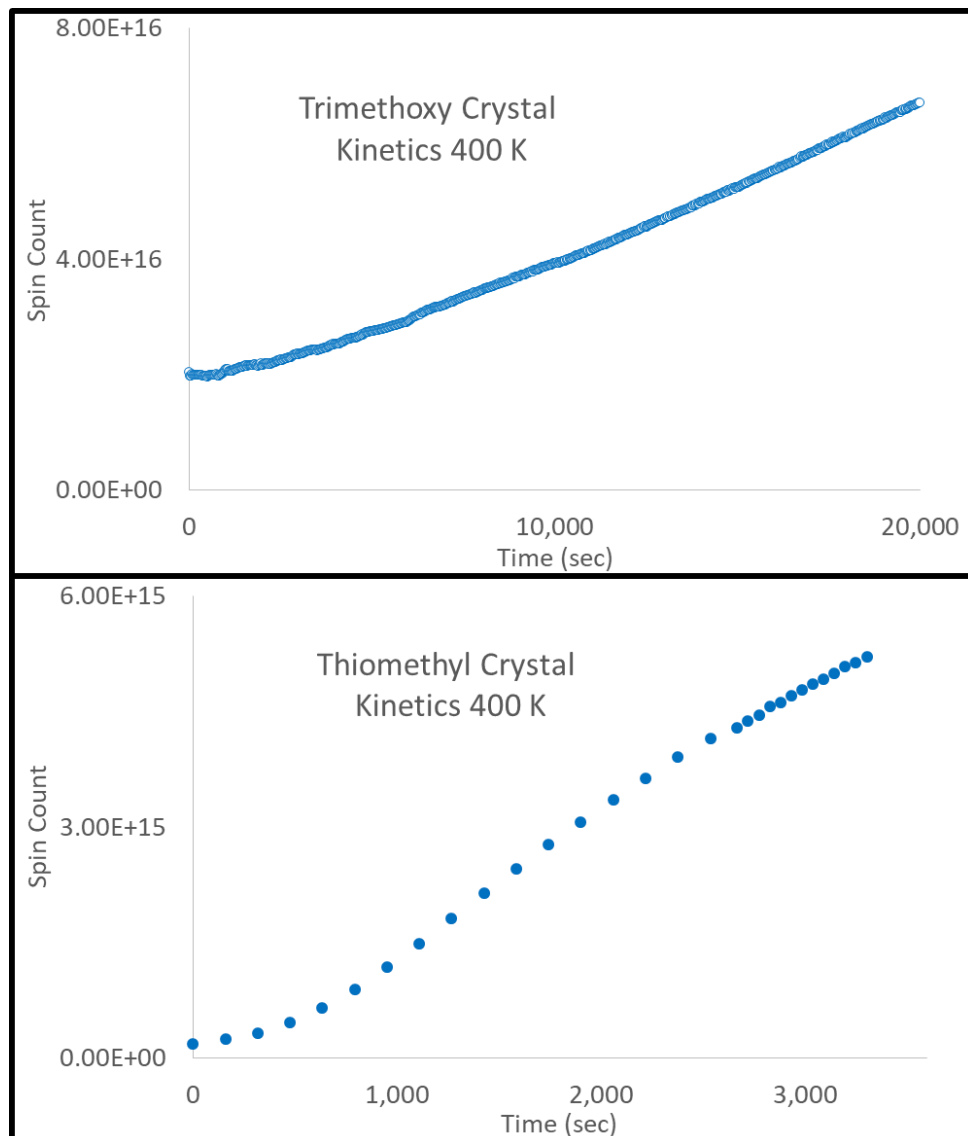
Identification code	Win015_233
Chemical formula	C ₂₀ H ₁₄ N ₄ S ₂
Formula weight	374.47 g/mol
Temperature	233(2) K
Wavelength	1.54184 Å
Crystal size	0.080 x 0.180 x 0.370 mm
Crystal habit	colorless plate
Crystal system	triclinic
Space group	P -1
Unit cell dimensions	a = 7.9861(3) Å α = 91.584(3)° b = 10.4323(4) Å β = 91.221(3)° c = 10.9003(4) Å γ = 93.952(3)°
Volume	905.39(6) Å ³
Z	2
Density (calculated)	1.374 g/cm ³
Absorption coefficient	2.748 mm ⁻¹
F(000)	388

Data collection and structure refinement for Win015_233.

Theta range for data collection	4.06 to 66.93°
Index ranges	-9<=h<=9, -12<=k<=12, -12<=l<=13
Reflections collected	11722
Independent reflections	3142 [R(int) = 0.0398]
Coverage of independent reflections	97.4%
Absorption correction	Multi-Scan
Max. and min.	0.8100 and 0.4300

transmission	
Structure solution technique	direct methods
Structure solution program	XT, VERSION 2014/5
Refinement method	Full-matrix least-squares on F^2
Refinement program	SHELXL-2016/6 (Sheldrick, 2016)
Function minimized	$\sum w(F_o^2 - F_c^2)^2$
Data / restraints / parameters	3142 / 0 / 237
Goodness-of-fit on F^2	1.051
Final R indices	2703 data; $I > 2\sigma(I)$ $R_1 = 0.0478, wR_2 = 0.1302$ all data $R_1 = 0.0534, wR_2 = 0.1367$
Weighting scheme	$w = 1/[\sigma^2(F_o^2) + (0.0970P)^2 + 0.0975P]$ where $P = (F_o^2 + 2F_c^2)/3$
Largest diff. peak and hole	0.586 and -0.253 e \AA^{-3}
R.M.S. deviation from mean	0.074 e \AA^{-3}

Figure S6: Kinetics EPR Plots

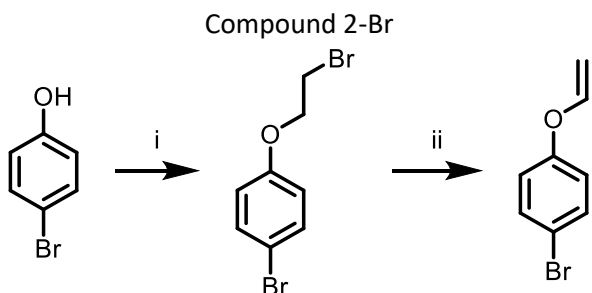


APPENDIX E. SUPPORTING INFORMATION FOR CHAPTER 6

Instrumentation and Chemicals. NMR spectra were acquired using either a Bruker NEO 400, Bruker DRX 500, or Bruker AV III 600. All EPR analysis was performed on a Bruker FT-EPR. UV-Vis spectra were recorded on an Agilent 8453 UV-Vis for room temperature acquisition and a Shimadzu UV 3101 PC for low temperature studies. All reagents were purchased through Oakwood Chemical, which were used without further purification.

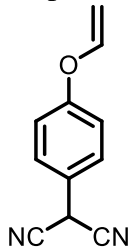
General Cross Coupling Procedure to Make Aryl Malonitriles from Aryl Bromides. To a 2-neck round bottom flask was added NaOtBu (4.4 equiv) and the flask was then sealed under an inert atmosphere. To the sealed flask was added by syringe 10-20 mL purged xylene. Melted malononitrile was then added via a syringe (2.2 equiv) and the reaction was allowed to mix with the xylene solution for 30 min. The aryl bromide (1 equiv) and 10 mol% Pd[(PPh₃)₂Cl₂] were then added to the reaction flask, which was placed under an inert atmosphere over a hot oil bath at 140° C and the reaction was monitored to completion by TLC. Reaction times varied from 15 min to 24 h (indicated for each below), depending on the aryl bromide. To work up the reaction, the reaction vessel was allowed to cool to room temperature with continued stirring. An equal portion of ethyl acetate and water (20-30 mL each) was added to the reaction vessel and the pH of the solution was brought to ~7 using a 10% HCl solution. The resulting mixture was extracted with water (3 x 50 mL) and then a final time with brine solution (50 mL). The organic solvent was dried with Na₂SO₄ and removed under reduced pressure and placed under vacuum until the product was dry. The final aryl malononitrile was purified with flash chromatography (80:20 Hexanes:EtOAc).

Procedures to synthesize each compounds aryl bromide are contained below with modified cross coupling procedure where necessary to generate the final aryl malononitriles.



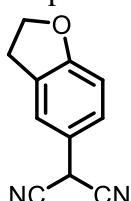
i. Dibromoethane (100 g) was added to a solution of 4-bromophenol (20 g) and K₂CO₃ (35 g) in acetone (200 mL) and refluxed overnight. The solvent was removed under reduced pressure and the crude mixture was extracted with water to remove inorganics, and 18 grams of product was recovered (53%). ii. The haloether (5.0 g) was added to a solution of NaOtBu (2.7 g) in THF (15 mL) and stirred overnight. The reaction mixture was filtered, and the organic solvent was removed by vacuum filtration. The allyloxy aryl bromide was purified by column chromatography (80:20 hexanes:ethyl acetate) to yield 2.8 g 2-Br (79%).

Compound 2



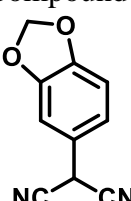
Compound 2 was synthesized from 2-Br using the general cross coupling procedure and a reaction time of 24 h (54%). ¹H NMR (400 MHz, CDCl₃) δ 7.46 (d, 2H); 7.11 (d, 2H); 6.63 (dd, 1H); 5.03 (s, 1H), 4.88 (dd, 1H); 4.58 (dd, 1H). ¹³C NMR (400 MHz, CDCl₃) δ 158.4, 147.0, 129.0, 120.5, 118.3, 111.9, 97.5, 27.7. HRMS (ESI-TOF) m/z calcd for C₁₁H₈N₂O 183.0564, found 183.0565 [M - H].

Compound 4

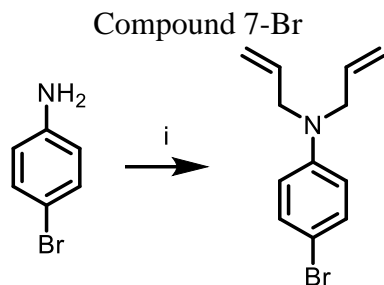


Compound 4 was synthesized following the general cross coupling procedure from the purchased aryl bromide after 8 h (55 %). ¹H NMR (400 MHz, CDCl₃) δ 7.32 (s, 1H); 7.20 (d, 1H); 6.84 (d, 1H); 4.96 (s, 1H); 4.65 (t, 2H); 3.27 (t, 2H). ¹³C NMR (400 MHz, CDCl₃) δ 161.9, 129.7, 127.7, 124.1, 117.8, 112.3, 110.6, 72.0, 29.6, 27.8. HRMS (ESI-TOF) m/z calcd for C₁₁H₈N₂O 183.0562, found 183.0564 [M - H].

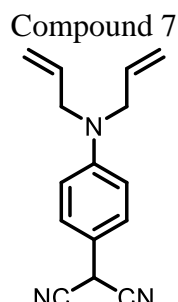
Compound 5



Compound 5 was synthesized following the general cross coupling procedure from the purchased aryl bromide after 8 h (31%). ¹H NMR (500 MHz, CDCl₃) δ 6.96 (d, 1H); 6.95 (s, 1H); 6.88 (d, 1H); 6.06 (s, 2H); 4.95 (s, 1H). ¹³C NMR (500 MHz, CDCl₃) δ 149.6, 149.3, 121.4, 119.5, 111.9, 109.4, 107.6, 102.3, 27.9. HRMS (ESI-TOF) m/z calcd for C₁₀H₆N₂O₂ 185.0357, found 185.0355 [M - H].

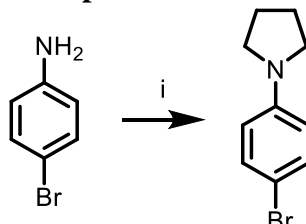


4-bromoaniline (5.1 g, 1 equiv) was dissolved in an 80:20 EtOH:Water solution with Na₂CO₃ (3.2 g, 4 equiv). After mixing for 10 min, allyl bromide (8.2 g, 4 equiv) was slowly added and the reaction was heated at 80 °C for 24 h. The reaction was worked up by extraction with dichloromethane and removal of solvent to yield 6.7 g 7-Br (89%). No further purification was conducted prior to the cross-coupling reaction.



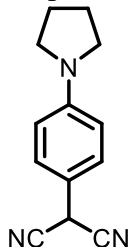
Compound 7 was synthesized from 7-Br following the general cross coupling procedure for 1 h (29%). ¹H NMR (600 MHz, CDCl₃) δ 7.28 (d, 2H); 6.75 (d, 2H); 5.87 (m, 2H); 5.23 (d, 2H); 5.20 (d, 2H); 4.97 (s, 1H); 3.98 (d, 4H). ¹³C NMR (600 MHz, CDCl₃) δ 149.8, 132.9, 128.2, 116.4, 112.9, 112.5, 112.4, 52.8, 27.4. HRMS (ESI-TOF) m/z calcd for C₁₅H₁₅N₃ 236.1193, found 236.1194 [M - H].

Compound 8-Br



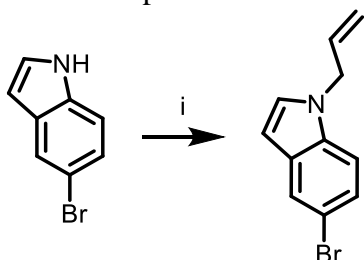
4-bromoaniline (4.3 g, 1 equiv) was added to a round bottom flask with K₂CO₃ (3.8 g, 3 equiv) in 25 mL DMF. After mixing for 10 min, 1,4-dibromobutane (3.3 mL, 1.1 equiv) was added to the reaction flask and allowed to react at 80° C overnight. The resulting solution was diluted with 100 mL water and acidified with HCl to a neutral pH. 3 extractions were performed with dichloromethane and the organics were combined, dried with Na₂SO₄, and solvent removed under reduced pressure. The crude product was purified by column chromatography (eluent 90:10 hexanes:ethyl acetate) to yield 3.8 g 8-Br (67%).

Compound 8



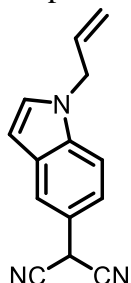
Compound 8 was synthesized from 8-Br following the general cross coupling procedure for 15 min (20%). In our hands, this compound auto-oxidized to the radical as it formed, so a quick reaction and resulting work-up minimizes auto-oxidation and possible decomposition.¹H NMR (400 MHz, CDCl₃) δ 7.27 (d, 2H); 6.57 (d, 2H); 4.93 (s, 1H); 3.30 (t, 4H); 2.03 (t, 4H). ¹³C NMR (400 MHz, CDCl₃) δ 148.9, 128.3, 112.7, 112.4, 111.4, 47.7, 27.7, 25.6. HRMS (ESI-TOF) m/z calcd for C₁₃H₁₃N₃ 210.1037, found 210.1040 [M - H].

Compound 9-Br



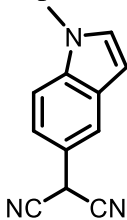
5-bromo-1H-indole (2.0 g, 1 equiv) was added to a round bottom flask with KOH (0.7 g) and allyl bromide (1.5 g) and 25 mL DMF as solvent. The reaction was carried out at 50°C overnight and work up consisted of extraction between dichloromethane and water (3 x 50 mL). The crude product was purified by column chromatography (90:10 hexanes:ethyl acetate) to yield 0.5 g 9-Br (21%).

Compound 9



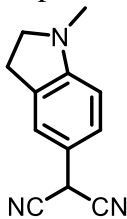
Compound 9 was synthesized from 9-Br following the general cross coupling procedure for 12 h (52 %).¹H NMR (400 MHz, CDCl₃) δ 7.75 (s, 1H); 7.41 (d, 1H); 7.23 (dd, 1H); 6.59 (d, 1H); 6.00 (m, 1H); 5.25 (d, 1H); 5.13 (s, 1H); 5.08 (d, 1H); 4.76 (dd, 1H). ¹³C NMR (400 MHz, CDCl₃) δ 136.4, 132.8, 130.1, 129.2, 120.3, 120.0, 117.7, 117.1, 112.7, 111.3, 102.0, 49.1, 28.3. HRMS (ESI-TOF) m/z calcd for C₁₄H₁₂N₃ 222.1026, found 222.1026 [M + H].

Compound 10



Compound 10 was synthesized following the general cross coupling procedure from the purchased aryl bromide after 16 h (29%). ^1H NMR (400 MHz, CDCl_3) δ 7.75 (d, 1H); 7.42 (d, 1H); 7.28 (dd, 1H); 7.17 (d, 1H); 6.55 (dd, 1H); 5.14 (s, 1H); 3.84 (s, 3H). ^{13}C NMR (400 MHz, CDCl_3) δ 137.2, 131.1, 129.2, 120.3, 120.1, 117.0, 112.7, 111.0, 101.7, 33.2, 28.5. HRMS (ESI-TOF) m/z calcd for $\text{C}_{12}\text{H}_9\text{N}_3$ 196.0869, found 196.0869 [M + H].

Compound 11



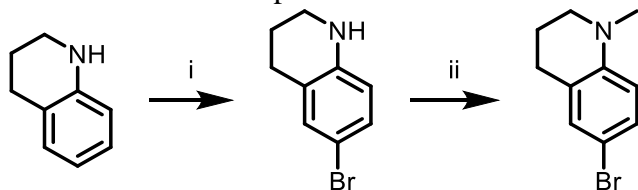
Compound 11 was synthesized by reduction of compound 10. To a solution of compound 10 (60 mg) in neat acetic acid (5 mL) was added NaBH_3CN (100 mg) and reacted for 3 h at room temperature. The reaction mixture was diluted with water and extracted with dichloromethane (3 x 25 mL). The resulting organic portions were combined and solvent was removed to yield crude compound 11, which was purified by flash chromatography with 80:20 hexanes:ethyl acetate to give 42 mg 11 (70 %).

^1H NMR (600 MHz, CDCl_3) δ 7.13 (m, 2H); 6.43 (d, 1H); 4.90 (s, 1H); 3.42 (t, 2H); 3.00 (t, 2H); 2.79 (s, 3H)

^{13}C NMR (600 MHz, CDCl_3) δ 154.9, 132.4, 127.2, 123.1, 113.9, 112.7, 106.9, 55.8, 35.4, 28.4, 27.9

HRMS (ESI-TOF) m/z calcd for $\text{C}_{12}\text{H}_{11}\text{N}_3$ 196.0880, found 196.0884 [M - H].

Compound 12-Br

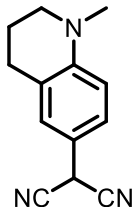


i: Tetrahydroquinoline (3.0 g, 1 equiv) was added to 60 mL acetonitrile and cooled to 0°C in an ice bath. To this cooled solution was added N-bromosuccinimide (4.0 g) and reacted for 3 h. Then, solvent was removed under reduced pressure and the resulting crude product was extracted between dichloromethane and water and the brominated product was used without further purification.

ii: The brominated THQ (3.0 g) was dissolved in 50 mL THF. NaH (0.6 g) was added to the

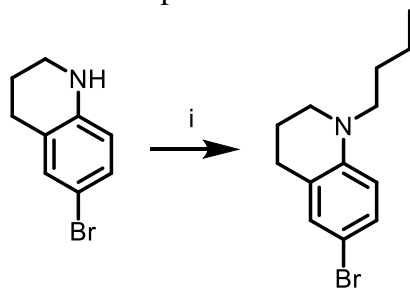
solution slowly and methyl iodide (4.0 g) was added over 15 min and left to react for 18 h. After quenching with water and extracting with dichloromethane, the product was purified by flash chromatography (80:20 hexanes:ethyl acetate) to give 2.0 g 12-Br (61%).

Compound 12



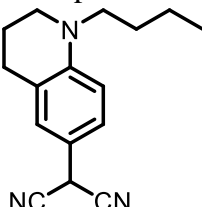
Compound 12 was synthesized following the general cross coupling procedure from compound 12-Br and reacted for 1 h (16 %). ^1H NMR (400 MHz, CDCl_3) δ 7.12 (d, 1H); 7.01 (s, 1H); 6.58 (d, 1H); 4.88 (s, 1H); 3.30 (t, 2H); 2.92, (s, 3H); 2.78 (t, 2H); 1.98 (p, 2H). ^{13}C NMR (400 MHz, CDCl_3) δ 130.5, 130.2, 127.5, 127.3, 126.3, 112.6, 111.5, 51.1, 39.1, 27.9, 27.6, 21.8. HRMS (ESI-TOF) m/z calcd for $\text{C}_{13}\text{H}_{13}\text{N}_3$ 210.1037, found 210.1021 [M - H].

Compound 13-Br



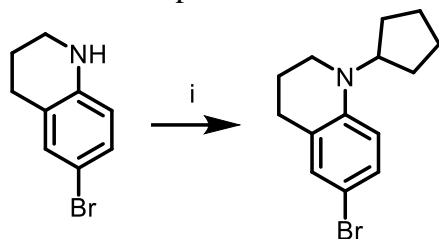
i: The brominated tetrahydroquinoline (1.0 g) was dissolved in 50 mL EtOH with DIPEA (1.35 g, 2.2 equiv) and K_2CO_3 (2.0 g). 1-bromobutane (1.3 g) was slowly added and left to react at 80° C overnight. The reaction mixture was extracted between dichloromethane (3 x 50 mL) and after solvent removal column chromatography was performed (90:10 hexanes:ethyl acetate) to isolate 0.43 g 13-Br (34%).

Compound 13



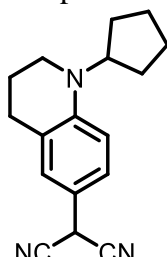
Compound 13 was synthesized following the general cross coupling procedure with a reaction time of 1 h (44 %). ^1H NMR (400 MHz, CDCl_3) δ 7.07 (d, 1H); 6.98 (s, 1H); 6.55 (d, 1H); 4.87 (s, 1H); 3.32 (t, 2H); 3.26 (t, 2H); 1.94 (p, 2H); 1.57 (p, 2H); 1.35 (p, 2H); 0.97 (t, 3H). ^{13}C NMR (400 MHz, CDCl_3) δ 146.6, 127.8, 126.2, 123.5, 112.7, 111.0, 110.8, 51.2, 49.5, 28.3, 28.2, 27.6, 21.7, 20.5, 14.1. HRMS (ESI-TOF) m/z calcd for $\text{C}_{16}\text{H}_{20}\text{N}_3$ 254.1652, found 254.1653 [M + H].

Compound 14-Br



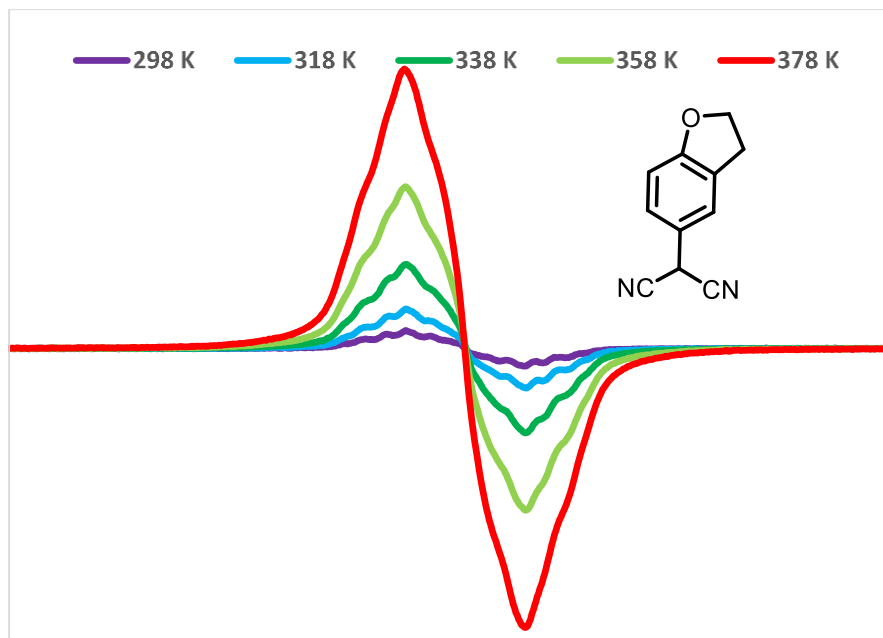
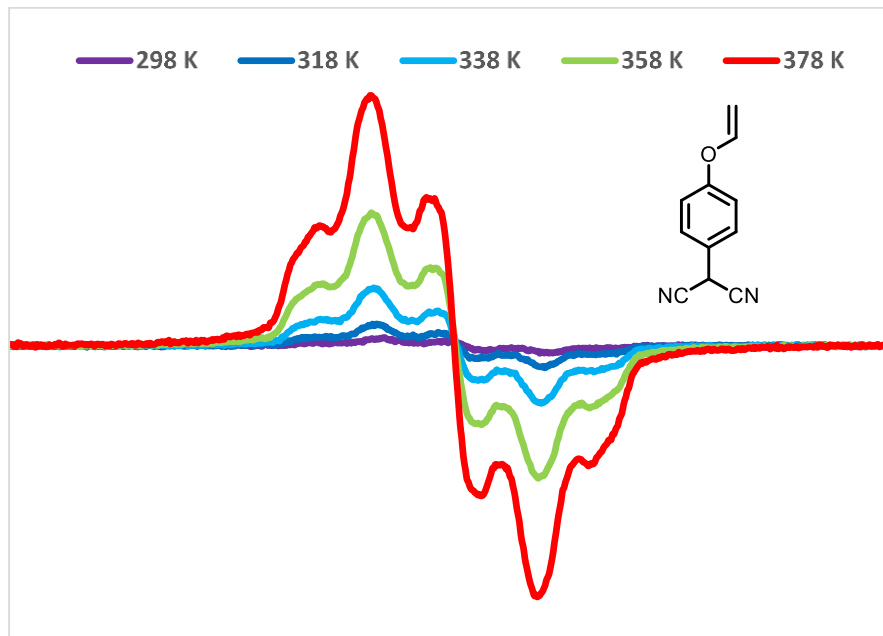
i: The brominated product (1.0 g) was dissolved in methanol (15 mL) and 0.5 mL of conc HCl was added, cyclopentanone (0.44 g, 1 equiv), InCl_3 (0.5 g, 0.5 equiv), and Et_3SiH (1.1 g, 2 equiv). The reaction was heated at 50° C for 72 h, then cooled and extracted between dichloromethane and water, the crude product was purified by column chromatography (90:10 hexanes:ethyl acetate) to yield 14-Br (0.7 g, 54%), which was used without further purification.

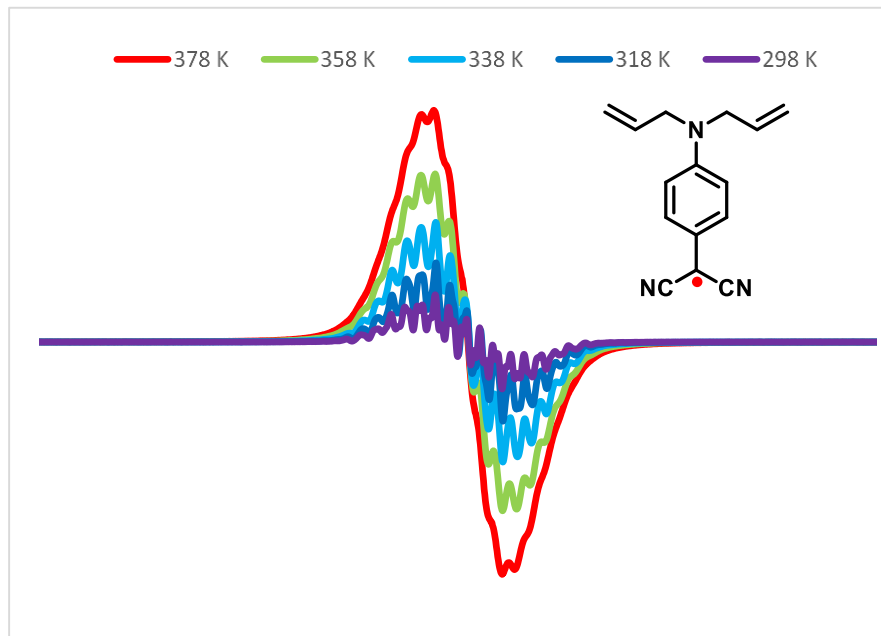
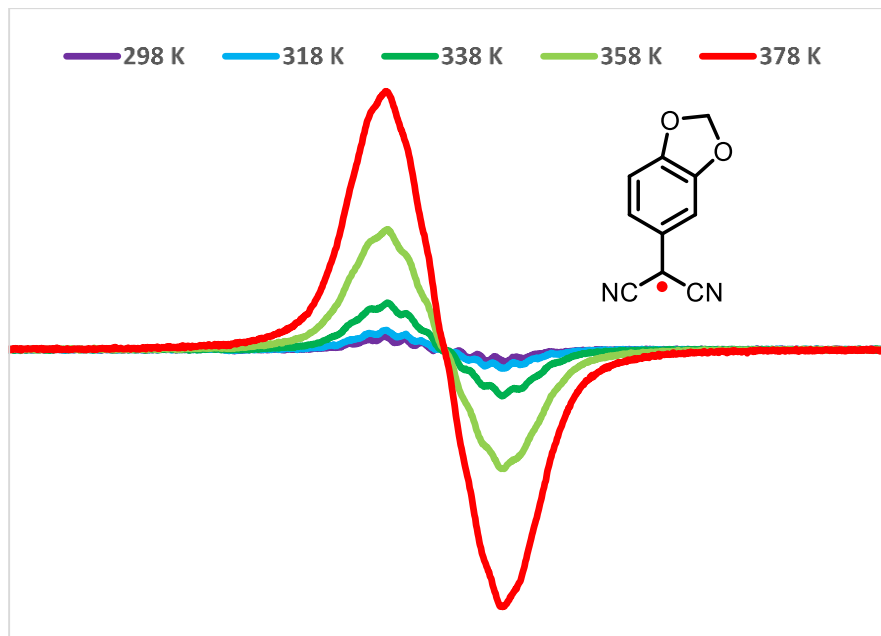
Compound 14

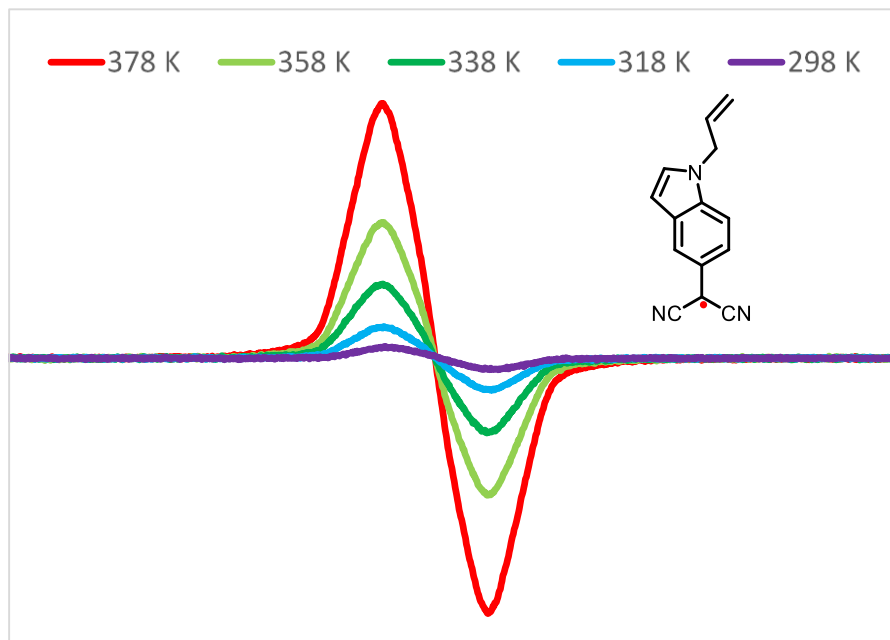
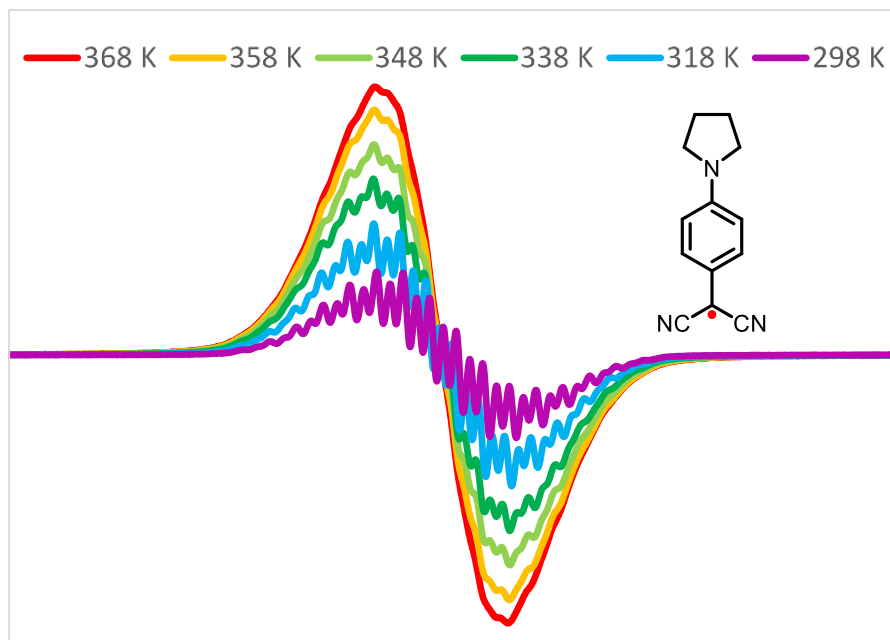


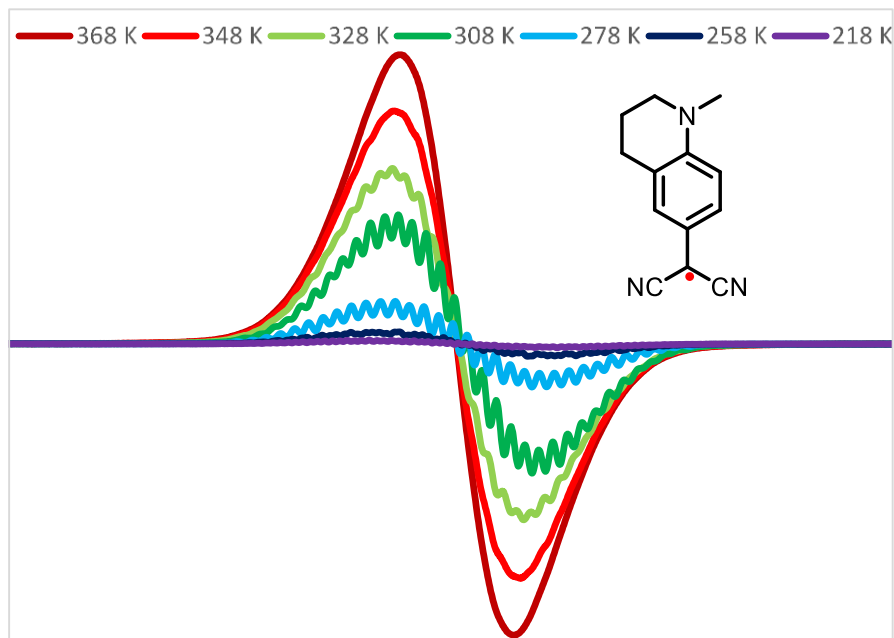
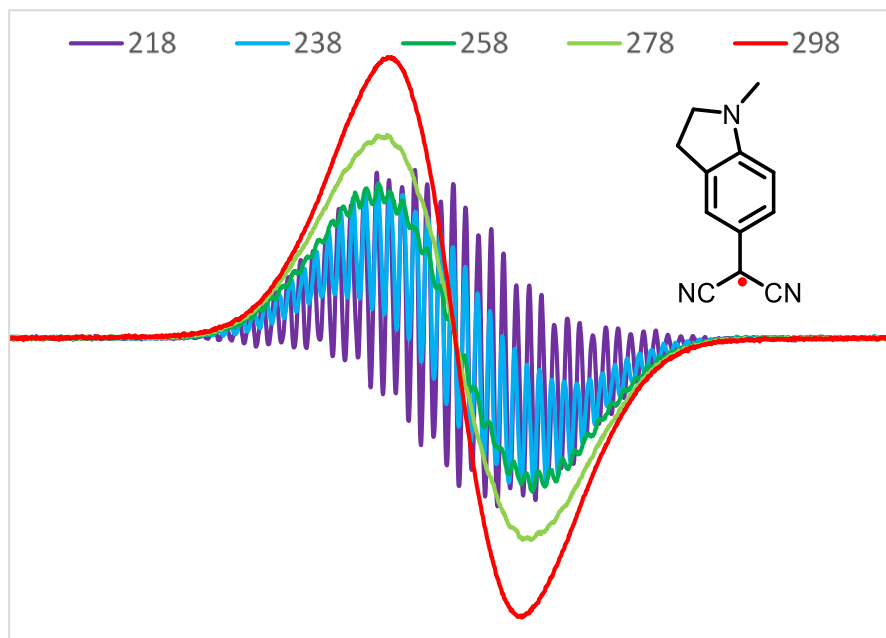
Compound 14 was synthesized following the general cross coupling procedure from 14-Br. Reaction time was 30 min (42%). ^1H NMR (500 MHz, CDCl_3) δ 7.08 (d, 1H); 6.99 (s, 1H); 6.71 (d, 1H); 4.87 (s, 1H); 4.15 (p, 1H); 3.23 (t, 2H); 2.74 (t, 2H); 1.88-1.93 (m, 4H); 1.58-1.78 (m, 6H). ^{13}C NMR (500 MHz, CDCl_3) δ 147.5, 127.6, 126.2, 124.6, 112.7, 111.5, 111.1, 58.8, 42.2, 28.5, 28.2, 27.5, 24.2, 22.1. HRMS (ESI-TOF) m/z calcd for $\text{C}_{17}\text{H}_{20}\text{N}_3$ 266.1652, found 266.1655 [M + H].

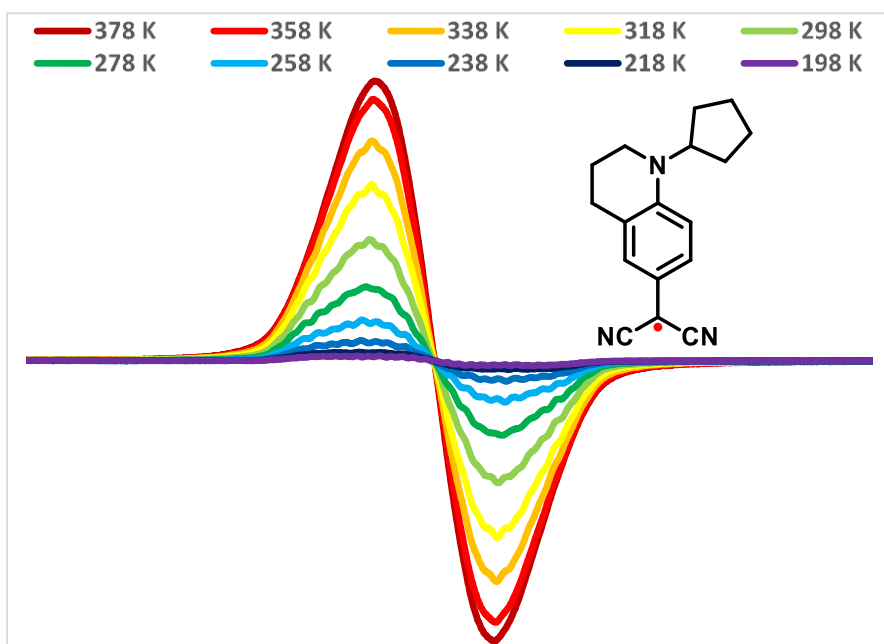
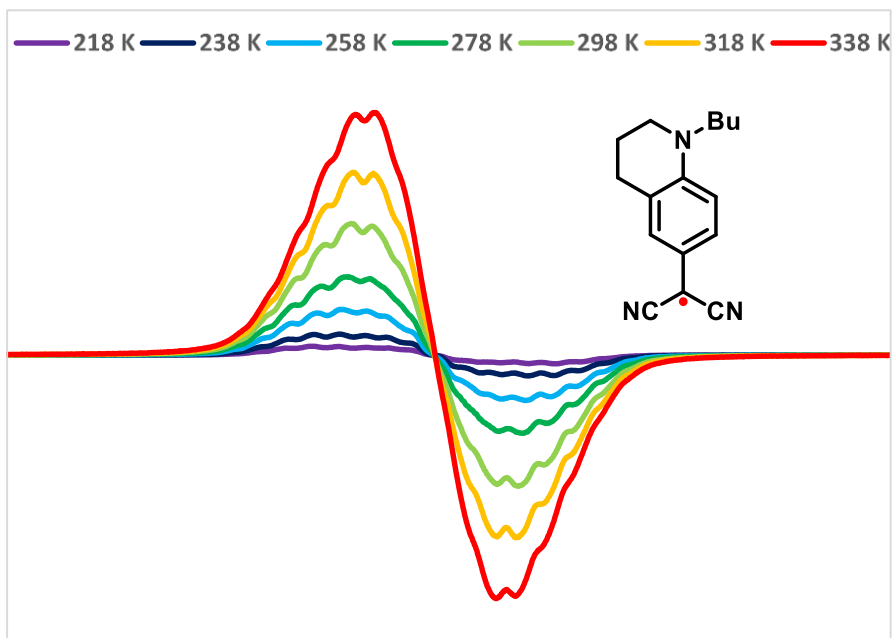
EPR Spectra









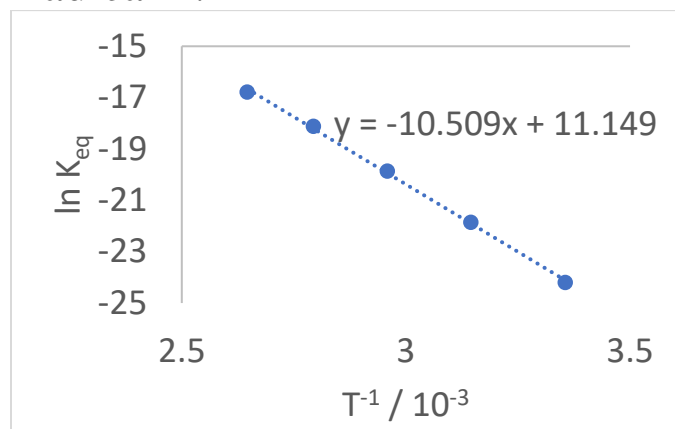


Generation of Van 't Hoff Plots:

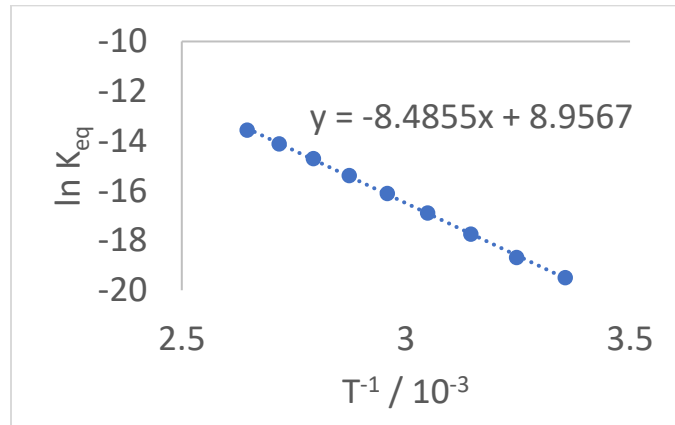
The van'T Hoff plots were made from a variable temperature EPR study. For a given radical, the double integration of each EPR spectrum provides the radical concentration at each temperature, which gives the equilibrium constant assuming a simple equilibrium between radical and dimer. This method is blind to the dimerization mode and simply gives an equilibrium between EPR silent and EPR active species. A plot of $\ln K_{eq}$ versus $T^{-1} / 10^{-3}$ gives the Van 't Hoff plot for each radical, from which the slope and intercept provide the ΔH and ΔS values, which can then be used to find ΔG and K_a .

Van 't Hoff plots for all new radicals:

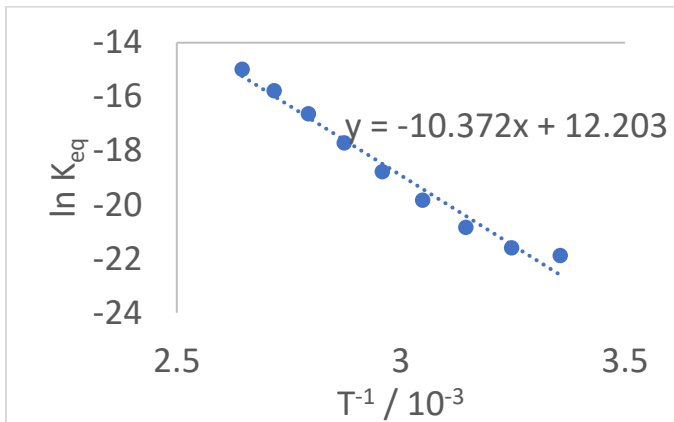
Radical 2:



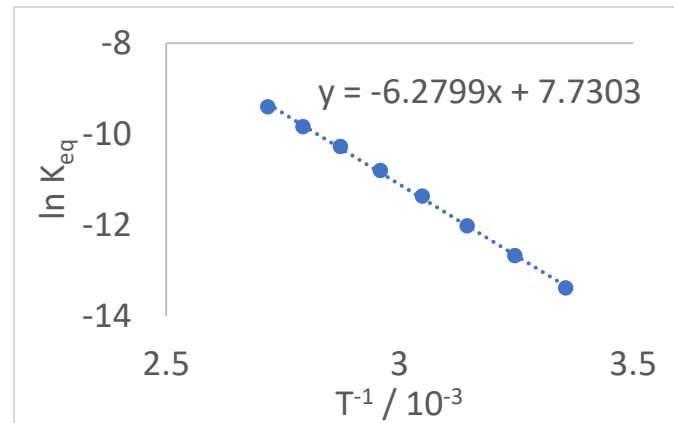
Radical 4:



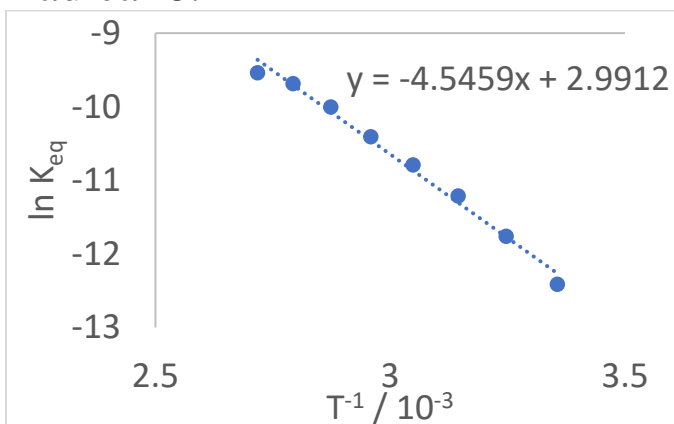
Radical 5:



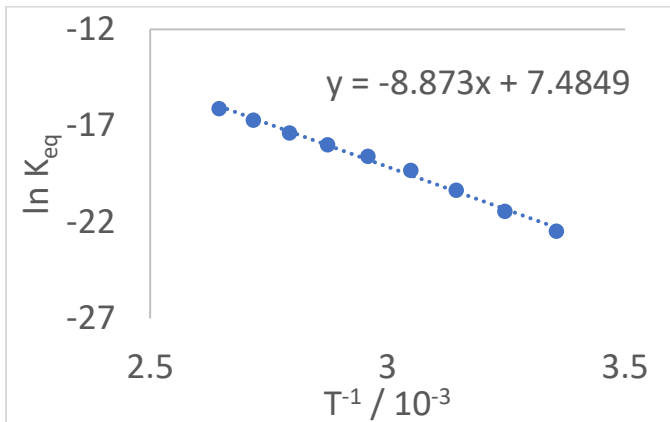
Radical 7:



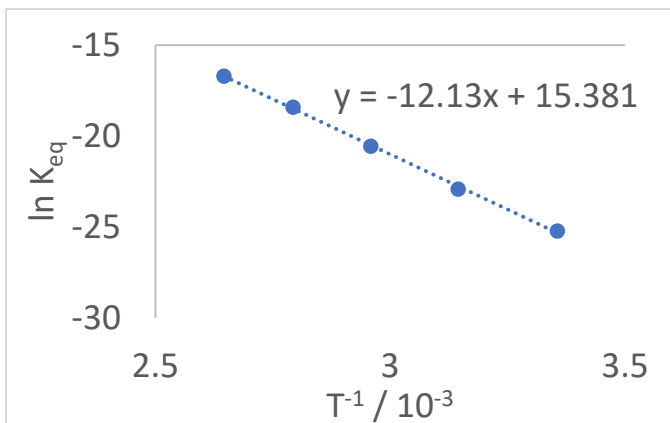
Radical 8:



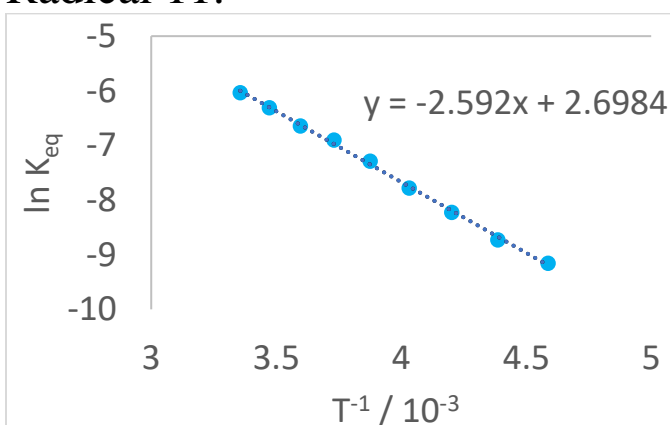
Radical 9:



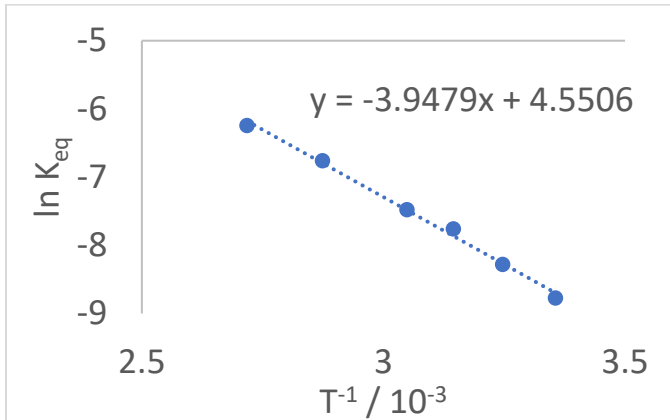
Radical 10:



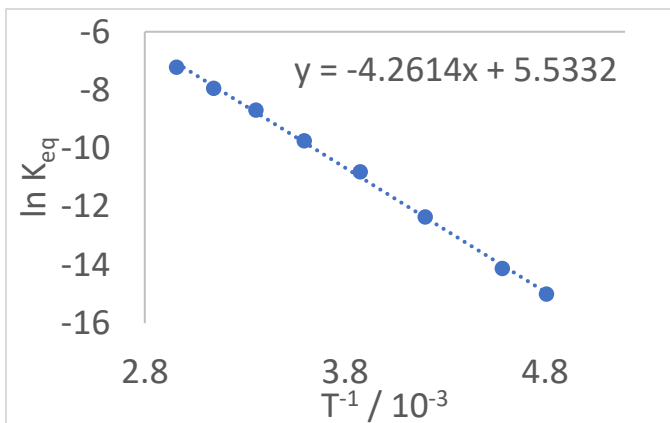
Radical 11:



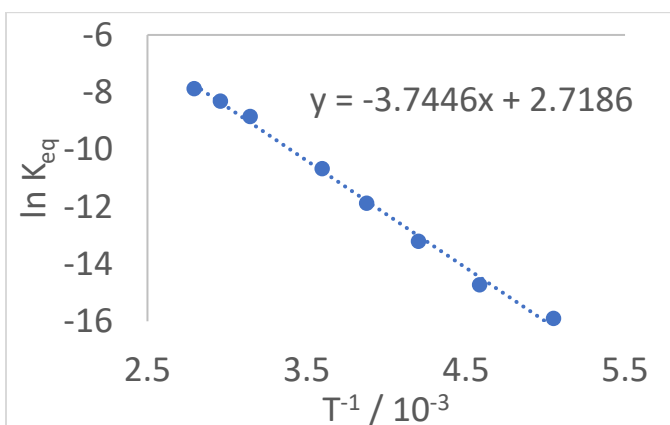
Radical 12:



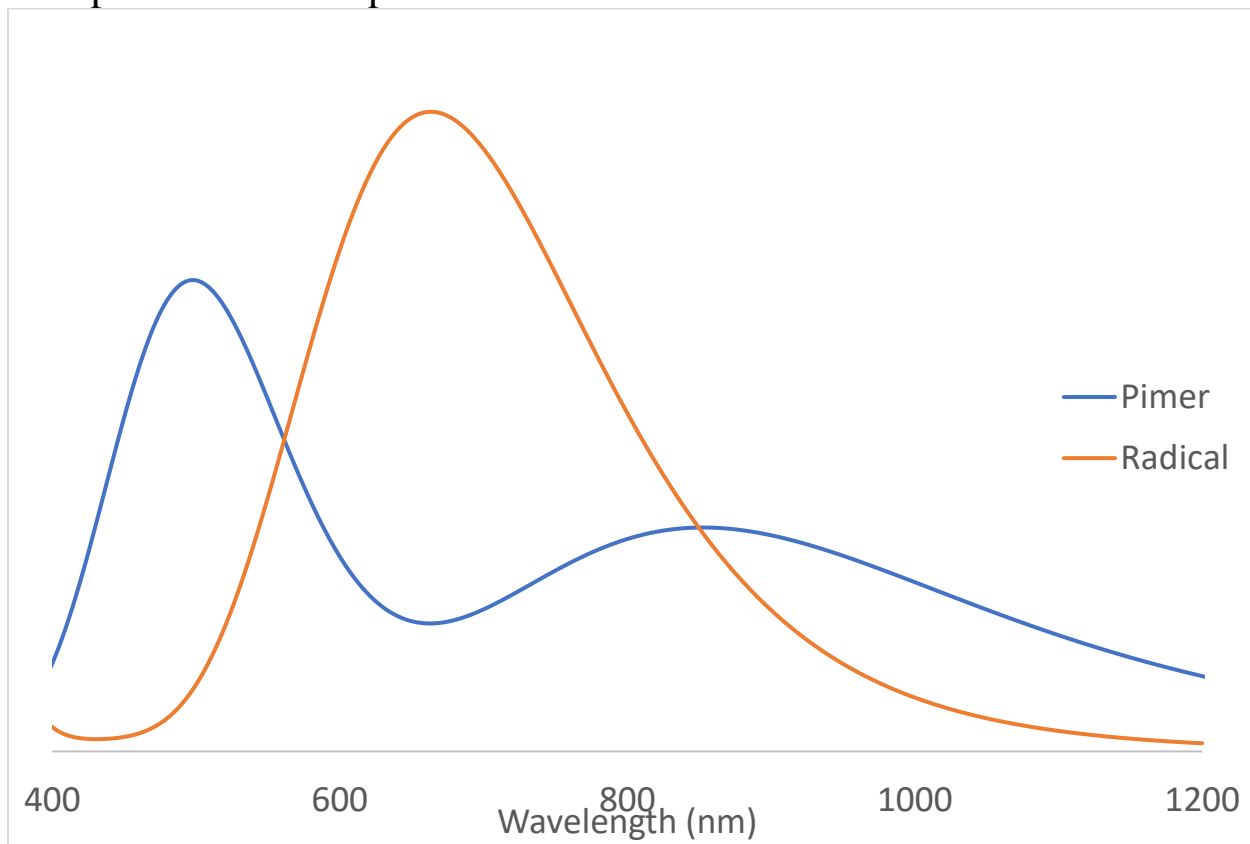
Radical 13:



Radical 14:



Computed TDDFT Spectra



TD-DFT computed absorption spectra for Radical 12 and pimer using TD-B3LYP/6-31+G(d,p)

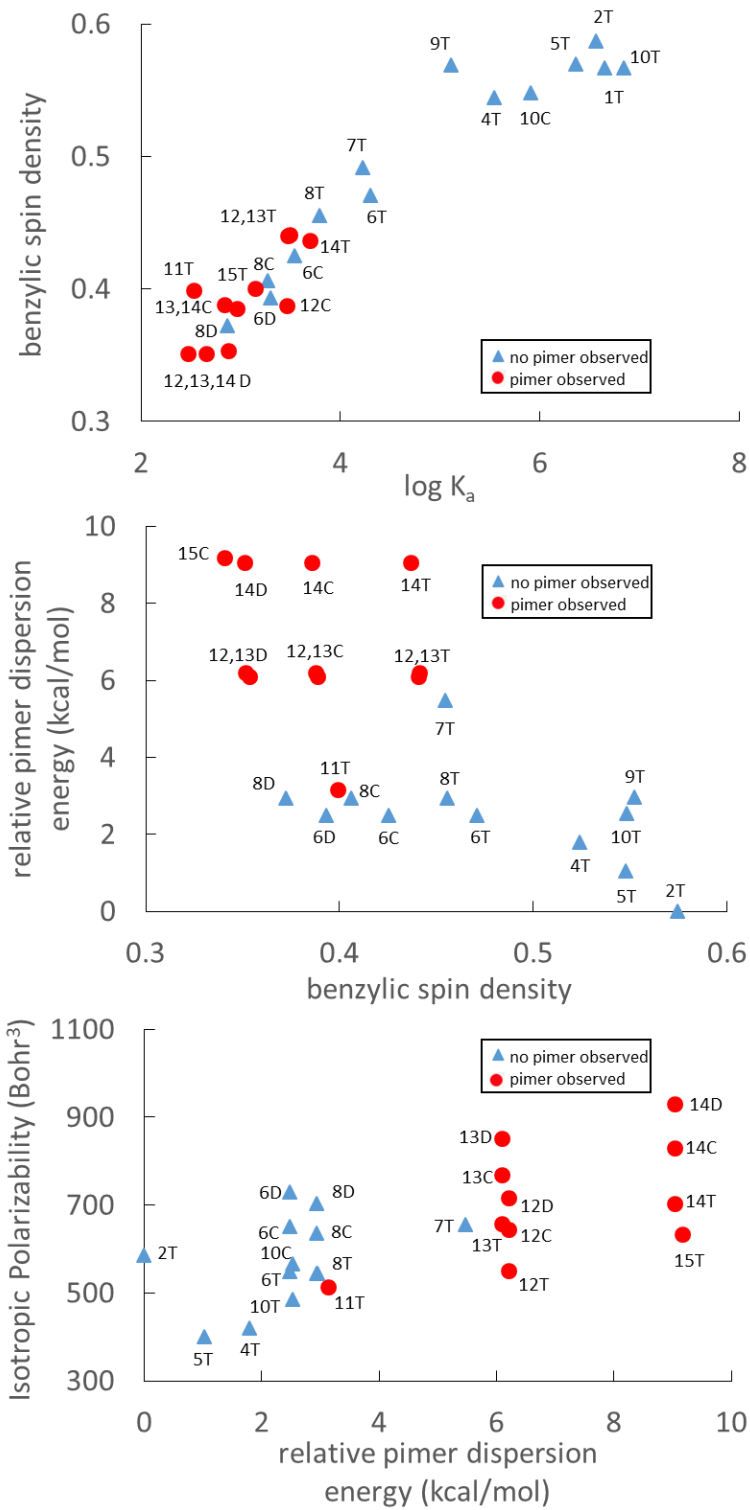
Computational data table

Radical	B97D Pimer (Hartrees)	B97D Sigma (Hartrees)	B98 Pimer (Hartrees)	B98 Sigma (Hartrees)	Δ B97 D (kcal/mol) Sigma-Pimer
2	-1215.2654	-1215.2600	-1215.6047	-1215.6314	3.4020
4	-1215.3387	-1215.3141	-1215.6868	-1215.6971	15.4635
5	-1287.0859	-1287.0636	-1287.4432	-1287.4547	13.9946
6	-1178.0517	-1178.0166	-1178.3763	-1178.3773	22.0274
7	-1487.4216	-1487.3860	-1487.8361	-1487.8413	22.3734
8	-1332.7990	-1332.7626	-1333.1858	-1333.1862	22.8916
9	-1406.4765	-1406.4595	-1406.8917	-1406.9115	10.6435
10	-1251.7906	-1251.7745	-1252.1580	-1252.1780	10.1082
11	-1254.2256	-1254.1845	-1254.5881	-1254.5841	25.8284
12	-1332.8157	-1332.7717	-1333.1935	-1333.1915	27.6230
13	-1568.5580	-1568.5139	-1569.0020	-1568.9997	27.6964
14	-1644.6877	-1644.6528	-1645.1628	-1645.1744	21.8930
15	-1487.5699	-1487.5252	-1488.0018	-1488.0038	28.0656
Compound	Δ B98 (kcal/mol) Sigma-Pimer	$\Delta\Delta$ (kcal/mol)	Benzylic Spin Density	ΔE normalized (kcal/mol)	Isotropic Polarizability (Bohr)
2	-16.7666	20.1686	0.5748	0.0000	431.2
4	-6.4922	21.9557	0.5241	1.7872	331.1
5	-7.2042	21.1988	0.5478	1.0302	318.2
6	-0.6272	22.6546	0.4253	2.4860	413.3
7	-3.2609	25.6343	0.4546	5.4657	507.5
8	-0.2158	23.1075	0.4063	2.9389	425.2
9	-12.4790	23.1226	0.5525	2.9540	430.3
10	-12.5820	22.6902	0.5484	2.5216	376.9
11	2.5202	23.3082	0.3992	3.1397	394
12	1.2555	26.3675	0.3878	6.1989	423.9
13	1.4372	26.2592	0.3889	6.0906	512.7
14	-7.3184	29.2114	0.3858	9.0429	541.5
15	-1.2727	29.3382	0.3411	9.1697	481

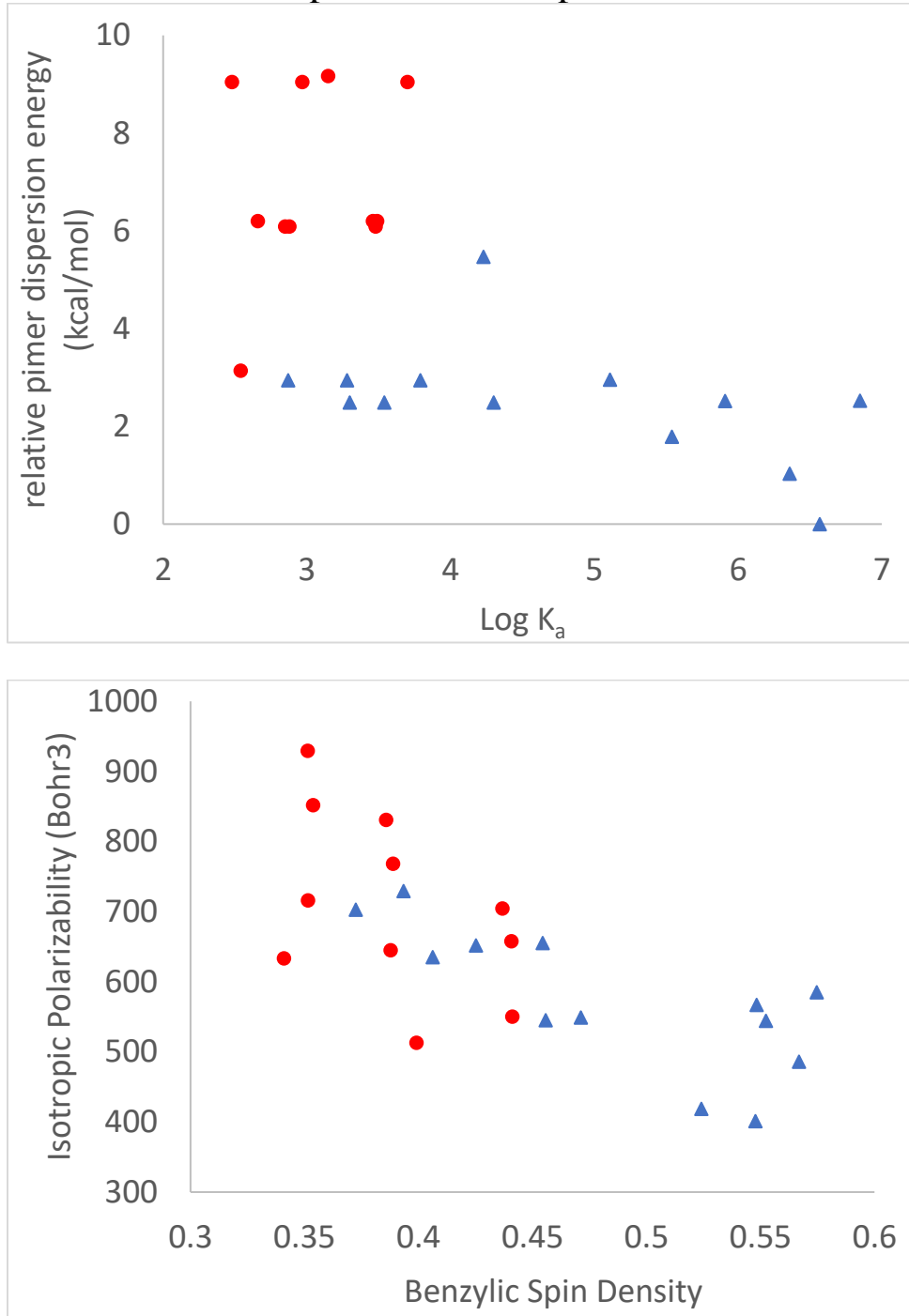
Solvent	Compound	Benzyllic Spin Density	ΔE solvation (kcal/mol)	log Ka	Isotropic Polarizability
Toluene	2	0.5748	0	6.57	585
Toluene	7	0.4546	5.4657	4.23	655.4
Toluene	4	0.5241	1.7871	5.54	419.1
Toluene	5	0.5478	1.0302	6.36	401.5
Toluene	10	0.5669	2.5215	6.85	486
Toluene	9	0.5525	2.9539	5.11	544.5
CHCl ₃	6	0.4253	2.4860	3.54	652.1
CHCl ₃	13	0.3889	6.0905	2.85	768.3
Toluene	15	0.3411	9.1696	3.15	633.7
CHCl ₃	12	0.3878	6.1989	3.46	645.2
CHCl ₃	8	0.4063	2.9388	3.28	635.3
CHCl ₃	14	0.38582	9.0428	2.97	831.2
CHCl ₃	11	0.39918	3.1396	2.54	513.1
Toluene	12	0.4412	6.1989	3.49	550.3
CHCl ₂	12	0.3516	6.1989	2.66	716.2
Toluene	14	0.43692	9.0428	3.70	704.7
CHCl ₂	14	0.35149	9.0428	2.48	929.6
Toluene	13	0.4408	6.0906	3.48	658
CHCl ₂	13	0.3538	6.0906	2.88	852.1
Toluene	6	0.4713	2.486	4.30	549
CHCl ₂	6	0.3935	2.486	3.30	729.7
Toluene	8	0.4559	2.9388	3.79	545.4
CHCl ₂	8	0.3726	2.9388	2.87	702.9
CHCl ₃	10	0.5484	2.52	5.91	567

Detailed Plots of Computational Benchmarks

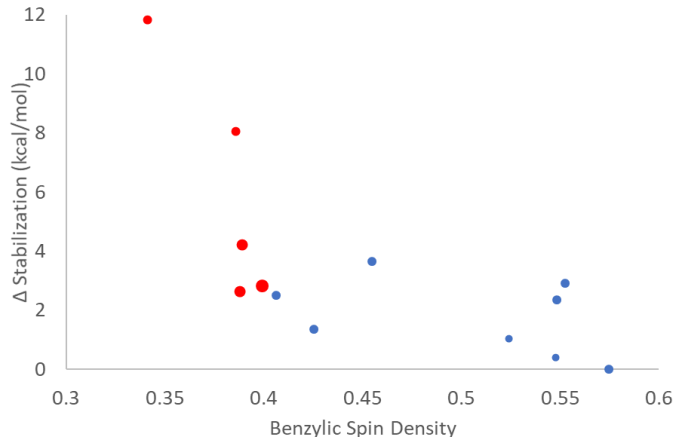
T = Toluene, C = Chloroform, D = Dichloromethane



Other Computational Comparison Tables

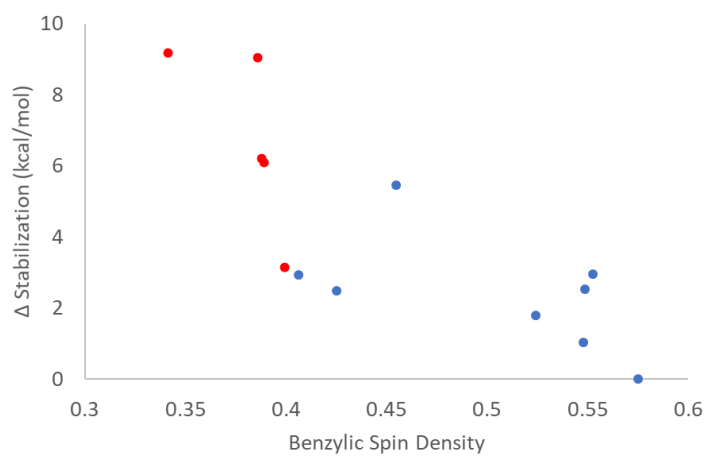


Unrestricted Dispersion

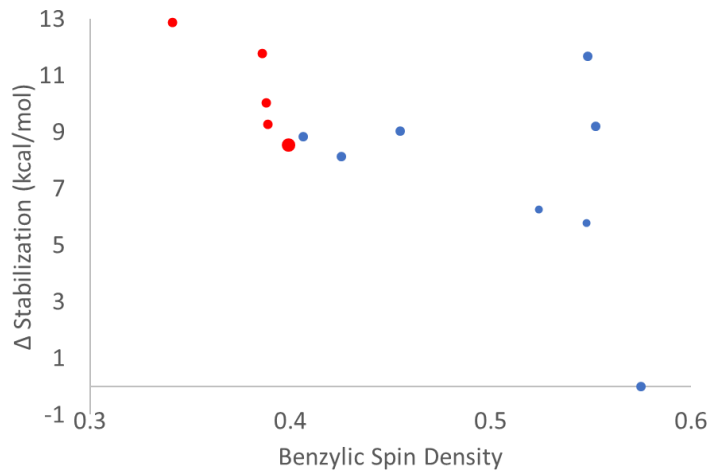


(In this plot, the pimers were optimized using an unrestricted singlet)

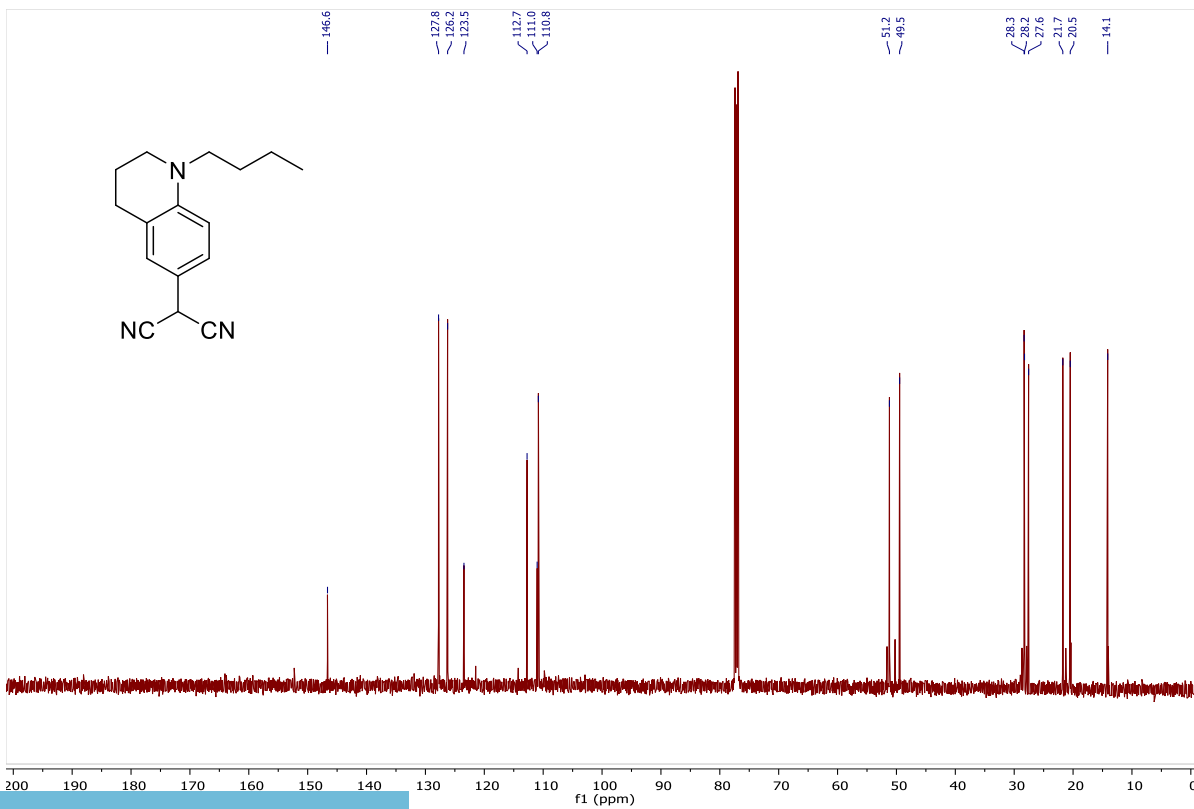
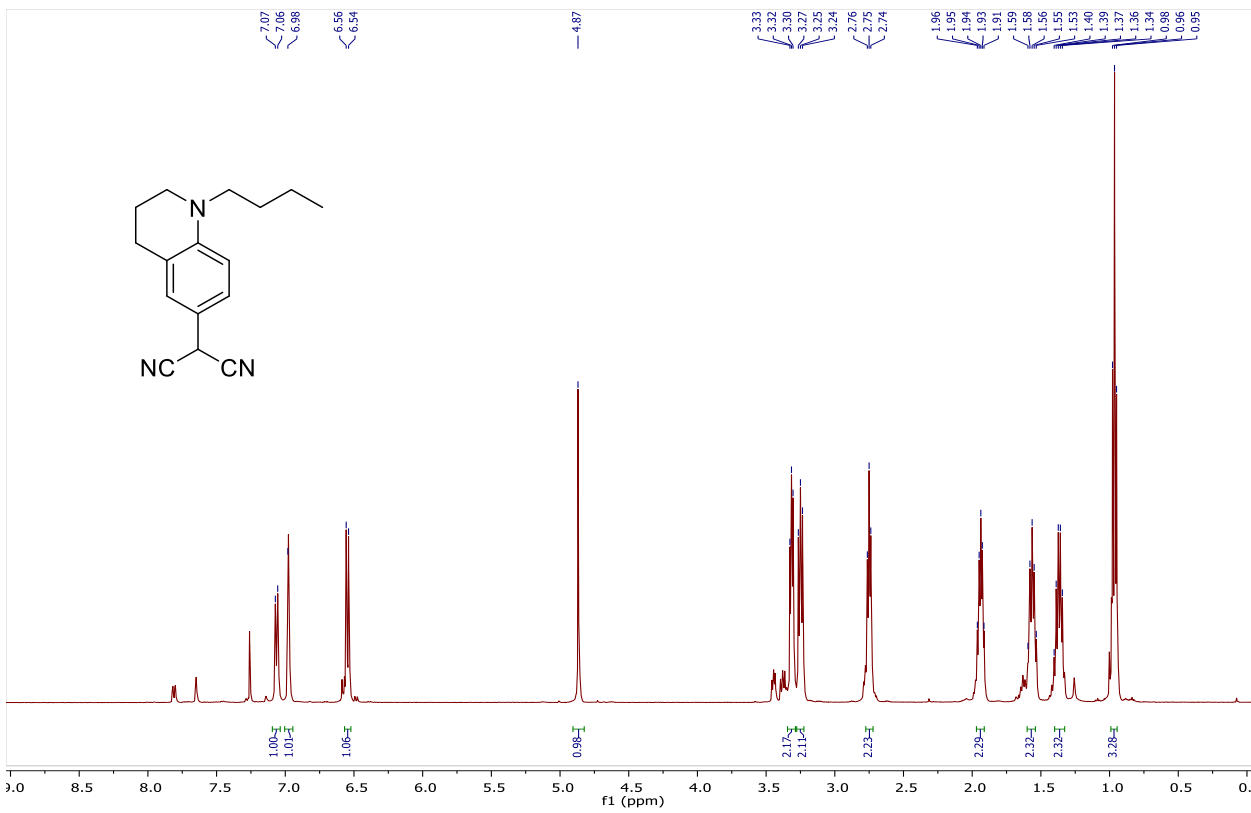
Restricted Dispersion

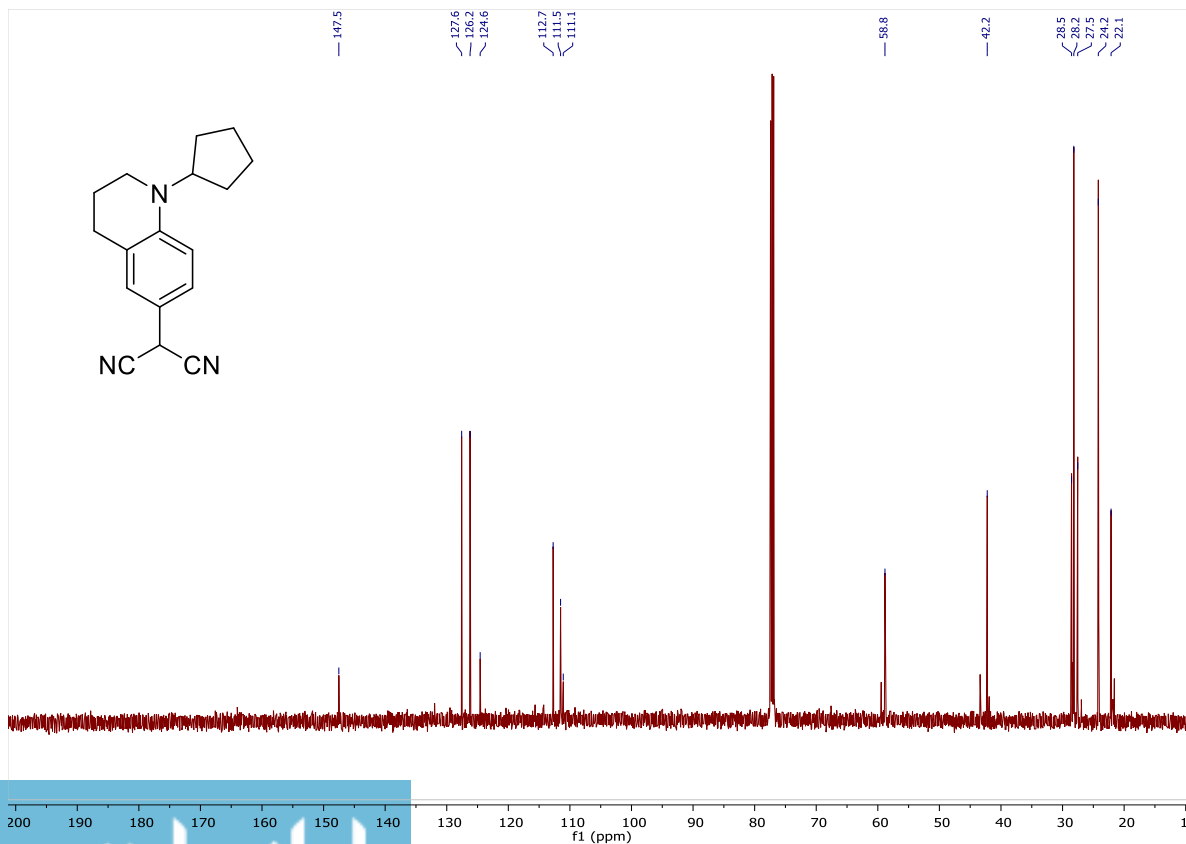
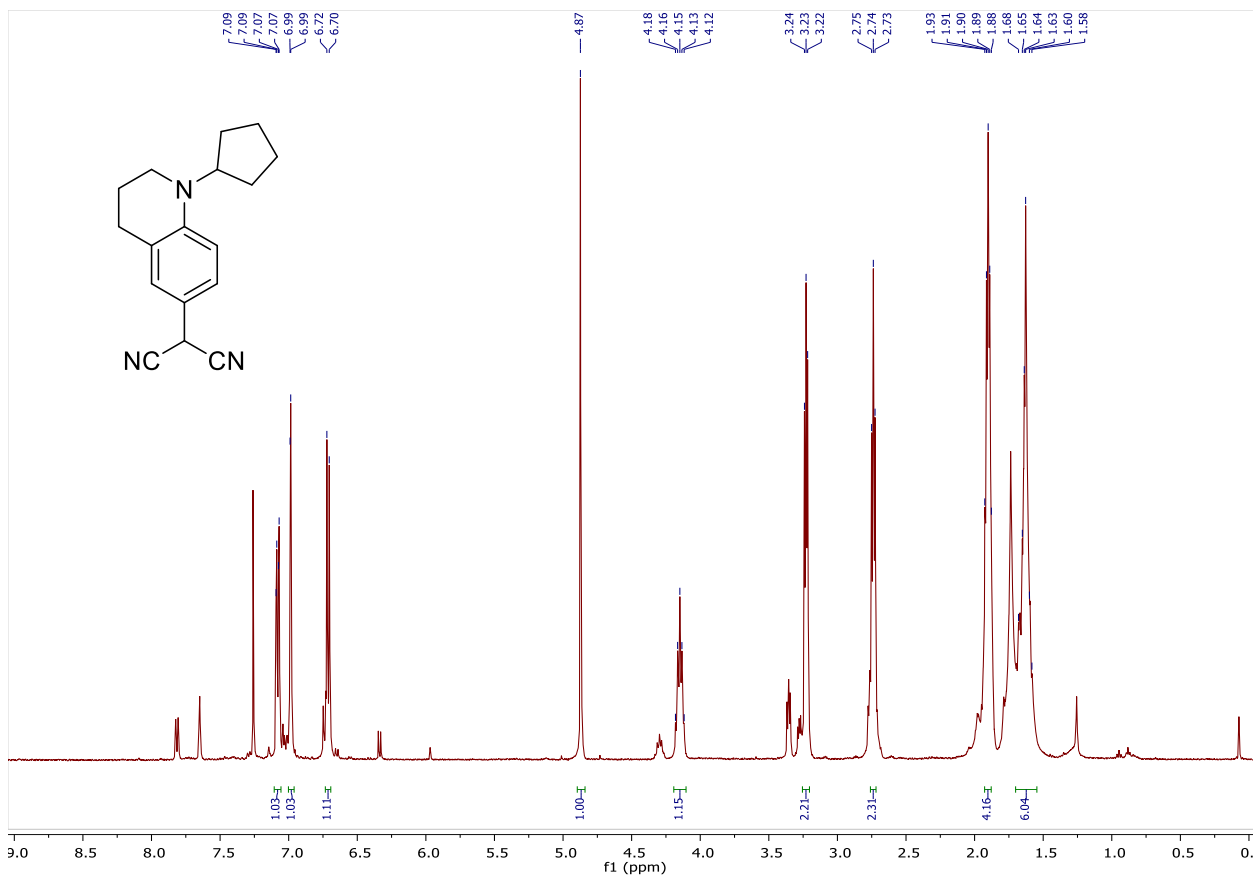


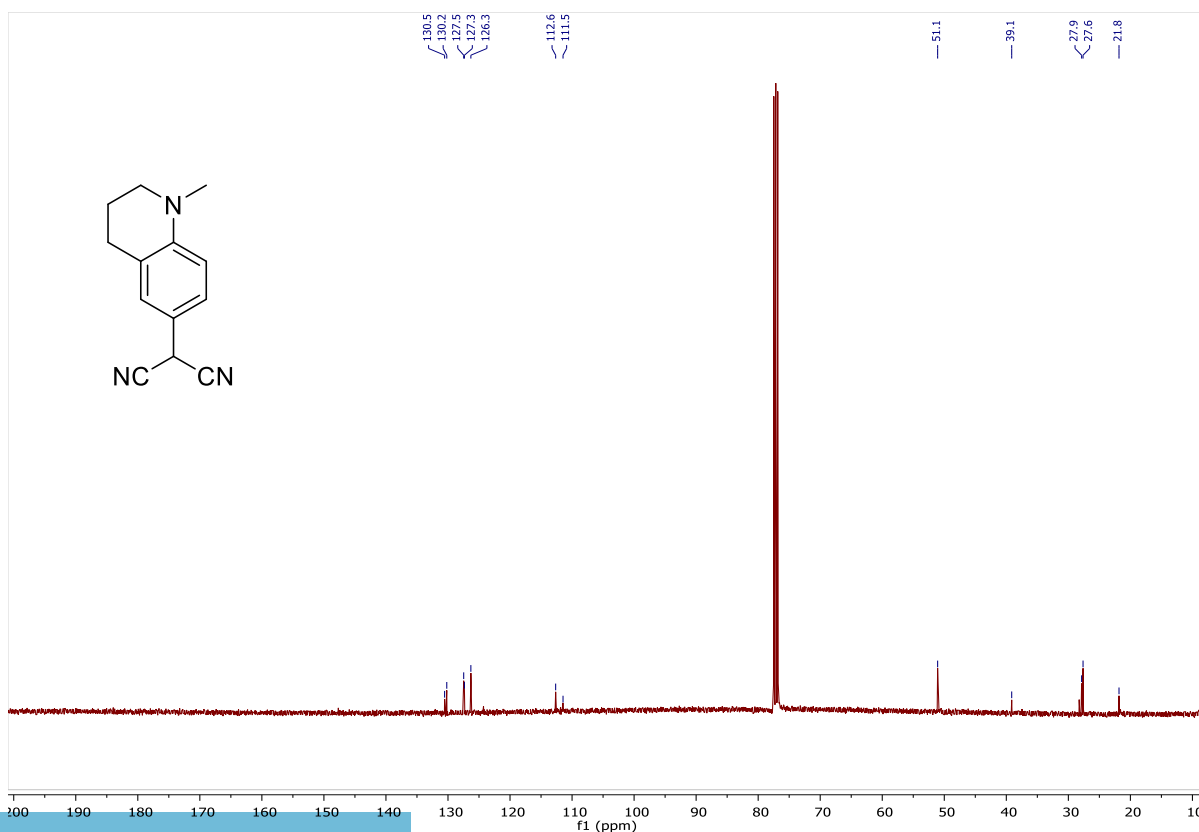
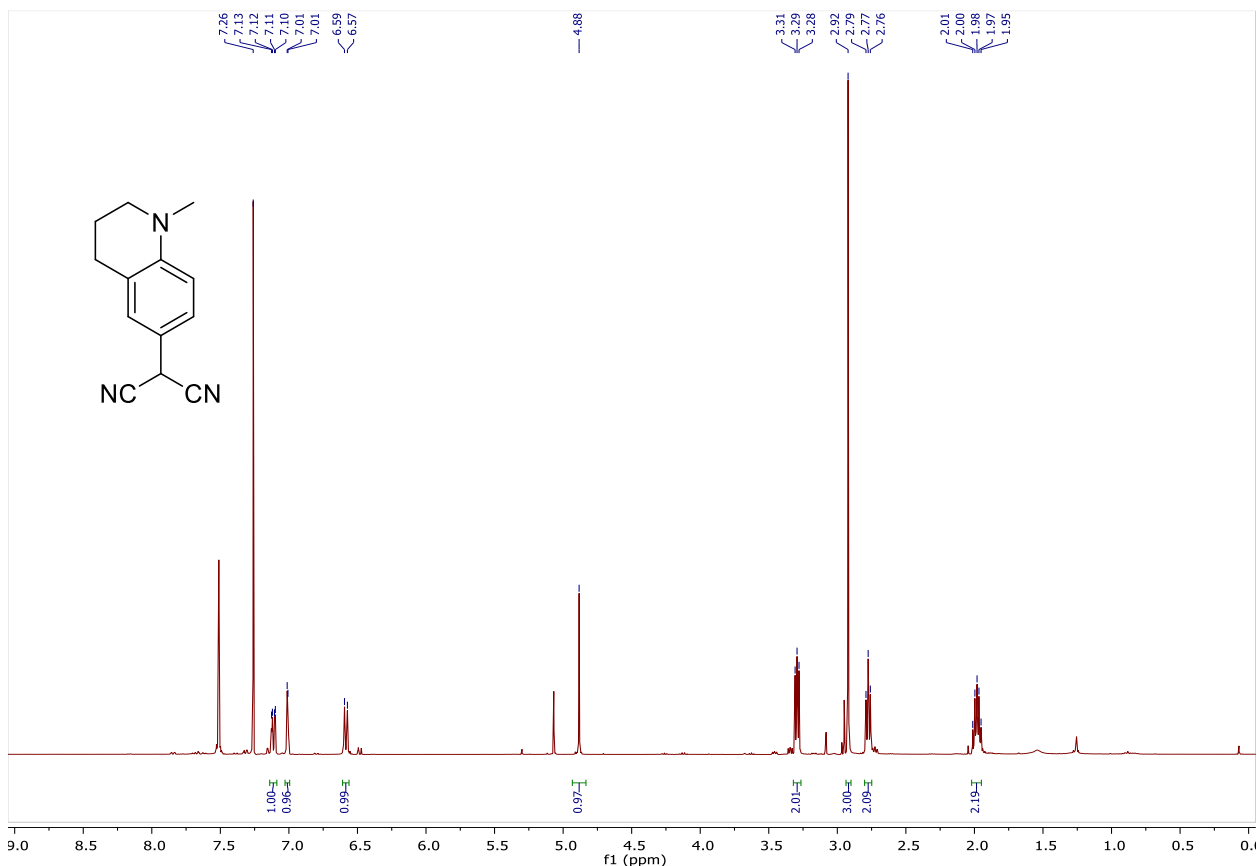
Restricted Dispersion (B97D3 Functional)

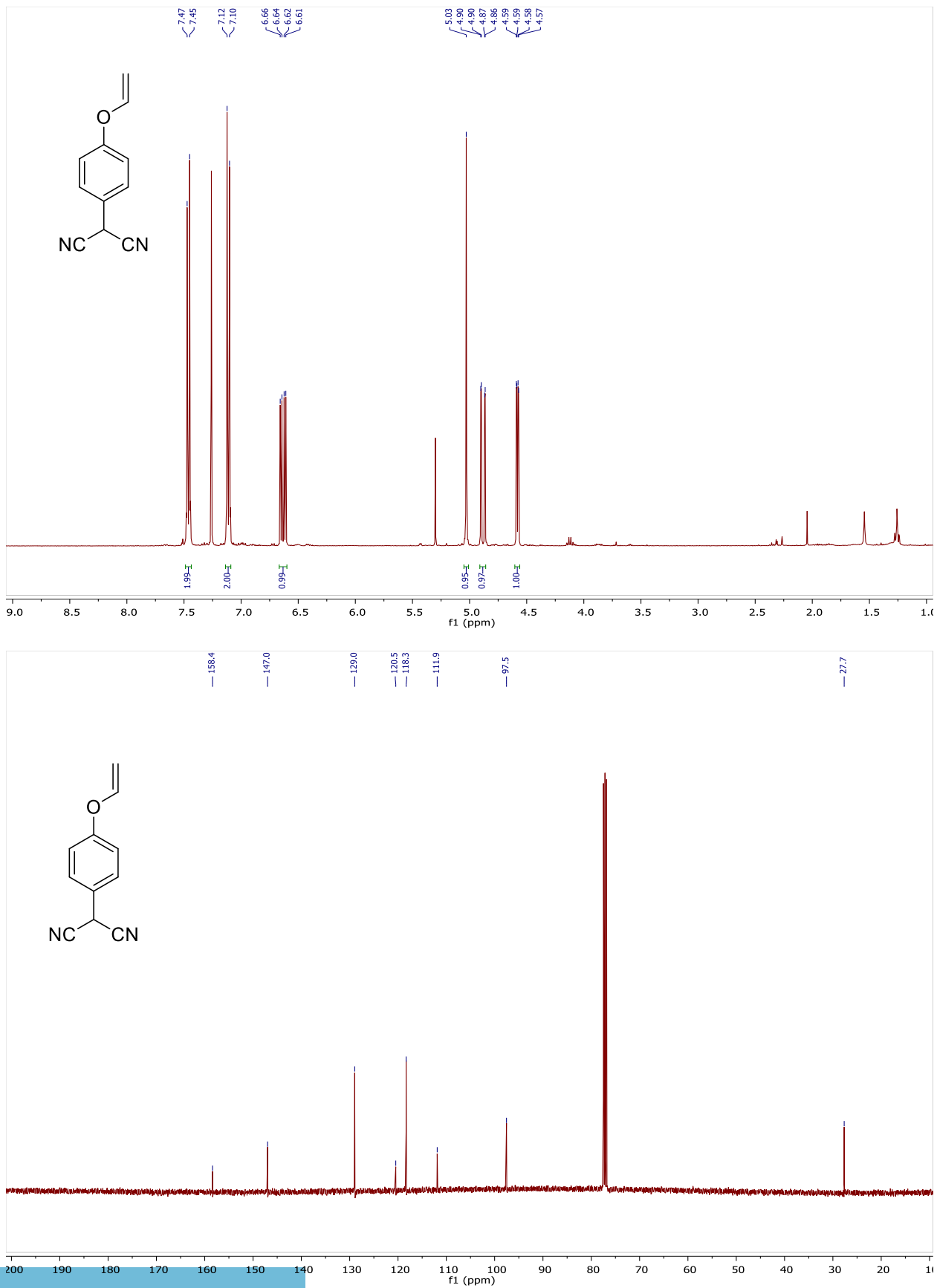


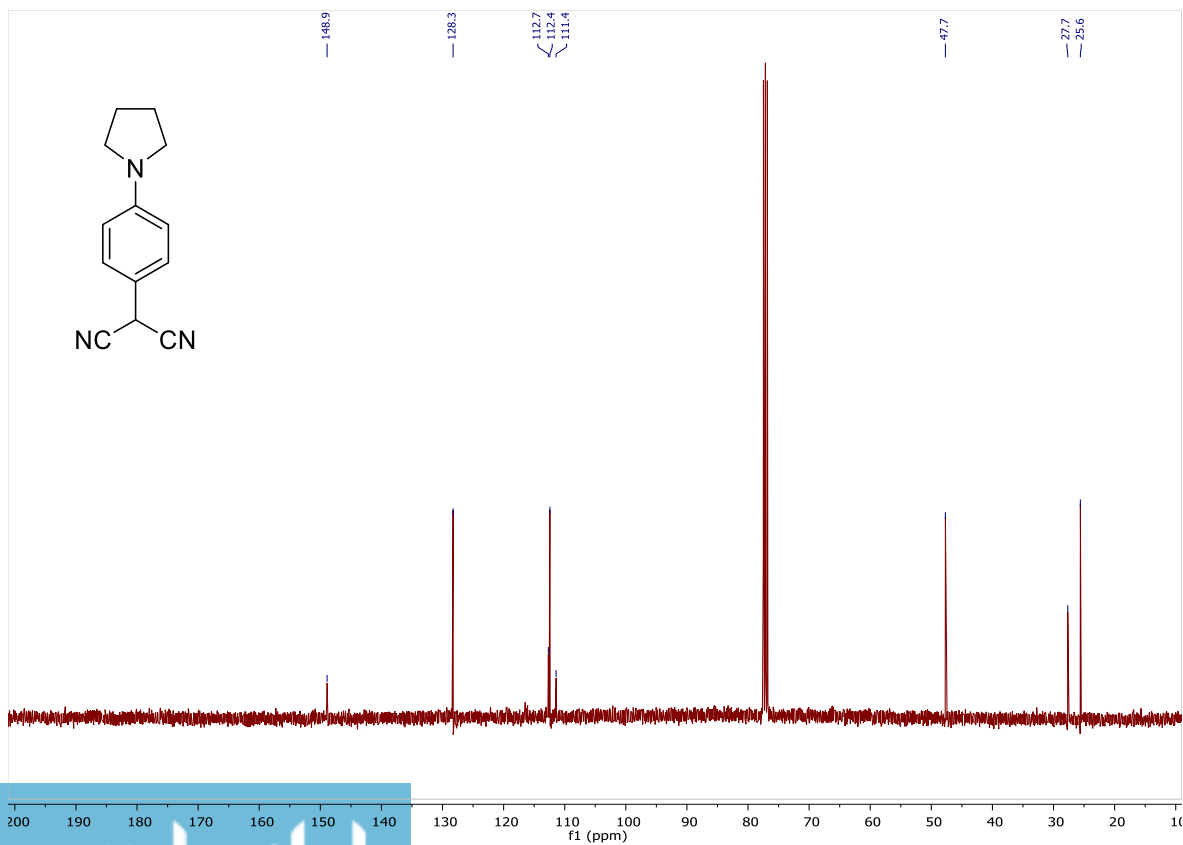
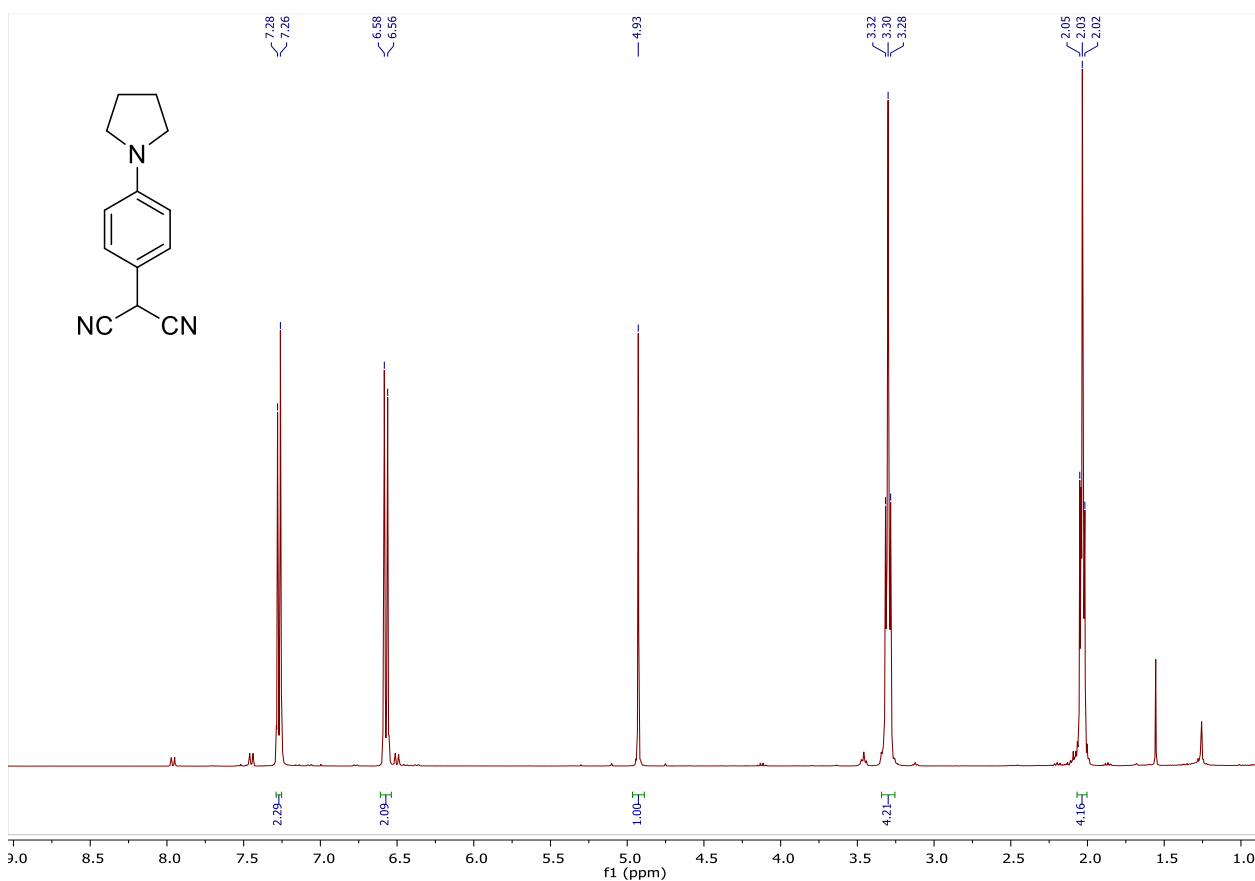
NMR Spectra:

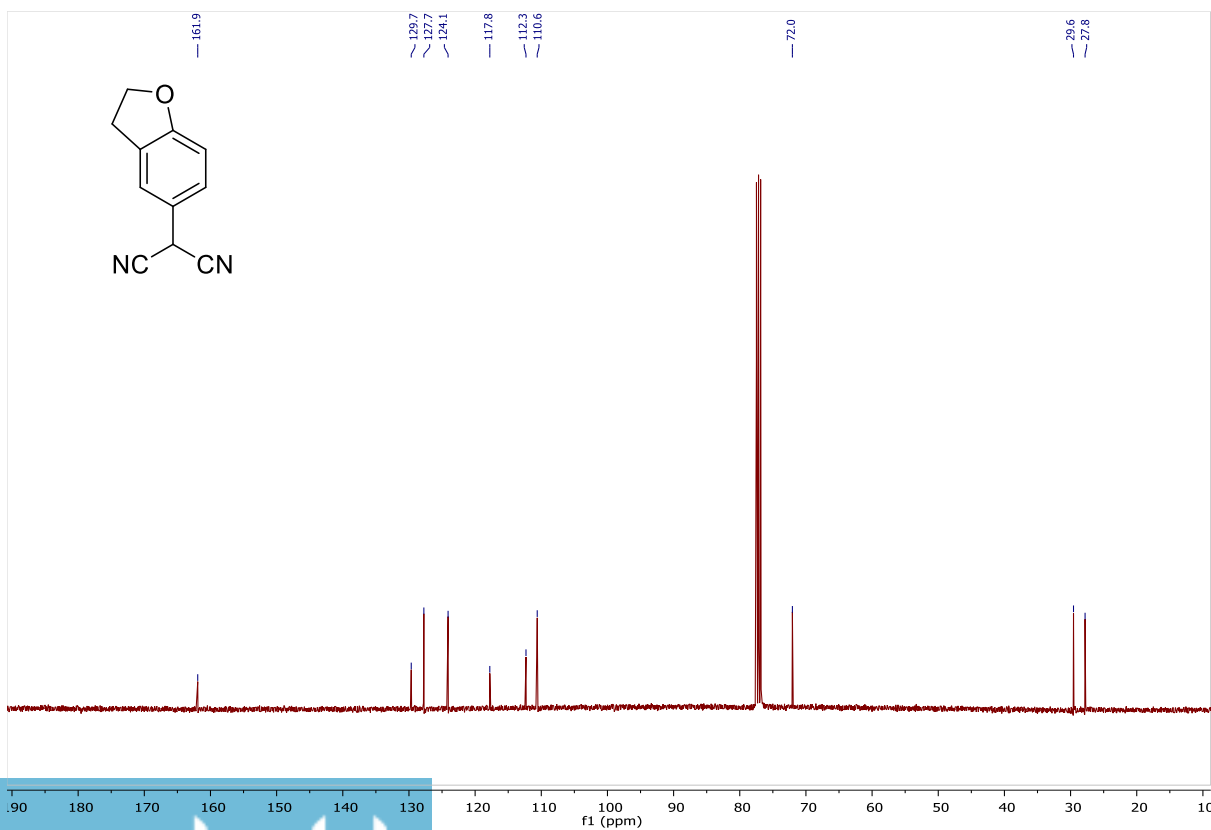
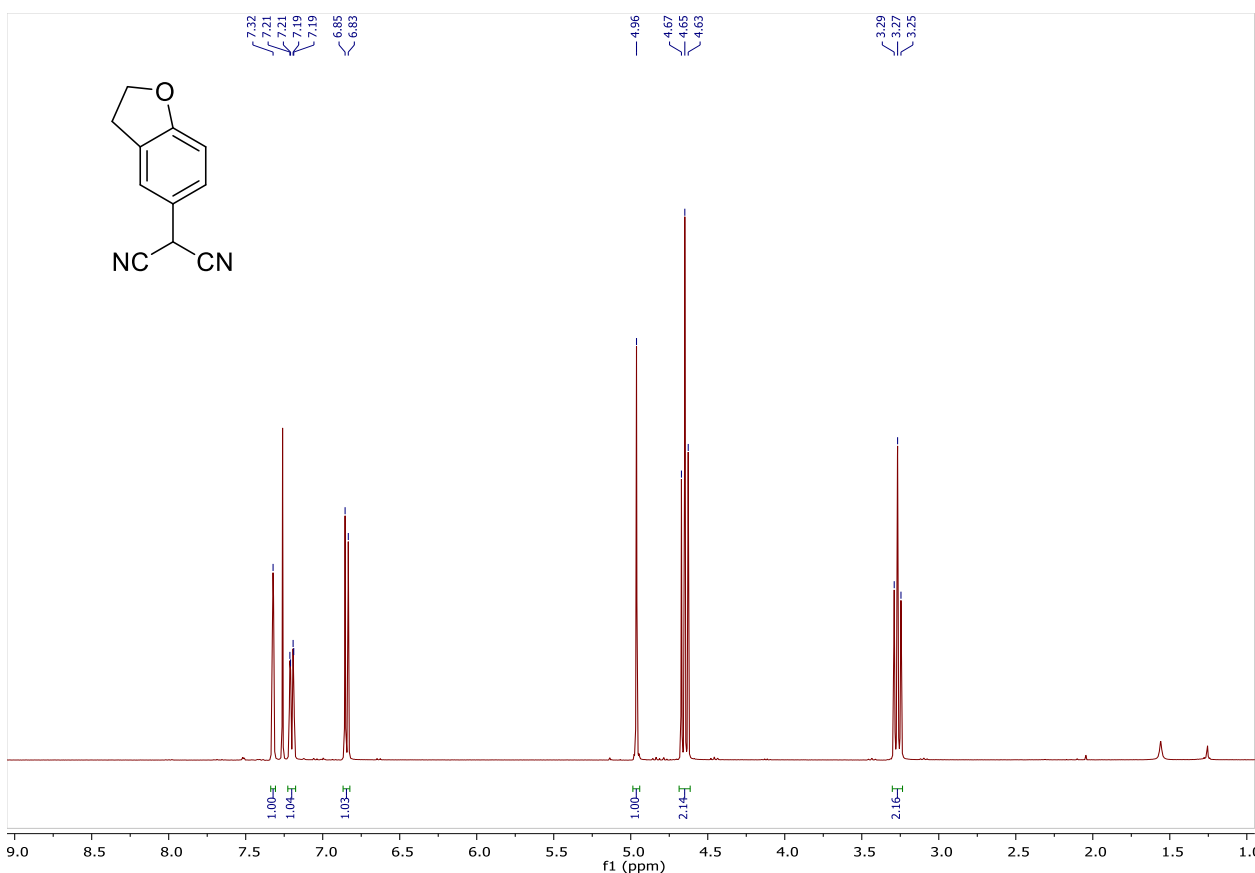


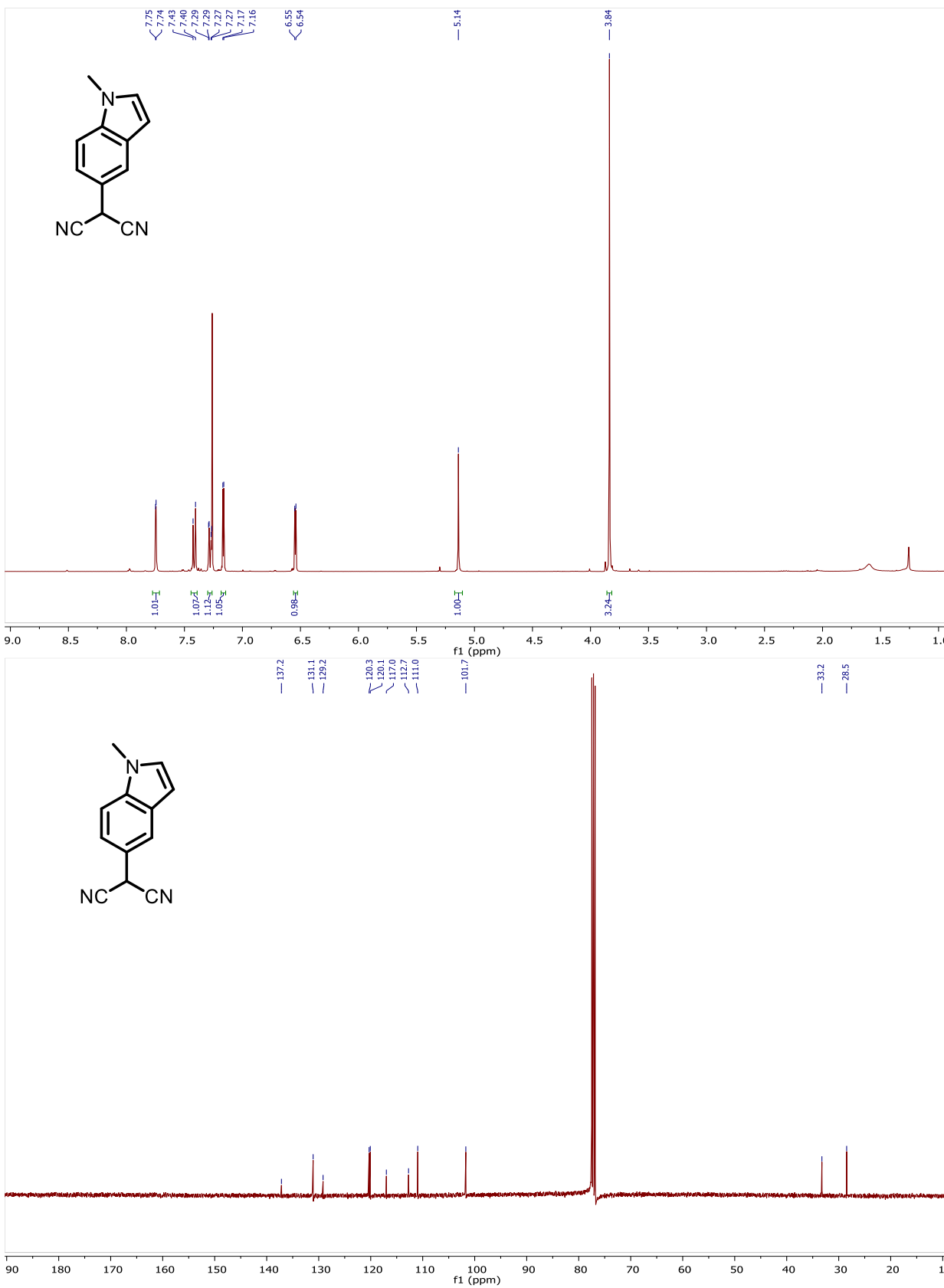


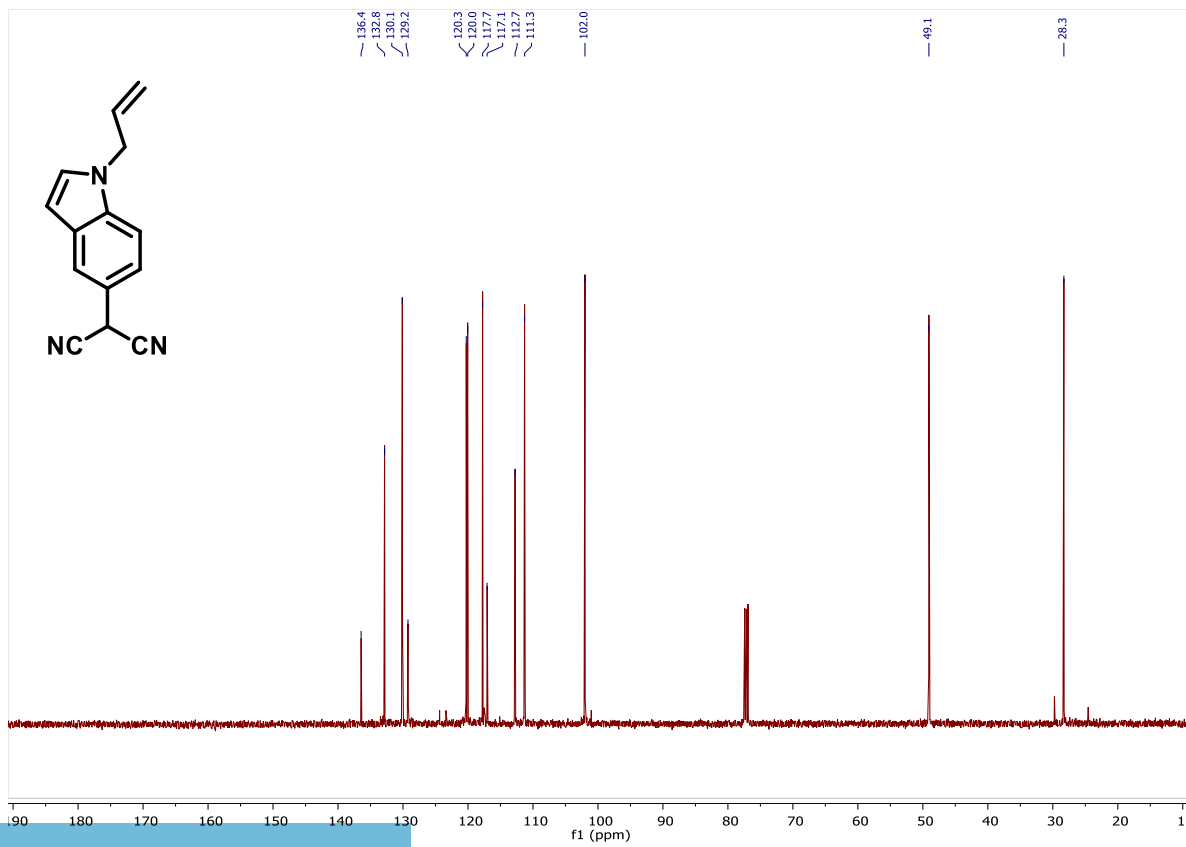
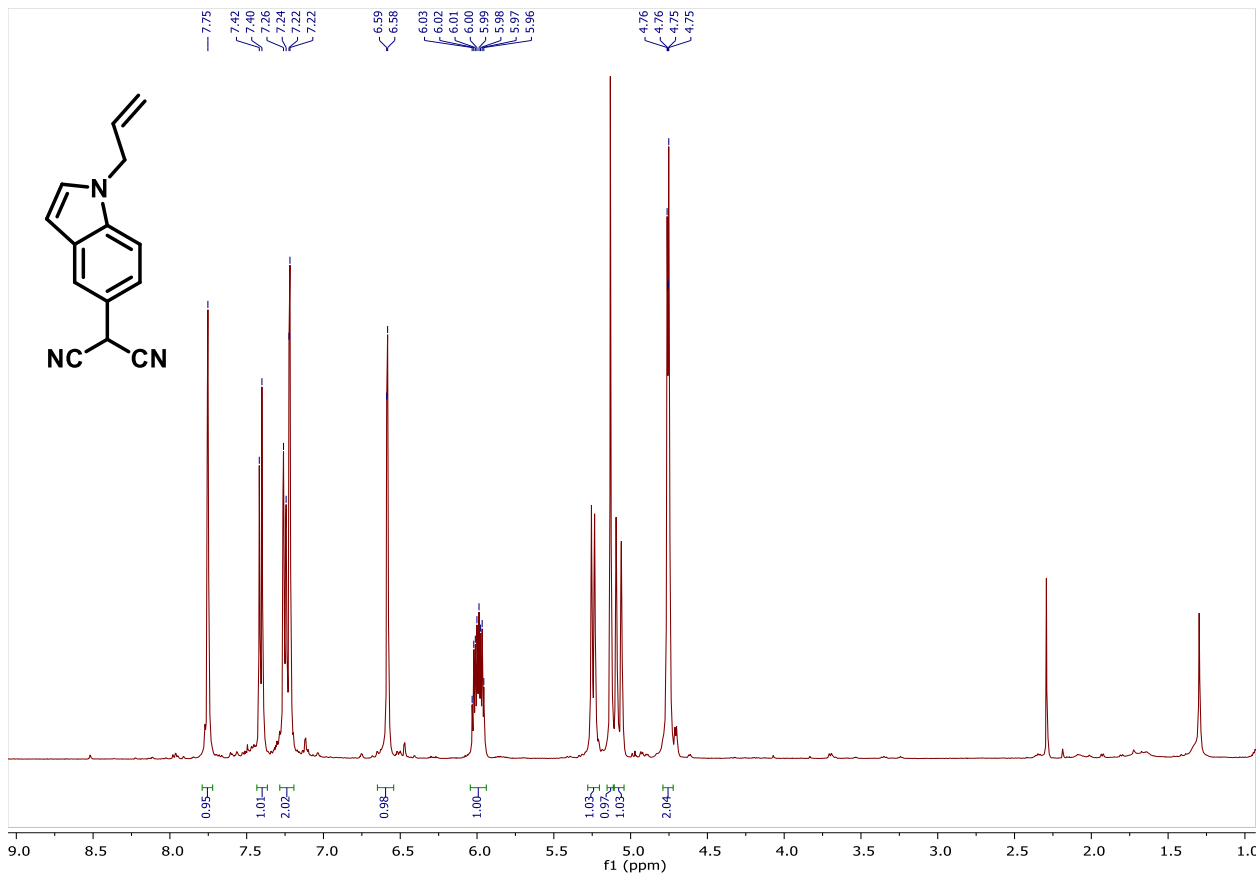


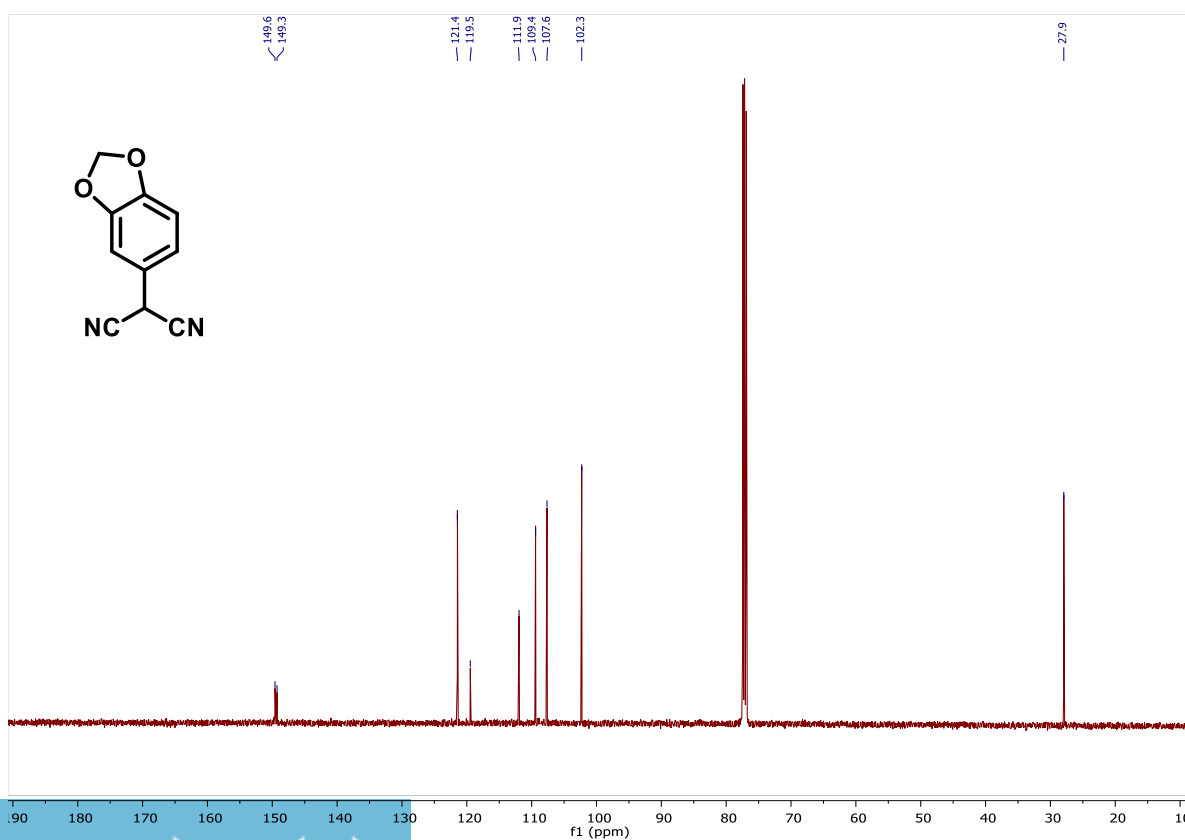
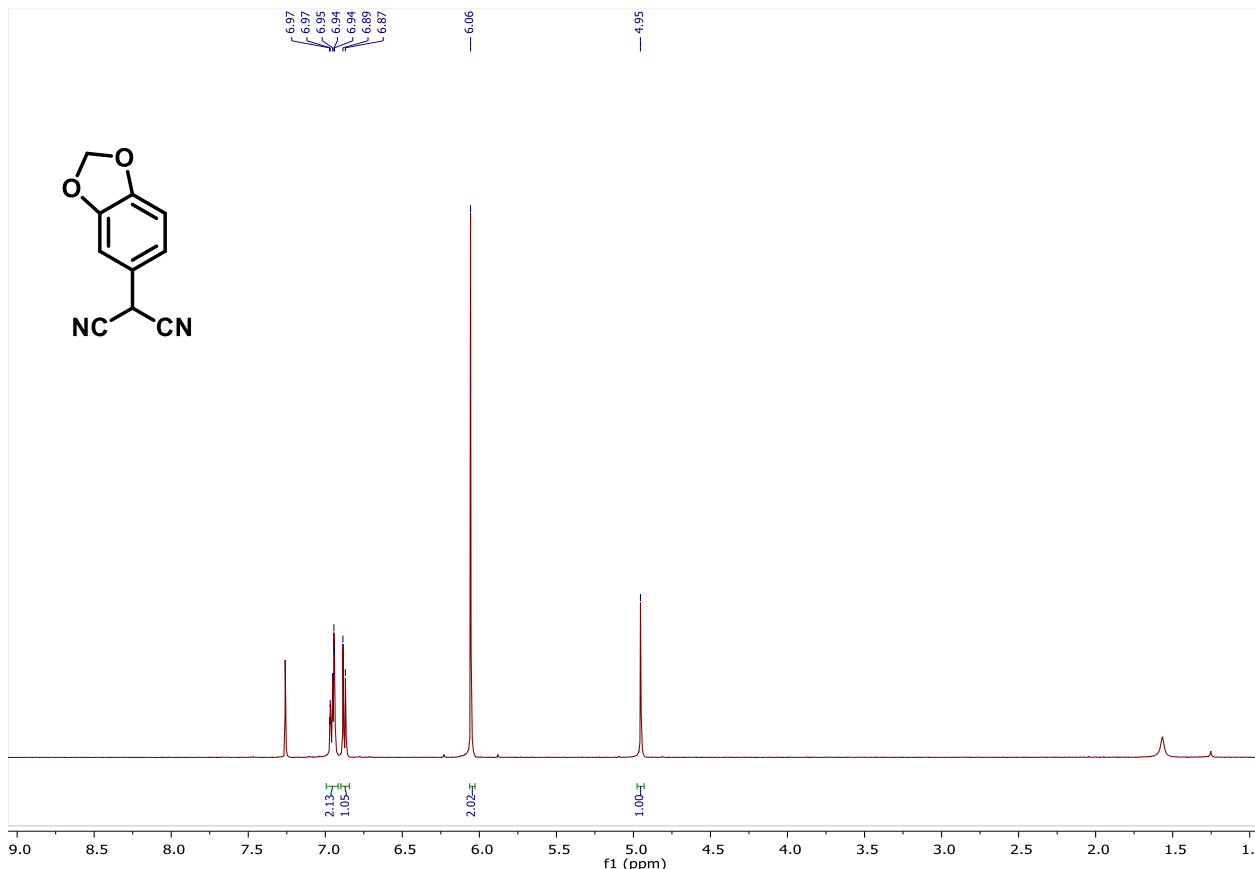


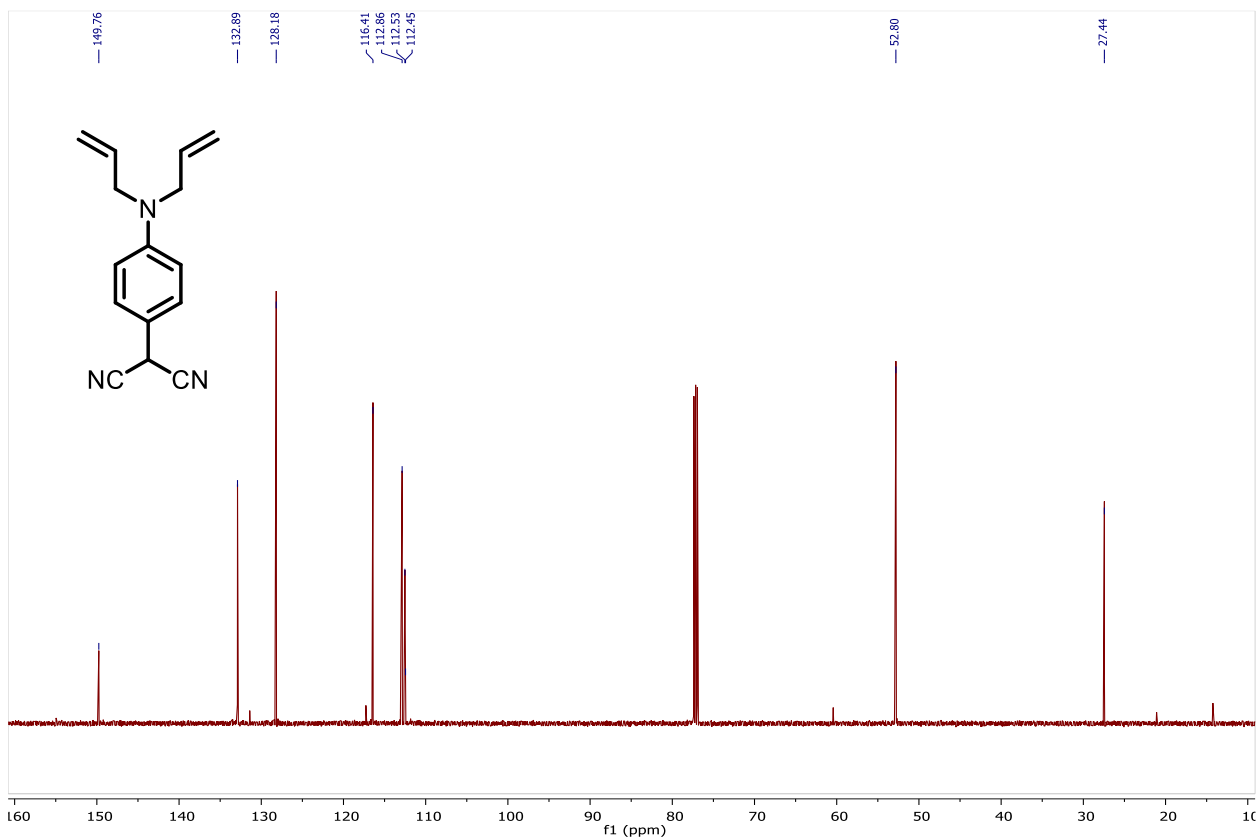
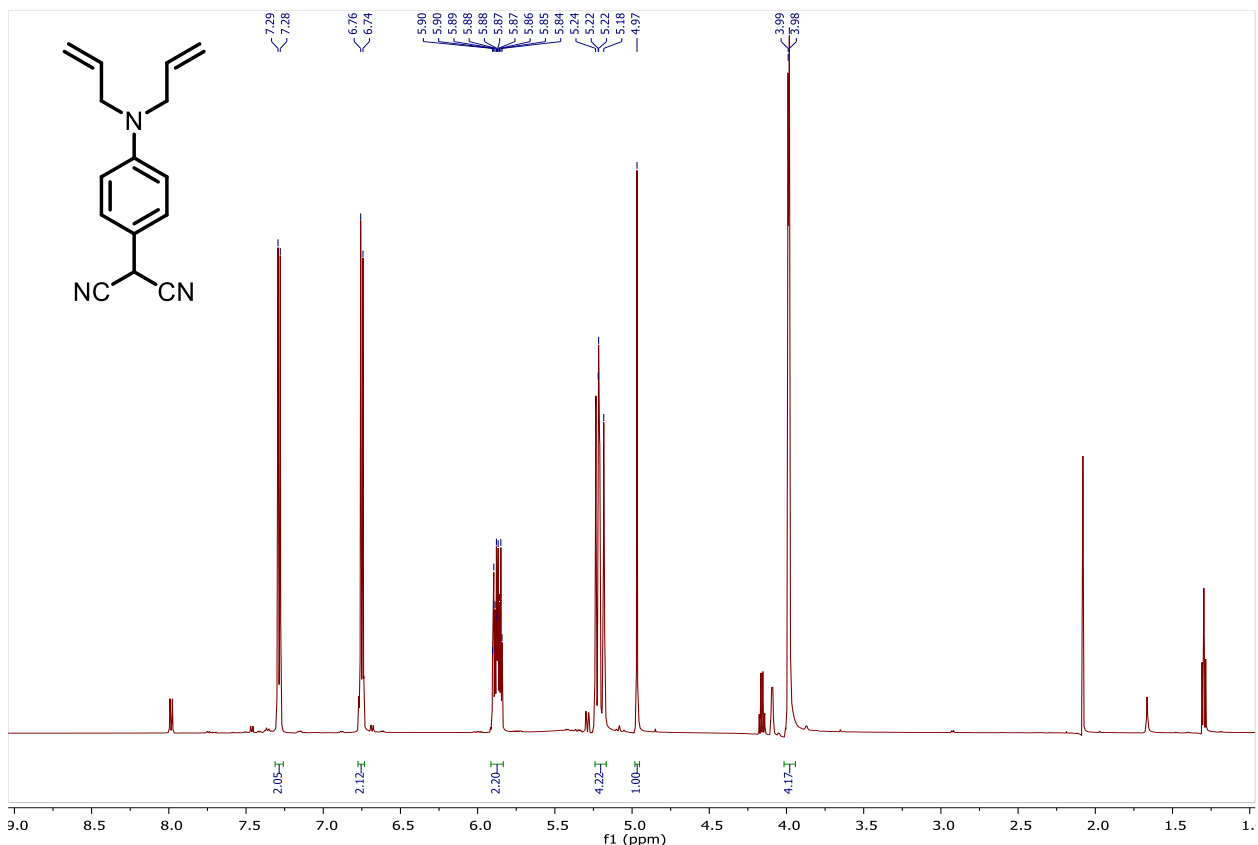


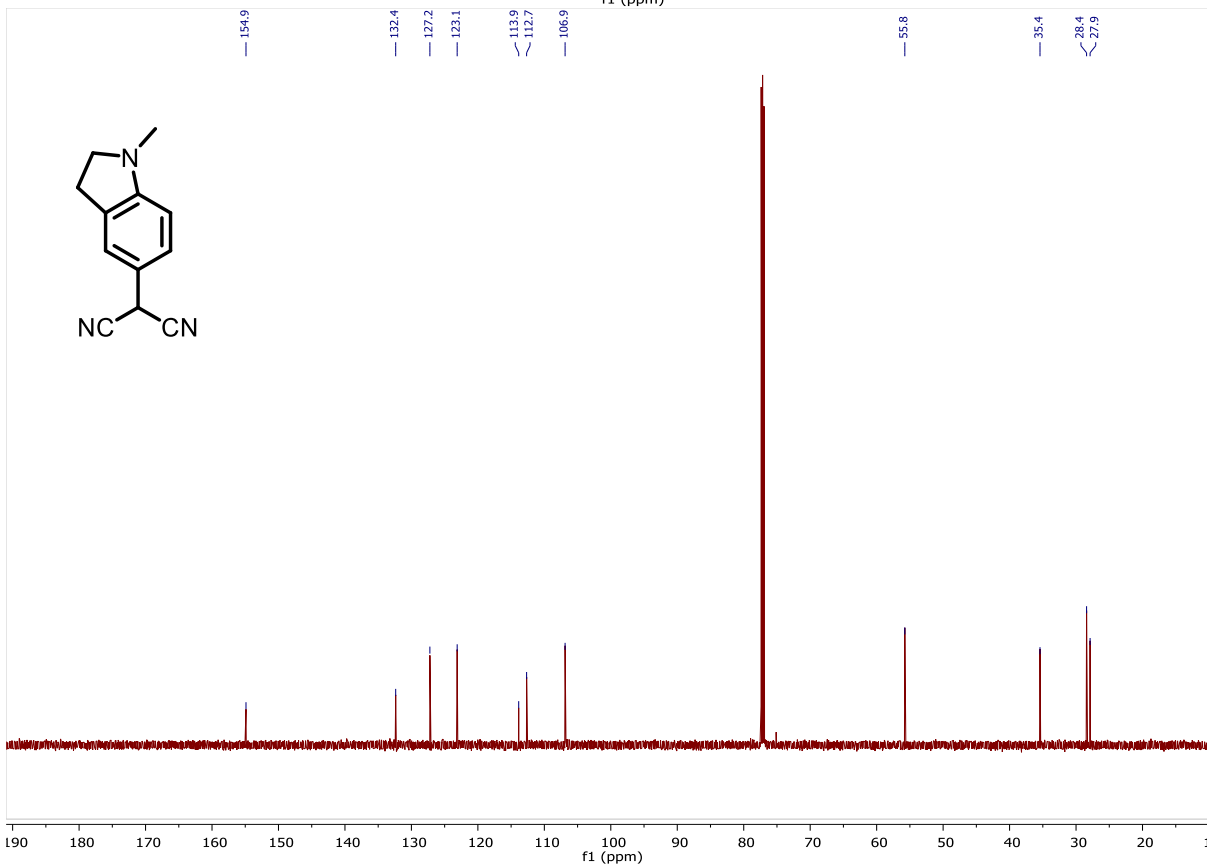
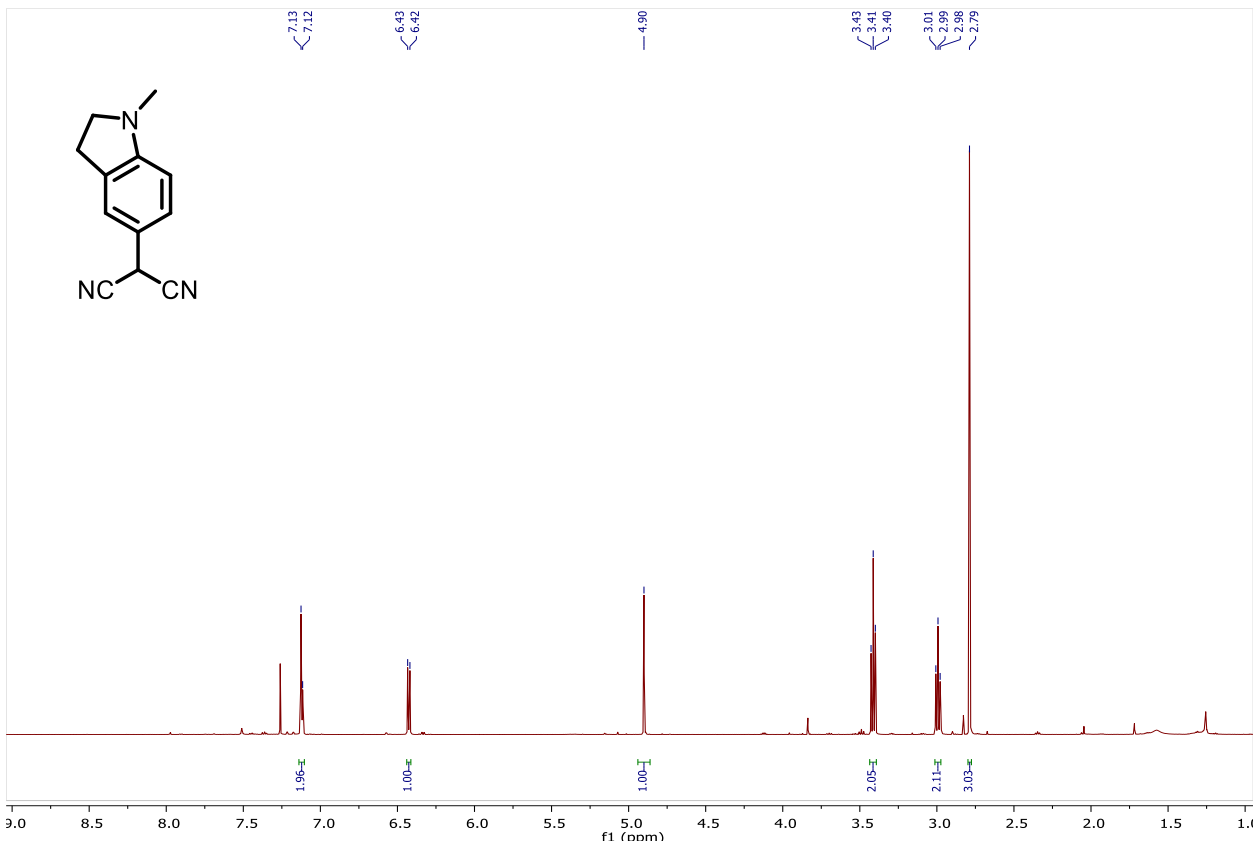




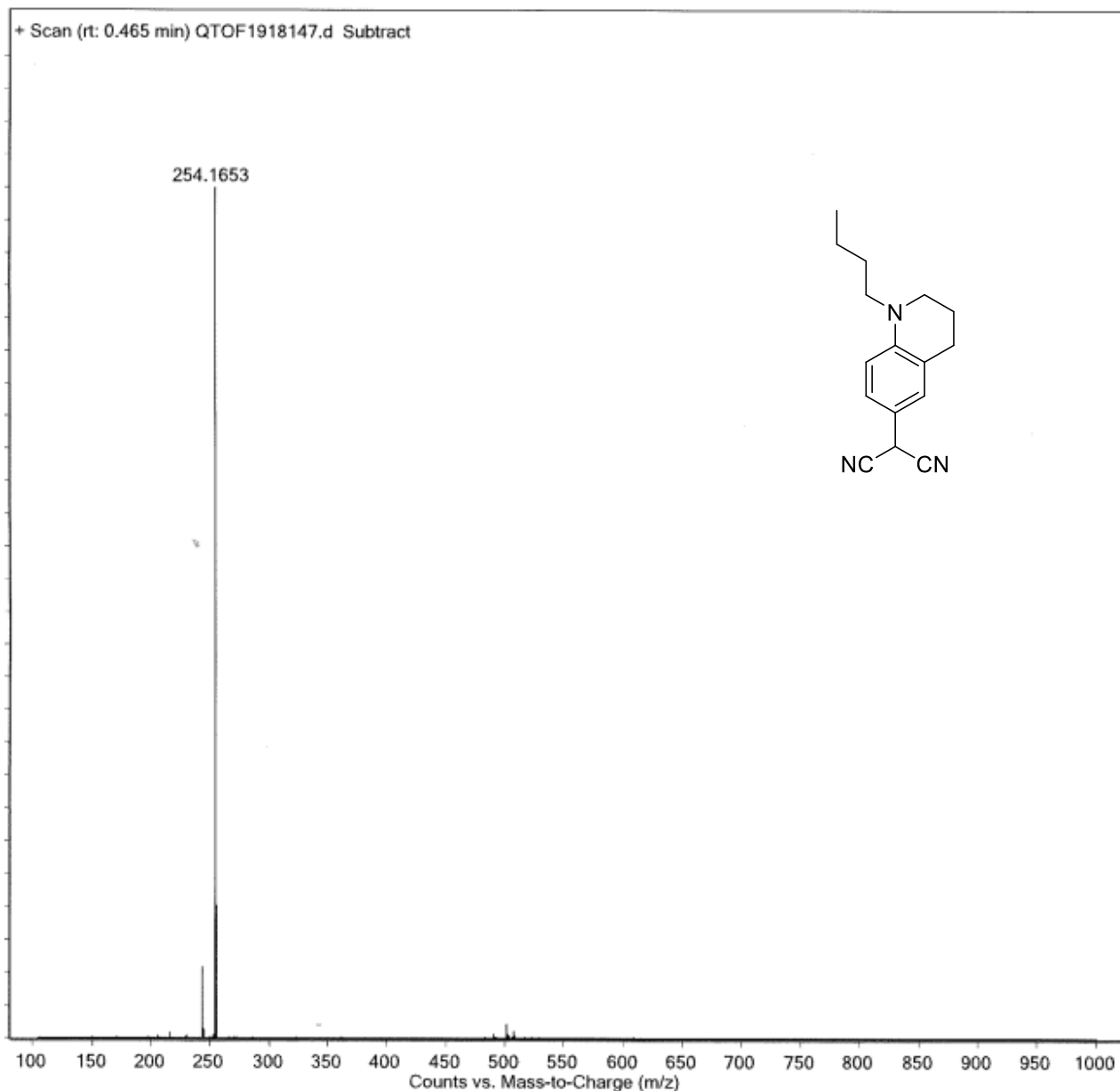


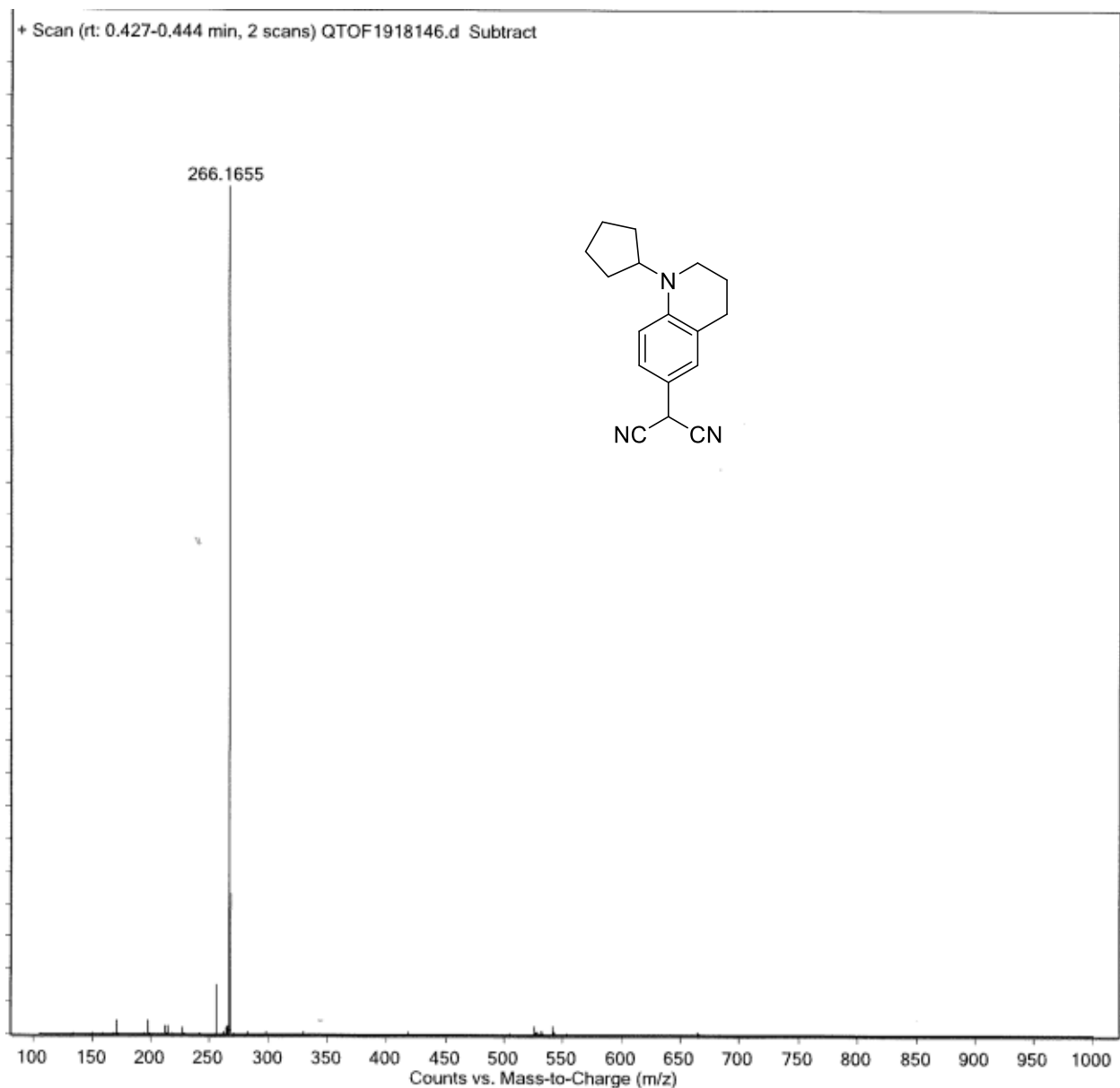


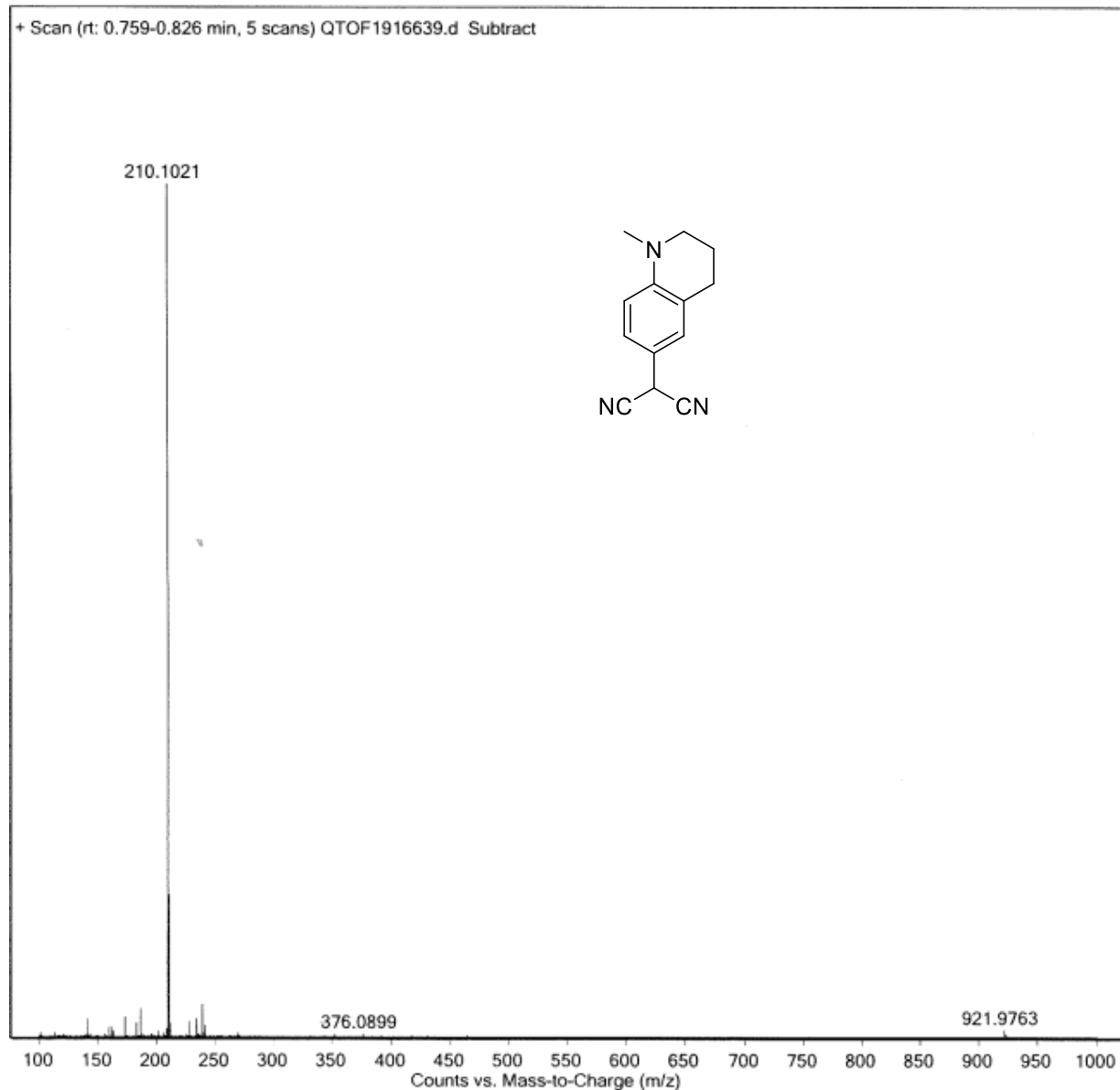


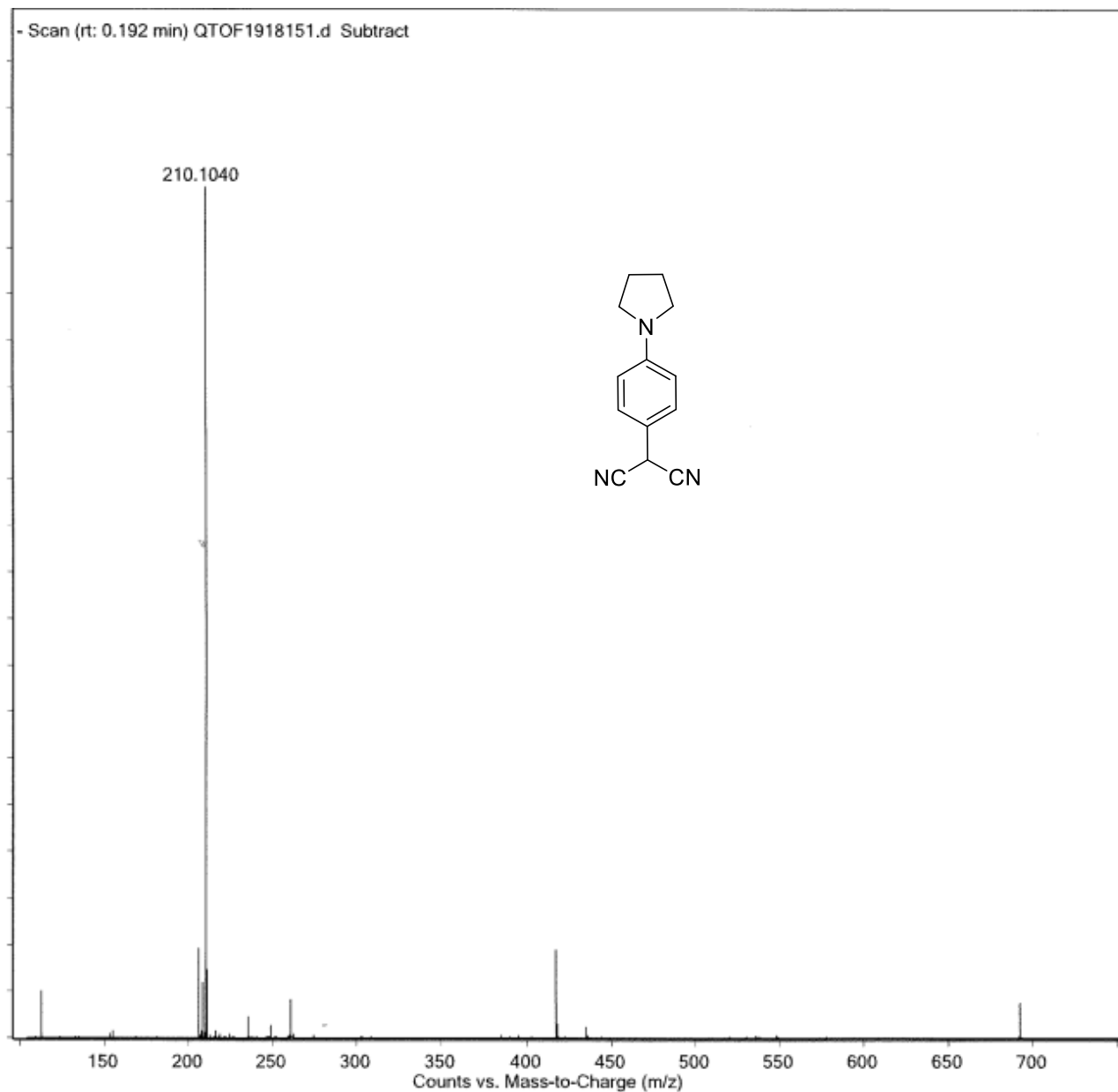


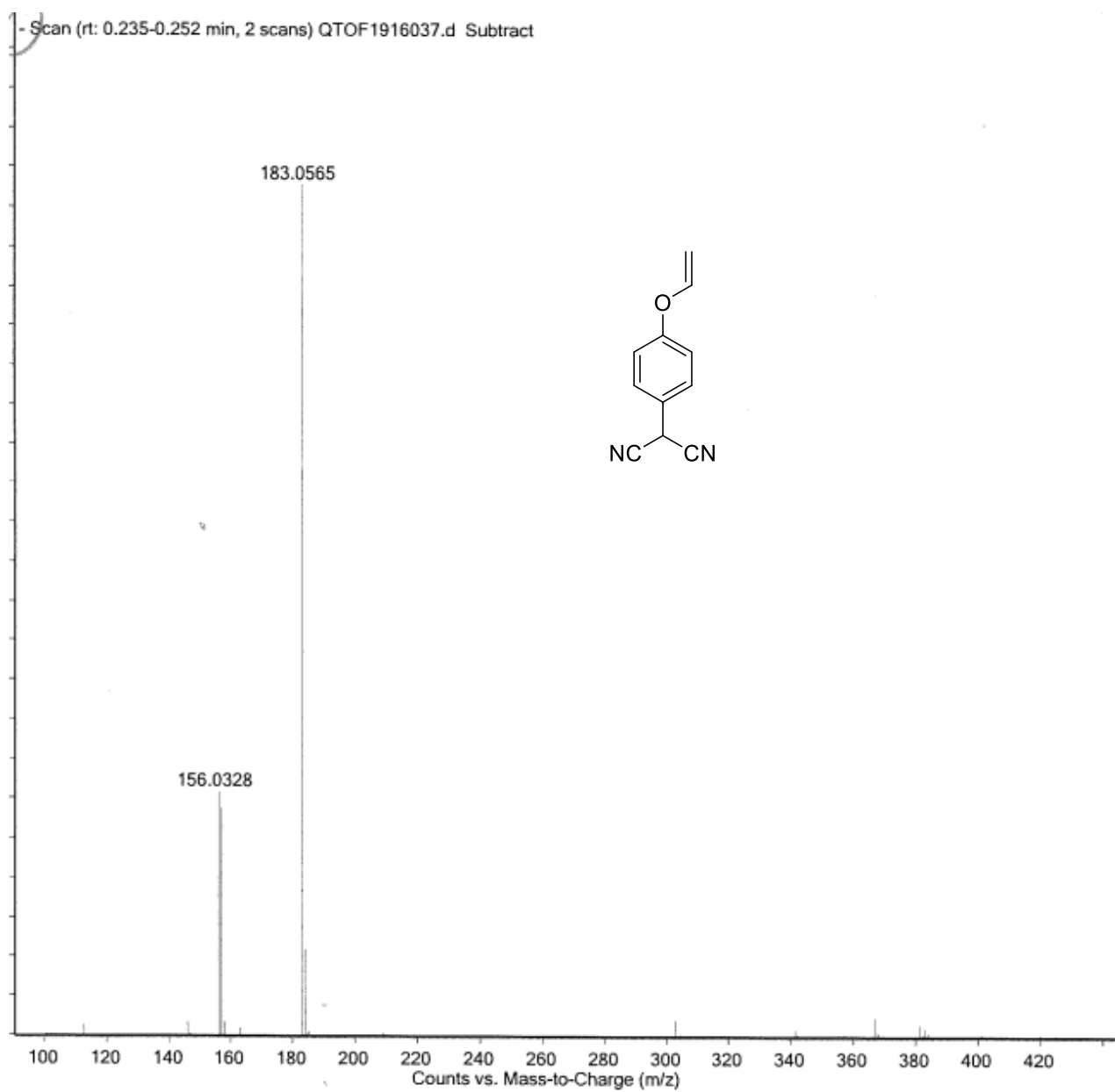
High Resolution Mass Spectra:

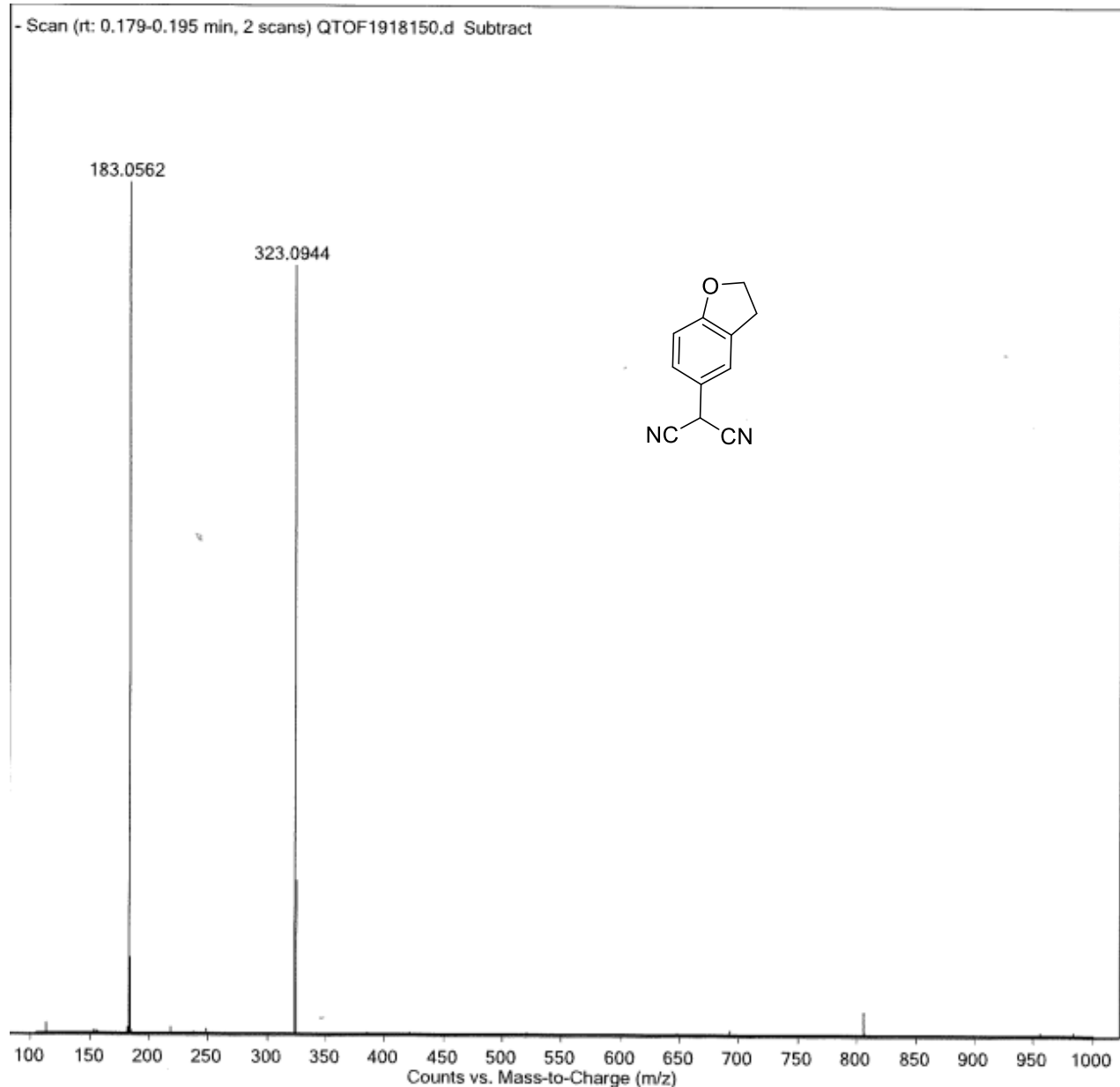


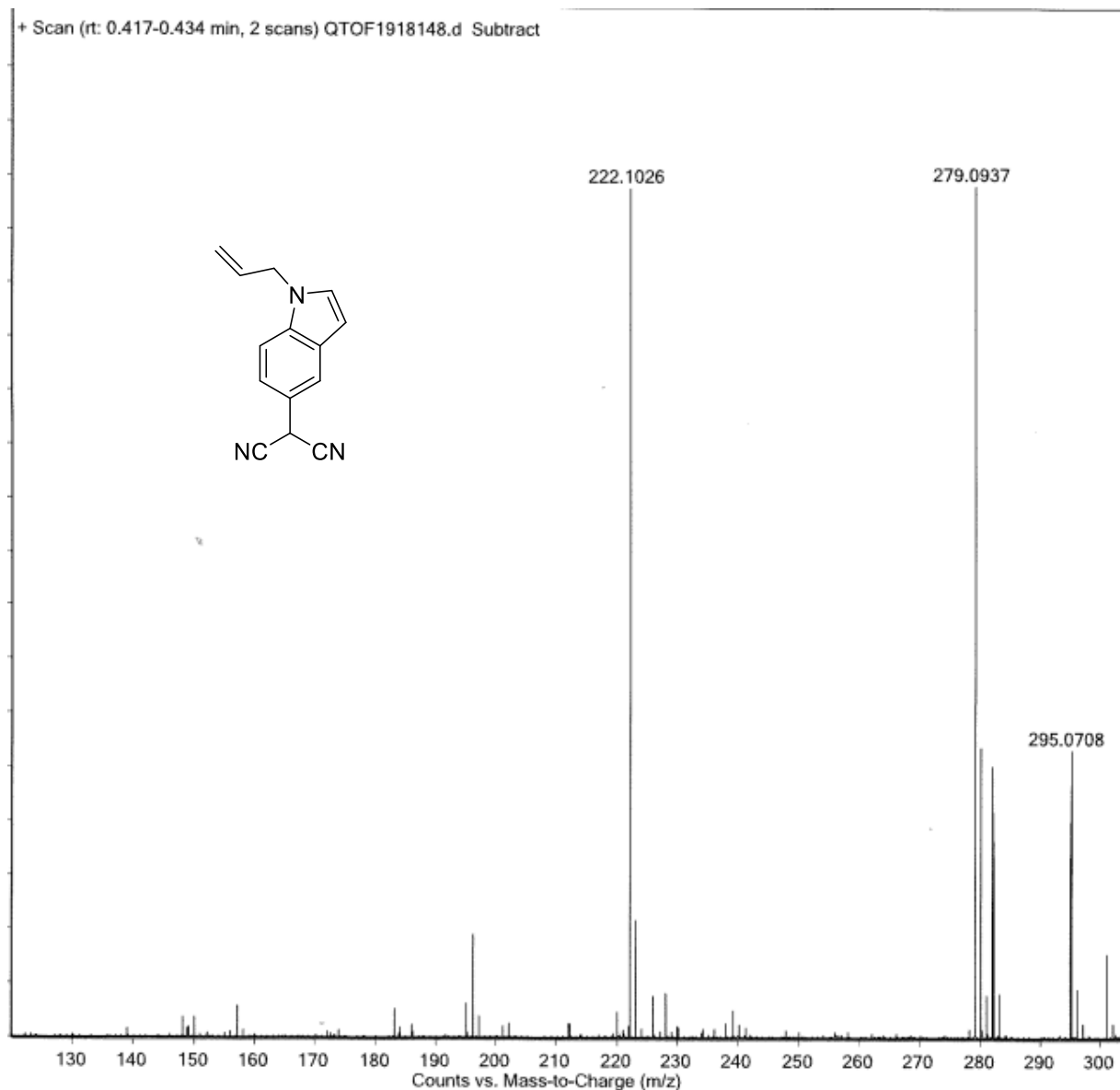




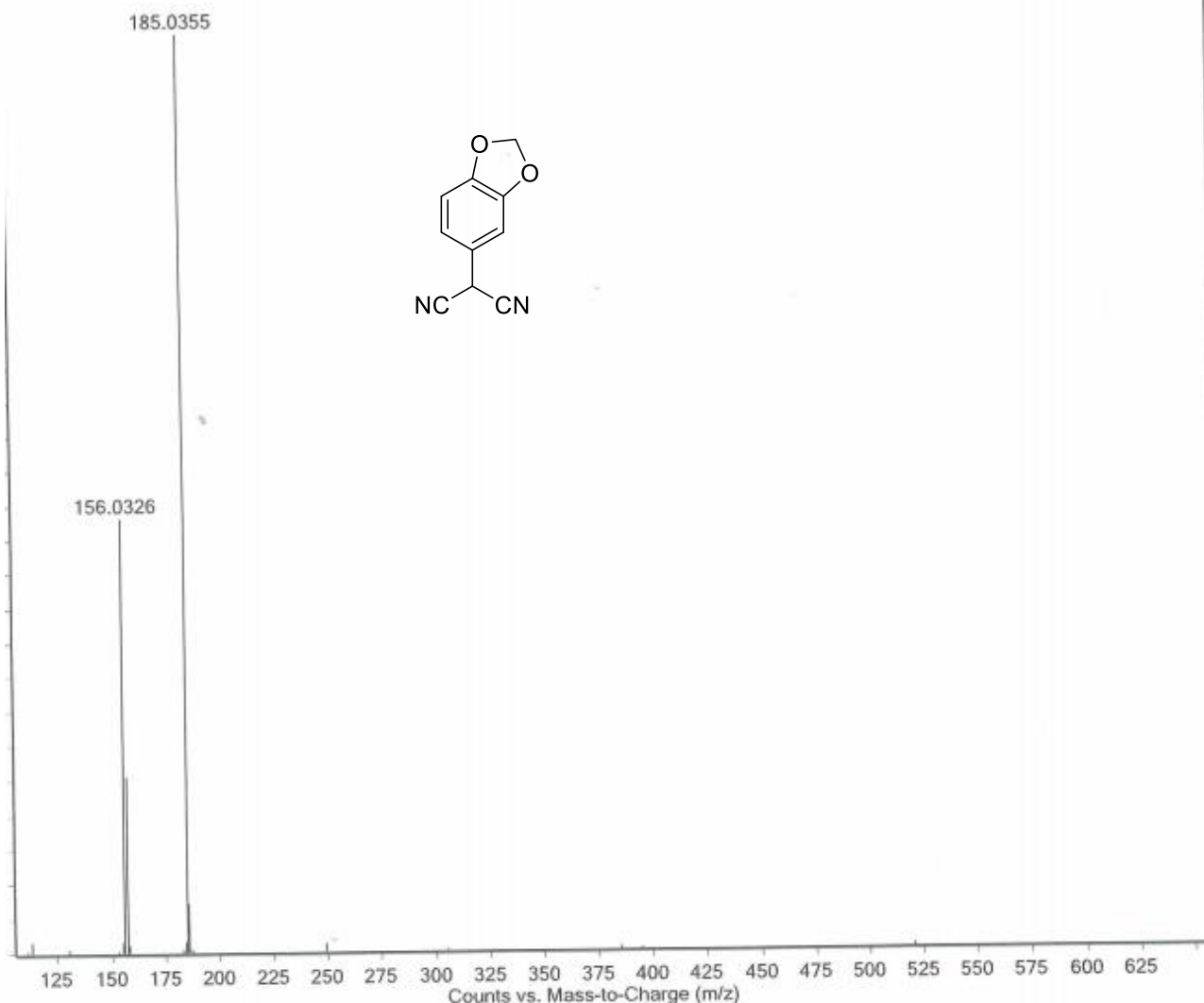


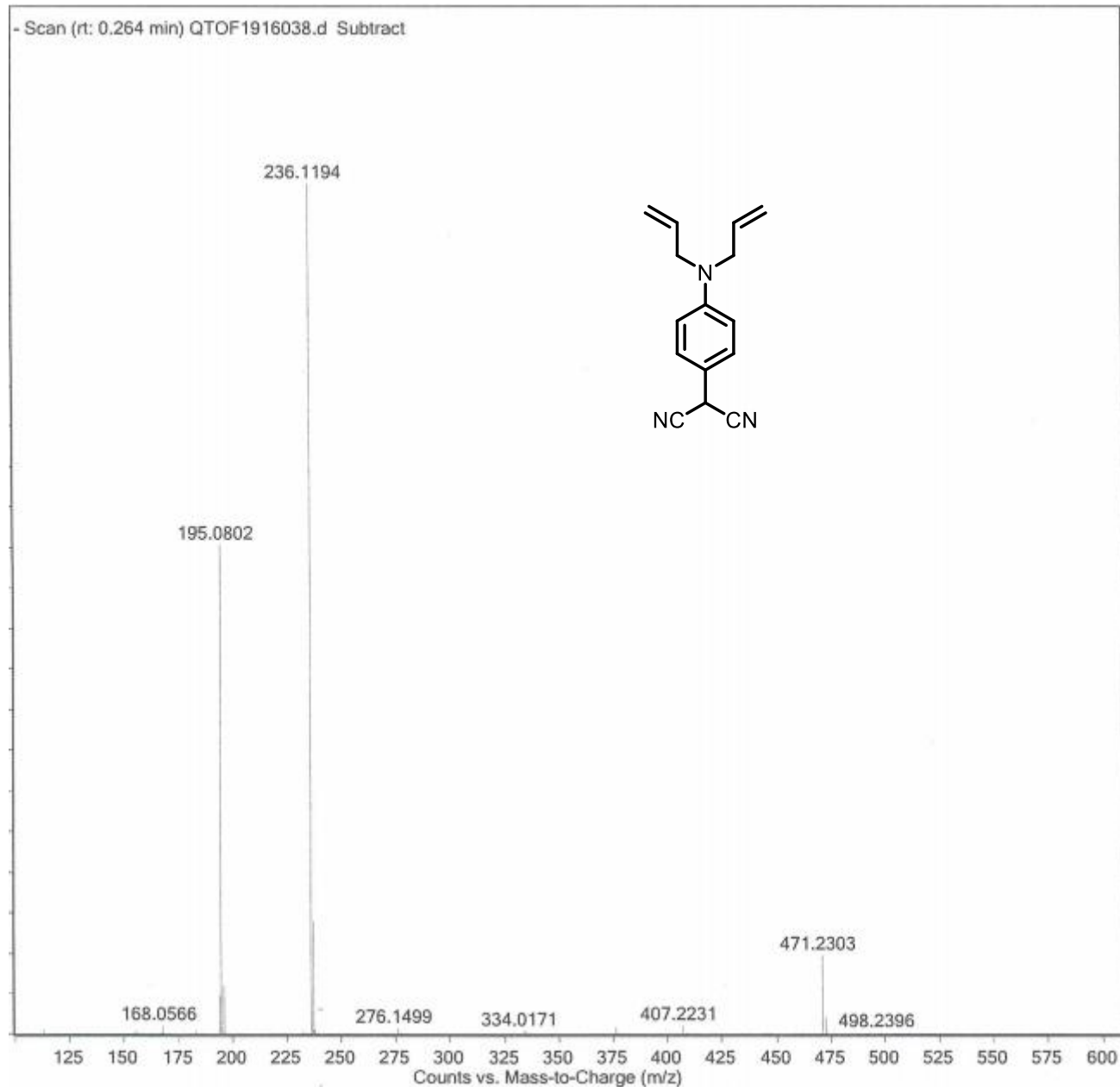


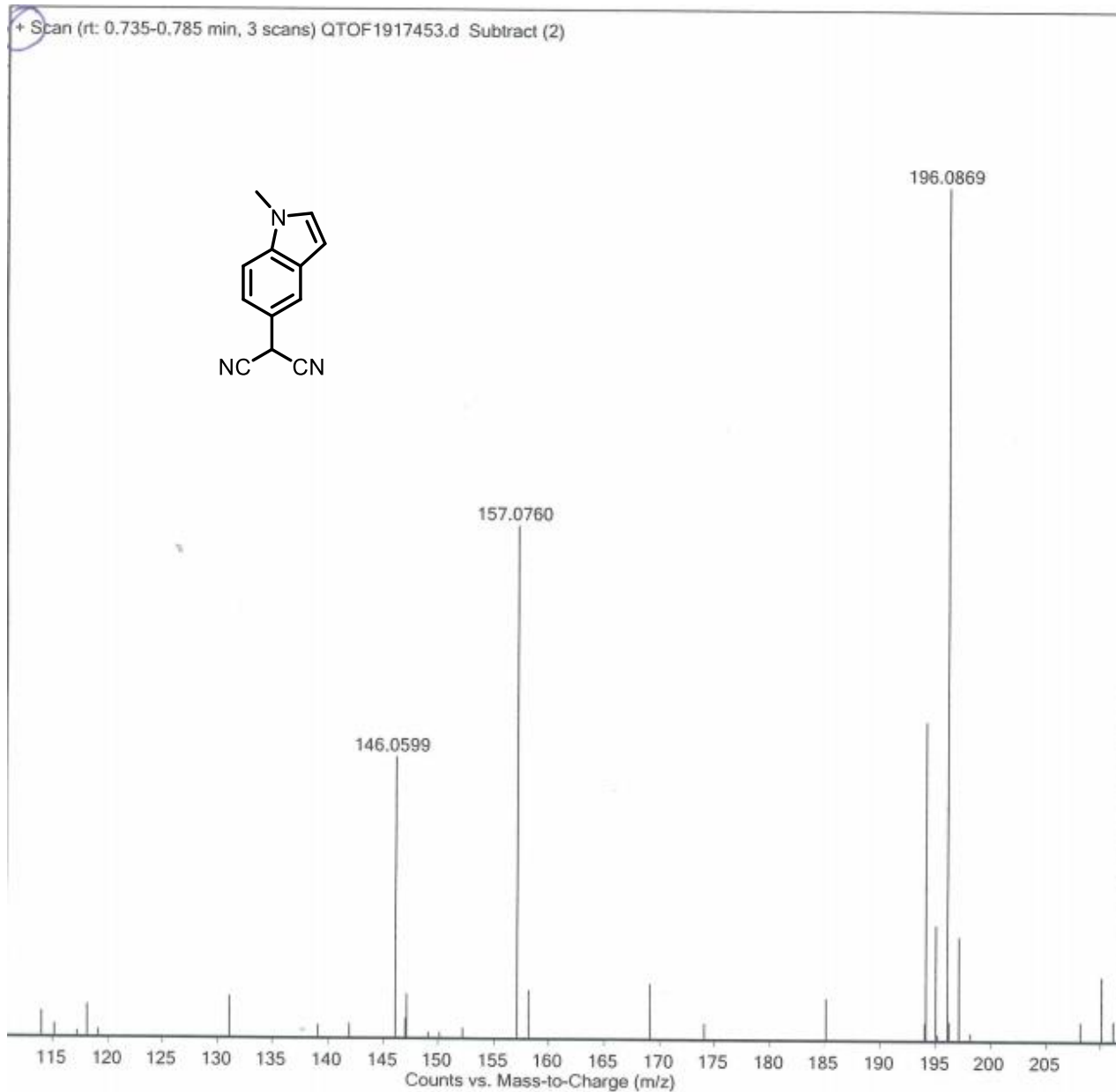


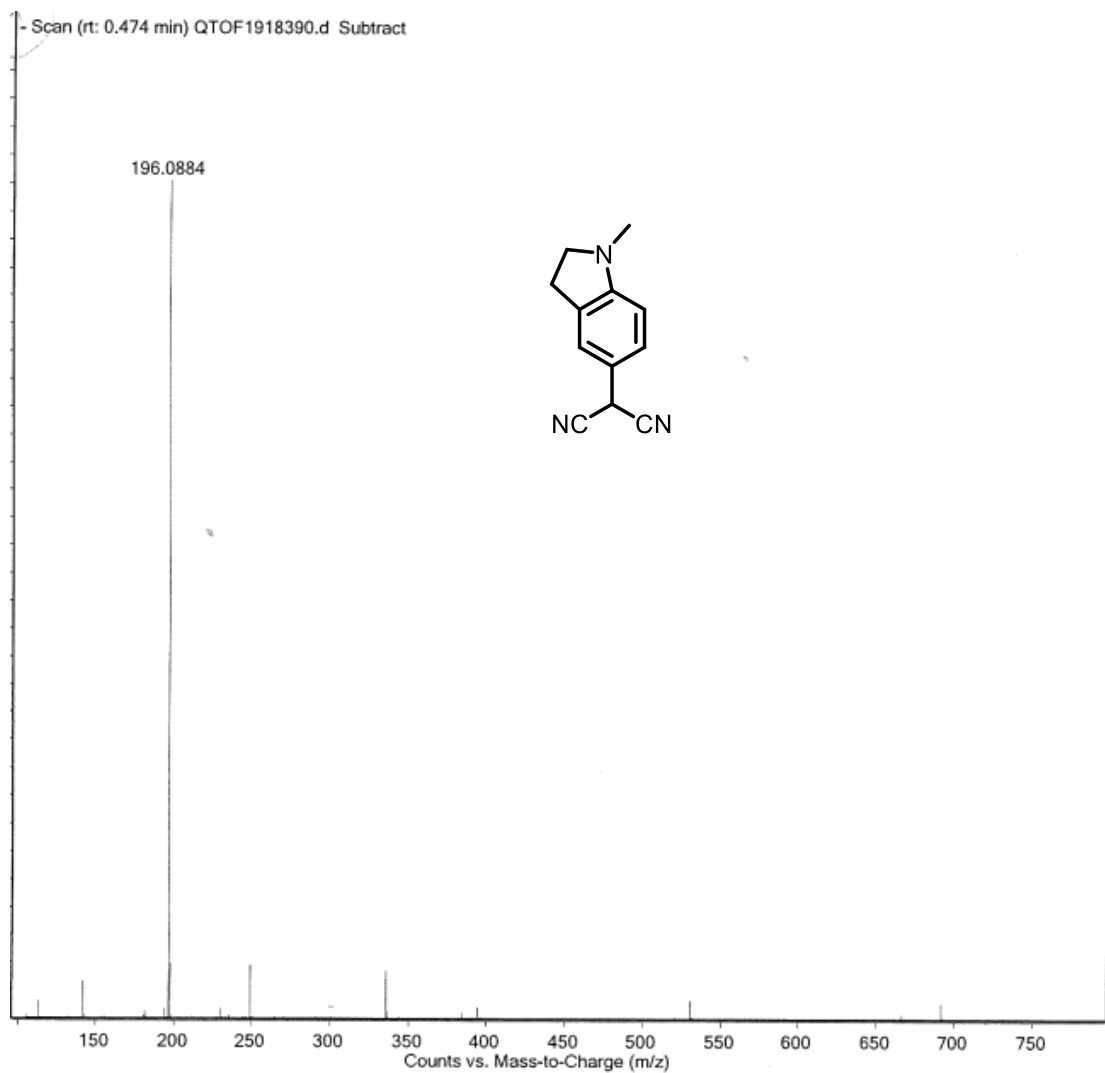


- Scan (rt: 0.233 min) QTOF1917700.d Subtract



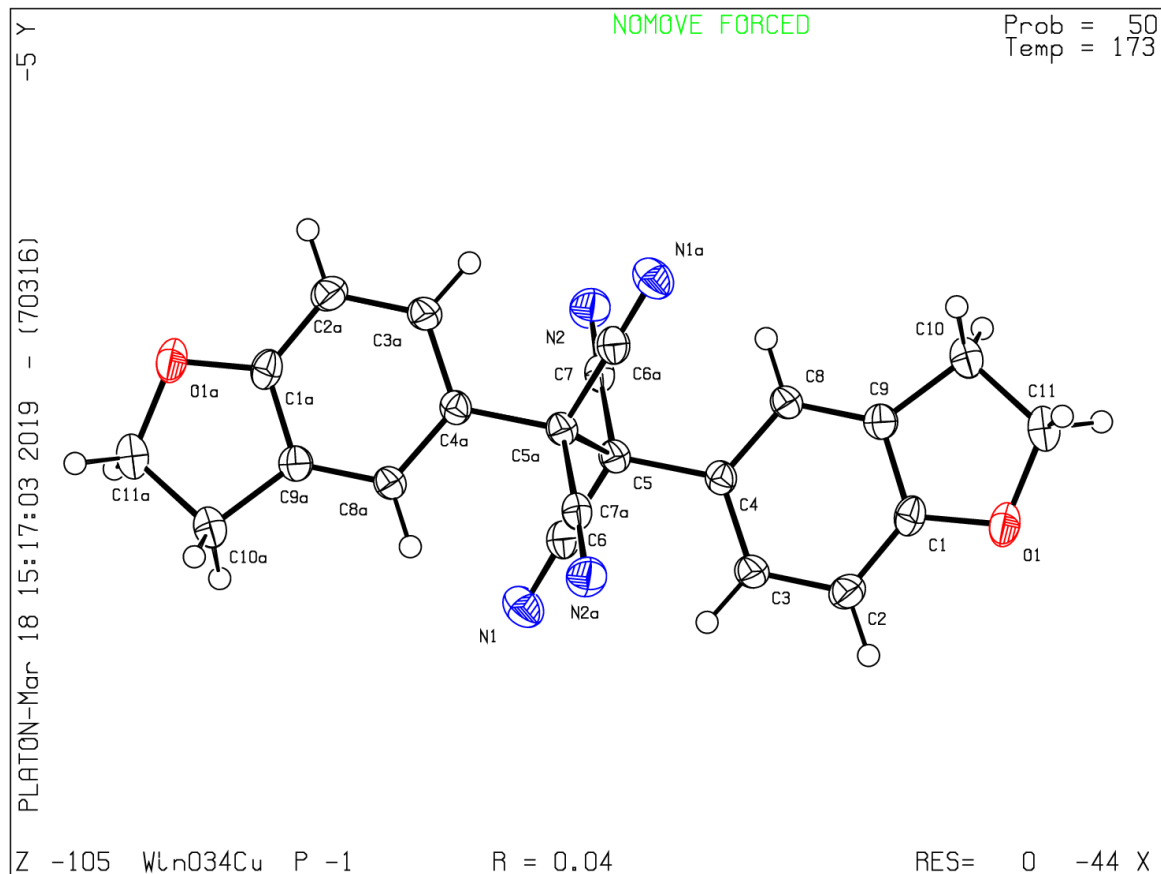






Crystallographic Ellipsoid Plots:

Compound 4 CIF



Datablock: Win034Cu (Benzofuran)

Bond precision: C-C = 0.0020 Å Wavelength=1.54178
 Cell: a=7.2535(2) b=7.5984(2) c=9.1524(2)
 alpha=73.700(1) beta=88.894(2) gamma=65.047(2)

Temperature: 173 K

	Calculated	Reported
Volume	436.11(2)	436.11(2)
Space group	P -1	P -1
Hall group	-P 1	-P 1
Moiety formula	C22 H14 N4 O2	?
Sum formula	C22 H14 N4 O2	C22 H14 N4 O2
Mr	366.37	366.37
Dx,g cm-3	1.395	1.395
Z	1	1
Mu (mm-1)	0.754	0.754
F000	190.0	190.0
F000'	190.58	
h,k,lmax	8,9,10	8,8,10
Nref	1532	1477
Tmin,Tmax	0.913,0.970	0.860,0.970
Tmin'	0.913	

Correction method= # Reported T Limits: Tmin=0.860 Tmax=0.970

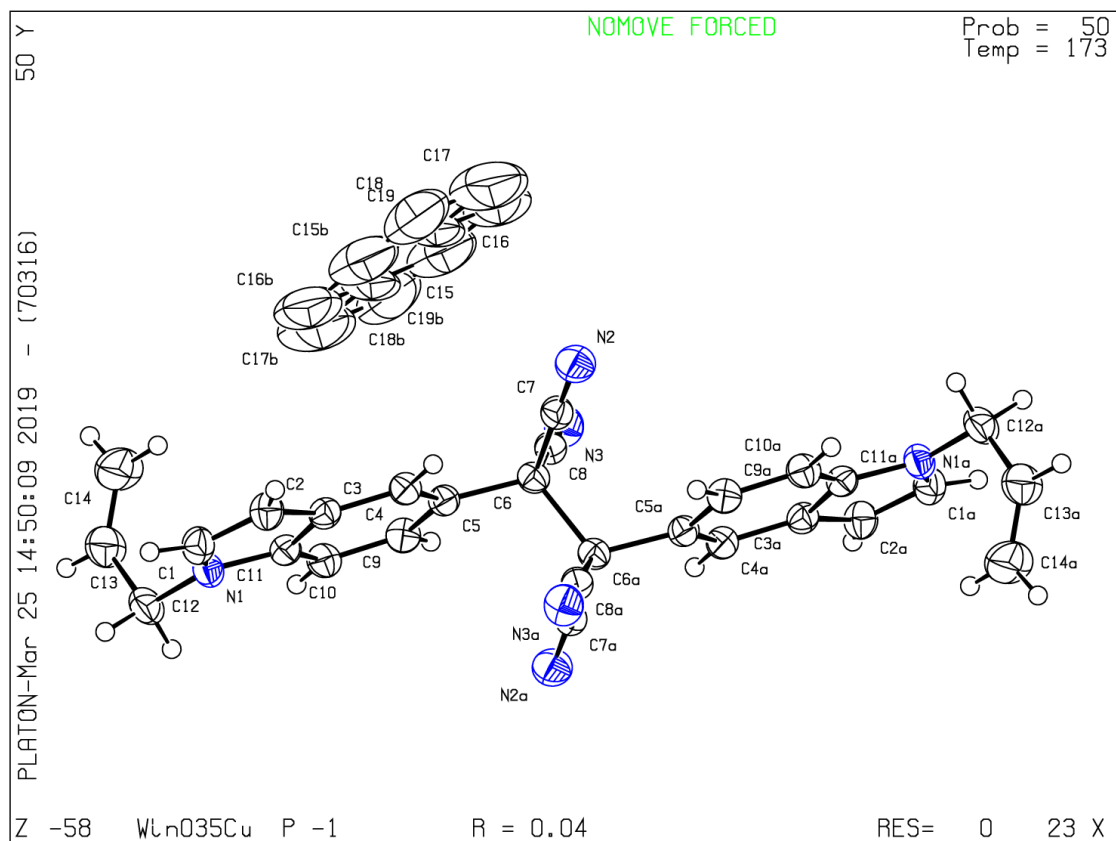
AbsCorr = MULTI-SCAN

Data completeness= 0.964 Theta(max)= 66.470

R(reflections)= 0.0380(1334) wR2(reflections)= 0.1427(1477)

S = 1.221 Npar= 127

Compound 9 CIF



Datablock: Win035Cu (Allyl Indole)

Bond precision: C-C = 0.0021 Å Wavelength=1.54178
 Cell: a=7.6280(3) b=10.0861(3) c=10.2848(3)
 alpha=74.527(2) beta=74.067(2) gamma=76.732(2)

Temperature: 173 K

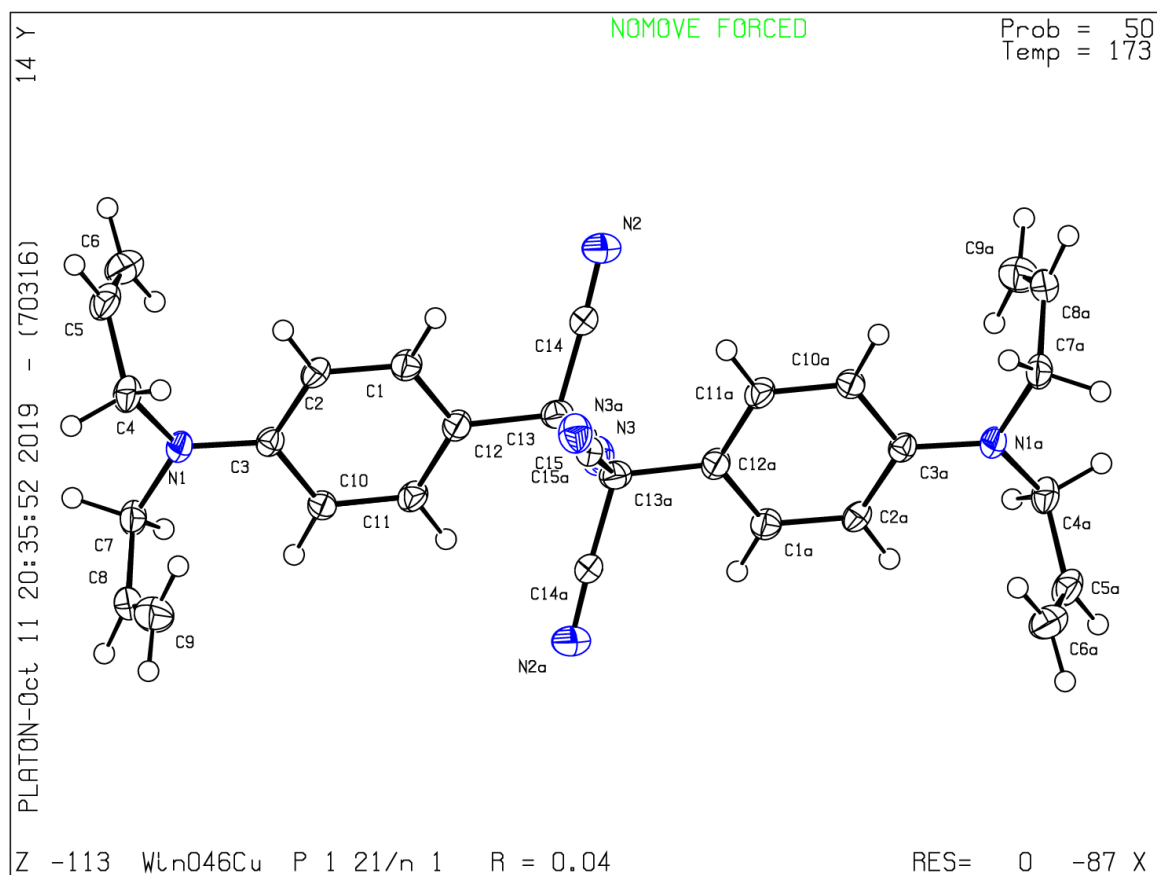
	Calculated	Reported
Volume	722.80(4)	722.80(4)
Space group	P -1	P -1
Hall group	-P 1	-P 1
Moiety formula	C28 H20 N6, C7 H8	?
Sum formula	C35 H20 N6	C35 H28 N6
Mr	524.57	532.63
Dx,g cm-3	1.205	1.224
Z	1	1
Mu (mm-1)	0.581	0.581
F000	272.0	280.0
F000'	272.76	
h,k,lmax	8,11,11	8,11,11
Nref	2297	2248
Tmin,Tmax	0.926,0.977	0.670,0.750
Tmin'	0.895	

Correction method= # Reported T Limits: Tmin=0.670 Tmax=0.750

AbsCorr = MULTI-SCAN

Data completeness= 0.979	Theta(max)= 62.380
R(reflections)= 0.0447(1987)	wR2(reflections)= 0.1507(2248)
S = 0.611	Npar= 199

Compound 7 CIF



Datablock: Win046Cu (Diallylamino)

Bond precision: C-C = 0.0018 Å Wavelength=1.54184
 Cell: a=7.9528(7) b=9.0316(17) c=18.0753(17)
 alpha=90 beta=94.632(3) gamma=90

Temperature: 173 K

	Calculated	Reported
Volume	1294.1(3)	1294.0(3)
Space group	P 21/n	P 1 21/n 1
Hall group	-P 2yn	-P 2yn
Moiety formula	C ₃₀ H ₂₈ N ₆	?
Sum formula	C ₃₀ H ₂₈ N ₆	C ₃₀ H ₂₈ N ₆
Mr	472.58	472.58
Dx,g cm ⁻³	1.213	1.213
Z	2	2
Mu (mm ⁻¹)	0.580	0.580
F000	500.0	500.0
F000'	501.34	
h,k,lmax	9,10,21	9,10,21
Nref	2202	2197
Tmin,Tmax	0.821,0.917	0.810,0.920
Tmin'	0.821	

Correction method= # Reported T Limits: Tmin=0.810 Tmax=0.920

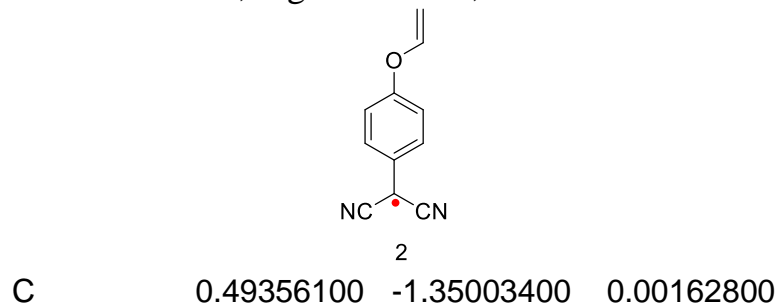
AbsCorr = MULTI-SCAN

Data completeness= 0.998 Theta(max)= 65.100

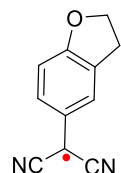
R(reflections)= 0.0396(2125) wR2(reflections)= 0.1068(2197)

S = 1.012 Npar= 164

XYZ Coordinates for Radicals, Sigma Dimers, and Pimers of all new compounds:



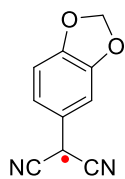
C	1.06588300	-0.05371700	0.01399400
C	0.20008300	1.06235400	0.04097200
C	-1.17327000	0.89890900	0.04772900
C	-1.71423000	-0.39255600	0.01640300
C	-0.87335700	-1.51541600	0.00319200
H	1.13933000	-2.22233600	-0.01437500
H	0.61775300	2.06384500	0.07012100
H	-1.82062100	1.76660000	0.10213000
H	-1.32084800	-2.50258700	-0.01210100
O	-3.04540100	-0.64430500	0.03483800
C	-3.92047500	0.34002300	-0.36011400
H	-3.58587900	0.93803800	-1.20478900
C	-5.10828100	0.46769700	0.21503200
H	-5.81165800	1.19831700	-0.16413300
H	-5.39923400	-0.15723900	1.05182500
C	2.48908100	0.12293600	0.00591500
C	3.37116800	-0.98586800	-0.01252900
C	3.07177500	1.41469200	0.01556400
N	4.07126800	-1.91519400	-0.02778900
N	3.51912300	2.48886200	0.02291900



4

C	-0.38137400	-1.49481700	-0.01223800
C	-0.83401300	-0.14958600	-0.00769300
C	0.12219700	0.90291900	-0.01820900
C	1.45913200	0.59344900	-0.02445700
C	1.87210400	-0.74666600	-0.02186500
C	0.96624400	-1.80606200	-0.02008100

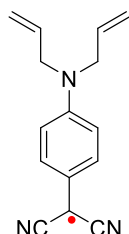
H	-1.11284600	-2.29655200	-0.00532300
H	-0.21057800	1.93666700	-0.02397500
H	1.31226800	-2.83279000	-0.01984500
C	-2.23478200	0.14224600	0.00556100
C	-2.70915900	1.47818900	0.01224700
C	-3.20731300	-0.88919000	0.01240900
N	-3.06481600	2.58616200	0.01785900
N	-3.98271500	-1.75674900	0.01755600
C	2.69339700	1.45728800	-0.07833100
H	2.77899800	1.95483100	-1.04953700
H	2.70623900	2.22737800	0.69630200
C	3.81247100	0.41363100	0.12912900
H	4.61947700	0.48481800	-0.60037100
H	4.23285000	0.45463800	1.13778800
O	3.20661100	-0.89291100	-0.03022100



5

C	-0.35217900	-1.49146200	-0.00473700
C	-0.80004100	-0.14678600	-0.00591800
C	0.14523800	0.92129600	-0.01559600
C	1.46531600	0.57597300	-0.01888300
C	1.89370300	-0.75820500	-0.01549600
C	1.00213200	-1.81385200	-0.01112100
H	-1.08537000	-2.29072200	0.00306800
H	-0.16952100	1.95845400	-0.02325900
H	1.34307800	-2.84179000	-0.01260500
C	-2.20226800	0.13836100	0.00269000
C	-2.68362100	1.47159800	0.00262900

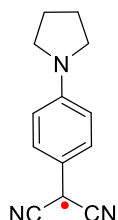
C	-3.17043400	-0.89751100	0.01230300
N	-3.04748900	2.57677800	0.00267100
N	-3.94434300	-1.76613200	0.02036200
C	3.69188700	0.55176300	0.09270700
H	4.41185900	0.77069800	-0.69703600
H	4.12636400	0.68827600	1.08904900
O	3.24420000	-0.80135300	-0.03996600
O	2.55305200	1.39304000	-0.05402200



7

C	-1.23161700	1.20869800	0.18646000
C	-1.96541900	-0.00006200	0.10334800
C	-1.23140200	-1.20873900	0.18609100
C	0.13308500	-1.21153900	0.35188800
C	0.86530600	0.00012300	0.45765800
C	0.13288400	1.21167400	0.35224900
H	-1.75476600	2.15694900	0.11070800
H	-1.75440600	-2.15704400	0.11001100
H	0.64078500	-2.16534500	0.38287100
H	0.64039700	2.16556600	0.38361100

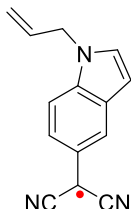
C	-3.38087500	-0.00017900	-0.06904900
C	-4.11273900	1.21120000	-0.15670000
C	-4.11250300	-1.21166200	-0.15716700
N	-4.68297800	2.22337800	-0.22505500
N	-4.68256900	-2.22391000	-0.22592800
N	2.22063600	0.00020600	0.67462500
C	2.96986600	1.25123600	0.73605500
H	3.93802400	1.01946100	1.19009600
H	2.47452200	1.95145400	1.41878600
C	2.97002500	-1.25071100	0.73620700
H	2.47464300	-1.95092500	1.41890800
H	3.93810100	-1.01879000	1.19034700
C	3.19708900	1.90104700	-0.60669600
H	3.55877300	1.24487600	-1.39676100
C	3.19755500	-1.90083400	-0.60635800
H	3.55896900	-1.24503800	-1.39687200
C	3.00336000	-3.19363900	-0.85251000
H	2.63367100	-3.86993800	-0.08425600
H	3.20706500	-3.62406400	-1.82721100
C	3.00218800	3.19361600	-0.85345800
H	2.63219400	3.87004900	-0.08546900
H	3.20557900	3.62370400	-1.82837200



8

C	-1.04295100	-1.21087300	-0.04835800
C	0.33075600	-1.21464800	-0.04936100
C	1.06551600	-0.00011400	-0.00042300
C	0.33093300	1.21441700	0.04901000
C	-1.04283800	1.21073200	0.04844400
H	-1.57447900	-2.15652600	-0.09174100
H	0.85138800	2.16307700	0.10242100
H	-1.57422100	2.15643900	0.09226000
C	3.23540700	-1.21299700	0.05737800
H	2.87856300	-1.88329900	0.84602800
H	3.18881200	-1.75464800	-0.89799500
C	3.23503600	1.21295800	-0.05778400
H	3.18696900	1.75393300	0.89797300
H	2.87890600	1.88364600	-0.84637200
N	2.42217100	-0.00019900	-0.00092100
C	-1.78057000	-0.00000500	0.00011900

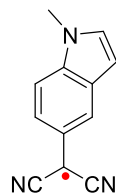
C	-3.20572100	0.00004000	0.00026800
C	-3.94316500	-1.21046900	-0.04081600
C	-3.94308200	1.21060400	0.04100300
N	-4.51736000	-2.22221400	-0.07430600
N	-4.51713400	2.22241200	0.07434700
C	4.64479400	-0.68746300	0.33736700
H	4.79399400	-0.57870700	1.41665900
H	5.41830100	-1.35603900	-0.04574000
C	4.64488000	0.68780700	-0.33624900
H	4.79495700	0.57873600	-1.41538400
H	5.41790500	1.35676100	0.04712800
H	0.85121600	-2.16328700	-0.10267000



9

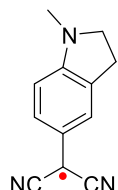
C	0.73515200	-1.19703700	0.27883300
C	1.60277300	-0.08419800	0.05110400
C	1.06422800	1.21099000	-0.08065700
C	-0.31238800	1.38836200	0.01739800
C	-1.14538900	0.26228000	0.24790200
C	-0.62605300	-1.03775200	0.37510100
H	1.16591000	-2.18829100	0.37395700
H	1.71923300	2.05920400	-0.25485300
H	-1.27438500	-1.89219600	0.53284300
C	3.02000100	-0.28993500	-0.04363200
C	3.91153600	0.78855200	-0.26974700
C	3.59464000	-1.57864800	0.08779300
N	4.62083800	1.69223900	-0.45560400
N	4.04263600	-2.64705800	0.19946400
N	-2.43828600	0.70326000	0.32016900
C	-3.61096200	-0.13255400	0.51978800
H	-4.44527000	0.54058500	0.74067200
H	-3.45930000	-0.76065100	1.40479200
C	-3.92771700	-0.98004600	-0.68373100
H	-4.00127600	-0.44880000	-1.63113900
C	-4.11975100	-2.29544600	-0.63245400
H	-4.04140800	-2.84534700	0.30298700

H	-4.36568800	-2.86642600	-1.52154300
C	-2.44508500	2.07490500	0.13165500
H	-3.38182500	2.61418800	0.15347200
C	-1.17551900	2.53496100	-0.05469800
H	-0.88511100	3.56204700	-0.21732400



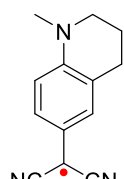
10

C	-0.46365700	-1.38998200	-0.00068800
C	0.90425500	-1.52444700	-0.00175200
C	1.67872400	-0.35173500	-0.00465500
C	1.09185400	0.94111800	-0.00220700
C	-0.29403500	1.06151500	-0.00083700
H	-1.08819100	-2.27731200	0.00081100
H	1.36293100	-2.50755800	0.00049100
H	-0.76300900	2.04059700	0.00061700
N	3.03602900	-0.19893400	-0.01000800
C	-1.08658500	-0.10374000	-0.00059800
C	-2.51850200	-0.00134300	0.00053000
C	-3.34600200	-1.15171700	-0.00196000
C	-3.16978500	1.25749500	0.00432200
N	-4.00361500	-2.11202800	-0.00413200
N	-3.67748700	2.30464100	0.00762100
C	4.00065900	-1.27773500	0.01467700
H	3.81914100	-1.97113800	-0.81130700
H	5.00136500	-0.85952300	-0.09710100
H	3.94944000	-1.82430700	0.96131800
C	2.17430200	1.88558600	-0.00200500
H	2.09937600	2.96263600	-0.00227000
C	3.32535300	1.15449300	-0.00495200
H	4.35496500	1.48380600	-0.00617700

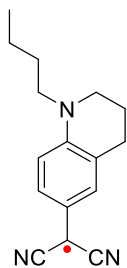


11

C	0.55115400	-1.40503700	-0.06391300
C	-0.82169400	-1.56014000	-0.09821900
C	-1.62160500	-0.40826300	-0.11084000
C	-1.03362500	0.88084600	-0.08262500
C	0.32270300	1.03208300	-0.04463700
H	1.18312300	-2.28761200	-0.04925000
H	-1.25764200	-2.55266500	-0.10622000
H	0.77080500	2.02102600	-0.01751100
N	-2.98436800	-0.31165100	-0.15138100
C	1.16098100	-0.12334700	-0.03308300
C	2.57884200	0.00753900	0.01622600
C	3.42823800	-1.12850300	0.02824100
C	3.19884500	1.28242700	0.05790500
N	4.09777300	-2.08020800	0.03726600
N	3.67289900	2.34473200	0.09227000
C	-3.86169300	-1.41388900	0.16338700
H	-3.85031100	-1.65515000	1.23687800
H	-4.88205400	-1.15321600	-0.12621300
H	-3.56995000	-2.30193900	-0.40169500
C	-3.38758300	1.05627100	0.19003200
H	-3.63456300	1.11458000	1.26161900
H	-4.27217900	1.34626400	-0.38280100
C	-2.14296300	1.90377400	-0.13671100
H	-2.00512600	2.72682100	0.56730700
H	-2.21583300	2.32922100	-1.14377800

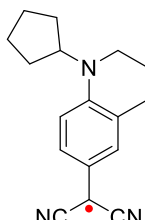


C	0.52586900	0.94811200	-0.06399700
C	-0.83895700	0.79287500	-0.08196800
C	-1.40026800	-0.51975600	-0.01984400
C	-0.51440000	-1.62533400	0.04334900
C	0.84881900	-1.44892700	0.04946600
H	0.93676600	1.95365200	-0.10542800
H	-0.90521000	-2.63371300	0.09465400
H	1.49777700	-2.31776600	0.09886800
C	-3.68202500	0.41775100	-0.10592600
H	-3.95628500	0.59335800	-1.15771100
H	-4.59517600	0.14131100	0.42944100
C	-3.31318500	-2.03973900	-0.13189500
H	-2.94130400	-2.55590600	-1.02510300
H	-3.08374500	-2.65030700	0.74906100
H	-4.39732400	-1.95987900	-0.21522200
N	-2.75412900	-0.70586200	-0.01576800
C	1.41831800	-0.15343200	-0.00408200
C	2.82896200	0.03902600	0.00377100
C	3.39519400	1.33827500	-0.04965500
C	3.72352900	-1.05998900	0.06281800
N	3.82441400	2.41915900	-0.09441600
N	4.42979600	-1.98366400	0.11126200
C	-1.75378800	1.98939300	-0.17326900
H	-1.92425000	2.24082200	-1.22849900
H	-1.27588700	2.85916100	0.28605000
C	-3.09020700	1.68361600	0.49415300
H	-3.79624300	2.50741500	0.35736600
H	-2.94684700	1.54320000	1.57144100

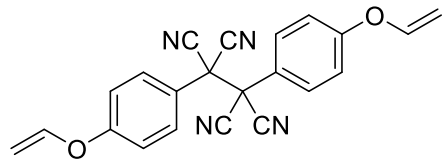


13

C	1.72976000	1.04221100	0.12497000
C	2.10705000	-0.31402800	-0.04482600
C	1.07270900	-1.24512000	-0.30765800
C	-0.23724100	-0.84289100	-0.40061100
C	-0.60936300	0.51784800	-0.23918900
C	0.42377400	1.46434100	0.04558800
H	2.50147200	1.77991800	0.32964000
H	1.31621400	-2.29490200	-0.43838700
H	-0.98874100	-1.59718100	-0.59442100
C	0.08006700	2.91904900	0.26170000
H	-0.04077200	3.10844300	1.33646100
H	0.90676200	3.54922100	-0.07830000
C	-1.21288500	3.27860300	-0.46037100
H	-1.06492900	3.23410600	-1.54516800
H	-1.53155700	4.29403500	-0.20876300
C	-2.30037700	2.29369600	-0.06092800
H	-2.52041100	2.39700300	1.01301200
H	-3.22540800	2.50560100	-0.60453300
N	-1.91179500	0.92129000	-0.37035100
C	3.46757200	-0.72247900	0.04600700
C	4.50128200	0.21270100	0.30695200
C	3.84054200	-2.08041800	-0.12307200
N	4.11043400	-3.20334800	-0.26650300
N	5.32312500	1.00814800	0.52221500
C	-2.99318800	-0.04419700	-0.50536800
H	-2.70570900	-0.79959800	-1.24098200
H	-3.85047600	0.48265400	-0.93739000
C	-3.40632600	-0.68976100	0.82203300
H	-2.52822600	-1.15750700	1.28447300
H	-3.73471100	0.10136700	1.50653600
C	-4.52024300	-1.72941700	0.66720500
H	-4.85024100	-2.03255700	1.66687100
H	-5.39124300	-1.26423000	0.18695700
C	-4.10241500	-2.97415900	-0.11854100
H	-4.89947500	-3.72278800	-0.11694100
H	-3.87612600	-2.74661800	-1.16520100
H	-3.21308000	-3.43546600	0.32526500



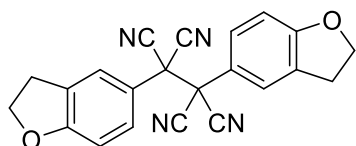
C	1.90629500	1.02753200	0.14175300
C	2.39834500	-0.28560400	-0.06447900
C	1.44277900	-1.29368800	-0.33939000
C	0.10216000	-1.00373100	-0.40504300
C	-0.38975500	0.31383700	-0.20306100
C	0.56769900	1.33549300	0.08946300
H	2.61388300	1.82347200	0.35963500
H	1.77252200	-2.31477000	-0.50397500
H	-0.57806000	-1.81640800	-0.62014300
C	0.10289300	2.74664800	0.34603300
H	-0.07123300	2.88846300	1.42093800
H	0.88382800	3.45492000	0.05575000
C	-1.18789500	3.00973400	-0.41453300
H	-0.99948100	2.97908100	-1.49375700
H	-1.59398100	3.99709500	-0.17743800
C	-2.22050200	1.95485500	-0.05330300
H	-2.51628600	2.06751500	1.00176900
H	-3.11359800	2.10794000	-0.66053800
N	-1.72982700	0.60032300	-0.29829600
C	3.78945500	-0.57595200	0.00368100
C	4.74131100	0.43933000	0.27721400
C	4.27933800	-1.89133000	-0.20059100
N	4.64733300	-2.98189900	-0.37267600
N	5.49418600	1.29734200	0.50415500
C	-2.70499100	-0.49170400	-0.28872000
H	-2.38826200	-1.22166200	-1.04221600
C	-2.85788200	-1.19843500	1.07312600
H	-2.00594900	-1.83907300	1.31309000
H	-2.91018600	-0.43040300	1.85358800
C	-4.19121800	-1.97317300	0.96623500
H	-4.02459600	-3.05093700	0.89230600
H	-4.80540500	-1.80931300	1.85554300
C	-4.89191800	-1.43168400	-0.30791600
H	-5.96294700	-1.27147800	-0.16403100
H	-4.78153500	-2.14275200	-1.13386900
C	-4.15255900	-0.13023500	-0.64072800
H	-4.52297800	0.66804600	0.01206600
H	-4.27890000	0.18854600	-1.67944500



2 σ

C	-2.49276600	-1.48729800	0.36577300
C	-1.89932700	-0.24226400	0.59806200
C	-2.69531900	0.90182900	0.62645700
C	-4.06541100	0.81531700	0.40893700
C	-4.64180500	-0.42807700	0.15140100
C	-3.85628800	-1.58152700	0.14193200
H	-1.89352200	-2.39189000	0.35084600
H	-2.25741000	1.87436300	0.82632200
H	-4.67653300	1.70879500	0.46389700
H	-4.32631100	-2.53981700	-0.04588500
O	-5.97590000	-0.59947700	-0.05781600
C	-6.70357200	0.45305600	-0.55346800
H	-6.17066900	1.08327500	-1.26248400
C	-7.98003600	0.61931300	-0.23275500
H	-8.54868200	1.41344200	-0.69993500
H	-8.47357000	-0.03452200	0.47731700
C	-0.37857500	-0.12663700	0.75587000
C	0.18192900	-1.34810700	1.36394400
C	-0.02519700	1.01163400	1.62522600
N	0.60730800	-2.32408600	1.81427700
N	0.23357300	1.92457100	2.28543500
C	2.47097200	1.47462300	-0.29198700
C	1.88687700	0.22384700	-0.51772200
C	2.69135500	-0.91435100	-0.53652900
C	4.06207600	-0.81549200	-0.32592600
C	4.63423100	0.43796100	-0.11154600
C	3.83652900	1.58323300	-0.09098700
H	1.86416600	2.37417500	-0.27689700
H	2.25732700	-1.89486500	-0.70331900
H	4.66876900	-1.71341800	-0.30751500
H	4.30097700	2.54753000	0.07909800
O	5.96237100	0.62285700	0.11936600
C	6.85010900	-0.32660700	-0.32054300
H	6.60447900	-0.77510500	-1.28102800
C	7.95645200	-0.59813500	0.35909900
H	8.67908800	-1.29409000	-0.04808100
H	8.16043900	-0.12551300	1.31320300
C	0.36664000	0.09731900	-0.67216500
C	-0.20162200	1.31307800	-1.28504700

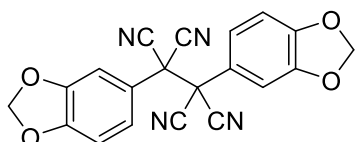
C	0.02008100	-1.04478000	-1.53935400
N	-0.63360100	2.28332100	-1.74148600
N	-0.23361200	-1.95909300	-2.19965100



4 σ

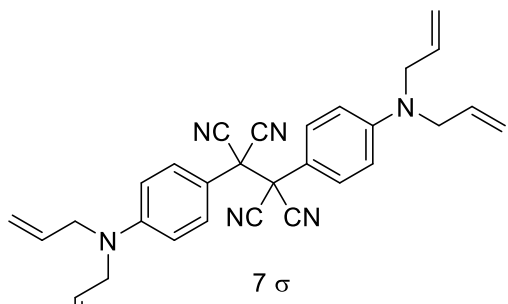
C	2.38378300	1.62692600	0.36428100
C	1.89413300	0.32950700	0.54005500
C	2.76477200	-0.76868900	0.47426000
C	4.10113100	-0.54345300	0.21330200
C	4.56911700	0.75730200	0.02885800
C	3.73197100	1.86034500	0.10623300
H	1.70950300	2.47536600	0.42008100
H	2.40020000	-1.78020500	0.62439500
H	4.11315500	2.86452300	-0.03431300
C	0.39136400	0.09590800	0.73012900
C	0.14532000	-1.10220800	1.55579700
C	-0.24065800	1.24135500	1.41240100
N	-0.02455200	-2.05960100	2.18109400
N	-0.72700800	2.15641800	1.92484000
C	5.28005800	-1.47840200	0.12358700
H	5.54292400	-1.87052000	1.11185600
H	5.10401100	-2.32703800	-0.54152600
C	6.36727900	-0.53213200	-0.42740400
H	7.33135900	-0.62761300	0.07247600
H	6.50471900	-0.66152700	-1.50572300
O	5.89762300	0.81776200	-0.20787400
C	-2.39307400	-1.62841800	-0.31107800
C	-1.88888900	-0.33804700	-0.49654700
C	-2.74736800	0.77016800	-0.44023700
C	-4.08898700	0.56079300	-0.19478000
C	-4.57428500	-0.73378700	-0.01273400
C	-3.74665100	-1.84557600	-0.06588000
H	-1.72814600	-2.48477400	-0.35889700
H	-2.36841800	1.77783300	-0.57995500
H	-4.14051300	-2.84486800	0.07454000
C	-0.38359700	-0.11972700	-0.68573500
C	-0.12667500	1.07207200	-1.51702500
C	0.23981400	-1.27383700	-1.36114600
N	0.05120700	2.02447500	-2.14770800
N	0.72039500	-2.19537300	-1.86740300
C	-5.23871400	1.51771100	-0.01137600

H	-5.14772400	2.04829000	0.94239600
H	-5.31375400	2.26278400	-0.80680000
C	-6.43756400	0.54639400	-0.01541900
H	-7.17174700	0.74644400	0.76519700
H	-6.93945900	0.52789200	-0.98823200
O	-5.90388300	-0.77692000	0.22180900

5 σ

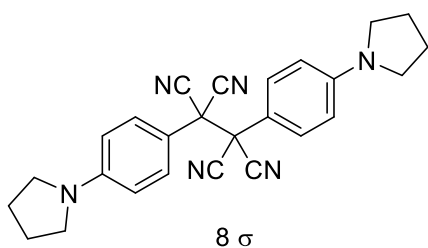
C	2.38894200	1.62260300	0.34719700
C	1.89953600	0.33068700	0.52825300
C	2.75338200	-0.78849900	0.46591700
C	4.07615400	-0.53587700	0.20065600
C	4.56418500	0.75431900	0.01255600
C	3.74533800	1.85756500	0.08541200
H	1.71738800	2.47230800	0.40223100
H	2.40049600	-1.80190100	0.61721700
H	4.12894300	2.86100500	-0.05070100
C	0.39441500	0.10743400	0.72763800
C	0.14579000	-1.08602900	1.55876900
C	-0.22308400	1.26011500	1.41031000
N	-0.02772000	-2.03907600	2.18951200
N	-0.69773800	2.17972400	1.92537400
C	6.21290100	-0.67909600	-0.37385800
H	7.10709000	-0.93052000	0.19654200
H	6.33961900	-0.88226800	-1.44469500
O	5.90790800	0.70432000	-0.19145100
O	5.10597300	-1.42532200	0.12435200
C	-0.38659600	-0.10631700	-0.68426100
C	-1.89208000	-0.32847200	-0.48566200
C	0.23035700	-1.25915200	-1.36744800
C	-0.13683000	1.08615600	-1.51653100
C	-2.38236600	-1.61968600	-0.30329000
C	-2.74639100	0.79091100	-0.43126400
N	0.70496700	-2.17754200	-1.88475000
N	0.03817200	2.03736400	-2.14965600
C	-3.74059600	-1.85393200	-0.04974700
H	-1.71101100	-2.46980000	-0.35459400
C	-4.07267300	0.53815100	-0.18387500
H	-2.39041200	1.80498100	-0.57016600
C	-4.56205000	-0.75149900	0.00258000
H	-4.12319400	-2.85619900	0.09729200

O	-5.09058900	1.43391700	-0.05171100
O	-5.89782300	-0.69782100	0.25100500
C	-6.28271200	0.65413500	-0.00243300
H	-6.91550400	1.00841100	0.81165100
H	-6.79465500	0.70883800	-0.97120400



C	-2.65259800	0.10918100	-1.19818800
C	-1.96442300	0.30273000	-0.00000600
C	-2.65265300	0.10922800	1.19815600
C	-3.97973300	-0.28577200	1.20395900
C	-4.67823400	-0.51649700	-0.00005100
C	-3.97967500	-0.28582600	-1.20403700
H	-2.15775100	0.26983500	-2.15084100
H	-2.15786500	0.26997100	2.15082400
H	-4.47133500	-0.39523000	2.16028000
H	-4.47122500	-0.39540500	-2.16037000
C	-0.47757600	0.65909000	0.00001200
C	-0.12829300	1.45816300	-1.19084600
C	-0.12829300	1.45822900	1.19083000
N	0.12831400	2.05995200	-2.14406700
N	0.12829300	2.06012600	2.14398900
N	-5.98548300	-0.96346500	-0.00008700
C	-6.69849500	-1.17425800	-1.25084300
H	-7.57539600	-1.78743800	-1.01926100
H	-6.08565600	-1.76916600	-1.93989700
C	-6.69828500	-1.17513400	1.25064200
H	-6.08500700	-1.76990000	1.93940900
H	-7.57481900	-1.78880300	1.01893700
C	-7.15899800	0.09446300	-1.92691000
H	-7.65569000	0.81947200	-1.28345800
C	-7.15950200	0.09306400	1.92718700
H	-7.65716700	0.81777500	1.28415000
C	-7.00838300	0.34950900	3.22400200
H	-6.50313400	-0.35108100	3.88609900
H	-7.38298600	1.26445300	3.67090900
C	-7.00833200	0.35102500	-3.22375400
H	-6.50401200	-0.34986000	-3.88624700

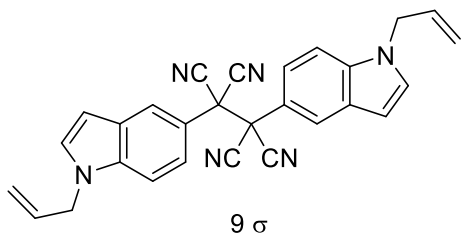
H	-7.38239000	1.26637000	-3.67029600
C	0.47757600	-0.65909000	0.00001200
C	1.96442300	-0.30273000	-0.00000600
C	0.12829300	-1.45816300	-1.19084600
C	0.12829300	-1.45822900	1.19083000
C	2.65259800	-0.10918100	-1.19818800
C	2.65265300	-0.10922800	1.19815600
N	-0.12831400	-2.05995200	-2.14406700
N	-0.12829300	-2.06012600	2.14398900
C	3.97967500	0.28582600	-1.20403700
H	2.15775100	-0.26983500	-2.15084100
C	3.97973300	0.28577200	1.20395900
H	2.15786500	-0.26997100	2.15082400
C	4.67823400	0.51649700	-0.00005100
H	4.47122500	0.39540500	-2.16037000
H	4.47133500	0.39523000	2.16028000
N	5.98548300	0.96346500	-0.00008700
C	6.69849500	1.17425800	-1.25084300
C	6.69828500	1.17513400	1.25064200
H	7.57539600	1.78743800	-1.01926100
H	6.08565600	1.76916600	-1.93989700
C	7.15899800	-0.09446300	-1.92691000
H	6.08500700	1.76990000	1.93940900
H	7.57481900	1.78880300	1.01893700
C	7.15950200	-0.09306400	1.92718700
H	7.65569000	-0.81947200	-1.28345800
C	7.00833200	-0.35102500	-3.22375400
H	7.65716700	-0.81777500	1.28415000
C	7.00838300	-0.34950900	3.22400200
H	6.50401200	0.34986000	-3.88624700
H	7.38239000	-1.26637000	-3.67029600
H	6.50313400	0.35108100	3.88609900
H	7.38298600	-1.26445300	3.67090900



C	2.60243900	1.19980700	0.50864500
C	3.97535200	1.20731900	0.33383900
C	4.70002600	-0.00042400	0.23420000
C	3.97526400	-1.20855900	0.32659200

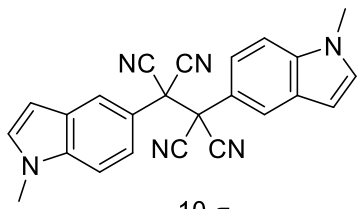
C	2.60266000	-1.20178900	0.50431800
H	2.08415700	2.15048400	0.58658000
H	4.48432300	-2.16140100	0.24774400
H	2.08367400	-2.15290000	0.57117000
C	6.83694600	1.20958300	-0.15959500
H	6.38086500	1.83582500	-0.93470700
H	6.90574400	1.80808000	0.76136800
C	6.86964200	-1.20664200	0.06810500
H	6.70907800	-1.79527100	-0.84764600
H	6.62158100	-1.84264900	0.92543900
N	6.05371700	0.00071700	0.06196700
C	1.89408700	-0.00121000	0.59243200
C	0.36959900	-0.00171400	0.71096600
C	-0.09859600	1.18909200	1.44664200
C	-0.09711200	-1.19208700	1.44823600
N	-0.44408100	2.14249100	2.00195600
N	-0.44108800	-2.14510600	2.00513800
C	8.20734200	0.67513000	-0.58413100
H	8.22511500	0.51653900	-1.66755800
H	9.01731600	1.36175300	-0.32859100
C	8.30004900	-0.66817600	0.14619300
H	8.57801900	-0.50838000	1.19341700
H	9.02707600	-1.35220500	-0.29702500
H	4.48823600	2.16027400	0.28718500
C	-2.60653500	-1.20123400	-0.52745200
C	-3.97818200	-1.20724100	-0.34221700
C	-4.70133900	0.00133100	-0.24333100
C	-3.97692400	1.20862700	-0.35027200
C	-2.60505100	1.20035500	-0.53284500
H	-2.08846400	-2.15264300	-0.59710000
H	-4.48937200	2.16178500	-0.30262400
H	-2.08677000	2.15070600	-0.61468800
C	-6.86723100	-1.20515300	-0.04186300
H	-6.64490700	-1.83867600	-0.90804700
H	-6.67752900	-1.79582400	0.86710600
C	-6.83142900	1.21086300	0.18900400
H	-6.92845800	1.81071200	-0.72837100
H	-6.35301200	1.83618800	0.95123700
N	-6.05330400	0.00337700	-0.05768400
C	-1.89762800	-0.00111500	-0.61846900
C	-0.37329300	-0.00250100	-0.73872200
C	0.09269500	-1.19416500	-1.47426500
C	0.09534600	1.18718800	-1.47583400
N	0.43629000	-2.14834200	-2.02941200
N	0.44140100	2.13987400	-2.03201500
C	-8.30047600	-0.66938200	-0.07386800

H	-8.61323300	-0.50986100	-1.11126500
H	-9.01119700	-1.35505000	0.39259500
C	-8.18742100	0.67352200	0.65426900
H	-8.17084700	0.51386500	1.73755800
H	-9.00616600	1.35897800	0.42477200
H	-4.48717000	-2.15995600	-0.26164300



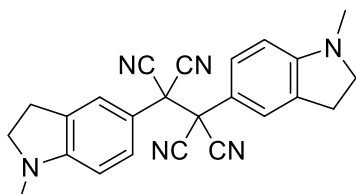
C	-2.63507000	-1.02805000	-0.36968800
C	-1.87128500	0.15947900	-0.37990200
C	-2.47163200	1.39763300	-0.19701900
C	-3.85335900	1.45406500	0.01228300
C	-4.60054300	0.25175200	0.02897700
C	-4.00144600	-0.99608500	-0.16705500
H	-2.15060000	-1.98572400	-0.52578100
H	-1.88944900	2.31355400	-0.21090100
H	-4.58007000	-1.91254000	-0.17614500
C	-0.34573500	0.07010200	-0.52860500
C	0.03657200	-1.08606200	-1.36275500
C	0.18732000	1.28080700	-1.18263600
N	0.31693300	-2.00916100	-1.99980300
N	0.58434700	2.24645100	-1.67897400
N	-5.91510400	0.57552600	0.26152100
C	-7.01909700	-0.36552100	0.32258900
H	-7.88462600	0.18251800	0.70837000
H	-6.78462900	-1.15243800	1.04873100
C	-7.33997000	-0.96445400	-1.02134600
H	-7.48044400	-0.25172800	-1.83244400
C	-7.45594500	-2.27085600	-1.24360500
H	-7.30648400	-2.99865900	-0.44876500
H	-7.70455100	-2.65938800	-2.22559900
C	-6.00913600	1.94784900	0.38156300
H	-6.96986300	2.40678500	0.56987700
C	-4.78031500	2.52471100	0.23767900
H	-4.55899400	3.57973600	0.29833000
C	0.40432900	-0.09088900	0.90529600
C	1.92971400	-0.18234200	0.75702400
C	-0.13308300	-1.30023800	1.55817600
C	0.02551500	1.06621500	1.73980800
C	2.69098100	1.00655900	0.72656700
C	2.53175800	-1.42172600	0.58912700

N	-0.53570500	-2.26466400	2.05235400
N	-0.25075400	1.99004900	2.37759300
C	4.05616700	0.97470800	0.51690200
H	2.20403600	1.96577800	0.86442100
C	3.91322500	-1.47833600	0.37723600
H	1.95135200	-2.33845000	0.61671300
C	4.65829500	-0.27509800	0.34426500
H	4.62734100	1.89515000	0.47927500
C	4.84329600	-2.55053000	0.17272700
N	5.97682300	-0.60083900	0.13919300
C	6.07249100	-1.97394200	0.03024500
H	4.62543000	-3.60740300	0.13639600
C	7.06570100	0.34724400	-0.01535400
H	7.03605100	-2.43432200	-0.13917100
H	7.99775900	-0.22437900	0.03914500
H	7.06292100	1.04336600	0.83127700
C	6.99080900	1.10049700	-1.31712400
H	6.89098300	0.48794100	-2.21167000
C	7.03776700	2.42650200	-1.41234900
H	7.12254800	3.05731400	-0.52992900
H	6.99157400	2.92738600	-2.37348700



C	-2.51159600	1.38872000	-0.45821000
C	-3.86995400	1.52224100	-0.24035000
C	-4.62606700	0.35305600	-0.11663400
C	-4.04260100	-0.93366200	-0.21327100
C	-2.66687600	-1.04442900	-0.43623800
H	-1.90655100	2.28328800	-0.55740100
H	-4.32123800	2.50609900	-0.16971500
H	-2.20786000	-2.02464500	-0.51578800
N	-5.97075900	0.19206200	0.09781000
C	-1.91063400	0.11451700	-0.55161500
C	-0.38744500	0.01150500	-0.71491600
C	-0.02124800	-1.21913300	-1.44265200
C	0.13746700	1.15296600	-1.48955600
N	0.24625700	-2.19855200	-1.99549800
N	0.53100200	2.06607200	-2.07936200
C	-6.92480700	1.26749100	0.25273900
H	-6.95498400	1.89044600	-0.64670800
H	-7.91529100	0.84123900	0.41541100

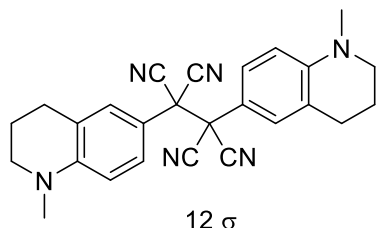
H	-6.66629100	1.89260500	1.11299200
C	-5.10231600	-1.88437200	-0.04563200
H	-5.02114100	-2.96092100	-0.05543200
C	-6.24504100	-1.15984600	0.14014000
H	-7.25840700	-1.49848600	0.30544900
C	0.38743500	-0.01141200	0.71486100
C	1.91062300	-0.11446700	0.55156200
C	-0.13752100	-1.15287400	1.48946100
C	0.02128600	1.21922400	1.44263600
C	2.51157400	-1.38869100	0.45836700
C	2.66687500	1.04445600	0.43600800
N	-0.53109000	-2.06598400	2.07923900
N	-0.24616400	2.19862000	1.99554900
C	3.86993600	-1.52225800	0.24056900
H	1.90652100	-2.28323900	0.55768300
C	4.04260200	0.93364000	0.21306500
H	2.20787000	2.02468700	0.51542800
C	4.62605900	-0.35309800	0.11666900
H	4.32122100	-2.50612800	0.17011600
C	5.10233500	1.88431500	0.04533900
N	5.97076400	-0.19215200	-0.09773100
H	5.02115800	2.96086600	0.05490600
C	6.24505900	1.15974600	-0.14028000
C	6.92482900	-1.26762100	-0.25228800
H	7.25843900	1.49834100	-0.30559800
H	6.66617300	-1.89317700	-1.11217100
H	7.91526800	-0.84141000	-0.41533500
H	6.95519400	-1.89012000	0.64747100



11 σ

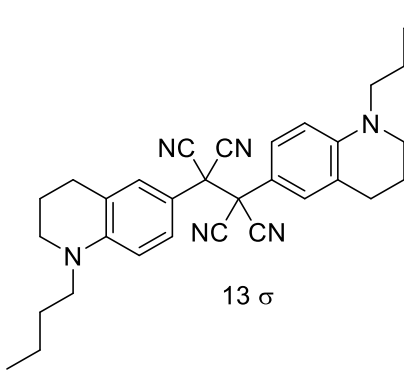
C	2.47928200	1.41532600	0.57300300
C	3.85365600	1.56010500	0.39180300
C	4.63033400	0.40958300	0.27045000
C	4.03406600	-0.86249400	0.31729200
C	2.67765600	-0.99911100	0.50180100
H	1.87216500	2.31035100	0.66344800
H	4.28948200	2.55139400	0.34443200
H	2.23131900	-1.98817100	0.54127200
N	6.00077200	0.29840400	0.11447400
C	1.88402400	0.15517300	0.62579200
C	0.36212300	0.02393000	0.72989000

C	-0.00965700	-1.21109800	1.44768700
C	-0.21626500	1.15846000	1.47550300
N	-0.27722500	-2.19685900	1.98930900
N	-0.65538800	2.06607800	2.04121900
C	6.77690300	1.38569400	-0.43399600
H	6.60061100	2.30133500	0.13522600
H	7.83940700	1.14458200	-0.35085800
H	6.53997100	1.57652600	-1.49332300
C	-0.36207000	-0.02360700	-0.72958900
C	-1.88396400	-0.15501700	-0.62556600
C	0.21654400	-1.15808600	-1.47510400
C	0.00952700	1.21143700	-1.44745800
C	-2.47920400	-1.41520100	-0.57361000
C	-2.67763300	0.99918800	-0.50092700
N	0.65580700	-2.06569200	-2.04073000
N	0.27694500	2.19719200	-1.98916700
C	-3.85361600	-1.56010800	-0.39272900
H	-1.87205700	-2.31016000	-0.66451600
C	-4.03405400	0.86243800	-0.31662500
H	-2.23133900	1.98828800	-0.53976700
C	-4.63032500	-0.40967700	-0.27078900
H	-4.28944600	-2.55143200	-0.34610700
N	-6.00080300	-0.29861300	-0.11510200
C	-6.77708100	-1.38630600	0.43237000
H	-6.54020900	-1.57808300	1.49154100
H	-7.83955200	-1.14499600	0.34941200
H	-6.60085900	-2.30145900	-0.13766100
C	-5.11922900	1.90160300	-0.17301100
H	-4.85009400	2.71769000	0.50084700
H	-5.36403400	2.33344100	-1.15049700
C	-6.29104000	1.05786900	0.36211600
H	-6.30685300	1.07406300	1.46503800
H	-7.26638200	1.39175400	-0.00140100
C	6.29083200	-1.05838700	-0.36195400
H	7.26631300	-1.39202900	0.00141000
H	6.30622000	-1.07533300	-1.46487300
C	5.11923300	-1.90173700	0.17419300
H	5.36437100	-2.33274300	1.15196800
H	4.84993800	-2.71842700	-0.49887400



C	-0.37538200	-0.04599500	-0.70666600
C	-1.88628900	-0.22917000	-0.56208500
C	0.22497000	-1.18054700	-1.43498100
C	-0.06425800	1.18170600	-1.46497700
C	-2.72600200	0.88141200	-0.45133300
C	-2.44830600	-1.50018300	-0.46904700
N	0.67957400	-2.08912500	-1.98679500
N	0.15465300	2.16111300	-2.03902200
C	-4.09024600	0.75516200	-0.24396000
H	-2.31430300	1.88416100	-0.53034400
C	-3.80990500	-1.65252800	-0.26141900
H	-1.83186200	-2.38903500	-0.55751500
C	-4.66123100	-0.53786700	-0.13213300
C	-4.95207700	1.99385100	-0.15052700
H	-4.20752800	-2.65701500	-0.19749700
N	-6.01224000	-0.69799500	0.10951000
H	-5.16550700	2.36555800	-1.16129400
H	-4.40190900	2.78702800	0.36531900
C	-6.26385100	1.69566100	0.56740100
C	-6.90011700	0.44763900	-0.02729000
C	-6.60860000	-2.01077800	-0.01990100
H	-6.95560700	2.53835500	0.47753700
H	-6.08033200	1.52676100	1.63420600
H	-7.15306100	0.62523800	-1.08662400
H	-7.83127600	0.21493600	0.49711700
H	-6.48072500	-2.43482800	-1.02734700
H	-6.18550000	-2.71140900	0.70750100
H	-7.67756400	-1.93165200	0.18365300
C	0.37945600	0.06544200	0.73275200
C	1.89115200	0.23992500	0.58491200
C	-0.21434900	1.20569800	1.45727300
C	0.06199300	-1.15942500	1.49265800
C	2.72468900	-0.87580900	0.48268600
C	2.45787700	1.50694100	0.46956500
N	-0.66433300	2.12000600	2.00337500
N	-0.16193300	-2.13796900	2.06621100
C	4.08647500	-0.75924300	0.25353600
H	2.30861200	-1.87545900	0.57703900
C	3.81845200	1.64975900	0.24847900
H	1.84502200	2.39950600	0.54487800

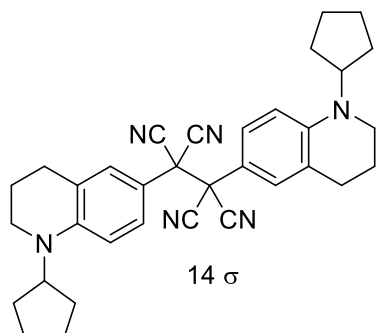
C	4.66508700	0.52968700	0.13757400
C	4.92973800	-2.00653100	0.11506300
H	4.21844000	2.65130100	0.15864000
N	6.02625000	0.67987600	-0.05482800
H	4.79328400	-2.42133600	-0.89212600
H	4.57771700	-2.76986500	0.81599100
C	6.40675200	-1.70589100	0.34596100
C	6.81142100	-0.47829900	-0.45782800
C	6.55550100	1.98226800	-0.40132700
H	7.02483100	-2.55903300	0.05088100
H	6.59214000	-1.51039300	1.40794900
H	6.69157500	-0.67911000	-1.53611500
H	7.86572200	-0.24681000	-0.28236700
H	6.13090600	2.37593800	-1.33727100
H	6.36888700	2.70858600	0.39619700
H	7.63654100	1.89992900	-0.52388800



C	2.37731500	-1.47839200	0.13345400
C	1.81739600	-0.21020700	0.29476700
C	2.66365800	0.89648200	0.26634500
C	4.02481200	0.73536600	0.06975600
C	4.59825400	-0.53982200	-0.11191300
C	3.73696900	-1.66581200	-0.06002700
H	1.74187300	-2.36005300	0.15511300
H	2.27040400	1.89957800	0.39805200
H	4.64218000	1.62426800	0.06376200
C	4.28201500	-3.06743200	-0.21441100
H	4.40992400	-3.52075800	0.77751100
H	3.55708700	-3.68659800	-0.75175400
C	5.62174800	-3.05617800	-0.94111300
H	5.47701800	-2.79734600	-1.99574200
H	6.09215600	-4.04298400	-0.90114300
C	6.53836600	-2.02728500	-0.29642700
H	6.74958900	-2.32064100	0.74554200
H	7.49658100	-1.98952600	-0.82346800
N	5.95011000	-0.69676100	-0.35619000
C	0.30405400	-0.03842200	0.41854100

C	-0.30638300	-1.20219300	1.09069300
C	-0.02593400	1.15751600	1.21825800
N	-0.26301600	2.11112500	1.82750500
N	-0.76505700	-2.13416100	1.59840300
C	6.86890300	0.41696700	-0.19144200
H	6.46593500	1.29072600	-0.71084300
H	7.79351900	0.15782800	-0.71994400
C	7.19499800	0.74665300	1.27041400
H	6.26376100	0.96243500	1.80894100
H	7.62597300	-0.14607500	1.73941400
C	8.16385100	1.92218300	1.42787200
H	8.43790600	2.00710500	2.48539600
H	9.09474300	1.70440400	0.88749600
C	7.59586200	3.26169500	0.95303200
H	8.28675400	4.08005100	1.17545400
H	7.41533000	3.27397500	-0.12651400
H	6.64627500	3.48133200	1.45395900
C	-0.424449800	0.12536400	-1.02980900
C	-1.93892000	0.28464300	-0.90216700
C	-0.08475200	-1.06699500	-1.83047600
C	0.17559500	1.29713300	-1.69663900
C	-2.50657600	1.54533400	-0.71230800
C	-2.77606400	-0.82914400	-0.88603800
N	0.16074900	-2.02073300	-2.43612100
N	0.62419500	2.23795300	-2.19693000
C	-3.86350600	1.71684800	-0.48532300
H	-1.87918300	2.43287100	-0.73059000
C	-4.13536000	-0.682666000	-0.66870700
H	-2.37531100	-1.82688200	-1.03427600
C	-4.71682800	0.58437000	-0.45907200
C	-4.41197700	3.10740100	-0.25839700
H	-4.74373500	-1.57766600	-0.65377700
N	-6.07895100	0.72939200	-0.26347600
H	-4.22655300	3.40191300	0.78280700
H	-3.87293800	3.82364500	-0.88620600
C	-5.90876400	3.15929600	-0.54170000
C	-6.59901500	2.01383900	0.18405100
C	-6.90539000	-0.43088700	0.02820400
H	-6.09433400	3.06314400	-1.61728700
H	-6.33302500	4.11234100	-0.21249300
H	-6.47197600	2.13719900	1.27254500
H	-7.67366200	2.02647200	-0.02195100
H	-6.71127200	-1.20297300	-0.72167700
H	-7.94963500	-0.13317600	-0.11889900
C	-6.72714800	-0.98373800	1.44782200
H	-5.66410400	-1.18829000	1.62566500

H	-7.01764200	-0.20485700	2.16297300
C	-7.54216400	-2.25244100	1.71615400
H	-7.47651600	-2.48647400	2.78450200
H	-8.60345000	-2.05853300	1.51040700
C	-7.07537800	-3.46748300	0.91109400
H	-7.62956900	-4.36578200	1.19845700
H	-7.21996600	-3.32798900	-0.16506000
H	-6.01115900	-3.66238400	1.08437100



C	-2.52111400	1.46606400	-0.67323300
C	-1.91592200	0.22324100	-0.85857700
C	-2.72369000	-0.91145000	-0.85121000
C	-4.08905000	-0.80127800	-0.64970100
C	-4.71296700	0.44761100	-0.44797500
C	-3.88478400	1.59973400	-0.46174600
H	-1.91954700	2.37137500	-0.68219600
H	-2.29607500	-1.89843600	-0.99654300
H	-4.66661500	-1.71542000	-0.64710200
C	-4.46829500	2.97454900	-0.24110200
H	-4.34355300	3.25791100	0.81222200
H	-3.91536700	3.71142300	-0.83173800
C	-5.94653300	2.98649500	-0.60049100
H	-6.07291000	2.87139000	-1.68302600
H	-6.41304500	3.93230900	-0.30970100
C	-6.65493500	1.84008300	0.10489400
H	-6.60774500	1.99009700	1.19677800
H	-7.70770700	1.84555700	-0.18014300
N	-6.08596600	0.55206800	-0.27249100
C	-0.39679700	0.10671100	-0.97623500
C	-0.02088700	-1.06953200	-1.78462000
C	0.17499500	1.30000600	-1.62963200
N	0.60095300	2.25693800	-2.11902900
N	0.25210400	-2.01123100	-2.39732300
C	-6.84519300	-0.65009200	0.05801700
H	-6.58117600	-1.41322900	-0.68346700
C	-6.60594100	-1.22178200	1.47042900
H	-5.62618700	-1.69365600	1.57595200

H	-6.64134700	-0.39475500	2.18933300
C	-7.77953800	-2.20159700	1.69689800
H	-7.44748100	-3.24214300	1.64538600
H	-8.21919800	-2.06058700	2.68808600
C	-8.81048200	-1.89286500	0.57697500
H	-9.83870700	-1.87201300	0.94665700
H	-8.76545500	-2.65955300	-0.20413100
C	-8.37313300	-0.53991200	0.00180800
H	-8.73037900	0.25907700	0.66111600
H	-8.75369700	-0.34837800	-1.00575800
C	0.32674400	-0.04730700	0.47519100
C	1.84581100	-0.16612100	0.35965900
C	-0.24671300	-1.23874500	1.13104900
C	-0.04822600	1.12899900	1.28400700
C	2.44857500	-1.41027600	0.17431000
C	2.65724500	0.96599500	0.36144400
N	-0.67494200	-2.19247000	1.62477200
N	-0.32057800	2.06871300	1.90005300
C	3.81516300	-1.54844000	-0.01181600
H	1.84380300	-2.31346700	0.17393800
C	4.02440700	0.85217200	0.17315300
H	2.23173500	1.95382500	0.50724900
C	4.64545300	-0.39779600	-0.03144700
C	4.40533300	-2.92462200	-0.19785600
H	4.60529100	1.76416400	0.18483200
N	6.00963500	-0.49886700	-0.26311600
H	4.60684000	-3.37793600	0.78183900
H	3.68253600	-3.57227200	-0.70329200
C	5.70015000	-2.83315900	-0.99107000
C	6.62894400	-1.81615200	-0.34642800
C	6.86698000	0.63435500	0.07228800
H	5.48721500	-2.52480300	-2.02089600
H	6.20467300	-3.80292400	-1.03309300
H	6.93451700	-2.17363200	0.65169000
H	7.53276200	-1.73181400	-0.95180000
H	6.44376200	1.52066300	-0.41510200
C	7.02493300	0.91904000	1.58057200
C	8.32263400	0.56058300	-0.40282700
H	6.12550200	1.35208700	2.02468700
H	7.20869800	-0.03297500	2.09256200
C	8.25701400	1.84721700	1.67656900
C	8.94618200	1.77975400	0.28662800
H	8.80726700	-0.34764300	-0.02752500
H	8.42137300	0.57602000	-1.49221200
H	7.96869900	2.87369800	1.91914800
H	8.93369300	1.51522500	2.46874400

H	10.03364800	1.70106800	0.36058900
H	8.72756700	2.68481000	-0.29071500

 2π

C	1.00842900	0.66454000	-1.42552200
C	1.65241400	1.46343000	-0.42893400
C	0.81528200	2.26183200	0.41799000
C	-0.54479300	2.25891900	0.28318400
C	-1.15289500	1.44837100	-0.71325700
C	-0.35488500	0.67121700	-1.56955600
H	1.61652500	0.07839500	-2.10674100
H	1.27656900	2.87176900	1.18809700
H	-1.15577600	2.84365200	0.96102900
H	-0.84500200	0.08338700	-2.33716300
O	-2.47381200	1.38860900	-0.93009200
C	-3.30759100	2.41225000	-0.52483000
H	-2.82383600	3.37125200	-0.37368500
C	-4.61192900	2.20912400	-0.41600200
H	-5.25544100	3.03520800	-0.14237700
H	-5.05834900	1.23792000	-0.59031400
C	3.04915300	1.45850100	-0.28209000
C	3.86985000	0.75316400	-1.19941700
C	3.68264500	2.17011700	0.77202100
N	4.48318100	0.14990900	-1.98313400
N	4.15893500	2.75520900	1.65676900
C	-3.02170500	-1.33601300	0.37480500
C	-1.62663300	-1.41584200	0.48828200
C	-3.72161900	-2.02594700	-0.65244800
C	-3.78656400	-0.56645000	1.28889500
C	-0.92105200	-0.64472600	1.46428400
C	-0.85414700	-2.27380300	-0.36281300
N	-4.26143400	-2.58929300	-1.51435500
N	-4.38132400	0.08004000	2.05176900
C	0.44308400	-0.70534400	1.56392700
H	-1.48415200	-0.01902000	2.14863800
C	0.50718400	-2.33461600	-0.26552700
H	-1.36962800	-2.89964800	-1.08445300
C	1.18073700	-1.51507000	0.68018800
H	0.98382000	-0.12623000	2.30360600
H	1.06865500	-3.01222600	-0.89760000
O	2.50278700	-1.52437100	0.87025800
C	3.34099500	-2.19550600	-0.00495300
H	3.14467300	-2.02108700	-1.05837300
C	4.36632700	-2.88965400	0.46178900
H	5.06341700	-3.33664000	-0.23568300
H	4.53748600	-3.00263800	1.52625300

4π

C	-0.19427800	-0.48539000	-1.81943700
C	0.20989100	-1.33754500	-0.73730400
C	-0.79253300	-1.81789200	0.16931600
C	-2.09809100	-1.46877300	-0.02543300
C	-2.44895200	-0.60490200	-1.08449300
C	-1.50631700	-0.12937900	-2.00985300
H	0.55991200	-0.13966100	-2.51842900
H	-0.50510200	-2.48711000	0.97417700
H	-1.81388500	0.51663400	-2.82316700
C	1.56287400	-1.68522400	-0.56318400
C	1.96970300	-2.56199700	0.48262200
C	2.54983200	-1.32013100	-1.51889300
N	2.26596800	-3.27309900	1.35307900
N	3.33821600	-0.99716800	-2.31095500
C	-3.36017100	-1.84397800	0.70236900
H	-3.51013600	-2.92654400	0.72034800
H	-3.35137200	-1.47816200	1.73339900
C	-4.44413500	-1.12303600	-0.12780000
H	-5.12875400	-1.80936200	-0.62947500
H	-5.00963300	-0.39557500	0.45418600
O	-3.75603900	-0.38497500	-1.17882200
C	0.19409000	0.48549700	1.81944500
C	-0.20989500	1.33751900	0.73712600
C	0.79265100	1.81760500	-0.16949300
C	2.09815300	1.46844300	0.02547600
C	2.44891000	0.60507200	1.08499100
C	1.50610800	0.12962400	2.01022600
H	-0.56022800	0.13982100	2.51832500
H	0.50535900	2.48664700	-0.97454900
H	1.81353200	-0.51622500	2.82372700
C	-1.56281700	1.68528000	0.56282800
C	-1.96946000	2.56221500	-0.48292300
C	-2.54996200	1.32003900	1.51828500
N	-2.26556100	3.27340400	-1.35336200
N	-3.33870000	0.99694200	2.30994200
C	3.36031900	1.84345800	-0.70228600
H	3.35168300	1.47727900	-1.73319300
H	3.51019700	2.92603300	-0.72055300
C	4.44417400	1.12287800	0.12831500
H	5.00960100	0.39488500	-0.45306800
H	5.12894100	1.80942900	0.62947100
O	3.75602200	0.38560800	1.17988000

5π

C	-0.17347800	0.48836700	1.80891300
C	0.22526000	1.35570600	0.73665500
C	-0.76650400	1.86784600	-0.16558300
C	-2.05622900	1.49263700	0.05302000
C	-2.41683800	0.59973500	1.07873600
C	-1.48795400	0.12372700	2.00406400
H	0.58535900	0.13128200	2.49650600
H	-0.49965700	2.55500100	-0.95964500
H	-1.79003200	-0.53609000	2.80783000
C	1.58382600	1.67758200	0.55617100
C	1.99733600	2.55858000	-0.48363000
C	2.58049600	1.27656300	1.48817900
N	2.30009700	3.26540200	-1.35513400
N	3.39319200	0.92591700	2.24191900
C	-4.27736800	1.25671800	0.03402000
H	-4.89953800	2.03318100	0.48769900
H	-4.82819900	0.63254500	-0.66914200
O	-3.74483400	0.42791400	1.08358700
O	-3.16815500	1.85856000	-0.62672700
C	-1.58392000	-1.67721700	-0.55647900
C	-0.22522400	-1.35554800	-0.73673800
C	-2.58024700	-1.27617000	-1.48883100
C	-1.99776000	-2.55827900	0.48314500
C	0.17377700	-0.48829900	-1.80890300
C	0.76627100	-1.86782900	0.16564800
N	-3.39250800	-0.92553800	-2.24305700
N	-2.30086200	-3.26521700	1.35444000
C	1.48836200	-0.12381100	-2.00381800
H	-0.58484900	-0.13104800	-2.49664000
C	2.05612400	-1.49284500	-0.05279700
H	0.49928500	-2.55497100	0.95967300
C	2.41700400	-0.59993200	-1.07834000
H	1.79059800	0.53601600	-2.80751600
O	3.16781700	-1.85894800	0.62723900
O	3.74504500	-0.42797800	-1.08270200
C	4.27726300	-1.25732100	-0.03338900
H	4.82832700	-0.63360600	0.66998200
H	4.89911000	-2.03388600	-0.48734700

 7π

C	0.03377200	-2.31719500	-0.38135200
C	-0.76243400	-1.89798000	0.73117200
C	-0.16553900	-0.96794800	1.63021400
C	1.09803800	-0.48494800	1.43497300

C	1.87769400	-0.87808100	0.30951300
C	1.29261600	-1.83367600	-0.58430900
H	-0.37174800	-3.04896800	-1.07326100
H	-0.72478300	-0.64348800	2.50174600
H	1.50006200	0.21095800	2.15733800
H	1.85863000	-2.20261200	-1.42829300
C	-2.06716900	-2.38614800	0.94166400
C	-2.68170300	-3.25056500	0.00089000
C	-2.80224400	-2.03855400	2.10263500
N	-3.16388200	-3.91208900	-0.82711100
N	-3.37582700	-1.71158100	3.06203600
N	3.12683700	-0.38565800	0.11417100
C	3.93524900	-0.80850800	-1.03312100
H	4.71654600	-0.05491200	-1.16206200
H	3.33526400	-0.75570100	-1.94589700
C	3.81101400	0.36730100	1.17266800
H	3.20242900	1.21862700	1.48999400
H	4.70670300	0.79851600	0.71831500
C	4.55808200	-2.17174300	-0.87337200
H	5.08725200	-2.35584400	0.05972600
C	4.19334200	-0.47027000	2.36673400
H	4.67336200	-1.42491600	2.16023500
C	3.99993700	-0.08406700	3.62496700
H	3.52078100	0.86419400	3.85927900
H	4.32297400	-0.69468600	4.46143700
C	4.52043600	-3.11668400	-1.80908600
H	4.00489000	-2.96039000	-2.75435500
H	5.01238900	-4.07344400	-1.66923500
C	2.06717200	2.38580700	-0.94177600
C	0.76243400	1.89767000	-0.73120300
C	2.80215500	2.03834100	-2.10284300
C	2.68179000	3.25021300	-0.00104200
C	0.16548900	0.96762700	-1.63019800
C	-0.03369200	2.31687800	0.38137000
N	3.37567900	1.71147500	-3.06231400
N	3.16406900	3.91172800	0.82690500
C	-1.09809900	0.48468600	-1.43490500
H	0.72472200	0.64309500	-2.50171000
C	-1.29256900	1.83343600	0.58436300
H	0.37188400	3.04862200	1.07327800
C	-1.87774100	0.87792400	-0.30946800
H	-1.50017900	-0.21127200	-2.15719100
H	-1.85852300	2.20235600	1.42839200
N	-3.12696300	0.38565800	-0.11418100
C	-3.81132100	-0.36698800	-1.17282000
C	-3.93530300	0.80844200	1.03319100

H	-4.70702000	-0.79819100	-0.71848300
H	-3.20287100	-1.21828600	-1.49042600
C	-4.19361300	0.47099700	-2.36659300
H	-3.33534700	0.75535800	1.94596500
H	-4.71668200	0.05490500	1.16202000
C	-4.55801200	2.17175600	0.87366700
H	-4.67411900	1.42532300	-2.15974000
C	-3.99956900	0.08564200	-3.62498600
H	-5.08730200	2.35598900	-0.05933800
C	-4.52015500	3.11663100	1.80943900
H	-3.51996000	-0.86228500	-3.85971800
H	-4.32253700	0.69666600	-4.46118700
H	-4.00451400	2.96023500	2.75463800
H	-5.01204800	4.07343700	1.66969000

 8π

C	1.53210000	1.78680100	0.21995500
C	0.15026500	1.53111400	0.12680100
C	2.33539500	2.02337100	-0.92783800
C	2.16507700	1.96485600	1.48176800
C	-0.66396500	1.36698500	1.28742400
C	-0.50376500	1.42540300	-1.14240600
N	2.99808900	2.21087100	-1.86616000
N	2.66718500	2.10151300	2.52262700
C	-2.00600100	1.11881300	1.19192600
H	-0.20637500	1.44680600	2.26799300
C	-1.84553900	1.19772400	-1.24349500
H	0.08257600	1.55569600	-2.04657100
C	-2.65210500	1.01480900	-0.07794100
H	-2.29808300	1.13894400	-2.22510700
N	-3.97717800	0.80792200	-0.17612000
C	-4.85923200	0.63441400	0.98460300
C	-4.70349000	0.66496800	-1.44420600
H	-4.60111300	-0.28969200	1.51460100
H	-4.88333500	1.65500800	-1.88676200
H	-4.13973600	0.05295400	-2.14866600
C	-1.53213900	-1.78675100	0.21950600
C	-0.15027800	-1.53102400	0.12644000
C	-2.16517100	-1.96510000	1.48123400
C	-2.33538400	-2.02305400	-0.92837800
C	0.50375000	-1.42492900	-1.14272200
C	0.66394000	-1.36721200	1.28710900
N	-2.66739300	-2.10197900	2.52201200
N	-2.99810700	-2.21019900	-1.86675000
C	1.84553500	-1.19722700	-1.24373500
H	-0.08257000	-1.55496700	-2.04693500

C	2.00599200	-1.11904200	1.19170000
H	0.20633800	-1.44730800	2.26765200
C	2.65210900	-1.01472400	-0.07813300
H	2.57804000	-0.97535200	2.09967100
N	3.97721200	-0.80795000	-0.17628100
C	4.70336600	-0.66420700	-1.44439000
C	4.85937800	-0.63496000	0.98440800
H	4.13967200	-0.05142500	-2.14824500
H	4.75230200	-1.47258200	1.68136700
H	4.60174600	0.28924000	1.51449600
H	2.29810000	-1.13814300	-2.22532200
H	4.88280700	-1.65394800	-1.88778600
C	6.00601200	0.01154900	-1.02434100
H	6.81797100	-0.18564000	-1.72721600
H	5.84976900	1.09374200	-0.97204400
C	6.26012400	-0.56234000	0.37211900
H	6.93364500	0.05041200	0.97429700
H	6.69160800	-1.56609500	0.29520800
H	-2.57802800	0.97474800	2.09984900
H	-4.75245400	1.47207500	1.68157200
C	-6.26002300	0.56127300	0.37241900
H	-6.93305300	-0.05232100	0.97428900
H	-6.69218300	1.56478900	0.29626700
C	-6.00582200	-0.01155600	-1.02446700
H	-6.81793300	0.18581600	-1.72711800
H	-5.84915200	-1.09372300	-0.97297600

 9π

C	0.87005400	1.62929900	0.46794000
C	0.06863600	1.39393500	-0.70965400
C	0.64469300	0.70091400	-1.81331900
C	1.95822300	0.29042400	-1.74874300
C	2.70534500	0.49753700	-0.54465000
C	2.16848800	1.20670700	0.55242200
H	0.42426100	2.16952600	1.29620500
H	0.05984700	0.54518600	-2.71405000
H	2.75577900	1.38732200	1.44457900
C	-1.26608600	1.83754700	-0.76718000
C	-1.83519800	2.68198900	0.22749800
C	-2.07504500	1.60278700	-1.91537600
N	-2.30305800	3.39153200	1.02086100
N	-2.73933200	1.38350900	-2.84479700
N	3.95354600	-0.00962400	-0.73849900
C	5.02976700	-0.03272100	0.24539800
H	5.78782600	-0.72264800	-0.13723100
H	4.64942600	-0.45457000	1.18065000

C	5.62344900	1.33046600	0.47692500
H	5.96618800	1.85972900	-0.41082900
C	5.74513900	1.88122500	1.68212900
H	5.39960200	1.36751600	2.57672200
H	6.19825400	2.85814200	1.81481100
C	4.01956400	-0.53740300	-2.02271800
H	4.92792300	-1.01981600	-2.35386500
C	2.83889600	-0.36940300	-2.67217100
H	2.60443000	-0.70530600	-3.67055900
C	1.42623700	-1.84736300	0.74748600
C	0.08620800	-1.43411000	0.61706900
C	2.15796100	-1.58569900	1.94168000
C	2.08542900	-2.67310600	-0.20393200
C	-0.64608000	-1.69808500	-0.59927100
C	-0.56316000	-0.74571700	1.67998300
N	2.75641000	-1.34496600	2.90968800
N	2.65233100	-3.35583000	-0.95579900
C	-1.95099700	-1.31635900	-0.75356800
H	-0.14304500	-2.23285400	-1.39811000
C	-1.88042600	-0.36593700	1.53928000
H	-0.03246300	-0.56612300	2.60916600
C	-2.56296800	-0.60948200	0.30323300
H	-2.47664500	-1.51820400	-1.67983100
C	-2.82763000	0.27388400	2.41116400
N	-3.83509500	-0.14326200	0.43192700
C	-3.98355700	0.38733000	1.70856200
H	-2.64973500	0.63326400	3.41300500
C	-4.89929200	-0.20309900	-0.56275600
H	-4.92905800	0.82564000	1.99378100
H	-5.37521600	0.78044100	-0.62175500
H	-4.43355600	-0.37919300	-1.53569000
C	-5.90676400	-1.27073700	-0.23642900
H	-5.50695100	-2.27488300	-0.10244900
C	-7.21147500	-1.04330000	-0.10922500
H	-7.62936900	-0.04694500	-0.23372900
H	-7.90757100	-1.84486200	0.11485800

 10π

C	0.35951900	-0.60583500	1.78192800
C	1.70325500	-0.35144800	1.82230200
C	2.49464100	-0.81767400	0.75088000
C	1.94343400	-1.60083400	-0.31341700
C	0.58651700	-1.84011200	-0.35047500
H	-0.28118200	-0.25668900	2.58469800
H	2.13652600	0.22347600	2.63299800
H	0.15012100	-2.43237700	-1.14807400

N	3.83853000	-0.73857700	0.56140800
C	-0.24009700	-1.36217500	0.70686100
C	-1.62334100	-1.62306600	0.705558500
C	-2.46429500	-1.31863200	1.81253100
C	-2.23055400	-2.37230700	-0.34262000
N	-3.16231000	-1.09639800	2.71552900
N	-2.72132900	-2.96658400	-1.21380000
C	4.77815800	-0.06296700	1.43718900
H	4.90334900	-0.61582400	2.37336400
H	5.74187100	0.00278800	0.93193500
H	4.43055900	0.94959600	1.65211900
C	3.04547800	-1.97837400	-1.15478900
H	3.00043800	-2.54172400	-2.07402500
C	4.15955700	-1.43765300	-0.59590700
H	5.18518700	-1.46557900	-0.93487000
C	1.62334200	1.62305900	-0.70560100
C	0.24009700	1.36217200	-0.70686900
C	2.46428700	1.31862300	-1.81255300
C	2.23056200	2.37229800	0.34260100
C	-0.35952800	0.60583300	-1.78193100
C	-0.58651000	1.84011400	0.35047100
N	3.16229400	1.09638700	-2.71555700
N	2.72134100	2.96657200	1.21378000
C	-1.70326500	0.35144900	-1.82229500
H	0.28116700	0.25668400	-2.58470400
C	-1.94342700	1.60084000	0.31342200
H	-0.15010700	2.43237900	1.14806700
C	-2.49464300	0.81767900	-0.75086900
H	-2.13654300	-0.22347700	-2.63298700
C	-3.04546500	1.97838600	1.15480000
N	-3.83853100	0.73858500	-0.56138800
H	-3.00041800	2.54173800	2.07403400
C	-4.15954900	1.43766500	0.59592600
C	-4.77816400	0.06297200	-1.43716000
H	-5.18517700	1.46559400	0.93489600
H	-4.43057100	-0.94959400	-1.65208300
H	-5.74187600	-0.00277400	-0.93190400
H	-4.90335500	0.61582000	-2.37334100

 11π

C	0.45661800	0.23220200	-1.81337800
C	1.78466100	-0.11049500	-1.78891000
C	2.63048500	0.53185300	-0.85483300
C	2.11872300	1.55519300	-0.00376000
C	0.79842100	1.88208900	-0.02431000

H	-0.20340600	-0.25184900	-2.52582600
H	2.16538900	-0.87162500	-2.45930500
H	0.40932000	2.65552100	0.63123700
N	3.95131800	0.37266100	-0.65832300
C	-0.09091900	1.22185200	-0.93653900
C	-1.46399300	1.54254600	-0.97210800
C	-2.34348200	0.98671700	-1.93647100
C	-2.01862700	2.53363400	-0.11623800
N	-3.06538300	0.51912000	-2.72155500
N	-2.46797300	3.33277200	0.60094600
C	4.82026700	-0.55400100	-1.34265200
H	5.36355700	-0.06336900	-2.16080300
H	5.54550100	-0.95659300	-0.62994900
H	4.24536500	-1.39224100	-1.73732200
C	1.46398400	-1.54224800	0.97216800
C	0.09086900	-1.22168000	0.93652500
C	2.34336300	-0.98642200	1.93663000
C	2.01888400	-2.53318200	0.11630300
C	-0.45682400	-0.23213100	1.81336500
C	-0.79832200	-1.88195400	0.02418000
N	3.06526300	-0.51879000	2.72169300
N	2.46856200	-3.33213300	-0.60088300
C	-1.78492200	0.11039900	1.78884000
H	0.20310700	0.25197800	2.52586100
C	-2.11866300	-1.55519800	0.00354600
H	-0.40907700	-2.65530700	-0.63137800
C	-2.63059200	-0.53203000	0.85469100
H	-2.16583700	0.87144800	2.45922600
N	-3.95142800	-0.37293600	0.65813600
C	-4.82040500	0.55312800	1.34326500
H	-4.24605900	1.39315800	1.73497500
H	-5.54817200	0.95309900	0.63170800
H	-5.36069200	0.06289800	2.16365100
C	-4.49110200	-1.36080100	-0.28081100
H	-5.05064300	-0.85053600	-1.06989200
H	-5.17392400	-2.03458100	0.25304500
C	-3.25056100	-2.09947900	-0.83009800
H	-3.10064400	-1.86123300	-1.88752500
H	-3.34317700	-3.18373900	-0.73166300
C	4.49111700	1.36052700	0.28053400
H	5.17394500	2.03419400	-0.25346200
H	5.05068600	0.85029900	1.06962200
C	3.25069400	2.09932700	0.82987100
H	3.34343600	3.18358600	0.73158300
H	3.10076500	1.86094600	1.88726600

12π

C	1.27810600	1.66892600	-1.09335900
C	-0.02933500	1.12232700	-1.04172100
C	2.28770900	1.14774900	-1.93663700
C	1.59176100	2.86982300	-0.40580800
C	-1.07157200	1.72971600	-0.28851400
C	-0.36545600	-0.05344500	-1.77973500
N	3.12256600	0.72020000	-2.62868200
N	1.82360000	3.85903000	0.16404700
C	-2.35932800	1.25289800	-0.28255000
H	-0.85298100	2.62444700	0.28847900
C	-1.63837500	-0.54780900	-1.79065300
H	0.40076800	-0.55225100	-2.36474200
C	-2.68624700	0.08640700	-1.05866200
C	-3.44544600	1.98006800	0.47189000
H	-1.84456100	-1.43998800	-2.36743400
N	-3.95393000	-0.37263300	-1.13966100
H	-3.75792500	2.85317000	-0.11594200
H	-3.04313400	2.35999600	1.41596000
C	-4.65028000	1.08204900	0.72703700
C	-5.06624200	0.37379700	-0.54906600
C	-4.30193700	-1.44584600	-2.06212200
H	-5.49386800	1.67099800	1.09701500
H	-4.41197000	0.33671000	1.49041300
H	-5.44607700	1.09583100	-1.28685100
H	-5.86565700	-0.33948400	-0.33785000
H	-4.11063000	-1.15605900	-3.10273400
H	-3.74864700	-2.35908600	-1.83182300
H	-5.36452400	-1.66203400	-1.95474500
C	-1.29612100	-1.19104400	1.52683100
C	0.05214400	-0.87291100	1.25927100
C	-2.01992900	-0.46691000	2.50787000
C	-1.95127500	-2.31210800	0.95742200
C	0.85140000	-1.67555500	0.38290700
C	0.68843900	0.23970400	1.88396800
N	-2.58143400	0.14040900	3.32739900
N	-2.49984600	-3.23060800	0.49708500
C	2.17051500	-1.41911400	0.14559000
H	0.39317500	-2.53320300	-0.10202300
C	2.00227800	0.52809400	1.64753600
H	0.12272600	0.86961600	2.56241800
C	2.79686300	-0.28658800	0.77871800
C	2.99290400	-2.26358900	-0.78447900
H	2.44900700	1.37961100	2.14505900
N	4.09796000	-0.02519900	0.57290800
H	2.99815900	-1.80012400	-1.78052500

H	2.54728600	-3.25683400	-0.88372100
C	4.42475800	-2.34028800	-0.26470700
C	4.99926800	-0.94017000	-0.14118400
C	4.69929300	1.21609700	1.03736600
H	5.05830400	-2.91836100	-0.94236000
H	4.44005600	-2.83907100	0.71108100
H	5.20444800	-0.51708700	-1.13116000
H	5.94043800	-0.96376700	0.41687500
H	4.07977800	2.07418800	0.76563400
H	4.85183200	1.20747400	2.12272000
H	5.66822300	1.33324400	0.55133900

 13π

C	-0.32811900	1.25967300	-2.03579400
C	-0.71852800	-0.11562700	-2.05153300
C	0.22414800	-1.05372600	-1.54934500
C	1.43154500	-0.65501500	-1.04670600
C	1.80132900	0.71983400	-0.99743400
C	0.87777600	1.67997000	-1.55029800
H	-1.01090900	1.99833200	-2.44824600
H	-0.01230900	-2.11209000	-1.58156700
H	2.11270700	-1.41288500	-0.68368900
C	1.28339800	3.12913700	-1.61492900
H	1.78816800	3.31454200	-2.57287000
H	0.39495600	3.76706500	-1.59893300
C	2.22906900	3.46933600	-0.47042400
H	1.71100000	3.41161200	0.49066500
H	2.61121500	4.48901300	-0.56625900
C	3.40795400	2.51232700	-0.45904500
H	4.06959500	2.70622100	-1.31549400
H	3.98519200	2.66170800	0.45806000
N	2.99492300	1.10704900	-0.48831400
C	-1.96453500	-0.53414800	-2.56754900
C	-2.91726700	0.40318200	-3.03908000
C	-2.30487500	-1.90537900	-2.62161200
N	-2.55865700	-3.04336700	-2.61567600
N	-3.69127200	1.20873700	-3.36788100
C	4.07312000	0.14419600	-0.25628600
H	3.67978900	-0.72585500	0.26737400
H	4.77980100	0.61172300	0.43553200
C	4.78754100	-0.27558800	-1.54272400
H	4.04879600	-0.67523600	-2.24968800
H	5.22946300	0.60996800	-2.01459800
C	5.87454700	-1.32559500	-1.29123300
H	6.40843700	-1.49755100	-2.23228600

H	6.61376500	-0.92520400	-0.58562400
C	5.33370700	-2.65761200	-0.76489200
H	6.12858500	-3.40690200	-0.71550100
H	4.91571900	-2.56550500	0.24249700
H	4.55154700	-3.04754000	-1.42698600
C	2.13474100	0.21033400	2.45391100
C	0.85404600	-0.07277500	1.93949600
C	2.58457300	1.53868700	2.65522000
C	3.04325400	-0.83710100	2.75094800
C	0.36037800	-1.41205500	1.83945300
C	-0.01656300	0.96642200	1.50295600
N	2.94089800	2.63783500	2.80627500
N	3.78016400	-1.72312500	2.91867000
C	-0.86820900	-1.70657100	1.32463200
H	0.99579000	-2.22622600	2.17784300
C	-1.25763500	0.69632700	1.00043500
H	0.30658700	1.99774800	1.59369200
C	-1.73818100	-0.63977600	0.88726000
C	-1.36174700	-3.12296300	1.20981200
H	-1.88202000	1.52530600	0.69613500
N	-2.97757600	-0.90706600	0.42178800
H	-1.17476500	-3.50029300	0.19568000
H	-0.81416700	-3.76668400	1.90300600
C	-2.86259300	-3.15452500	1.48060200
C	-3.57031500	-2.24865800	0.48743000
H	-3.06204900	-2.82239200	2.50625600
H	-3.26058000	-4.16675200	1.37306700
H	-3.53972500	-2.69587100	-0.51463100
H	-4.62080500	-2.12419800	0.76553800
C	-3.91140500	0.15925600	0.06158700
H	-3.38600500	0.93967300	-0.49227300
H	-4.63034000	-0.26685800	-0.64440400
C	-4.63770200	0.75285800	1.26964400
H	-3.90132300	1.13387600	1.98840000
H	-5.19539900	-0.03859800	1.78735600
C	-5.59130400	1.87451200	0.85907700
H	-5.02741000	2.65130100	0.32725100
H	-6.32337300	1.48572900	0.14036300
C	-6.31785800	2.49367800	2.05135900
H	-5.60727300	2.92125900	2.76690100
H	-6.99363400	3.29166900	1.73142700
H	-6.91411000	1.74377000	2.58234800

 14π

C	0.48558300	-2.34484900	-0.05368200
C	0.86974900	-1.60826900	-1.21602000

C	-0.07878500	-0.68099000	-1.72114700
C	-1.31493800	-0.53597500	-1.14993500
C	-1.69921100	-1.27461100	0.00234000
C	-0.73140900	-2.19194800	0.55094200
H	1.18082800	-3.07550800	0.35310600
H	0.16016100	-0.111173800	-2.61307800
H	-2.00850500	0.15462800	-1.60445100
C	-1.10788700	-3.01067100	1.75684100
H	-1.57483600	-3.94895800	1.42743300
H	-0.20957600	-3.28441900	2.31768900
C	-2.09128600	-2.23202000	2.61972200
H	-1.61906300	-1.33647500	3.03226100
H	-2.43494700	-2.82917200	3.46851300
C	-3.29937700	-1.83662000	1.79236900
H	-3.90681100	-2.72683700	1.57137400
H	-3.91714900	-1.13433500	2.36348100
N	-2.95264400	-1.18340900	0.52477700
C	2.11219600	-1.81584200	-1.85939600
C	2.98050000	-2.87272900	-1.48220900
C	2.49046200	-1.01740000	-2.96214300
N	2.77252200	-0.30533100	-3.84195500
N	3.67319400	-3.74642500	-1.14744400
C	-4.13973700	-0.83592300	-0.28001900
H	-4.97306800	-1.02108400	0.40150100
C	-4.34593900	-1.73884300	-1.51486900
H	-3.39285600	-1.90248700	-2.02939100
H	-4.74875000	-2.71834300	-1.24128200
C	-5.27826400	-0.91106300	-2.40196200
H	-5.30746800	-1.26693000	-3.43522700
H	-6.30264000	-0.94850700	-2.01066800
C	-4.71214000	0.50999600	-2.26786800
H	-5.42297500	1.28617800	-2.56000700
H	-3.83848300	0.61195300	-2.92346300
C	-2.16765800	2.15440100	1.43214800
C	-0.89682200	1.80708000	0.94206300
C	-2.72074200	1.51890200	2.57243700
C	-2.92889100	3.19019200	0.82541100
C	-0.35293400	2.39790000	-0.24169100
C	-0.06146300	0.87991600	1.63057000
N	-3.15262600	0.97149900	3.50597700
N	-3.52664000	4.03682800	0.29681500
C	0.89605200	2.10583000	-0.70664400
H	-0.96921600	3.09359000	-0.80486600
C	1.21909500	0.63459400	1.22758700
H	-0.42485800	0.42091200	2.54298500
C	1.76901400	1.23592500	0.05775100

C	1.41467800	2.71654800	-1.97736300
H	1.82318000	-0.01487500	1.83848800
N	3.06295900	1.06478200	-0.29777700
H	1.32623300	1.99631200	-2.80086300
H	0.81949200	3.59447000	-2.24151400
C	2.88299600	3.07013100	-1.78670300
C	3.65747300	1.81813700	-1.41760300
H	2.98456000	3.82578800	-0.99860000
H	3.31158100	3.48316900	-2.70351000
H	3.72580200	1.15307600	-2.28805600
H	4.67325200	2.08992900	-1.12089400
C	4.07661200	0.41164400	0.55799700
H	4.95828500	0.36404200	-0.08300200
C	4.43648700	1.25149500	1.80483500
H	3.52806700	1.68630800	2.23675700
H	5.11357400	2.07559400	1.56204800
C	5.03619500	0.22434600	2.76783000
H	6.06454300	-0.01634600	2.47154500
C	-4.29366100	0.62491300	-0.78987800
H	-3.38223900	1.20277900	-0.65898300
H	-5.05974700	1.13875300	-0.20366600
H	5.06732300	0.58178700	3.80042800
C	4.13245700	-1.00251700	2.57991900
H	3.21022300	-0.86445000	3.15861100
H	4.59107400	-1.93013000	2.93038000
C	3.83622800	-1.03730600	1.06868600
H	2.83995000	-1.41125000	0.83988000
H	4.52991600	-1.70927800	0.56040900

The following table contains the absolute energies for the dispersion calculation comparison. All structures, sigma dimers and pimers, were optimized using ω B97XD/6-31+G(d,p) using the chloroform SMD solvent model. Single point energy calculations were run on the optimized sigma dimers and pimers using both B97D/6-31+(d,p) and B98/6-31+(d,p). The pimer energy under each functional was subtracted from the sigma dimer energy, converted into kcal/mol and then the B98 difference was subtracted from the B97D difference. These absolute dispersion energies were then normalized to the lowest dispersion energy (compound 2).

Compound	B97D Pimer (Hartrees)	B97D Sigma (Hartrees)	B98 Pimer (Hartrees)	B98 Sigma (Hartrees)	Δ B97 D (kcal/mol) Sigma-Pimer
2	-1215.2654	-1215.2600	-1215.6047	-1215.6314	3.4020
4	-1215.3387	-1215.3141	-1215.6868	-1215.6971	15.4635
5	-1287.0859	-1287.0636	-1287.4432	-1287.4547	13.9946
6	-1178.0517	-1178.0166	-1178.3763	-1178.3773	22.0274
7	-1487.4216	-1487.3860	-1487.8361	-1487.8413	22.3734
8	-1332.7990	-1332.7626	-1333.1858	-1333.1862	22.8916
9	-1406.4765	-1406.4595	-1406.8917	-1406.9115	10.6435
10	-1251.7906	-1251.7745	-1252.1580	-1252.1780	10.1082
11	-1254.2256	-1254.1845	-1254.5881	-1254.5841	25.8284
12	-1332.8157	-1332.7717	-1333.1935	-1333.1915	27.6230
13	-1568.5580	-1568.5139	-1569.0020	-1568.9997	27.6964
14	-1644.6877	-1644.6528	-1645.1628	-1645.1744	21.8930
15	-1487.5699	-1487.5252	-1488.0018	-1488.0038	28.0656
Compound	Δ B98 (kcal/mol) Sigma-Pimer	$\Delta\Delta$ (kcal/mol)	Benzylic Spin Density	ΔE normalized (kcal/mol)	
2	-16.7666	20.1686	0.5748	0.0000	
4	-6.4922	21.9557	0.5241	1.7872	
5	-7.2042	21.1988	0.5478	1.0302	
6	-0.6272	22.6546	0.4253	2.4860	
7	-3.2609	25.6343	0.4546	5.4657	
8	-0.2158	23.1075	0.4063	2.9389	
9	-12.4790	23.1226	0.5525	2.9540	
10	-12.5820	22.6902	0.5484	2.5216	
11	2.5202	23.3082	0.3992	3.1397	
12	1.2555	26.3675	0.3878	6.1989	
13	1.4372	26.2592	0.3889	6.0906	
14	-7.3184	29.2114	0.3858	9.0429	
15	-1.2727	29.3382	0.3411	9.1697	